LUMBOSACRAL TRANSITIONAL VERTEBRAE MORPHOLOGY: A SOUTH AFRICAN POPULATION

By

Glen James Paton

SUBMITTED TO THE UNIVERSITY OF CAPE TOWN

In fulfilment of the requirements for the degree

DOCTOR OF PHILOSOPHY (PhD) in Clinical Anatomy

Date of submission 19 July 2021

Supervisor: Emeritus Professor Graham J. Louw (UCT)

Co-supervisors: Associate Professor Scott A. Williams (NYU)

Associate Professor Shahed Nalla (UJ)

Department of Human Biology

Faculty of Health Sciences

DECLARATION

I, Glen James Paton, hereby declare that the work on which this dissertation/thesis is based is my original work (except where acknowledgements indicate otherwise) and that neither the whole work nor any part of it has been, is being, or is to be submitted for another degree in this or any other university.

I empower the university to reproduce for the purpose of research either the whole or any portion of the contents in any manner whatsoever.

Signature: Signed by candidate Date: 19/7/2021

ABSTRACT

Lumbosacral transitional vertebrae (LSTV) are defined as congenital anatomical variations, observed unilaterally or bilaterally, in which the transverse process of the last lumbar vertebra exhibits signs of dysplasia evident as increased craniocaudal height, with varying degrees of articulation or fusion to the 'first' sacral vertebra. Such variations give rise to vertebral morphology that may display lumbar or sacral characteristics at the terminal lumbar spine, together with subsequent enumeration variation.

The purpose of this study was to establish baseline data on the prevalence rates of LSTV and to describe the morphological characteristics (Type, subtype, frequency of side and spinal enumeration) of LSTV in the South African population. This study was subdivided into two main sections, namely Part 1: medical imaging appraisal and Part 2: osteological morphology appraisal.

In Part 1, both retrospective and prospective cohort randomised sampling methods of data collection of medical images were used. The appraisal of the medical images included radiographs, magnetic resonance imagers and computerised tomography scans. Prevalence rates, utilising the Castellvi et al. (1984) classification, were established via radiographs only. Additionally, lumbar spine enumeration, namely lumbarisation and sacralisation, was made through the appraisal of lumbar radiographs. Images were obtained from medical radiology practices located at Groote Schuur Hospital in Cape Town, Western Cape Province and Charlotte Maxeke Johannesburg Academic Hospital in Johannesburg, Gauteng Province.

The total imaging cohort included 3096 individuals of which 308 individuals (10%) were found to contain LSTV. Prevalence rates were further evaluated by subdivision of the three largest ancestries in South Africa. Ancestries were classified as African (n=1032), Mixed (n=1032) and European (n=1032). The prevalence of LSTV in the three ancestral groups was 10.5%, 9.3% and 9.9% respectively and the sex distribution was greater in females (52.1%) then in males (47.9%). The morphological assessment found the prevalence of LSTV by Type was Type II (67.9%) followed by Types III (27.6%) and IV (4.5%). The most frequent subtype by prevalence was Type IIA (41.9%) followed by Type IIB (26%), Type IIIB (21.8%), and Type IV (5.8%). Additionally, the frequency of side was bilateral (47.7%), left (26.6%), right (21.1%), and other (4.5%).

Comparison of ancestry and spinal enumeration analyses established statistical significance for individuals of African-ancestry (67.0%) and Mixed-ancestry (72.9%) both of which demonstrated a greater affinity of prevalence for sacralisation (p=0.008), with a small effect size (V=0.178) over the European-ancestry subgroup (52.4%). Furthermore, a statistical significance with a medium effect size (V=0.256) was found in males (p=0.010) when comparing ancestry and spinal enumeration between sexes.

In Part 2, a systematic search of the total cadaveric skeletal collection housed at the University of Witwatersrand (the Dart Collection of skeletons) yielded 1797 human skeletal specimens of between 21 and 65 years of age at time of death. One-hundred and fourteen skeletal remains were identified as containing LSTV. Damage and loss of vertebral elements resulted in a subset of 91 LSTV for study. A sex balanced control group cohort of 30 males and 30 females was selected at random from the Dart Collection for comparative analyses. A number of osteometric measurements were evaluated comparing the LSTV and control group cohorts. Numerous osteometric comparisons were statistically significant highlighting the many changes in lumbar and sacral morphology associated with LSTV.

There are several original findings to emerge. This is the first study to establish the prevalence of LSTV in a large sample from the South African population, subdivided into the three largest ancestral groups. Novel findings associated with LSTV include iliolumbar articulation, bipartition of the sacral foramen, intra-articular vacuum phenomenon of accessory articulations of LSTV, enlargement of the contralateral TVP associated with Types III and IV LSTV, lumbar ossified bridging syndrome and a novel complex named by the researcher as the transverso-sacro-iliac articulation. Furthermore, the researcher has proposed three modifications to the Castellvi et al. (1984) classification, namely (1) that there should be a sub-classification of the Type IV LSTV into right and left nomenclature, (2) the inclusion of a new subtype of Type II LSTV morphology, a unilateral right or left iliolumbar articulation associated with contralateral Type IIA morphology, and (3) a modified morphological classification of LSTV based on the presence of an extended sacroiliac articulation either directly or via the transverso-sacro-iliac articulation. The latter effectively increases the size of the sacroiliac joint and is thought to increase spinopelvic stability. The transverso-sacro-iliac articulation was demonstrated for all clinically significant LSTV Types (II-IV), both unilateral (right or left) and bilateral. Finally, this is the first study to incorporate an *in situ* and an *ex situ* study in the same population by examining spinal morphology of LSTV using medical images and skeletal remains for descriptive analyses.

ACKNOWLEDGEMENTS

To my supervisor, Professor Graham Louw, I owe a greatest debt of gratitude to you! Graham, your vast knowledge, coupled with your endless patience, makes you a remarkable supervisor. Thank you for guiding me through often unfamiliar terrain while allowing me to find me own way. This thesis is only possible because you saw potential in me and my concept.

To my Co-supervisors, Associate Professor Scott Williams and Associate Professor Shahed Nalla, you both contributed invaluably to the research. I was fortunate enough to spend time with both of you in your 'natural-environments', the Skeletal Collection, examining bones.

Nicole, you have been my soundboard for my thoughts, an active participant in my deliberative process, and you reviewed my seemingly endless work. You have supported me throughout. Thank you for all your love, support, and assistance with my work and keeping me grounded. I am a better person because of you. I dedicate this thesis to you.

Jaclyn de Klerk, thank you for the hours spent assisting me with the convoluted world of statistics. Little did I know, the months it would take to decipher and write-up the numerous statistics for this research. You were always willing and available to assist me at every point.

Dewald Basson, thank you for your wonderful hospitality and incredible assistance with the navigating the PACS imaging software at Groote Schuur Hospital, Radiology Department. You made feel at home.

Associate Professor Mgomezulu, Head of Department of Radiology at the University of Witwatersrand, thank you for your assistance and willingness to help me gain access to the medical images necessary for this study.

Professor Beningfield, Head of Department of Radiology, Groote Schuur Hospital, thank you for allowing me access to your department and assisting with institutional access via the Department of Health in the Western Cape.

To my colleagues, past and present, at the University of Cape Town. Doctors Devin Finaughty, Kentse Mpolokeng, Francesca du Toit, you all played a meaningful role in helping me along the way. Thank you.

Doctor Brendon Billings, thank you for all the assistance you provided as the curator of the Dart Skeletal Collection at the University of Witwatersrand.

Doctor Nicholas Bacci, thank you for inadvertently inspiring me to conceptualise the redesign of the lumbosacral transitional vertebrae classification.

Leann Morecroft-Davies, thank you for the endless hours of proof reading all while trying to make sense of the many intricate concepts throughout the thesis writing.

Peet Beneker, thank you for your fantastic artistic contributions to the thesis. You were able to take my ideas and turn them into wonderful stylistic creations. It was a great collaborative effort.

Mashudu Malaudzi, thank you for your technical assistance with Dart Collection.

To my brother, Ian, thank you for the use of your digital camera used to take the images for this thesis. It proved invaluable in illustrating the skeletal measurements.

Doctor Markus Linzbacher, thank you for being a great friend. You allowed me to vent my frustration, bounce ideas off of you, and was always willing to listen to my ramblings of my thesis and its process throughout the many years of hard work. Thank you.

To my Mom and Dad, thank you for your ongoing support over the many years it has taken to complete this thesis.

Thank you to the three examiners for their valuable feedback on my thesis.

I wish to express my sincere gratitude to each person whose remains I was able to study in depth in order to ensure the success of this research project.

TABLE OF CONTENTS

LIST OF FIGURES

Chapter 1

Chapter 2

Chapter 3

Chapter 4

Chapter 5

LIST OF TABLES

Chapter 1

Chapter 2

Chapter 3

Chapter 4

Chapter 5

LIST OF APPENDICES

CHAPTER 1

INTRODUCTION and LITERATURE REVIEW

CONTEXT AND BACKGROUND

Congenital anatomical variations of the spine are important to anatomists, anthropologists, clinicians and surgeons alike. Congenital morphological variation of the lumbosacral junction gives rise to vertebral morphology that may display lumbar or sacral characteristics at the terminal lumbar spine, together with subsequent enumeration variation. These morphological variations of the lumbosacral junction are known broadly as lumbosacral transitional vertebrae (LSTV).

Lumbosacral transitional vertebrae are defined as congenital anatomical variations, observed unilaterally or bilaterally, in which the transverse process of the last lumbar vertebra exhibits signs of dysplasia (increased craniocaudal height), with varying degrees of articulation or fusion to the 'first' sacral vertebra (Southworth and Bersack, 1950; Hughes and Saifuddin, 2004; Jancuska et al., 2015).

There are two descriptive terms associated with LSTV and vertebral enumeration in the literature, namely lumbarisation and sacralisation. These terms allude to the number of motion segments contained within the lumbar spine and by implication the segments contained within the sacrum (assuming no sacrococcygeal transitional segment present). Lumbarisation refers to a caudal shift where there is separation or partial separation of the first sacral vertebra (S1) by which it gains characteristics of a lumbar vertebra (Savage, 2005; Konin and Walz, 2010; Mahato 2010; Barnes, 2012). Sacralisation is a cranial shift where fusion or partial fusion of the last lumbar vertebra (usually L5) gains characteristics of a sacral vertebra (Savage, 2005; Konin and Walz, 2010; Mahato, 2010; Barnes, 2012). Note: sacralisation *here* must not be confused with sacrococcyx border shifting in which the term sacralisation refers to the incorporation of the first coccyx to the sacrum (O'Rahilly et al., 1990). For the context of this study, all references of sacralisation will pertain to the lumbosacral junction only.

Lumbosacral transitional vertebrae were first described in the early 1800s (Wenzel, 1824), and have since gained notoriety in 1917 due to the descriptions of Italian physician Mario Bertolotti for its reported association with LBP (Bertolotti, 1917; Blumensaat and Clasing, 1932; Elster, 1989; Dzupa et al., 2014). The condition of LBP with concomitant positive identification of LSTV attracted the eponym 'Bertolotti's syndrome' (Bertolotti, 1917). Researchers and clinicians have long thought that the presence of LSTV may increase the likelihood of LBP, and in some cases, may be the direct cause of LBP (Castellvi, Goldstein and Chan, 1984; Jönsson et al., 1989; Avimadje et al., 1999; Nardo et al., 2012; Jancuska et al., 2015). This may be due to pseudo-articulation arthrosis, bone trabeculae alteration, bone marrow oedema, disc degeneration, disc herniation, spinal stenosis, spondylolisthesis above the LSTV, muscle strains, sacroiliitis (sacroiliac joint inflammation which may cause pain) and nerve impingement (Nachemson, 1975; Castellvi et al., 1984; Hughes 2004; Savage, 2005; Konin and Walz, 2010; Jancuska et al., 2015; Nevalainen et al., 2018). Correct identification of an LSTV is essential as inaccurate or misidentification may lead to incorrect vertebral level surgery or error in anaesthetic procedures such as infiltrations (cortisone and local anaesthetic combinations) for pain management (Malanga and Cooke, 2004; Konin and Walz, 2010; Apazidiset al., 2011; Sharma et al., 2011; Nakagawa et al., 2017). Lumbosacral transitional vertebrae are a clinically relevant anatomical variation of interest for professionals involved in managing of lumbar spine conditions including pain management. These practitioners may include manual therapists and medical practitioners namely chiropractors, physiotherapists, osteopaths, sports physicians, orthopaedic surgeons and neurosurgeons.

As a chiropractor, the author had seen many patients with medical imaging containing LSTV and had recognised there was paucity in South African-specific literature on prevalence and morphology. Anecdotally, the author had seen low back pain in association with LSTV although this was not the focus of the study.

Aims of the study

This study aims to establish baseline data on the prevalence rates of LSTV and describe the morphological characteristics of LSTV in a South African population.

Objectives of the study

- Investigate the prevalence rate of LSTV in a sample of the South African population
- Within the context of prevalence rates, investigate if ancestry and sex plays a role in the prevalence of LSTV. Ancestries were classified as African, Mixed and European within a South African sample.
- Evaluate osteological morphology of LSTV *in situ* and *ex situ*. The *ex situ* anthropological portion of the study was to evaluate what changes may occur over time in various anatomical structures of the bony elements associated with LSTV.

ANATOMY OF THE LUMBAR SPINE AND SACRUM

In order to understand lumbosacral anatomical variation, it is important to understand the embryological development process and structural anatomy of the lumbar spine, sacrum and surrounding connective tissue.

Genetics of the lumbar spine and sacrum

Tini et al. (1977) found that LSTV has a genetic link with hereditary familial traits. Genes are pivotal in the formation of anatomic variations and at the centre are *Hox* genes (Pilbeam, 2004).

Hox genes are a sub-class of homeobox genes which are transcription factors involved in axial patterning in ontogenesis and embryogenesis. These genes are a regulatory family of genes, 39 *Hox* genes arranged in four clusters, expressed along the anterior to posterior (A-P) axis in all metazoans (Burke et al., 1995; Forlani et al., 2003; Pilbeam, 2004; Wellik, 2007).

Hox genes control many factors, including the development of the appendicular and post-cranial axial skeleton, the body wall and connective tissue of the limbs and have been a major contributor (although not the only contributor) to the morphological identity of the vertebrae through their effect on the somites and vertebrogenesis (Fromental-Ramain et al., 1996; Burke and Nowicki, 2001; Pilbeam, 2004; Carapuço et al., 2005; Wellik, 2007). The primary function of *Hox* genes is the segmentation of the body plan, including the vertebral column, while the secondary function is the second layer of patterning that is required to achieve the final segmented morphology of the vertebral column. The secondary morphological characteristics distinguish the vertebrae by region based on their macroscopic appearance (Wellik, 2009). *Hox* gene expression is directly linked to the progression of embryogenesis and follows the third 'three prime' and fifth 'five prime' (3'-to-5') carbon numbers in the deoxyribose order, expressing an A-P order of appearance in a cranial to caudal order of development (Fromental-Ramain et al*.,* 1996; Forlani et al*.,* 2003; Pilbeam, 2004; Wellik, 2007).

Lumbar and sacral vertebral formation in humans is thought to be via the *Hox* genes, namely *Hoxa-9* for levels one through to three of the lumbar vertebrae (L1-L3) and *Hoxd-9* for levels from the third lumbar vertebra through to the first coccyx (L3-Cy1) (Fromental-Ramain et al*.,* 1996). Evolutionary changes of the post-cranial axial formula likely represent perturbations of *Hox* gene expression. Perturbations in *Hox* gene expression had been demonstrated to result in segmental homeotic transformations of one vertebra into another (Burke et al*.,* 1995, Forlani et al*.,* 2003). Changes in arrangement and proportions of the *Hox* genes may account for the morphological variation and segmental homeotic shift that occurs during the course of vertebrate evolution (Burke et al*.,* 1995; Burke and Nowicki, 2001; Wellik, 2007; Williams et al., 2019). Therefore, it is theorized that LSTV are partly as a result of perturbations in *Hox* gene expression (Pibeam, 2004; Williams et al., 2019).

It appears *Hox 10* paralogous group genes are essential to lumbar vertebrae morphology as studies have found that omission of these genes created thoracic-like morphological changes at the lumbosacral segments, including rib development (Scaal, 2016). *Hox 11* has also been implicated in axial patterning along with *Hox* 10 (Jancuska et al., 2015; Du Plessis, 2017). Essentially, *Hox 10* paralogous genes suppress rib formation (and create lumbar vertebrae), while *Hox 11* acts to suppress *Hox 10*, so the sacrum develops (McIntyre et al., 2007; Wahba et al., 2001; Wellik & Capecchi, 2003; Williams, SA. 2020, personal communication, 5 October 2020). As demonstrated by Fromental-Ramain et al*.* (1996), the *Hox* genes affect the coronal orientation of homeotic transformations of the vertebral column. Anteriorisation is one such process whereby a change in orientation, in the axial plane, is towards an anterior bias. Fromental-Ramain et al. (1996) expose that H*ox* genes influence post-cranial formula via homeotic shift both segmentally and axially.

In humans, the boundary between primary gastrulation (the first twenty-eight pairs of somites formed from the primitive streak) and secondary gastrulation, (somites found posteriorly that develop from the tail bud) lies at the level of the fifth lumbar vertebra (Christ et al., 2000).

Early human embryonic development

The development of the vertebral column contains a number of phases that must occur throughout the embryonic development process. These phases include (Dias, 2007; Du Plessis, 2017):

1. Gastrulation;
2. Formation of the somitic mesenchyme and notochord;
3. Differentiation of cells to form the sclerotome, dermomyotome and syndetome from somites;
4. Resegmentation of the somites to form vertebrae;
5. Vertebral chondrification, and
6. Ossification.

Williams and Russo (2015) defined a homeotic shift as the transformation of one segment into a different segment. Lumbosacral transitional vertebrae indicate a homeotic shift at the lumbosacral border both segmentally and axially (left or right or both). The lumbosacral region is susceptible to malformations and is a common site of spina bifida amongst other variations (Christ et al., 2000). Neural tube development is also known as neurulation has two phases, primary and secondary.

Pang et al. (2011) described primary neurulation, as the formation of the primary (cranial) neural tube, whereas the secondary (caudal) neural tube transforms from the caudal cell mass (caudal eminence or tail bud) into a compact epithelial rod known as the medullary cord. The medullary cord undergoes partial regression, degeneration and cavitation to form the lower conus medullaris and the filum terminale in the adult. Closure of the caudal neuropore marks the start of secondary neurulation. The caudal eminence gives rise to the caudal notochord, tail gut, caudal somites and the urogenital tracts in the caudal end of the embryo (Pang et al., 2011). It is thought that failure of closure of the caudal neural tube is, in part, responsible for a portion of the malformations seen in the lumbosacral region, including spina bifida (Deora et al., 2019).

Human development begins after fertilisation when a diploid zygote is formed by the fusion of two haploid gametes. During cell proliferation, the zygote forms a morula and ultimately a blastocyst. The blastocyst becomes the bilaminar embryo suspended between two cavities, the amniotic and yolk sacs (Du Plessis, 2017). Thereafter, gastrulation occurs to create a trilaminar embryo (Keller, 2005). During development, there is a myriad of cell types that must be formed. Besides the requirement of a cell's fate, development must occur in a context-appropriate for its surroundings; 'positional information'. Coined by Lewis Wolpert (1969), positional information describes the translation of genetic information into reproducible spatial patterns of cellular differentiation (Wolpert, 1969; Wellik, 2009).

In the early stages of cell formation, the bilaminar embryo is transformed into a trilaminar cellular structure through the process of gastrulation. During gastrulation, cells are directed into one of three primitive cell layers: ectoderm, endoderm and mesoderm through the process of infolding of the blastocyst. The epidermis, nervous system, as well as retina and ear development (in part), are derived from the ectoderm. The gastrointestinal lining as well as the urinary bladder, and organs such as the lungs, liver and pancreas, are derived from the endoderm. The mesoderm gives rise to the dermis, hypodermis and the muscular wall of the gastrointestinal tract as well as the axial and appendicular skeleton, tendons and musculature. In addition, the mesoderm gives rise to the cardiovascular system, kidneys and immune system. The vertebrate musculoskeletal system arises from two populations of embryonic mesoderm; paraxial and presomitic mesoderm (Christ et al., 2000; Pilbeam, 2004; Figure 1.1). The ectoderm, endoderm and mesoderm, as well as their derivatives, arise from the paired somites (Fleming et al., 2001; Bogduk, 2005; Kaplan et al., 2005; Keller, 2005; Wellik, 2009).

Embryology of the lumbar spine and sacrum

Somites are commonly described as block-like or spherical-shaped structures (Figures 1.4 and 1.5) that are paired segmental units found in the paraxial mesoderm (Fleming et al., 2001; Brent et al., 2003; Figure 1.2). The somites are found on either side of the developing notochord and give rise to the appendicular and axial skeleton (includes the skull).

Likewise, with the exception of certain groups of muscles in the head and neck which arise from branchial arches, the somites give rise to striated muscle (Burke and Nowicki, 2001; Carapuço et al., 2005).

The 42 to 44 somites of the human embryo are divided into groups: 4 occipital, 8 cervical, 12 thoracic, 5 lumbar, 5 sacral and 8-10 coccygeal somites (O'Rahilly and Müller, 2003) (Figure 1.2). The 7th and 8th paired coccygeal somites regress and do not contribute to the vertebral column, while the first pair of occipital somites gives rise to the muscles of the tongue and basi-occipital cartilage, respectively (Bogduk, 2005; Kaplan et al., 2005).

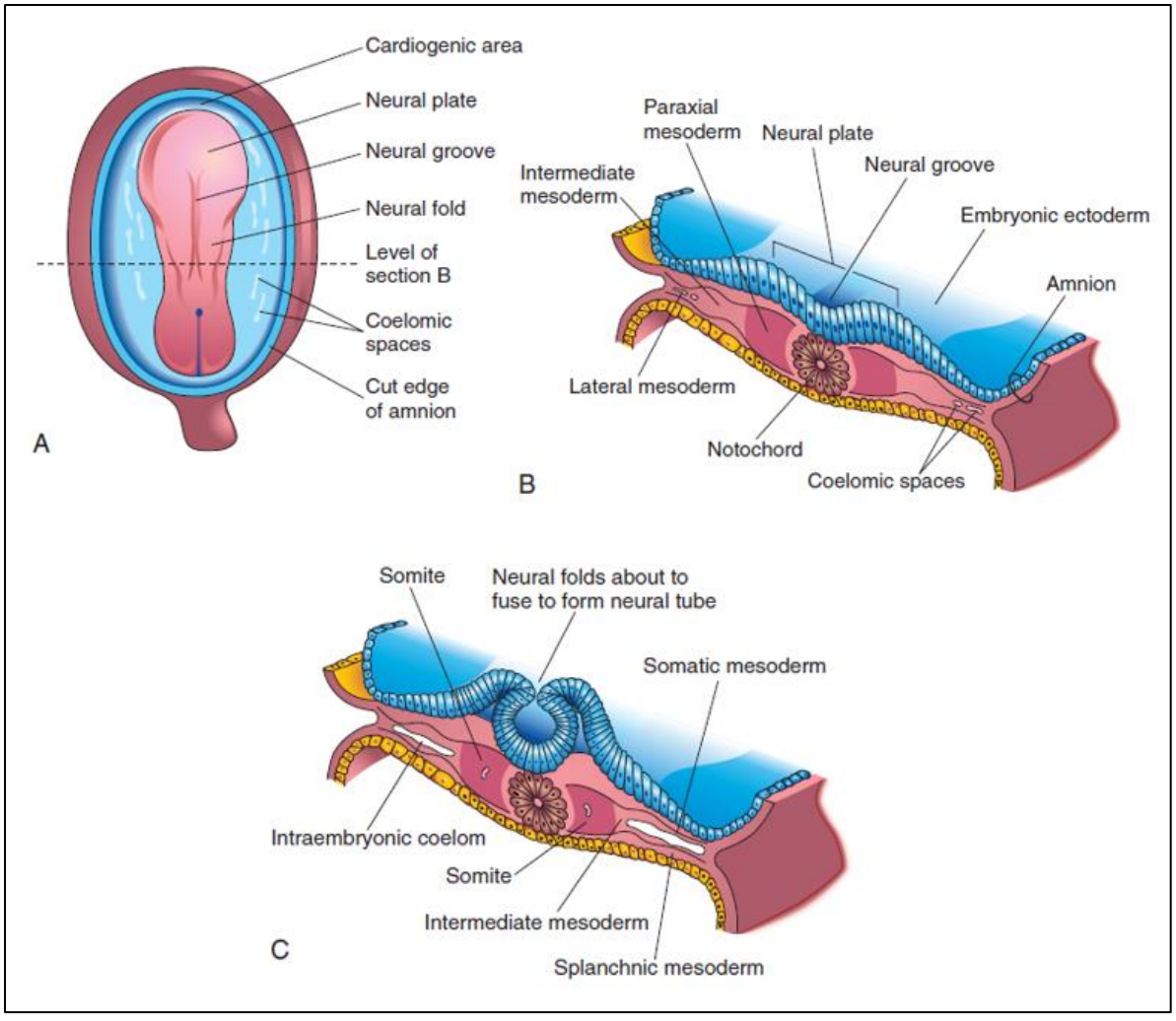

Figure 1.1: *Formation and early differentiation of somites within the blastocyst embryo.* ***A)*** *Posterior view of an approximate 18-day embryo.* ***B)*** *Transverse section of an embryo (seen In* ***A****) illustrating the paraxial mesoderm from which somites are derived. Forty-two to forty-four pairs of somites are created by further differentiation from the paraxial mesoderm.* ***C)*** *The Transverse section of an approximate 22-day embryo with somite appearance noticeable (Adapted from Moore et al., 2018). Used with permission from Elsevier.*

Somitic mesenchyme

Mesenchyme is made up of loose connective tissue cells located within the mesoderm layer. The somites are originally of an epithelial cell type but gradually undergo epithelial-to-mesenchymal transition (EMT). This differentiation of EMT is a central process that affects specific progenitor cells of all three germ layers in the fourth week of development (Fleming et al., 2001; Savage, 2005; Dias, 2007; Kalchiem, 2015).

The somites contain two clusters of cells, which can be divided into four tissue types (Figure 1.2). The somitic mesenchyme arises from columnar epithelial cells to form the first cluster and tissue type, the sclerotome. The sclerotome forms the axial and appendicular skeleton, specifically the vertebral column, namely the lumbar spine and sacrum in the context of this study (Brent et al., 2003). The other cluster, the dermomyotome gives rise to the trunk and musculature of the skin, that is to say, the erector pili muscles and specifically the dermis and hypodermis. The dermomyotome comprises two tissue types, the dermatome and myotome (Fleming et al., 2001; Bogduk, 2005; Dias, 2007). The fourth tissue type, the syndetome, lies at the interface of the myotome and sclerotome and gives rise to tendons (Brent et al., 2003; Dubrulle and Pourquie, 2003).

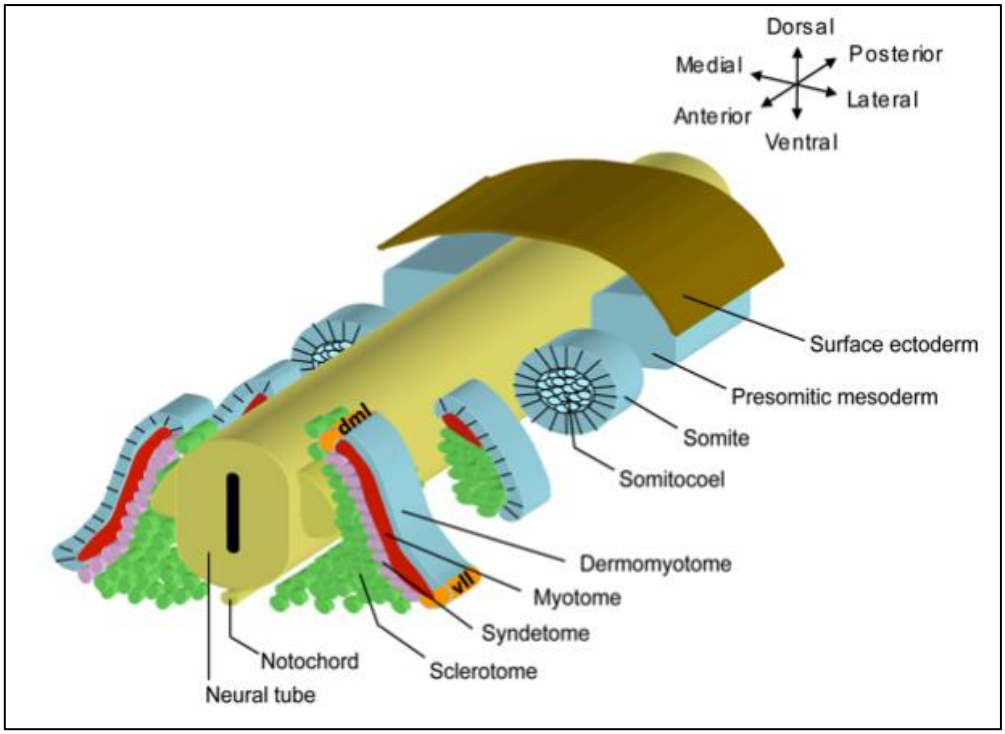

***Figure 1.2**: The tissues of the musculoskeletal system of embryonic origin. Starting at the anterior end of the embryo, in a caudal (posterior) direction, the presomitic mesoderm is segmented and epithelialised in a mesenchymal-to-epithelial transition to form somites. The epithelialisation of somites is imperative to the patterning of its derivatives. Maturing somites then undergo epithelial-to-mesenchymal transition to form four tissue-specific compartments. The sclerotome gives rise to the axial cartilage and bone. The syndetome gives rise to tendons. The dermatome gives rise to adipocytes and endothelial cells and the myotome gives rise to skeletal muscle and the dermis (Adapted from Rowton, 2013). Used with permission from the author.*

An important mesoderm-derived structure, the notochord, provides structural support as the centre axis of development for the axial skeleton of the embryo (Stemple, 2005). The notochord is a transient embryonic structure that regresses during vertebral column formation. As the notochord regresses, its original position is marked by the position of the vertebral bodies and contributes directly to the NP of the vertebral column. The vertebrae originate from either side of the notochord via the unsegmented paraxial or presomitic mesoderm. The roles of the notochord include the following: provide rigidity to the developing embryo, initiate neurulation (neural tube development) in the overlying ectoderm, axial patterning, the release of signalling proteins which support chondrification precursor cell development, the timing of segmentation of the axial skeleton as well as a direct component of NP development (Stemple, 2005; Christ et al., 2000; Burke and Nowicki, 2001; Pilbeam, 2004; Corallo et al., 2015; Ramesh et al., 2017).

Resegmentation

As far back as the mid-1800s Remak (1850) proposed the idea that one vertebra is not directly derived from one pair of somites. The concept of resegmentation of the sclerotome (vertebral formation) was derived over many years (Scaal, 2016). Resegmentation occurs after the metameric patterning that has taken place from individual somites to condensed layers of somitic mesenchyme of varying cell densities forming the sclerotome. The dense caudal somite domain coalesces with the less dense rostral somite domain to form a single vertebra. During the resegmentation process, the boundaries of the somite domains are shifted in a craniocaudal direction by roughly a half-segment frameshift (Huang, et al., 2000; Keynes, 2018; Figure 1.5A). The finalised contribution pattern of the vertebrae has a composition made up of roughly two thirds caudal and one-third rostral somite domain consolidation. Thus, a single pair of somites is not responsible for a single vertebra (Figures 1.3, 1.4 and 1.5)**.** The boundary between the prospective vertebrae lies in the sclerotome delineated by von Ebner's fissure, also known as the intervertebral fissure (Figures 1.3, 1.4A and 1.5D). It is at this junction there is the formation of the intervertebral foramen by which the spinal nerves grow outward towards the myotome which later becomes the striated muscles innervated by the spinal nerves, (Wolpert, 1969; Christ et al., 2000; Bogduk, 2005; Christ et al., 2007; Chal and Pourquié, 2009; Scaal, 2016; Keynes, 2018; Figure 1.3).

Additionally, the bilateral arterial supply to the somites originally emerges between adjacent blocks of somites but after the resegmentation processes cease, they then emerge at the level of each vertebra (Schoenwolf et al., 2009)

Segmentation and resegmentation are complicated fields of study in humans that form the basis of understanding vertebral formation of the spinal column. The knowledge relies on model species, mouse and chicken embryos, and it is still unclear at which stage of the development process, including tissue remodelling, apoptosis or tissue loss, is responsible for the finalised somitic contribution to human vertebral morphology. The evidence is inferred by the lineage tracing (Chal, J. 2020, personal communication, 30 May). The analogy is represented in colour coded human models seen in Figures 1.4, 1.5 and 1.6. The somites that contribute to the various segments of the vertebral column include somites 5 and 6 through to 11 and 12, which form the seven cervical vertebrae.

The somites 12 and 13 through to the 23rd and 24th somites form the twelve thoracic vertebrae, 24 and 25 through to 28 and 29 paired somites form the lumbar vertebrae and somites 30 and 31 through to the 33 and 34 pair form the sacrum. The somites 34 and 35 through to approximately 39 and 40 form the four segmented coccyx (variation in coccyx number exists) (Schmorl, 1971 adapted by Savage, 2005; Pang et al., 2011).

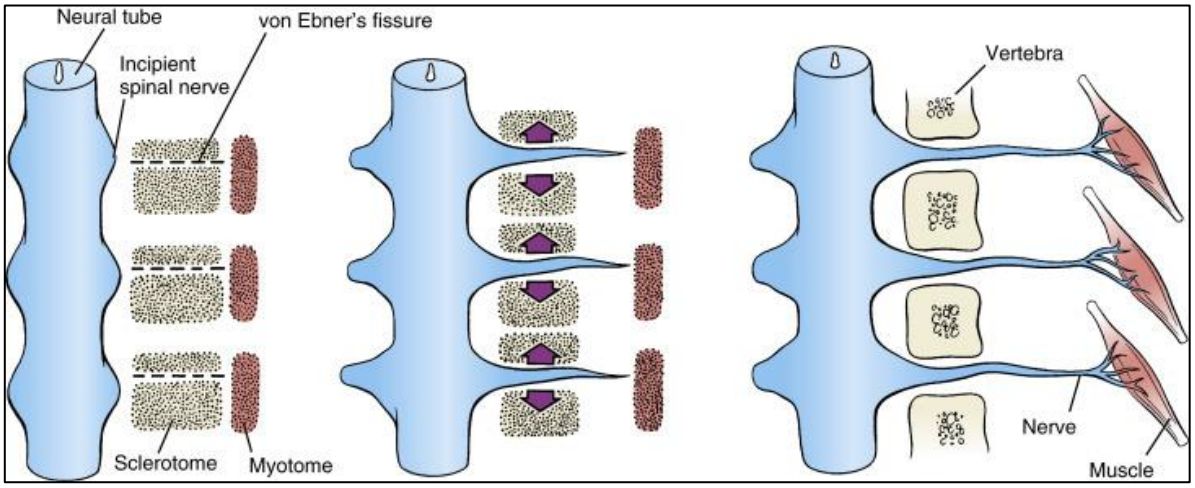

Figure 1.3: *Spinal nerve growth and resegmentation of the sclerotomes forming vertebrae.* ***Left)*** *Each sclerotome is separated by the von Ebner's fissure by which the segmental spinal nerves grow towards the cranial domain end of the somite in the direction of the myotome.* ***Middle)*** *Each sclerotome is divided into rostral and caudal domains in a 2/3 rostral and 1/3 caudal somite ratio, and each recombine to form the vertebral rudiment.* ***Right)*** *The adult macroscopic structure of the vertebrae and the spinal nerves extension to the muscles (Adapted from Schoenwolf et al., 2009). Used with permission from Elsevier.*

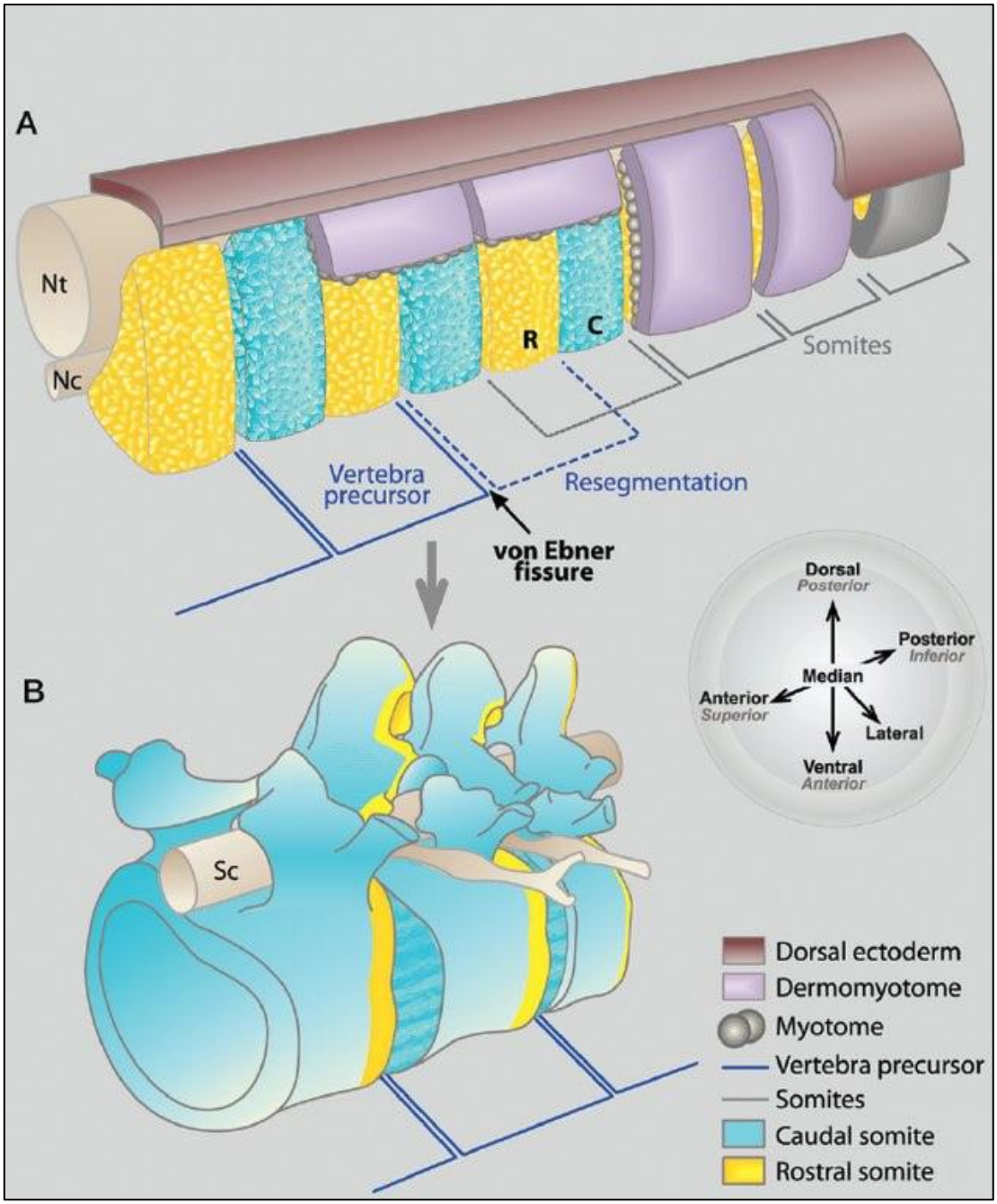

Figure 1.4: *Sclerotome resegmentation process and its contribution to vertebrae.* **A*)*** *Schematic temporal sequence (oblique side view) of resegmentation of the sclerotome. The rostral and caudal domains of the somite are divided by von Ebner's fissure. One somite (yellow) rostral compartment coalesces to the caudal compartment of the consecutive somite (blue) to form a single vertebra. Furthermore, the somites and the vertebral precursor are out of register by a half-segment after caudal and rostral somite fusion. Dorsal ectoderm (brown) and dermomyotome (purple) and the myotome, have been removed to aid the visualisation of sclerotome.* **B*)*** *Adult human vertebrae with a colour-coded projected overlay of the fate of the rostral and caudal sclerotome segments.* ***Note:*** *the illustration is to support the resegmentation concept and approximate boundaries. The finalised contribution pattern of the vertebrae is seen in* **B***. The final composition of vertebrae is made up of 2/3 caudal and 1/3 rostral somite domain consolidation. Orientation of the embryonic axis is indicated in the bubble in black.* ***R=*** *Rostral somite sclerotome segments.* ***C=*** *Caudal somite sclerotome segment.* ***NT=*** *Neural tube****. Nc=*** *Notochord.* ***Sc=*** *Spinal cord (Modified with permission from Chal and Pourquié, 2009).*

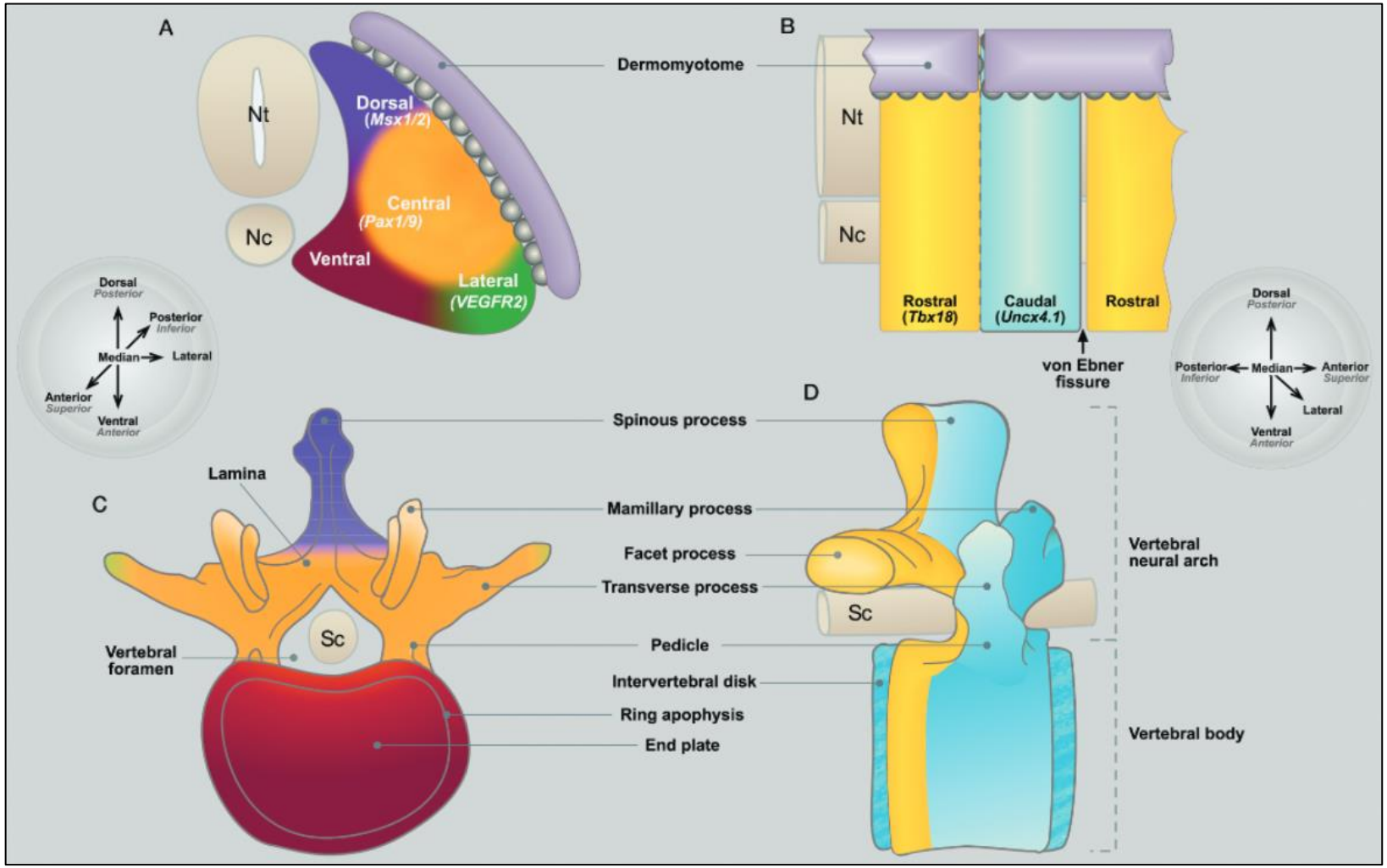

Figure 1.5: *The compartments of the sclerotome and their contribution to the vertebrae.* ***A)*** *Transverse view, sclerotome compartments and fate map indicating the molecular markers.* ***B)*** *Lateral view, sclerotome and von Ebner's fissure; dermomyotome has been removed to aid visualisation.* ***C)*** *Axial (superior view) and* ***D)*** *Lateral (right) view.* ***C and D)*** *Adult human vertebrae with colour-coded projection overlay of the sclerotome compartments, as seen in* ***A*** *and* ***B****, respectively.* ***Note:*** *the finalised contribution pattern of the vertebrae seen in* ***D****. The composition is made up of 2/3 caudal and 1/3 rostral somite domain consolidation. Orientation of the embryonic axis is indicated in the bubble in black. (R) Rostral somite sclerotome segments. Orientation of the embryonic axis is indicated in the bubbles, either side of the image, in black.* ***NT=*** *Neural tube****. Nc=*** *Notochord.* ***Sc=*** *Spinal cord (Adapted with permission from Chal and Pourquié, 2009).*

Chondrification and Ossification

Chondrification is a differentiation of mesenchymal cells along the A-P axis. The prechondrogenic cells migrate to surround the neural tube, condense to form prevertebral structures and ultimately form centres for chondrification (Wellik, 2009; Figure 1.6). The cartilaginous phase of vertebral development commences between the fifth and sixth weeks of gestation. Primary chondrification centres are found throughout the mesenchymal vertebra at the centrum, costal processes and neural arch, which gradually coalesce with time (Bogduk, 2005; Moore et al., 2018). These fused centres form the cartilaginous vertebra that then acts as the cartilage scaffold for the ossification phase (Moore et al., 2018).

Ossification of the lumbar spine and sacrum occurs between nine and eleven weeks of gestation. It is the gradual change of chondrocytes (cartilaginous matrix) to osteocytes forming bone via endochondral ossification (Figures 1.6 and 1.8). The secondary ossification centres are located in the superior and inferior ring epiphyses of the VBs, tips of the spinous process and transverse processes (Figure 1.7). Ossification ends at the 25th year (Cochard, 2012; Skórzewska et al., 2013).

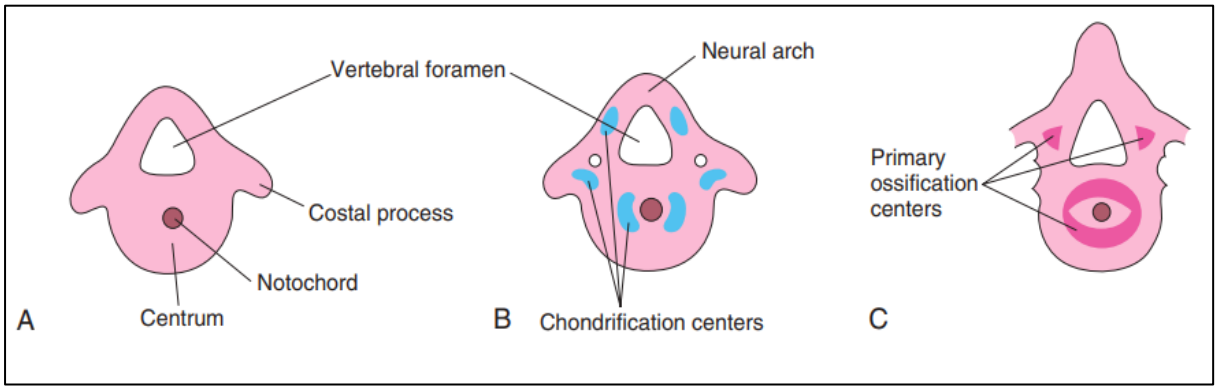

***Figure 1.6**: Chondrification and Ossification centres in vertebrae and the stages of development. **A)** Mesenchymal vertebra at 5 weeks gestation. **B)** Mesenchymal vertebra at 6 weeks demonstrating the three chondrifiaction centres; the centrum, costal process and neural arch. The neural arch is the primordium of the vertebral arch. **C)** Cartilaginous vertebra at 7 weeks containing the primary ossification centres (Adapted from Moore et al., 2018). Used with permission from Elsevier.*

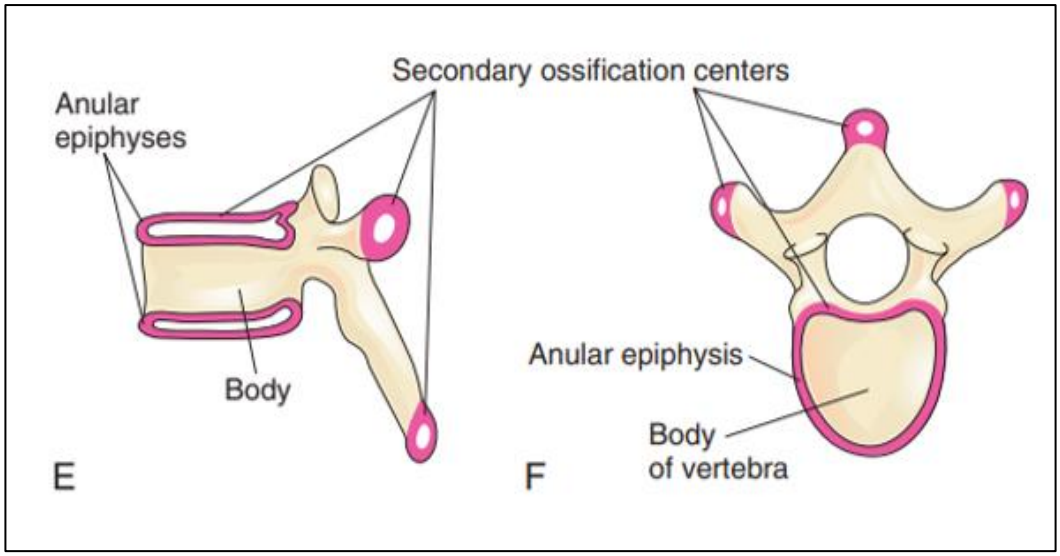

Figure 1.7: *Secondary Ossification centres of vertebrae.* ***E and F)*** *Side view and superior view showing the location of the secondary ossification sites depicted on a thoracic vertebra (analogous to lumbar vertebra in their locations respectively) (Adapted from Moore et al., 2018). Used with permission from Elsevier.*

O'Rahilly et al. (1990) stated that the study of embryonic development of the human sacrum had been neglected compared to the vertebral column. A cartilaginous sacrum is a definitive unit with five separate vertebrae, each containing a future centrum, bilateral neural processes and bilateral transverse processes (costal element) by which ossification, both primary and secondary, occurs similarly to the lumbar spine. Secondary ossification centres are located in the annular, sacroiliac and lower lateral margin epiphyses (Figure 1.8). The auricular surface comprises the first three sacral segments (O'Rahilly et al., 1990; Cochard, 2012).

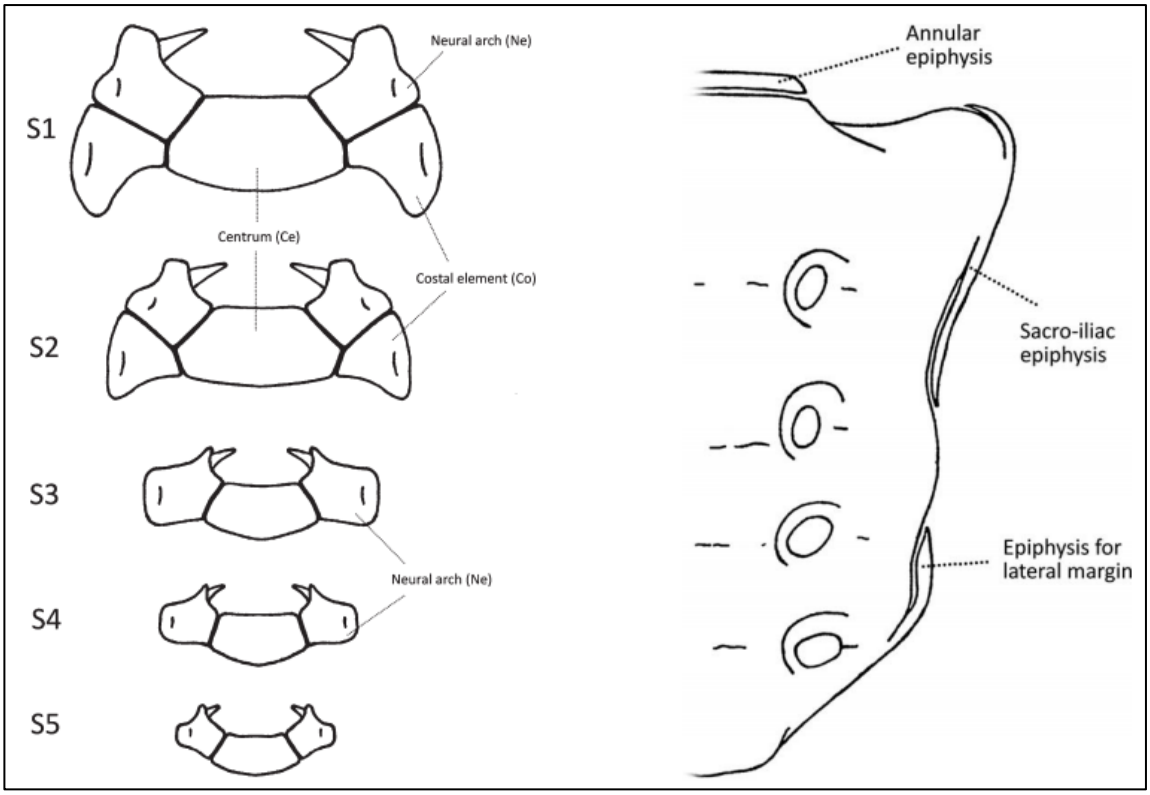

Figure 1.8: *Illustration of the primary ossification centres of the sacrum* ***(left)*** *and secondary ossification centres of the sacrum* ***(right)****.* ***(NE)*** *Neural arch.* ***(Co)*** *Costal element.* ***(Ce)*** *centrum.* ***S1*** *to* ***S5*** *represenets the five vertebrae of the sacrum (Adapted from Cardoso et al., 2014). Used with permission from Wiley-Liss, Inc.*

Development of the intervertebral disc

The vertebral column and its embryonic development revolve around the rod-like structure of mesoderm-derived cells known as the notochord (Smith et al., 2011; Figure 1.9). As discussed earlier, the notochord is an important structure that gives rise to the NP of the IVD, mediates cell migration and cell signalling as well as differentiation and survival of cells of the vertebral column (Stemple, 2005; Smith et al., 2011; Ramesh et al., 2017). At the end of the sixth week the notochord undergoes regression at the VBs' level until it disappears. This regression is known as ‘involution’ of the notochord (Savage, 2005; Smith et al., 2011; Scaal, 2016; Figure 1.9). The notochord then broadens at the level of the IVD to form the NP (Smith et al., 2011). Scaal (2016) confirms that at the lumbar region of the vertebral column, the classical resegmentation model for the origin of the IVD arising from the caudal somite holds true (Figures 1.4B and 1.5D). The annulus fibrosus and cartilaginous endplates of the vertebral bodies form from the inferior one-third of caudal somites after resegmentation (Chal and Pourquié, 2009; Figures 1.4 and 1.5).

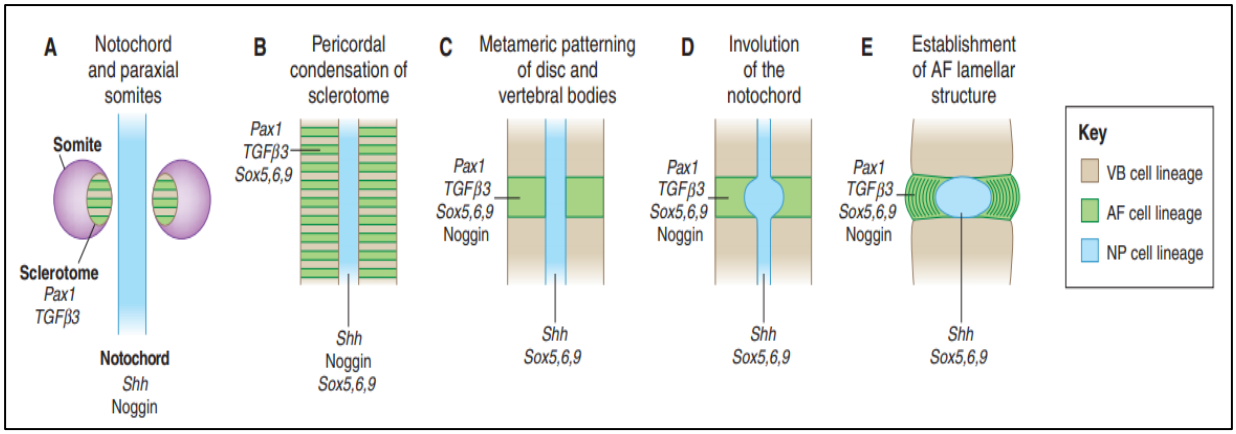

Figure 1.9: *Schematic representation of intervertebral disc embryonic morphogenesis. Colours represent origins and cell fates through embryonic development. Indicated are significant morphogens and transcriptional regulators implicated in the differentiation and growth of the intervertebral disc structures at each developmental stage.* ***A)*** *Paired paraxial somites containing the sclerotome cells medially and epithelial cells laterally, adjacent to the notochord.* ***B)*** *Condensed sclerotome cells around the notochord.* ***C)*** *Metameric patterning of condensed (green) and less condensed (brown) regions that give rise to the intervertebral disc and vertebral bodies, respectively.* ***D)*** *Contraction of the notochord within the vertebral bodies and expansion within the future site of the intervertebral disc to form the nucleus pulposus.* ***E)*** *Basic intervertebral disc structures with the annulus fibrosus adopt orientation alignment to form the template for the lamellar structure seen in mature intervertebral discs.* ***VB=*** *Vertebral body.* ***AF=*** *Annulus fibrosus.* ***NP=*** *Nucleus pulposus (Adapted from Smith et al., 2011). Image obtained from an open access publication, creative commons licence.*

Osteology of the lumbar spine

The lumbar vertebrae are the largest of all the unfused segments of the spine. As with cervical and thoracic vertebrae, lumbar vertebrae progressively increase in size caudally, i.e. superior to inferior (White et al., 2012; Moore et al., 2014). The lumbar vertebrae has the following components (Figures 1.10, 1.11 and 1.12; White et al*.,* 2012; Moore et al., 2014):

i. **Vertebral bodies**: large ovoid or kidney-shaped structures when viewed superiorly which lack costal facets and transverse foramina. The largest of the vertebral bodies found in the vertebral column;

ii. **Vertebral foraminae**: triangular in shape and are small relative to their corresponding vertebral bodies. The vertebral foramina are larger in the thoracic spine when compared to the lumbar but smaller than that of the cervical spine;

iii. **Spinous processes**: short, hatchet-shaped blunt projections, orientated horizontally, orthogonal to the coronal plane;

iv. **Transverse processes**: long slender processes that lack articulation facets. Transverse processes may contain an accessory process at their bases, on the posterior aspect;

v. **Articular processes**: the superior and inferior articulation facets are almost vertical in orientation. Superior articulating processes face posteromedially while the inferior articulating processes face anterolaterally. The facets progressively change orientation from a coronal orientation superiorly to that of sagittal at the lumbosacral region;

vi. **Mammillary processes**: elongated tubercles originating from the posterolateral boundary of both superior articular processes;

vii. **Accessory processes**: minute tubercles, variable in occurrence, that arise from the base on the posterior aspect of both transverse processes.

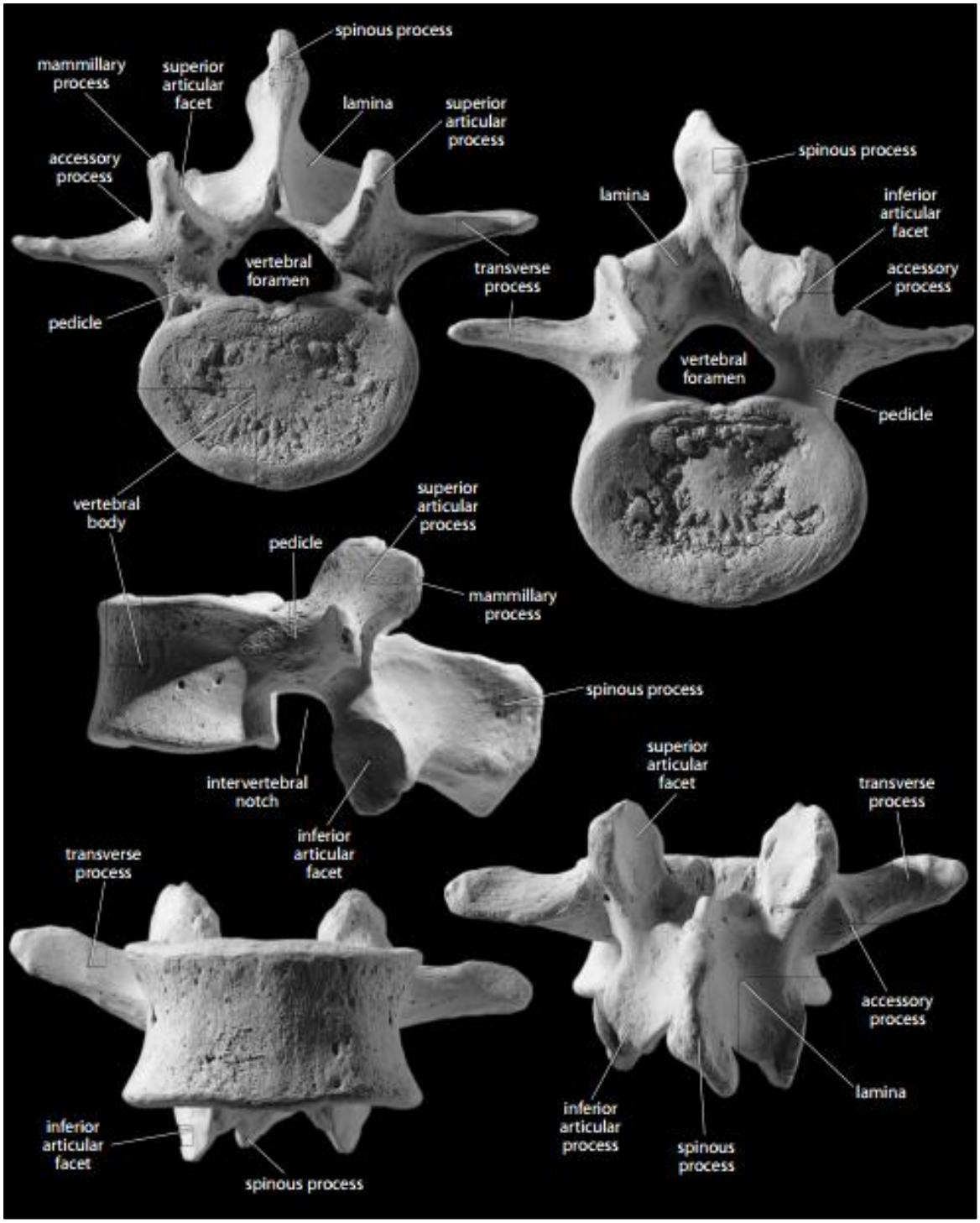

Figure 1.10: *Multiple view of typical anatomy of lumbar vertebrae, seen from all aspects, namely the superior (top left), inferior (top right), lateral (middle), anterior (bottom left) and posterior (bottom right) views (Adapted from White et al., 2012). Used with permission from Elsevier.*

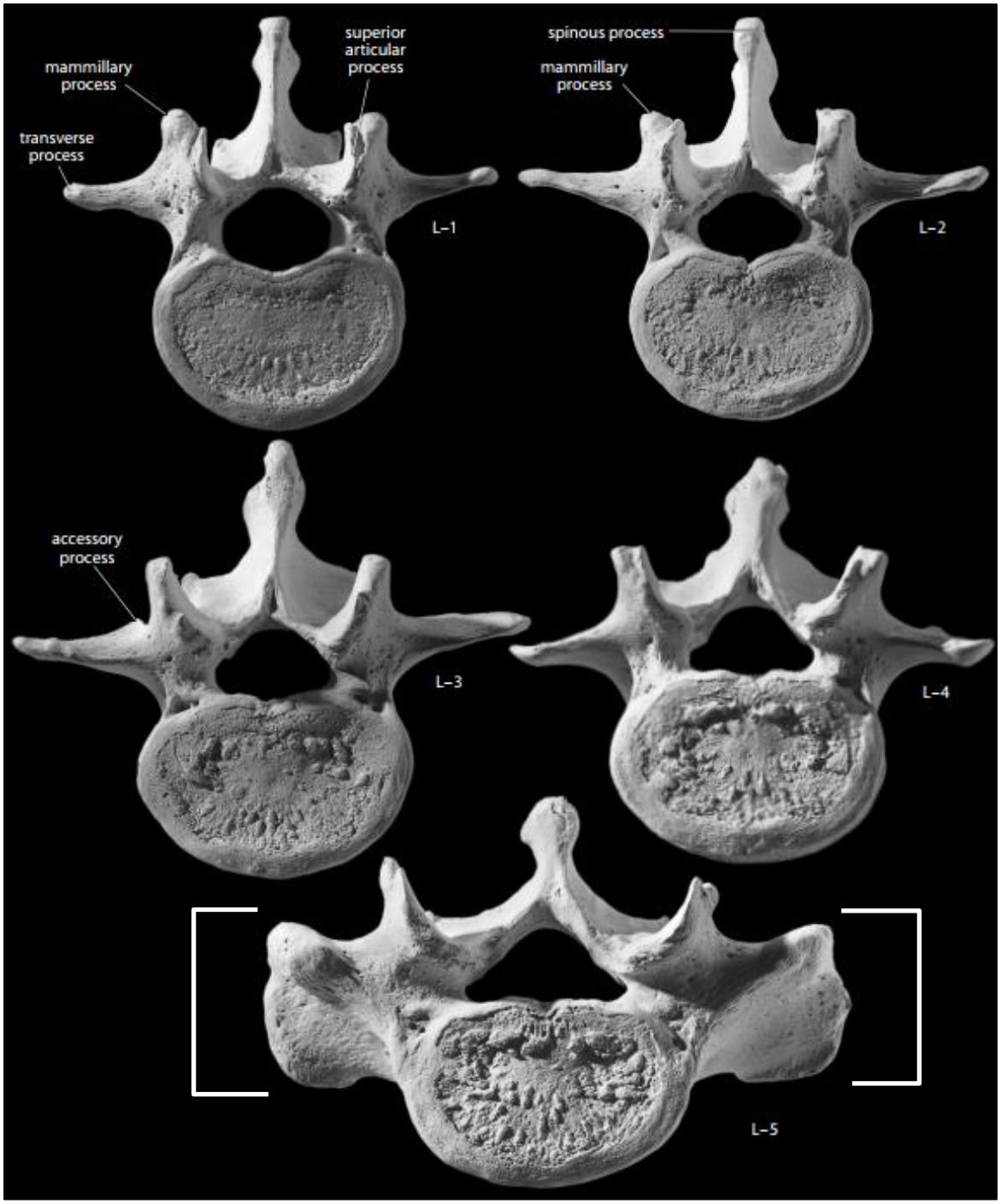

Figure1.11: Superior view of lumbar vertebrae L1 through L5. **Note:** the fifth lumbar vertebra (labelled L-5) specimen (illustrated above) is of a lumbosacral transitional vertebra, Type IIB, sacralisation. The L5 lumbosacral transitional vertebra has enlarged bilateral transverse processes (demonstrated with large brackets) in the axial plane (Adapted from White et al., 2012). Used with permission from Elsevier.

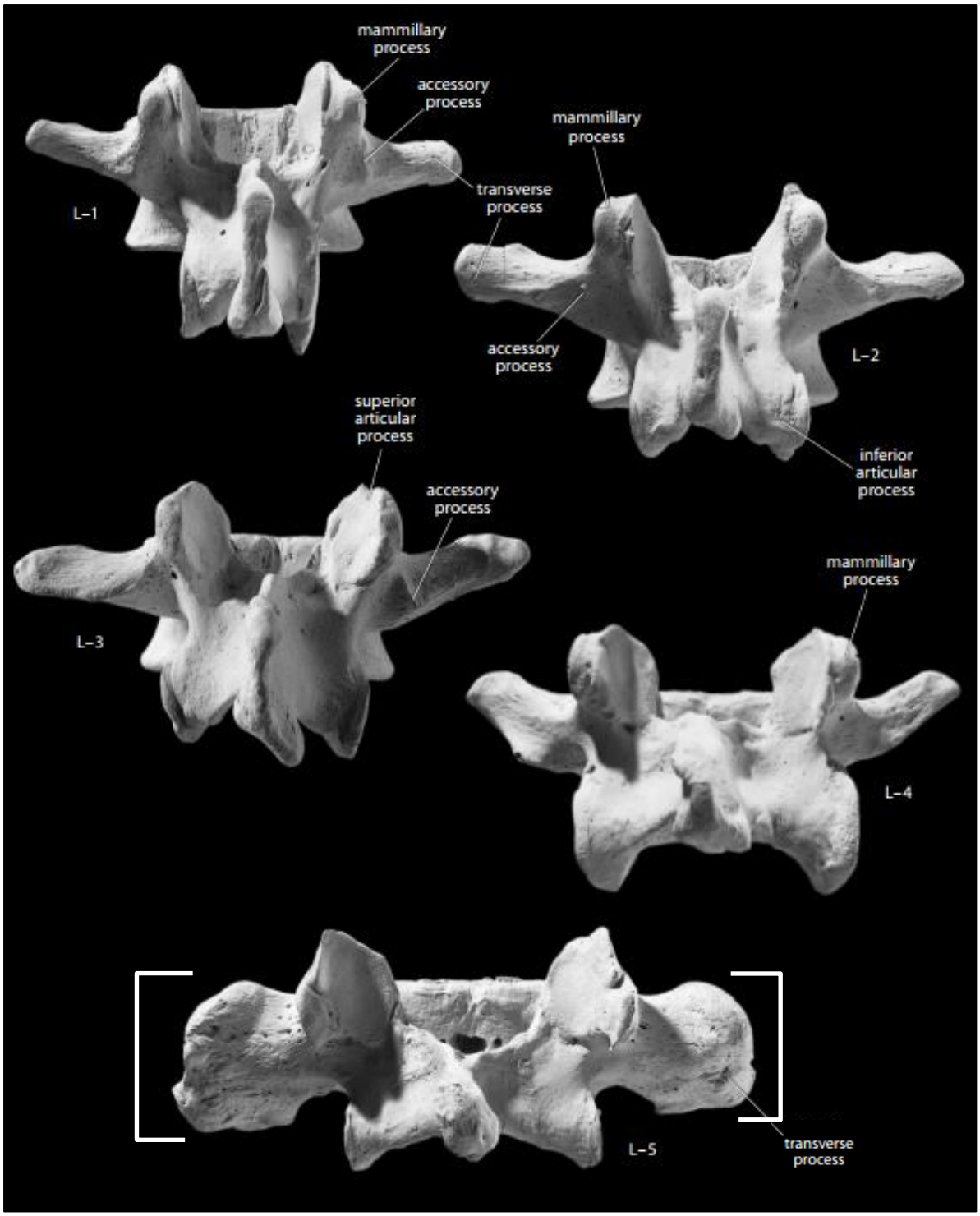

Figure 1.12: *Posterior view of lumbar vertebrae L1 through L5.* ***Note:*** *the L5 vertebra is that of a lumbosacral transitional vertebra, Type IIB, sacralisation. The L5 lumbosacral transitional vertebra has macroscopically enlarged (increased craniocaudal height) bilateral transverse processes (demonstrated with large brackets). Comparison of the size difference of the L5 transverse processes relative to the adjacent vertebrae L1 through to L4 can be seen in this image (Adapted from White et al., 2012). Used with permission from Elsevier.*

Osteology of the sacrum

The sacrum is typically formed from a fusion of five vertebrae into a single, wedge-shaped, immobile compound bone. Variation in sacral segment numbers from four to six segments has been observed. It is located at the base of the vertebral column between the ilia of the pelvis, with which it articulates laterally, and the coccyx located distally, with which it articulates inferiorly (White et al., 2012; Moore et al., 2014). The sacrum has the following components (Figures 1.13, 1.14 and 1.15; White et al*.,* 2012; Moore et al., 2014):

I. **Sacral base:** superior, broad surface comprising the uppermost alae and the plateau of the first sacral vertebra;

II. **Sacral plateau:** anterosuperiorly inclined, broad, flat surface of the first sacral centrum (akin to a vertebral body) that articulates with the last lumbar vertebra;

III. **Sacral promontory:** found on the body of S1, the anterior projection in the midline of the sacral plateau;

IV. **Alae (ala** singular**):** wing-like structures that extend laterally from the sacral plateau and constitute the fusion of the transverse processes of the sacral vertebrae. They articulate with the ossa coxae, forming the sacroiliac joints;

V. **Sacral canal:** the continuation of the vertebral canal;

VI. **Pelvic surface:** anterior surface of the sacrum that faces inward to the pelvis;

VII. **Posterior surface:** posterior-facing, rough convex surface of sacrum;

VIII. **Transverse ridges:** lines of fusion on the pelvic surface;

IX. **Auricular surface:** the sacral contribution to the sacroiliac joint that is an ear-shaped articular surface;

X. **Sacral tuberosity:** a roughened, irregular, non-articular area immediately posterior to the auricular surface. The sacral tuberosity forms the attachment site for the sacroiliac ligaments;

XI. **Anterior and posterior sacral foramina:** foramen on the anterior and posterior surfaces of the sacrum through which the anterior divisions of the sacral nerves and lateral sacral arteries pass (anterior foramina) and the posterior divisions of the sacral nerves pass (posterior foramina);

XII. **Intervertebral foramina:** internal foramina found between fused superior and inferior notches that lie medial to the anterior and posterior sacral foramina. They occupy a similar position to the lumbar intervertebral foramina;

XIII. **Median crest:** posterior ridge running vertically formed by fusion of the spinous processes of the sacral vertebrae;

XIV. **Intermediate sacral crests:** located medial to the posterior sacral foramina. These are the remnants of the sacral articular processes;

XV. **Lateral sacral crests:** located laterally to the posterior sacral foramina. These are the remnants of the fused sacral transverse processes;

XVI. **Sacral hiatus:** area, usually at the level of fourth or fifth sacral vertebrae, where the posterior wall is missing forming an arch-like opening;

XVII. **Sacral cornua (**singular: **cornu):** two small processes that extend inferiorly on either side of the sacral hiatus;

XVIII. **Facet for coccyx:** distal surface of the last sacral vertebra, and

XIX. **Sacral apex:** distal tip of the sacrum that includes an articular facet for the coccyx.

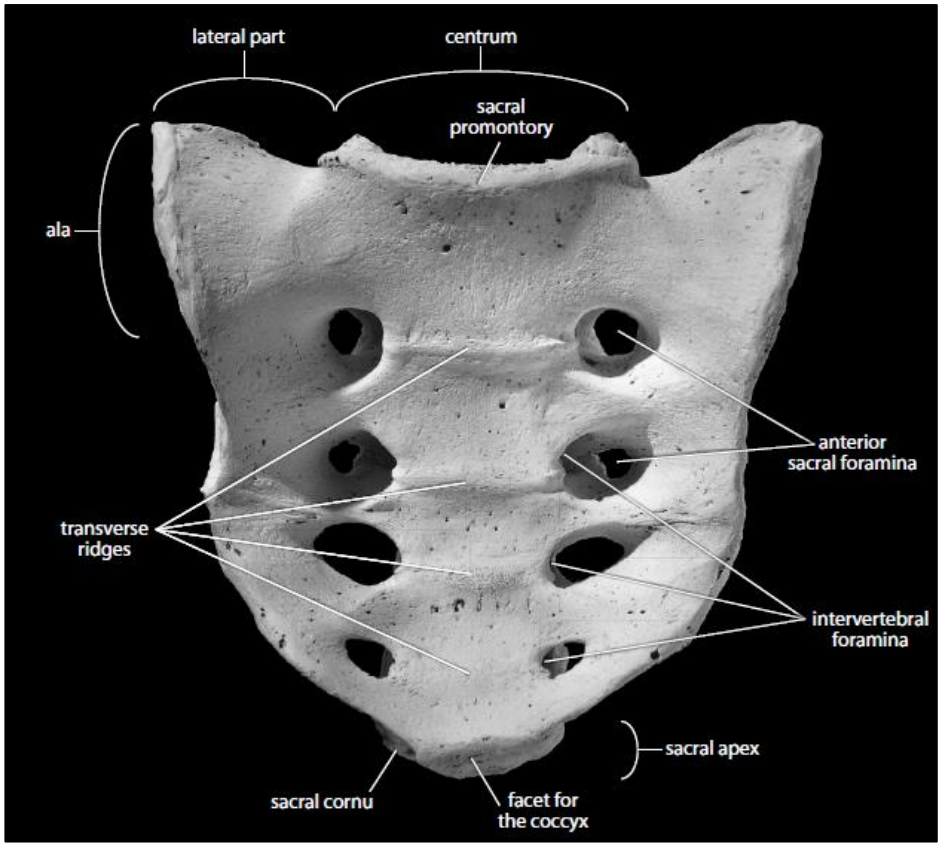

Figure 1.13: Anterior view of the sacrum (Adapted from White et al., 2012). Used with permission from Elsevier.

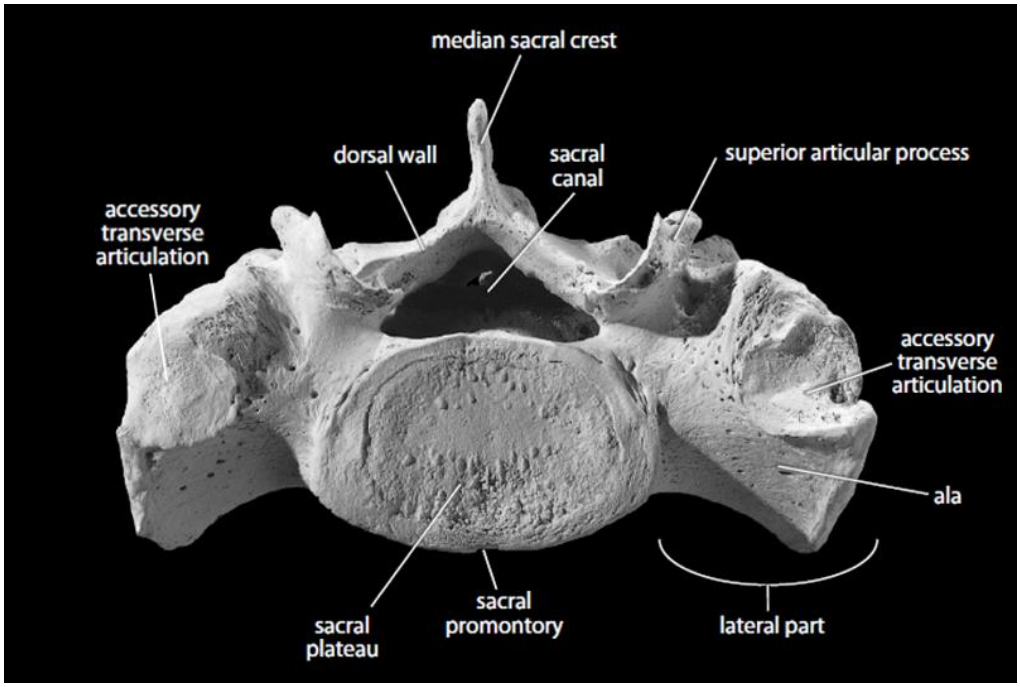

Figure 1.14: *Superior view of the sacrum.* ***Note:*** *that the sacrum articulates with a lumbosacral transitional vertebra, Type IIB, sacralisation. Bilateral accessory articulations are present on the sacral alae's superior surface, which correspond to articulations with the enlarged transverse processes of the fifth lumbar vertebra superior to it, Figure 1.12 and Figure 1.13 (Adapted from White et al., 2012). Used with permission from Elsevier.*

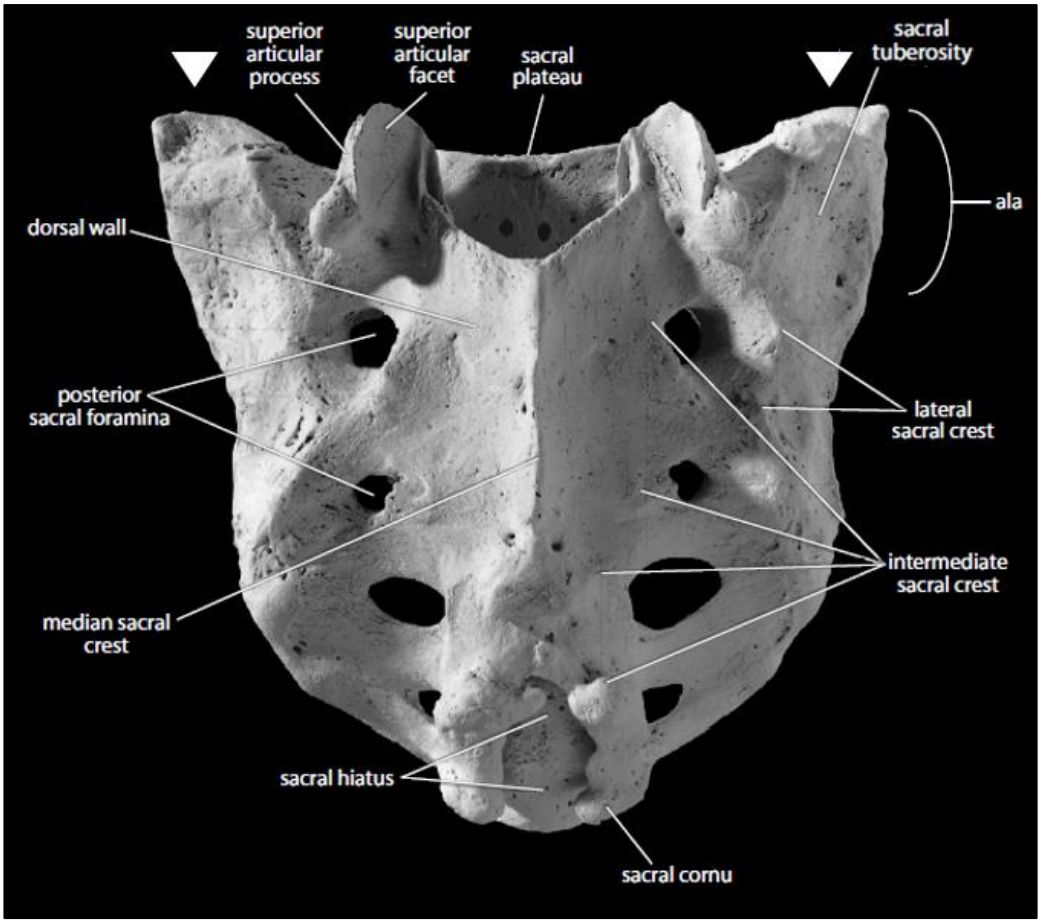

Figure 1.15: *Posterior view of the sacrum.* ***Note:*** *that the sacrum articulates with a lumbosacral transitional vertebra, Type IIB, sacralisation. Bilateral accessory articulations (arrowheads) are present on the sacral alae's superior surface, which correspond to articulations with the enlarged transverse processes of the fifth lumbar vertebra superior to it (Adapted from White et al., 2012). Used with permission from Elsevier.*

Sexual dimorphism in male and female skeletal geometry

Sexual dimorphism is described as differences in shape and size between males and females of the same species (Nikitovic, 2018). Although not as pronounced as other species, humans exhibit numerous differences between males and females (Nikitovic, 2018). Differences may be seen in females whereby they are shorter, smaller proportions and contain gracile postcranial features. Men tend to be taller, contain larger muscle mass and contain a robust spinal column (Nikitovic, 2018; Zlolniski et al., 2019). Although height varies, globally all human populations exhibit a mean adult height of men greater than the mean height of women (Dunsworth, 2020). Epiphyseal closure, especially of the long bones, is highly dependent on oestrogen levels (Dunsworth 2020).

Oestrogen has been demonstrated to accelerate progenitor cell loss in the epiphyses, which leads to senescence of the growth plates leading to growth arrest. Women have greater quantities of oestrogen, up to eight times the amount when compared to men, therefore experience earlier growth arrest (Dunsworth 2020). Subsequently, men are on average taller than women, have larger bone geometry, increased bone density and larger body mass due to an extended growth period (Nieves 2017; Nikitovic, 2018; Zlolniski et al., 2019). Sexual dimorphism of the vertebral column reflects growth and development factors that have their origin in genetic and environmental influences (Ubelaker et al., 2017). Additionally, sacral dimorphism exists between African-ancestry and European-ancestry. European sacra, both male and female, measure wider and contain significantly longer costal processes than their African counterparts. This is theorised as an adaptation to climate (Bergman's rule) and is found in both South African and North American individuals of European-ancestry (Wayne, 2016).

Bipartition of foramen of the spine

The existence of a double vertebral foramen is known as bipartition (Rios et al., 2014). It has also been referred to as an accessory foramen (Sangari et al., 2015). Bipartite foramina of the spine have been described as having two forms, partial or complete osseous separation (Rios et al., 2014). In some cases, bipartition may be seen in the form of non-osseous connective tissue namely ligaments or cartilaginous septum (Marić et al., 2015; Umeh et al., 2016). In the literature, osseous bipartition has been described at multiple different spine regions, namely the cervical and thoracic spine. In the cervical spine it has been described occurring at the retrotransverse foramen, the transverse foramen and the vertebral foramen (Rilliet, 2008; Rios et al., 2014; Sanchis-Gimeno et al., 2081).

In the thoracic and upper lumbar spine, bipartition has been seen in the vertebral canal associated with diastematomyelia (Mamo et al., 2021; Tom et al., 2021). In the lumbar spine, description exists for soft tissue separation in the form of transforaminal ligaments of the intervertebral foramen (Marić et al., 2015; Umeh et al., 2016).

Intervertebral disc anatomy

The joints between the vertebral bodies of the lumbar spine are referred to as intervertebral discs (IVD). They are considered symphyses (secondary cartilaginous joints) structured for weight bearing and shock absorption. The IVDs account for 20-25% of the total length of the vertebral column. The IVDs consist of three parts: the annulus fibrosus (AF), the nucleus pulposus (NP) and vertebral endplates (Bogduk, 2005; Moore et al., 2014; Figure 1.16).

Annulus fibrosus

A ring-like structure on the circumference of the IVD comprising a highly ordered pattern of concentric lamellae composed of collagen. These lamellae insert onto the rounded, smooth epiphyseal rims on the articular sides of the VBs. These 10 to 20 sheets are oriented in an oblique fashion, alternating in opposite directions from 60 to 65 degrees from vertical layer by layer. The fibre arrangement allows limited rotation of the spine between vertebrae and is a very strong construct (Bogduk, 2005; Moore et al., 2014; Figure 1.16).

Nucleus pulposus

A semifluid mass of mucoid material composed of up to 88% water at birth that constitutes the centre of the IVD. In the adult, the nucleus pulposus (NP) is a remnant of the notochord (Figure 1.14). The NP is avascular and relies on diffusion for its nutrition, known as imbibition (Bogduk, 2005; Moore et al., 2014; Figure 1.16).

Vertebral endplates

The vertebral endplates are a layer of cartilage covering the superior and inferior aspects of the vertebral bodies surrounded by the ring apophysis. They cover the NP completely, superiorly and inferiorly, but peripherally they fail to cover the entire area of the AF. Towards the periphery of the endplates, the collagen fibres of the AF insert onto the ring apophysis and bone of the vertebral bodies. The vertebral endplates are considered part of the IVD due to the strong attachment of the AF fibres.

Paradoxically the endplates are weakly attached to the VB and can be avulsed from the vertebral bodies in spinal trauma cases. For the above reasons the vertebral endplates are considered morphologically part of the IVD and not the vertebral bodies (Bogduk, 2005; Figure 1.16).

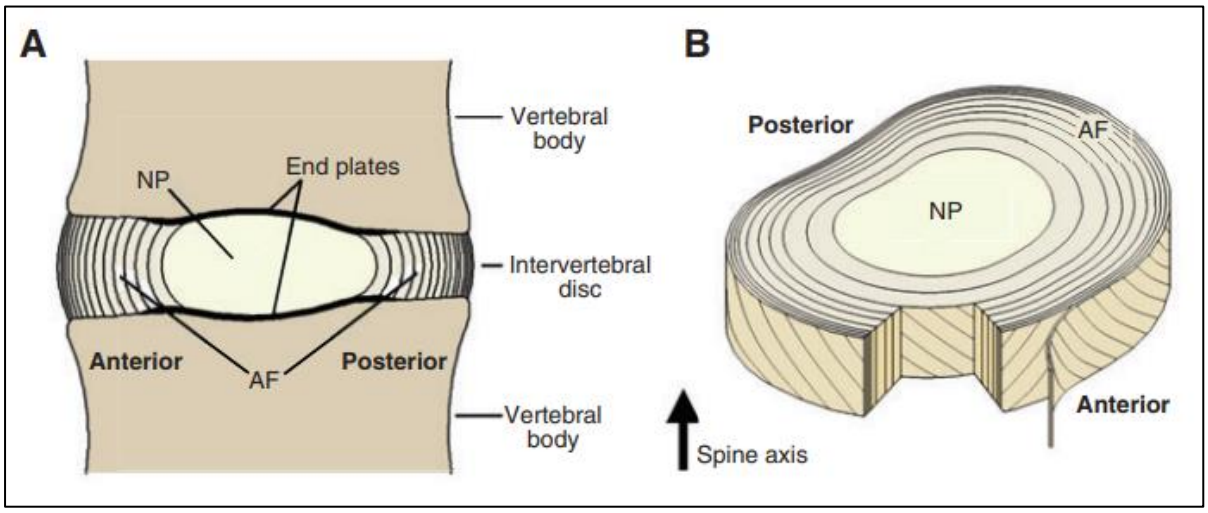

Figure 1.16: *Schematic adult lumbar intervertebral disc.* ***A)*** *A cross-sectional mid-sagittal view illustrating the various portions of the intervertebral disc.* ***B)*** *A three-dimensional view illustrating the annulus fibrosus lamellar structure.* ***NP)*** *Nucleus pulposus.* ***AF)*** *Annulus fibrosus (Adapted from Smith et al., 2011). Image obtained from an open access publication, creative commons licence.*

Ligaments of the lumbar and lumbosacral junction

Three ligaments connect the axial skeleton to the pelvis, namely the sacrotuberous, sacrospinous and iliolumbar ligaments (Wang et al., 2018).

Sacrotuberous and sacrospinous ligaments

Extrinsic to the capsule of the sacroiliac joint. They prevent posterior displacement of the sacral apex during flexion (nutation) of the sacral promontory. The sacrotuberous ligament attaches medially to the lateral sacral crest from the third to fifth sacral segments respectively. The sacrotuberous ligament forms the boundary of the greater and lesser sciatic foramen and in addition it provides insertion sites for the gluteus maximus and biceps femoris muscles. Additionally, the sacrotuberous ligament contains long fibres originating from the posterior superior iliac spine and joining the lower fibres to course inferiorly, laterally and anteriorly to attach to the medial aspect of the ischial tuberosity.

The fibres of the sacrotuberous ligament blend with the posterior sacroiliac fibres as well as with the sacrospinous ligament (Cox, 2012; Moore et al., 2014). The sacrospinous ligament is triangular in shape with the fibres attaching to the anterolateral border of the sacrum at the level of the third to the fifth sacral segments and course laterally and anteriorly to reach the ischial spine. The sacrospinous ligament forms the boundary separating the greater and lesser sciatic foreman (Cox, 2012; Moore et al., 2014).

Iliolumbar ligament

Arguably one of the most important ligaments of the lumbosacral junction (Bogduk, 2005), the iliolumbar ligament (ILL) is a set of bilateral ligaments that connect almost exclusively to the transverse processes of the fifth lumbar vertebra to the ilia (Hughes and Saifuddin, 2006). In some cases, the ILL may attach to the transverse process of the fourth lumbar vertebra (L4) (Pool-Goudzwaard et al., 2003; Tureli et al., 2014). In the literature, the presence of the ILL has been reported as a reliable way to identify the last lumbar vertebra in the absence of lumbosacral variation. However, in the presence of LSTV the ILL reliability as a landmark for lumbar spine enumeration is inconsistent for identifying the L5 vertebra (Hughes and Saifuddin, 2006; Carrino et al., 2011; Farshad et al., 2013). It has been suggested that the ILL, unlike most ligaments, are formed in childhood and adolescence by metaplasia of muscle fibres. This hypothesis has been met with disagreement (Luk et al., 1986; Uhthoff, 1993; Sims and Moorman, 1996; Wang et al., 2018). By contrast, Uhthoff (1993) and Sims and Moorman (1996) found that the ILL formed by the twelfth week of gestation.

The ILL radiates distally from the tips of the L5 transverse processes to the anteromedial surface of the ilia and medial lips of the iliac crests. Controversy surrounds the amount of components contained within the ILL complex (Rucco et al., 1996). Early anatomists described the ILL as having five parts, namely the anterior and posterior, superior and inferior, and the vertical iliolumbar ligament divisions.

The superior ILL is the anterior fascia of the quadratus lumborum muscle and therefore lacks the characteristics of a true ligament. The vertical and inferior iliolumbar divisions attach to the lumbar and iliac bones and not the sacrum and ilia respectively.

Therefore the vertical and iliolumbar divisions should be considered part of the ILL and not part of the anterior sacroiliac ligament (Shellshear, 1949; Alderink, 1991; Bogduk, 2005). The ILL has two main constituents: the anterior and posterior bands, respectively (Basadonna et al., 1996; Fujiwara et al., 2000; Hammer et al., 2010; Figure 1.17).

The posterior band of the ILL gives rise to the deep fibres of the longissimus lumborum muscle, part of the erector spinae group of muscles (Alderink, 1991). The main function of the ILL is to restrain the L5 from anterior shearing forces while also providing stability to the lumbosacral junction segment in all directions (Aihara et al., 2005; Bogduk, 2005; Figure 1.17).

The ILL has been a readily identifiable structure on axial and coronal lumbar spine MR images and is a realiable indicator of the L5 (95-100%) in individuals without an LSTV (Hughes and Saifuddin, 2006; Farshad-Amacker et al., 2014a; Naciye and DÜzkalir, 2017). In individuals with LSTV however, the ILL may be difficult to locate or even absent. This difficulty is attributed to enlargement of the transverse processes leading to underdevelopment or lack of development of the ILL (Hughes and Saifuddin, 2004; Hughes and Saifuddin, 2005; Farshad-Amacker et al., 2014a). Interestingly, Tureli et al. (2014) found that the origin of the ILL associated with LSTV was that of the L4 vertebra in 23.4% of 94 individuals (n=22). By comparison, not one of the 411 non-LSTV containing individuals had an ILL of L4 origin (Tureli et al. 2014).

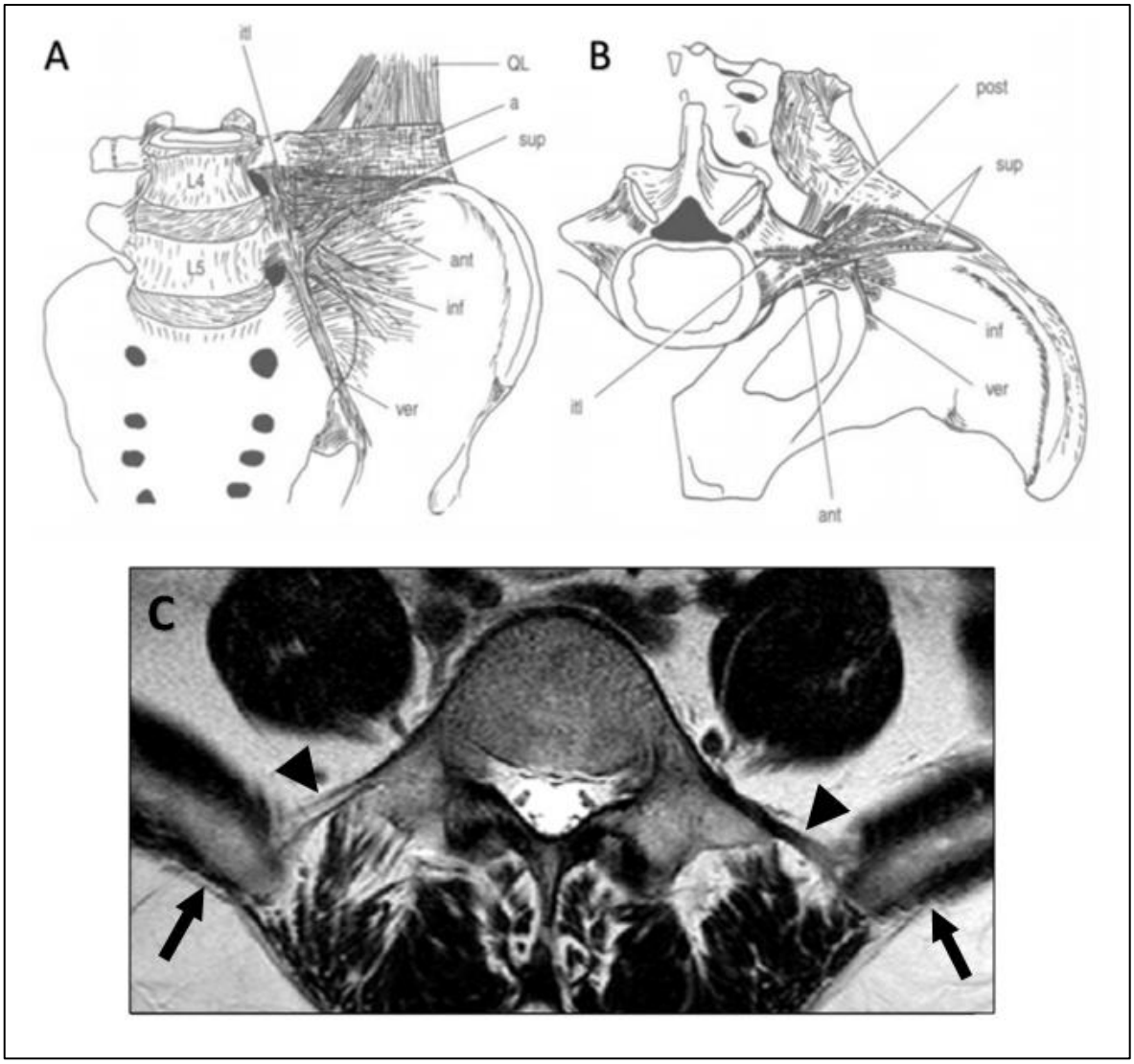

Figure 1.17: *The iliolumbar ligaments.* ***A)*** *Anterior view of the lower lumbar vertebrae and left iliolumbar ligament in situ.* ***B)*** *Superior view of the left iliolumbar ligament in situ.* ***a)*** *anterior layer of the thoracolumbar fascia;* ***ant)*** *anterior iliolumbar ligament;* ***inf)*** *inferior iliolumbar ligament;* ***itl)*** *intertransverse ligament;* ***post)*** *posterior iliolumbar ligament;* ***QL)*** *quadratus lumborum muscle;* ***sup)*** *superior iliolumbar ligament;* ***ver)*** *vertical iliolumbar ligament (Adapted from Bogduk, 2005 after Shellshear, 1949). Used with permission from Elsevier.* ***C)*** *Axial T2-weighted magnetic resonance imaging of the fifth lumbar vertebra demonstrating low-signal-intensity of the iliolumbar ligaments* ***(arrowheads)*** *and the iliac bones* ***(black arrow)****. Note: The right iliolumbar ligament's anterior and posterior bands are seen on the left side of the image. Image from the current research project.*

Biomechanical principles

Lumbosacral transitional vertebrae alter the biomechanics of the lumbar spine and lumbosacral junction directly. To understand the effects LSTV has on spinal biomechanics, it is necessary to understand basic biomechanical concepts and the biomechanics pertinent to the lumbar spine and lumbosacral junction, free of congenital anatomical variations such as LSTV (Elster, 1989; Susai Manickam and Dhason, 2006; Mahato, 2013b; Jancuska et al., 2015).

Basics biomechanics

There are two types of motion the vertebral column experiences: translation and rotation (Bogduk, 2005; Figure 1.18).

Translation

For translation to occur, the entire bone must move in the same direction and to the same extent. Forces acting on the bone that cause the translation are known as shear forces (Bogduk, 2005).

Rotation

Rotation is characterised as the entire bone moving in parallel around a fixed point on a curved path. The various points of the bone move in a similar direction, but the extent to which is dependent on the radial distance from the fixed point which acts as the centre of rotation. The force acting on the bone that creates the rotation is known as torque (Bogduk, 2005).

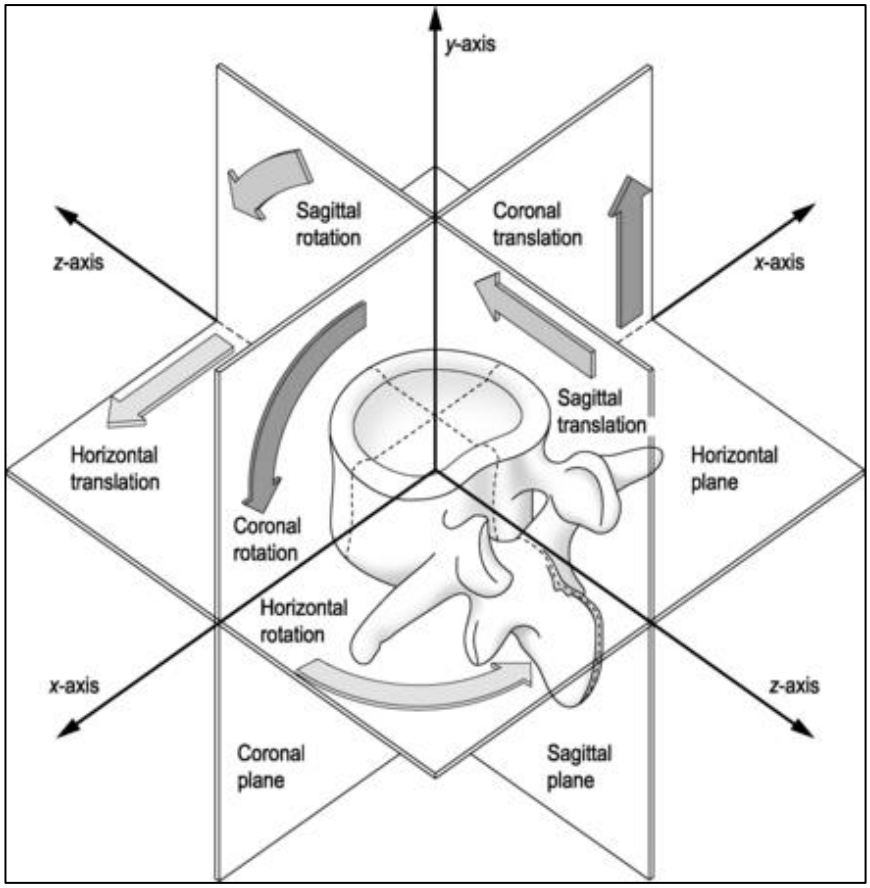

Figure 1.18: *The planes and directions of motion, translation and rotation of a vertebra (Adapted from Bogduk, 2012). Used with permission Elsevier.*

Planes of movement

Rotation is a circular movement around a fixed-axis. Translation can be defined as every point on a vertebra or bone moves the same amount in any direction, creating a shear force. These motions can be described as anterior or posterior, superior or inferior and clockwise or anticlockwise, to name a few. Furthermore, as movement occurs in three-dimensional space, rotation and translation can occur in any of the three fundamental planes, namely the coronal, sagittal or horizontal (axial) planes, respectively (Figure 1.18). Flexion and extension occur in the sagittal plane while rotation occurs in the horizontal or axial plane and lateral flexion occurs in the coronal plane. Understanding the direction and plane of movement allows for accurate descriptions and removes ambiguity (Bogduk, 2005).

Biomechanics of the lumbar spine and lumbosacral junction

Mechanical properties of the intervertebral disc

The IVD can absorb and transmit forces by developing a hydraulic effect, facilitated through the NP when loaded. The IVD acts as a physical spacer to maintain adjacent vertebral body separation through the hydraulic-like effect and allow deformation in all planes of motion. The IVD is subjected to external forces, these include: compression, tension, rotation and bending. In order for the IVD to accomplish intervertebral movement with stability it must tolerate vertically applied compression while withstanding the circumferentially applied tension on the annulus fibrosus fibres (Bogduk, 2005; Oatis, 2017).

The vertical to circumferential force absorption is achieved via a phenomenon known as *hoop stress*. Pascal's law states that 'pressure applied to a confined incompressible liquid is distributed equally in all directions' (Oastis, 2017). As water, the main the main constituent of the nucleus pulposus is incompressible, the compressive load applied to the IVD increases pressure in the NP. The NP in turn, through a process known as *radial expansion*, exerts pressure against the adjacent surrounding annulus fibrosus. In this manner *hoop stress* maintains the turgidity of the IVD through all range of motion (ROM), Figure 1.19 (Oatis, 2017).

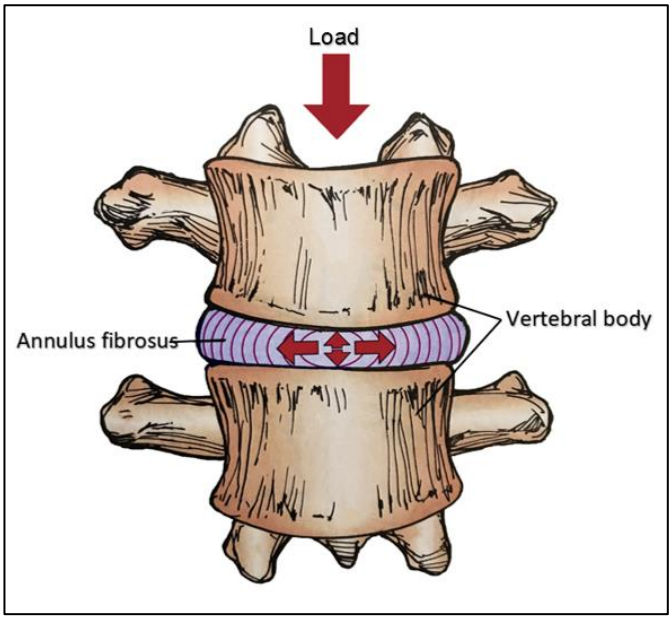

Figure 1.19: 'Hoop Stress' within the intervertebral disc during compressive load bearing (Adapted from Oatis, 2017). Used with permission from Wolters Kluwer Health Inc.

Rotation of the vertebral column

The superior articulating processes of the lumbar vertebrae face posteromedially, coronally biased in the higher cranial levels and more sagitally orientated at the inferior vertebrae. They are concave in the axial plane and straight vertically. These are akin geometrically to a cylinder with its centre point (**+** on Figures 1.20 and 1.21) found posteriorly towards the base of the spinous process as it meets the lamina. At the superior lumbar (L1-3) vertebrae, the centre of rotation of the cyclinder lies marginally posterior to a line connecting the distal aspects of the superior zygapophyseal joints.

By contrast, the inferior lumbar (L4-5) vertebrae have a larger diameter for this cylinder (orientation change and increased distance apart) and therefore, the centre of rotation lies more posteriorly (Kapandji, 2008; Figure 1.20).

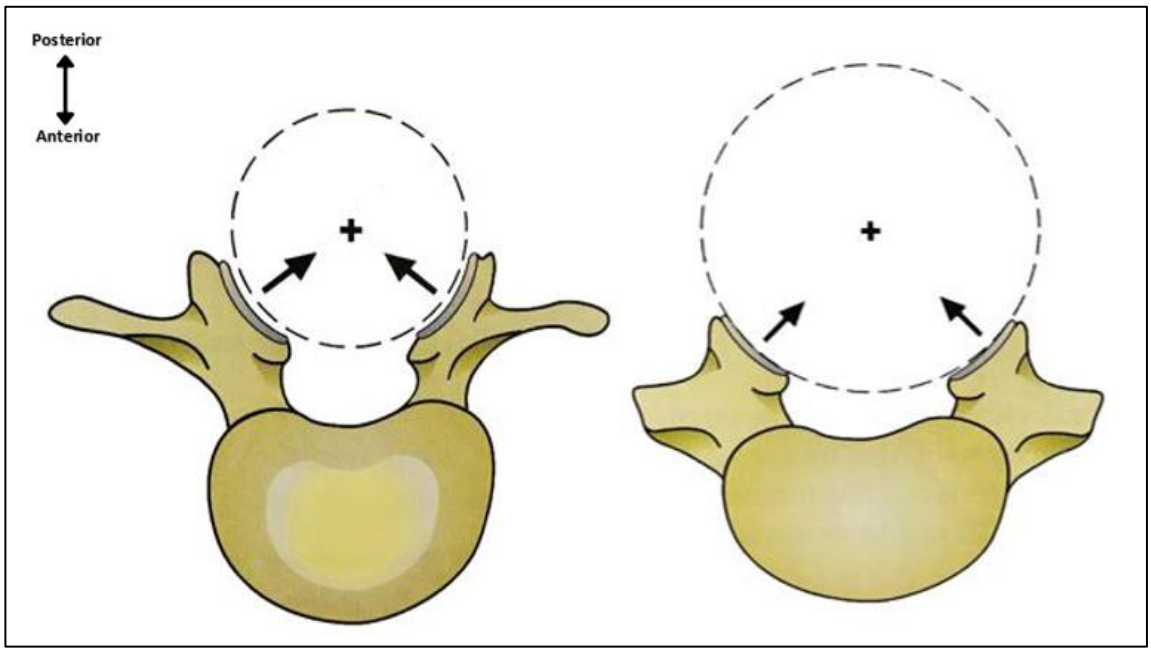

Figure 1.10: *Superior view of superior articulating zygapophyseal joints of the cranial* ***(left)*** *vs the inferior* ***(right)*** *lumbar vertebrae. Both lamina and spinous processes removed to aid visualisation.* ***Left:*** *upper lumbar vertebrae (L1-3) and* ***Right:*** *lower lumbar vertebrae (L4-5). Images depicted are representative of the biomechanics that occur at the lumbar spine and lumbosacral junction respectively (Adapted from Kapandji, 2008. Used with permission from Éditions Maloine, The Physiology of the Joints vol. 3, Figures 14 and 15, page 95).*

It is worth noting that the centre of the rotation occurs at the centre of the cylinder and does not occur around the centre of the IVDs (Kapandji, 2008). Therefore, when the superior vertebra rotates on the inferior vertebra, it is associated with a gliding movement (label **a**, Figure 1.21) of the superior vertebra relative to the inferior vertebra. The total rotation available at the lumbosacral junction is 1°-3° (Kapandji, 2008; Oatis, 2017).

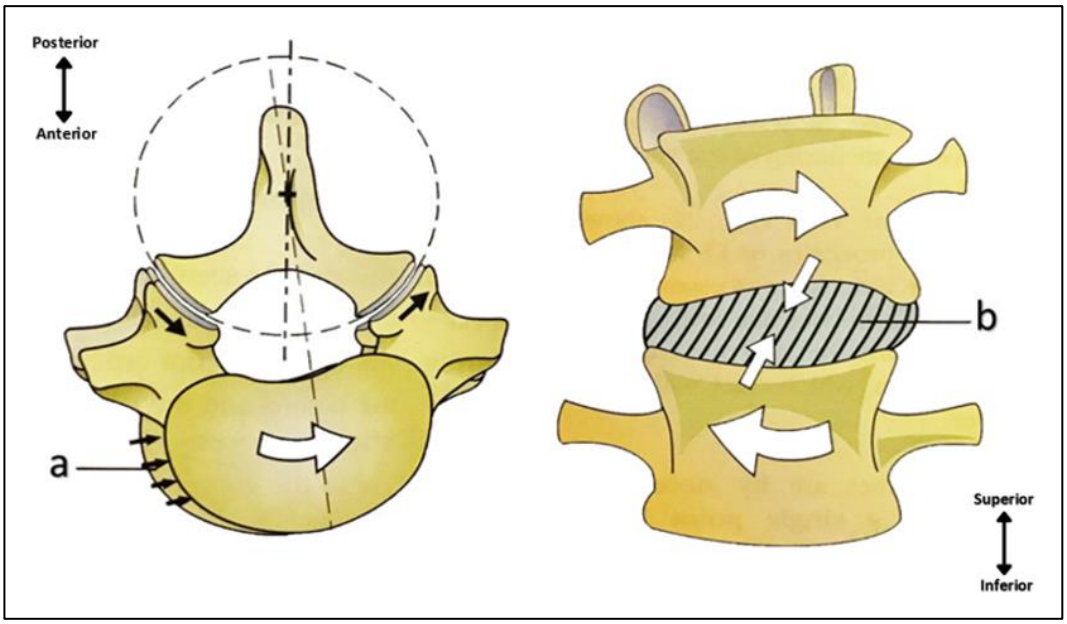

Figure 1.21: *Superior view of lumbar vertebrae* ***(left)*** *and anterior view* ***(right)*** *during rotation.* ***Left:*** *During rotation there is a gliding movement* ***(a)*** *created because of mismatched centres of pivot and rotation.* ***Right:*** *The rotation of the superior vertebra relative to the inferior vertebra places torsional stress on the intervening intervertebral disc* ***(b)****. Images depicted represent of the biomechanics that occur at the lumbar spine and lumbosacral junction, respectively (Adapted from Kapandji, 2008. Used with permission from Éditions Maloine, The Physiology of the Joints vol. 3, Figures 16 and 17, page 95).*

Segmental motion of the lumbar spine and lumbosacral junction

Flexion-extension of the vertebral column

During flexion, the superior vertebral body slopes and glides slightly anteriorly (direction of arrow ***F,*** Figure 1.22, left*)*. This will reduce the craniocaudal distance of the IVD anteriorly while widening it posteriorly. Simultaneously, the inferior articulating zygapophyseal joints separate from the superior articulating joints of the level below. The interspinous ligament, joint capsule, ligamentum flavum and posterior longitudinal ligament stretch as the spinous processes move apart (red arrows) thus increasing the interspinous space (label **a**, Figure 1.22).

The converse is true for extension with the direction of slant posteriorly (direction of arrow ***E,*** Figure 1.22, right*)*. The superior vertebra slopes and glides slightly posteriorly with reduction in the craniocaudal distance of the IVD posteriorly and widening anteriorly (Kapandji, 2008). The inferior articulating zygapophyseal joints of the vertebra above approximate the vertebra's superior articulating joints inferiorly, thereby limiting extension. The interspinous ligament, joint capsule, ligamentum flavum and posterior longitudinal ligament slacken as the spinous processes move towards each other (blue arrows) thus diminishing the interspinous space (label **b**, Figure 1.22).

Flexion and extension are at their maximum between the ages of two and thirteen years and decreases with age due to the stiffening of connective tissue. The segment that allows the greatest movement, especially in younger individuals, occurs at the L4-5 level with 20°-24° of available flexion-extension. The total flexion-extension movement available at the lumbosacral junction is 15°-18° between 35 and 77 years (Kapandji, 2008; Oatis, 2017).

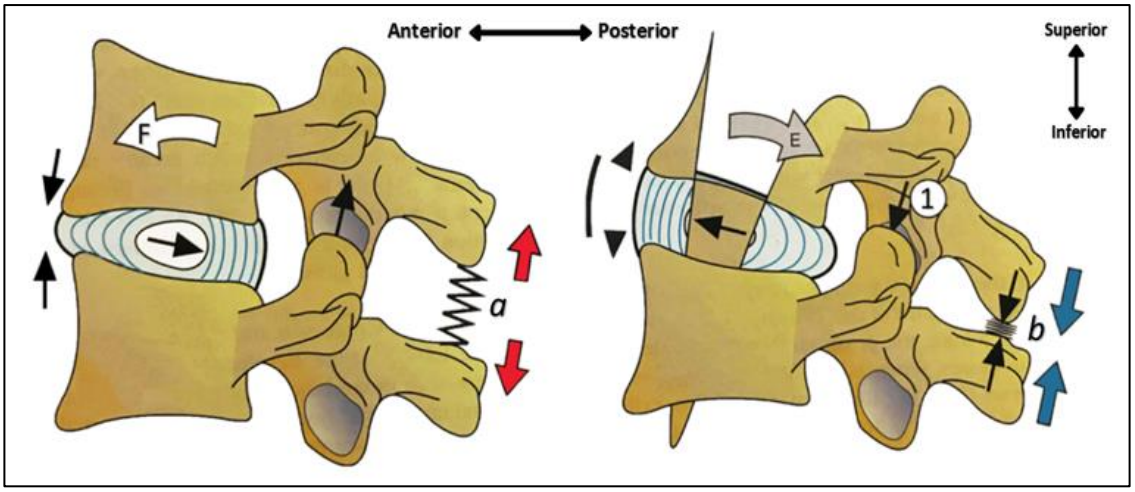

Figure 1.22: *Lateral view of lumbar vertebrae during flexion* ***(left)*** *and extension* ***(right)****.* ***Left:*** *During* ***flexion (left, F)****, the body of the superior vertebra slants anteriorly with wedging of the intervertebral disc, decreasing in craniocaudal height anteriorly. The interspinous space expands posteriorly (red arrows) with stretching of the interspinous ligament* ***(a)****.* ***Right:*** *During extension* ***(right, E)*** *the body of the superior vertebra slants posteriorly with wedging of the intervertebral disc, decreasing in craniocaudal height posteriorly. The interspinous space diminishes posteriorly (blue arrows) with compression of the interspinous ligament* ***(b)****. The facet joints approximate maximally* ***(1)****. Images depicted represent the biomechanics at the lumbar spine and lumbosacral junction respectively (Adapted from Kapandji, 2008. Used with permission from Éditions Maloine, The Physiology of the Joints vol. 3, Figures 10 and 11, page 93).*

Lateral flexion of the vertebral column

The body of the superior vertebra slopes toward the side of the lateral flexion while the IVD becomes wedge-shaped, wider (craniocaudally) on the contralateral side of lateral flexion. Furthermore, there is the displacement of the nucleus pulposus (NP) away from the side of lateral flexion.

The ipsilateral transverse process space diminishes, and the intertransverse ligament slackens (label **b**, Figure 1.23), while the contralateral transverse process space and intertransverse ligament (label **a**, Figure 1.23) are stretched (Kapandji, 2008).

Lateral flexion follows a similar pattern to flexion-extension characteristics of motions. The most mobile segment of the lumbar spine is L3-4, with L4-5 following closely behind. Maximum movement is found between the ages of two and thirteen years of age. The lumbosacral articulation has the least functional movement, with 7° in youth and diminishing to 2° in later years (Kapandji, 2008; Oatis, 2017).

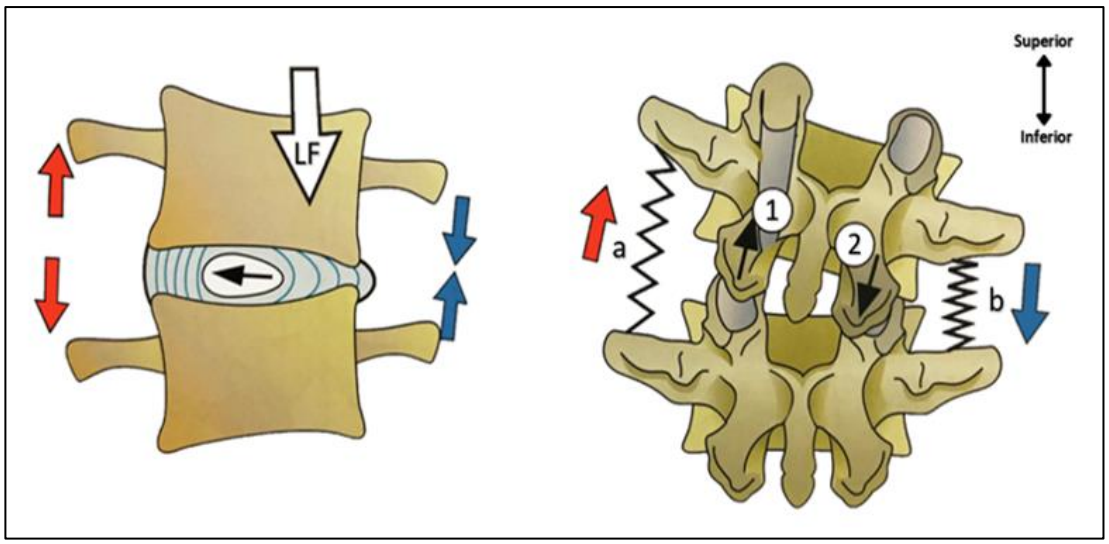

Figure 1.13: *Mid-coronal view* ***(left)*** *and posterior view* ***(right)*** *of lateral flexion of the lumbar spine.* ***Left:*** *The body of the superior vertebra slants toward the side of the lateral flexion* ***(LF)*** *with a loss in transverse process space (blue arrow), while the contralateral side demonstrates transverse process separation (red arrow).* ***Right:*** *The ipsilateral intertransverse ligament slackens* ***(b)****, while the contralateral intertransverse ligament* ***(a)*** *is stretched. The contralateral zygapophyseal joint separates* ***(1)*** *while the ipsilateral zygapophyseal joint approximates* ***(2)*** *Images depicted represent of the biomechanics that occur at the lumbar spine and lumbosacral junction, respectively (Adapted from Kapandji, 2008. Used with permission from Éditions Maloine, The Physiology of the Joints vol. 3, Figures 12 and 13, page 93).*

Lumbosacral hinge of the vertebral column

The lumbosacral hinge is composed of the last lumbar vertebra (most often L5) and the superior surface of the sacrum (S1 segment). As a result of the downward and anterior inclination of the superior surface of the sacrum, the lumbosacral hinge is a weak point in the vertebral column (Figure 1.24). The body of L5 has a predisposition to glide anteriorly and inferiorly. The vertebral column weight (**P**) acting through the L5 segment can be divided into four forces:

- A force (**G**) acts parallel to the upper surface of the sacrum with translation force at the L5 segment anteriorly.
- A force (**N**) acts perpendicular to the superior surface of the sacrum
- The gliding translation force (**G'**) of the L5 vertebra on the sacrum
- A reaction force (**R**) that restrains and limits the gliding force (**G'**)

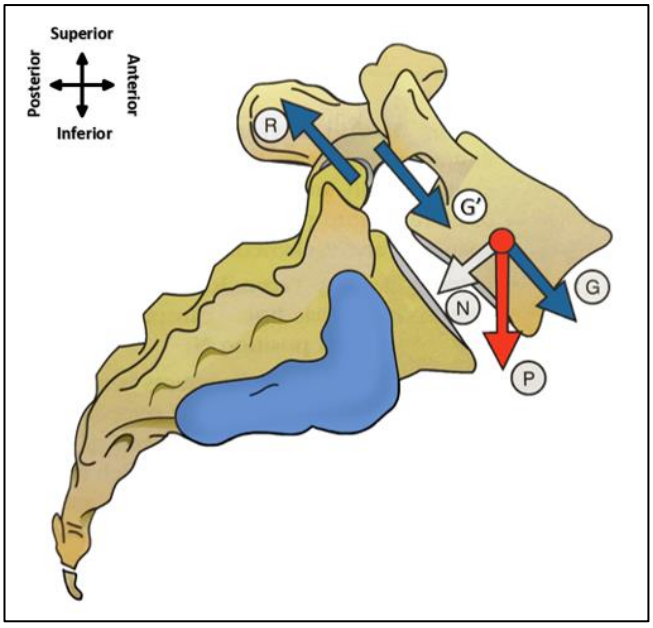

Figure 1.24: *Lateral view of the lumbosacral hinge. The arch of L5 restrains the gliding force* ***(G')*** *by force* ***(R)****. The vertebral column weight* ***(P)*** *acting through the L5 segment is divided into two forces, namely forces acting perpendicular to the sacrum* ***(N)*** *and a forces acting parallel to the superior sacrum, anteriorly* ***(G)*** *(Adapted from Kapandji, 2008. Used with permission from Éditions Maloine, The Physiology of the Joints vol. 3, Figure 20, page 97).*

The gliding translation force (**G'**) of the L5 vertebra on the sacrum is prevented by the robust vertebral arch of L5 (Figures 1.24 and 1.25). Reaction forces (**R**) exerted by the superior articulating facets of the sacrum restrain and react to prevent anterior migration (Kapandji, 2008).

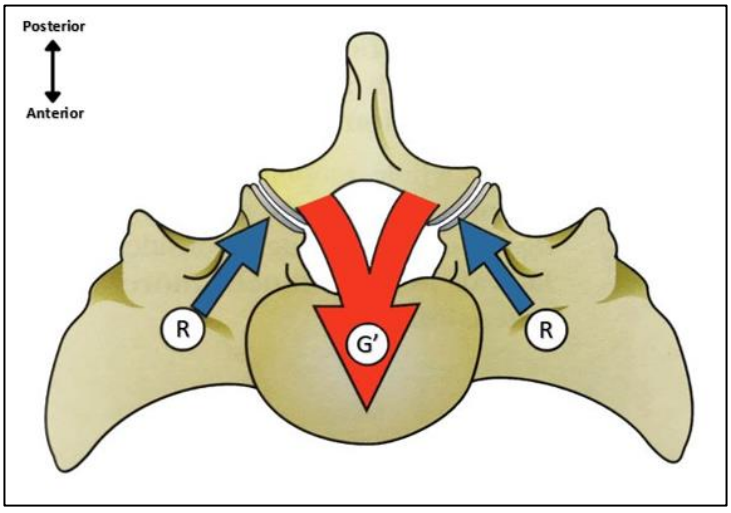

Figure 1.25*: Superior view of the lumbosacral hinge. The L5 inferior articulating processes are featured in situ, fitting congruently into the superior articulating processes of S1. The gliding force* ***(G')*** *exerts an anteriorly orientated compression force of the articular processes of L5 against superior articulating processes of the sacrum, which restrain and react with force* ***(R)*** *bilaterally (Adapted from Kapandji, 2008. Used with permission from Éditions Maloine, The Physiology of the Joints vol. 3, Figure 22, page 97).*

In spinal biomechanics, a distinction is made between the lumbar spine and the pelvis (Kapandji, 2008; Oatis, 2017). It is accepted that the lumbar spine articulates with the sacrum and the sacrum, in turn, articulates with ossa coxae. The transfer of forces is transmitted into the lower limbs in an upside-down 'Y' pattern. This pattern of load transmission starts centrally through the spinal column, IVDs, sacrum and moves to the SIJs and then via the hip joints to the lower limbs (Kapandji, 2008). Only by extension, through the ILLs, is there a direct connection from the lumbar vertebrae to the pelvis. The ILLs may influence lumbopelvic motion and act as stabilisers for orthograde locomotion (Bogduk, 2005; Hughes and Saifuddin, 2006; Kapandji, 2008; Vleeming et al., 2012; Oatis, 2017). As a result of the morphology of the pelvic ring anatomy, throughout bipedal walking, stress is concentrated at the SIJs with the SIJs demonstrating a shock absorption mechanism (Toyohara et al. 2020). Therefore, the SIJs therefore play an important part in orthograde posture and bipedal locomotion connecting the trunk to the lower limbs.

Spinal enumeration and human evolutionary hypothesis

The post-cranial axial skeleton variability is of great importance and is close to the ideal model system for evolutionary developmental studies (Pilbeam, 2004). The oldest assumed evidence of LSTV was found in the 3.7 million-tear-old KSD-VP-1/1 (Kadanuumuu) skeleton. Kadanuumuu is a large *Australopithecus afarensis* with the first suspected lumbarisation of the first sacral segment of a hominin fossil (Lovejoy et al., 2016).

Modern humans have five distinct groups of post-cranial vertebrae, namely cervical (C), thoracic (T), lumbar (L), sacral (S) and coccygeal (Cy) in a modal distribution of 7C:12T:5L:5S:4Cy. The modal number of lumbar vertebrae in modern humans is five. That is to say, the mode or modal number is the most common number contained within a dataset (Pilbeam, 2004).

Although moderate, there is variation in the number of lumbar vertebrae in humans (Mahato, 2010, 2011, 2013a and b). The lumbar vertebral number varies between four (sacralisation of last lumbar vertebra) and six (lumbarisation of the first sacral vertebra) vertebrae with a prevalence rate of LSTV at approximately 3.3% to 35.6%, depending on the geographic region of study and data acquisition method (Erken, 2002; Bron et al., 2007; Apazidis, 2011; Dharati et al., 2012; Table 1.10).

There are two evolutionary pathways hypothesised by which human lumbar vertebral enumeration arose, namely the long and short-backed hypotheses; these will be described later in the text. These two evolutionary pathways attempt to describe the number of lumbar vertebrae possessed by the last common ancestor (LCA) of hominins, humans and chimpanzees. Importantly, it may help extrapolate the total numerical composition of the vertebral formula (total number of post-cranial vertebrae) of the LCA. On the one hand, the lumbar vertebrae in extant African apes (gorillas and chimpanzees) vary between three and four (Pilbeam, 2004; McCollum et al., 2010; Williams et al., 2016). On the other hand, a more generalised LCA exists whereby it is believed early hominins (australopiths and early *Homo* species) possessed a long lumbar spine (six vertebrae).

These six vertebrae modal number of the lumbar spine in early hominins (A. *africanus* and H. *erectus*) are believed to have been reduced in later *Homo* species with a shorter lumbar spine composed of 5 vertebrae (Latimer and Ward, 1993; Ward and Latimer, 2005; McCollum et al., 2010; Whitcome, 2012).

Two methods of enumeration exist as to the reconstruction of the lumbar spine. Each method bears its own merits. Paleoanthropologists assessing the prezygapophyses (superior articulating zygapophyseal joints) categorise joints that face posteriorly as an indicator of the presence of a diaphragmatic vertebra. The term *diaphragmatic vertebra* represents the last thoracic vertebra considered to be T12. In contrast, the sagittal facing postzygapophyses (inferior articulating zygapophyseal joints) are considered the first lumbar vertebra (L1). Therefore, a plausible 6-element lumbar spine may exist in some early hominins depending on the method of enumeration (Robinson, 1972; Haeusler et al., 2002; Whitcome, 2012; Williams et al., 2013). On the other hand, lumbar identification utilising the absence of rib facets of the vertebral bodies, which lumbar vertebrae do not possess, indicates only five lumbar vertebrae may have been present in these early hominins (Haeusler et al*.,* 2002).

Australopithecus africanus (Sts 14), *Homo erectus* (KNM-WT 1500) and *Australopithecus sediba* (MH2*)* have been proposed to possess 5 lumbar segments if judged by costal facets, and 6 lumbar segments by facet orientation (Robinson, 1972; Haeusler et al., 2002; Whitcome, 2012; Williams et al., 2013; Williams and Russo, 2015; Williams et al., 2016).

The assessment of fossil taxa presents a challenge as multiple lumbar segments must be present from the same individual to conduct an accurate appraisal. Even when present, these segments from a single individual may have damage or natural biological variation that may make vertebral morphology interpretation problematic (Williams et al., 2016).

Cranial-caudal homeotic shifting of the lumbosacral segment

A homeotic shift, also known as border shift, is the transformation of one segment into a different segment without change in vertebral number (Williams and Russo, 2015).
This may affect one or more spinal column segments, targeting the transitional areas of regional change. These include: occipital-cervical, cervical-thoracic, thoracic-lumbar, lumbar-sacral and sacral-coccyx junctions. Vertebral homeotic shifting is controlled by genetic regulators and spinal precursor genes known as the *Hox* genes.

Homeotic shifting occurs during embryogenesis but may only be appreciated after ossification of the spinal column. The central concept to understanding homeotic shifting lies in that the vertebral segment remains static. It is the border, an imaginary line delineating the lumbosacral junction, which moves in a caudal or in a cranial direction.

A cranial shift is when the border moves upwards when altered by the ‘‘gain-of-function’’ gene (Barnes, 2012. p61). A cranial homeotic shift affects the vertebral level above the given border. The characteristics of the vertebral segment involved gain the features of the segment joined below (Figure 1.26).

A caudal shift is when the border moves downward when altered by the ‘‘loss-of-function’’ gene (Barnes, 2012. p61). A caudal homeotic shift affects the vertebral level below the given border. The characteristics of the vertebral segment involved gains the features of the segment that it has joined above it (Figure 1.27).

Cranial and caudal homeotic shifts may occur simultaneously at different segments of the vertebral column in a single individual. Homeotic shifts can be asymmetrical (unilateral or bilateral) with expressions of variation ranging from incomplete to complete changes in characteristics (Barnes, 2012).

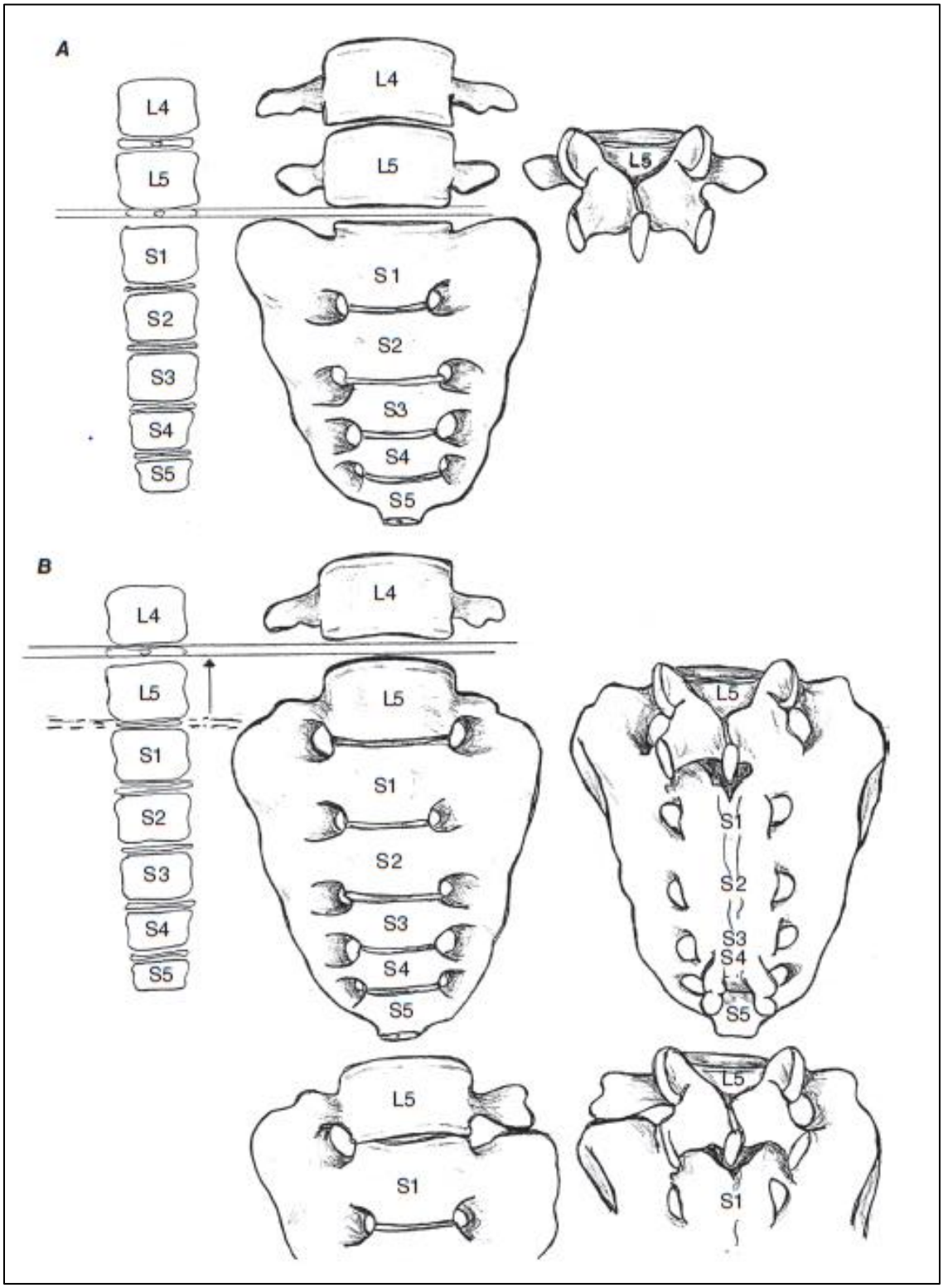

Figure 1.26: *Cranial homeotic shift in the lumbosacral border.* ***A)*** *The typical border between the last lumbar vertebra (usually the fifth segment) and the first sacral vertebra.* ***B)*** *Cranial border shift upward between the fourth and fifth lumbar vertebrae, demonstrating a lumbosacral transitional vertebra, partial and complete sacralisation of the fifth lumbar vertebra, respectively (Adapted from Barnes 2012). Used with permission from Wiley books.*

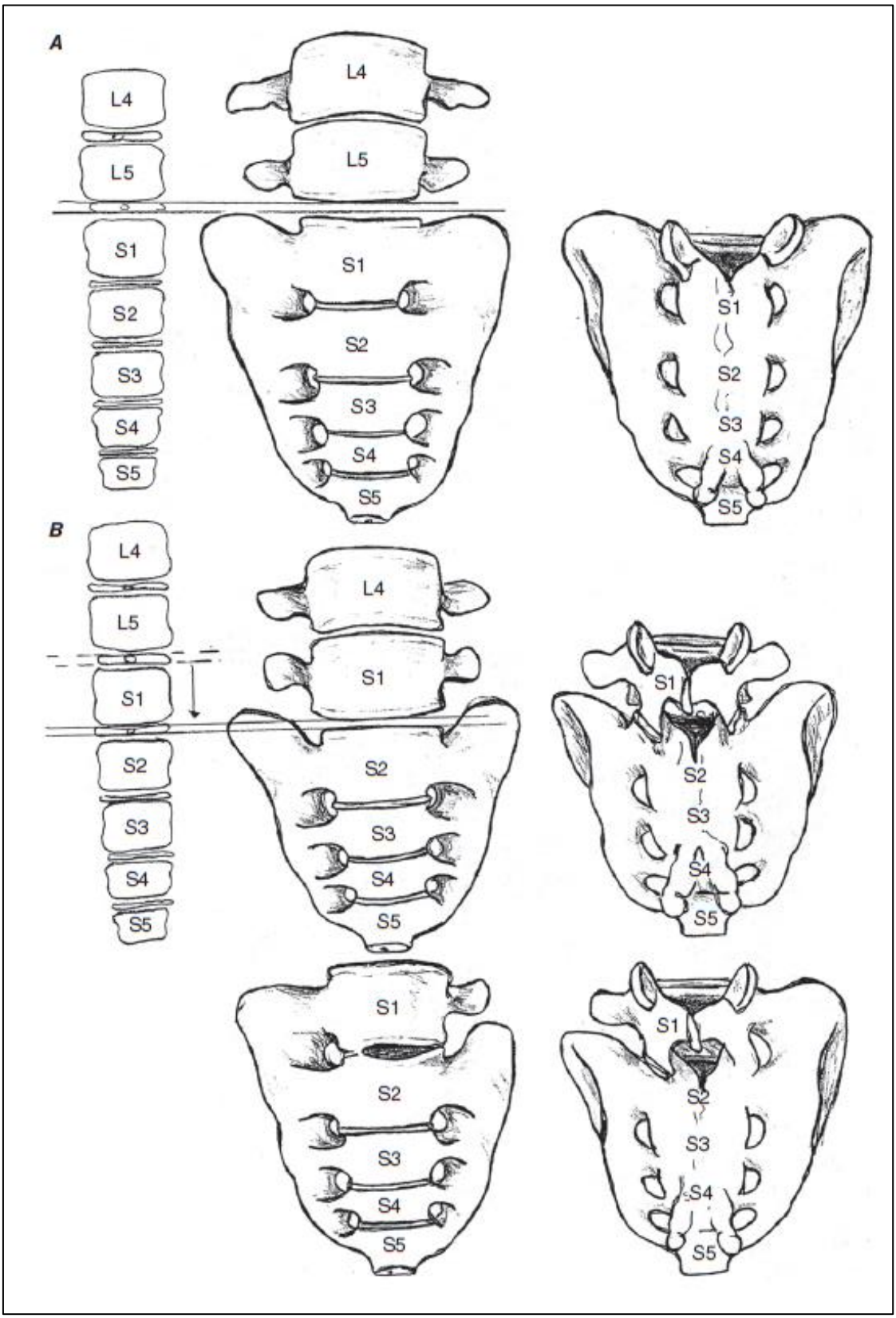

Figure 1.17: *Caudal homeotic shift in the lumbosacral border.* ***A)*** *The typical border between the last lumbar vertebra (usually the fifth segment) and the first sacral vertebra.* ***B)*** *Caudal border shift downward between the first and second sacral vertebrae, demonstrating a lumbosacral transitional vertebra, partial and complete lumbarisation of the first sacral vertebra, respectively (Adapted from Barnes 2012). Used with permission from Wiley books.*

There exist two main schools of thought as to evolutionary change of the axial vertebral column, namely the '*short-backed*' and the '*long-backed*' ancestry hypotheses:

Short-backed hypothesis

In contrast to homeotic shift whereby transformation of one segment into a different segment occurs without a vertebral enumeration change, a meristic shift is defined as the change in number by either the addition or the subtraction of segments. Meristic changes of the vertebral column result in a vertebral number change through the production or reduction of embryonic vertebral stem cells contained within somites (Williams and Russo, 2015). However, many evolutionary paleoanthropologists argue that hominids evolved not by meristic change but by homeotic change over time after tail loss. It is proposed that homeotic shifts of the thoracolumba vertebrae led to lumbar vertebrae reduction through sacralisation or Keith's (1902) 'posterior transmutation' into increased sacral numbers. The lumbar column reduction adapted hominid ancestors to increase their truncal stability to upright posture (Keith, 1902; Pilbeam, 2004; Williams, 2011, 2012).

Furthermore, it is hypothesized that the number reduction of the lumbar elements occurred in a stepwise fashion of evolution. Lumbar number reduction of the LCA of hominids was likely to have evolved from the base configuration of a relative 'short-backed' ancestor (Pilbeam, 2004; Williams, 2011, 2012; Williams and Russo, 2015; Williams et al*.,* 2016). It is further proposed that the lumbar column in subsequent species experienced a homeotic shift at the thoracolumbar border, resulting in 12T:5L configuration (from 13T:4L). Hominins are proposed to have evolved a fifth lumbar vertebra from a great ape-like configuration (7C:13T:4L:5S) to a modern hominin (7C:12T:5L:5S) configuration (Keith, 1902, 1923; Pilbeam, 2004; Williams and Russo, 2015). The decrease in numerical length of the pre-sacral vertebrae is classified as 'lipospondylous' (Williams et al*.,* 2016). There is support for the ape-like archetypal lipospondylous LCA from which modern humans perhaps evolved (Pilbeam, 2004; Williams, 2011, 2012; Williams and Russo, 2015; Williams et al., 2016).

Long-backed hypothesis

The increase in numerical length of the pre-sacral vertebrae is classified as 'auxispondylous' (Williams et al*.,* 2016). Lovejoy et al. (2009) and McCollum et al. (2010) view hominoid change as an evolutionary reduction in lumbar numbers from an auxispondylous 'long-backed' LCA possessing six or more lumbar vertebrae. Various ape taxa, namely African apes (gorillas, chimpanzees and bonobos), are hypothesized to have evolved independently, in parallel of each other, rather than sharing a common ancestor with this morphology (homology).

Lovejoy et al. (2009, 2010) and McCollum et al. (2010) contend that increased sacral numbers preceded lumbar reduction through meristic loss of a tail and concomitant homeotic change at the lumbosacral border. Lovejoy et al. (2009) and McCollum et al. (2010) argue that homeotic change was driven by LSTV formation, namely sacralisation, that lead to a dominance of 5 element modal lumbar number in modern humans from an ancestral 6 element lumbar spine. This evolution is hypothesized to be an extensive form of homoplasy (''similarity due to independent evolution''; Williams, 2011 p.1). Thoracic trunk reduction is believed to have occurred from 13 to 12 segments as seen in fossil hominins and orangutans while great apes (orangutans and African apes) re-evolved from 12 to 13 thoracic vertebrae. The thoracic change is hypothesised to have occurred via natural selection for decreased lumbar numbers as well as prevalent thoracic variation in favour of 13 vertebrae as it was advantageous for suspensory locomotion (Williams et al*.,* 2016; Williams et al., 2019).

Vertebral numbers in the sacrum

When dealing with asymmetrical vertebrae that display features from two adjacent regions, Schultz (1930 and 1960) formalised criteria for assigning the vertebrae to one region or another. The criteria define the thoracic vertebral column as rib-bearing-vertebrae while vertebrae that contribute to the sacral foramina are classified as sacral vertebrae. The cervical and lumbar vertebrae are distinct due to the absence of rib articulation facets and the lack of contribution to the sacral foramina. Furthermore, Tague (2011) stated that if a sacrum contains an extra-modal element (also known as a supernumerary vertebra) that does not include an assimilated lumbar vertebra, then the terminal vertebra is identified as a fused first coccygeal vertebra (Cy1).

Imaging of the spine

X-ray imaging

X-rays were discovered on 8 November 1895 by Wilhelm Röntgen for which he received the first Nobel Prize in Physics (Mould, 1995). X-rays are produced within a vacuum tube by the emission of electrons directed from the cathode to a rotating anode. Around 99% of the energy from the electron bombardment into the anode is transformed into heat. The remaining 1% of the energy converted to diverging X-rays towards the area of interest (Hermanek et al., 2018). The workflow of X-ray image production is described in the following order: X-ray generation, attenuation of X-rays as they pass through the body or body part, signal detection/ acquisition of projection, and finally reconstruction as an image on a screen as a two-dimensional radiograph (Hermanek et al., 2018). Radiographs are images produced by computer software measuring the strength of the X-rays on a detector plate after passing through a body part. The relative impedance of X-rays passing through tissue is directly proportional to the tissues' density. The denser the tissue, the whiter the image. The terminology for describing X-ray greyscale is based on density. Bone will appear white (hyperdense) whereas air will appear black (hypodense). Soft tissues vary in density and will appear in various shades of grey (isodense).

Computerised tomography imaging (CT)

Computerised tomography (CT) is also known as computerised axial tomography or X-ray computerised tomography and was first introduced into clinical practice in 1972 (Kalender, 2006). It is a medical technique that utilises rotating X-rays around a stationary supine patient for multiplane imaging and three-dimensional imaging. The invention of the CT scanner was credited to British engineer Godfrey Hounsfield and South African physicist Allan Cormack for which they won the Nobel Prize in Medicine in 1979. As with static X-ray production, CT images are produced by the relative impedance of X-rays passing through patient tissues as the X-ray tube rotates around a patient in a corkscrew-like fashion. A multidetector-row of sensors will measure the incoming X-rays of varying attenuation levels and convert the data into images, creating slices (axial, coronal or sagittal) and volumetric rendering images (3D images) of internal tissues or organs.

The multiplanar slices can be set to various values measured in millimetres of thickness as required for the region of the body and all images are viewed on a diagnostic imaging monitor. The computer software allows the user to adjust contrast settings to enhance visualisation of various bodily tissues.

The clinical application of CT includes traumatology (fast evaluation of bone and soft tissue following injury), provision of great bone-imaging detail, and multiplane image acquisition (Kalender, 2006; Hermanek et al., 2018). As with X-rays, the terminology for describing CT image greyscale is based on density. Density can be objectively measured using the Hounsfield unit (HU) named after Godfrey Hounsfield. A HU is a scale representing an index for X-ray attenuation from -1000HU defined for air, 0HU for water at standard temperature and pressure. Bone typically ranges between 300HU and 2000HU.

Magnetic resonance imaging (MRI)

Magnetic resonance imaging (MRI) is a non-invasive, ionising-radiation-free medical technique that utilises a very powerful magnetic field, radio waves, and computer software for the visualisation of the body tissues. Magnetic resonance imaging relies on computer software reconstruction of signals emitted by the various tissues in the body while in a magnetic field for image production (Khanna, 2014; Caverly, 2015). The chief component in MRI production utilises the most abundant substance in the human body, water, for which the principal constituent is hydrogen atoms (Khanna, 2014). Using the energy emitted by the change in position of hydrogen atoms in a magnetic field and very complex algorithms, various weighted-sequences can be produced favouring visualisation of certain structures over others. This allows MRI to be a highly sensitive soft tissue imaging modality of spinal anatomy and morphology. The invention of the MRI scanner was credited to Paul Lauterbur and Peter Mansfield for which they won the Nobel Prize in Physiology or Medicine in 2003 (Caverly, 2015). The terminology for MRI is *intensity*, varying from bright (hyperintense), grey (isointense), and dark (hypointense) on a greyscale.

Lumbosacral transitional vertebra morphology

Morphological classification

Morphological classification of LSTV involves describing the appearance of the lumbosacral transverse processes, articulation, and the fusion thereof, based on an anteroposterior view or coronal plane imaging (Blumensaat and Clasing, 1932; Southworth and Bersack, 1950; Tini et al., 1977; Mcculloch and Waddell (1980); Castellvi et al., 1984; Santavirta et al. 1993; Hanhivaara et al., 2020).

Two main morphological classification methods exist in the literature:

i. Medical imaging appraisal (*in situ*)

a) X-ray imaging appraisal: X-rays (radiographs), Lodox® Statscan® full body scanning (trauma focused imaging) and CT imaging; and

b) MR imaging appraisal.

ii. Osteological appraisal (*ex situ*)

The appraisal of *ex situ* skeletal remains housed mainly in University skeletal repositories around the world. This may provide information on prevalence rates in past populations, evolutionary hypotheses and metric and non-metric features associated with LSTV.

Lumbosacral transitional articulation

In the literature lumbosacral transitional articulation associated with LSTV has been interchangeably referred to as one of six descriptions: pseudoarticulation, pseudoarthrosis, accessory articulation, anomalous articulation, nearthrosis, and megatransversus (Jönsson et al., 1989; Konin and Walz, 2010, Mahato, 2013; Dzupa et al., 2014; Kanematsu at al., 2020). No clearly defined descriptions exist for the use of one term over another. Pseudoarticulation and accessory articulation are the most frequently used terms (Jönsson et al., 1989; Konin and Walz, 2010, Mahato, 2013a; Kanematsu at al., 2020).

Medical imaging appraisal (in situ)

Medical imaging appraisal may be subdivided further into two subcategories:

i. Anteroposterior and coronal-plane imaging appraisal

ii. Lateral and sagittal-plane imaging appraisal

These imaging modalities are an *in situ* assessment of LSTV in a living individual that may identify and inform: pain generation aetiology, conservative care planning strategies as well as surgical planning strategies (Konin and Wlaz, 2010; Nardo et al., 2012; de Bruin et al., 2017; Matson et al., 2020).

Anteroposterior and coronal-plane imaging

It has been reported by Blumensaat and Clasing (1932) that one of the earliest recorded accounts relating to lumbosacral transitional vertebrae development and classification was by the anatomist Emil Rosenberg in the mid-1870s. Rosenberg's theory was that LSTV was an effort to stabilise the vertebral column by undergoing a shortening process (Stinchfield and Sinton, 1955). Since then, many clinicians and anatomists have tried to develop a universal, easy-to-understand classification that could be used in clinical practice.

This section details the background on the proposed morphological classifications found throughout the recent literature:

- Blumensaat and Clasing (1932);
- Southworth and Bersack (1950);
- Tini, Wieser and Zinn (1977);
- McCulloch and Waddell (1980);
- Castellvi, Goldstein and Chan (1984);
- Santavirta, Tallroth, Ylinen and Suoranta (1993), and
- Hanhivaara, Määttä, Niinimäki and Nevalainen (2020).

Blumensaat and Clasing (1932)

Blumensaat and Clasing (1932) developed a system based on the anatomical changes observed on radiographs for clinical purposes. Their classification system consisted of 3 groups (Table 1.1).

Table 1.1: Blumensaat and Clasing (1932) classification of lumbosacral transitional vertebra.

Classification	Features
Group I	Complete, symmetrical sacralisation or lumbarisation
Group II	Partial sacralisation or lumbarisation a) Bilateral forms b) Unilateral c) Combination of sacralisation and lumbarisation
Group III	Transverse hyperplasia of costal processes without connection to the sacrum.

Blumensaat and Clasing (1932) proposed a confusing classification system with an inherent vagueness as to sacralisation and lumbarisation defining characteristics. Furthermore, their classification system did not differentiate between fusion and articulation-contact of the transverse process of the LSTV with the sacrum, nor did it consider the number of lumbar motion segments.

Southworth and Bersack (1950)

Southworth and Bersack (1950) appraised upper abdominal and lumbar spine radiographs. Subsequently, they described dysplasia of transverse processes, unilaterally or bilaterally, of the last lumbar vertebra as a form of '*fruste forme'*, that is to say, a crude unfinished form of dysplasia. Values of craniocaudal height of 19mm appeared to be a more reliable criterion than corresponding values for the length of the transverse process, from the medial aspect of the pedicle to the tip of the transverse processes of L5. They argued that transverse processes measuring 19 mm of craniocaudal height or more ''should be presumed as evidence of an attempt at sacralisation'' (Southworth and Bersack, 1950, p.631). This classification didn't consider the morphological changes toward a wing-shaped configuration, articulation with the sacrum or continuity (fusion) with the sacrum. Subsequent authors (Tini et al., 1977; Castellvi et al., 1984; Mahato, 2013a) have included this figure, 19mm, within the context of their proposed classifications of LSTV.

Tini, Wieser and Zinn (1977)

Incorporating the work from Southworth and Bersack (1950), Tini et al. (1977) proposed a classification of LSTV based on the ''radiomorphological changes of the transverse processes of transitional vertebra'' (Tini et al., 1977, p.180). They subsequently divided LSTV findings into four large groups based on 4000 radiographs appraised. Furthermore, they described dysplastic transverse processes (increase in craniocaudal height) as hereditary or genetic components. Tini et al. (1977) described a prevalence rate of LSTV at 6.7% (Types II-IV), Table 1.2 and Figure 1.28.

Table 1.2: Tini et al. (1977) classification of lumbosacral transitional vertebrae.

Classification	Features
Type I	**Dysplastic transverse process (DTP):** A transverse process measuring at least 19mm in craniocaudal height, as described by Southworth and Bersack (1950). **a)** Asymmetrical (DTPR or DTPL); **b)** Symmetrical (SDTP).
Type II	**Symmetrical lumbosacral transition vertebra (STV)** Dysplastic transverse processes (increased craniocaudal height) of the last lumbar vertebra, with an appearance of enlarged wing-like structures that articulate with the sacrum. **a)** Bony fusion between the transverse process to the sacrum (STVB); **b)** Articulation between transverse process and sacrum (STVA) present.
Type III	**Asymmetrical lumbosacral transition vertebra (ATV)** **a)** Ipsilateral articulation (left or right) with the sacrum and contralateral bony fusion of the transverse process with the sacrum (ATVAR/ ATVBL). **b)** Ipsilateral bony fusion (left or right) of the transverse process of the last lumbar vertebra with the sacrum. The contralateral transverse process shows no signs of dysplasia (ATVBR or ATVBL). **c)** Ipsilateral articulation (left or right) of the transverse process of the last lumbar vertebra with the sacrum. The contralateral transverse process shows no signs of dysplasia (ATVAR or ATVAL).
Type IV	**Combined disturbances of lumbosacral junction** **Mixed morphology:** A combination of a dysplasia of the transverse process on one side with an articulation or bony fusion on the contralateral side (DTPR/TVBL). **Note:** Spina bifida occulta or other dyplasias of the posterior arch were not considered in their study.

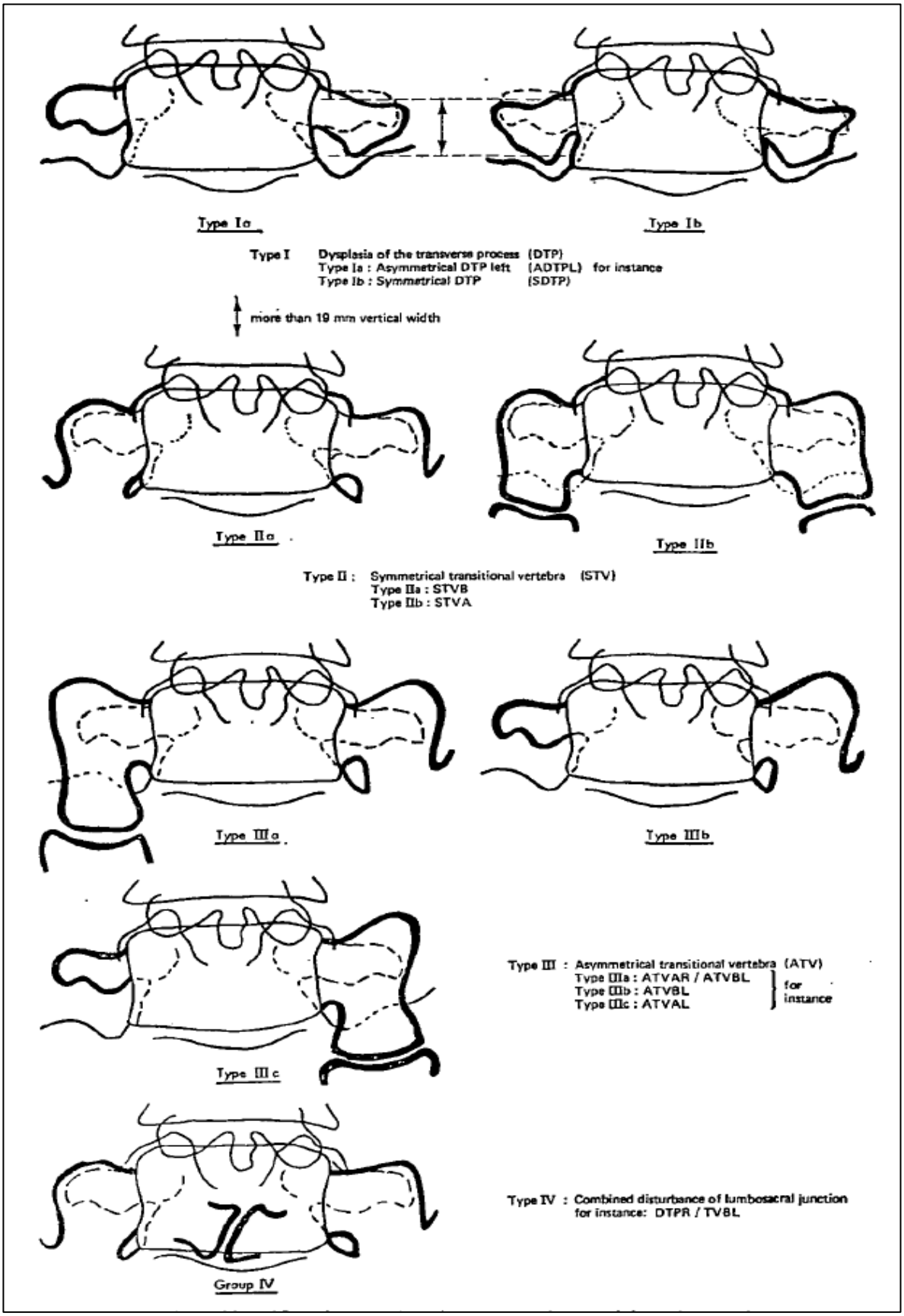

Figure 1.28: *Classification of lumbosacral transitional vertebrae based on morphological appearance on radiographs (Adapted from Tini et al., 1977). Used with permission from Oxford University Press.*

McCulloch and Waddell (1980)

With no detailed description of how the classification was devised, McCulloch and Waddell (1980) depicted eight categories (A to H) of LSTV which they utilised in their study on ''variation of the lumbosacral myotomes with bony segmental anomalies'' (McCulloch and Waddell, 1980, p.1), Table 1.3 and Figure 1.29. The LSTV features represented a spectrum from lack of variation to varying vertebral numbers, transverse process dysplasia represented by either an articulation and fusion, and finally intervertebral disc space appearance. No subsequent mention of their classification of LSTV appears to exist in the literature.

Table 1.3: McCulloch and Waddell (1980) classification of lumbosacral transitional vertebrae.

Classification	Features
A	Normal or varying numbers of vertebrae (unspecified)
B	Unilateral articulation of transverse process with the sacrum
C	Bilateral articulation of transverse process with the sacrum
D	Unilateral articulation of transverse process with sacrum and ilium
E	Bilateral articulation of transverse process with sacrum and ilium
F	Unilateral fusion of transverse process to the sacrum
I	Bilateral fusion of transverse process to the sacrum
H	Almost complete incorporation in sacrum: rudimentary intervertebral disc space and/ or incomplete segmentation of posterior arch

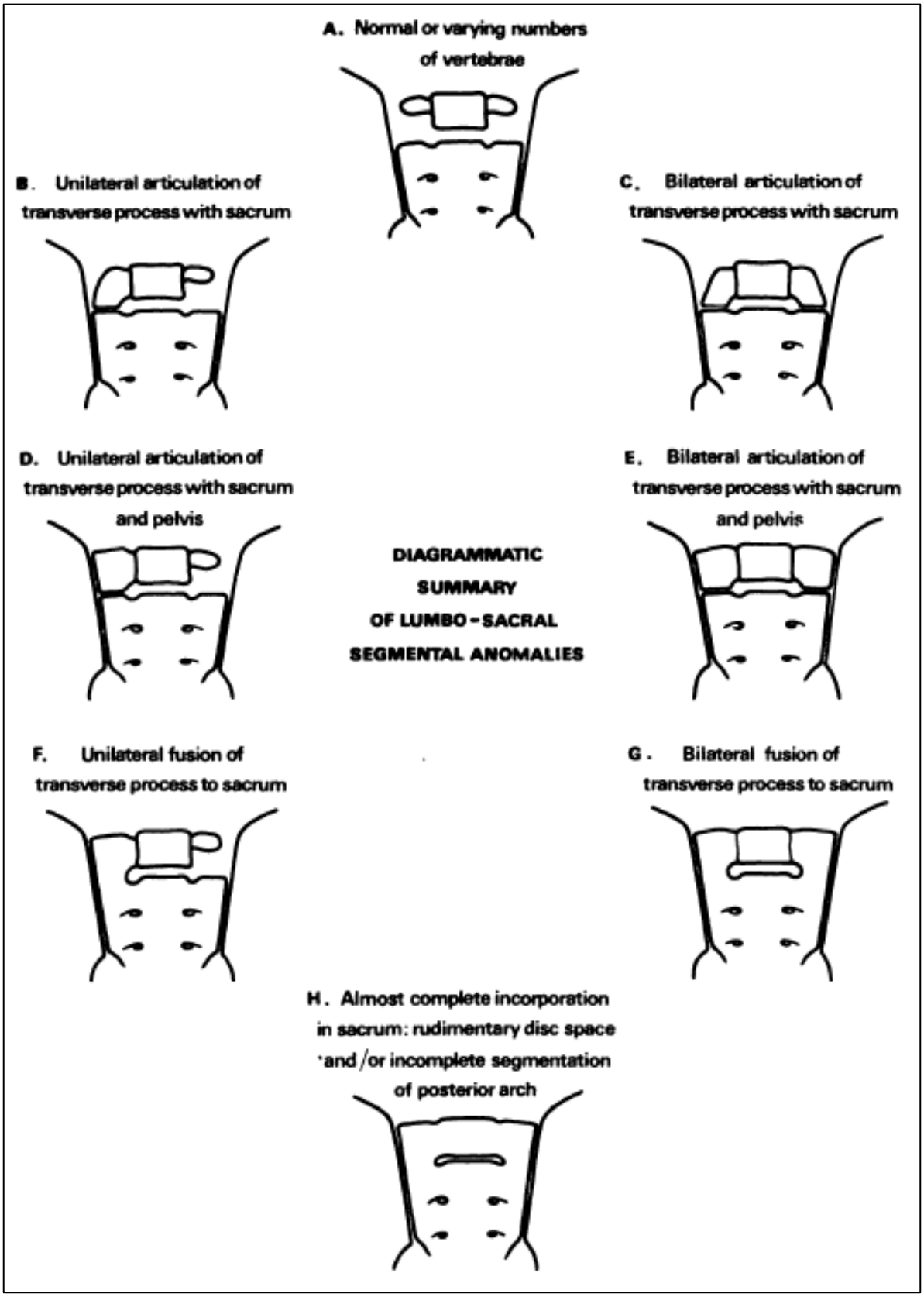

Figure 1.29: *Diagrammatic representation of the 8 subtype-classification of lumbosacral transitional vertebrae as described by McCulloch and Waddell (1980) (Adapted from McCulloch and Waddell 1980). Used with permission from British editorial Society of Bone & Joint Surgery Ltd.*

Castellvi, Goldstein and Chan (1984)

The Castellvi et al. (1984) classification system was based on their exploration of LSTV (conducted in 1979) incorporating the work from Southworth and Bersack (1950). Castellvi et al. (1984) classified LSTV according to morphological and clinical characteristics associated with IVD herniation. With similarity to Tini et al. (1977) classification, Castellvi et al. (1984) simplified LSTV classification making it more useable. The most commonly used morphological classification for LSTV is the Castellvi et al. (1984) radiographic classification, Tables 1.4 and Figure 1.30 (Kassir, 2015; Hanhivaara, 2020).

Table 1.4: Castellvi et al. (1984) classification of lumbosacral transitional vertebrae.

Classification Type	Features
Type I	**Dysplastic transverse process:** A transverse process measuring at least 19mm in craniocaudal height, as described by Southworth and Bersack (1950). **A**, *unilateral*; **B**, *bilateral*.
Type II	**Incomplete ***lumbarisation/ sacralisation**:** Dysplastic transverse process (increased craniocaudal height) of the last lumbar vertebra, with an appearance of enlarged wing-like structures that articulate with the sacrum. **A**, *unilateral*; **B**, *bilateral*.
Type III	**Complete *** lumbarisation/ sacralisation **:** Similar to Type II presentation except there is true bony fusion of the transverse process with the sacrum. **A**, *unilateral*; **B**, *bilateral*.
Type IV	**Mixed morphology:** spinal anatomy that exhibits <u>both</u> *unilateral* **Type II** and **Type III** categories concomitantly.

* ***Note:*** *Catsellvi et al. (1984) used the terminology 'lumbarisation and sacralisation' interchangably as they ''were not able to determine the total number of vertebrae in the patient's spines'' (Castellvi et al., 1984, p.494). These terms were not used as consideration for lumbar vertbral enumeration in their study. See section 2.1.8.1 for an updated, concise version.*

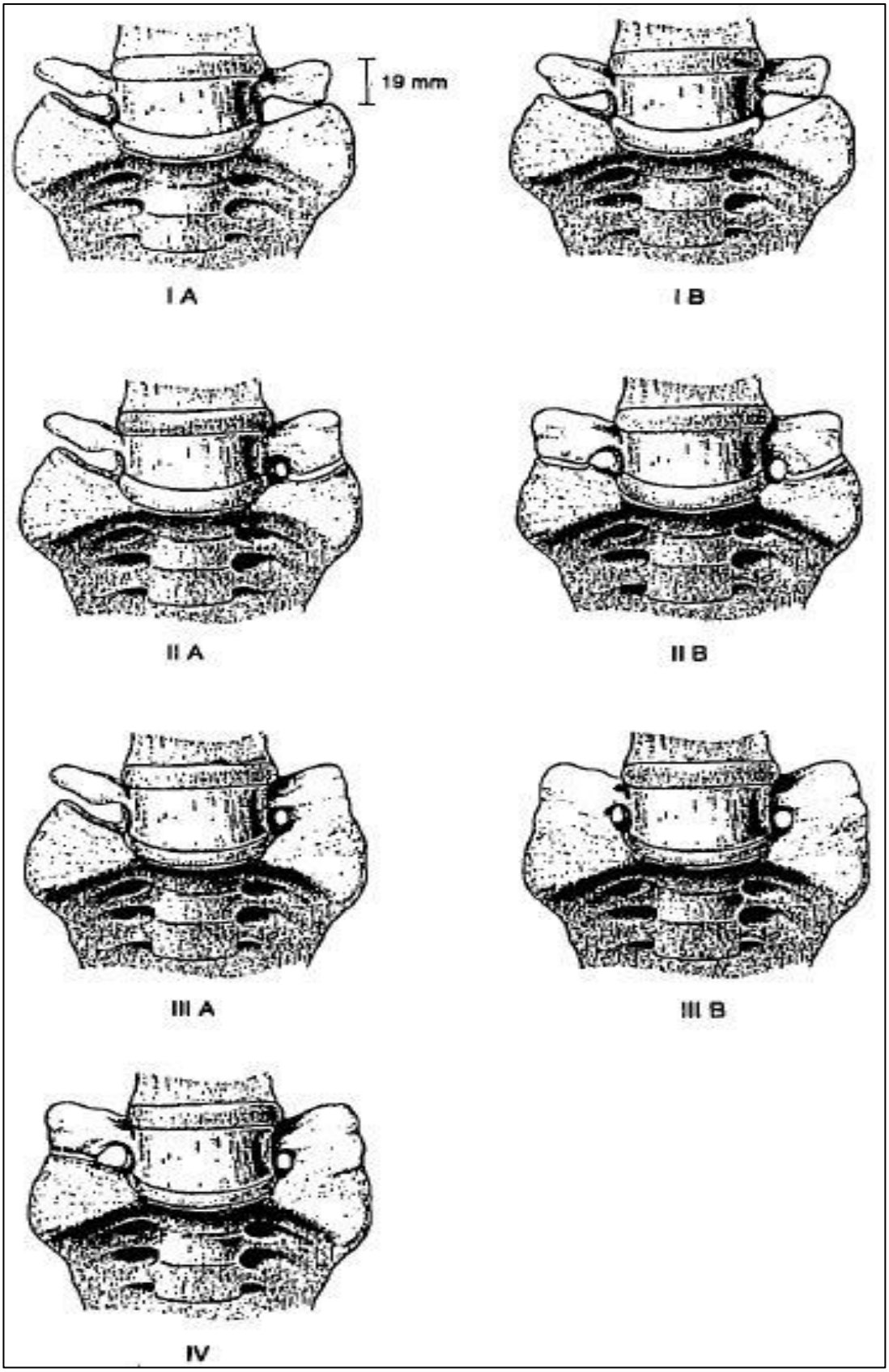

***Figure 1.10**: Classification of lumbosacral transitional vertebrae based on morphological appearance on radiographs (Adapted from Castellvi et al., 1984). Used with permission from Wolters Kluwer Health Inc.*

Santavirta, Tallroth, Ylinen and Suoranta (1993)

Santavirta et al. (1993) published an LSTV classification with a visual representation but no explanation was forthcoming on their rationale for LSTV classification (Santavirta et al., 1993). Described solely as ‘‘according to the classification used in our hospital’’ (Santavirta et al., 1993, p.82) and referenced to an illustration with the subscription of ‘’a modified LSTV classification after Tini et al. (1977) and McCulloch and Waddell (1980)’’ (Santavirta et al., 1993, p. 83), see Figure 1.31. The classification seems to hinge on ideas from both Tini et al. (1977) and McCulloch and Waddell (1980) to the exclusion of the more widely accepted Castellvi et al. (1984) classification.

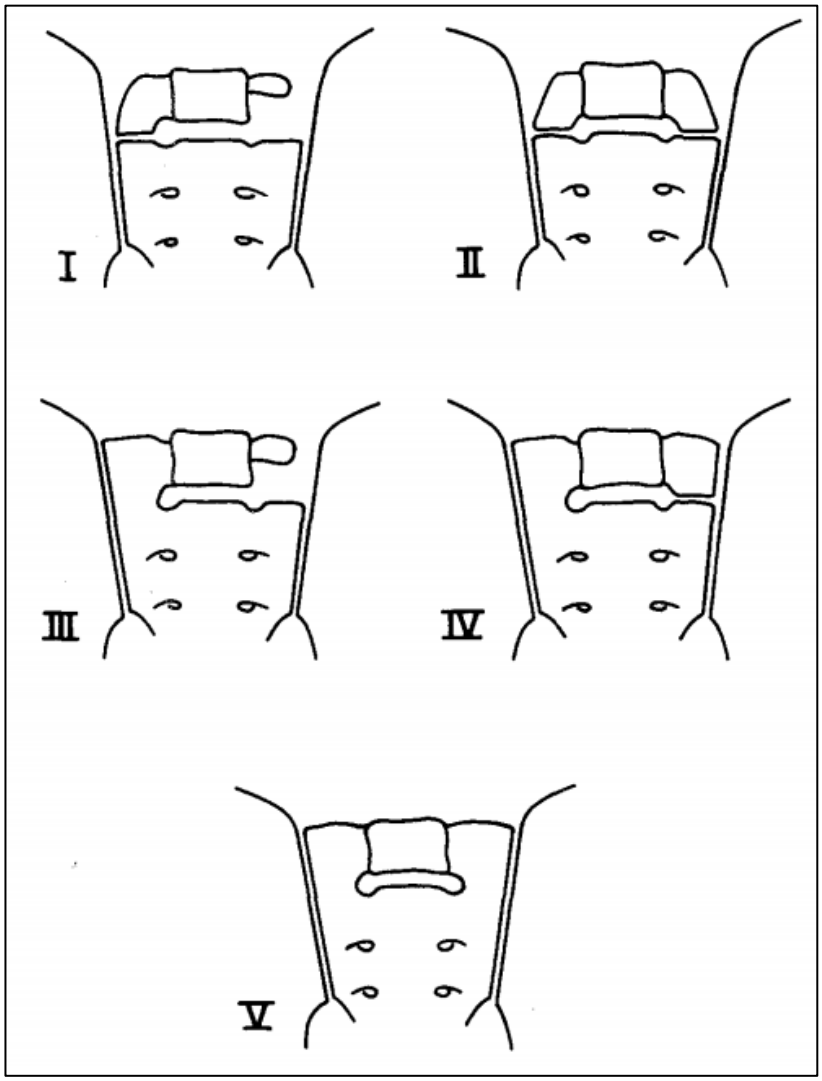

Figure 1.31: Diagrammatic representation of the modified 5 subtype-classification of lumbosacral transitional vertebrae as described by Santavirta et al., (1993) (Adapted from Santavirta et al. 1993). *Used with permission from Springer Nature.*

Hanhivaara, Määttä, Niinimäki and Nevalainen (2020)

The study by Hanhivaara et al. (2020) consisted of an evaluation on LSTV utilising CT scans. Vertebral enumeration was calculated using the method of counting down from the last pair of ribs (which define the last thoracic vertebra or T12). The LSTV was considered to be the fifth lumbar vertebra according to the study. They did not describe the enumeration of the lumbar spine, lumbarisation or sacralisation in their study.

Hanhivaara et al. (2020) proposed a new subtype to the Castellvi et al. (1984) classification describing the presence of a dyplastic TVP, a Type IA (arrow in Figure 1.33), on the side opposite a Type IIA or Type IIIA LSTV. They termed these new proposed subtypes as a Type IIC or Type IIIC (Figure 1.32). That is to say, the simultaenous presence of both a Type IA with either a Type IIA or Type IIIA LSTV.

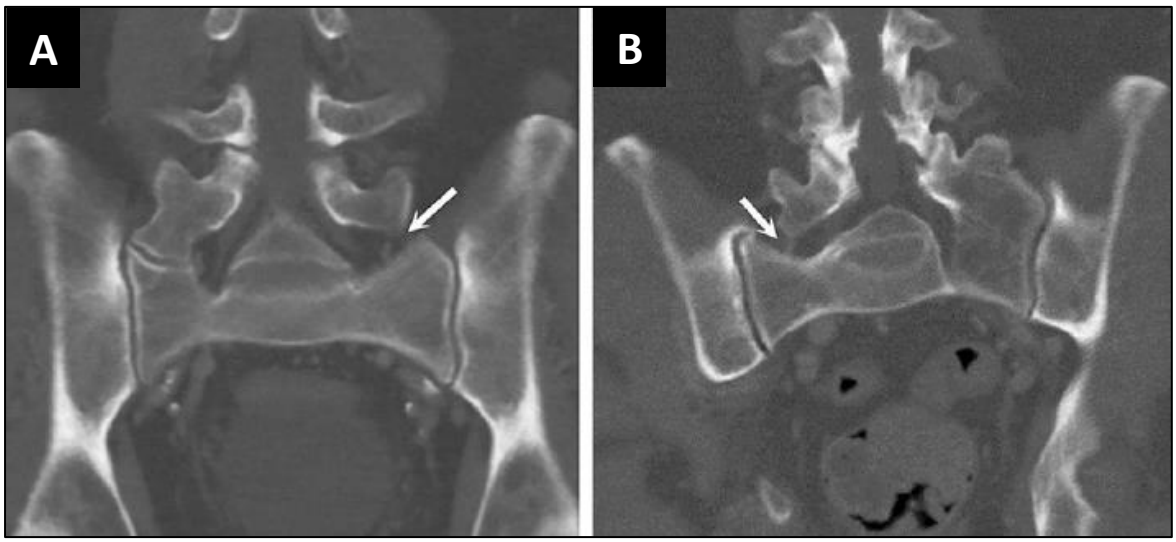

Figure 1.32: *A coronal CT scan of the lumbosacral junction. Hanhivaara et al. (2020) proposed new subtypes to the Castellvi et al. (1984) classification.* ***A)*** *Suggested* ***Type IIC*** *lumbosacral transitional vertebra showing a pseudoarticulation on the patient's right side and a dysplastic transverse process (increased craniocaudal height) without articulation on the patient's left side* ***(arrow)****.* ***B)*** *Suggested* ***Type IIIC*** *lumbosacral transitional vertebra showing complete bony fusion on the patient's left side and a dysplastic transverse process (increased craniocaudal height) without articulation on the patient's right side* ***(arrow)*** *(Adapted from Hanhivaara et al., 2020). Images obtained from an open access publication.*

Lateral and sagittal-plane imaging

The following are the proposed morphological classifications in the recent literature for lateral imaging appraisal of the IVD appearance:

- Wigh and Anthony (1981);
- Nicholson, Roberts and Williams (1988); and
- O'Driscoll, Irwin and Saifuddin (1996).

Intervertebral disc appearance

Intervertebral disc space narrowing is a known finding on lumbar spine images. However, IVD narrowing may not imply degeneration in the setting of LSTV. Developmental or congenital IVD height loss at the LSTV segment has been well documented (Nicholson et al., 1988, Hsieh et al., 2000, Luoma, et al., 2004).

Wigh and Anthony (1981)

Wigh and Anthony (1981) classified IVD appearances (height appraisal) associated with LSTV, seen on lateral radiographs, into four categories (Figure 1.33, Table 1.5). These demonstrated varying stages of fusion and hypoplasia. The proposed classification should be seen as a tool for identifying LSTV from the lateral radiograph. The use of Wigh and Anthony (1981) classification within LSTV studies has not been adopted with advanced imaging methods, CT and MRI scans are preferred means of IVD appraisal over radiographs (Luoma et al., 2004; Konin and Walz, 2010; Mahato 2011a and b, 2013a; Paik et al., 2013; Hanhivaara et al., 2020).

Table 1.5: Wigh and Anthony (1981) classification of intervertebral disc appearance on lateral radiographs.

Classification Type	Features
Type I	A slender biconvex IVD appearance, thicker centrally than peripherally, can be described as a synostotic intervertebral disc.
Type II	An IVD appearance that is rectangular but is short of height and is surrounded by a thin osseous capsule.
Type III	Similar to a Type II or greater in height without a bony capsule. It may be mistaken for a degenerative IVD.
Type IV	An IVD of similar height and shape to a conventional lumbar IVD. It may be mistaken, as seen on lateral radiograph, for last true lumbar IVD.

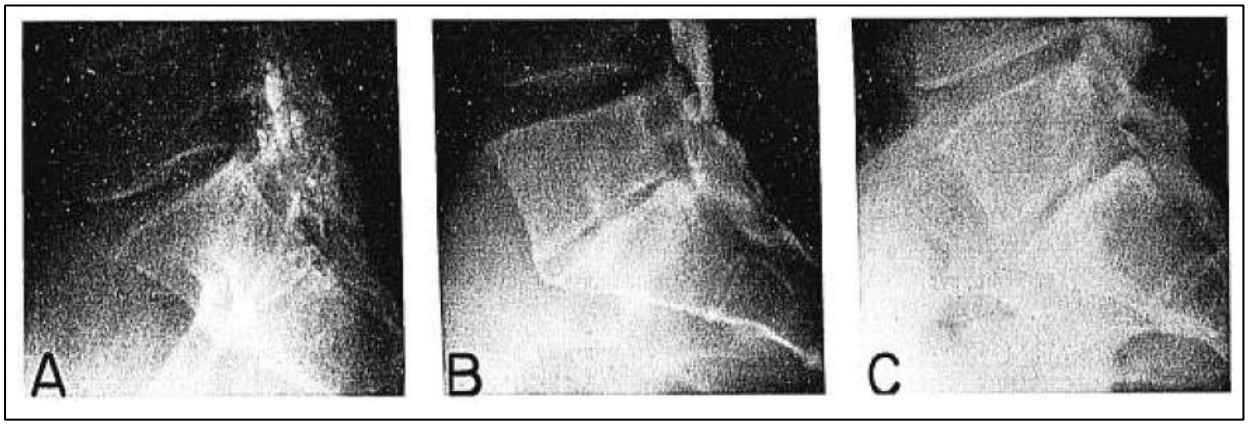

Figure 1.33: *The appearance (original images) of intervertebral discs viewed on lateral radiographs beneath the transitional vertebra.* ***A)*** *Type I,* ***B)*** *Type II,* ***C)*** *Type III. Type IV not depicted as it has a normal intervertebral disc appearance (Adapted from Wigh and Anthony, 1981). Used with permission Wolters Kluwer Health Inc.*

Nicholson, Roberts and Williams (1988)

Nicholson et al. (1988) described significant narrowing of the lumbosacral IVD in the presence of LSTV as an identifying feature of LSTV presence on lateral radiographs. They caution that this finding should not be viewed as a degenerative process. Likewise, numerous authors have reported observing IVD height loss at the LSTV segment (Wigh and Anthony 1981; O'Driscoll et al., 1996; Hsieh et al., 2000; Luoma et al., 2004; Konin and Walz, 2005; Mahato, 2011).

O'Driscoll, Irwin and Saifuddin (1996)

The objective of O'Driscoll et al. (1996) was to identify the features on lumbar spine MRI scans that indicated the presence of LSTV. Their classification system consists of a graded score between I and IV that describes IVD material between the uppermost sacral segment and the remainder of the sacrum (sacralised lumbar vertebra) using T2-weighted midsagittal MR images (Figure 1.34 and Table 1.6, respectively). Lumbosacral transitional vertebrae can be identified on mid-sagittal MRI scans owing to a high correlation between the presence of a fused LSTV and the O'Driscoll et al., (1996) Type 4 MRI appearance.

Table 1.6: O'Driscoll et al. (1996) classification of S1-S2 intervertebral disc.

Type	Features of S1-S2 intervertebral disc
1	No disc between S1 and S2. Thin, hypointense line on sagittal MRI
2	Small disc between S1 and the sacrum, which does not extend the entire sacral AP diameter
3	Well-formed intervertebral disc between S1 and the sacrum, which extends the entire sacral AP diameter
4	Well-formed intervertebral disc between S1 and the sacrum, which extends the entire sacral AP diameter, with 'squaring' of the upper sacral border

Figure 1.34: *Midsagittal T1 and T2-weighted MRI scan of the lumbar spine illustrating classification of sacral morphology.* ***A)*** *Type 1: No disc between S1 and S2. A thin, hypointense line on sagittal MRI.* ***B)*** *Type II: Small disc between S1 and the sacrum, which does not extend the entire sacral AP diameter.* ***C)*** *Type III: Well-formed intervertebral disc between S1 and the sacrum, extending the entire sacral AP diameter.* ***D)*** *Well-formed intervertebral disc between S1 and the sacrum, extending the entire sacral AP diameter, with 'squaring' of the upper sacral border (Adapted from O'Driscoll et al., 1996). Used with permission from Springer Nature.*

Lumbar vertebral body and sacral morphology

Lumbar vertebral body and sacral morphology differ in appearance on medical imaging depending on the spinal enumeration, sacralisation or lumbarisation.

Squaring of the sacralised segment

Wigh and Anthony (1981) described a 'squared' appearance of the vertebral body of an LSTV on lateral radiographs. They considered a vertebra to be transitional when a ratio made up of the AP diameter of the superior vertebral body to that of the inferior vertebral body as ≤1.38. They also stated that there were numerous instances when a vertebral body viewed on a lateral radiograph had neither a conventional relatively square shape of a lumbar body, nor the prominent wedge shape of a sacral vertebral body. There may be an intermediate vertebral body shape associated with LSTV. Furthermore, Konin and Walz (2010) found squaring of the upper sacral segment when a lumbarised LSTV presented (Figure 1.35A).

Wedging of the lumbarisation segment

Konin and Walz, (2010) found wedging of the upper sacral segment when there was a sacralisation LSTV present (Figure 1.35B).

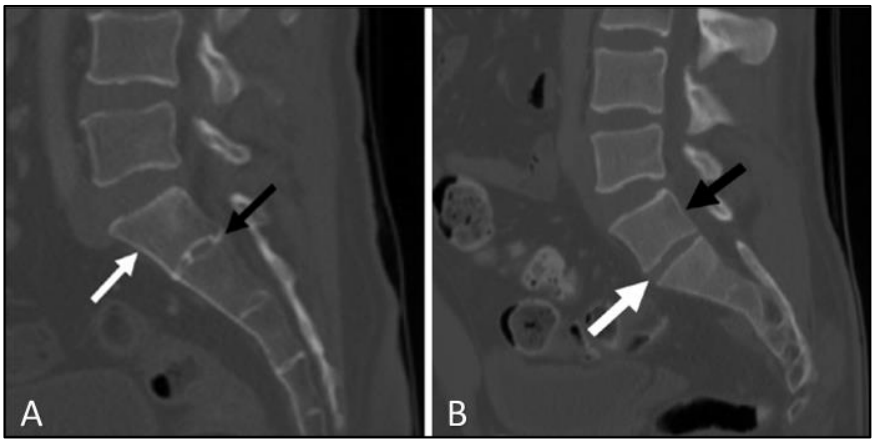

Figure 1.35: *Sagittal computerised tomography images of lumbosacral transitional vertebrae.* ***A)*** *A lumbosacral transitional vertebra demonstrating 'wedging' of a sacralised fifth lumbar (L5) vertebral body* ***(white arrow)*** *and diminished intervertebral disc height* ***(black arrow)****;* ***B)*** *a lumbosacral transitional vertebra demonstrating 'squaring' of a lumbarised first sacral (S1) vertebral body* ***(black arrow)*** *and moderately sized intervertebral disc between S1 and the second sacral (S2) l vertebral body* ***(white arrow)*** *(Adapted from Konin and Walz, 2010). Images obtained from an open access publication, creative commons licence.*

Novel techniques for Lumbosacral transitional vertebrae identification

- Spinal curve measurements: A-angle and B-angle
- Vertical mid-vertebral angle
- Iliac crest tangent line

Spinal curve measurements: A-angle and B-angle

Chalian et al. (2012) proposed a novel radiographic method for the identification of LSTV and enumeration of LSTV. Chalian et al. (2012) measured two spinal curves on T2-weighted mid-sagittal MRIs associated with LSTV (Figure 1.36). The 'A-angle' is the angle formed by a line parallel to the superior surface of the sacrum and a line perpendicular to the axis of the scan table (vertical line on a supine individual). The 'B-angle' is the angle formed by the intersection of a line parallel to the superior endplate of L3 vertebral body and a line parallel to the superior surface of the sacrum. They found increased angles in the A and/or B-angles in individuals with LSTV. Optimal cut-off value for prediction of LSTV of A-angle was 39.8° with a sensitivity of 80% and specificity of 80%. The B-angle cut-off value was set at 35.9° with a sensitivity of 80% and specificity of 54%. Therefore, an A-angle of greater than 40° or a B-angle of greater than 36° may suggest the radiologists as to the presence of a possible LSTV. This method is an easy-to-perform method that may be used as a guide (Figure 1.36).

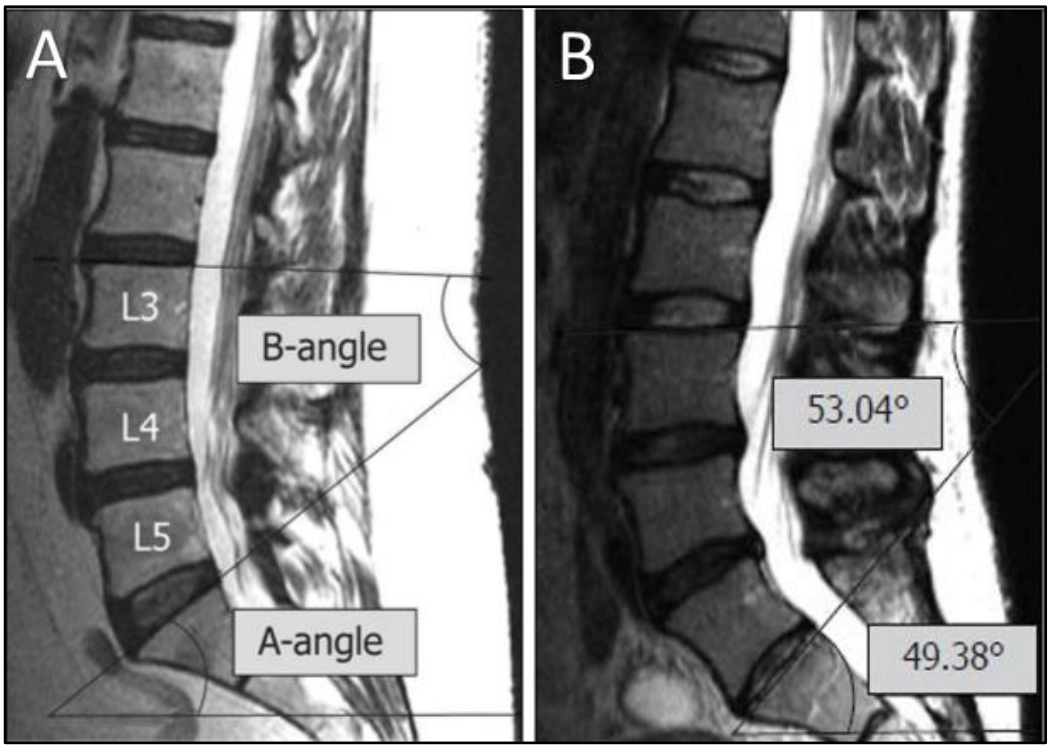

Figure 1.36: *Angle measurements of the vertebral column**. A)** Mid-sagittal T2-weighted image of the lumbar spine illustrating the A-angle and B-angle measurements. **B)** Mid-sagittal T2-weighted image of the lumbar spine illustrating the A-angle and B-angle measurements of an individual with a lumbosacral transitional vertebra (Type IIB in this case) (Adapted from Chalian et al., 2012). Images obtained from an open access publication, creative commons licence.*

Vertical mid-vertebral angle

Farshad et al. (2013) devised a simple yet reliable radiological method of identifying LSTV with a solid bony bridge (Castellvi at al. 1984 Type IIIA, B and Type IV) on both sagittal MR and lateral radiograph images (Figure 1.37). The vertical mid-vertebral angle (VMVA) was defined as ‘’the angle between the vertical mid-vertebral lines of a segment on a single-slice midsagittal MR scan or lateral radiograph’’ (Farshad et al., 2013, p.1534). The mid-vertebral line was drawn through the midpoint each vertebral body's upper and lower endplates (bisects the vertebral body). Measurements were taken at the lowest segment with a fully developed IVD (an IVD that extended across the full width of a segment) as well as the two cephalad segments. The differences per segment (Diff-VMVA) method can identify an LSTV with 100% sensitivity and specificity of 89% on MRI and 94% and 74% respectively on lateral lumbar radiographs. In order to achieve a 100% sensitivity their analysis revealed an optimal cut-off value of the Diff-VMVA of +10°. Therefore, a Diff-VMVA of ≤10° identified with bony bridging indicates an LSTV Type III and IV.

A Diff-VMVA ≤10° was found to identify bony bridging of the posterior elements of a non-mobile LSTV, and by association, the first adjacent mobile segment, without the need for additional imaging. The Diff-VMVA of Type II (A and B) LSTV were found to have lower angulation, 16° (SD 9) compared to the control group (free of LSTV) at 25° (SD 8).

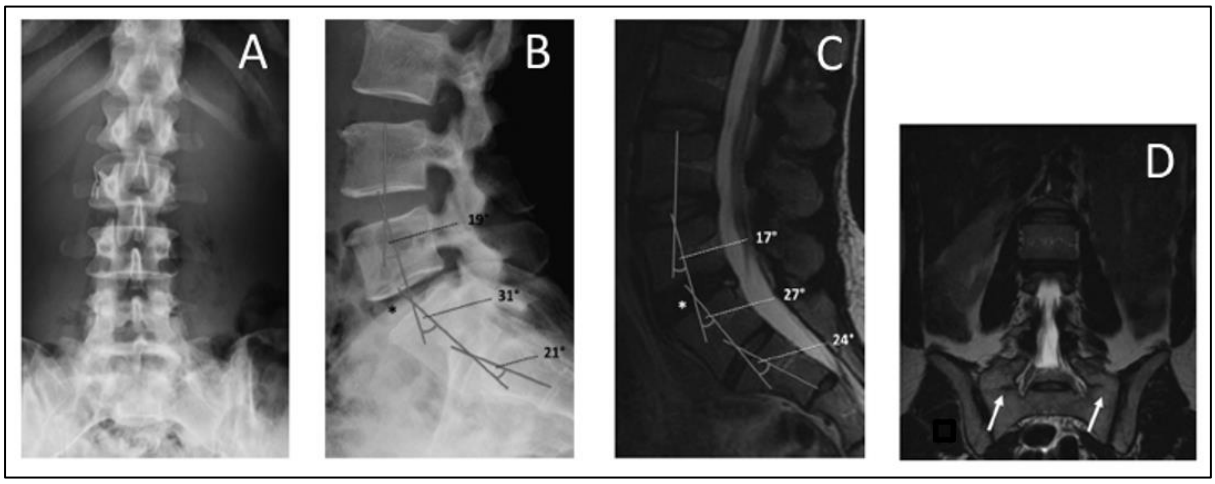

Figure 1.37: *Lumbosacral transitional vertebra images containing solid bony bridging.* ***A)*** *Anteroposterior lumbar radiograph indicating the presence of an LSTV.* ***B)*** *A lateral lumbar radiograph demonstrating the measurement of the vertical mid-vertebral (VMVA) angle with the difference per segment (Diff-VMVA) of <+10° (e.g. -10°) demonstrating a posterior mechanical connection (*, first mobile segment).* ***C)*** *Sagittal MRI displaying a Diff-VMVA < +10° (e.g. -3°) denotes a posterior mechanical connection (*, first mobile segment).* ***D)*** *Coronal MRI verifies the bony bridge of the LSTV (Type IIB), arrows indicate bony bridging of the LSTV to the sacrum (Adapted from Farshad et al., 2013). Images obtained from an open access publication, creative commons licence.*

Iliac crest tangent line

The iliac crest tangent line is based on a technique whereby a line is constructed joining the superior aspect of the iliac crests otherwise known as the intercrestal line (Kim et al., 2003). The intercrestal line may also be described by various other names such as Tuffier's line (Tuffier, 1900), intercristal line (Frymoyer et al., 1984), supracristal line (Jacoby, 1895) and Jacoby's line (Kubota et al., 1992). The intercrestal line crosses the vertebral column at L4-5 level in individuals free of LSTV (Chakraverty et al., 2007; Snider et al., 2008; Mirjalili et al., 2012; Chowdhury and Sharma, 2018). The iliac crest tangent (ICT) is a novel technique proposed by Farshad-Amacker et al. (2015) in which a line is constructed on a coronal lumbar spine MR image by joining the top of the iliac crests on individuals containing a suspected LSTV. The ICT is used to describe the ''iliac crest tangent sign'' (Farshad-Amacker et al., 2015, p.600) based on the number of vertebrae the ICT crosses.

The sign was defined as positive if more than one and a quarter ($1^1/_4$) vertebral bodies were visible below the tangent. If so, the most inferior vertebra was considered to be a lumbarised S1. A negative sign is defined as less than one and a quarter ($1^1/_4$) vertebral bodies visible below the tangent. The last vertebra was then considered to be a sacralised L5 (Figure 1.38). For reproducible measurements, the sagittal MR image of the lumbar spine was set to the posterior half of the second last lumbar vertebral body to which the coronal view is maintained. This technique may be used when there is a lack of complete vertebral column images available and more accurate than other anatomical landmarks (listed earlier) for correct numbering of the lumbar vertebrae in individuals with LSTV. It may be used with CT or MR images. The ICT sensitivity and specificity found were 81% and 64-88% respectively. Farshad-Amacker et al. (2015) found the inter-reader agreement was good at Cohen's kappa coefficient = 0.75. Gündüz et al. (2019) found ICT is highly reproducible with an excellent inter-observer agreement in individuals with lumbarisation but moderate in those with sacralisation. Interestingly, the correct numbering was notably higher in those with lumbarisation as opposed to sacralisation. The ICT relies on limited to no IVD degeneration as this alters vertebral body positioning relative to the iliac crests.

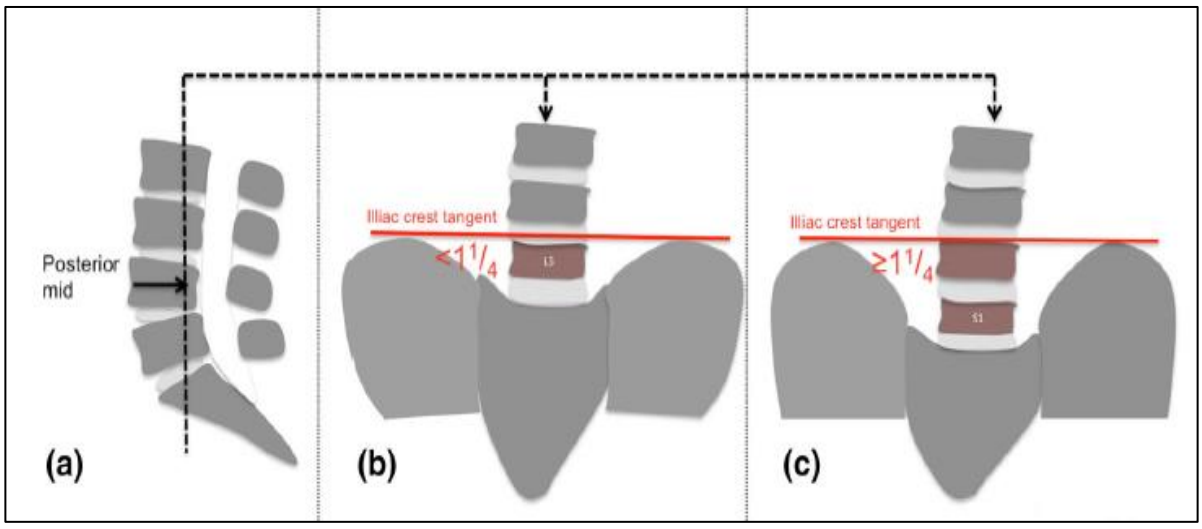

Figure 1.18: Schematic representation of the iliac crest tangent sign. **a)** On coronal images, a tangent (red line) is drawn with the cursor (black dotted line) in a sagittal view set to the posterior half of the second last lumbar vertebral body. **b)** A negative iliac crest sign with less than $1^1/_4$ lumbar vertebral bodies below the tangent. The last vertebra is considered a sacralised L5. **c)** A positive tangent sign with more than $1^1/_4$ lumbar vertebral bodies below the tangent. The last vertebra is considered a lumbarised S1 (Adapted from Farshad-Amacker et al., 2015*). Used with permission from Springer Nature.*

Osteological appraisal (*Ex situ*)

Ex situ osteological appraisal of LSTV have been described by a number of authors whom proposed classification alterations. Three variations in the classification of LSTV have been described by the following authors:

- Savage (2005)
- Mahato (2013)
- Mahato (2016)

Savage (2005)

Savage (2005) developed a three-tiered osteological classification system based on twelve different combinations found associated with LSTV morphology. Savage (2005) compared macroscopic nonmetric observations, rated in six structures of the relevant vertebral elements, namely the last lumbar vertebra and sacrum. The six structures were rated for the presence of bony fusion, contact or open space between the affected vertebra and sacrum. The six structures included (Figure 1.39 and Table 1.7 respectively):

1. **Transverse process (left and right):** fused, contact or open
2. **Vertebral Body (left and right):** fusion, contact or open
3. **Facets (zygapophyseal joints):** fusion, contact or open

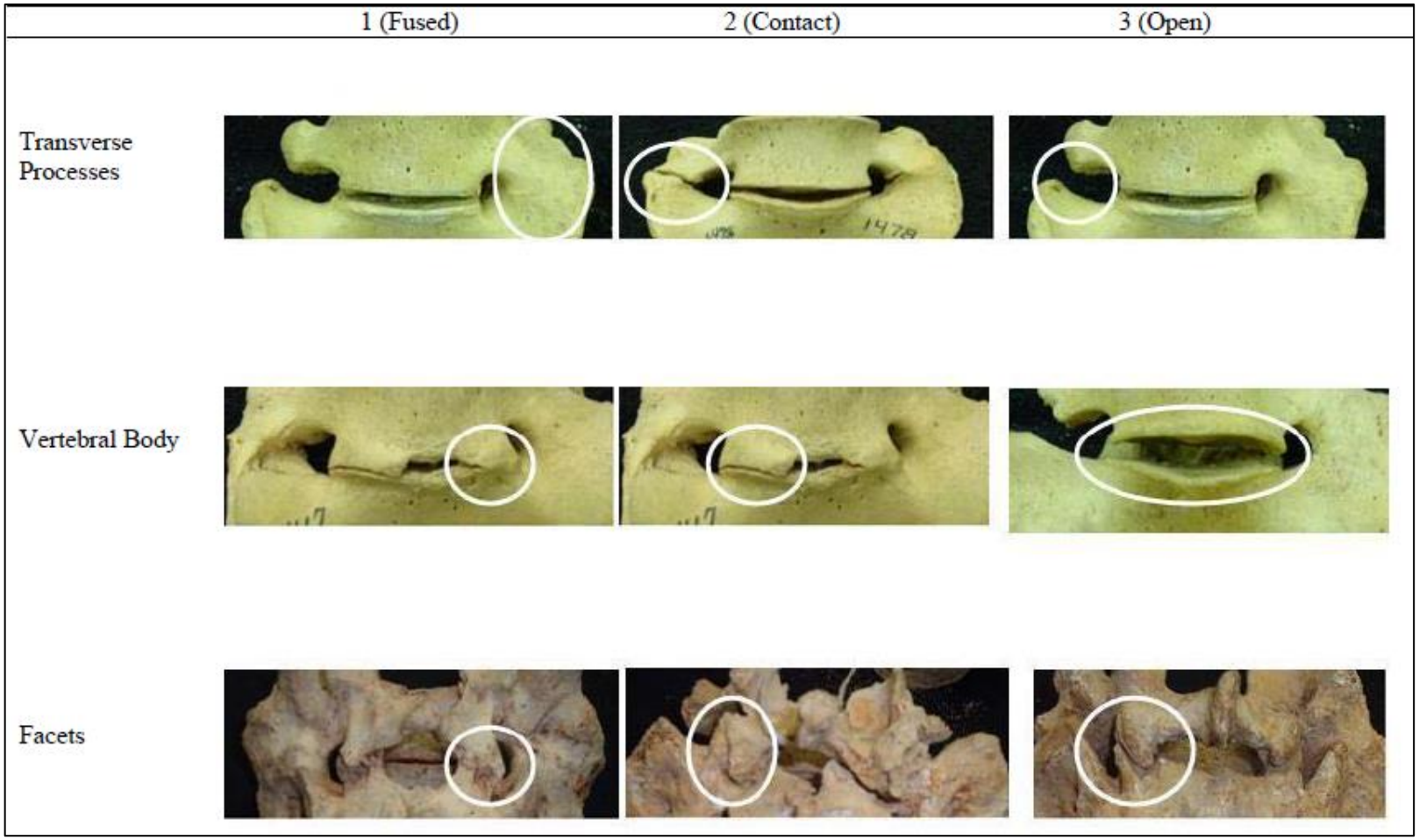

Figure 1.39: *Proposed osteological classification method that appraises transverse process morphology (classical criteria), vertebral body fusion and facet joint morphology of lumbosacral transitional vertebrae (Adapted from Savage 2005). Used with permission from the author.*

Table 1.7: Classification of lumbosacral transitional vertebrae (Adapted from Savage, 2005).

1. Fused (no joint space)

A. >6 motion segments – counted from thoracic transition to affected lumbar segment (i.e. T12 to an affected L5 = 5 motion segments)
- **b**. bilateral
- **u**. unilateral

B. 6 motion segments (normal)
- **b**. bilateral
- **u**. unilateral

C. <6 motion segments
- **b**. bilateral
- **u**. unilateral

2. Contact/Pseudapophysis (touching but not fused/some joint space)

A. >6 motion segments – counted from thoracic transition to affected lumbar segment (i.e. T12 to an affected L5 = 5 motion segments)
- **b**. bilateral
- **u**. unilateral

B. 6 motion segments (normal)
- **b**. bilateral
- **u**. unilateral

C. <6 motion segments
- **b**. bilateral
- **u**. unilateral

Mahato

Mahato (2013b and 2016) has proposed two variations on the lumbosacral junction and sacrum morphological classification that may contain LSTV.

Mahato (2013a)

This study proposed modifying to the Castellvi et al. (1984) classification for improved clinical and biomechanical correlation of LSTV subtypes. Mahato (2013a) argued that the classical methods used (Castellvi et al. 1984) do not include variations in the neural arch components and sacral auricular surfaces, which are functionally important structures (Figure 1.40 and Table 1.8).

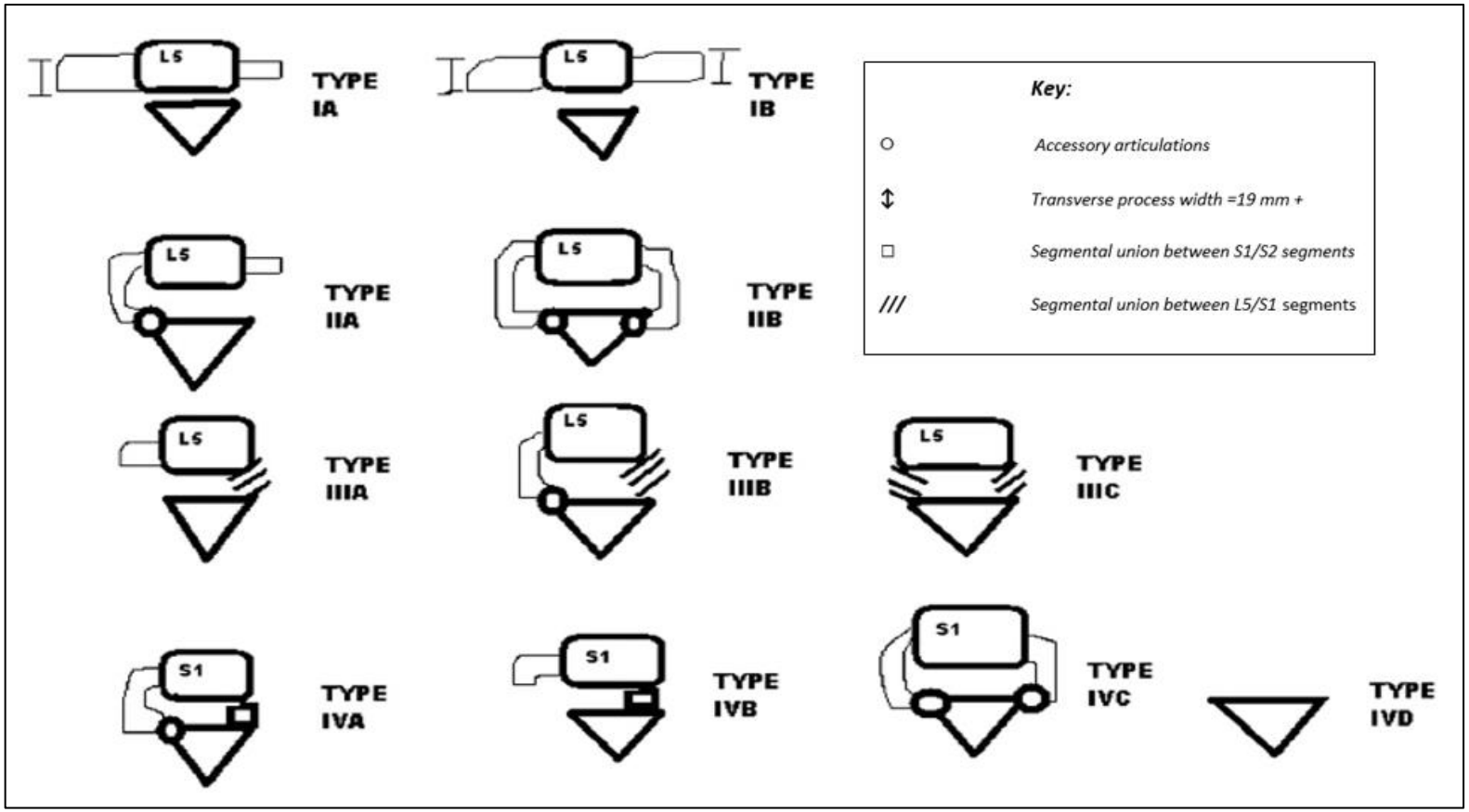

Figure 1.40: A schematic representation of a modified classification system proposed by Mahato (2013a). Sacralisation seen as the assimilation of the last lumbar (L5) to the first sacral segment (S1). Lumbarisation is the separation of the first sacral segment from the body of sacrum. See Table 1.8 for correlation (Adapted from Mahato, 2013). *Used with permission from Elsevier.*

Table 1.8: Table describing the Mahato (2013) proposed modified classification (Adapted from Mahato, 2013a; Figure 1.41).

Dysplastic Transverse Process (TP)	**Type I A** Unilateral TP ≤ 19 mm in width*	**Type I B** Bilateral TPs ≤ 19 mm in width*	**Type I A F(i/c) or Type I B F(i/c)** With presence of ipsi/contra lateral rudimentary facet to the side of the L5 enlargement	**Type I A F2 or Type I B F2** With presence of bilateral rudimentary facets	–	
Accessory articulations	**Type II A** Unilateral L5-S1 accessory articulation	**Type II B** Bilateral L5-S1 accessory articulations	**Type II A F(i/c) or Type I B F(i/c)** With presence of ipsi/contralateral rudimentary facet to the side of the diarthrosis	**Type II A 2F or Type II B 2F** With the presence of bilateral rudimentary facets	–	
Sacralisation	**Type III A** Unilateral L5-S1 sacralisation	**Type III B** Unilateral complete sacralisation with contralateral L5-S1 pseudo-arthrosis	**Type III C** Bilateral complete L5-S1 sacralisation	**Type III A F(i/c) or Type III B F(i/c) or Type III C F**	**Type III A 2F or Type III B 2F or Type III C 2F**	–
Lumbarisation	**Type IV A** Incomplete/ partial lumbarisation of S1 as an accessory S1-S2 articulation	**Type IV B** Unilateral complete separation of S1 from sacral mass	**Type IV C** Bilateral S1/S1 accessory articulation	**Type IV D** Complete sacralisation with residual four-segment sacrum	**Type IV A F(i/c) or Type IV B F(i/c) or Type IV C F or Type IV D F** With presence of ipsi/contra lateral rudimentary facet to the side of the diarthrosis	**Type IV A 2F or Type IV B 2F or Type IV C 2F or Type IV D 2F** With the presence of bilateral rudimentary facets

Mahato (2016)

Mahato (2016) proposed an anatomical classification of sacral variability based on specific criteria that were screened for:

1. The number of segments in the sacral mass
2. The position of the auricular surfaces (three groups)
3. Size and symmetry of the facet joints
4. Other anomalies: laminar hypoplasia, hiatal defects, accessory articular surfaces and rare segment numbers or hemi-sacra

This five-group classification and coding system (Figure 1.41) incorporated the structural characteristics of the sacra with subtypes described in Table 1.9. The drawback of Mahato's (2016) proposed classification system is its complexity as it contains many subtypes and variations.

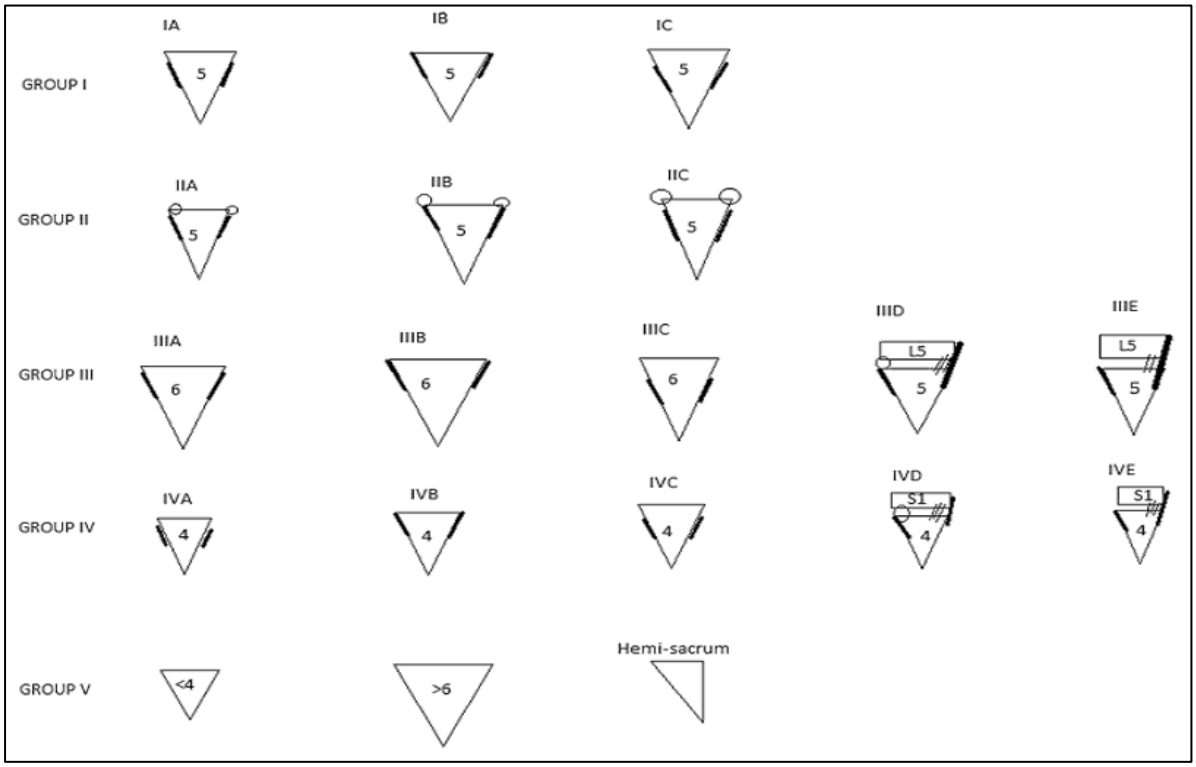

Figure 1.41: *Mahato (2016) proposed osteological classification of LSTV. Numbers inside the triangles denoted the number of segments in the sacral mass; bold lines show positions of the auricular surfaces on the sacrum. Cross-hatches in Groups III and IV indicate bony union between the appropriate segments (L5 in Group III and S1 Group IV) and the remaining sacrum, and circles denote accessory lumbosacral articulation (Adapted from Mahato, 2016). Used with permission from Springer Nature.*

Table 1.9: Mahato (2016) proposed anatomical classification of human sacrum, breakdown of the various subtypes (Adapted from Mahato, 2016).

Group I (5 segment sacrum)	**Group IA** Standard number of segments Standard position of auricular surfaces	**Group IB** Standard number of segments High-up auricular surfaces	**Group IC** Standard number of segments Low-down auricular surfaces	–	
Group II (5 segment sacrum with accessory articulations)	**Group IIA** Standard number of segments Standard position of auricular surfaces Unilateral or bilateral L5-S1 accessory articulation	**Group IIB** Standard number of segments High-up auricular surfaces Unilateral or bilateral L5-S1 accessory articulation	**Group IIC** Standard number of segments Low-down auricular surfaces Unilateral or bilateral L5-S1 accessory articulation		
Group III (sacralisation with 6 segment sacrum)	**Group IIIA** Six sacral segments Complete/bilateral sacralisation Standard position of auricular surfaces	**Group IIIB** Six sacral segments Complete/bilateral sacralisation High-up auricular surfaces	**Group IIIC** Six sacral segments Complete/ bilateral sacralisation Low-down auricular surfaces	**Group IIID** Six sacral segments Incomplete/unilateral sacralisation Sacralised side with low-down auricular surface (opposite side low-down) Low-down auricular surfaces	**Group IIIE** Six sacral segments Incomplete/ unilateral sacralisation Sacralised side with low-down auricular surface (opposite side high-up) Opposite side with L5/ S1 separation
Group IV (lumbarisation)	**Group IVA** Four sacral segments Complete/bilateral sacralisation with S1 detachment Standard position of auricular surfaces	**Group IVB** Four sacral segments Complete/bilateral sacralisation with S1 detachment High-up auricular surfaces	**Group IVC** Four sacral segments Complete/bilateral sacralisation with S1 detachment S1 detached side with high-up auricular surface (opposite side with high-up) Opposite side with accessory S1/S2 accessory articulation	**Group IVD** Five sacral segments Incomplete/ unilateral lumbarisation S1 detached side with high-up auricular surface (opposite side high-up) Opposite side with accessory S1/S2 accessory articulation	**Group IVE** Six sacral segments Incomplete/ unilateral sacralisation Sacralisation side with low-down auricular surface (opposite side low-down) Opposite side with S1/ S2 separation
Group V	Exceptionally rare segment in sacrum (>6<4segments) or hemi-sacra.				

Sex prevalence for lumbosacral transitional vertebrae

The prevalence of sex distribution in individuals with LSTV in a search of the literature revealed that males are more commonly affected than females (Castellvi et al., 1984; O'Driscoll et al., 1996; Apazidis, 2011; Dharati et al., 2012; Nardo et al., 2012; Uçar 2013; Dzupa, 2014; Tang et al., 2014; Gopalan and Yerramshetty, 2018; Alblas, 2019; Park et al., 2019). By contrast, only a few studies have found in favour of higher female LSTV prevalence rates over the male (Mahato, 2011a; Masud et al., 2016; Sekharappa et al., 2017).

Lumbar vertebral enumeration

Lumbarisation and sacralisation qualifiers are useful in understanding the direction of homeotic shifting associated with the lumbosacral junction and lumbar spine. (Tini et al*.,* 1977; Castellvi et al*.,* 1984; Savage, 2005; Konin and Walz, 2010; Barnes, 2012; Mahato 2013a; Mahato 2016). Additionally, these terms, lumbarisation and sacralisation, by association allude to the sacral mass and morphology with the addition or subtraction of vertebrae. Changes in sacral mass may impact biomechanics of the sacroiliac joint (Mahato, 2016).

The terms lumbarisation and sacralisation lack a description as to their degree of fusion or separation associated with the sacrum. For this reason these terms may be useful, to a degree, in biomechanical reasoning and should be viewed as an adjunct enumeration qualifier to LSTV morphology categorisation. However, these are not stand-alone descriptions for LSTV.

As alluded to earlier, **lumbarisation** refers to a caudal shift where there is separation or partial separation of the first sacral segment by which it gains characteristics of a lumbar vertebra (Savage, 2005; Konin and Walz, 2010; Mahato 2010; Barnes 2012). **Sacralisation** is a cranial shift where fusion or partial fusion of the last lumbar vertebra gains characteristics of a sacral vertebra (Savage, 2005; Konin and Walz, 2010; Mahato, 2010; Barnes, 2012).

Numbering technique for the lumbar spine in the setting of lumbosacral transitional vertebrae

There are four methods commonly used for lumbar spine enumeration utilising medical imaging (Lee et al., 2007; Thawait et al., 2012; Farshad-Amacker et al., 2014a; Dulhunty, 2015).

1. Plain film radiographs of the lumbar spine – counting from the last rib (T12 level).
2. Computerised tomography – counting from C2 inferiorly.
3. Mid-sagittal complete vertebral column MRI – counting from C2 inferiorly.
4. Anatomical landmarks – use of an anatomical landmark to identify a vertebral level.

Anatomical landmarks for vertebral enumeration may include vascular, intraspinal, spinal, paraspinal and pelvic structures.

Vascular structures used as landmarks include the aortic bifurcation (AB), right renal artery (RRA), coeliac trunk (CT), superior mesenteric artery (SMA) and inferior vena cava (IVC). The site of the AB may be variably located, spanning the L3-5 IVD levels. The AB may be found in between L3-4 IVD level, the lower half of L4 vertebral body or between the L4-5 IVD level (Lee et al., 2004; Lee et al., 2007; Mirjalili et al., 2012; Tureli et al., 2014). The proximal RRA may be variably located in an area spanning the lower half of the L1 vertebral body, the L1-2 IVD level and the upper half of the vertebral body of L2 (Lee et al., 2004; Lee et al., 2007; Tureli et al., 2014). The RRA has been found as high as the T12-L1 IVD level (Lee et al., 2004). The CT arises off the abdominal aorta and is most commonly located in the lower half of the T12 vertebral body and the T12/L1 IVD level (Lee et al., 2007). The SMA root is variably located between the T12-L1 IVD level and the upper half of the L1 vertebral body (Lee et al., 2007; Mirjalili et al., 2012; Tureli et al., 2014). The IVC confluence may be variably located in an area spanning the lower half of the L4 vertebral body, the L4-5 IVD level and the upper half of the L5 vertebral body (Lee et al., 2007; Mirjalili et al., 2012).

An intraspinal structure such as the conus medullaris (CM) is variably located in an area spanning the T12-L1 IVD level, the upper half of the L1 vertebral body, the lower half of the vertebral body of L1, the L1-2 IVD level and the upper half of L2 vertebral body (Lee et al., 2004; Tureli et al., 2014).

The longest lumbar transverse process is a spinal structure that is easily measured and is found most frequently at the L3 vertebral level (Guan, 2018). The ILL (as discussed earlier) is a paraspinal structure that is readily identifiable and reliable structure in the identification of the lowest lumbar vertebra, usually L5, in the setting of a lumbar spine free of LSTV. However, the presence of LSTV significantly reduces the accuracy of ILL identification (Carrino et al., 2011; Farshad-Amacker et al., 2014a and b). The pelvic structure commonly referred to as the intercristal line (Tuffier's line), is most commonly found in men at the level of the L4 vertebral body or at the inferior endplate of L4. In women, the intercristal line intersects the superior end plate of L5 or the vertebral body of L5 (Snider et al., 2008; Mirjalili et al., 2012).

These five landmarks collections have shown varying degrees of variability, in some cases increased variability in the presence of LSTV, and thus are not recommended as stand-alone anatomical landmarks for accurate vertebral enumeration associated with LSTV (Lee et al., 2004; Hughes and Saifuddin, 2006; Snider et al., 2008; Konin and Walz, 2010; Apazidis et al., 2011; Carrino et al., 2011; Mirjalili et al., 2012; Farshad et al., 2013; Farshad-Amacker et al., 2014a; Tureli et al., 2014; Dulhunty, 2015; Farshad-Amacker et al., 2015; Sarawagi et al., 2016; Guan et al., 2018; Lian et al., 2018).

The most accurate method and therefore the gold standard for enumeration of the lumbar spine is to image the entire vertebral column and count inferiorly from C2 (Hahn et al., 1992; Farshad-Amacker et al., 2015; Sarawagi et al., 2016; Tins and Balain, 2016; Lian et al., 2018). Counting of vertebrae is performed from the C2 vertebra moving inferiorly. To count from the last lumbar vertebra moving superiorly infers that the last lumbar vertebra is the L5 vertebra (Hahn et al., 1992).

The effect of lumbosacral transitional vertebrae on adjacent anatomical structures

Lumbosacral transitional vertebrae have been found to affect adjacent anatomical structures (Jancuska et al., 2015). Benlidayi et al. (2015) found a significant difference ($p=0.001$) in favour of LSTV sacral tilt (vertical orientation of the sacrum) compared to a control group with no difference found between the various LSTV subtypes (Castellvi et al., 1984; Types I, II, III and IV). Mahato's (2011a, b) observations found increases in the following features: lordotic curves, L5 vertebral body height, pedicle sloping of sacralised L5 and sacral auricular length associated with LSTV.

Furthermore, Ono (2018) found a significant difference ($p<0.001$) in pedicle asymmetry (9.29%) between LSTV (n=70) specifically Types II, III and IV, compared to 0.54% of the control group representing a non-LSTV sample (n=227). The Iliac crest height is raised 12mm (mean value) above the L4-5 IVD space compared to a 4mm drop in the iliac crest height in the control group (Josiah et al., 2017). Additionally, the union of the internal and external iliac veins was 8mm (mean value) above the L4-5 IVD space compared to 2.7mm below the L4-5 IVD space in the control group (Josiah et al., 2017). The iliac bifurcation exhibited an alteration in height with 23mm (mean value) above L4-5 IVD space against an 11mm drop in controls (Josiah et al., 2017). Furthermore, Josiah et al. (2017) found that the psoas muscle was separated from the lumbar spine, vertebral body and IVD with vasculature occupying this separation (space) known as the 'safe corridor' or the 'safe zone' in cases of LSTV (Lian et al., 2018). This 'safe corridor' is typically used in a lateral trans-psoas approach to vertebral column surgery (Josiah et al., 2017).

The terminal level of the CM have also shown variation associated with LSTV presence. It was found to terminate significantly higher ($p<0.001$) in the LSTV sacralisation group (upper third L1 vertebral body) and significantly lower (lower third of L1 vertebral body) with LSTV lumbarisation ($p<0.001$) when compared to the control group (mid- L1 vertebral body) (Morimoto et al., 2013). This height change of the CM is hypothesised due to the addition or subtraction of vertebrae of the lumbar spine associated with lumbarisation or sacralisation (Lee et al., 2004; Tureli et al., 2014).

Intra-articular vacuum phenomenon and lumbosacral transitional vertebrae

A collection of gas within a joint, which is visible on medical imaging, is known as intra-articular vacuum phenomenon (Gohil et al., 2014). The contained gas comprises at least 90% nitrogen, with the remainder constituting oxygen, carbon dioxide and other trace amounts of gases (Ford et al. 1977; Yoshida et al., 1997). The observation of the vacuum phenomenon have been demonstrated on radiographs, CT images, MRI scans and ultrasound images within a joint. Intra-articular vacuum phenomenon have been described in multiple joints in the human body, including the shoulder, knee, wrist, sacroiliac, hip and subtalar joints (Yanagawa et al., 2016). Sakamoto et al. (2011) and Lo et al. (2011) have noticed low reporting rates on vacuum phenomenona during medical imaging appraisal.

The underlying cause of the vacuum phenomenon is still under debate (Gohil et al., 2014; Yanagawa et al., 2016) and its presence is largely associated with degeneration that may accompany degenerative joint arthrosis (Faflia et al., 1998; Lo et al., 2011; Gohil et al., 2014; Yanagawa et al., 2016; Laloo et al., 2017). Other causes may include incidental finding from joint motion or traction applied across the joint, bone fracture, osteomyelitis, osteonecrosis, and iatrogenic gas (Lo et al., 1999; Gohil et al., 2014; Yanagawa et al., 2016). Females have a higher incidence of vacuum phenomenon within the sacroiliac joints than men (Faflia et al., 1998; Lo et al., 2011; Gohil et al., 2014; Takata et al., 2016). It is also reported that prevalence of sacroiliac vacuum phenomenon is significantly higher in middle-aged to older persons, from around the age of 60 years and older (Faflia et al., 1998; Lo et al., 2011; Gohil et al., 2014; Takata et al., 2016). There is paucity in the literature describing the vacuum phenomenona associated with LSTV.

Lumbar osseous bridging syndrome associated with lumbosacral transitional vertebrae

Lumbar osseous bridging syndrome (LOBS) is defined as the osseous bridging between two or more contiguous transverse processes, of the lumbar spine, containing a pseudoarthrosis at its point of contact (Yoslow and Becker, 1968; Sahin, et al., 2007). The most common aetiology includes the congenital origin and post-traumatic heterotopic ossification of soft tissues such as myositis ossificans (Yoslow and Becker, 1968; Sahin et al., 2007; Kim et al., 2012). It is considered rare, with an estimated prevalence of 0.45 per million population in Germany (Billet et al., 1991). Yoslow and Becker (1968) and Sahin et al. (2007) reported that LSTV has been found in association with LOBS. Sahin et al. (2007) proposed if the TVP of the last lumbar vertebra (usually L5) demonstrated a downward concavity that forms an articulation with the ala of the sacrum, it represents LSTV. If the converse occurred whereby the lumbar TVP is upswept and forms an articulation or fusion to the immediate level above it (usually the L4), it might represent a form of LOBS.

Pain associated with lumbosacral transitional vertebrae

The association between the presence of LSTV and LBP, coined Bertolotti's syndrome, is a controversial topic of discussion.

Since Bertolotti (1917) described the syndrome, it has been both disputed and supported in the literature (Wigh and Anthony, 1981; Castellvi et al., 1984; Frymoyer et al., 1984; Jönsson et al., 1989; Vergauwen et al., 1997; Chang and Nakagawa, 2004; Luoma et al., 2004; Taskaynatan et al., 2005; Peterson et al., 2005; Delport et al., 2006; Bron et al., 2007; Konin and Walz, 2010; Tang et al., 2014; Avimadje et al., 2015; Illeez et al., 2018; Apaydin et al., 2019, Kanematsu et al., 2020; Shinonara et al., 2021).

Type II and Type IV as defined in the Castellvi et al. (1984) classification, have been associated with pain generation (Castellvi et al., 1984; Jönsson et al., 1989; Avimadje et al., 1999; Hughes, 2004; Nardo et al., 2012; Tang et al., 2014; Jancuska et al., 2015; Shinonara et al., 2021). It is theorised that pain generation associated with LSTV is as result of abnormal weight bearing and motion at the lumbosacral segment, which may lead to degeneration at the pseudoarticulation (Jancuska et al., 2015; Al Riyami et al., 2017). Furthermore, the unilateral Type III LSTV classification has been associated with pain generation (Adams et al., 2018). The pain generation associated with the Type III LSTV classification is theorised due to mechanical stress applied to the bony bridge (the anomalous bridging TVP) that links the lumbar vertebra to the sacrum, leading to a form of stress fracture (Adams et al., 2018). Skeletal scintigraphy and single-photon emission tomography with computed tomography (SPECT/CT) scanning techniques have demonstrated an increased uptake of intravenous radiopharmaceutical agent at the anomalous articulation, unilateral or bilateral, between the transverse process and sacrum associated with LSTV (Types II and IV). This supports the physiological basis for direct pain generation due to stress or motion at the pseudoarticulation associated with LTV. Additionally, increased uptake of radiopharmaceutical agents has been seen at the *pars interarticularis* of the vertebrae articulating with an LSTV (Connolly et al., 2003). Skeletal scintigraphy and SPECT/CT remain valuable tools in providing physiological information and potentially directing treatment at the appropriate site (Avimadje et al., 1999; Connolly et al., 2003). Avimadje et al. (1999) found a relationship between the side of LBP experienced and the site of the anomalous articulation of the LSTV.

In addition, Avimadje et al. (1999) found improvement in LBP after infiltration at the site of the unilateral anomalous articulations using a steroid injection. These results mimic those previously obtained by Jönsson et al. (1989) with positive responses to diagnostic anaesthetic infiltration of the unilateral anomalous articulations (LSTV Type II morphology). This led Jönsson et al. (1989) to perform transverse process resection surgery to the pain-provoking anomalous articulations resulting in either total alleviation of pain (n=7) or significant reduction in pain (n=2) of the 11 patients operated upon. In the modern era, Shinonara et al. (2021) used 3-dimensional (3D) printing of the patient's LSTV spinal anatomy to practice the resection of the accessory articulation before performing the operation. Jönsson et al. (1989) stated that patients presenting with LBP and unilateral anomalous articulation of the lumbosacral junction, in whom an intra-articular local anaesthetic infiltration alleviated their pain, may benefit substantially from resection of the transverse process as it may be therapeutic or even curative. Likewise, Il Ju et al. (2017) had an 86.89% satisfactory result when performing L5 transverse processectomy for Bertolotti's syndrome. Multiple studies have found similar results to Jönsson et al. (1989) and Il Ju et al. (2017) that pain reduction following diagnostic infiltration may lead to improved surgical outcomes, measured as favourable to excellent in grading when treating LSTV induced mechanical LBP syndrome (Li et al., 2014, Manmohan et al., 2015; Shinonara et al., 2021).

Worthy of a mention, Santavirta et al. (1993) took a different approach to surgical treatment of Bertolotti's syndrome whereby a segmental fusion of the LSTV segment was performed as a treatment preference, which had mixed outcomes. The findings of persistent pain or sciatica symptoms were attributed to adjacent segmental degeneration of the facet joints and IVD degeneration following surgical arthrodesis at the LSTV segment (Santavirta et al. 1993).

An interesting example in the literature exists of Bertolotti syndrome in which pain was not experienced at the site of the accessory articulation (Brault et al., 2001). It was hypothesised that the right-sided Type II LSTV created abnormal stresses on the contralateral facet joint (left) at the L6-S1 level leading to recalcitrant facetogenic pain. Surgical resection of the accessory articulation resolved the facetogenic pain (Brault et al., 2001).

Since the initial description of this LBP syndrome by Bertolotti, it is now considered to be multifactorial in aetiology. Varying aetiologies arising at one or more locations around the LSTV segment have been proposed (Konin and Walz, 2010; Jancuska et al., 2015).

These locations include IVD degeneration and herniation, zygapophyseal joint arthrosis, central or foraminal stenosis, nerve root irritation, bone marrow oedema and sacroiliac dysfunction and sacroiliitis (Elster 1989; Otani et al., 2001; Bron et al., 2007; Apazidis et al., 2011; Porter et al., 2013; Illeez et al., 2018; Nevalainen et al., 2018; Abbas et al., 2019; Kanematsu et al., 2020; Hanhivaara et al., 2020). All these aetiologies may result in LBP associated with the identification of LSTV on imaging.

Almeida et al. (2009) proposed a diagnostic-therapeutic algorithm for evaluation and treatment of Bertolotti's syndrome, Figure 1.42.

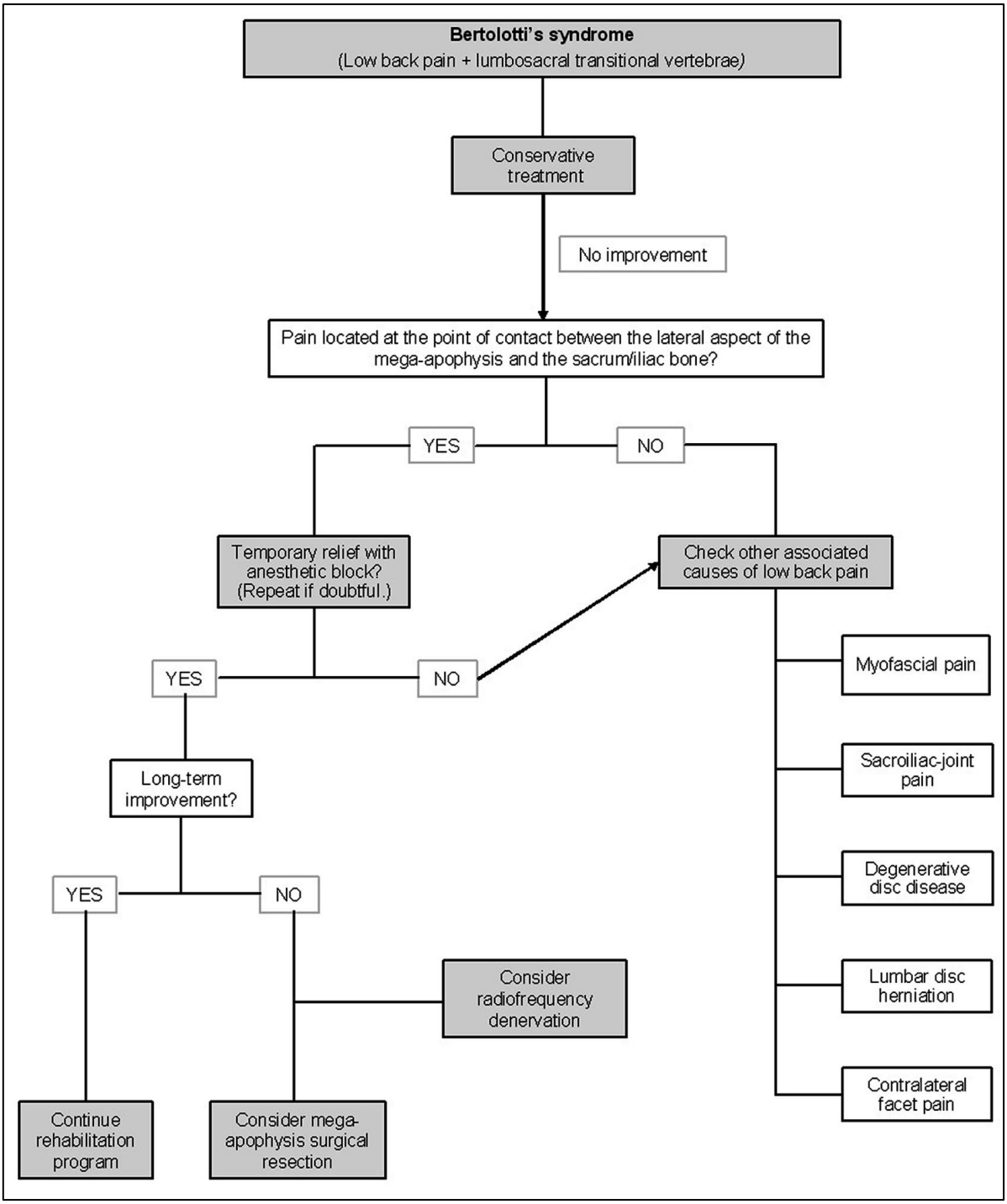

Figure 1.42: *A diagnostic-therapeutic algorithm for evaluation and treatment of Bertolotti's syndrome. The flow diagram depicts the proposed course of both diagnostic and therapeutic interventions that may help in the decision-making process for managing low back pain associated with lumbosacral transitional vertebrae (Adapted from Almeida et al., 2009). Figure obtained through creative commons licence from Arquivos de Neuro-Psiquiatria.*

Prevalence of lumbosacral transitional vertebrae

The prevalence rate of LSTV in the literature varies greatly, ranging from 3.3% to 35.6% (Erken, 2002; Apazidis, 2011; Uçar et al., 2013; Table 1.10). The three largest studies by sample size globally are:

- Park et al. (2019) with 9709 individuals;
- Paik et al. (2013) with 8260 individuals; and
- Tang et al. (2014) with 5860 individuals.

Table 1.10 represents the LSTV prevalence rates in 77 studies undertaken between the years 1925 and 2021. The mean sample size of the studies displayed in Table 1.10 is ±1400 individuals. The global average prevalence rate for LSTV is 12.6% based on a collective sample size of 101624 individuals (Table 1.10).

South Africa

There is a paucity of prevalence rate data on LSTV for the South African population. Research containing LSTV samples from South African authors on the South African population include: Wells (1963); De Beer Kaufman (1974); Einstein (1978), Morris (1984), Du Plessis (2017) and Alblas (2019). The aforementioned authors have provided a a generalised indication of the possible prevelence rate within the South African population.

Wells (1963) described a selection of LSTV based on macroscopic osteological appearance within the University of Cape Town's (UCT) osteology collection. Wells described ''variation of the fulcral vertebra'' (Wells, 1963, p.61) with no indication of the prevalence rates associated with the LSTV sample. Wells' (1963) report did not contain sample numbers, therefore it is not included in Table 1.10.

De Beer Kaufman (1974) appears to hold the largest LSTV-containing data-set sample of a South African population, 79 individuals with LSTV. However, de Beer Kaufman did not describe LSTV morphology but rather examined pre-sacral numbers in vertebral columns. De Beer Kaufman (1974) examined 462 vertebral columns containing lumbarisation in 59 (12.7%) as opposed to sacralisation in 17 (3.7%) of the sample, respectively (Table 1.10).

Einstein (1978) remarked (as a side note) on LSTV found in a selected sample of 485 skeletons while investigating spondylolysis contained within the Raymond A. Dart Collection at the University of Witwatersrand. A prevalence rate of 27 (5.6%) for LSTV was found in his research sample with no breakdown of the morphological classification or vertebral enumeration specifics outlined (Table 1.10).

Morris (1984) commented on variation in the number of lumbar vertebrae present in a sample composed of peoples from the Northern Cape and Western Free State. Variation in lumbar spine enumeration was categorised as either ''L5 fused to sacrum'' or ''six lumbar vertebrae'' (Morris 1984, p.270). No detailed morphological description was given as to the completeness of the L5 fusions observed. The presacral count was limited to lumbar spine enumeration and not the entire vertebral column. Morris examined 158 vertebral columns with a finding of LSTV in 14 (8.9%) of the sample (Table 1.10).

Du Plessis (2017) found 14 (40%) LSTV-containing samples of the 35 samples inspected, obtained from the Kirsten Skeletal Collection contained at the University of Stellenbosch, Western Cape Province, South Africa. The total sacralisation found in the sample was 12 (34%), while lumbarisation was found in 2 (6%) of the sample. The most common LSTV morphology (as graded using the Castellvi et al. (1984) classification) was Type IIIB (n=5) followed by Type IIA (n=3) respectively (Table 1.9). The inclusion of Du Plessis (2017) is for the sake of completeness. It represents a diminutive sample size obtained from the same collection as Ablblas (2019), for which, Alblas (2019) study represents superior regional representation (Table 1.10).

Finally, Alblas (2019) remarked on the prevalence of LSTV in dry bones, lumbar vertebrae and sacra, in a Western Cape population contained within the Kirsten Skeletal Collection at Stellenbosch University, Western Cape Province, South Africa. The sample of 506 individuals was found to contain an LSTV prevalence of 16.3% (n=83). The total number of individuals with sacralisation was 40 (7.9%) while lumbarisation was found in 43 (8.5%) of the sample (Table 1.9). Alblas (2019) described lumbarisation or sacralisation as the primary feature and then utilised the Castellvi et al. (1984) classification as the secondary feature, e.g. a Castellvi et al. (1984) Type IIIB LSTV lumbarisation was represented as a ''lumbarisation IIIb'' (Ablas, 2019, p.118).

Noteworthy to mention, Alblas (2019) made no mention of the subtype Type IIIA LSTV and only reported the presence of the Castellvi et al. (1984) Type IIIB within her sample. Furthermore, there may have been a misinterpretation of the LSTV morphology of the Castellvi et al. (1984) classification Type III and Type IV.

Table 1.10: Survey of the prevalence of lumbosacral transitional vertebrae in 77 observational studies 1925 to 2021.

First Author	Year	Sample Size	Transitional Vertebrae	Lumbarisation	Sacralisation
Haffer	2021	819	53 (6.5%)	*	*
Luo	2021	1880	262 (13.9%)	*	*
Doo	2020	1034	111 (8.3%)	43 (38.7%)	68 (61.3%)
Hanhivaara	2020	3855	1101 (29%)	*	*
Alblas **	2019	506	83 (16.3%)	43 (51.8%)	40 (48.2%)
Park[1]	2019	9709	367 (3.77%)	221 (60.2%)	146 (39.8%)
Tucker	2019	560	71 (12.7%)	*	*
Apaydin	2018	1875	600 (32%)	*	*
Illeez	2018	500	130 (26%)	*	*
Ono	2018	347	70 (20.17%)	*	*
Khan	2018	4939	574 (11.6%)	102 (17.8%)	472 (82.2%)
Njeze**	2018	333	27 (8.1%)	*	*
Du Plessis**	2017	35	14 (40%)	2 (14.3%)	12 (85.7%)
De Bruin	2017	273	68 (24.9%)	*	*
Shaikh	2017	504	75 (15%)	*	*
Sarawagi	2016	317	81 (25.5%)	68 (84%)	13 (16.0%)
Tins	2016	418	12 (2.9%)	4 (33.3%)	8 (66.7%)
Benlidayi	2015	1588	96 (6.1%)	*	*
Sekharappa	2014	3000	390 (13%)	60 (15.4%)	330 (84.6%)
Tureli	2014	505	94 (18.6%)	44 (46.8)	50 (53.2%)
Tang[3]	2014	5860	928 (15.8%)	*	*
Radulovska-Chabukovska	2014	200	64 (31.5%)	54 (84.4%)	10 (14.1%)
French	2014	5429	540 (9.9%)	315 (58.3%)	225 (41.7%)
Dzupa	2014	1513	417 (27.6%)	*	*
Bulut	2013	1000	190 (19.0%)	*	190 (100%)
Uçar	2013	3607	683 (18.9%)	12 (1.7%)	118 (17.3%)
Paik[2]	2013	8280	877 (10.6%)	438 (49.9%)	439 (51.1%)
Nardo	2012	4636	841 (18.1%)	*	*
Dharati	2012	189	24 (12.7%)	3 (12.5%)	21 (87.5%)

Table 1.10: (continued)

First Author	Year	Sample Size	Transitional Vertebrae	Lumbarisation	Sacralisation
Mohammed Abith Ali	2011	244	32 (13.1%)	10 (31.3%)	22 (68.8%)
Sharma	2011	206	38 (18.6%)	9 (23.7%)	29 (76.3%)
Apazidis	2011	211	75 (35.6%)	*	*
Mahato	2010	332	42 (12.7%)	*	*
Wu	2009	203	34 (16.7%)	9 (26.5%)	25 (73.5%)
Oyinloye* **	2009	561	51 (9.1%)	*	*
Tague	2009	2086	131 (6.3%)	*	*
Lee	2007	534	127 (23.8%)	53 (41.7%)	74 (58.3%)
Quinlan	2006	769	35 (4.6%)	*	*
Hughes	2006	500	67 (13.4%)	21 (31.3%)	46 (68.7%)
Delport	2006	300	90 (30%)	*	*
Savage	2005	2803	196 (6.9%)	*	*
Peterson	2005	353	43 (12.2%)	*	*
Taskaynatan	2005	881	41 (4.7%)	*	*
Chang	2004	62	10 (116%)	10 (100%)	0
Luoma	2004	163	49 (30%)	*	*
Steinberg	2003	464	85 (18.3%)	20 (23.5%)	65 (76.5%)
Chithriki	2002	441	37 (8.4%)	15 (40.5%)	22 (59.5%)
Erken	2002	729	260 (35.6%)	*	*
Otani	2001	1009	119 (11.8%)	*	*
Santiago	2001	138	26 (18.4%)	10 (38.5%)	16 (61.5%)
Hsieh	2000	1668	67 (4.0%)	*	*
Dai	1999	460	126 (27.4%)	*	*
Peh	1999	129	17 (13.2%)	9 (52.9%)	8 (47.1%)
Cadeddu	1997	299	16 (5.4%)	*	*
Vergauwen	1997	350	53 (15%)	*	*
O'Driscoll	1996	100	15 (15%)	*	*
Kim	1995	182	33 (18.1%)	12 (36.4%)	21 (63.6%)
Hald	1995	5781	792 (13.7%)	341 (43.1 %)	451 (56.9%)
Olofin* **	1994	300	112 (37%)	40 (35.7%)	72 (64.3%)
Barzó	1993	1500	107 (7.13%)	*	*
Hahn	1992	200	24 (12%)	9 (37.5%)	15 (62.5%)
Leboeuf	1989	530	61 (11.5%)	32 (52.5%)	29 (47.5%)
Elster	1989	2000	140 (7%)	*	*
Morris**	1984	158	14 (8.9%)	5 (35.7%)	9 (64.3%)
Frymoyer	1984	292	17 (5.8%)	12 (70.6%)	5 (29.4%)

Table 1.10: (continued)

First Author	Year	Sample Size	Transitional Vertebrae	Lumbarisation	Sacralisation
Castellvi	1984	200	60 (30%)	*	*
Wigh	1981	200	42 (21%)	*	*
Einstein**	1978	485	27 (5.6%)	*	*
Tini	1977	4000	269 (6.7%)	*	*
De Beer Kaufman**	1974	462	76 (16.5%)	59 (77.6%)	17 (22.4%)
Zinn	1972	786	44 (5.6%)	*	*
Lawrence	1966	423	18 (4.3%)	*	*
Kellgren	1956	1873	94 (5%)	*	*
Stinchfield	1955	920	100 (10.9%)	27 (27%)	73 (73%)
Hasner	1953	400	40 (10%)	10 (25%)	30 (75%)
Southworth	1950	550	46 (8.4%)	11 (23.9%)	35 (76.1%)
Giles	1931	1122	103 (9.2%)	*	*
Moore	1925	87	3 (3.4%)	*	3 (100%)
TOTAL		**101957**	**12842 (12.6%)**	**2686/5702[a] (47.1%)**	**3016/5702 [a] (52.9%)**

** – Lack of detailed information regarding sacralisation and / or lumbarisation numbers.*

***– Indicates South African-based studies.*

****– Indicates African-based LSTV studies (outside of South Africa). All three studies were conducted in Nigeria.*

a – Indicates the total LSTV sample size (N=5702) that contains information on lumbarisation (n=2686) and sacralisation (n=5702) numbers. Bulut et al., (2013) was excluded due to a lack of information on sacralisation.

Authors in bold font with superscript numerals (one, two and three) indicate the three largest studies globally by sample size.

CHAPTER 2

MATERIALS AND METHODS

Introduction

This study was divided into two main parts, each containing sub-objectives:

Part I: Medical imaging

a) Prevalence of LSTV in the South African population

b) Morphological characteristics of LSTV in the South African population

Part II: Osteological morphology

a) Metric observations

b) Non-metric observations

For this methodology Chapter, Part I and Part II are discussed separately.

Nomenclature used for ancestry

Non-metric observations were made from radiographs, CT and MRI scans, as well as osteological samples. As listed in Table 1.10, many studies have investigated Asian-descent populations, namely Chinese and Indian specific-population prevalence rates. Therefore the prevalence amongst Asian ethnic groups can be estimated with greater confidence using the available global data obtained from large sample sizes. The results of the South African mid-year population estimate (SAPSS, 2019) projected the ethnic groups in South Africa to consist of 'Black African' at 80.7%, 'Coloured' at 8.8% and 'White' at 7.9%, while 'Indian/Asian' was estimated at 2.6% of the total population. Females accounted for 51.2% of the total population. The total South African population for the year 2019 was estimated at 58 775 022 people (SAPSS, 2019).

The population ancestry nomenclature used in this study will differ from that used in the South African population statistics survey in the following ways:

i. African-ancestry will replace ‘Black African’

ii. Mixed-ancestry will replace ‘Coloured’

iii. European-ancestry will replace ‘White’

These ancestral population groups consisted of the first, second and third largest proportions in the South African population (SAPSS, 2019). The total sample for this study, therefore, represented 97.4% of the South African ethnic diversity. The various South African tribal ethnic groups that constitute the African-ancestry population were considered homogenous for this study. Therefore, Zulu, Xhosa, Sotho, Pedi, Ndebele, Tswana, Tsonga, Venda, Thembu, Bhaca and Mpondo tribes, amongst others, were recorded under the population group of African-ancestry (Dayal et al. 2009). The Mixed-ancestry population did not specify the ethnic group, tribes or cultures from which the individual may have been associated with or originated from. This could include Middle Eastern and/or Khoi or San heritage and/or offspring from people of different ancestries/ ethnicities. In addition, the European ancestry population affinity did not specify origin (e.g. American, European or Island countries such as Australian and New Zealand, etc.).

Part I: Medical imaging of lumbosacral transitional vertebrae

Study Sample

Both retrospective and prospective cohort randomised sampling methods of data collection of medical images were used in this study. The appraisal of the medical images included radiographs, MRI and CT scan images. Prevalence rates, utilising the Castellvi et al. (1984) classification, were established via radiographs only. Additional qualification of the lumbar spine enumeration, namely lumbarisation and sacralisation, was made through the appraisal of lumbar radiographs counting from the last rib bearing vertebra, which was determined as the twelfth thoracic vertebra (T12). If present for the individual that contained LSTV, MRI and CT scans were used to aid in the identification of LSTV.

Images were obtained from the medical radiology practices located within South African public government hospitals: Groote Schuur Hospital (GSH) in Cape Town, Western Cape Province and Charlotte Maxeke Johannesburg Academic Hospital (CMJAH) in Johannesburg, Gauteng Province.

Consecutive medical imaging records were retrieved from the picture archiving and communication system (PACS) and appraised between 10 November, 2017 and 18 May, 2019 at CMJAH and GSH between 1 December, 2017 and 20 March, 2019.

The total imaging cohort included 3096 individuals (n=3096). The imaging cohort included radiographs of the lumbar spine, and of the abdomen performed part of a kidney, ureter and bladder (KUB) X-ray investigation. The sample was selected to cover the three largest subgroups of the South African population.

i. African-ancestry sample included 1032 radiographs (1032/3096)

ii. Mixed-ancestry sample included 1032 radiographs (1032/3096)

iii. European-ancestry sample included 1032 radiographs (1032/3096)

Materials for the medical imaging cohort

Imaging Centres Used

Charlotte Maxeke Johannesburg Academic Hospital (Gauteng Province)

Charlotte Maxeke Johannesburg Academic Hospital, formerly known as the Johannesburg General Hospital, is an almost 1100 bed tertiary hospital servicing the Johannesburg Metropole and surrounds. The University of Witwatersrand Parktown Health Sciences Campus is adjoined to the hospital and houses multiple X-ray machines, two CT scanners and one MRI machine.

Groote Schuur Hospital (Western Cape Province)

Groote Schuur Hospital is a tertiary hospital servicing Cape Town Metropole and surrounds it with approximately 900 beds. The University of Cape Town's Health Sciences Campus is across the road from this hospital. Groote Schuur Hospital houses numerous X-rays machines, two CT scanners and two MRI scanners.

Inclusion criteria

Individuals had to demonstrate sufficient radiographic skeletal ossification to determine LSTV morphology to be included in this study. Similar LSTV radiographic imaging investigations found from the age of ages 16 years to be suitable for inclusion (de Bruin et al. 2017, Khan et al., 2018). This study inclusion criteria consisted of males and females aged 16 years and older.

Ancestry was categorised according to the hospital records of the individuals. Furthermore, as this study targeted a sample of the South African population, individuals had to be South African-born as determined from their hospital record declaration and by verification of their ID number (*Decoding your South African ID number,* 2019).

Exclusion criteria

Exclusion criteria consisted of any disease entity, pathological process and/ or artefacts that obscured classification of LSTV and prevented accurate numbering/ enumeration of the relevant vertebrae.

These included metal artefacts from surgery or clothing, poor image quality to the extent that the vertebral anatomy was rendered inaccurate and images that did not contain clear thoracolumbar and lumbosacral junctions. Additionally, images were excluded if they contained severe deformity of the spinal column and age-related degeneration that obscured the vertebral anatomy.

Sample summary

The study involved evaluating radiographs taken for various primary investigations, including but not limited to LBP, KUB imaging, and abdomen X-ray imaging. The images were obtained from hospitalised (inpatient) imaging as well as out-of-hospital (outpatient) imaging. It is an ethical conundrum to expose public members with no valid medical complaints to the ionising radiation used in radiograph production. For this reason the sample data-set represented an alternative use for previously acquired medically-necessitated imaging for the study of LSTV. It was evident that the radiographs were used for diagnostic purposes as well as for post-intervention appraisal. The radiographs contained examples that included healthy spinal columns free of pathology, pre-intervention images, post-surgical spine surgery, abdominal surgery, vascular surgery, spinal malignancy and infection of the spine. The radiographic images containing LSTV morphology with MRI and/or CT scans were used to appraise LSTV morphology. Classification, sex and ancestry were recorded on *Microsoft Excel*® spread sheet at the sites of measurement, namely GSH and CMJAH.

Research method

Measuring equipment and unit of measure

All images were viewed on radiology quality 2-3 megapixel greyscale monitors in a dim-lit image reporting room.

In order to maintain the anonymity of the patients, names of individuals were not used in this study and each individual was assigned a reference number. Radiographs of interest were saved as a JPEG file and used in the appraisal of LSTV morphology.

To ensure no duplication of information of an individual occurred, cross-referencing was performed whereby an individual 'A' was checked against the individual's hospital file numbers on a data-base, located on the *Microsoft Excel*® spreadsheet, before recording the information. This was a safeguard to ensure that no duplication or replacement of information for any individual took place.

The prevalence of LSTV was determined by radiographs only. Computerised tomography and MRI scans were assessed and recorded if available for the individual with the presence of LSTV to be used in the discussion of LSTV morphology.

Intra-observer error for the imaging cohort

To minimise the intra-observer error, the following steps were taken:

1. Twenty percent of the LSTV radiographic cohort (62 radiographs) was appraised by the author and then re-appraised two weeks later. This allowed for sufficient time to pass to mitigate any short-term memory of radiographic features associated with the sample of appraised images.
2. The categorical data was analysed using Cohen's Kappa coefficient on the number of each LSTV category, and sub-category found.
3. Agreement for the intra-observer error for all categories of LSTV was in the range of 'almost perfect agreement'. Therefore, the interpretation of the remaining 80% of the images could be taken with confidence regarding their accuracy and precision. Refer to Table 2.1, which displays the degree of agreement across six categories of Cohen's kappa coefficient. Table 2.2 reports the intra-observer error agreement for Types IIA, B, IIIA, B and IV.

Table 2.1: Cohen's kappa coefficient values for intra-observer error assessment (Adapted from Rafieyan, 2016).

Values	Interpretation
Smaller than 0.00	No agreement
0.00 to 0.20	Poor agreement
0.21 to 0.40	Fair agreement
0.41 to 0.60	Moderate agreement
0.61 to 0.80	Substantial agreement
0.81 to 1.00	Almost perfect agreement

Cohen's kappa coefficient is a statistical measure for intra-observer and inter-observer agreement for qualitative items. It is seen as a more robust measure than simple percentage agreement calculation as it takes into account the agreement occurring by chance (Vieira et al., 2010). The closer the value of Cohen's kappa coefficient to 1, the higher the agreement between observers and/ or observations (Rafieyan, 2016).

Table 2.2: Intra-observer error utilising radiographs.

Type of LSTV	Cohen's Kappa coefficient
Type II	0.964 (95% CI 0.934 to 0.995)
Type IIA	0.942 (95% COI 0.905 to 0.979)
Type IIB	0.896 (95% CI 0.835 to 0.956)
Type III	0.968 (95% CI 0.936 to 0.999)
Type IIIA	0.941 (95% CI 0.860 to 1.000)
Type IIIB	0.991 (95% CI 0.972 to 1.000)
Type IV	0.868 (95% CI 0.741 to 0.995)

Inter-observer error assessment of the imaging cohort

Inter-observer error was minimised by performing the following steps:

1. A research volunteer in the field of medicine, external to the study, was trained by the principal investigator (author) on the morphological classification of LSTV.
2. One hundred percent of the entire LSTV radiographic cohort (308 radiographs) was appraised by the external researcher and compared to the author's findings.
3. The categorical data was analysed using Cohen's kappa coefficient on the number of each LSTV category, and sub-category found.
4. Agreement for all categories of LSTV for inter-observer error was in the range of 'almost perfect agreement', Tables 2.1 and 2.3. Therefore, the interpretation of the images was taken with confidence regarding their accuracy and precision.

When advanced imaging was available and appraised (CT and MRI scans), the inter-observer error rate was 0%. Therefore, there was a 100% agreement on the classification of LSTV between both observers. The categorical results of this study were, in part, informed through the concomitant use of advanced imaging with the radiographs to ensure the classification was as accurate as possible.

Table 2.3: Inter-observer error using radiographs.

Type of LSTV	Cohen's Kappa coefficient
Type II	0.937 (95% CI 0.996 to 0.977)
Type IIA	0.949 (95% COI 0.914 to 0.984)
Type IIB	0.951 (95% CI 0.908 to 0.994)
Type III	0.984 (95% CI 0.962 to 1.000)
Type IIIA	0.941 (95% CI 0.860 to 1.000)
Type IIIB	0.981 (95% CI 0.956 to 1,.000)
Type IV	0.805 (95% CI 0.731 to 0.936)

Defining the non-metric features

Lumbosacral Transitional Vertebrae morphology and classification

Castellvi, Chan and Goldstein (1984) classification

Castellvi et al. (1984) used a classification system that clustered LSTV into four groups based on radiographic morphology (Figures 2.1 to 2.4). It is the most widely used classification system for LSTV worldwide (Konin & Walz 2010; Mahato 2013a; Jancuska et al., 2015; Matson et al., 2020). The Type I LSTV (Figure 2.1) was not considered for this study for various reasons that will be explained. The craniocaudal measurement of the last lumbar TVP relies heavily on radiographic technique and positioning of the individual to obtain a true perpendicular central ray (the centre of the X-ray beam) to the lumbosacral junction. This assertion is supported by Hou et al., (2020) in which standard lumbar spine imaging may produce false-positive findings due to the overlap effect of the TVP on ala of the sacrum. The radiographic imaging cohort included lumbar, abdomen and KUB imaging which all utilise a central ray considerably higher than the lumbosacral junction, at approximately at the level of the L3 (Figure 2.1A).

Therefore, the radiographs were not suitable for accurate measurement of last lumbar TVPs. An anteroposterior X-ray with 20°-30° cranial tilt of the central ray (Ferguson view) is best suited to visualise L5 TVP height (Figure 2.1B). The Ferguson view improves the visualisation of the enlarged TVP/s for accurate measurement of radiographs (Stinchfield & Sinton, 1955; Castellvi et al., 1984; O'Driscoll et al., 1996; Hughes & Saifuddin, 2006; Konin & Walz, 2010; Lian et al., 2018; Kanematsu et al., 2020). It has been reported that standard anteroposterior lumbar radiographs achieve 76-84% accuracy for LSTV recognition (Farshad-Amacker, 2014b; Kanematsu et al., 2020).

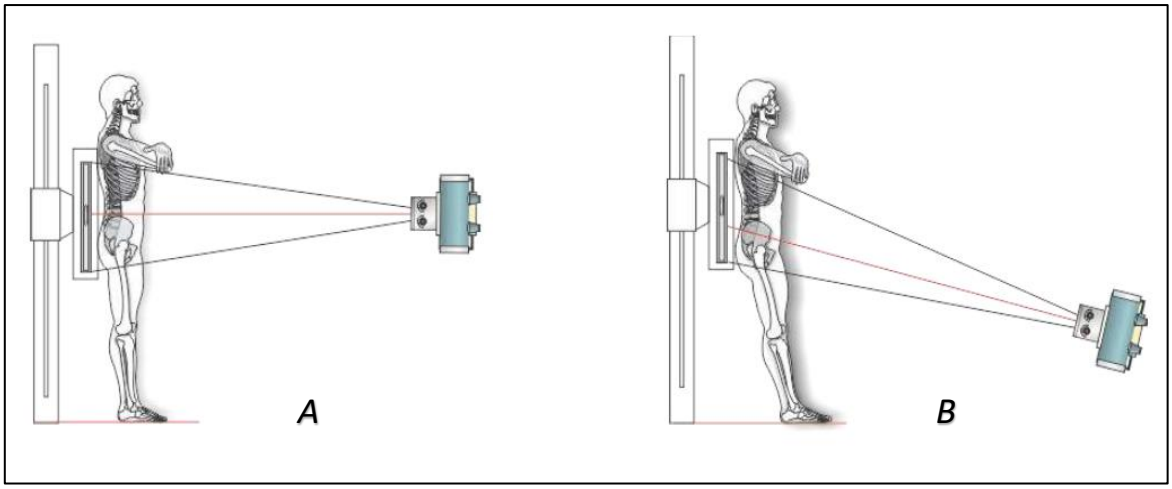

Figure 2.1: *Anteroposterior X-ray technique for imaging the lumbar spine. A) Anteroposterior lumbar spine X-ray technique with a central ray perpendicular at the level of L3, erect positioning. B) Anteroposterior lumbosacral X-ray technique with 20°-30° cranial tilt of the central ray (Ferguson view), erect positing (Adapted from Dulhunty, 2015). Used with permission form from the author.*

Furthermore, it can be argued that the Type I LSTV inclusion bears no clinical relevance to pain generation as it represents no alteration in biomechanics at the lumbosacral junction due to its lack of articulation between both lumbar TVPs and the alae of the sacrum (Castellvi et al., 1984, Konin & Walz, 2010, Paik et al., 2013, Hanhivaara et al., 2020, Hou et al., 2020). Huo and colleagues (2020) reports that many medical field specialists do not consider the Type I LSTV as a true form of the LSTV morphological classification. Therefore, the Type I LSTV presence would not benefit clinicians in diagnostic assessment nor decision-making strategies. Lumbosacral transitional vertebrae Types II and IV have been implicated in symptomology and pain generation (Castellvi et al., 1984; Hughes & Saifuddin, 2004; Savage, 2005; Hughes & Saifuddin, 2006; Konin & Walz, 2010; Morimoto et al., 2013; Tang et al., 2014; Benlidayi et al., 2015; Farshad-Amacker et al., 2015; Jancuska et al. 2015; Nevalainen et al., 2018; Ono et al., 2018; Gündüz et al., 2019).

This study informs clinicians about the prevalence of LSTV in the South African population, the morphological classification and characteristics thereof, and its potential to influence spinal biomechanics based on the spinal morphological changes associated with LSTV. The hope is that this study may aid diagnosis and treatment strategies for LBP in the presence of LSTV.

Described below is Castellvi et al. (1984) classification of LSTV with diagrams reflecting the four main Types and their subtypes. Due to its lack clinical significance in pain generation (Castellvi et al., 1984, Konin & Walz, 2010, Hanhivaara et al., 2020, Hou et al., 2020), the Type I morphology (Figure 2.1) is included with no further discussion in subsequent chapters. The LSTV Types II, III and IV were considered in this study (Figures 2.3 to 2.5).

Type I

Dysplastic transverse process: A, unilateral; **B**, bilateral.

A dysplastic TVP is one or both TVPs measuring at least 19mm, in craniocaudal height, as described by Southworth & Bersack (1950; Refer to Figure 2.2).

For the thesis and to avoid confusion on definitions, the Castellvi et al. (1984) classification was modified for a concise description of LSTV morphology. This revised version is free of the terms lumbarisation and sacralisation as they are seen as adjuncts to the LSTV morphology because they describe vertebral numbers and not vertebral morphology.

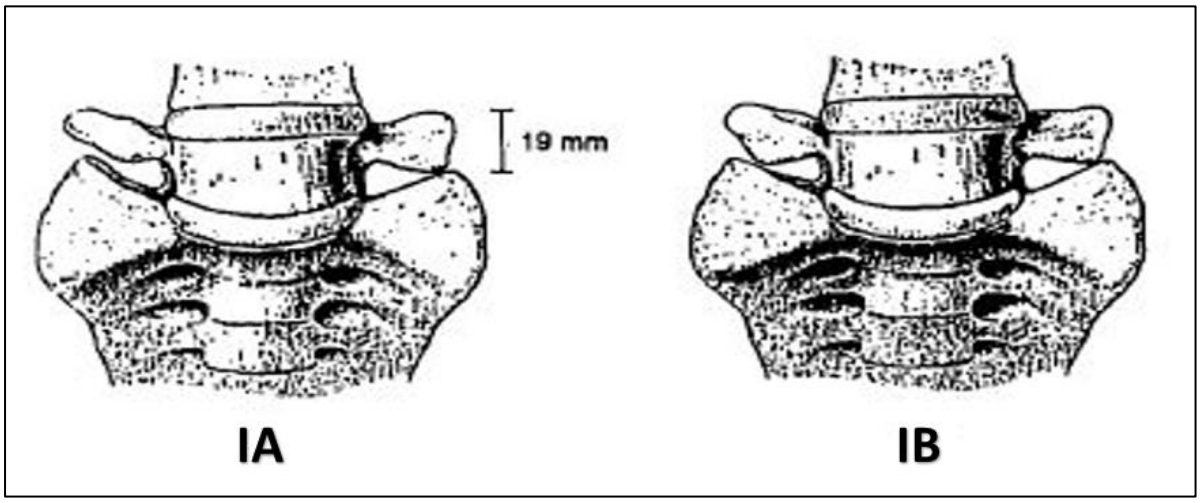

Figure 2.2: *Type I classification of lumbosacral transitional vertebrae.* ***Left:*** *Left-sided enlargement of the TVP of the last lumbar vertebra.* ***Right:*** *Bilaterally enlarged TVPs of the last lumbar vertebra (Adapted from Castellvi et al., 1984). Used with permission from Wolters Kluwer Health Inc.*

Type II

Incomplete fusion, articulation/s between TVP and sacrum present: A, unilateral; **B**, bilateral.

A vertebra containing one or both dysplastic TVPs (increased craniocaudal height) of the last lumbar vertebra appears as an enlarged wing-like structure /s that may articulate with the ala/e of the sacrum (Refer to Figure 2.3).

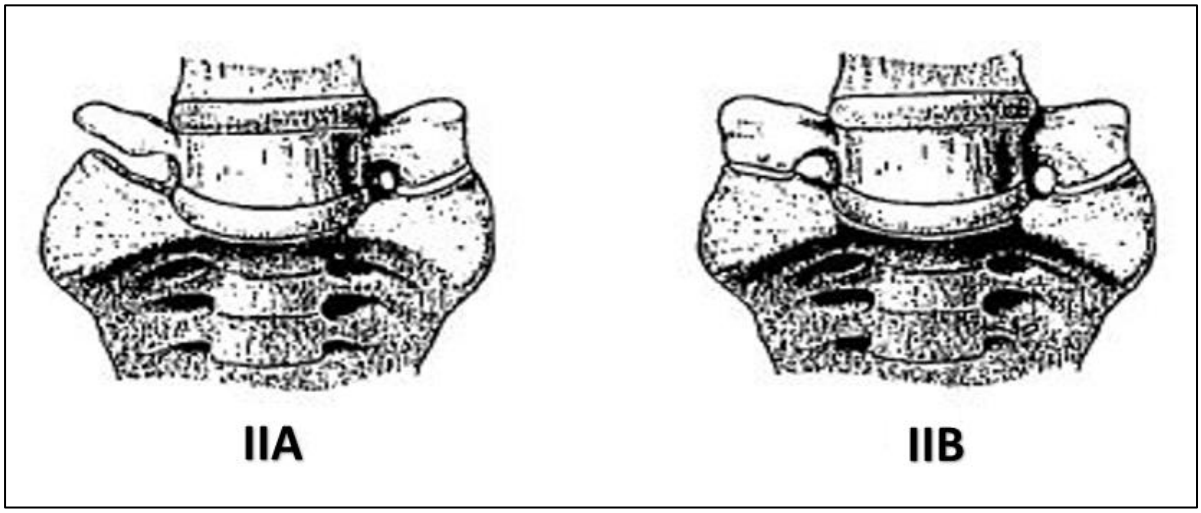

Figure 2.3: *Type II classification of lumbosacral transitional vertebrae.* ***Left:*** *Left-sided enlargement of the lumbar TVP of the last lumbar vertebra with articulation/ contact with ala of the sacrum.* ***Right:*** *Bilaterally enlarged lumbar TVPs of the last lumbar vertebra with articulation/ contact with the alae of the sacrum (Adapted from Castellvi et al., 1984. Used with permission from Wolters Kluwer Health Inc.*

Type III

Complete fusion: A, unilateral; **B**, bilateral.

This type is similar to Type II presentation except there is bony fusion of one or both TVPs of the last lumbar vertebra with the ala/e sacrum (Refer to Figure 2.4).

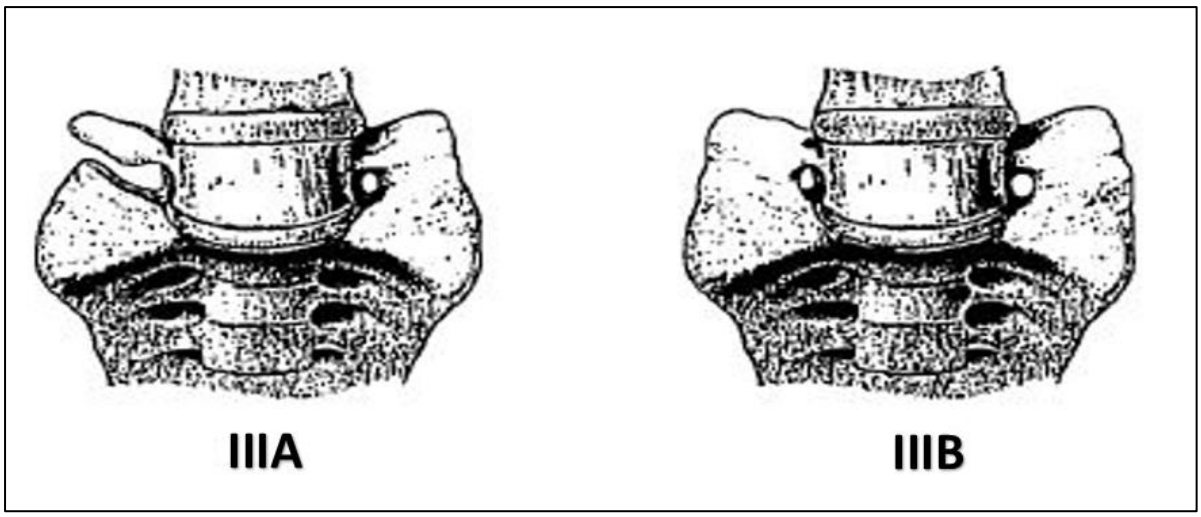

Figure 2.4: *Type III classification of lumbosacral transitional vertebrae.* ***Left:*** *Left sided unilateral enlargement of the transverse process of the last lumbar vertebra with articulation / contact with the sacrum.* ***Right:*** *Bilaterally enlarged TVPs of the last lumbar vertebra with articulation / contact with the alae of the sacrum (Adapted from Castellvi et al., 1984). Used with permission from Wolters Kluwer Health Inc.*

Type IV

Mixed morphology: No side preference. No subtype classification.

The Type IV LSTV morphology exhibit the features of both Type IIA and Type IIIA LSTV characteristics. The Type IV LSTV characteristics include enlargement of both of the TVPs of the last lumbar vertebra. In addition, one side displays an articulation of the TVP with the ala of the sacrum whereas the opposite side displays a fusion of the TVP with the ala of the sacrum. Two morphological variants exist within this single classification (Refer to Figure 2.6).

Unique to the Type IV LSTV, there is no subtype description or classification. That is to say, in the literature, there is no distinction between the two figures in Figure 2.5. No classification exists on how to describe the frequency of side of a Type IV LSTV.

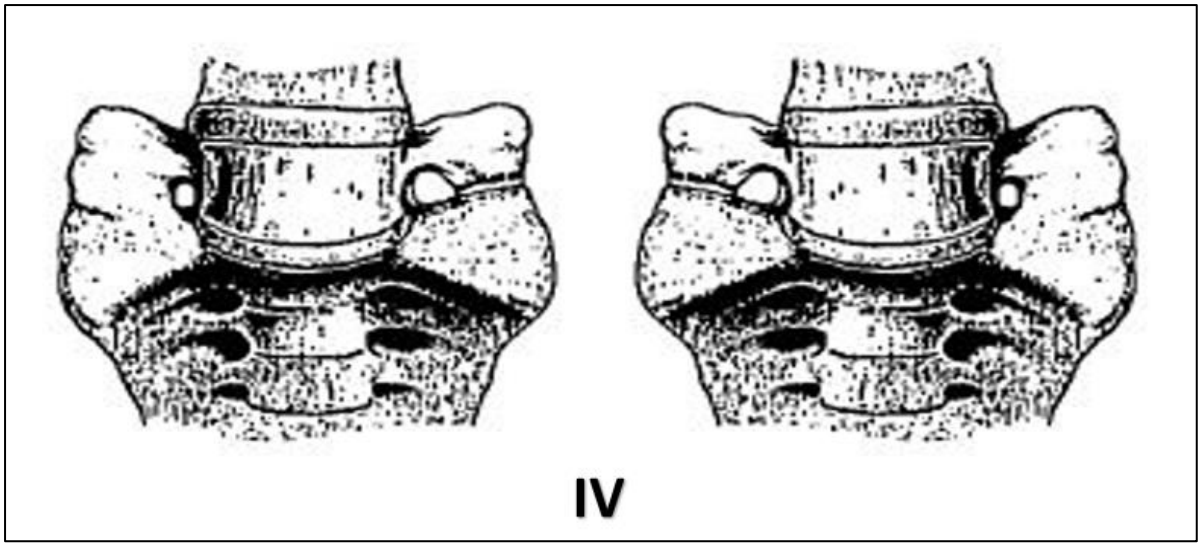

Figure 2.5: *Type IV classification of lumbosacral transitional vertebrae.* ***Left:*** *Bilateral enlargement of the TVP of the last lumbar vertebra with a unilateral articulation/ contact with the ala of the sacrum on the left side and fusion of the lumbar TVP to the ala of the sacrum on the right side.* ***Right:*** *Bilateral enlargement of the TVPs of the last lumbar vertebra with unilateral articulation/ contact with the alae of the sacrum on the right side and fusion of the lumbar TVP to the ala of the sacrum on the left side (Adapted from Castellvi et al., 1984). Used with permission from Wolters Kluwer Health Inc.*

Vertebral enumeration

Vertebral enumeration is the process of counting presacral vertebrae. Of particular interest to this study was the lumbar vertebrae count. The last rib bearing-vertebra was used to define the twelfth thoracic vertebra (T12). Therefore, lumbar vertebral enumeration was determined by counting the number of lumbar vertebrae present inferiorly from the first non-rib bearing vertebra (L1) down to the last vertebra before the sacrum on an AP lumbar radiograph. Lumbarisation represented six vertebrae where the last vertebra displayed signs of LSTV, i.e. lack of fusion of S1 to the remainder of the sacral vertebra. Sacralisation represented four lumbar vertebrae where the fifth lumbar vertebra displayed signs of LSTV i.e. signs of contact or fusion of L5 to the sacrum.

Lumbarisation and sacralisation are adjunct qualifiers to the LSTV morphology. That is to say, lumbarisation and sacralisation are supplementary information suggesting lumbar vertebral count. Lumbarisation and sacralisation serve as an indicator for the number of mobile segments present in association with LSTV. As a stand-alone description, lumbarisation and sacralisation hold little value in understanding LSTV morphology.

Statistical analyses

Statistical analyses were performed using IBM® Statistical Product and Service Solutions SPSS® (formerly Statistical Package for the Social Sciences) software for Windows operating system, version 25.0 (IBM Corp. 2015). The probability value or *p*-value is an estimated value for the null hypothesis to be rejected. The *p*-value was set at $p \leq 0.05$ for significance for all tests in the thesis.

Statistical tests

Cross tabulation of categorical variables was performed with:

Chi-squared test (X^2)

This is a non-parametric test that can be used for two purposes: G*oodness of fit* test and a Test of *Homogeneity* and Test of *Independence*. The X^2 of independence test compared if two or more categorical variables were related (Pallant, 2013; Durrheim and Tredoux, 2014).

Cramer's V test

Cramer's V test is a post-hoc test used to determine the strength of association between two categorical variables after the X^2 test found a significant relationship between the variables that existed, used in tables 3x3 (3 rows and 3 columns) or bigger. Cramer's V test is an effect size measurement represented as a number between zero and one. The higher the number towards one, the greater is its significance (Pallant, 2013; Durrheim and Tredoux, 2014). The effect size for Cramer's V is displayed in Table 2.4.

Table 2.4: Effect size values for Cramer's V test (Adapted after Kotrlik et al., 2011; Brezina, 2018).

Degrees of freedom (table type)	Effect size		
	Small	Medium	Large
1 (2x2)	0.10	0.30	0.50
2 (3x2 or 2x3)	0.07	0.21	0.35
3 (4x2 or 2x4)	0.06	0.17	0.29
4 (5x2 or 2x5)	0.05	0.15	0.25
5 (6x2 or 2x6)	0.04	0.13	0.22

Phi Correlation Coefficient

Phi correlation coefficient is a post-hoc test used to determine the strength of association between two categorical variables in a two column and two-row (2x2) contingency table after the X^2 test had found a significant relationship. Condition for use requires no expected counts should be less than 5. The Phi coefficient effect size measurement is represented as a number between -1, 0 and 1 (Pallant, 2011; Kim, 2017). A negative represents a negative correlation, while a positive number represents a positive correlation. Zero indicates no correlation (Durrheim and Tredoux, 2014; Kim, 2017). The effect size categorisation is shared with the Pearson's coefficient effect seen in Table 3.10.

Fisher's exact test

In practice, Fisher's exact test is applied in the analysis of small samples sizes but is valid for all sample sizes. It is an exact test comparing two nominal variables in a 2x2 contingency table that measures the deviation from the null hypothesis, which states that variables are independent (Kim, 2017).

Part II: Osteological morphology cohort

Materials for osteological cohort

The cadaveric skeletal specimens of known sex, age and ancestry recorded in accession registers were selected for this study. The skeletal remains used in this study were obtained from the University of the Witwatersrand (WITS).
Metric data were collected and non-metric observations were made on the axial skeletons of dried preserved sacra and the last two lumbar vertebrae.

Skeletal collection used

The Raymond A. Dart Collection of Modern Human Skeletons

The Raymond A. Dart Collection of modern human skeletons known simply as ''the Dart Collection'', is part of the School of Anatomical Sciences, Faculty of Health Sciences, University of Witwatersrand, Johannesburg, South Africa. It is the oldest skeletal collection in South Africa and largest on the African continent, founded in 1923. This collection contains predominantly cadaveric skeletal specimens (N=~3000). The collection functioned as the selected population for the osteometric study of LSTV and consists of individuals with a predominance of individuals of African-ancestry.

Ancestry in Dart Collection

Earlier cadaver collection methods were largely derived from unclaimed bodies from regional hospitals in South Africa (Dayal et al., 2009; Kramer et al., 2019). From the collection methods used, the Dart Collection of modern human skeletons is mainly comprised of African-ancestry (≈71%) (Dayal et al., 2009). More recently however, there has been a change in population demographics associated with a change in the cadaveric collection of skeletal remains. This is likely, wholly or partly, due to a shift in global acquisition of human cadavers towards bequests and body donation (Kramer et al., 2019) instead of unclaimed bodies. Recent additions to the WITS School of Anatomical Sciences and ultimately into the Dart Collection constitutes individuals of European-ancestry, 'South African White', at 98.2%, while individuals of African-ancestry only accounted for 0.8% during the years 2013-2017 (Kramer et al., 2019).

The factors that have affected this change in cadaver acquisition may include the ethical sourcing of cadavers whereby cadavers are donated with an individual's and/or family's consent. The change in donated/bequeathed cadavers currently is up to 97.5% compared to unclaimed individuals at 2.5%. This in contrast to the early practices of medical schools (Kramer et al., 2019). This in contrast to the early practices of medical schools (Kramer et al., 2019).

Inclusion criteria

Skeletal remains undergo maceration and drying that removes connective tissue and may allow unfused sacral vertebrae to separate. Lumbar and sacral epiphyseal activity has been found to cease early in the third decade of life, i.e. at around 21 years of age (Rios et al., 2008; Cardoso and Rios, 2011). Therefore, specimens younger than 21 years were not included to avoid mistaking the first sacral segment as an LSTV if found separated.

The inclusion criteria consisted of skeletal remains of males and females of skeletal remains aged 21 to 65 years old at the age of death (AD).

The natural history of spinal degeneration accelerates with advancing age and enhances the likelihood of vertebral degeneration including facet hypertrophy, osteophytosis and IVD degeneration (Eubanks et al., 2007; Brinjikji et al., 2015). Furthermore, ageing may lead to osteoporosis with associated sequelae (Benoist, 2005; Papadakis et al., 2011; Brinjikji et al. 2015).

The spinal degenerative changes described would influence the metric features associated with LSTV in this investigation. Therefore, it was decided upon to set a cut-off point of 65 years at AD to avoid the chances of an altered vertebral column due to age-related changes. In turn, this allowed for a wide range of samples across a broad age spectrum.

Exclusion criteria

The exclusion criteria consisted of skeletons that showed loss of normal ante-mortem anatomical architecture, non-fusion of the sacral vertebrae below the first sacral vertebra (S1), fractures and spinal deformities.

The exclusion criteria extended to the presence of exuberant osteophyte/syndesmophyte spur formation, surgical interventions that distorted normal anatomy, post-mortem damage to the samples, and missing bones, namely the sacrum and last two lumbar vertebrae.

Sample summary

The osteological morphological study aimed to measure and analyse the sacra and lumbar vertebrae's osteometric and morphometric traits exist between LSTV and non-LSTV skeletal samples.

A systematic search of the total cadaveric skeletal collection housed at WITS yielded 1797 human skeletal specimens (N_t=1797) from 21 to 65 years at AD. One-hundred and fourteen skeletons were identified as containing LSTV.

Due to damage or loss of vertebrae, a subset of 91 LSTV (N=91) was studied. Osteometric linear measurements, measurement of angles and surface area measurements were performed on the LSTV specimens. The LSTV descriptive information data were recorded, including determining the sex distribution (male versus female ratio). Ancestry was determined via accession records kept by the Dart Collection.

Ancestry was recorded but not compared in the osteological analyses due to low numbers of LSTV found in Mixed-ancestry and European-ancestry samples contained within the Dart Collection. A summary of the total study cohort and the LSTV cohort is displayed in Chapter 4, Tables 4.1 and 4.2.

A sex-balanced comparative control cohort sample composed of 30 males and 30 females, free of LSTV variation, was preselected. Sixty individuals for the control sample was deemed satisfactory against an LSTV comparative sample of 91. This would allow for statistical analyses to be performed with confidence. A summary of the control cohort is displayed in Chapter 4, Table 4.3.

Data Collection

The study investigated the dimensions of the last two lumbar vertebrae and sacrum of LSTV and was compared with the non-LSTV sample (normal anatomical architecture).

Research method

The research methodology involved photography, and linear and surface area measurements of a distinct list of dimensions for the LSTV cohort compared to a control cohort list of measurements.

Measuring equipment and unit of measure

i. Photographic equipment

A high-resolution digital camera (Canon EOS 650D with an EF-S 18-55mm lens) was mounted on a height-adjustable fixed-base photographic frame seen in Figure 2.6. Images were recorded as high-resolution JPEG files.

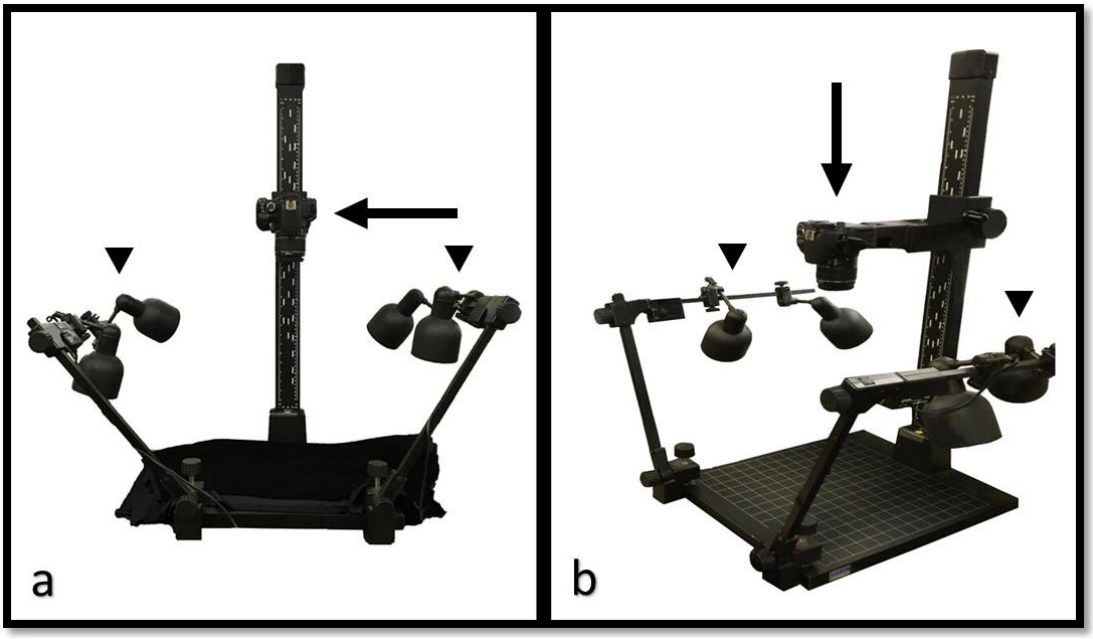

Figure 2.6: P*hotography jig set-up used to photograph skeletal materials****. (a)*** *Anterior and* ***(b)*** *left anterior oblique view of the equipment. The camera is mounted* ***(arrow)*** *on a height-adjustable fixed vertical track while there are four multidirectional adjustable lights paracentral* ***(arrowhead)*** *to the jig base.* ***Note:*** *black velvet material (seen in image* ***a****) was used to cover the base of the jig to act as a contrast medium (absorbs ambient light) and reduce the glare when flash photography was employed. Furthermore, the velvet acted as a soft surface on which the skeletal materials were placed.* ***Photography and editing:*** *GJ Paton.*

ii. Linear and surface area measurements of bone:

Osteometric linear measurements were recorded using digital Vernier callipers (with a sensitivity of 0.01mm).

The measurements included linear sacral and lumbar vertebral dimensions as well as surface areas. Surface area and angles were calculated using scaled photographs with the aid of an open-source computer scientific-tool software programme known as ImageJ created by Wayne Rasband (Schneider et al., 2012). Surface areas were measured directly with the aid of ImageJ and recorded in the format of mm^2.

The measurements were entered and recorded in *Microsoft Excel*® spread sheet at the site of measurement. In addition to the physical measurements, the pre-sacral vertebral count was recorded.

Method for measurement of photographs

All photographs of bone specimens were taken in the photography-jig displayed in Figure 2.6. The sacra and lumbar vertebrae were placed so that the area to be measured would be aligned perpendicular to the line of sight of the camera lens. A scale bar was positioned next to the specimen at the height of the surface to be measured. A scale bar depicts lengths of known distance which was used to set the scale for the photographs. Using the ImageJ software in conjunction with the scale bar, dimensions could be calculated and recorded from the photographs, such as linear distance (mm), surface area (mm^2) and angles (degrees).

Osteometric measurements

The osteometric linear measurements and surface area measurements utilised for the study represent a combination of corresponding measures found in the literature and measures incorporated by the author for investigative purposes (Savage, 2005; Mahato, 2010; Mahato 2011a and b). Twenty-three separate sets of measurements were labelled one to twenty-three for each of the dimensions (D). Refer to Table 2.5 and Figure 2.7 for the summary and illustrations of the dimensions.

Table 2.5: Dimensions of the lower lumbar column and sacrum in the lumbosacral transitional vertebrae cohort.

Dimension	Description	Definition
D1	**Sacral height (SH)**	One measurement. The anterior sacral surface, measured as a linear distance from the superior aspect of anterior edge of the sacral promontory to the distal aspect of the articular surface for the coccyx articulation, in non-LSTV individuals. For cases of LSTV, the Type III and IV LSTV were measured as a linear distance from the superior tip of the LSTV superior aspect of the vertebral body to the distal aspect of the last sacral vertebra.
D2	**Sacral body width (SBW)**	One measurement. The maximum width of the vertebral body measured on the superior aspect, in the coronal plane.
D3	**Sacral body length (SBL)**	One measurement. The maximum length of the vertebral body, anterior to posterior, measured in the sagittal plane.
D4	**Inter-alae distance (IAD)**	One measurement. The maximum distance between the alae, measured from the auricular surface on one side to the auricular surface on the other side.

Table 2.5: (Continued).

Dimension	Description	Definition
D5	**Inter-facet distance, lateral (IFD*lat*)**	One measurement. The lateral edge of the sacral facet joint one side to the lateral edge of the sacral facet joint on the other side, measured in the coronal plane.
D6	**Inter-facet distance, medial (IFD*med*)**	One measurement. It is the medial edge of the sacral facet joint one the one side to the medial edge of the sacral facet joint of the other side, measured in the coronal plane.
D7	**Facet distance (FD)**	One measurement. The maximum distance posteriorly of the sacral facet joints. Measured from the anterior aspect of the sacral canal to a projected line connecting the posterior aspect of the sacral facet joints.
D8	**Sacral facet height (SFH)**	Two measurements. Right and left sides. The maximum height of the articular surface of the sacral superior articulating processes (facets), measured superior to inferior.
D9	**Sacral facet width (SFW)**	Two measurements. Right and left sides. The maximum width of the articular surface of the sacral superior articulating processes (facets), measured medial to lateral.

Table 2.5: (Continued).

Dimension	Description	Definition
D10	**Auricular length (AL)**	Two measurements. Right and left sides. The maximum length of the auricular surface of the sacrum, measured from superior to inferior.
D11	**Facet joint angle (FA)**	Two measurements. Right and left sides. The angle formed between the mid-sagittal plane and a line that interacts with the plane of the articular surface of the superior articulating processes (facets). Facet joint angle was only measured on specimens with Type II LSTV in the LSTV cohort.
D12	**Sacral hiatus length (SHL)**	One measurement. The length of the sacral hiatus from the superior arch which intersects a line produced by connecting the distal aspect of the cornu, measured in the mid-sagittal plane.
D13	**Length of last lumbar transverse process (TVPL)**	Two measurements. Right and left sides. In the axial plane, a line bisecting the TVP is measured from the tip of the TVP to the junction of the pedicle (defined by a line from the lateral aspect of the vertebral body to the lateral aspect of the facet joint) on the same side.
D14	**Vertical height of last lumbar transverse process (TVPH)**	Two measurements. Right and left sides. The maximum height of the TVP, measured superior to inferior.

Table 2.5: (Continued).

Dimension	Description	Definition
D15	**Auricular surface area (ASA)**	Two measurements. Right and left side. The sacral auricular surface area, right and left.
D16	**Lumbar transverse process contribution to ASA**	Two measurements. Right and left. The surface area contribution to the ASA from the lumbar TVP.
D17	**Sacral facet surface area (FSA)**	One measurement. The sacral superior articulating (facet) surface area, right and left. Sacral facet surface area was only measured on specimens with Type II LSTV in the LSTV cohort.
D18	**Sacral body surface area (BSA)**	One measurement. The surface area of the superior aspect of the first sacral vertebra. Only measured on Type II LSTV.
D19	**Accessory facet surface area (AFSA)**	One or two measurements. The surface area of the accessory facet on the superior surface of the sacrum, right and / or left. Accessory facet surface was only measured on specimens with Type II LSTV in the LSTV cohort.
D20	**Vertebral body height 1 (VBH1)**	One measurement. The vertical height of the last lumbar vertebra. In the LSTV cohort it is the vertebral body height of the LSTV segment, measured superior to inferior, on the anterior aspect of the LSTV.

Table 2.5: (Continued).

Dimension	Description	Definition
D21	**Vertebral body height 2 (VBH2)**	One measurement. The vertical height of the second last lumbar vertebra. In the LSTV cohort it is the vertebral body height of the vertebra superior to the LSTV segment, measured from the anterior aspect of the lumbar vertebral body.
D22	**Thoracolumbar enumeration (TLE)**	One measurement. The total vertebral count for the thoracolumbar vertebral column.
D23	**Thoracolumbar vertebral contribution to TLE**: **D23T** – Thoracic (T) vertebrae count. **D23L** – Lumbar (L) vertebrae count.	Two measurements. Sub-classification of the TLE. The vertebral count for the spinal vertebrae of the thoracic and lumbar vertebral column separately.

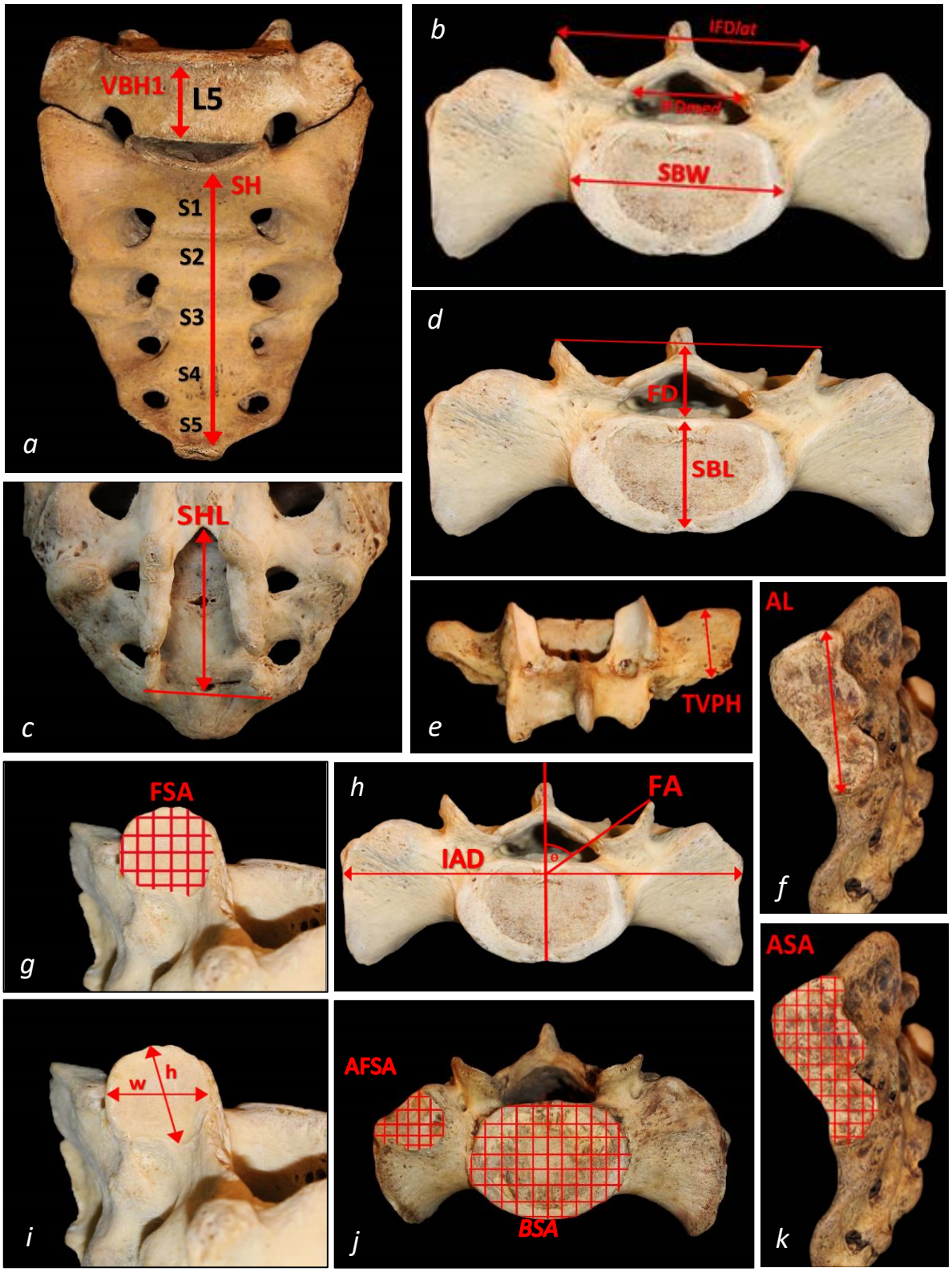

Figure 2.7: *Views of a sacrum and last lumbar vertebra demonstrating a selection of the various dimensions used in measurement data-set. These included:* ***(a)*** *Sacral Height (SH), Vertebral Body Height (VBH1);* ***(b)*** *Sacral Body Width (SBW), Inter-Facet Distance: lateral (IFDlat); and Inter-Facet Distance: medial (IFDmed).* ***(c)*** *Sacral Hiatus length (SHL);* ***(d)*** *Sacral Body Length (SBL), Facet Distance (FD);* ***(e)*** *Transverse process height of the last lumbar vertebra (TVPH);* ***(f)*** *Sacral Auricular Length (AL), right and left;* ***(g)*** *Sacral facet surface area (FSA), right and left;* ***(h)*** *Inter-Alae Distance (IAD) and Sacral Facet Angle (FA);* ***(i)*** *Sacral Facet Height (SFH) and width (SFW) - labelled (h) and (w) for presentation aesthetics,* ***(j)*** *Sacral Body Surface Area (BSA) and Accessory Facet Surface Area (AFSA);* ***(k)*** *Sacral Auricular Surface Area (ASA).* ***Photography and editing:*** *GJ Paton.*

Intra-observer error assessment of the osteometric cohort

Intra-observer error was assessed by performing the following steps:

1. Ten percent of the osteological cohort (10 skeletal specimens) was appraised by the author and then re-appraised a week later. This allowed for sufficient time to pass to mitigate any bias in landmark location selection.
2. The numerical data was analysed using Lin's concordance correlation coefficient (CCC) on the mean value for each osteometric measurement selected.
3. Agreement for the intra-observer error for all categories of LSTV was in the range of 'almost perfect agreement'. Therefore, the interpretation of the remaining 90% of the images could be taken with confidence regarding their accuracy and precision. Refer to Table 2.6, which displays the degree of agreement across four categories of Lin's correlation coefficient. Table 2.7 reports the intra-observer error agreement for 12 osteological measurements.

Table 2.6: Interpretation of Lin's correlation coefficient (Adapted from McBride, 2005).

Value of Lin's CCC	Interpretation
> 0.99	Almost perfect
0.95 to 0.99	Substantial
0.90 to 0.95	Moderate
< 0.90	Poor

Lin's CCC measures the agreement between two variables (Akoglu, 2018). The closer the value of Lin's CCC is to 1, the higher the agreement between observers and/or observations. McBride (2005) suggested a modified level of agreement scale seen in Table 2.6. (McBride, 2005).

Table 2.7: Results of intra-observer test of osteometric assessment.

Number of samples	Variable	Lin's concordance correlation coefficient
10	D1	0.999
10	D2	0.996
10	D4	0.999
10	D5	0.999
10	D6	0.999
10	D7	0.997
10	D8	0.996
10	D11	0.999
10	D14	0.999
10	D11	0.996
10	D17	0.997
10	D22	0.999

Inter-observer error

Inter-observer error was minimised by performing the following steps:

1. A research volunteer external to the study was trained by the principal investigator (author) on how to perform the necessary measurements both physically and using computer software.

2. Ten percent of the osteological cohort (10 skeletal specimens) were measured for twelve variables by a second observer. Physical measurements (using digital Vernier callipers) and photographic measurements were performed (using the software programme ImageJ) were performed for surface area calculations and degrees of angulation.

3. The measurements obtained by the second observer were compared to those of the author using Lin's CCC. Agreement for all measurements for the inter-observer error assessment was in the range of 'almost perfect agreement'. Therefore, the measurements performed by the author could be taken of the remaining 90% of the osteological cohort with confidence regarding their accuracy and precision. Refer to Table 2.6 which displays the degree of agreement across four categories of Lin's correlation coefficient. Table 2.8 reports the inter-observer error agreement for Types IIA, B, IIIA, B and IV.

Table 2.8: Results of inter-observer test of osteometric assessment.

Number of samples	Variable	Lin's concordance correlation coefficient
10	D1	0.999
10	D2	0.988
10	D4	0.999
10	D5	0.999
10	D6	0.999
10	D7	0.996
10	D8	0.977
10	D11	0.999
10	D14	0.999
10	D11	0.997
10	D17	0.998
10	D22	0.999

Osteological Paradox

Osteological paradox has gained wide recognition with the seminal paper by Wood et al. (1992) whereby they describe inherent fundamental problems to analyses of past populations. Wood et al. (1992) defined the osteological paradox as a false inference of heterogeneous prehistoric health from skeletal samples due to many of factors.

The three main principles of the osteological paradox include: Firstly, ''demographic non-stationarity,'' or in other words, populations that move and experience changing fertility rates. Secondly, ''selective mortality'' whereby individuals who die at a given age do not represent the entire living population at risk of death at that age. Lastly, ''heterogeneous fragility'' is an inherent vulnerability or susceptibility to disease and death (Woods et al, 1992, p.344). Inferences, therefore, are made with the knowledge that findings may be influenced by one or more of the listed factors (DeWitte and Stojanowski, 2015).

Statistical analyses

Statistical analyses were performed using IBM® Statistical Product and Service Solutions SPSS® (formerly Statistical Package for the Social Sciences) software for Windows operating system, version 25.0 (IBM Corp. 2015). The alpha was set at $p \leq 0.05$ for significance for all tests in the thesis.

Statistical tests

Cross-tabulation of categorical variables was performed on lumbar spine enumeration using the Chi-squared test (X^2), Cramer's V test and Fisher's exact test.

Tests for normality

These are tests to determine if the data is normally distribution within the population sample. Parametric tests assume normality therefore, a normal distribution is required to analyse the data utilising parametric testing methods. There are seven tests available for data normality (Durrheim and Tredoux, 2014). Two tests for normality were selected based on the number of sample measurements collected per group (D1, D2, D3 etc.).

The Kolmogorov-Smirnov test was used to test for normality in groupings larger or equal to 50 samples, and the Shapiro-Wilk test was used with groupings less than 50 samples or data found to be distributed non-parametrically (distribution-free) (Shapiro and Wilk, 1965).

The *null hypothesis* for a population states that the population is normally distributed. The *alternative hypothesis* is that it is not normally distributed and would require certain tests in response to the findings (Durrheim and Tredoux, 2014).

Based on the findings of the tests for normality two options exist. A parametric test is used if the data is normally distributed namely the Mann-Whitney U test and a nonparametric test if the data is found to be non-normal namely an unpaired t-test.

Student's t-test (t-test)

The independent samples t-test (also known as unpaired samples t-test) is a parametric test used to test how significant the differences between groups are (measured in means). It is an indicator that reveals to a researcher whether the differences could have happened by chance (Pallant, 2013; Durrheim and Tredoux, 2014).

Mann-Whitney U Test

This is a non-parametric test used to determine the differences between unrelated samples. It is used when there are two groups of scores that are independent of each other. The Mann-Whitney U test is based on mean ranks or medians. This is also known as the Wilcoxon rank-sum test (Verma et al. 2019).

Pearson's correlation coefficient

The Pearson's correlation coefficient (*r*) measures how strong a relationship exists between two variables. The correlation coefficient values range from -1 to 1. The number one indicates a positive relationship while a negative one indicates a strong negative relationship. A zero indicates no relationship at all. A positive correlation means for every positive increase in one variable, there is a positive increase in the correlating variable.

A negative correlation coefficient is the converse of a positive result, see Table 2.9 for strength of variables (Pallant, 2013; Durrheim and Tredoux, 2014).

Table 2.9: Pearson's correlation coefficient (Hinkle and Wiersma, 2009).

Size of Correlation	Interpretation
0.90 to 20.00 (-0.90 to -1.00)	Very high positive (negative) correlation
0.70 to 0.90 (-0.70 to -0.90)	High positive (negative) correlation
0.50 to0.70 (-0.50 to -0.70)	Moderate positive (negative) correlation
0.30 to 0.50 (-0.3.0 to -0.50)	Low positive (negative) correlation
0.00 to 0.30 (0.00 to -0.30)	Negligible correlation

Analysis of variance (ANOVA) test

Analysis of variance (ANOVA) is a parametric test used to test differences between mean averages measurements for more than two groups. The assumption for parametric tests is that the sample groups are of equal variance. That is to say, that the variability of scores for each of the groups is comparable. As part of the t-tests performed, the Levene's test for equality of variances was conducted (Pallant, 2013; Durrheim and Tredoux, 2014).

Kruskal-Wallis test

This is a non-parametric test that is analogous to the ANOVA testing methods. The Kruskal-Wallis test is used to determine the differences between three or more groups. It is an extension of the Mann-Whitney U test to determine the differences between unrelated samples for three or more independent samples (Pallant, 2013; Durrheim and Tredoux, 2014).

Ethical considerations

Confidentiality and anonymity: All personal identifiers were removed. The LSTV-containing images was stored on the principal investigator's computer using a password protected folder for use in the thesis. The data were stored by the principal investigator (the author of this study) with no access available to any individual outside of the research team.

The author of this study maintained the anonymity of the images displayed. No names or identifiers were displayed that could be used to recognise any individual in the study. Importantly, any findings in the images remained confidential and no mention of any disease or disease-like process was linked to the individual of origin.

Ethical clearance was granted via UCT Human Research Ethics Committee (HREC) before the commencement of this study. Human Research Ethic's clearance number was *HREC REF: 195/2017* (**Appendix 1A and Appendix 1B**). Likewise, permission with ethical clearance was granted via the School of Anatomical Sciences Collections Committee at WITS, no reference number, the permission letter displayed in **Appendix 2**.

Continuing approval was obtained through the annual progress report submitted to the HREC by which an extension of the data collection period was granted for an additional year due to time-constraint difficulties experienced by the author. Additionally, study continuity was obtained by the Head of Department of Human Biology, University of Cape Town through the process of the annual progress reports.

The heads of department for radiology at CMJAH, Adjunct Professor Mngomezulu, and Professor Beningfield at GSH granted permission for use of the radiology facilities prior to the author's Provincial-level ethics request for access to the hospitals records.

Permission with ethical clearance was granted by the Department of Health in Gauteng and Western Cape Provinces at CMJAH, Ref number: GP_201807_050 (**Appendix 3**) and GSH, application number: WC_201807_030 (**Appendix 4**).

CHAPTER 3

RESULTS

Introduction

This study was divided into two main parts that each contained sub-objectives:

Part I: Medical imaging

a) Prevalence and morphological characteristics of LSTV in the South African population

Part II: Osteological morphology

b) Metric observations

c) Non-metric observations

For the purposes of this results chapter, Part I and Part II will be discussed separately.

Part I: Medical imaging of lumbosacral transitional vertebrae

Prevalence and morphological characteristics of LSTV in the South African population

Frequencies and percentages

Study Sample

The Castellvi et al. (1984) classification was used when categorising LSTV into its Types and subtypes. The total number of individuals for this study was 3096 (N_t=3096). The total cohort was comprised of three equal groups of 1032 individuals reflecting the ancestry of the three largest ethnic cohorts in South Africa, namely African-ancestry, Mixed-ancestry and European-ancestry (SAPSS, 2019).

The total prevalence of LSTV in the South African cohort was 10% (Types II, III and IV, N=308). The result discussions listed in this chapter were ordered from the greatest number to the least number.

A summary of the total cohort for the study categorised by ancestry and sex is presented in Table 3.1 and Table 3.2.

Table 3.1: Summary of total sample in the imaging cohort.

ANCESTRY	SEX	SEX DISTRIBUTION		SUB-TOTAL
		Number of Individuals	PERCENT	
AFRICAN	MALE	516	50.0	1032
	FEMALE	516	50.0	
MIXED	MALE	446	43.2	1032
	FEMALE	586	56.8	
EUROPEAN	MALE	520	50.4	1032
	FEMALE	512	49.6	
TOTAL (N_t)				**3096**

Table 3.2: Summary of the lumbosacral transitional vertebrae in the imaging cohort.

ANCESTRY	SEX	FREQUENCIES			RADIOGRAPGHS	
		NUMBER OF INDIVIDUALS	PERCENTAGE WITHIN ANCESTRY	PERCENTAGE WITHIN LSTV COHORT	TOTAL NUMBER OF INDIVIDUALS	LSTV FREQUENCY (PERCENT)
AFRICAN	MALE	48	44	**15.6**	**109**	**10.6%**
	FEMALE	61	56	**18.2**		
MIXED	MALE	42	43.75	**13.6**	**96**	**9.3%**
	FEMALE	54	56.25	**17.5**		
EUROPEAN	MALE	52	50.5	**16.9**	**103**	**10.0%**
	FEMALE	51	49.5	**16.6**		
TOTAL (N)					**308**	

Age and sex

The average age for the total sample group was 45.10 years (standard deviation 15.26 years) (N_t=3096). The total imaging cohort had a sex distribution of 1482 (47.9%) males and 1614 (52.1%) females. The imaging cohort that contained LSTV had a sex distribution of 142 males (46.1%) and 166 females (53.9%). Within age distribution by sex, the average age of males without LSTV was 47.31 years (n=1340) (standard deviation 15.23 years) and the average age of females without LSTV was 47.13 years (n=1448) (standard deviation 14.62 years). By contrast, the males within the LSTV cohort had an average age of 45.90 years (n=142) (standard deviation 16.08 years) and the average age of females with LSTV cohort was 47.40 years (n=166) (standard deviation 13.03 years).

The age range for males and females in the cohort without LSTV was between 16 and 88 years. The age range found for the males in the LSTV cohort was between 16 and 85 years while females in the LSTV cohort was between 16 and 82 years. The total age distribution for the study is displayed in Figure 3.1.

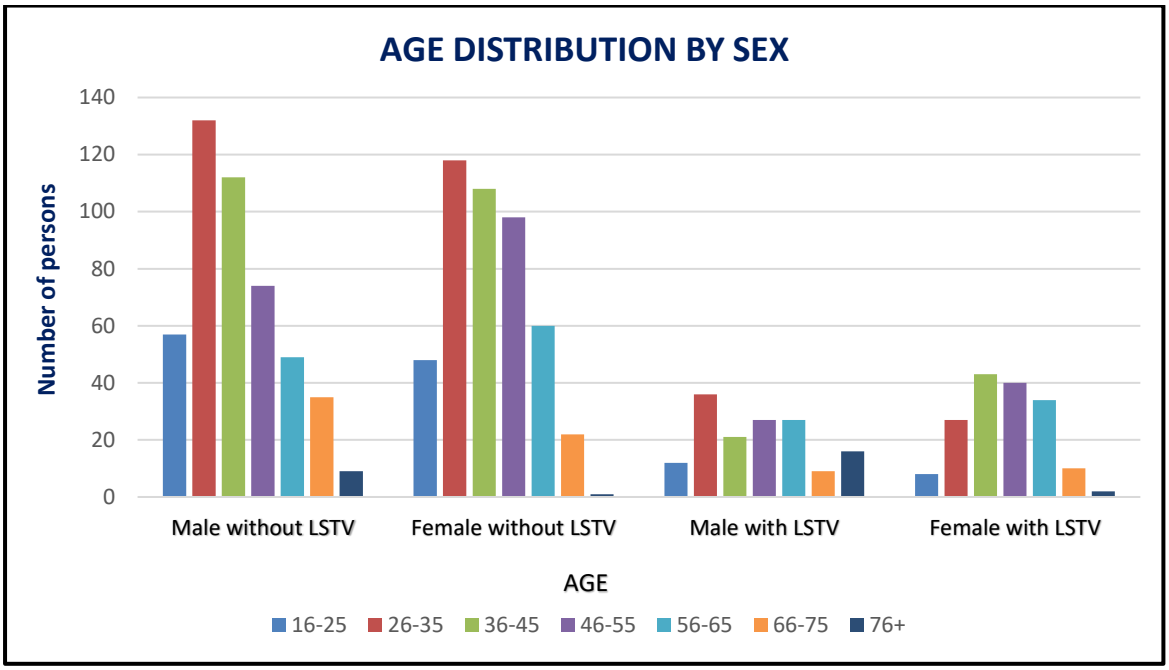

Figure 3.1: *Age distribution of the total study cohort. Comparison was made between the age distribution range of the lumbosacral transitional vertebrae and non-lumbosacral transitional vertebrae cohorts.*

Age and ancestry

In the African-ancestry cohort, the average age without LSTV was 42.0 years (n=923) (standard deviation 14.35 years), and the average age for the LSTV cohort was 41.10 years (n=108) (standard deviation 12.34 years). The age range for the African-ancestry cohort without LSTV was between 16 and 88 years, while the LSTV cohort age range was between 16 and 70 years.

In the Mixed-ancestry cohort, the average age was 49.80 years (n=936) (standard deviation 15.01 years) and the average age for the LSTV cohort was 50.52 years (n=96) (standard deviation 14.10 years). The age range for the Mixed-ancestry cohort without LSTV was between 16 and 88 years, while the LSTV cohort age range was between 18 and 85 years.

In the European-ancestry cohort, the average age without LSTV was 49.5 years (n=929) (standard deviation 15.36 years), and the average age for the LSTV cohort was 48.18 years (n=103) (standard deviation 15.48 years). The age range for the European-ancestry cohort without LSTV was between 16 and 88 years, while the LSTV cohort age range was between 17 and 82 years.

Sex

The total number of males and females in the study was 1482 (48%) and 1614 (52%), respectfully (Table 3.1). The LSTV cohort (n=308) demonstrated a sex distribution of 142 males (46%) and 166 females (54%). The sex distribution in the African-ancestry cohort (n=109) consisted of 48 males (44%, 15.5% of 308) and 61 females (56%, 18.2% of 308). The Mixed-ethnicity cohort contained a sex content of 42 males (44%, 13.6% of 308) and 54 females (56%, 17.5% of 308). Finally, the European-ancestry cohort exhibited a sex distribution of 52 males (50.5%, 16.9% of 308) and 51 females (49.5%, 16.6% of 308). A summary of the total sample for the study categorised by sex is displayed in Figure 3.2.

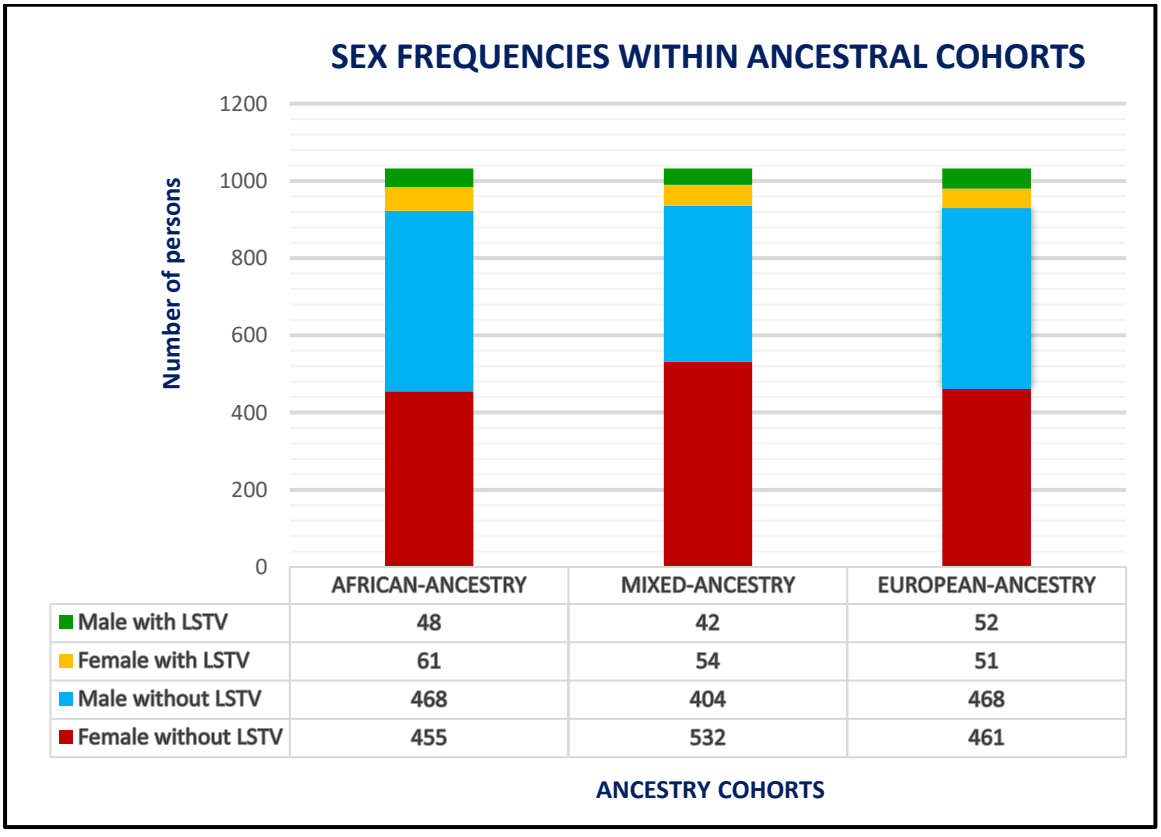

Figure 3.2: *Sex frequencies of each ancestral cohort in the total study sample.*

Imaging modalities

Three imaging modalities of the lumbar spine and pelvis were utilised for this study, namely radiographs, CT scans and MRI scans. The images that met the inclusion criteria for the study consisted of 308 radiographs (n=308 LSTV), 51 CT scans and 38 MRI scans. The total number of images used in this study was 397 separate imaging sequences (not including the multiple images per modality such as axial and sagittal imaging on CT or MRI scans). Refer to Table 3.3 for a summary of the total imaging cohort.

Table 3.3: Summary of the imaging cohort for lumbosacral transitional vertebrae.

ETHNICITY	IMAGING MODALITY			FREQUENCIES
		ADDITIONAL IMAGING		
	RADIOGRAPHS	CT	MRI	
AFRICAN	109	25	3	137
MIXED	96	7	23	126
EUROPEAN	103	19	12	134
TOTAL	**308**	**51**	**38**	**397**

Examples of LSTV found in the imaging appraisal

A selection of radiographic images, namely radiographs and CT images, as chosen to provide examples of the three main Types and subtypes of LSTV found in the study. Computerised tomography images were chosen to contrast the radiographs and highlight the benefit of advanced imaging for its clarity to display superior quality resolution of vertebral anatomy. Types II, III and IV as well their subtypes are displayed in Figures 3.3 to 3.8.

Type IIA: Right and left-sided lumbosacral transitional vertebrae

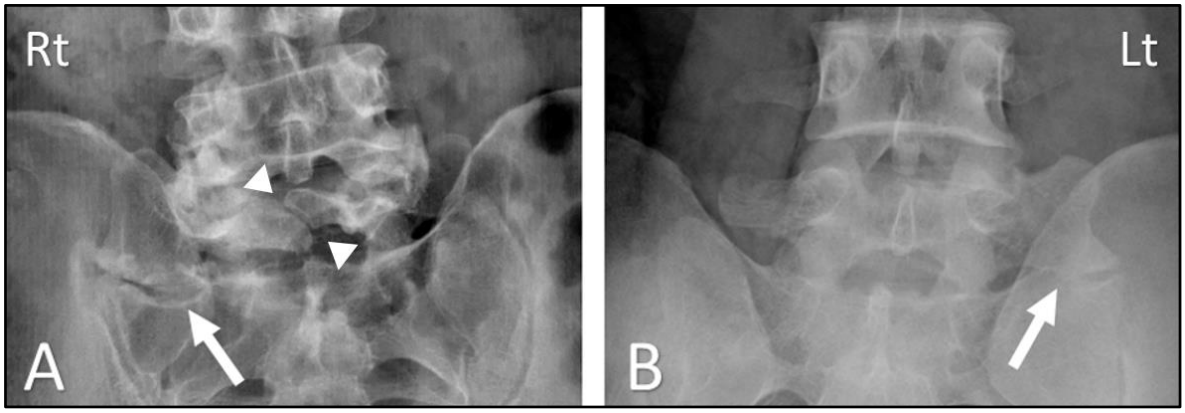

Figure 3.3: *Unilateral Type II lumbosacral transitional vertebrae.* ***A)*** *An anteroposterior lumbosacral radiograph demonstrates a right-sided Type IIA LSTV. The arrow indicates articulation of the right transverse process of the last lumbar vertebra with the right ala of the sacrum.* ***B)*** *An anteroposterior lumbosacral radiograph demonstrates a left-sided Type IIA LSTV. The arrow indicates articulation of the left transverse process of the last lumbar vertebra with the left ala of the sacrum.* ***Rt*** *= Right side.* ***LT*** *=Left side. Note: A spina bifida occulta is seen in Figure* ***A*** *as a cleft of the posterior arch on the last lumbar vertebra (****arrowheads****).*

Type IIB lumbosacral transitional vertebra

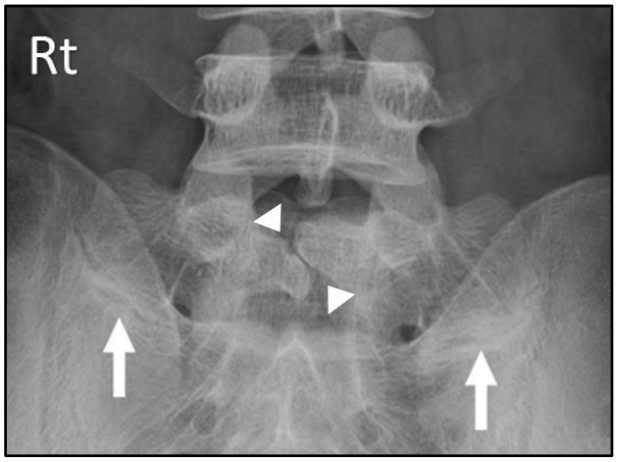

Figure 3.4: *Bilateral Type II lumbosacral transitional vertebra. An anteroposterior lumbosacral radiograph demonstrates a Type IIB LSTV. The arrows indicate the sites of articulation of both transverse processes of the last lumbar vertebra with the alae of the sacrum.* ***Rt*** *= Right side. Note: A spina bifida occulta* ***(arrowheads)*** *is seen as a cleft of the posterior arch on the last lumbar vertebra.*

Type IIIA: Right-sided lumbosacral transitional vertebrae

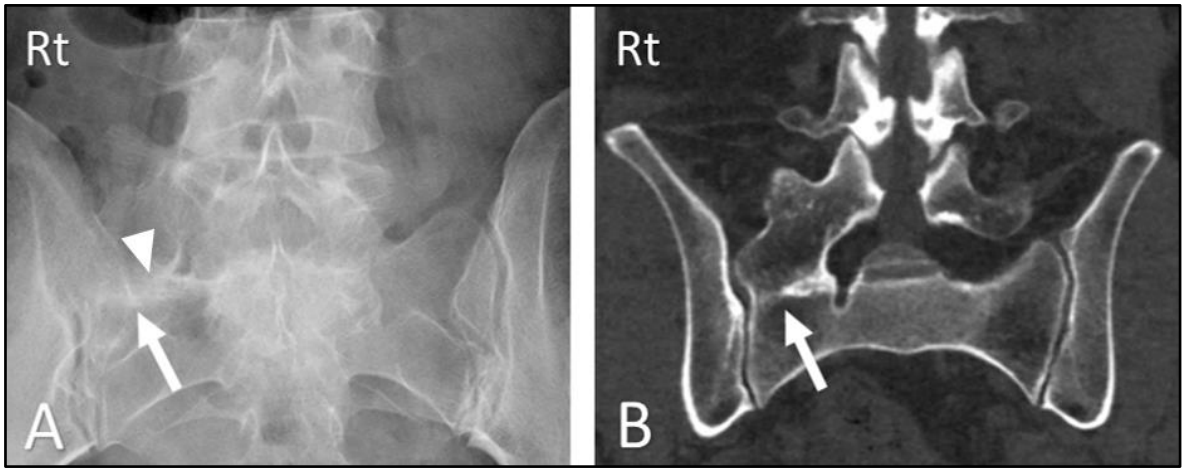

Figure 3.5: *Right-sided Type IIIA lumbosacral transitional vertebra.* ***A)*** *An anteroposterior lumbosacral radiograph demonstrates a right-sided Type II LSTV. The arrow indicates the site of fusion of the right transverse process of the last lumbar vertebra with the right ala of the sacrum. A thin sclerotic band* ***(arrowhead)*** *is seen on the medial half of the LSTV which may give the impression this is a site of articulation.* ***B)*** *A coronal CT scan of the lumbosacral junction of the same individual seen in* ***A****. The arrow indicates the site of fusion of the right transverse process of the last lumbar vertebra with the right ala of the sacrum.* ***Rt*** *= Right side. Note: the medial half at the site of fusion of the transverse process and the ala of the sacrum demonstrates increased density and only partial fusion on image* ***B****. This explains the increased density seen as a thin sclerotic line* ***(arrowhead)*** *on the radiograph on image* ***A****.*

Type IIIA: Left-sided lumbosacral transitional vertebra

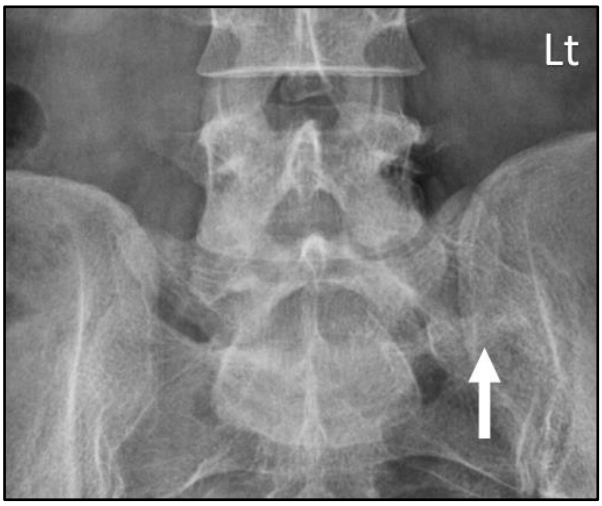

Figure 3.6: *Left-sided Type IIIA lumbosacral transitional vertebra.* ***A)*** *An anteroposterior lumbosacral radiograph demonstrates a right-sided Type II LSTV. The arrow indicates the fusion of the left transverse process of the last lumbar vertebra with the left ala of the sacrum.* ***LT*** *= Left side.*

Type IIIB lumbosacral transitional vertebrae

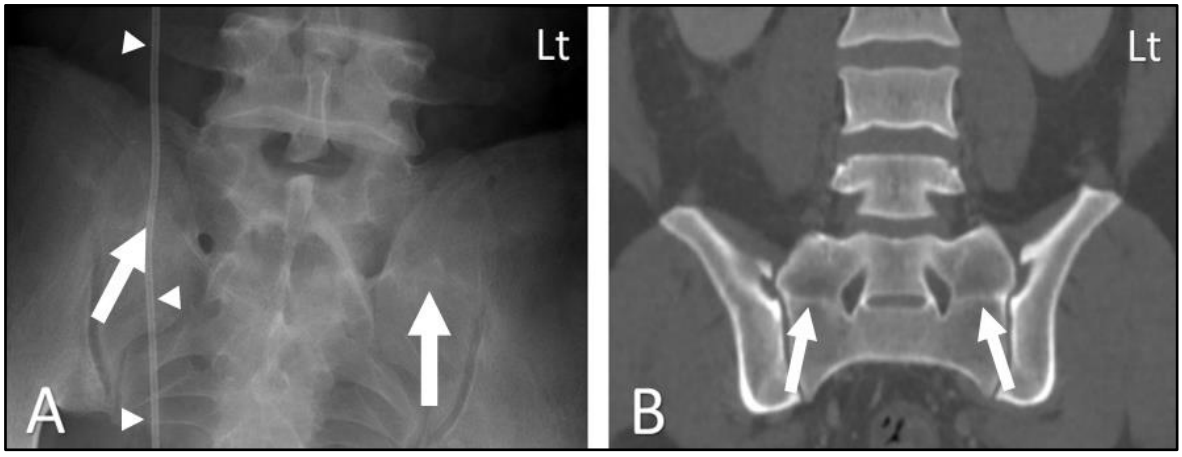

Figure 3.7: *Bilateral Type III lumbosacral transitional vertebra.* ***A)*** *An anteroposterior lumbosacral radiograph demonstrates a bilateral Type III LSTV. The arrows indicate the sites of fusion of both transverse processes of the last lumbar vertebra with the alae of the sacrum. A tubular artefact is seen running down the right side of the radiograph in front of the sacrum* ***(arrowheads)****. This artefact represents a ureteric stent maintaining the patency of the ureter from the right renal pelvis of the right kidney to the urinary bladder. It is the likely reason the X-ray was taken.* ***B)*** *A coronal CT scan of the lumbosacral junction of the same individual seen in* ***A****. The arrows indicate the sites of fusion of both transverse processes of the last lumbar vertebra with the alae of the sacrum.* ***Lt*** *= Left side.*

Type IV lumbosacral transitional vertebrae

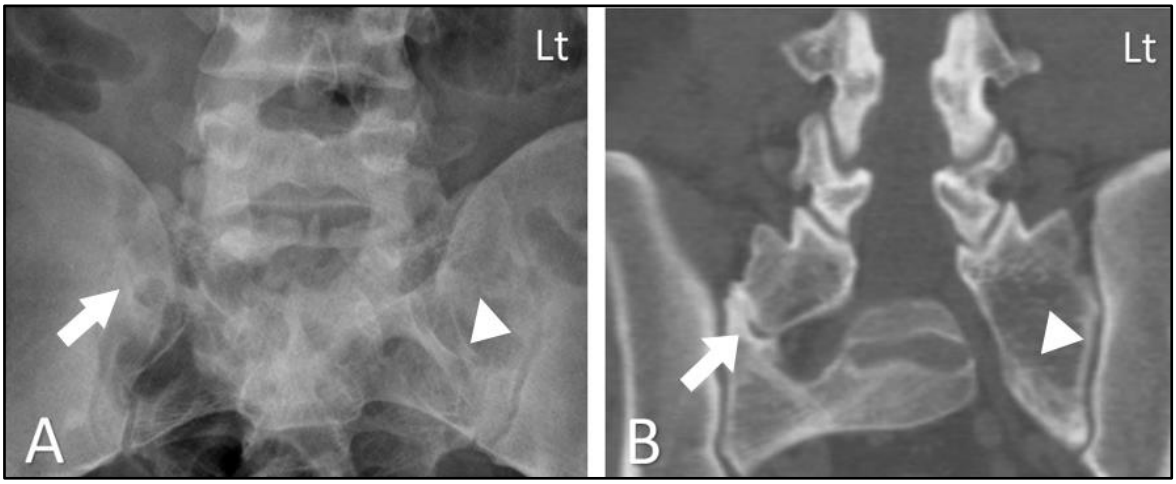

Figure 3.8: *Type IV lumbosacral transitional vertebra.* ***A)*** *An anteroposterior lumbosacral radiograph demonstrates a Type IV LSTV. The articulation site is the right transverse process of the last lumbar vertebra with the right ala of the sacrum (****arrow****). The left transverse process of the last lumbar vertebra is fused to the left ala of the sacrum* ***(arrowhead)****.* ***B)*** *A coronal image of a CT scan of the lumbosacral junction of the same individual as* ***A****. The articulation site is the right transverse process of the last lumbar vertebra with the right ala of the sacrum* ***(arrow)****. The left transverse process of the last lumbar vertebra is fused to the left ala of the sacrum (arrowhead).* ***Lt*** *= Left side.*

Types of lumbosacral transitional vertebrae

The following was found for the evaluation of the LSTV by Type classification: the largest category of LSTV found was the Type II at 67.9% (n=209) of the sample, which contained an articulation of one or both the lumbar TVPs with the alae of the sacrum. The second-largest category was the Type III accounting for 27.8% (n=85) of the sample which contained a fusion of one or both the lumbar TVPs with the alae of the sacrum. The Type IV LSTV was the smallest category, accounting for only 4.5% (n=14) of the sample, which consisted of a unilateral articulation of the lumbar TVP with the ala of the sacrum and sharing a contralateral fusion of the lumbar TVP to the ala of the sacrum. Refer to Table 3.4 for summary of the Types of LSTV found in the LSTV cohort.

Table 3.4: Type of lumbosacral transitional vertebrae in the imaging cohort.

TYPE	Frequency	Percentage	Cumulative percentage
TYPE II	209	67.9	67.9
TYPE III	85	27.6	95.5
TYPE IV	14	4.5	100
TOTAL	**308**	100	

Types and ancestry of lumbosacral transitional vertebrae

The following were the results for the evaluation of the LSTV by Types and ancestry classification: regarding Type II, the African-ancestry cohort (n=109) contained the greatest number, namely 81, which was 74.3% of its cohort. The Mixed-ancestry (n=96) and European-ancestry (n=103) cohorts each comprised the same number at 64 individuals, but they varied in their prevalence rate for each of the cohorts. The Mixed-ancestry's cohort made up 66.7% of the sample while the European-ancestry cohort comprised 62.1% of this Type.

The European-ancestry, Mixed-ancestry and African-ancestry cohorts contained 33.0% (n=34), 27.1% (n=26) and 22.9% (n=25) of Type III, respectively.

The Type IV LSTV was the least common of the three main Types of LSTV. It was found in the greatest number in the Mixed-ancestry cohort at 6.3% (n=6) followed by the European-ancestry cohort at 4.9% (n=5) and the African-ancestry cohort demonstrated the least with 2.8% (n=3). Refer to Figure 3.9 to compare the LSTV Types found in each of the three ancestry cohorts.

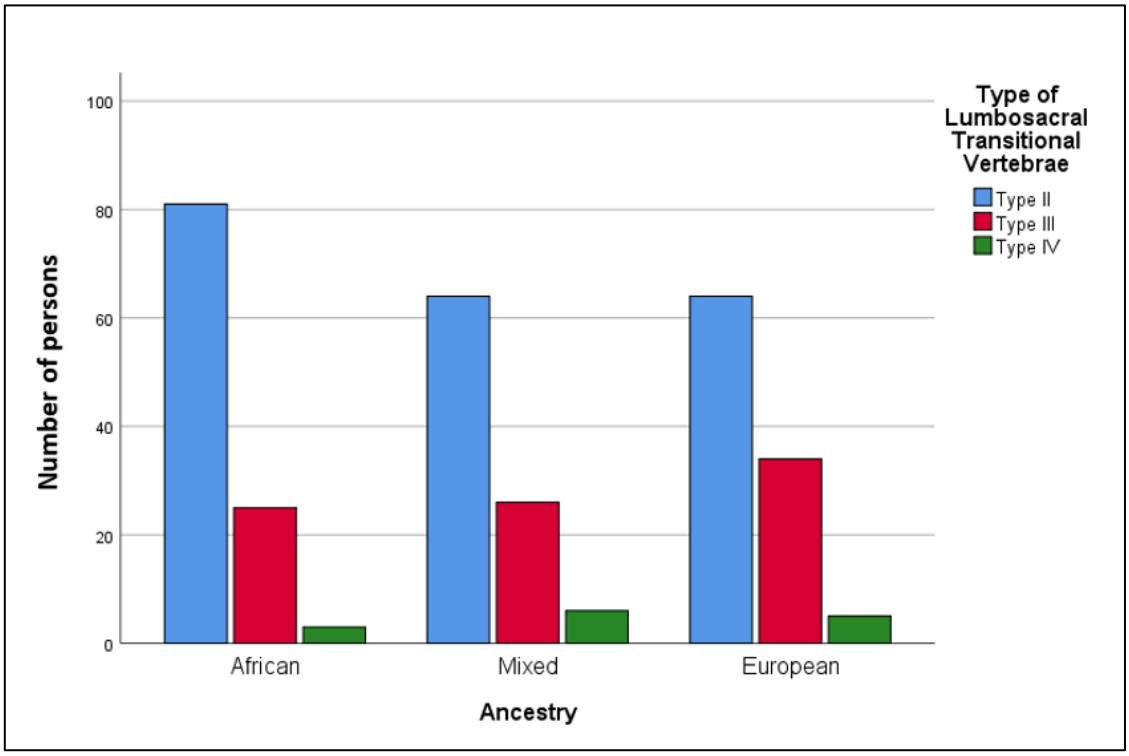

Figure 3.9: *Types of lumbosacral transitional vertebrae grouped by ancestry. The key is in the top right corner.*

Subtypes of lumbosacral transitional vertebrae

The evaluation of LSTV by its subtypes found the following: the largest category found was the Type IIA with 41.9% (n=129) of the sample containing a unilateral articulation, right or left, whereby the lumbar TVP made contact with one of the alae of the sacrum. The frequency of the side will be discussed in the next section.

The Type IIB accounted for the second-largest category at 26.0% (n=80) of the sample and contained articulations of both lumbar TVPs with the alae of the sacrum.

The third most common Type found was Type IIIB which accounted for 21.8% (n=67) of the sample with bilateral lumbar TVP fusion to the alae of the sacrum. Type IIIA was present in 5.8% (n=18) of the sample while Type IV was the least common at 4.5% (n=14). Refer to Table 3.5 for a summary of the findings of LSTV subtypes contained within this cohort.

Table 3.5: Subtypes of lumbosacral transitional vertebrae in the imaging cohort.

Subtypes	Frequency	Percentage	Cumulative percent
TYPE IIA	129	41.9	41.9
TYPE IIB	80	26	67.9
TYPE IIIA	18	5.8	73.7
TYPE IIIB	67	21.8	95.5
TYPE IV	14	4.5	100
TOTAL	**308**	100	

Subtypes and ancestry of lumbosacral transitional vertebrae

For the evaluation of LSTV by their subtypes and ancestry, the following was found: regarding Type IIA LSTV, the African-ancestry, Mixed-ancestry and the European-ancestry cohorts consisted of 41.3% (n=45), 45.8% (n=44) and 38.8% (n=40), respectively.

Concerning Type IIB LSTV, the African-ancestry cohort had the greatest number at 33.0% (n=36) of its cohort, while the European-ancestry and Mixed-ancestry cohorts consisted of 23.3% (n=24) and 20.8% (n=20), respectively.

The Type IIIA LSTV was the most prevalent in the Mixed-ancestry cohort at 9.4% (n=9) while the European-ancestry and African-ancestry cohorts consisted of 5.8% (n=6) and 2.8% (n=3), respectively.

The Type IIIB LSTV was most prevalent in the European-ancestry cohort accounting for 27.2% (n=28) of its cohort. The African-ancestry and Mixed-ancestry cohorts consisted of 20.2% (n=22) and 17.7% (n=17) respectively.

The least common of the subtypes of LSTV, the Type IV LSTV was found in the greatest number in the Mixed-ancestry cohort at 6.3% (n=6) while the European-ancestry cohort had 4.9% (n=5) and the African-ancestry cohort accounted for 2.8% (n=3). Refer to Figure 3.10 to compare the LSTV Types found in each of the three ancestral cohorts.

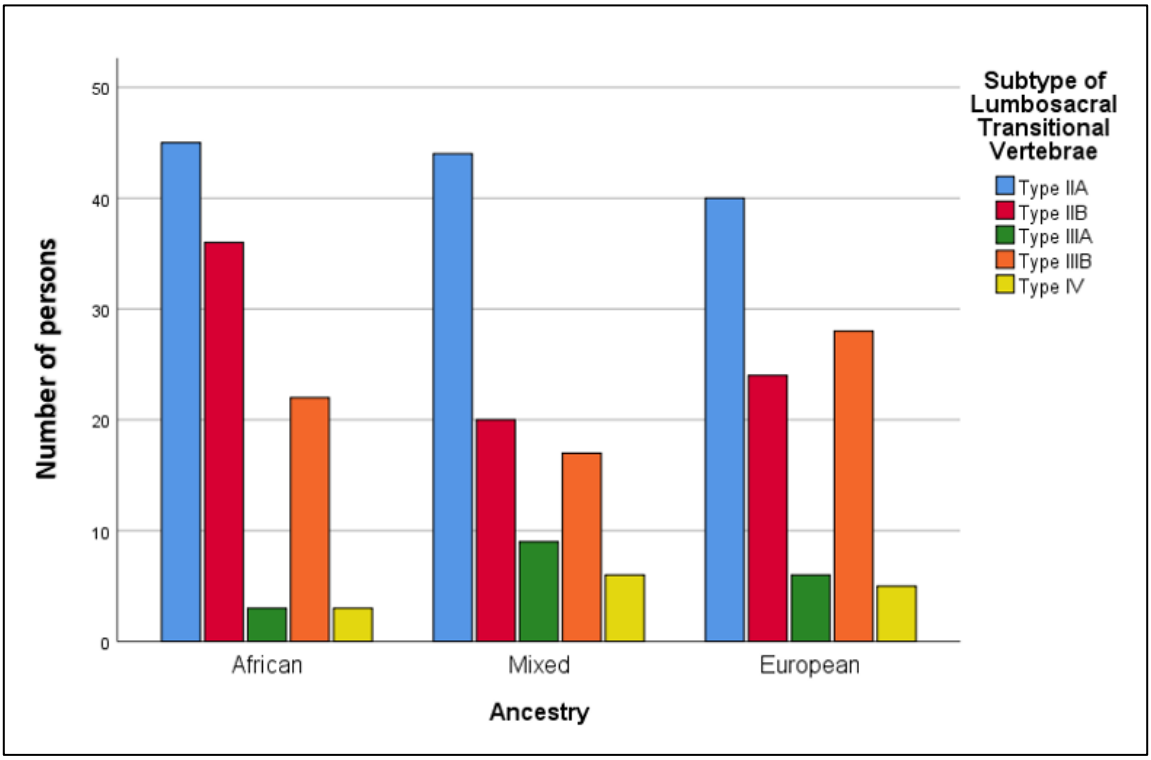

Figure 3.10: *Subtype of lumbosacral transitional vertebrae cohort by ancestry. The key is in the top right corner.*

Frequency of side of lumbosacral transitional vertebrae

The following were the results for the evaluation of LSTV by their frequency of side: the largest category for frequency of side location was 'bilateral' which accounted for 47.7% (n=147) of the sample.

The second-largest category for frequency of side was the 'left' side in 26.6% (n=82) while the 'right' side accounted for 21.1% (n=65) of the sample.

The least by number was classified as 'other', representing a Type IV LSTV at 4.5% (n=14) in the sample. The Type IV could not be categorised by side. Refer to Table 3.6 to summarise the findings for frequency of side associated with LSTV within this cohort.

Table 3.6: Frequency of side of lumbosacral transitional vertebrae in the imaging cohort.

Side	Frequency	Percentage
Left	82	26.6
Right	65	21.1
Bilateral	147	47.7
Other*	14	4.5
Total	**308**	100

** 'Other' represents a Type IV LSTV. There is no designated frequency of side nomenclature for this LSTV subtype. Therefore, it could not be assigned a side.*

Frequency of side and ancestry of lumbosacral transitional vertebrae

For the evaluation of LSTV concerning their frequency of side and ancestry, the following were the results: regarding a single side presentation for frequency of side, the largest category was 'bilateral'. The African-ancestry, European-ancestry and Mixed-ancestry cohorts contained 53.2% (n=58), 50.5% (n=52) and 38.5% (n=37) respectively.

The 'left' side was the second-largest category. The Mixed-ancestry cohort contained 33.3% (n=32), while the African-ancestry and European-ancestry cohorts represented 25.7% (n=28) and 21.4% (n=22) of the sample with a left-sided LSTV.

The third-largest category of frequency of side was classified as 'right'. The European-ancestry cohort had the largest representation at 23.3% (n=24) while the Mixed-ancestry and African-ancestry cohorts consisted of 21.9% (n=21) and 18.3% (n=20) of the sample representing a right-sided LSTV.

Regarding 'other', the Mixed-ancestry cohort accumulated the greatest quantity with 6.3% (n=6) while the European-ancestry and African-ancestry cohorts amounted to 4.9% (n=5) and 2.8% (n=3) of the sample. Refer to Figure 3.11 to compare the LSTV Types found in each of the three ancestral cohorts. Refer to Figure 3.11 to compare the frequency of the side found in each of the three ancestral cohorts.

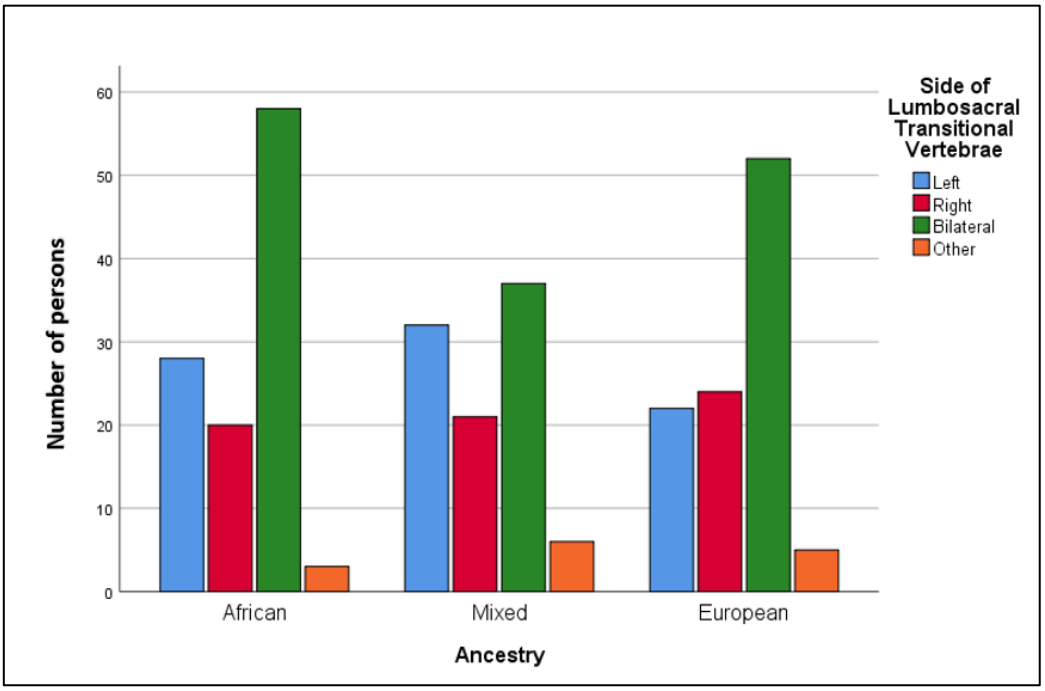

Figure 3.11**:** *Frequency of side of lumbosacral transitional vertebrae grouped by ancestry. The key is in the top right corner.*
Other: *Refers to the Type IV lumbosacral transitional vertebrae morphology which has no designated preference of side.*

Subtypes and frequency of side of lumbosacral transitional vertebrae

Lumbosacral transitional vertebrae subtypes and their frequency of side were found in the following proportions: the largest category for subtypes of LSTV and their frequency of side was the 'Type II bilateral' at 26.0% (n=80) of the sample.

The second-largest number was the 'Type IIA left' and the third-largest number 'Type III bilateral' consisted of 23.1% (n=71) and 21.8% (n=67) of the sample.

The ‘Type IIA right’ accounted for 18.8% (n=58) of the sample. Lastly the ‘Type IIIA left’ (n=9) and the ‘Type IIIA right’ (n=9) contained the least number with 2.9% of the sample.

The Type IV could not be listed for frequency of side. Type IV LSTV contributed to 4.5% (n=14) of the sample. Refer to Table 3.7 for a summary of the findings of LSTV Subtype and frequency of side consisted of within this cohort.

Table 3.7: Subtypes and frequency of side of lumbosacral transitional vertebrae in the imaging cohort.

	SUBTYPES AND FREQUENCY OF SIDE							TOTAL
	TYPE IIA LEFT	TYPE IIA RIGHT	TYPE IIB	TYPE IIIA LEFT	TYPE IIIA RIGHT	TYPE IIIB	TYPE IV	
COUNT	71	58	80	9	9	67	14	**308**
PERCENTAGE	23.1%	18.8%	26.0%	2.9%	2.9%	21.8%	4.5%	100.0%

Subtypes, ancestry and frequency of side of lumbosacral transitional vertebrae

For the evaluation of LSTV subtypes by their frequency of side and ancestry, the following were the results: regarding ‘Type II Bilateral’, the African-ancestry cohort consisted of 33.0% (n=36), the European-ancestry cohort consisted of 23.3% (n=24) and the Mixed-ancestry cohort consisted of 20.8% (n=20) of the sample.

The second-largest category was the ‘Type IIA Left’. The Mixed-ancestry cohort consisted of 27.1% (n=26) while the African-ancestry cohort consisted of 23.9% (n=26), and the European-ancestry cohort consisted of the least at 18.4% (n=19) of the sample.

The ‘Type IIA Right’ was found in the European-ancestry cohort at 20.4% (n=21), the Mixed-ancestry cohort accounted for 18.8% (n=18), and the African-ancestry cohort consisted of 17.4% (n=19) of the sample.

With regards to the ‘Type III Bilateral’, the European-ancestry cohort consisted of 27.2% (n=28), the African-ancestry and Mixed-ancestry cohorts contained 20.2% (n=22), and 17.7% (n=17) of the sample, respectively.

The ‘Type IIIA Left’ was found in the Mixed-ancestry cohort at 5.2% (n=5), the European-ancestry cohort consisted of 1.9% (n=2), and the African-ancestry cohort consisted of 1.8% (n=2) of the sample.

The ‘Type IIIA Right’ was found in the Mixed-ancestry cohort at 4.2% (n=4), the European-ancestry and African-ancestry cohorts consisted of 3.9% (n=4), and 0.9% (n=1) of the sample, respectively.

Regarding the ‘Type IV’, this was found in the greatest number in the Mixed-ancestry cohort with 6.3% (n=6) while the European-ancestry and African-ancestry cohorts comprised of 4.9% (n=5), and 2.8% (n=3) of the sample, respectively.

Refer to Figure 3.9 for a comparison of the LSTV Types found in each of the three ancestral cohorts, while Figure 3.12 provides a comparison of the frequency of the side found in each of the three ancestral cohorts.

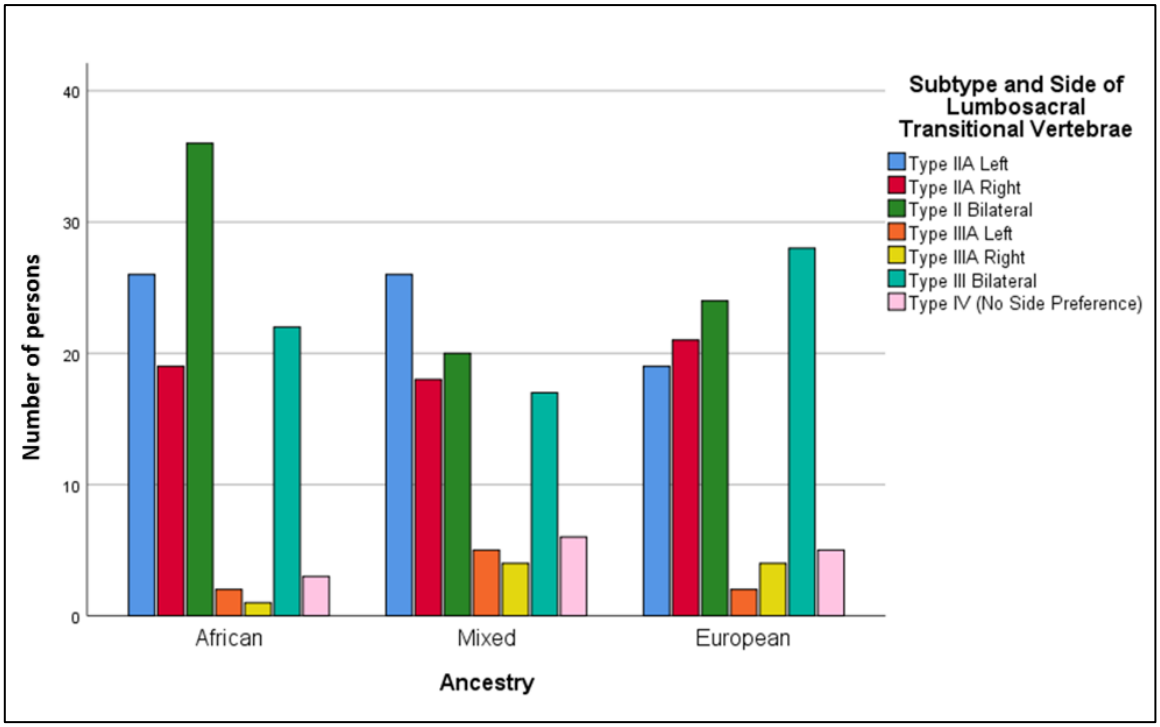

Figure 3.12: *Subtypes and frequency of side of lumbosacral transitional vertebrae grouped by ancestry. The key is in the top right corner.*

Spinal enumeration of lumbosacral transitional vertebrae

Lumbar spine enumeration was subdivided into sacralisation and lumbarisation. The majority of spinal enumeration associated with LSTV was sacralisation representing 64.0% (n=197/308), while lumbarisation accounted for 36.0% (n=111/308) of the sample.

Spinal enumeration and ancestry of lumbosacral transitional vertebrae

Sacralisation in the African-ancestry cohort consisted of the greatest proportion by number at 67.0% (n=73) while the Mixed-ancestry cohort consisted of the greatest proportion by percentage at 72.9% (n=70). Lastly, the European-ancestry cohort consisted of the least in both number and percentage at 52.4% (n=54) of the sample.

Lumbarisation was found in the European-ancestry cohort in the greatest number at 47.6% (n=49). The African-ancestry cohort consisted of 33.0% (n=36) and the Mixed-ancestry cohort consisted of 27.1% (n=26) of the sample. Refer to Figure 3.13 to compare of the frequency of side of LSTV found in each of the three ancestral cohorts.

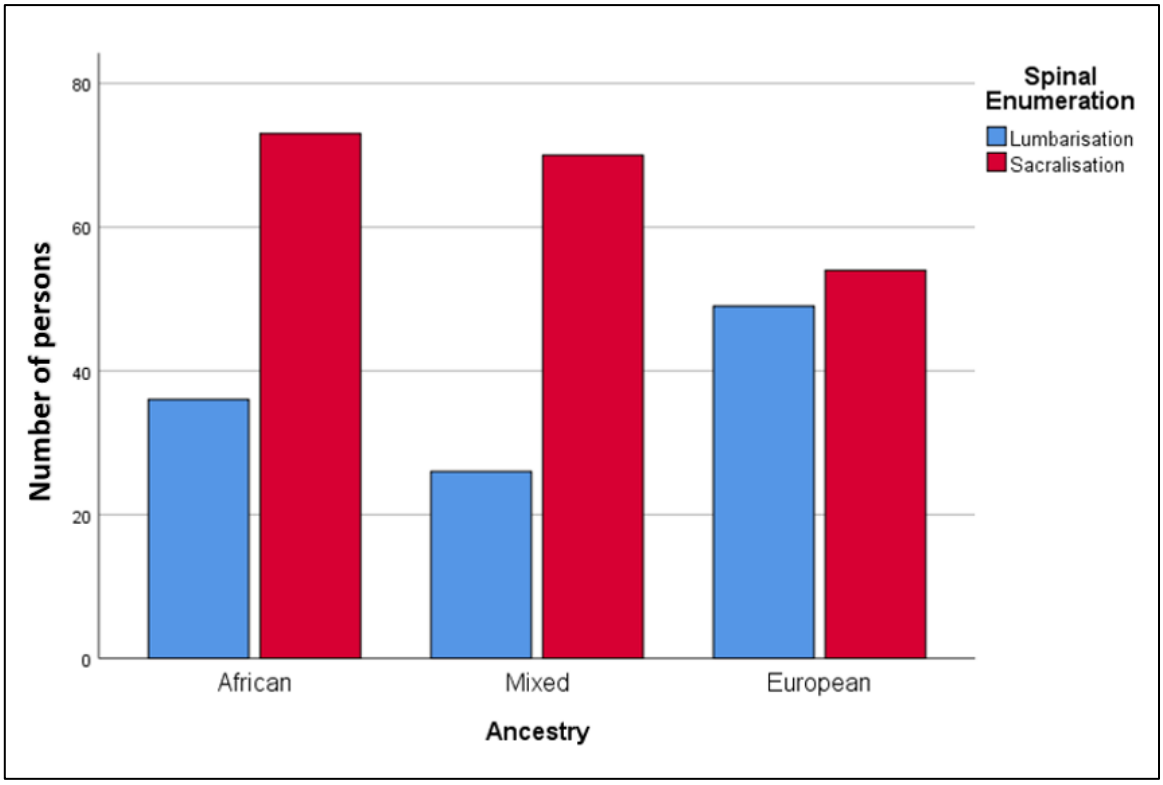

Figure 3.13: *Spinal enumeration of lumbosacral transitional vertebrae grouped by ancestry. The key is located in the top right corner.*

A summary of the ancestry, sex, subtypes, frequency of side and spinal enumeration of the lumbosacral transitional vertebrae cohort is displayed in Table 3.8.

Table 3.8: Summary of ancestry, sex, subtype, frequency of side and spinal enumeration of the lumbosacral transitional vertebrae in the imaging cohort.

SEX	ANCESTRY		SUBTYPE and FREQUENCY OF SIDE							ENUMERATION		TOTAL
			TYPE IIA LEFT	TYPE IIA RIGHT	TYPE IIB	TYPE IIIA LEFT	TYPE IIIA RIGHT	TYPE IIIB	TYPE IV	SACRALISATION	LUMBARISATION	
FEMALE	AFRICAN	Count	10	12	23	1	1	12	2	39	22	61
		% within ancestry	16.4%	19.7%	37.7%	1.6%	1.6%	19.7%	3.3%	63.9%	36.1%	100.0%
	MIXED	Count	14	9	11	2	3	9	6	37	17	54
		% within ancestry	25.9%	16.7%	20.4%	3.7%	5.6%	16.7%	11.1%	68.5%	31.5%	100.0%
	EUROPEAN	Count	7	15	9	1	3	14	2	28	23	51
		% within ancestry	13.7%	29.4%	17.6%	2.0%	5.9%	27.5%	3.9%	54.9%	45.1%	100.0%
SUB-TOTAL		Count/ % Total	31 18.7%	36 21.7%	43 25.9%	4 2.4%	7 4.2%	35 21.1%	10 6.0%	104 62.7%	62 37.3%	166 100.0%
MALE	AFRICAN	Count	16	7	13	1	0	10	1	34	14	48
		% within ancestry	33.3%	14.6%	27.1%	2.1%	0.0%	20.8%	2.1%	70.8%	29.2%	100.0%
	MIXED	Count	12	9	9	3	1	8	0	33	9	42
		% within ancestry	28.6%	21.4%	21.4%	7.1%	2.4%	19.0%	0.0%	78.6%	21.4%	100.0%
	EUROPEAN	Count	12	6	15	1	1	14	3	26	26	52
		% within ancestry	23.1%	11.5%	28.8%	1.9%	1.9%	26.9%	5.8%	50.0%	50.0%	100.0%
SUB-TOTAL		Count/ % Total	40 28.2%	22 15.5%	37 26.1%	5 3.5%	2 1.4%	32 22.5%	4 (2.8%	93 65.5%	49 34.5%	142 100.0%
TOTAL		Count/ % Total	71 23.1%	58 18.8%	80 26.0%	9 2.9%	9 2.9%	67 21.8%	14 4.5%	209 67.9%	85 27.6%	308 100.0%

Statistical analyses of the lumbosacral transitional vertebrae

Statistical analyses were performed on the imaging cohort using IBM® SPSS® statistics software version 25.0 (IBM Corp. 2015). In the reporting of the results of the analyses, two decimal places were retained throughout. For statistical analyses of the imaging sample, the LSTV sample was divided into categorical cohorts, namely Type, subtype and frequency of side, etc., and these were reflected in Tables 3.5 to 3.9. Cross-tabulation describes the relationships between categorical variables. The categorical variables included ancestry, sex, LSTV Type, LSTV subtype, side and spinal enumeration. The following combinations were used in the statistical analyses performed.

- Ancestry (independent variable);
- Sex (independent variable); and
- Sex and ancestry (dual variable).

The above-mentioned factors, ancestry, sex and a combination of the ancestry with sex were compared against:

- Types of LSTV;
- Subtypes of LSTV;
- Frequency of side of LSTV;
- Subtypes and frequency of side of LSTV; and
- Spinal enumeration of LSTV.

Age was not considered in the analyses as LSTV is congenital, and therefore age has no direct bearing on the presence of LSTV. This being said, Jancuska et al. (2015) stated that pseudo-articulation is susceptible to arthritic changes so it is possible that ageing may affect accessory articulation appearance on radiographs. A wide range of age was accepted for the investigation to mitigate age-related degenerative changes that may obscure accurate classification LSTV.

The assumptions for non-parametric techniques

Non-parametric techniques have less stringent assumptions over parametric techniques and there are general assumptions to be complied with. These assumptions are listed below (Pallant, 2013).

1. Randomness

The term randomness refers to a random sample drawn from the population, free of selection bias. It is one of the essential assumptions for valid statistical results (Verma et al. 2019).

2. Independent observation

Only a single case, person or sample can be counted at any point in the analyses. They cannot appear in more than one cohort or category and the data from one subject cannot influence the data from another. There may be exceptions in certain repeated measurement techniques such as the Wilcoxon Signed Rank and Friedman Tests (Pallant, 2013; Verma et al., 2019).

Chi-squared test (X^2)

The X^2 test is a non-parametric test that can be used to test three types of statistical tests: Goodness of Fit, Independence, and *Homogeneity*. The X^2 test of independence test was used in the statistical analyses to compare if two or more categorical variables were related (Pallant, 2013; Durrheim and Tredoux, 2014; Verma et al., 2019). This testing method compares the observed frequencies or proportions of cases in each category (Pallant, 2013). A p-value was set at $p \leq 0.05$, indicating statistical significance (Pallant, 2013). Tables must be greater than two columns and two-rows (2x2). The null hypothesis associated with the X^2 test states that variables are unrelated. Therefore, a statistically significant test result rejects the null hypothesis and reveals a relationship between variables.

Two conditions need to be met for the use of X^2 test (Pallant, 2013; McHugh, 2013; Durrheim and Tredoux, 2014; Verma et al., 2019):

1. Each observation is independent of others (one observation being tested at a time).

2. The data in cells should be represented as counts or frequencies and not as percentages. The expected counts per cell should not be less than five for two categories.

For more than two categories, the expected per-cell count cannot be less than one and is not cannot have more than 20% of the categories with expected counts less than five. In other words, 80% of cells must contain counts of five or more.

Fisher's Exact Probability Test

If a table did not meet the second condition of use for the X^2 test, then Fisher's Exact Probability Test was used. Categorical data that displayed cohorts that were too small to make statistical inferences were then described according to the general trends observed.

Ancestry

Ancestry and Types of lumbosacral transitional vertebrae

The African-, Mixed- and European-ancestry cohorts were compared to the Type of LSTV found on radiographs (Types II-IV). The X^2 test could not be used for statistical inference as it did not meet the second condition for its use, namely that the expected per-cell count was lower than five for 33.3% of cells (X^2=4.553, df=4, p=0.336). The general trend across the three cohorts demonstrated comparable numbers for each LSTV Type. The African-ancestry cohorts consisted of the greatest number for the Type II LSTV.

The European-ancestry cohort consisted of the highest number of Type III LSTV and the Mixed-ancestry consisted of the greatest number of Type IV LSTV.

Further analysis was performed with the removal of the Type IV LSTV cohort and the result was that no statistically significant difference could be attributed to ancestry and LSTV Type (X^2=3.058, df=2, p=0.217). Therefore, the null hypothesis stands, i.e. no relationship is demonstrated between ancestry and LSTV Type (Types II and III). Refer to Table 3.8.

Ancestry and Subtype of lumbosacral transitional vertebrae

The African-, Mixed- and European-ancestry cohorts were compared to the LSTV subtype found on radiographs (Types IIA, B, IIIA, B and Type IV). The X^2 test could be conducted as it met the necessary parameters for statistical inference.

No significant statistical significance could be attributed to ancestry and LSTV subtype (X^2=11.423, df=8, p=0.179). Therefore, the null hypothesis stands, i.e. no relationship is demonstrated between ancestry and LSTV subtype. Refer to Table 3.8.

Ancestry and frequency of side of lumbosacral transitional vertebrae

The African-, Mixed- and European-ancestry cohorts were compared to the frequency of side of the LSTV found on radiographs (left, right, bilateral and other). The X^2 test could not be used for statistical inference as the expected count did not meet the second condition for its use; the expected per-cell count was lower than five for 25.0% of cells (X^2=7.341, df=6, p=0.290). The general trend across the three cohorts was bilateral presentation as the largest component in number with the African-ancestry cohort, consisting of the greatest number of bilateral presentations followed by European-ancestry and then Mixed-ancestry. Right-sided frequency of preference showed comparable numbers throughout the ancestry cohorts.

Further analyses were performed with the removal of the Type IV LSTV cohort. No significant statistical significance could be attributed to ancestry and frequency of side (X^2=5.912, df=4, p=0.206). Therefore, the null hypothesis stands, i.e. no relationship is demonstrated between ancestry and LSTV frequency of side (left, right and bilateral).

Ancestry, Subtype and frequency of side of lumbosacral transitional vertebrae

The African-, Mixed- and European-ancestry cohorts were compared to the frequency of sides found on radiographs (left, right, bilateral and other). The X^2 test could not be used for statistical inference as the expected count did not meet the second condition for its use; the expected per cell was lower than five for 42.0% of cells (X^2=13.728, df=12, p=0.318).

The general trend across the three cohorts was that the European-ancestry cohort consisted of the greatest percentage of Type IIA right and Type IIIB LSTV while the Mixed-ancestry cohort consisted of the greatest percentage of Type IIA left, Type IIIA left, Type IIIA right, and Type IV LSTV and the African-ancestry cohort consisted of the greatest percentage of Type IIB LSTV. There is not enough evidence to suggest an association between ancestry, subtype and frequency of side of LSTV.

Ancestry and spinal enumeration of lumbosacral transitional vertebrae

The African, Mixed and European-ancestry cohorts were compared to the difference in the proportion of spinal enumeration found on radiographs (sacralisation and lumbarisation). The X^2 test could be conducted as it met the necessary parameters for statistical inference. A statistical significance was identified between ancestry and spinal enumeration (X^2=9.713, df=2, p=0.008), with a small effect size (V=0.178) as indicated by the Cramer's V test and effect size table (Table 2.4). This may be interpreted as a difference between the African-ancestry and Mixed-ancestry cohort when compared to the European-ancestry cohort. The African-ancestry (67.0%) and Mixed-ancestry (72.9%) demonstrated a greater propensity for sacralisation, while the European-ancestry demonstrated only marginally in favour of sacralisation (52.4%) preference. Therefore, the null hypothesis is rejected, and a relationship with small effect size is established between the spinal enumeration for the African-ancestry and Mixed-ancestry cohorts demonstrating sacralisation compared to the European-ancestry cohort demonstrating lumbarisation predilection. Refer to Figure 3.21 and Table 3.8.

Sex

Sex and Type of lumbosacral transitional vertebrae

The sex was compared to the Type of LSTV found on radiographs (Types II, III and Type IV). The X^2 test could be conducted as it met the necessary parameters for statistical inference. No significant statistical significance could be attributed to sex and Type of LSTV (X^2=1.868, df=2, p=0.393).

Further analysis was performed with the removal of the Type IV LSTV cohort, and the result was such that there was no change to the statistical analysis outcome for the female cohort (X^2=2.181, df=2, p=0.336) or the male cohort (X^2=1.015, df=2, p=0.602).

Therefore, the null hypothesis stands, i.e. no relationship is demonstrated between sex and LSTV Type. Refer to Figure 3.14.

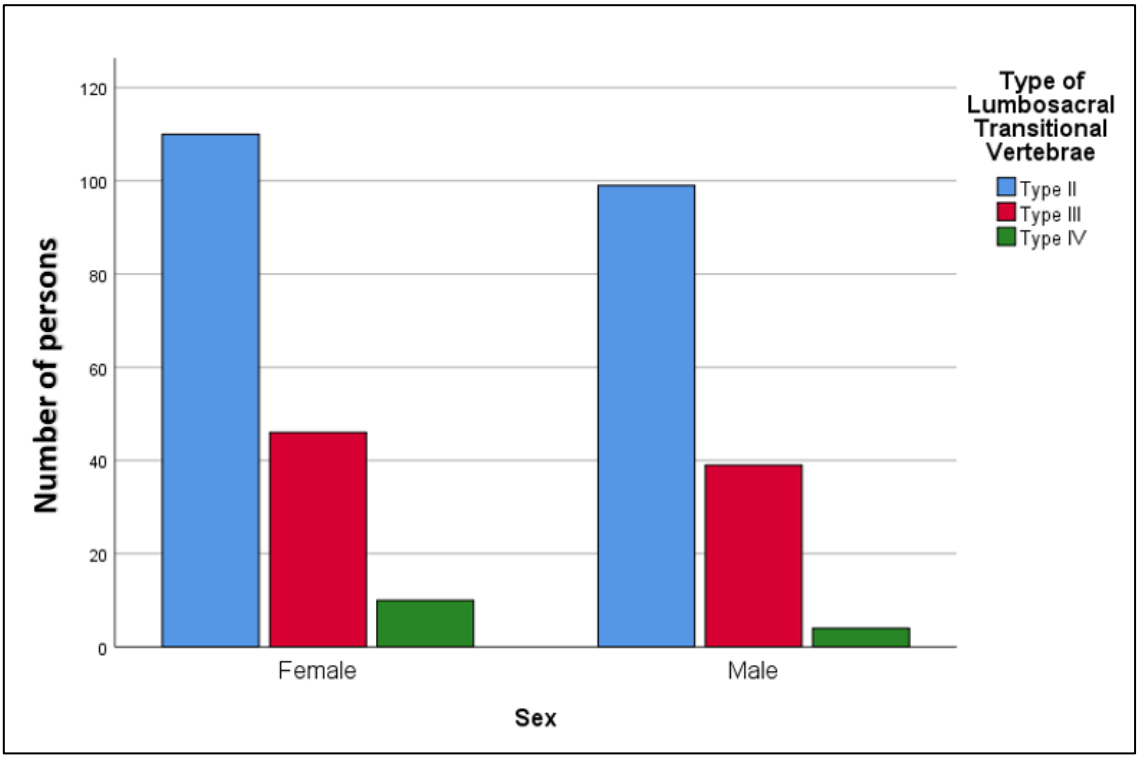

Figure 3.14: *Sex and Type of lumbosacral transitional vertebrae. The key is located in the top right corner.*

Sex and subtype of lumbosacral transitional vertebrae

The sex was compared to the subtype of LSTV identified on radiographs (Types IIA, B, IIIA, B and IV). The X^2 test could be conducted as it met the necessary parameters for statistical inference. No significant statistical significance could be attributed to ancestry and LSTV subtype (X^2=2.383, df=4, p=0.666). Therefore, the null hypothesis stands, i.e. no relationship is demonstrated between sex and LSTV subtype. Refer to Figure 3.15.

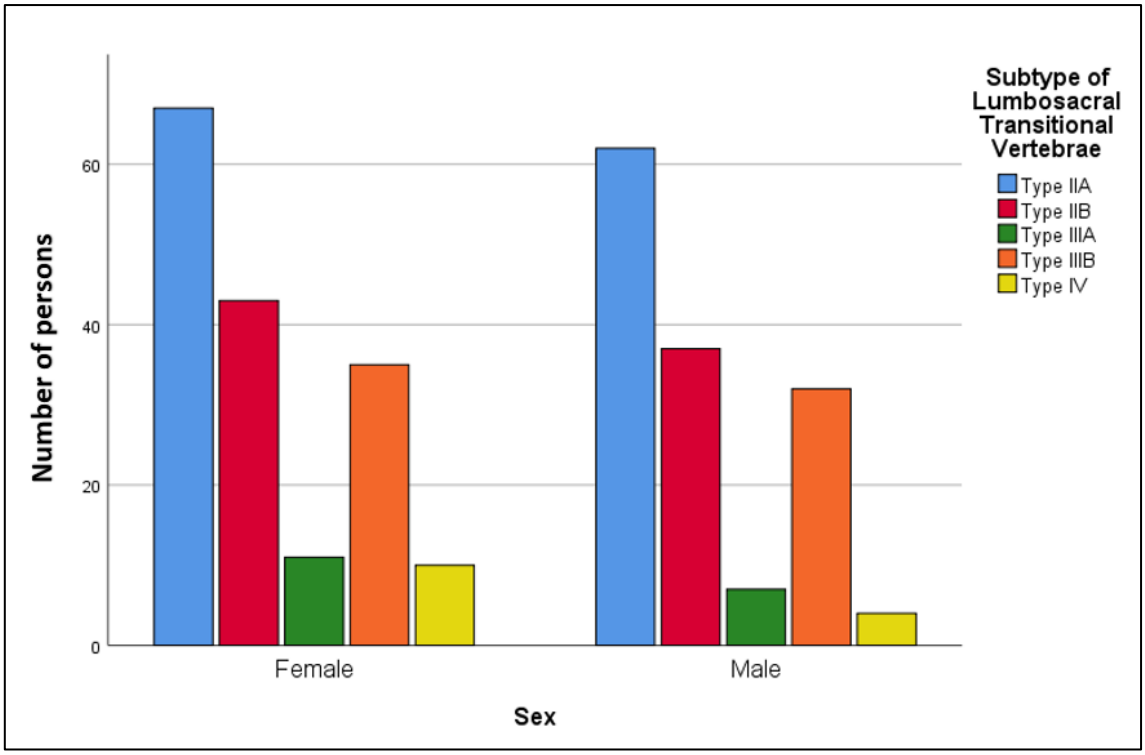

Figure 3.15: *Sex and subtype of lumbosacral transitional vertebrae. The key is located in the top right corner.*

Sex and frequency of side of lumbosacral transitional vertebrae

The sex was compared to the frequency of the side of LSTV found on radiographs (right, left, bilateral and other). '*Other*' refers to the Type IV LSTV which has no preference of side. The X^2 test could be conducted as it met the necessary parameters for statistical inference. No significant statistical significance could be attributed to ancestry and frequency of side of LSTV (X^2=6.519, df=3, p=0.089). Therefore, the null hypothesis stands, i.e. no relationship is demonstrated between sex and the frequency of side. Refer to Figure 3.16.

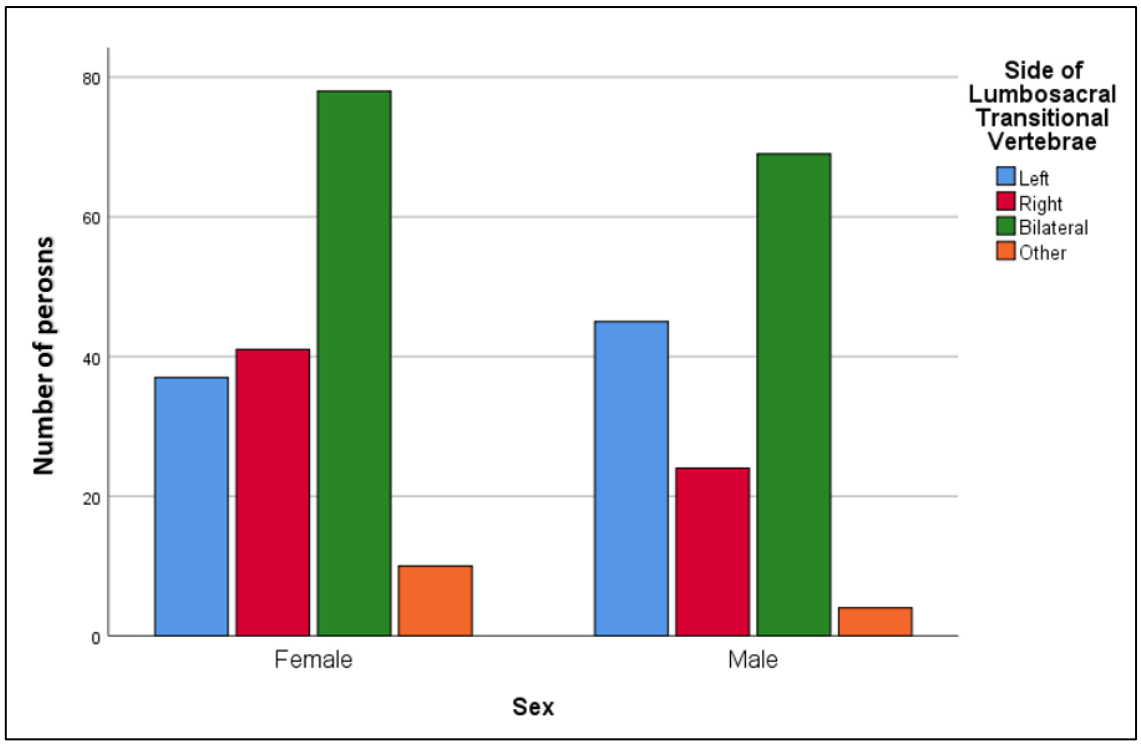

Figure 3.16: *Sex and frequency of side of lumbosacral transitional vertebrae.* ***Other:*** *Refers to the Type IV lumbosacral transitional vertebrae morphology which has no preference of side. The key is located in the top right corner.* ***Other:*** *Refers to the Type IV lumbosacral transitional vertebrae morphology which has no designated preference of side.*

Sex, subtype and frequency of side of lumbosacral transitional vertebrae

The sex was compared to the frequency of side (left, right, bilateral and other) and Type of LSTV identified on radiographs (Types IIA, B, IIIA, B and IV). The X^2 test could not be used for statistical inference on all LSTV Types as the expected count did not meet the second condition for its use; the expected per cell were lower than five for 28.6% of cells (X^2=8.748, df=6, p=0.188). The general trend found that the female cohort consisted of the greatest number of Type IIB followed by right-sided Type IIA and Type IIB. The general trend in the male cohort was that men consisted of the largest number of left-sided Type IIA followed by Type IIB and then Type IIIB. There is not enough evidence to suggest an association between sex, subtype and frequency of the side of LSTV. Refer to Figure 3.17.

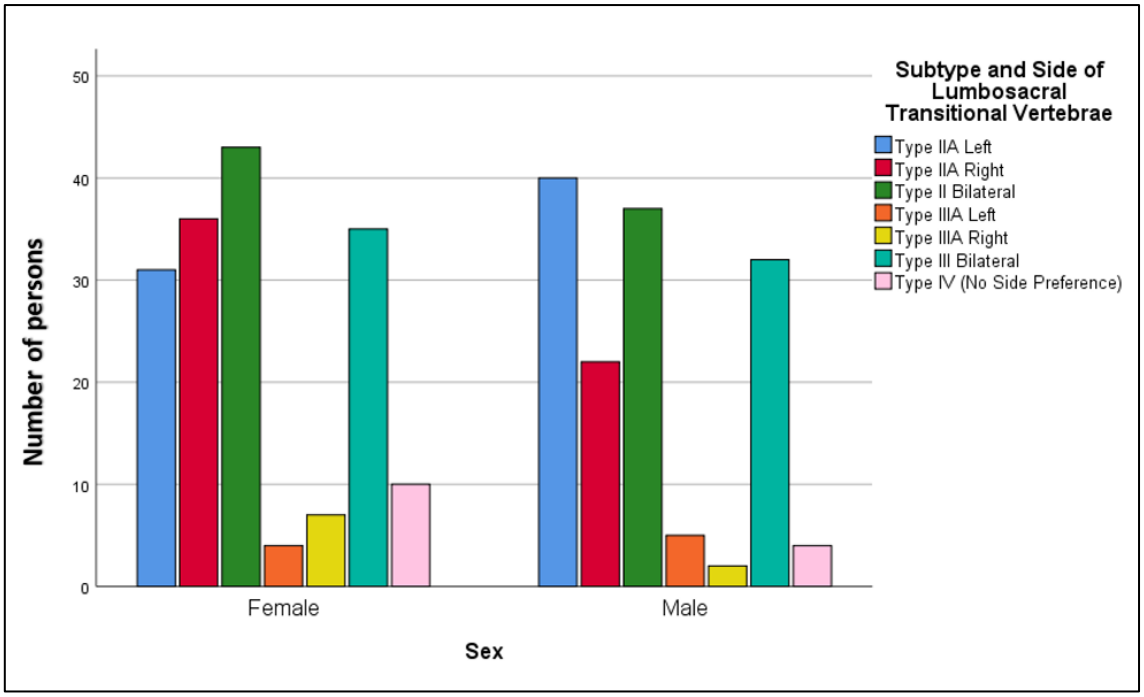

Figure 3.17: Sex and subtype of lumbosacral transitional vertebrae. The key is located in the top right corner.

Sex and spinal enumeration of lumbosacral transitional vertebrae

The sex was compared to spinal enumeration found on the radiographs (sacralisation and lumbarisation). The X^2 test could be conducted as it met the necessary parameters for statistical inference. Fisher's exact test was used for the analysis of the double column and row contingency table. No significant statistical significance could be attributed to sex and spinal enumeration (X^2=0.268, df=1, p=0.635). Therefore, the null hypothesis stands, i.e. no relationship is demonstrated between sex and spinal enumeration. Refer to Figure 3.18.

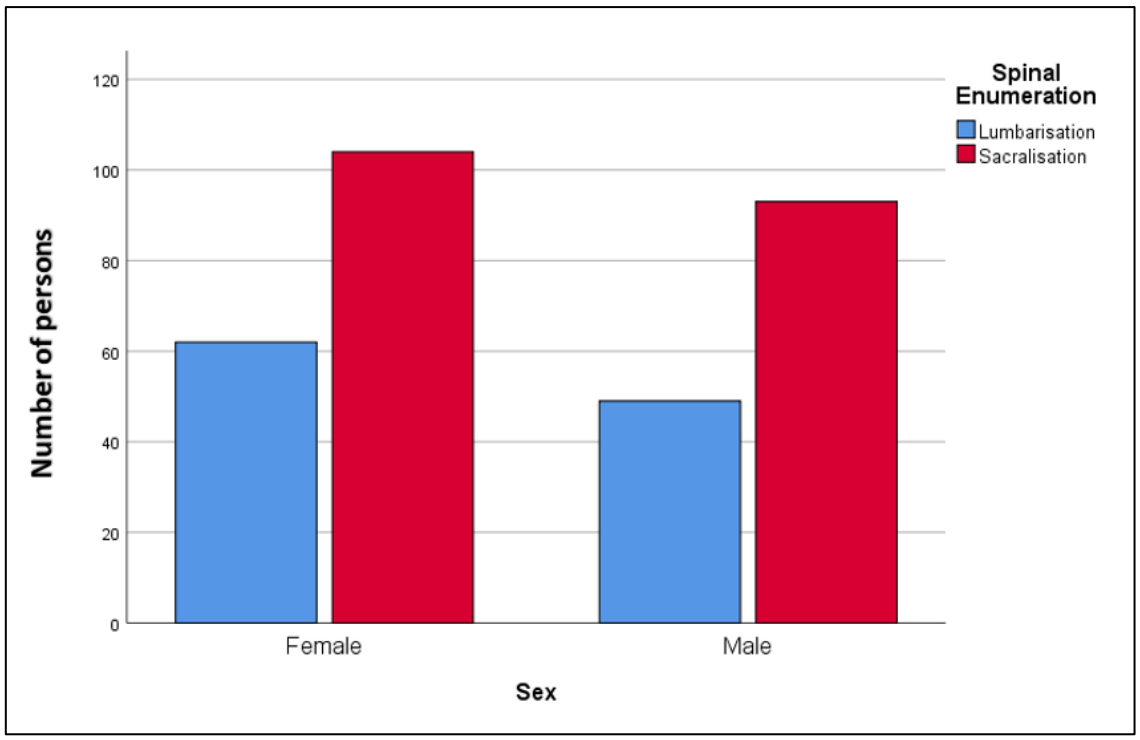

Figure 3.18: *Sex and spinal enumeration of lumbosacral transitional vertebrae. The key is located in the top right corner.*

SEX AND ANCESTRY (Cross-Tabulations Subdivided By Sex)

Sex, ancestry, and Type of lumbosacral transitional vertebrae

The sex and Type of LSTV (Types II, III and IV) were compared and assessed in the African-, Mixed- and European-ancestry cohorts. The X^2 test could not be used for statistical inference for the two sexes as the expected count did not meet the second condition for its use; the expected per-cell count for male and female was lower than five for 33.0% of cells, females (X^2=5.915, df=4, p=0.206) and males (X^2=3.972, df=4, p=0.410). Further analysis was performed with the removal of Type IV LSTV cohort, and the result was no change to the statistical analysis outcome in the female cohort (X^2=2.181, df=2, p=0.336) and in male cohort (X^2=1.015, df=2, p=0.602). The general trend in males and females was Type II accounted for the greatest number, followed by Type III and IV. The African-ancestry cohort consisted of the greatest number of Type II in both sexes while the European-ancestry consisted of the greatest number for Type III. There is not enough evidence to suggest an association between sex, ancestry and Type of LSTV. Refer to Figures 3.19 and 3.20.

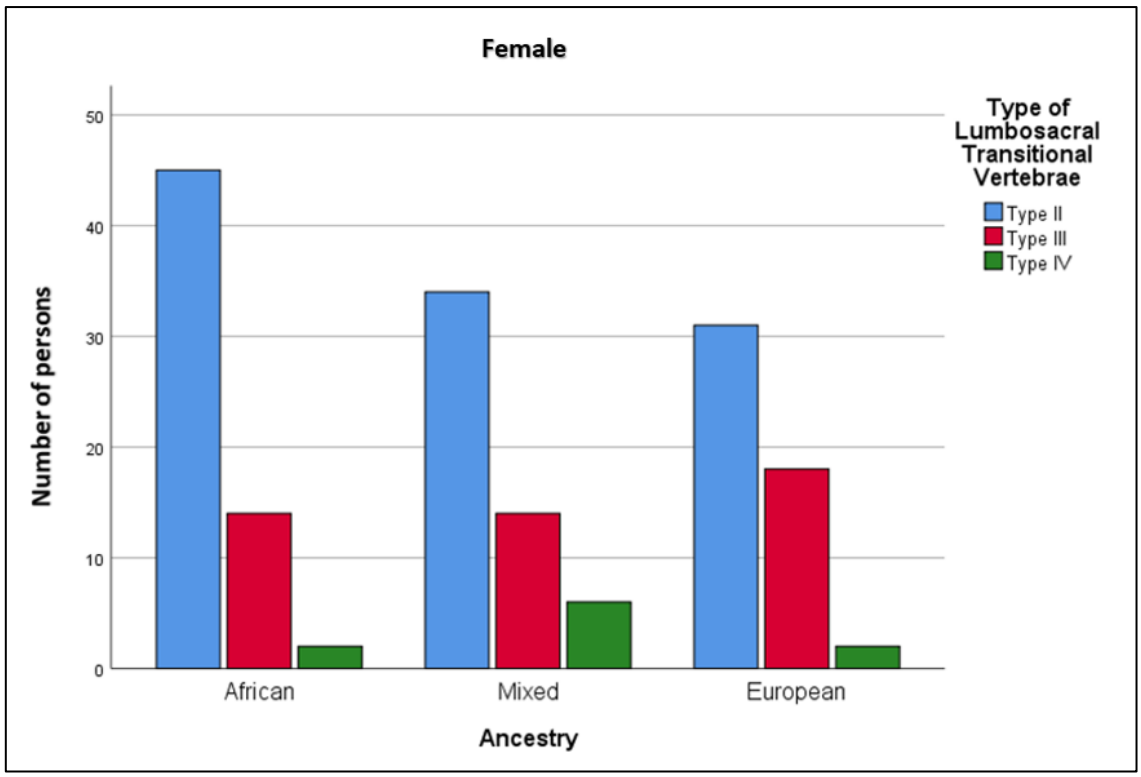

Figure 3.19: *Type of lumbosacral transitional vertebrae of women in the African, Mixed and European-ancestry cohorts. The key is located in the top right corner.*

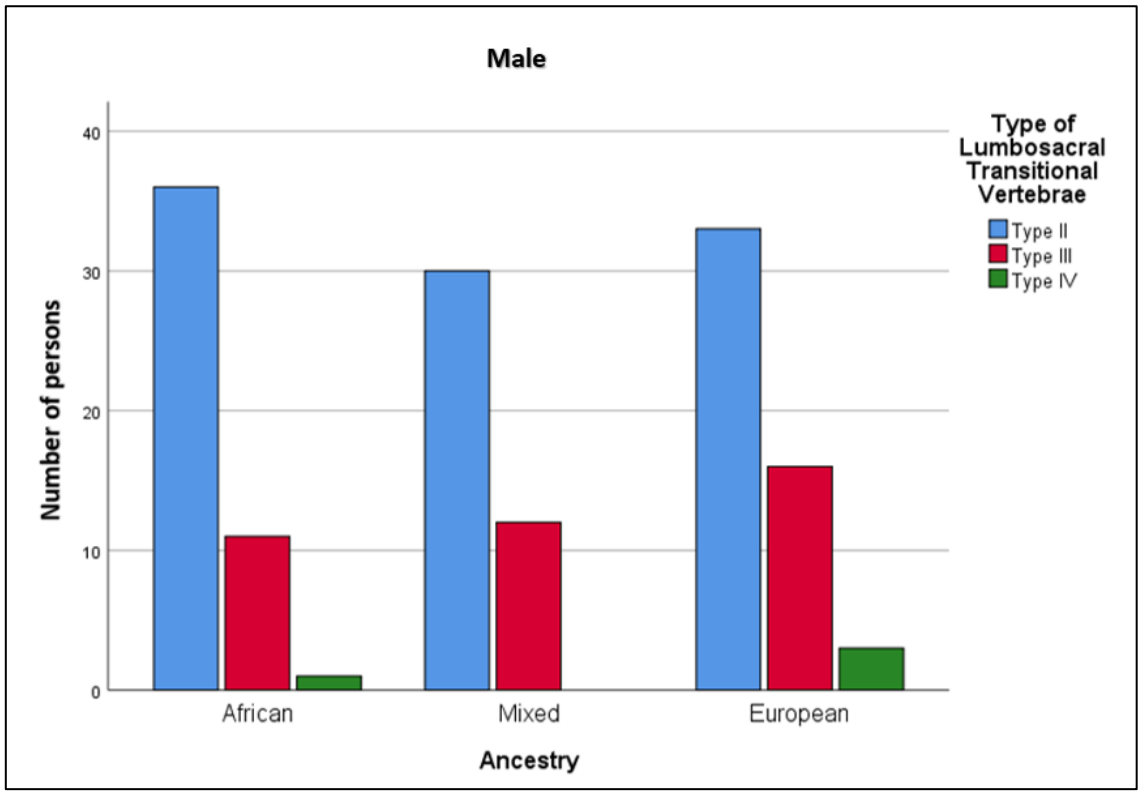

Figure 3.20: *Type of lumbosacral transitional vertebrae of men in the African, Mixed and European-ancestry cohorts. The key is located in the top right corner.*

Sex, ancestry and subtype of lumbosacral transitional vertebrae

The sex and subtype of LSTV (Type IIA, B; IIIA, B and IV) were compared and assessed in the African-, Mixed- and European-ancestry cohorts. The X^2 test could not be used for statistical inference for the two sexes as the expected count did not meet the second condition for its use; the expected per-cell count for male and female was lower than five for 40.4% of cells females (X^2=12.409, df=8, p= 0.134) and males (X^2=8.408, df=8, p=0.395). The general trend in males and females was Type II which accounted for the greatest number, followed by Type III and IV. The African-ancestry cohort consisted of the greatest number of Type II in both sexes while the European-ancestry consisted of the greatest number for Type III. There is not enough evidence to suggest an association between sex, ancestry and subtype of LSTV. Refer to Figures 3.21 and 3.22.

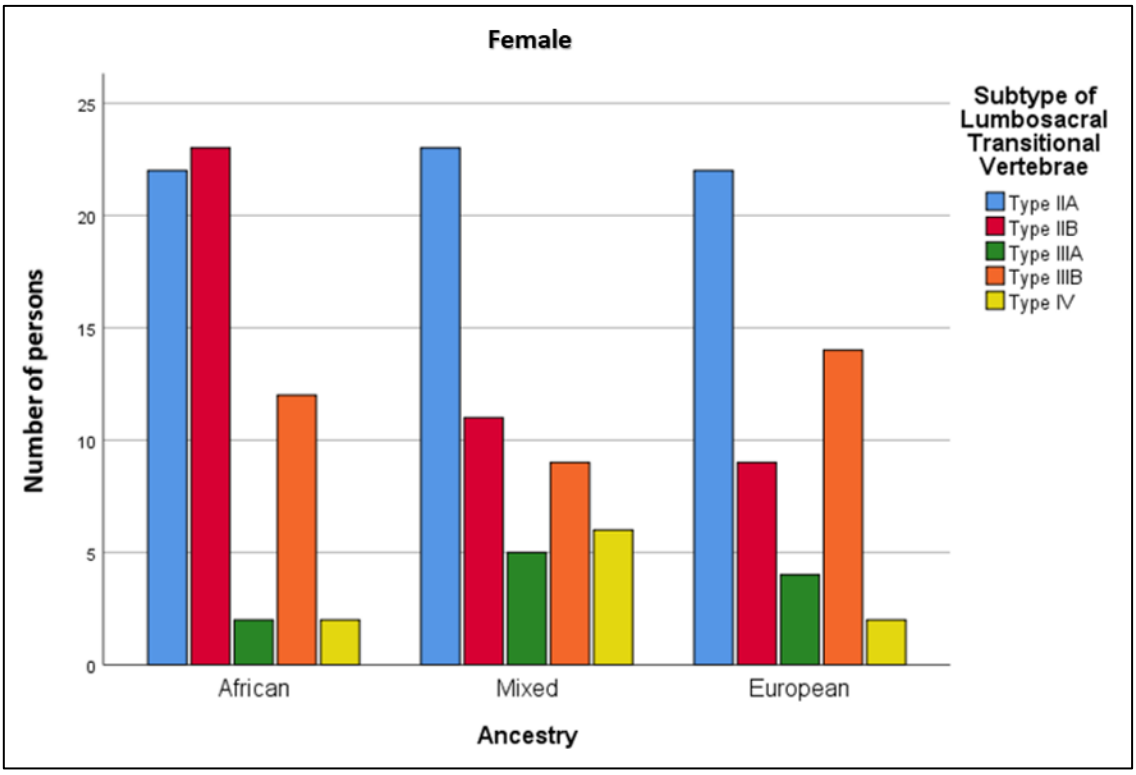

Figure 3.21: *Subtype of lumbosacral transitional vertebrae of women in the African, Mixed and European-ancestry cohorts. The key is located in the top right corner.*

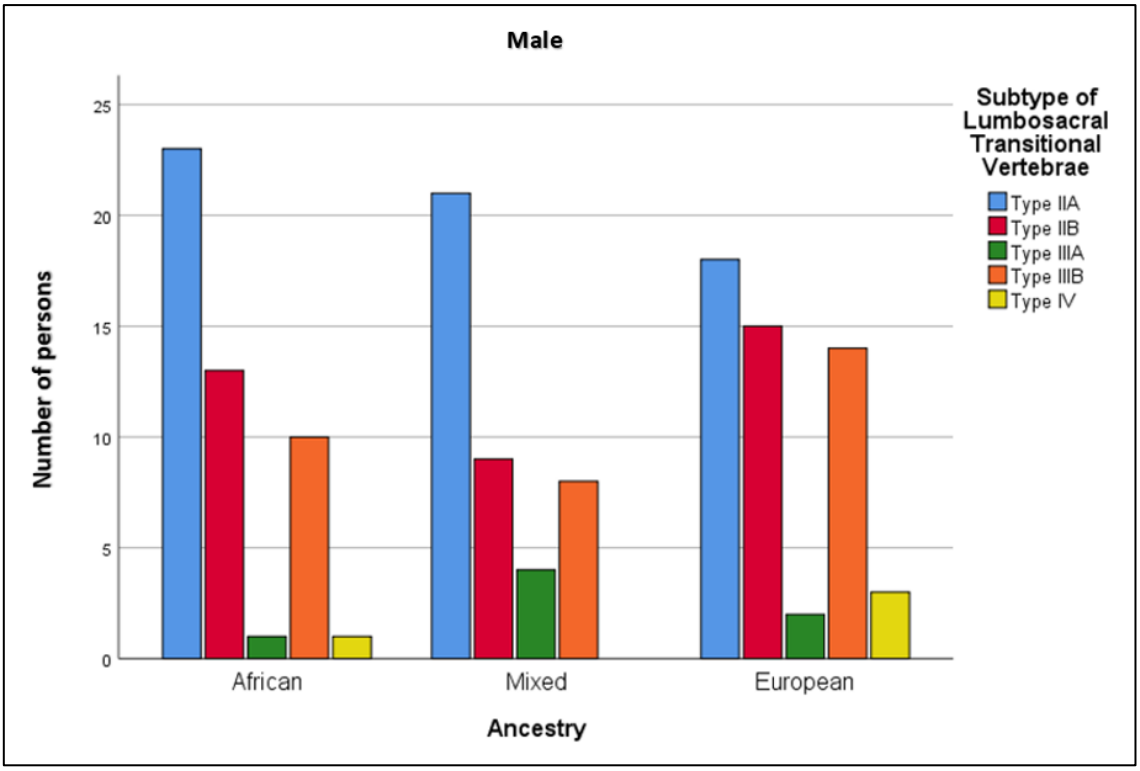

Figure 3.22: *Subtype of lumbosacral transitional vertebrae of men in the African, Mixed and European-ancestry cohorts. The key is located in the top right corner.*

Sex, ancestry and frequency of side of lumbosacral transitional vertebrae

The sex and the frequency of side (left, right, bilateral and other) of LSTV were compared and assessed in the African-, Mixed- and European-ancestry cohorts. The X^2 test could not be used for statistical inference for the sexes as the expected count did not meet the second condition for its use; the expected per-cell count for female (X^2=11.304, df=6, p=0.079) and male (X^2=6.871, df=6, p=0.333) were lower than five for 25.0% of cells. Further analysis was performed with the removal of the Type IV LSTV cohort ('other') and the result was no change to the statistical analysis outcome in the female cohort (X^2=7.717, df=4, p=0.103) and the male cohort (X^2=3.896, df=4, p=0.420).The general trend in males and females was Type II which accounted for the greatest number followed by Type III and IV. The African-ancestry cohort consisted of the greatest number of Type II in both sexes while the European-ancestry consisted of the greatest number for Type III. Refer to Figures 3.23 and 3.24.

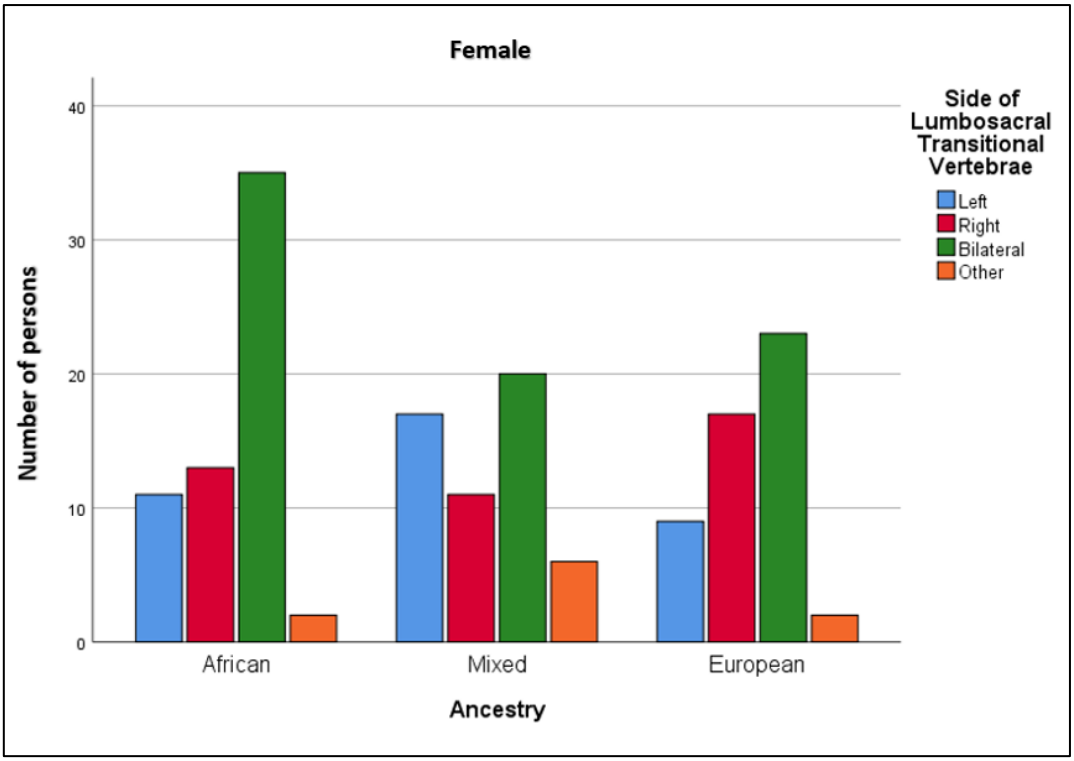

Figure 3.23: *Frequency of side of lumbosacral transitional vertebrae of women in the African, Mixed and European-ancestry cohorts. The key is located in the top right corner.* ***Other:*** *Refers to the Type IV lumbosacral transitional vertebrae morphology which has no designated preference of side.*

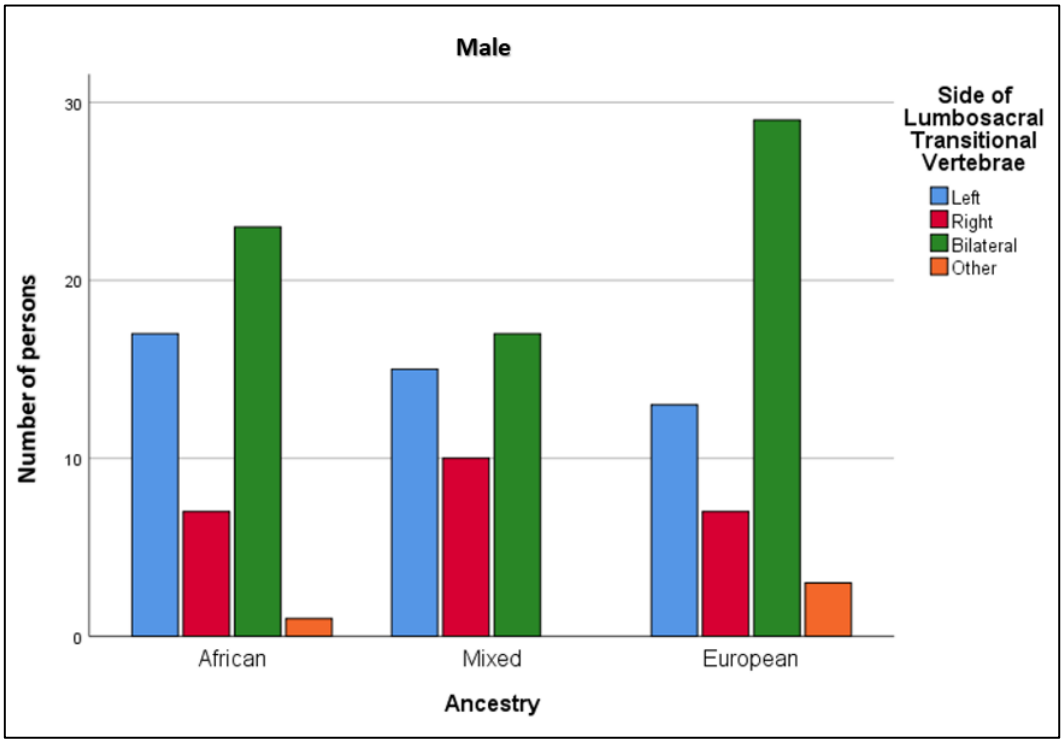

Figure 3.24: *Frequency of side of lumbosacral transitional vertebrae of men in the African, Mixed and European-ancestry cohorts. The key is located in the top right corner.* ***Other:*** *Refers to the Type IV lumbosacral transitional vertebrae morphology which has no designated preference of side.*

Ancestry, sex, subtype and frequency of side of lumbosacral transitional vertebrae

The sex and the frequency of side (left, right, bilateral and other) were compared and assessed in the African-, Mixed- and European-ancestry cohorts from the radiographs. The X^2 test could not be used for statistical inference for the two sexes as the expected count did not meet the second condition for its use; the expected per-cell count for male and female was lower than five for 42.9% of cells in females (X^2=16.854, df=12, p=0.155) and males (X^2=9.857, df=12, p=0.629). The findings were fluctuant, with no single trend seen between the sexes and ancestry cohorts. A consistent finding was that Type IIIA left and Type IIIA right were among the lowest in both sexes and all ancestry cohorts. There is not enough evidence to suggest an association between sex, ancestry, subtype and frequency of side of LSTV. Refer to Figures 3.25 and 3.26.

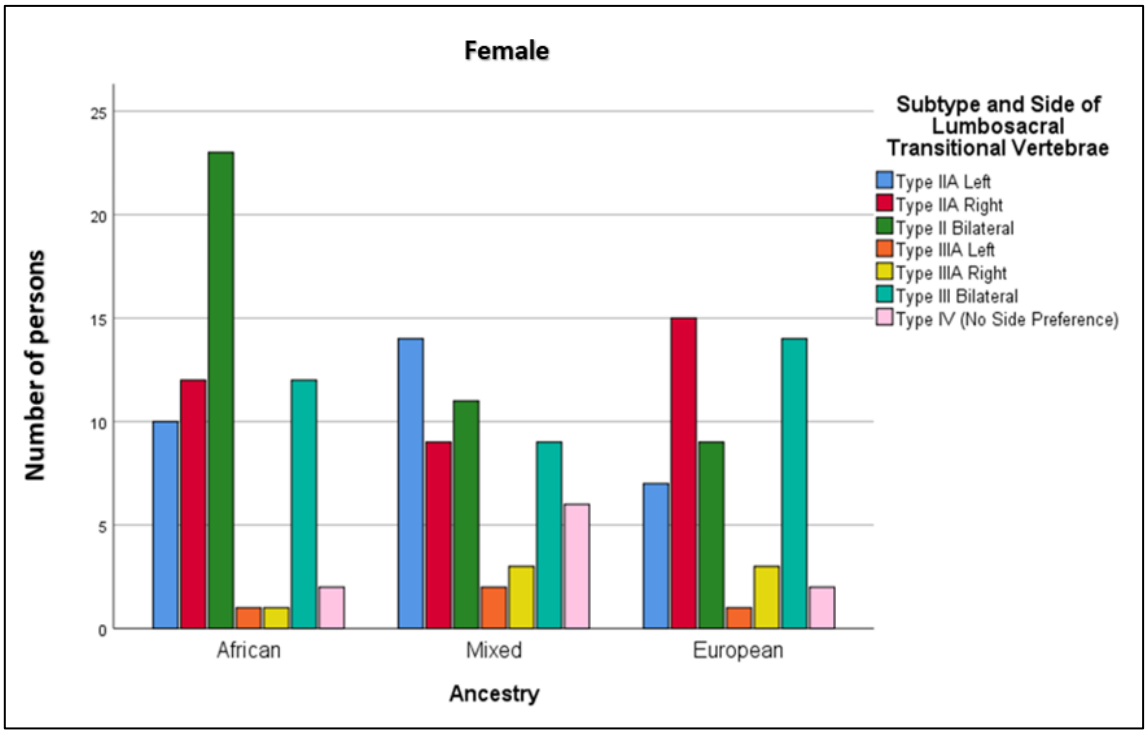

Figure 3.25: *Subtype and frequency of side of lumbosacral transitional vertebrae of women grouped by ancestry. The key is located in the top right corner.*

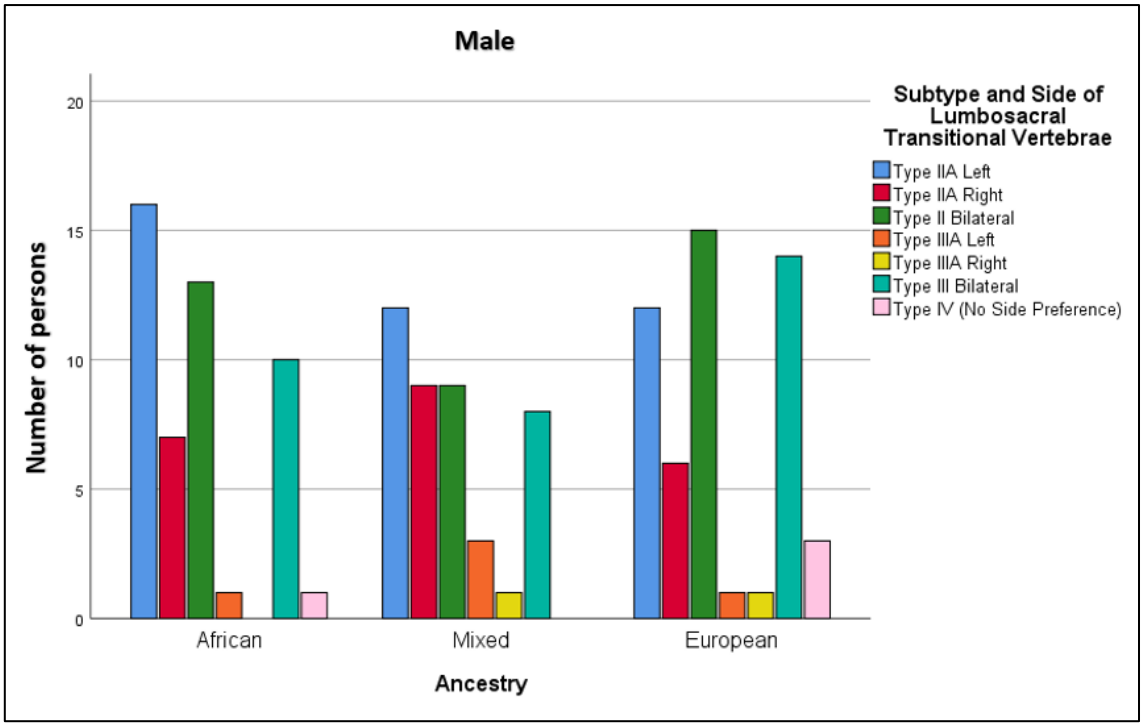

Figure 3.26: *Subtype and frequency of side of lumbosacral transitional vertebrae of men grouped by ancestry. The key is located in the top right corner.*

Sex, ancestry and spinal enumeration of lumbosacral transitional vertebrae

The sex and ancestry were compared to the proportions of spinal enumeration (sacralisation and lumbarisation). The X^2 test could be conducted as it met the necessary parameters for statistical inference. No statistical significance was found in females (X^2=2.146, df=2, p=0.342) when comparing ancestry and spinal enumeration of LSTV. However, statistical significance was found in males (X^2=9.307, df=2, p=0.010) when comparing ancestry and spinal enumeration, with a medium effect size as indicated by the Cramer's V test (V=0.256) and effect size table (Table 3.4). This was interpreted as a difference existed in the spinal enumeration in the male sex cohort between the three ancestral cohorts. The African-ancestry (n=34/48) and Mixed-ancestry (n=33/42) contained 71% and 79% in favour of sacralisation. The European-ancestry had less propensity for sacralisation (n=26/52), accounting for only 50% in favour of sacralisation. Therefore, the null hypothesis is rejected, a relationship is demonstrated with a medium effect size between males in all ancestry groups and spinal enumeration, demonstrating predilection for sacralisation. Refer to Figures 3.27 and 3.28.

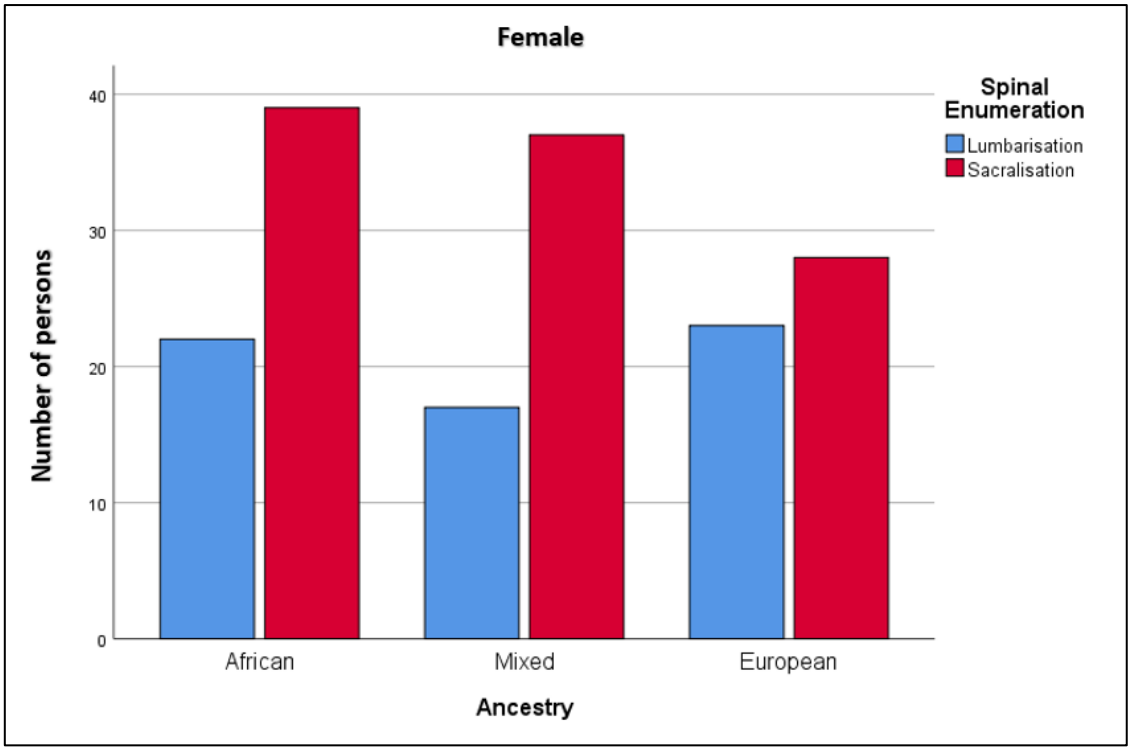

Figure 3.27: Spinal enumeration of lumbosacral transitional vertebrae of women found in the African, Mixed and European-ancestry cohorts. The key is located in the top right corner.

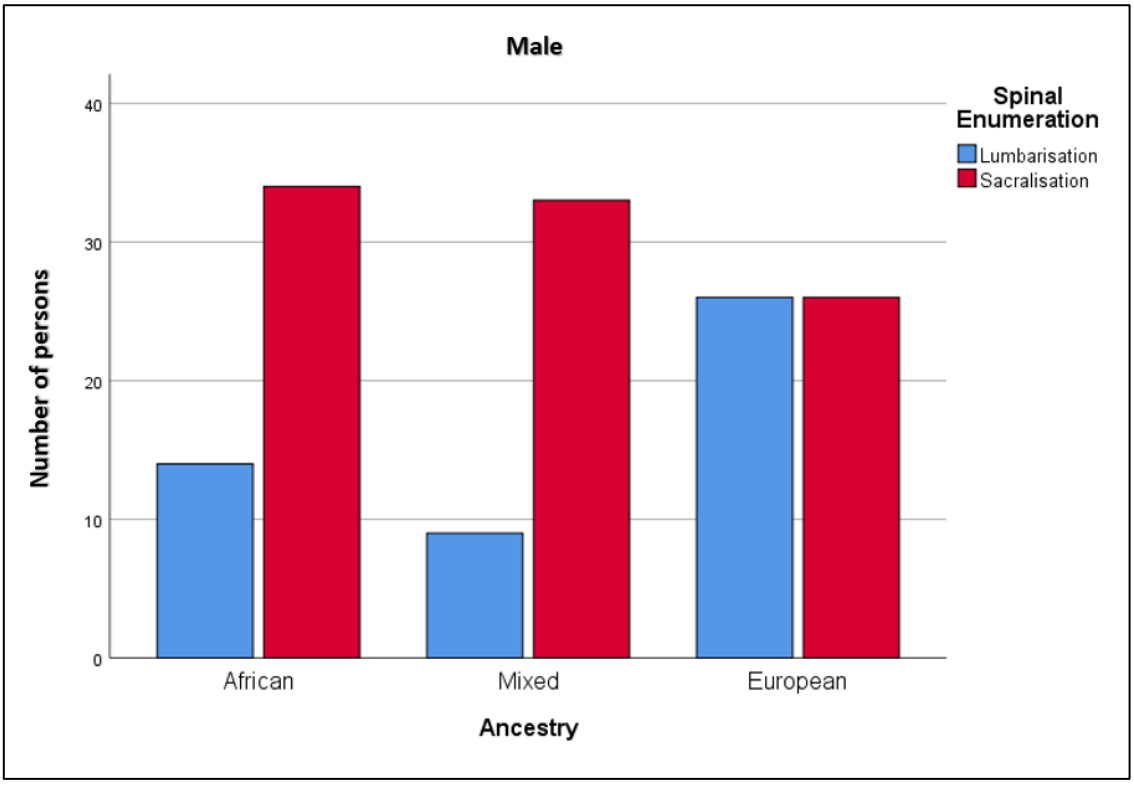

Figure 3.28: *Spinal enumeration of lumbosacral transitional vertebrae of men found in the African, Mixed and European-ancestry cohorts. The key is located in the top right corner.*

ANCESTRY AND SEX (Cross-Tabulations Subdivided By Ancestry)

Ancestry, sex and Type of lumbosacral transitional vertebrae

The African-, Mixed- and European-ancestry cohorts were compared to sex and Type of LSTV (Types II, III and IV). The X^2 test could not be used for statistical inference for the ancestry cohorts as the expected count did not meet the second condition for its use; the expected per-cell count for all three cohorts (African-ancestry, X^2=0.145, df=2, p=0.930; Mixed-ancestry, X^2=4.982, df=2, p=0.083; and European-ancestry, X^2=0.370, p=0.831) was lower than five for 33.3% of cells. Further analysis was performed by removing of the Type IV LSTV cohort and using Fisher's exact test for analysis of the double column and row contingency table. No significant statistical significance could be attributed to ancestry, sex and Type of LSTV for the African-ancestry (X^2=0.145, df=1, p=1.000), Mixed-ancestry (X^2=4.982, df=1, p=1.000) and European-ancestry (X^2=0.370, df=1, p=0.832) cohorts. Therefore, the null hypothesis stands, i.e. no relationship is demonstrated between ancestry, sex and Type of LSTV. Refer to Figures 3.29 to 3.31.

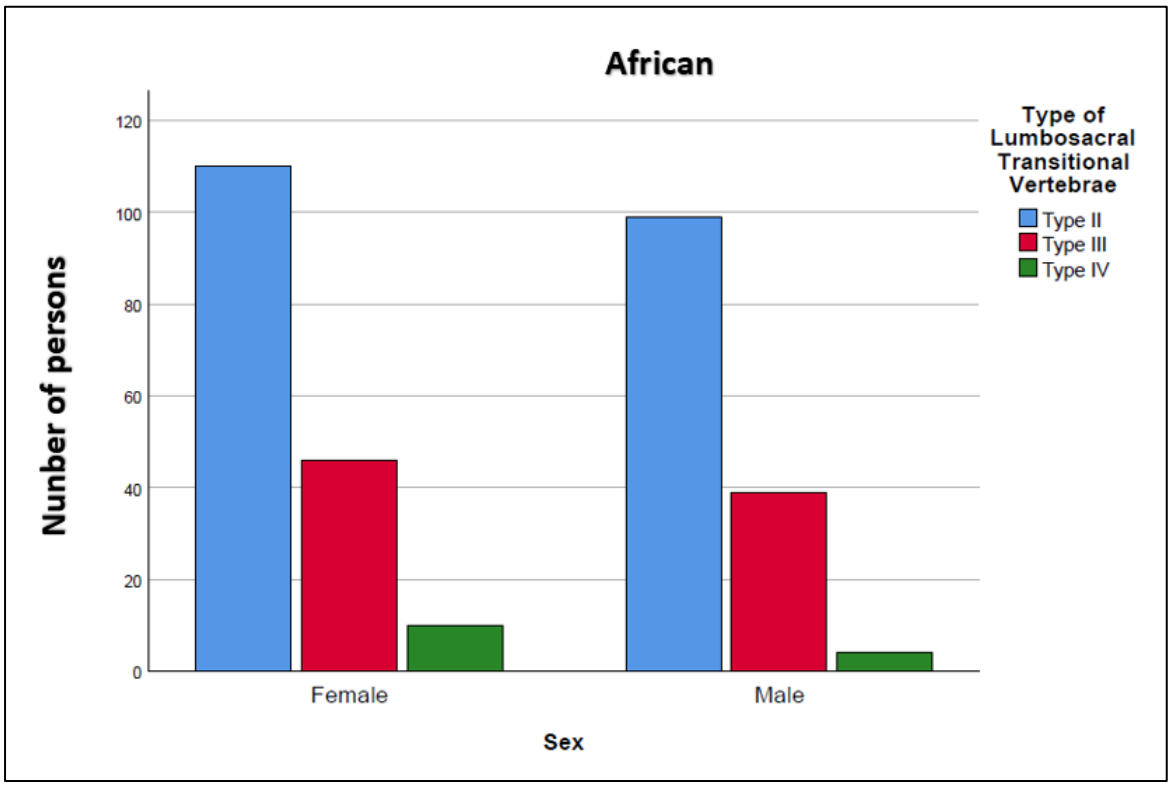

Figure 3.29: *Type of lumbosacral transitional vertebrae found in the African-ancestry cohort. The key is located in the top right corner.*

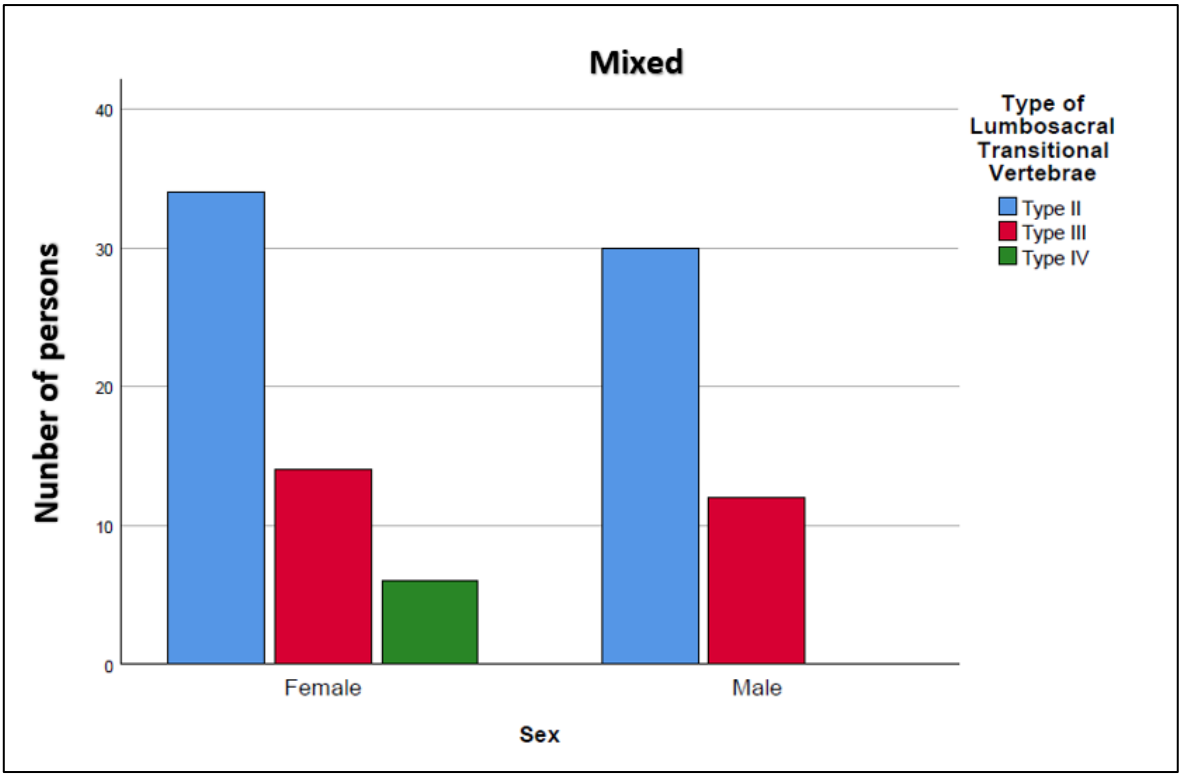

Figure 3.30: *Type of lumbosacral transitional vertebrae found in the Mixed-ancestry cohort. The key is located in the top right corner.*

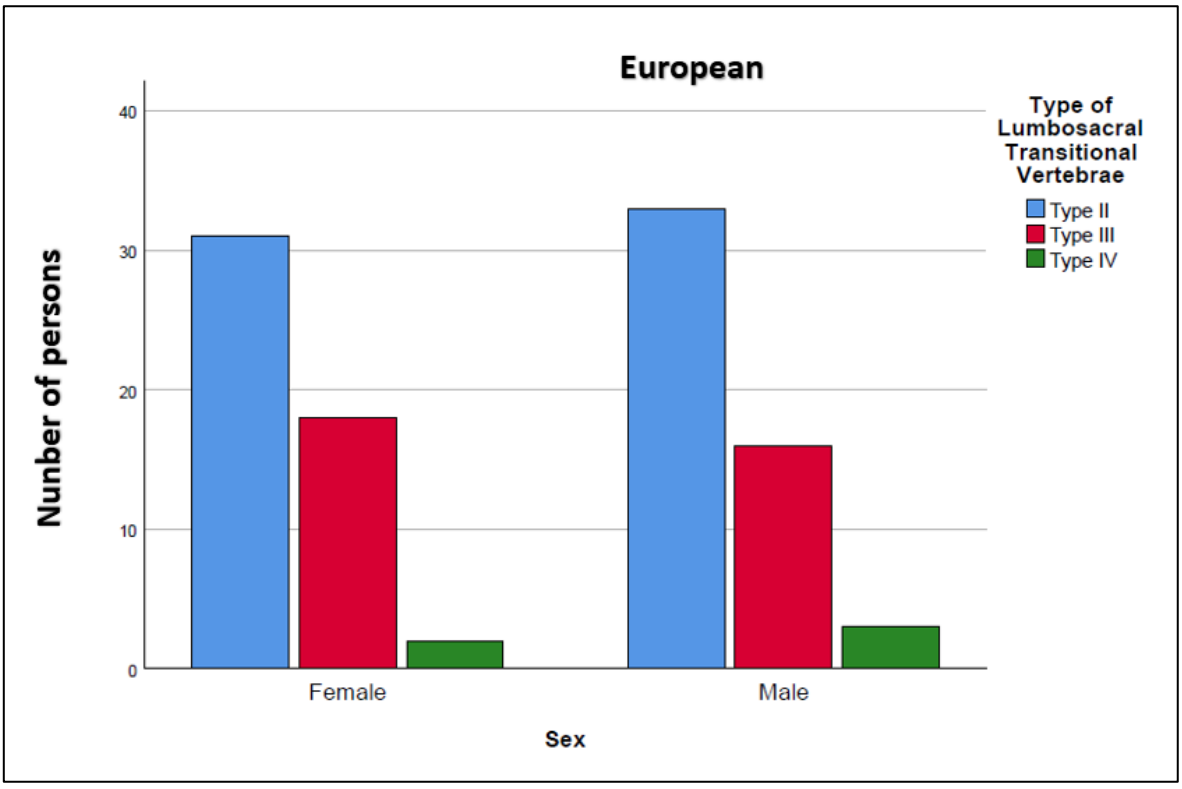

Figure 3.31: *Type of lumbosacral transitional vertebrae found in the European-ancestry cohort. The key is located in the top right corner.*

Ancestry, sex and subtype of lumbosacral transitional vertebrae

The African-, Mixed- and European-ancestry cohorts were compared to sex and subtype of LSTV from the radiographs. The X^2 test could not be used for statistical inference for the ancestry cohorts as the expected count did not meet the second condition for its use; the expected per-cell count for all three cohorts which were lower than five, 40.0% of cells for the African-ancestry (X^2=1.128, df=4, p=0.712) and Mixed-ancestry (X^2=5.040, df=4, p=0.283) cohorts while the European-ancestry (X^2=2.757, df=4, p=0.599) cohort did not meet the condition with 30.0% of cells. There is not enough evidence to suggest an association between ancestry, sex and subtype of LSTV. Refer to Figures 3.32 to 3.34.

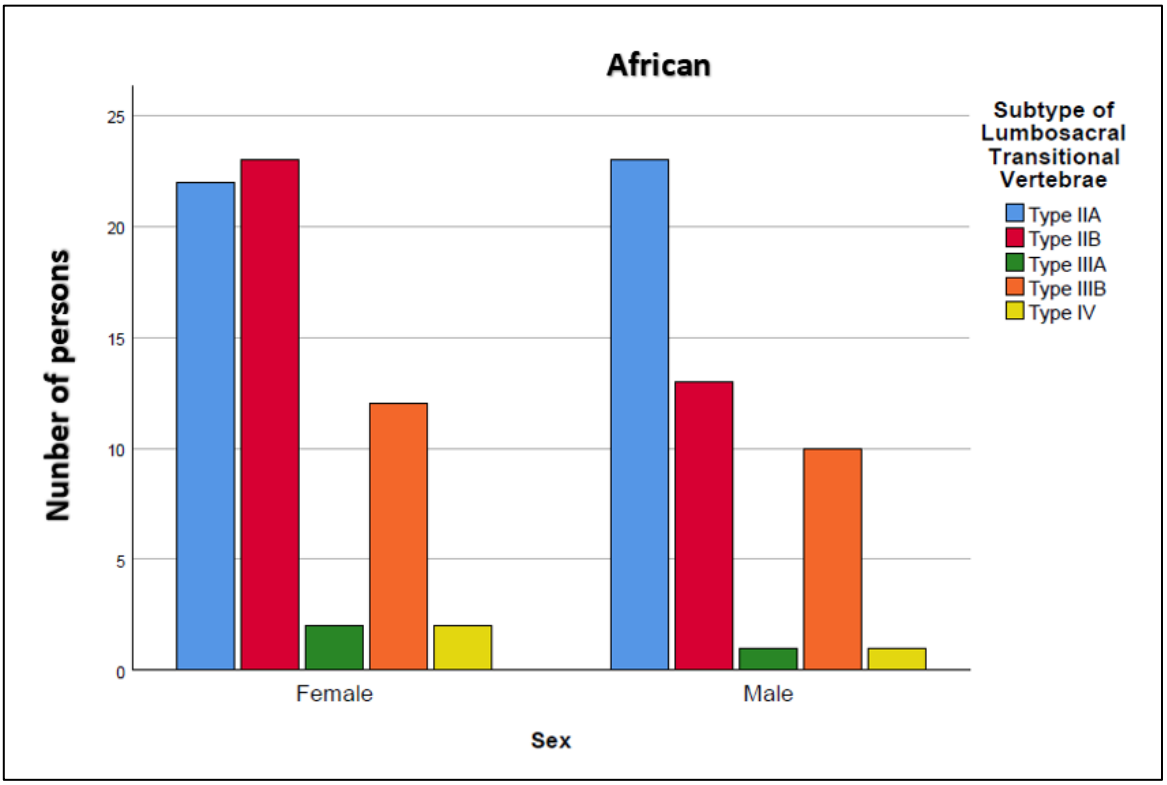

Figure 3.32: *Subtype of lumbosacral transitional vertebrae found within the African-ancestry cohort. The key is located at the top right corner.*

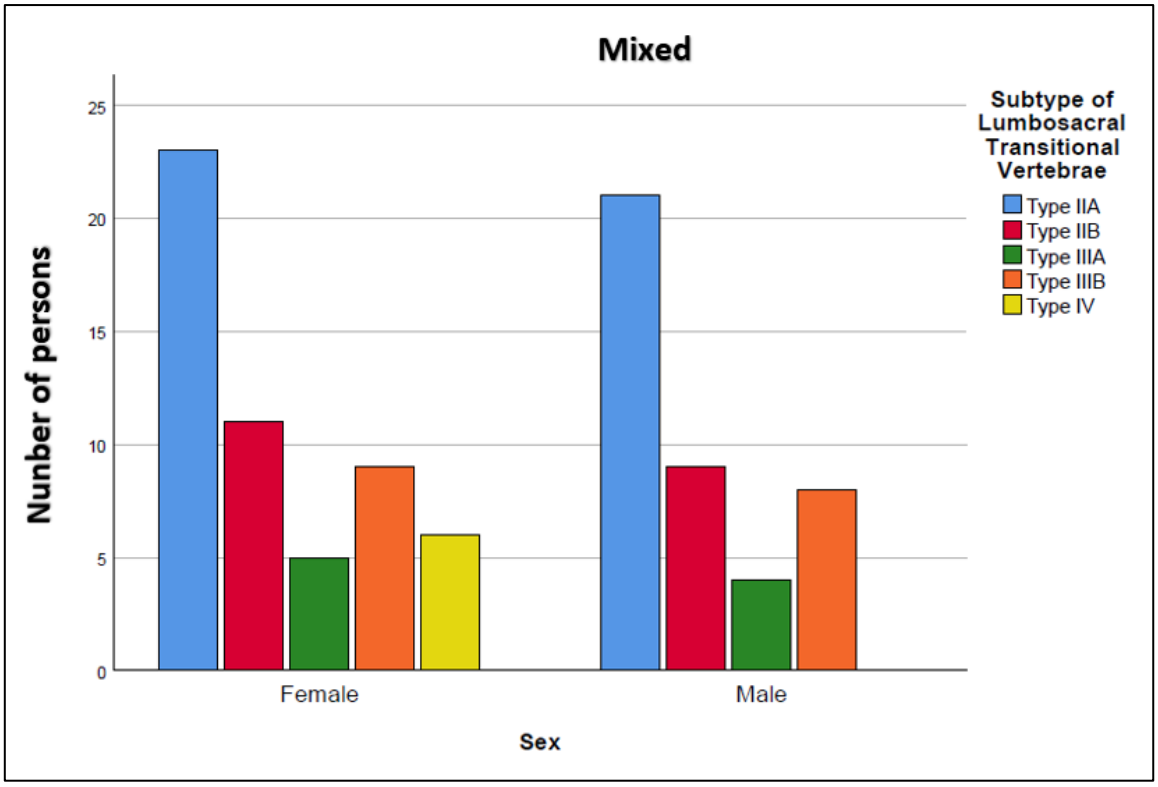

Figure 3.33: *Subtype of lumbosacral transitional vertebrae found in the Mixed-ancestry cohort. The key is located at the top right corner.*

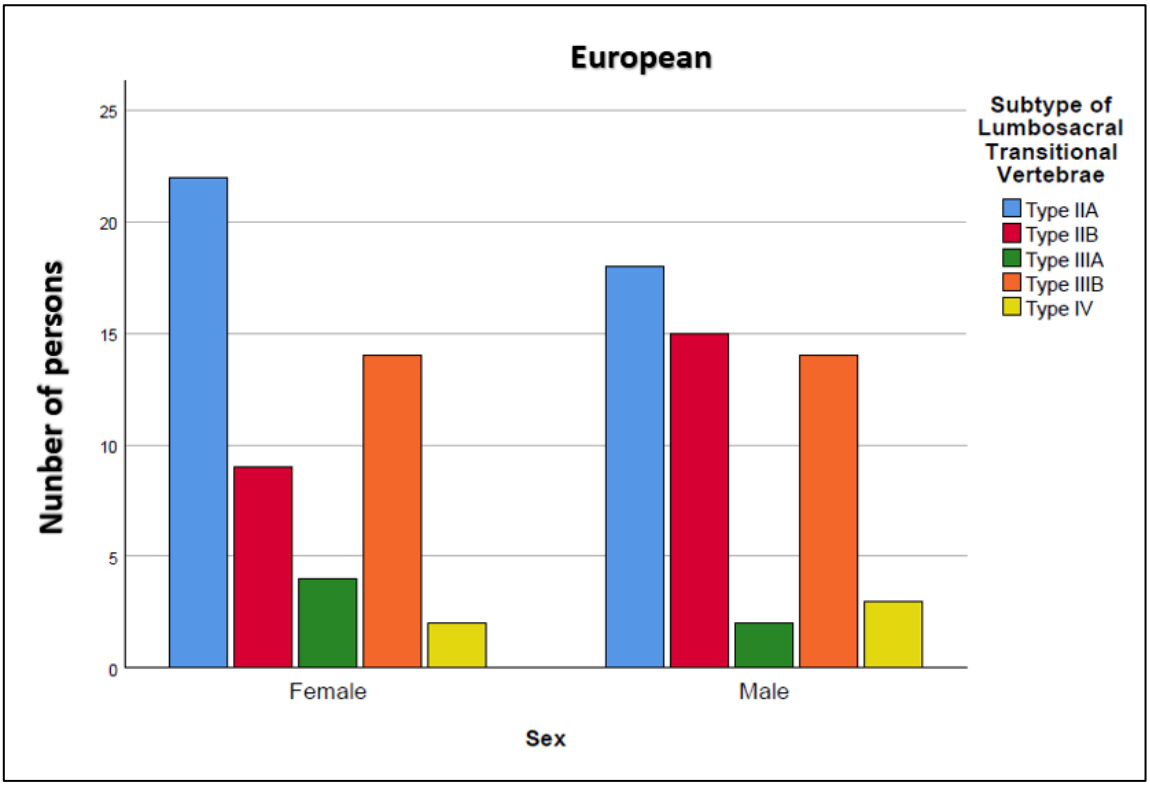

Figure 3.34: *Subtype of lumbosacral transitional vertebrae found in within the European-ancestry cohort. The key is located at the top right corner.*

Ancestry, sex and frequency of side of lumbosacral transitional vertebrae

The African-, Mixed- and European-ancestry cohorts were compared to sex and frequency of side from radiographs. The X^2 test could not be used for statistical inference for the ancestry cohorts as the expected count did not meet the second condition for its use; the expected per-cell count for the African-ancestry (X^2=4.414, df=3, p=0.220), Mixed-ancestry (X^2=4.994, df=3, p=0.172) and European-ancestry (X^2=5.777, df=3, p=0.123) cohorts was lower than five in 25.0% of cells. Further analysis was performed with the Type IV cohort removed, this did not affect the statistical significance outcome for the African ancestry (X^2=4.265, df=2, p=0.119), the Mixed-ancestry (X^2=0.016, df=2, p=0.992) and for the European-ancestry (X^2=5.586, df=2, p= 0.061) cohorts. Therefore, the null hypothesis stands i.e. no relationship is demonstrated between ancestry, sex and frequency of side of LSTV. Refer to Figures 3.35 to 3.37.

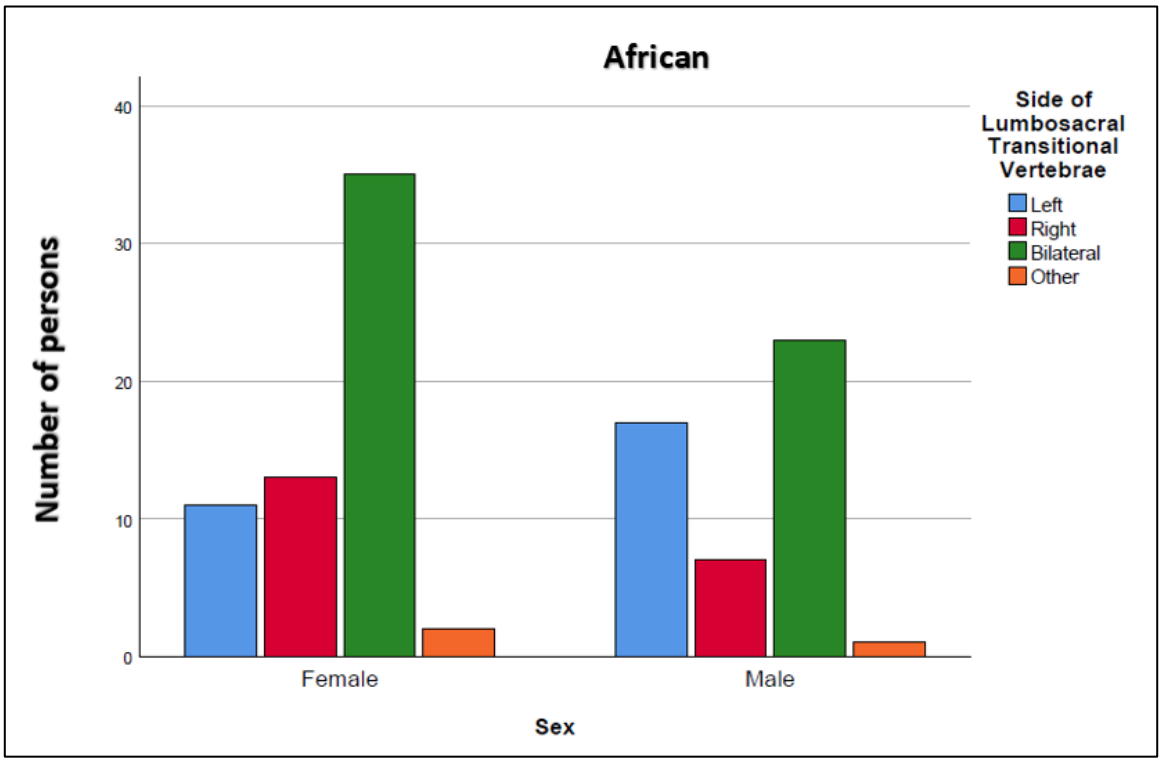

Figure 3.35: *Sex and frequency of side of lumbosacral transitional vertebrae found in the African-ancestry cohort. The key is located at the top right corner.* ***Other:*** *Refers to the Type IV lumbosacral transitional vertebrae morphology which has no designated preference of side.*

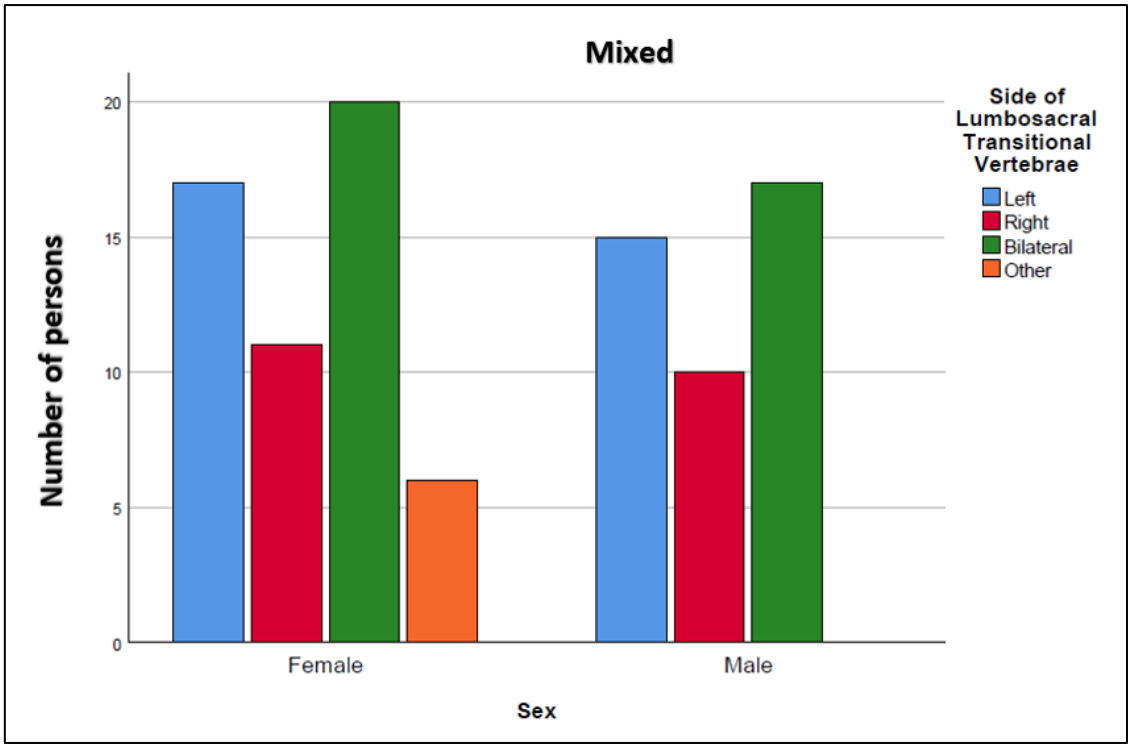

Figure 3.36: *Sex and frequency of side of lumbosacral transitional vertebrae found in the Mixed-ancestry cohort. The key is located at the top right corner.* ***Other:*** *Refers to the Type IV lumbosacral transitional vertebrae morphology which has no designated preference of side.*

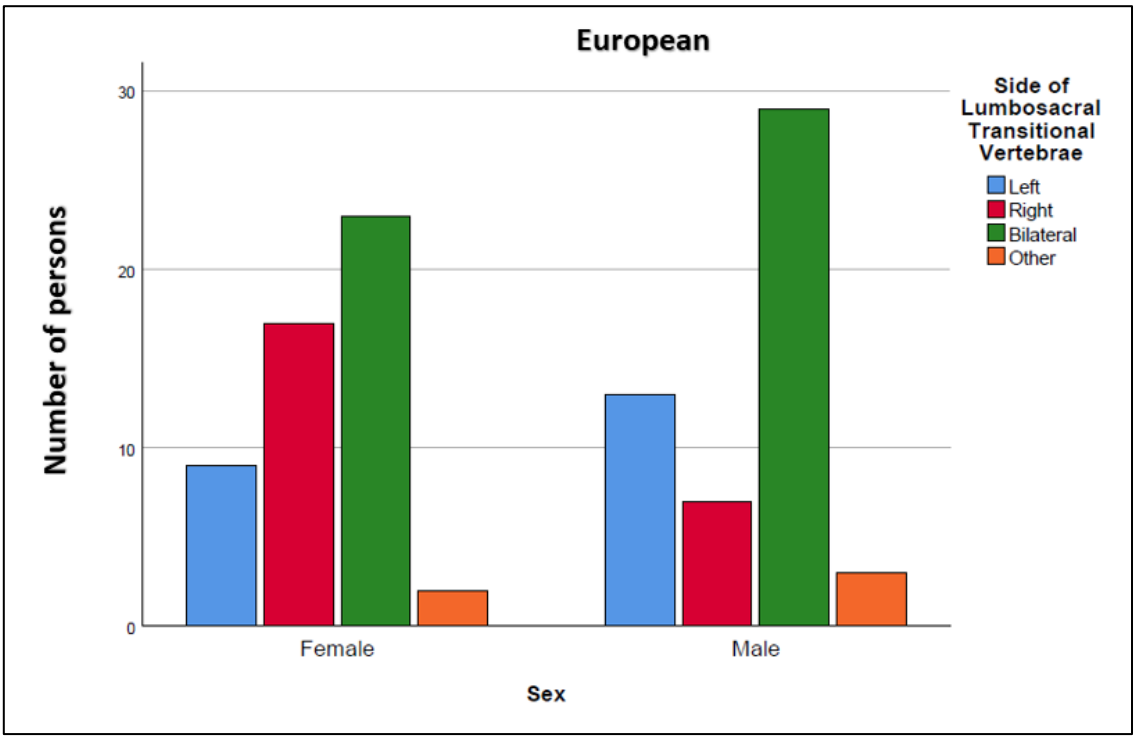

Figure 3.37: Sex and frequency of side of lumbosacral transitional vertebrae found in the European-ancestry cohort. The key is located at the top right corner. ***Other:*** *Refers to the Type IV lumbosacral transitional vertebrae morphology which has no designated preference of side.*

Ancestry, sex, subtype and frequency side of lumbosacral transitional vertebrae

The African-, Mixed- and European-ancestry cohorts were compared to sex and subtype of LSTV from radiographs. The X^2 test could not be used for statistical inference amongst the ancestry cohorts as the expected count did not meet the second condition for its use; the expected per-cell count for the African-ancestry (X^2=5.521, df=6, p=0.479), Mixed-ancestry (X^2=6.210, df=6, p=0.400), and European-ancestry (X^2=7.864, df=6, p=0.248) cohorts was lower than five in 42.9% of cells. There is not enough evidence to suggest an association between ancestry, sex, subtype and frequency of side of LSTV. Refer to Figures 3.38 to 3.40.

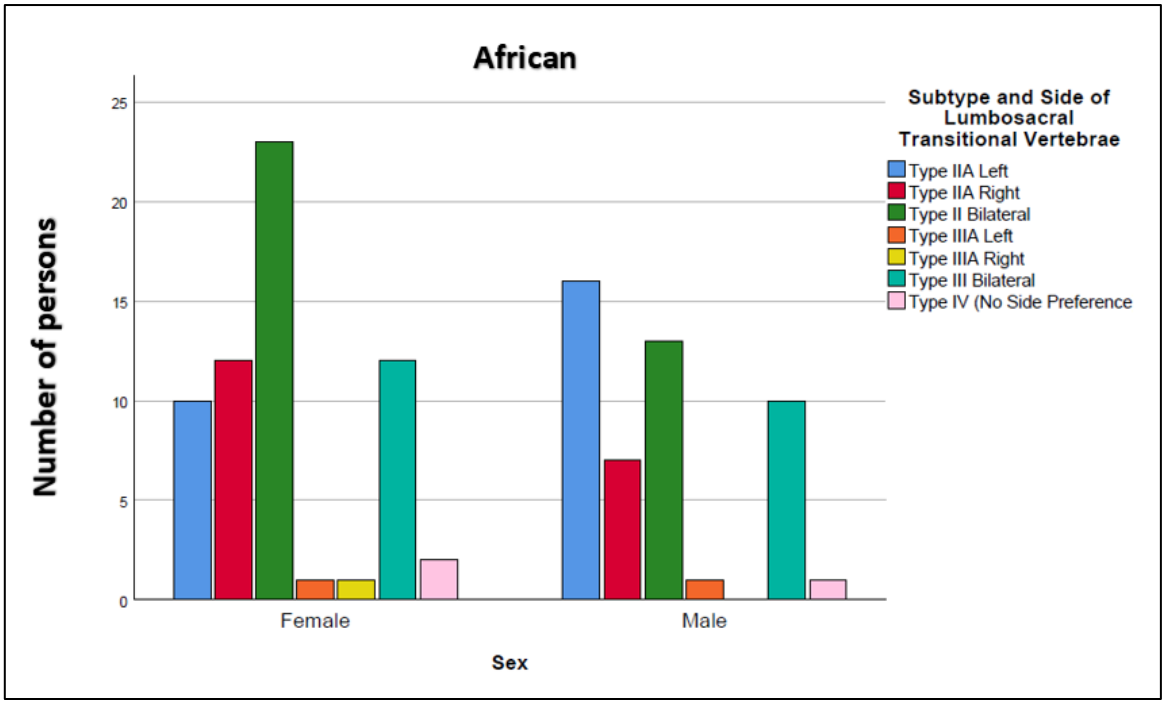

Figure 3.38: *The sex, subtype and frequency of side of lumbosacral transitional vertebrae found in the African-ancestry cohort. The key is located at the top right corner.*

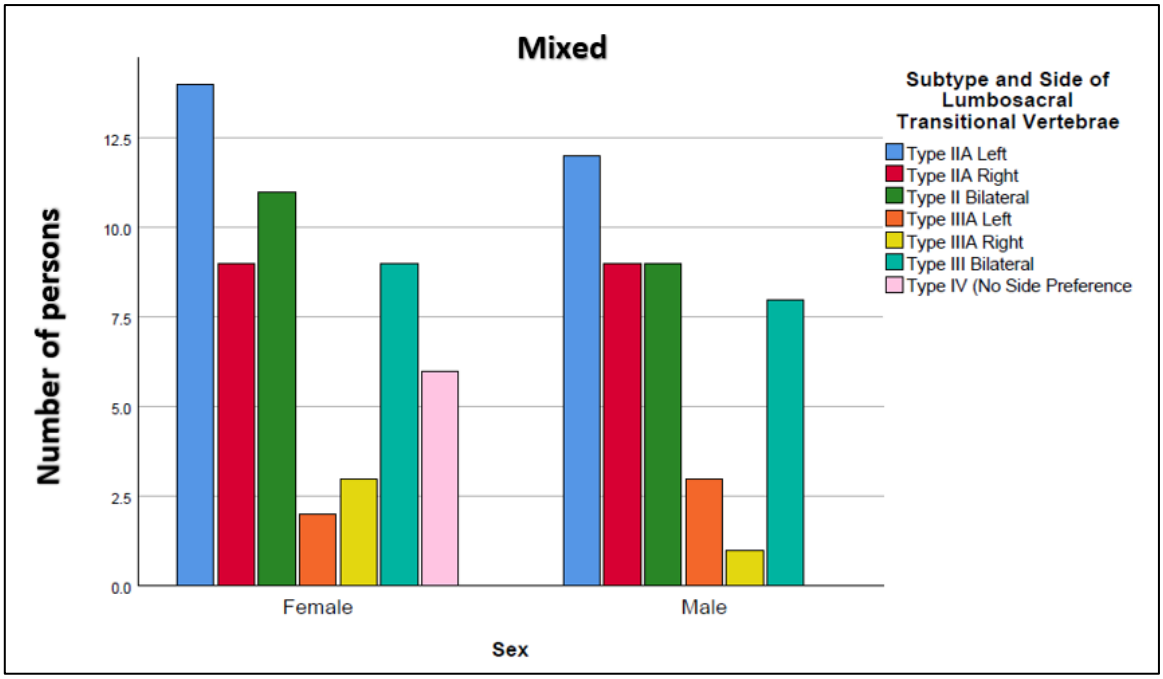

Figure 3.39: *The sex, subtype and frequency of side of lumbosacral transitional vertebrae found in the Mixed-ancestry cohort. The key is located at the top right corner.*

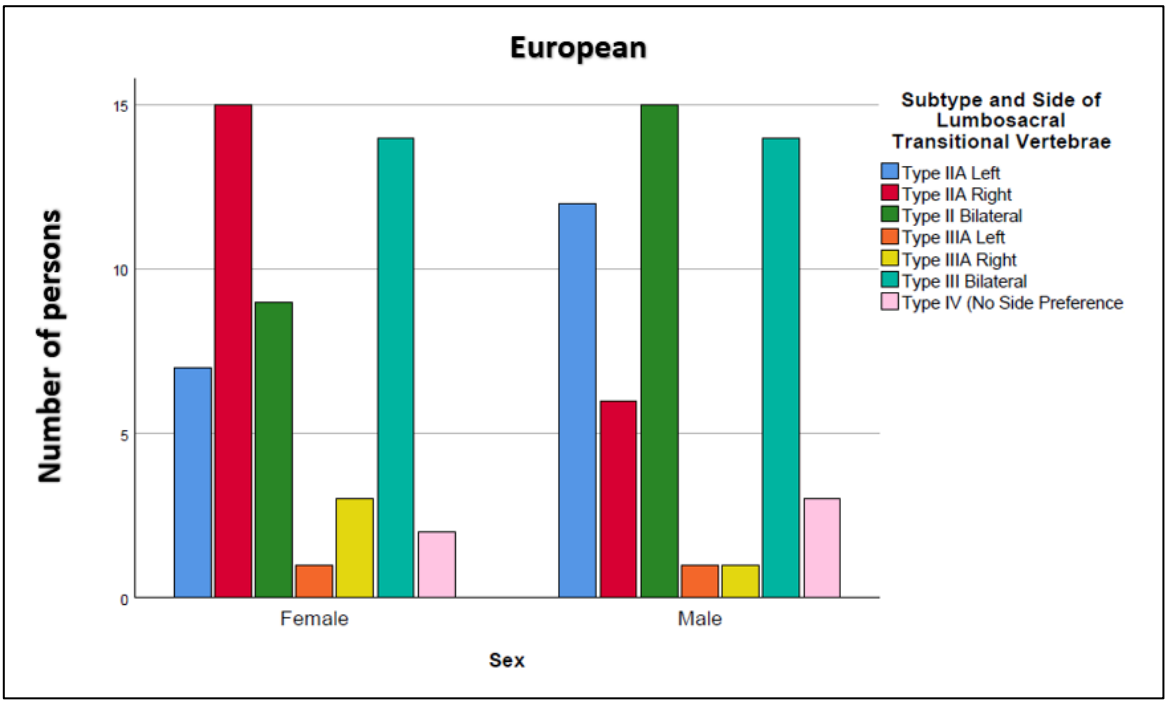

Figure 3.40: *The sex, subtype and frequency of side of lumbosacral transitional vertebrae found in the European-ancestry cohort. The key is located at the top right corner.*

Ancestry, sex and spinal enumeration of lumbosacral transitional vertebrae

The sex and ancestry were compared to the spinal enumeration found on radiographs (sacralisation and lumbarisation). The X^2 test could be conducted as it met the necessary parameters for statistical inference. No statistical significance was found in the African-ancestry (X^2=0.578, df=1, p=0.447), Mixed-ancestry (X^2=1.209, df=1, p=0.272) and European-ancestry (X^2=0.248, df=1, p=0.618) cohorts. Further analysis was performed by removing of the Type IV LSTV cohort and using Fisher's exact test to anayise the double column and row contingency table. No significant statistical significance between sex and spinal enumeration could be attributed to the African-ancestry (X^2=0.02, df=1, p=1.000), Mixed-ancestry (X^2=0.04, df=1, p=1.000) and European-ancestry (X^2=0.180, df=1, p=0.832) cohorts. Therefore, the null hypothesis stands, i.e. no relationship is demonstrated between ancestry, sex and spinal enumeration. Refer to Figures 3.41 to 3.43.

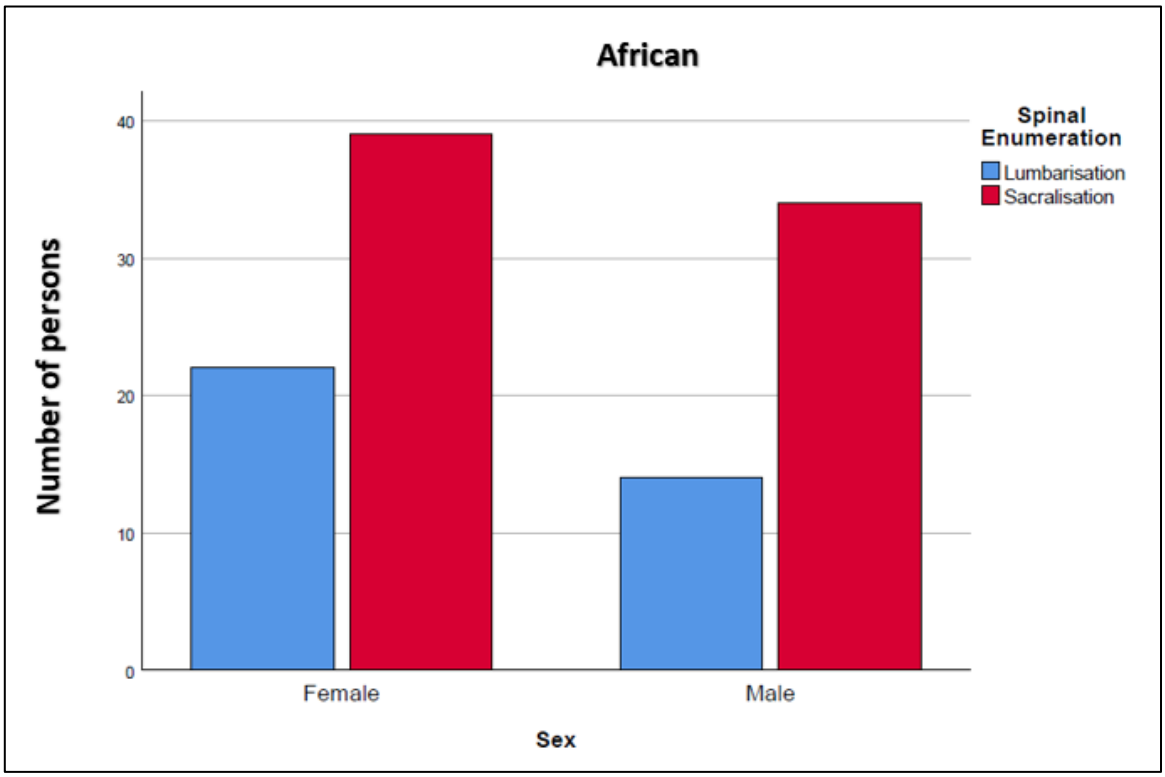

Figure 3.41: *Sex and spinal enumeration of lumbosacral transitional vertebrae found in the African-ancestry cohort. The key is located at the top right corner.*

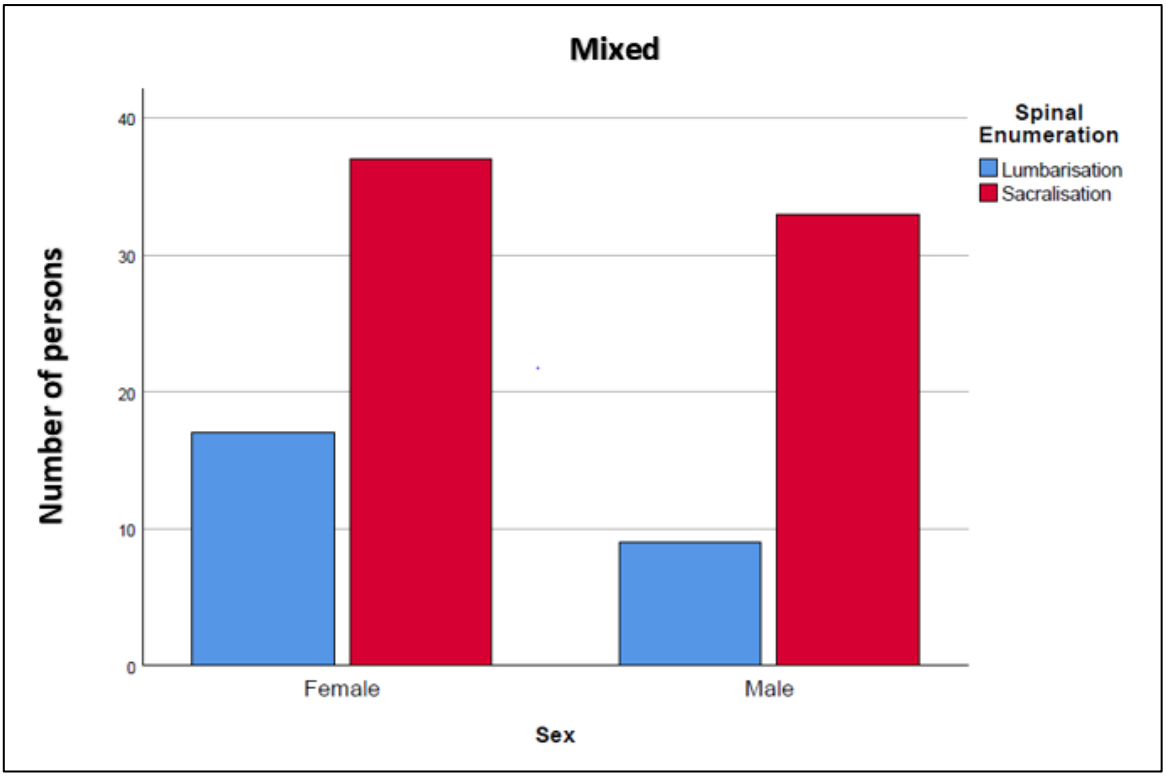

Figure 3.42: *Sex and spinal enumeration of lumbosacral transitional vertebrae found in the Mixed-ancestry cohort. The key is located at the top right corner.*

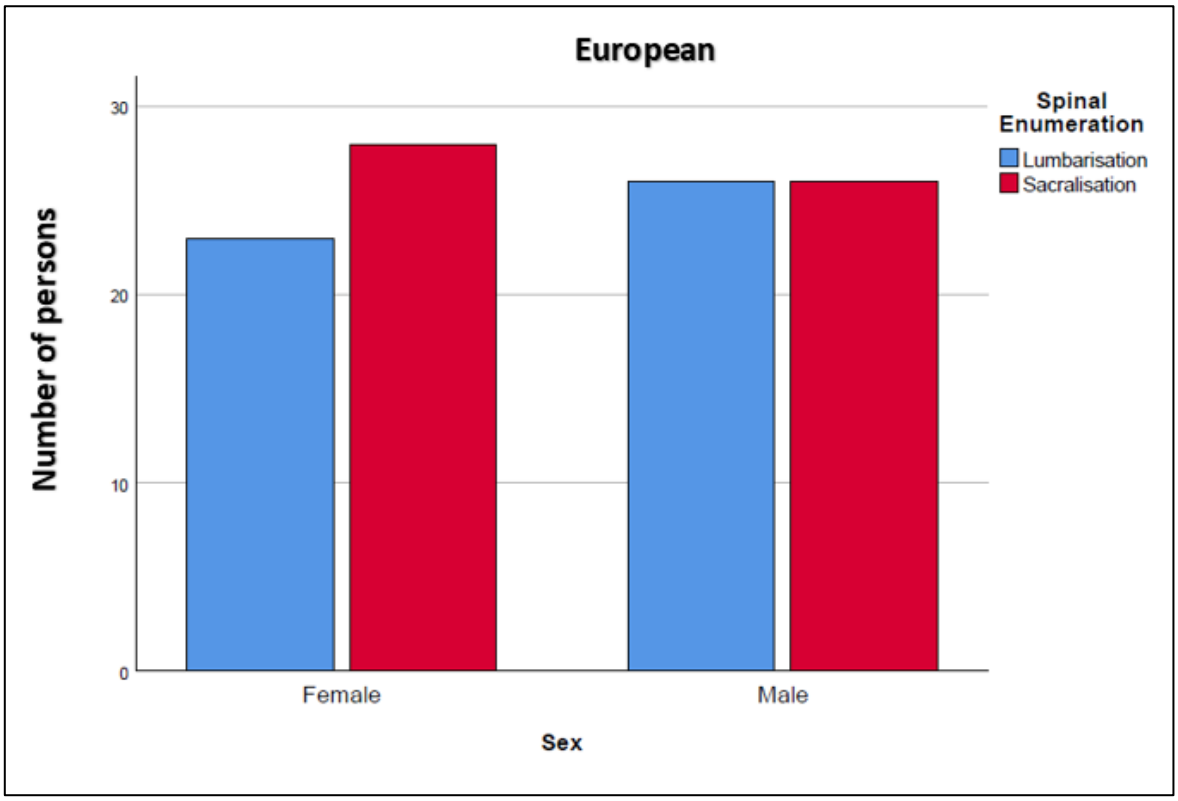

Figure 3.43: *Sex and spinal enumeration of lumbosacral transitional vertebrae found in the European-ancestry cohort. The key is located at the top right corner.*

Non-metric observations

Noteworthy and novel non-metric observations are listed below and will be discussed in Chapter 5.

Iliolumbar articulation

Additional findings in the imaging cohort were two left-sided Type IIA LSTV with a right-sided articulation between the lumbar transverse process and the ilium seen on a radiograph. Figure 3.44 was a supplementary finding that did form part of the LSTV cohort while Figure 3.45 was found in the imaging cohort. These were not reflected in the statistical data analyses due to their limited quantity and novelty.

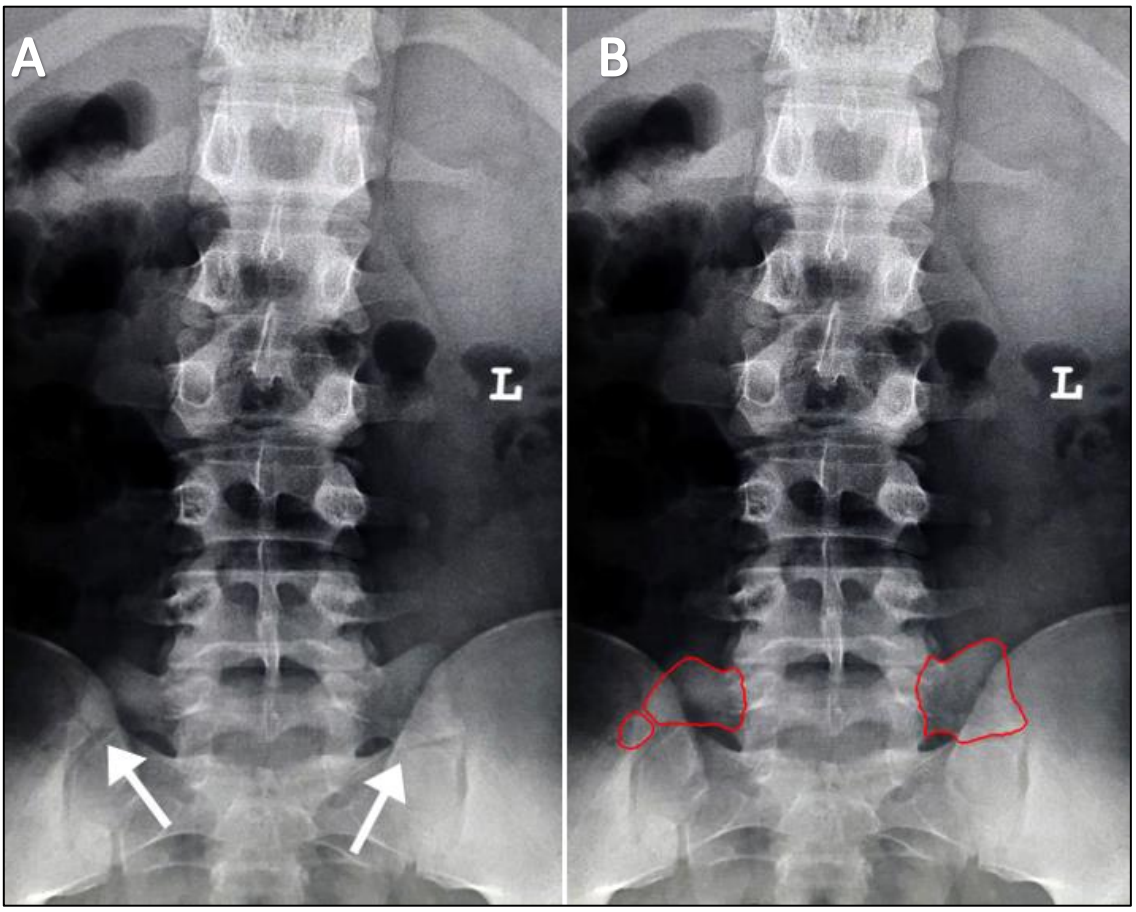

Figure 3.44: *An anteroposterior lumbar radiograph of atypical left-sided Type IIA lumbosacral transitional vertebra, sacralisation.* ***A)*** *An anteroposterior lumbar radiograph containing an unclassified lumbosacral transitional vertebra. The arrows indicate the articulation of the transverse processes of the L5 lumbosacral transitional vertebra with the ala of the sacrum on the left and with the ilium of the pelvic girdle on the right.* ***B)*** *The articulation of the transverse process of the L5 with the ala of the sacrum on the left and the articulation of the transverse process with the ilium of the pelvic girdle on the right are highlighted in red. Both images* ***A*** *and* ***B*** *are of the same individual with different visual aids.* ***L****= left.*

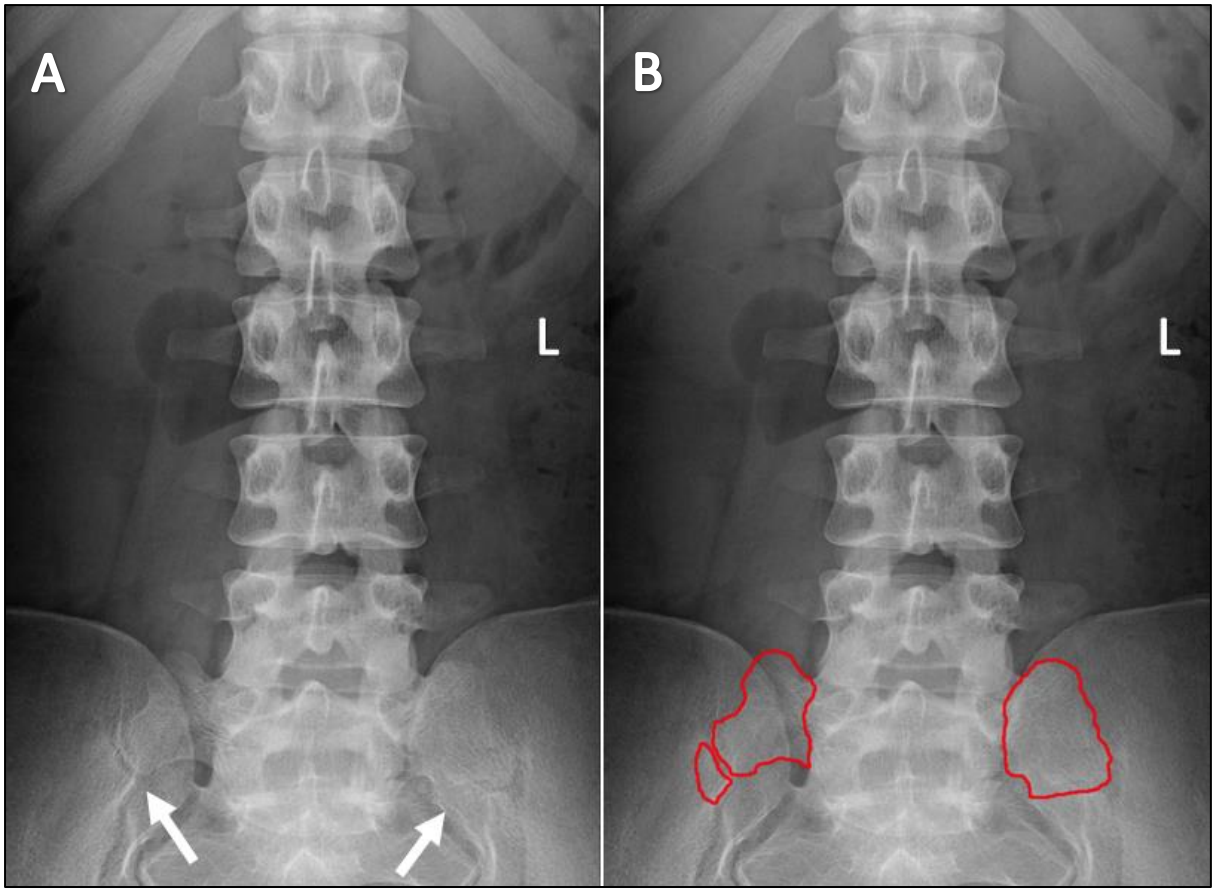

Figure 3.45: *An atypical anteroposterior lumbar radiograph left-sided Type IIA lumbosacral transitional vertebra, lumbarisation.* ***A)*** *An anteroposterior lumbar radiograph containing an unclassified lumbosacral transitional vertebra. The arrows indicate the articulation of the transverse processes of the L6 lumbosacral transitional vertebra with the ala of the sacrum on the left and with the ilium of the pelvic girdle on the right.* ***B)*** *The articulation of the transverse process of the L6 with the ala of the sacrum on the left and the articulation of the transverse process with the ilium of the pelvic girdle on the right are highlighted in red. Both images* ***A*** *and* ***B*** *are of the same individual with different visual aids.* ***L****= left*

Bipartition of the sacral foramen

An unusual finding in the imaging cohort was a bipartition of the left anterior sacral foramen formed by a Type IIIB LSTV seen on a lumbosacral radiograph. The appearance is in keeping with a bony septum (calcified/ ossified connective tissue or ligament) that separates the left first sacral foramen into two foramina. Refer to Figure 3.46.

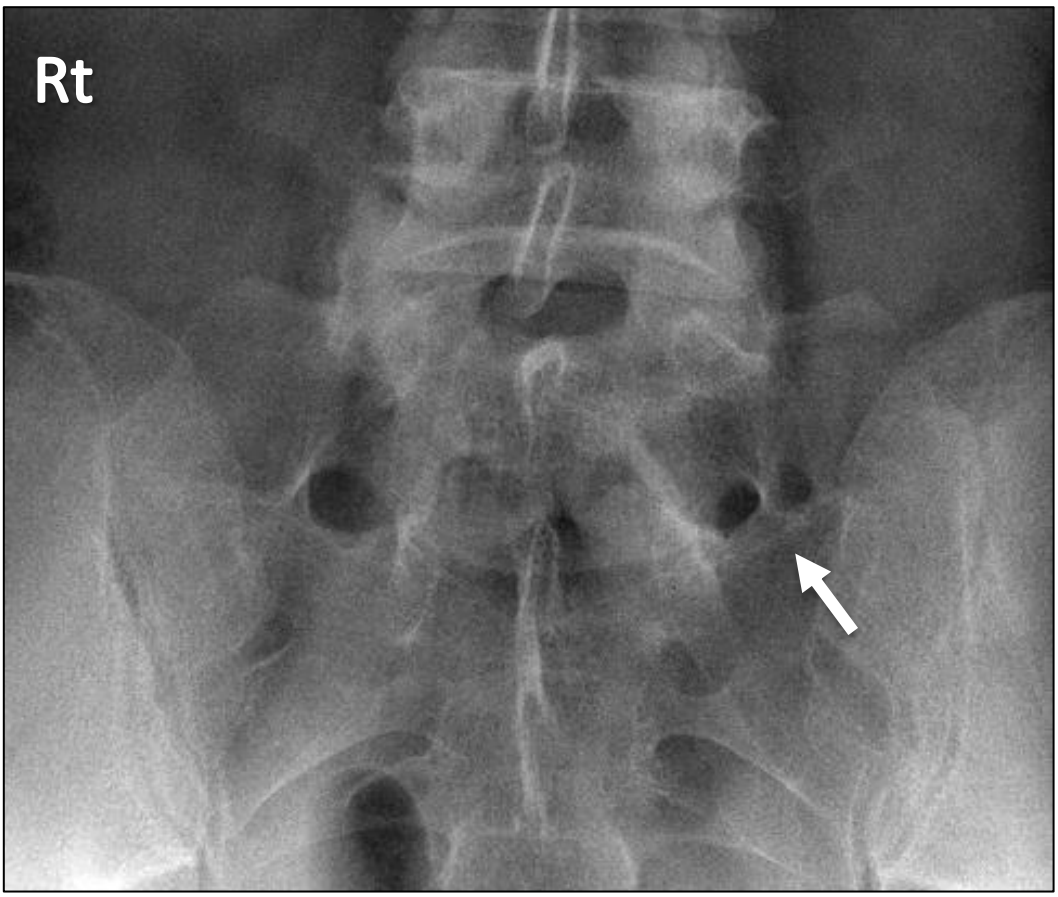

Figure 3.46: *A bipartite sacral foramen associated with a Type IIIB lumbosacral transitional vertebra. An anteroposterior lumbosacral radiograph contained a left-sided bipartite first sacral foramen. The arrow indicates the bony septum that separates the left anterior first sacral foramen into two foramina.* ***Rt****= right.*

Intra-articular vacuum phenomenon

While appraising advanced imaging scans associated with LSTV, hypodense areas were identified which represents the intra-articular vacuum phenomenon. This was seen in association with LSTV on a number of different coronal CT scan images. Refer to Figure 3.47.

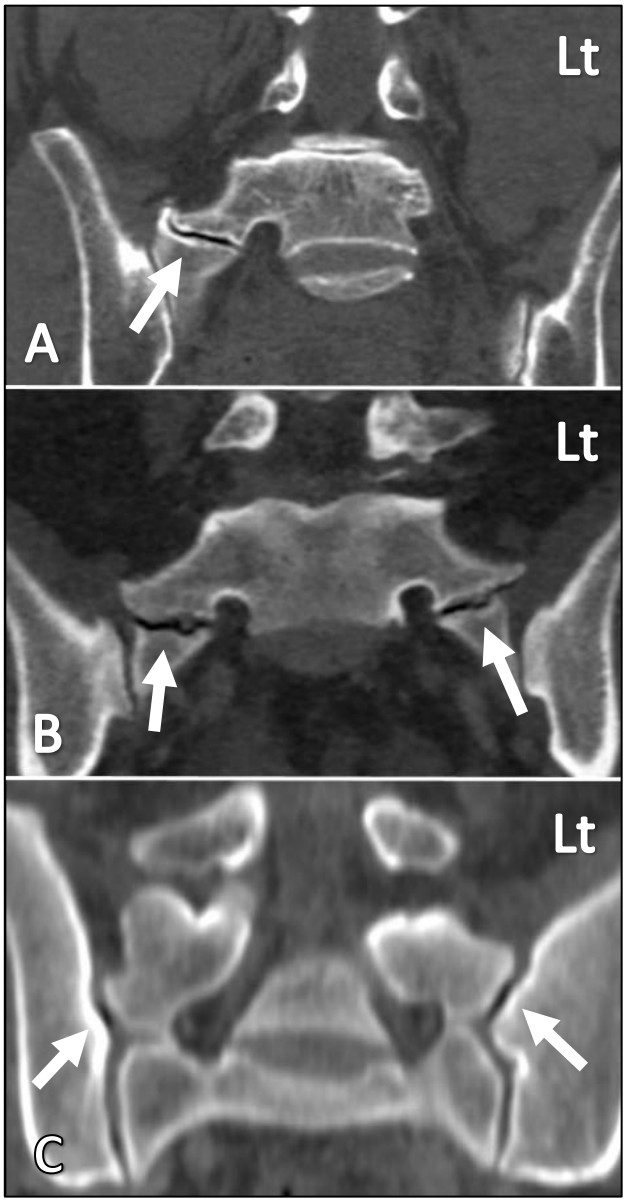

Figure 3.47: Computerised tomographic images i*ntra-articular vacuum phenomenon accompanying lumbosacral transitional vertebrae.* ***A)*** *A right-sided Type II lumbosacral transitional vertebra displaying hypodensity (dark line) seen between the articulation of the lumbar transverse process and the ala of the sacrum of a 55 year-old female.* ***B)*** *A Type IIB lumbosacral transitional vertebra displaying hypodensity (dark lines) seen between the articulations of the lumbar transverse processes and the alae of the sacrum of a 52 year-old male.* ***C)*** *A Type IIB lumbosacral transitional vertebra displaying areas of hypodensity (dark spots) seen between the articulation of the lumbar transverse processes and the ilia of the pelvic girdle of a 41 year-old female. The white arrows indicate the intra-articular vacuum phenomenon.* ***Lt****= Left.*

Enlargement of the lumbar transverse process without articulation

Lumbar TVP enlargement without articulation was seen on the opposite side to the dysplastic TVP of the LSTV on both radiographs and CT scan images. This Type I LSTV morphological characteristic was seen in association with the Type II and III LSTV classifications. Refer to Figure 3.48.

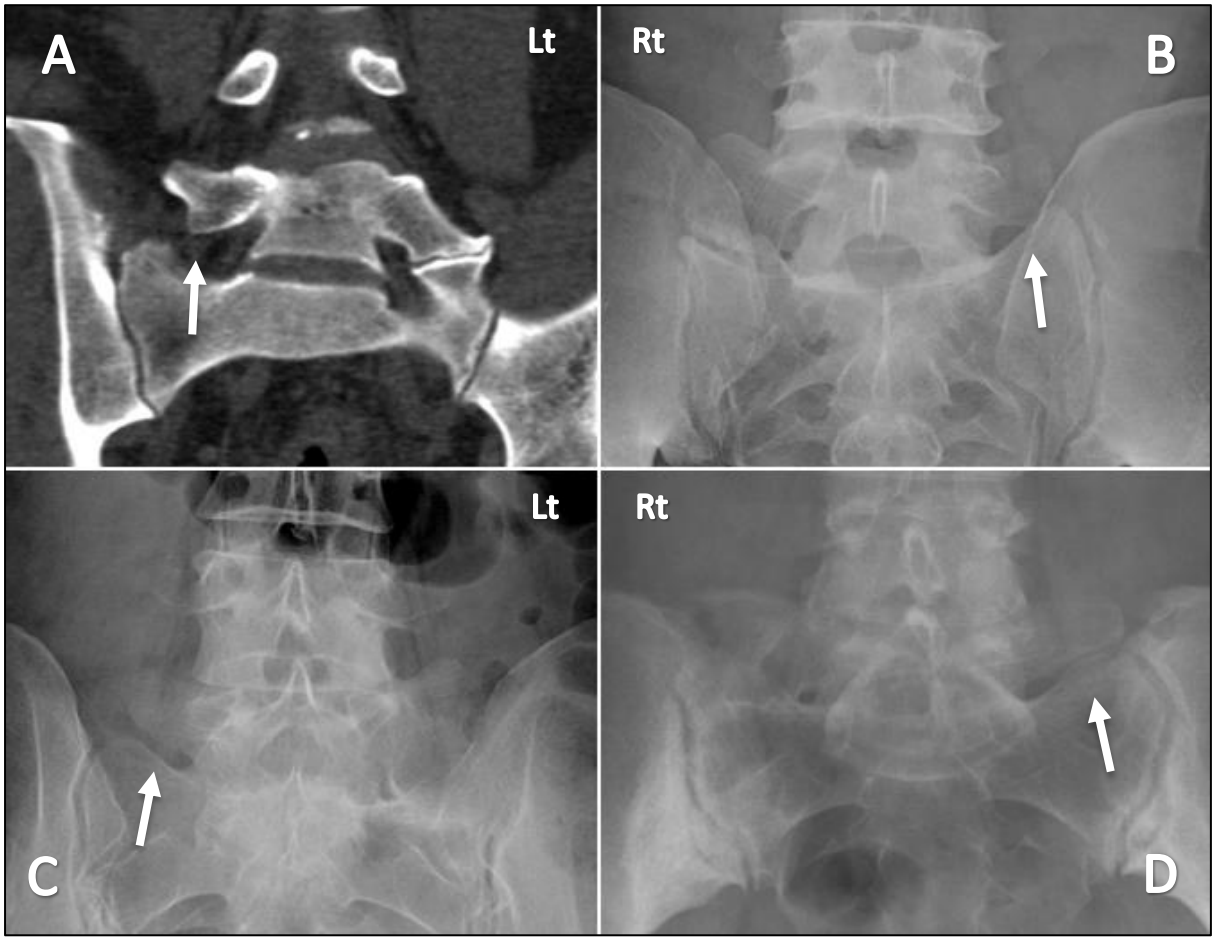

Figure 3.48: *An atypical subtype of lumbosacral transitional vertebrae.* ***A)*** *A coronal CT scan of the lumbosacral junction of the left-sided Type IIA lumbosacral transitional vertebra.* ***B)*** *An anteroposterior radiograph of the lumbosacral junction of a right-sided Type IIA lumbosacral transitional vertebra.* ***C)*** *An anteroposterior radiograph of the lumbosacral junction of a left-sided Type IIIA lumbosacral transitional vertebra.* ***D)*** *An anteroposterior radiograph of the lumbosacral junction of a right-sided Type IIIA lumbosacral transitional vertebra. The arrows indicate an enlarged lumbar transverse process of 19mm or more in height.* ***Rt****= Right.* ***Lt****= Left.*

Lumbar ossified bridging syndrome

While appraising advanced imaging scans associated with LSTV, coronal CT scan images of a 53 year-old female demonstrated a left-sided accessory articulation of the L4 TVP with the TVP of a left-sided Type IIA LSTV of L5. This is a condition known as lumbar ossified bridging syndrome (LOBS). Refer to Figure 3.49.

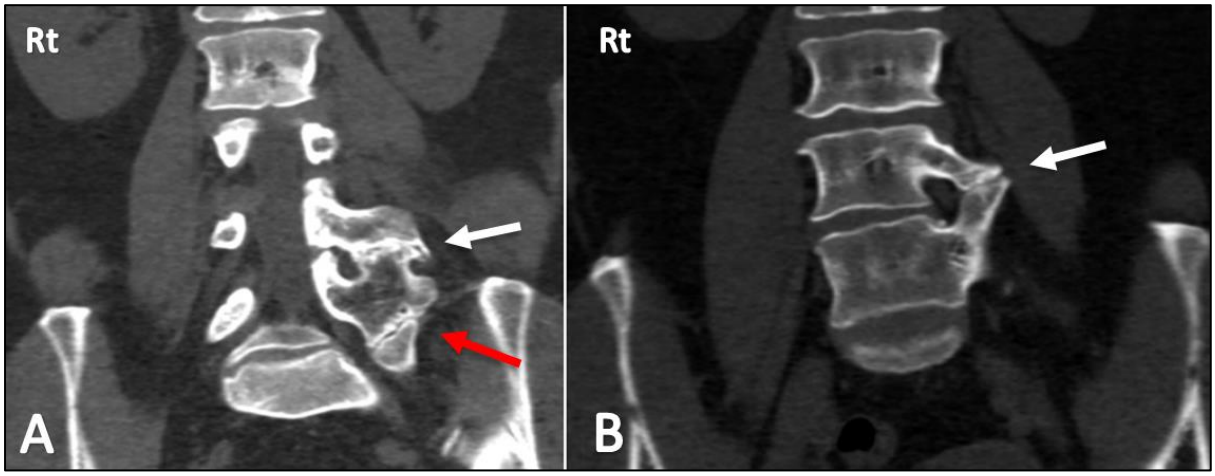

Figure 3.49: *An accessory articulation of the lumbar transverse processes of L4 and lumbosacral transitional vertebra.* ***A)*** *A coronal CT scan image of the lumbar spine displays an accessory articulation of the lumbar transverse processes of L4 with a lumbosacral transitional vertebra of L5.* ***B)*** *A coronal CT scan image of the lumbar spine displays an accessory articulation of the lumbar transverse processes of L4 with a lumbosacral transitional vertebra of L5. The white arrows indicate the accessory articulation between the L4 and L5 transverse processes. The red arrow indicates the articulation of the lumbar transverse process of the lumbosacral transitional vertebra with the ala of the sacrum. Both images* ***A*** *and* ***B*** *are of the same individual.* ***Rt****= Right.*

Transverso-sacroiliac articulation

Coronal CT scan images of a Type IIB LSTV of L5 displayed three articulations. Firstly, the articulation of the auricular surface of the sacrum with the ilium of the pelvis forming the sacroiliac articulation which is a normal spinopelvic joint found bilaterally. Furthermore, two additional accessory joints were identified, namely an articulation between the L5 lumbar transverse process and the alae of the sacrum known as the lumbosacral articulation and an articulation of the lumbar transverse process with the ilium of the pelvis known as the iliolumbar articulation. These were found unilaterally (right and left) and bilaterally in the imaging cohort. These articulations form a complex which the author has named the transverso-sacro-iliac articulation complex. Refer to Figure 3.50.

Additionally, a tongue-in-groove appearance is seen bilaterally in A and B whereby the iliolumbar joint and the sacroiliac joints have a prominent ridge-like profile when viewed on coronal images.

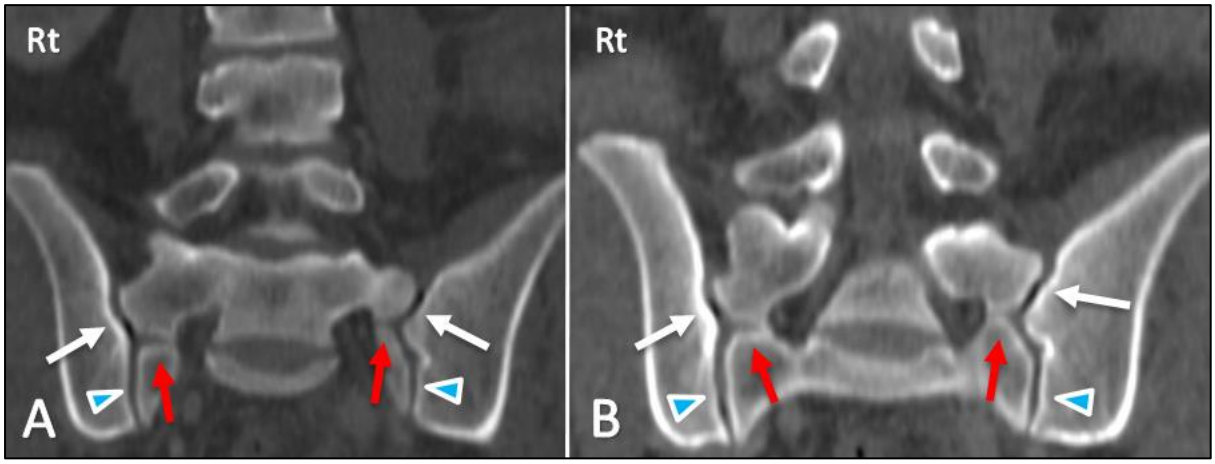

Figure 3.50: *A lumbosacral transitional vertebrae displaying an articulation of the transverse process with the alae of the sacrum and the ilium.* ***A and B)*** *Coronal CT scan images of the lumbosacral junction and lower lumbar spine display concomitant articulation of the lumbar transverse processes of the lumbosacral transitional vertebra with the ilia of the pelvis in addition to the lumbosacral transitional vertebra articulation. Note: there are areas of hypodensity (dark spots) seen between the articulations of the lumbar transverse processes and the ilia of the pelvis on both sides. This represents the finding of intra-articular vacuum phenomenon. The white arrows indicate the transverso-iliac articulation between the transverse process of the lumbosacral transitional vertebra and the ilia of the pelvis. The red arrows indicate the lumbosacral articulation of the transverse processes of the lumbosacral transitional vertebra with the alae of the sacrum. The arrowheads indicate the sacroiliac articulation between the auricular surface of the sacrum and the ilia of the pelvis. Both images* ***A*** *and* ***B*** *are of the same individual. Note: a tongue-in-groove appearance is seen bilaterally in A and B formed by the ilio-transverse joint, and the sacroiliac joint which have a prominent ridge-like profile when viewed on coronal images.* ***Rt****= Right.*

CHAPTER 4

RESULTS CONTINUED

Part II: OSTEOLOGICAL MORPHOLOGY

Introduction

This study was divided into two main parts, each containing sub-objectives:

Osteological morphology contained:

a) Metric observations; and

b) Non-metric observations.

Ancestry was recorded and reported under frequencies but was not evaluated in the statistical analyses due to the Dart Collection containing an assemblage dominated by African-ancestry skeletal remains at 83.4% of the total sample and 92.3% of the LSTV cohort. Refer to Tables 4.1 and 4.2.

Frequencies and percentages

A systematic search of the WITS' Dart Collection of Human Skeletons found 1797 cadaveric human skeletal specimens (N_t=1797) from the ages of 21 to 65 years at AD, of which 114 skeletal remains were identified as containing LSTV. Damage and loss of vertebral elements resulted in a subset of 91 LSTV for the study (N=91). The total number of males found was 1308 (72.8%) compared to 489 (27.2%) females.

A sex balanced control group cohort (N=60), 30 males (n=30) and 30 females (n=30), was selected at random from the Dart Collection. This group represents the non-variation representation within the general population (Table 4.3). A summary of the total sample of the study as well as the LSTV cohort according to ancestry and sex, tabulated in Tables 4.1 and 4.2.

Table 4.1: Summary of the total study cohort.

ANCESTRY	SEX	SEX DISTRIBUTION		SUB-TOTAL
		Frequency	Percentage	
AFRICAN	MALE	1135	74.9%	1515
	FEMALE	380	25.1%	
MIXED	MALE	61	59.8%	103
	FEMALE	42	41.2%	
EUROPEAN	MALE	110	61.5%	179
	FEMALE	69	38.5%	
TOTAL (N_t)				**1797**

The average age at death (AD) for the total sample group was 45.10 years (standard deviation 12.23 years) (N=1797). The minimum AD was 21 years, and the maximum age was 65 years old for both male and female cohorts. The average AD for the male cohort was 45.63 years (standard deviation 11.81 years). The average AD for the female cohort was 43.62 years (standard deviation 13.18 years).

Table 4.2: Summary of the lumbosacral transitional vertebrae cohort.

ANCESTRY	SEX	SEX DISTRIBUTION		SUB-TOTAL
		Frequency	Percentage	
AFRICAN	MALE	63	69.2%	84
	FEMALE	21	23.1%	
MIXED	MALE	2	2.2%	4
	FEMALE	2	2.2%	
EUROPEAN	MALE	1	1.1%	3
	FEMALE	2	2.2%	
TOTAL (N)				**91**

The average age at death for the LSTV cohort was 42.70 years (N=91) (standard deviation 12.41 years). The minimum AD was 21 years, and the maximum age was 65 years old. The average AD for the male sample was 43.5 years (standard deviation 11.76 years). The average AD for the female sample was 40.67 years (standard deviation 12.99 years).

Table 4.3: Summary of the control group cohort.

ANCESTRY	SEX	SEX DISTRIBUTION		SUB-TOTAL
		Frequency	Percent	
AFRICAN	MALE	23	36.7%	48
	FEMALE	25	43.3%	
MIXED	MALE	2	3.3%	5
	FEMALE	3	5%	
EUROPEAN	MALE	5	8.3%	7
	FEMALE	2	3.3%	
TOTAL				60

Within the sex balanced control sample, 30 males and 30 females, an average age at death was 37.71 years old (standard deviation 9.83 years). The minimum AD was 21 years old and the maximum age was 60 years old. The average AD for the male cohort was 39.70 years (standard deviation 10.21 years). The minimum AD for the male cohort was 25 years old and the maximum age was 60 years old. The average AD for the female cohort was 35.50 years (standard deviation 9.47 years). The minimum AD for the female cohort was 21 years old and the maximum age was 55 years old.

Examples of LSTV found in the osteological cohort appraisal

A selection of osteological images was chosen for display to provide examples of the various types and subtypes of LSTV found in the study. Types II, III and IV as well as their subtypes are displayed in Figures 4.1 to 4.3.

Type II lumbosacral transitional vertebrae

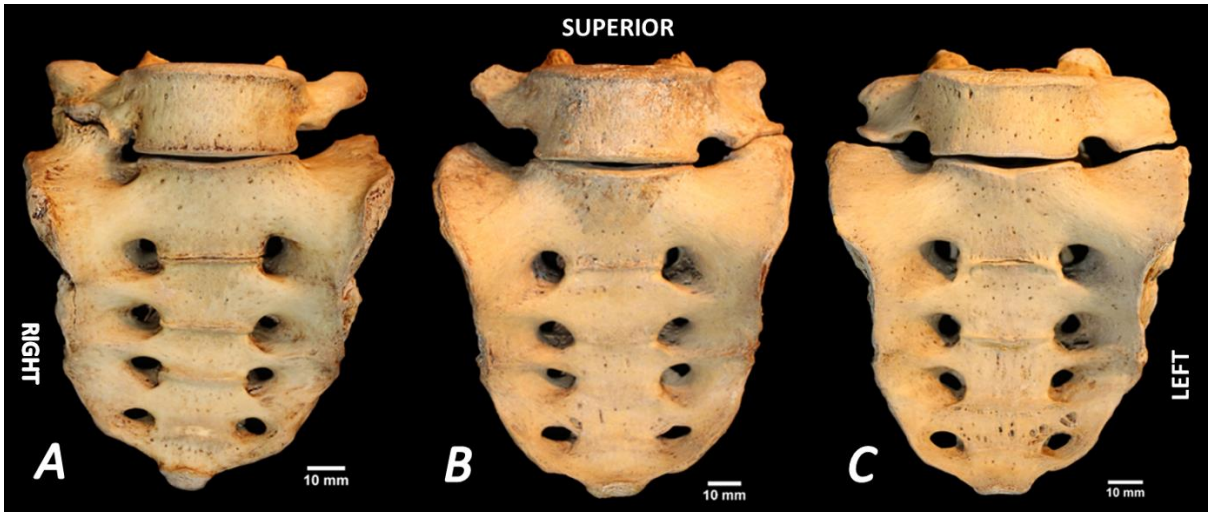

Figure 4.1: *Anterior view of Type II lumbosacral transitional vertebrae.* ***A)*** *Right-sided type IIA lumbosacral transitional vertebra.* ***B)*** *Left-sided Type IIA lumbosacral transitional vertebra.* ***C)*** *Type IIB lumbosacral transitional vertebra.* ***Photography and editing:*** *GJ Paton.*

Type III lumbosacral transitional vertebrae

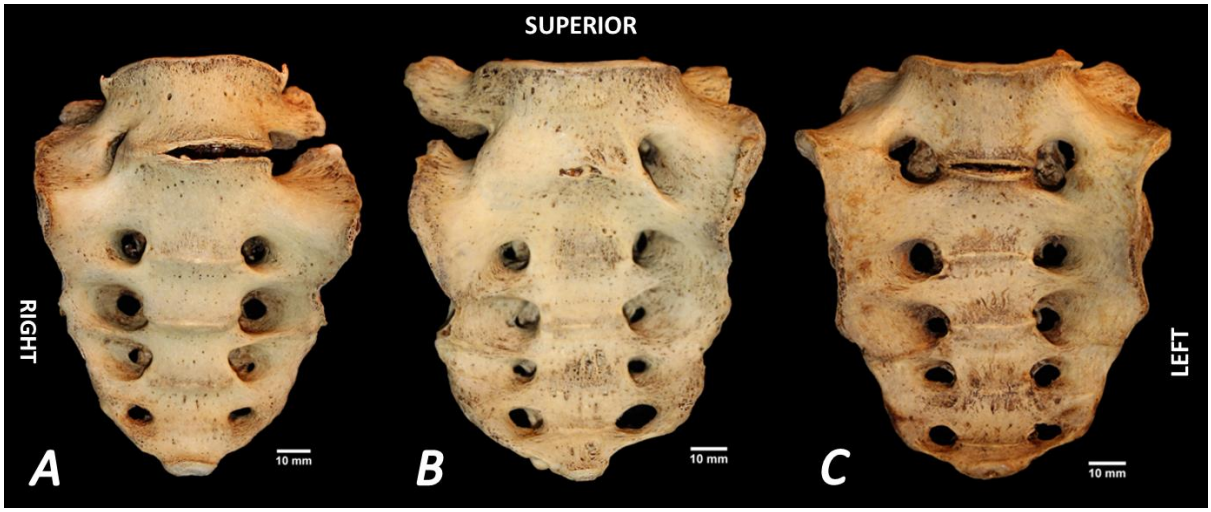

Figure 4.2: *Type III lumbosacral transitional vertebrae.* ***A)*** *Right-sided type IIIA lumbosacral transitional vertebra.* ***B)*** *Left-sided Type IIIA lumbosacral transitional vertebra.* ***C)*** *Type IIIB lumbosacral transitional vertebra.* ***Photography and editing:*** *GJ Paton.*

TYPE IV lumbosacral transitional vertebrae

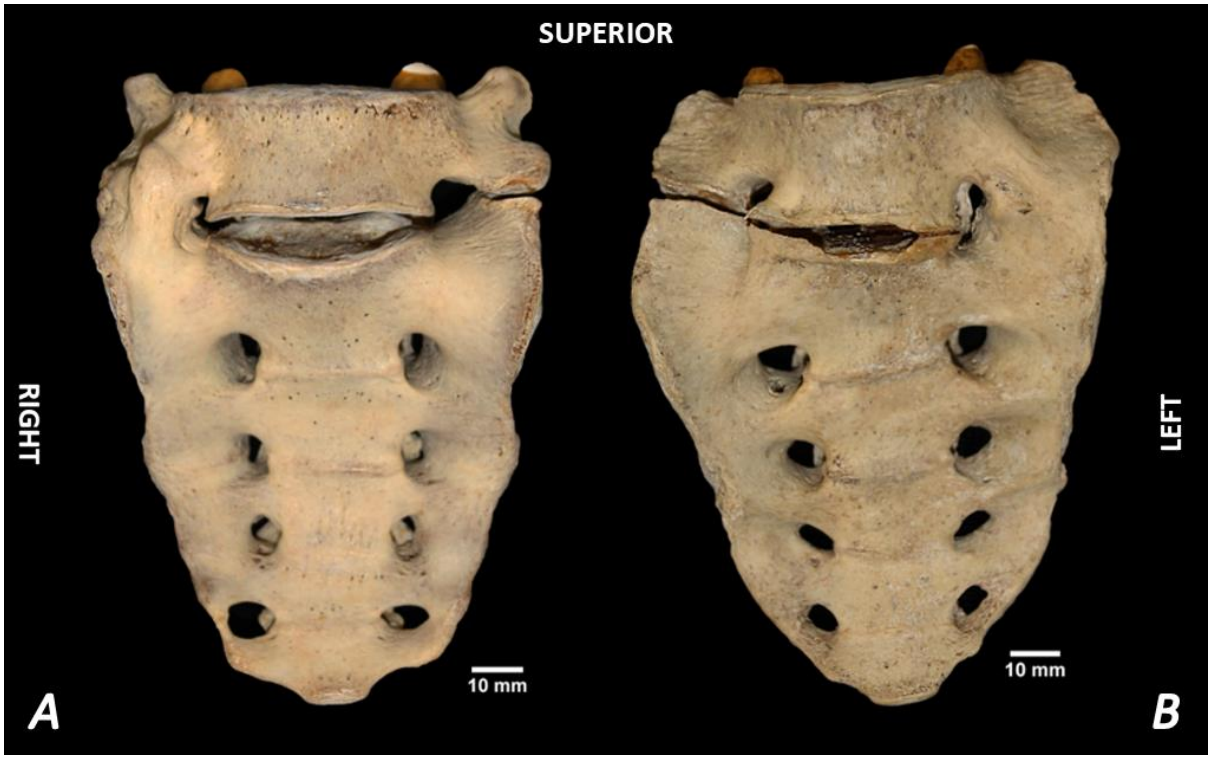

Figure 4.3: Type IV lumbosacral transitional vertebrae. **A)** Right-sided fusion of the transverse process to the ala of the sacrum with left-sided contact/ articulation of the transverse process to the ala of the sacrum. **B)** Left-sided fusion of the transverse process to the ala of the sacrum with right-sided contact/ articulation of the transverse process to the ala of the sacrum. ***Photography and editing:*** *GJ Paton.*

Type of lumbosacral transitional vertebrae

The largest category found was the Type II LSTV at 64.8% (n=59/91) of the sample, which consisted of articulation of one or both the lumbar TVPs with the alae of the sacrum. The second-largest category found was the Type III LSTV, accounting for 22.0% (n=20/91) of the sample, containing a fusion of one or both lumbar TVPs with the alae of the sacrum. The Type IV LSTV was the smallest category, accounting for only 13.2% (n=12/91) of the sample, which consisted of a unilateral articulation of the lumbar TVP with ala of the sacrum while concomitantly sharing a contralateral fusion of the lumbar TVP to the ala of the sacrum. Table 4.4 summarises the frequencies of three major types of LSTV categorised within this cohort.

Table 4.4: Classification of lumbosacral transitional vertebrae by Type.

TYPE of LSTV	Frequency	Percent
Type II	60	65.9
Type III	19	20.9
Type IV	12	13.2
Total (N)	91	100.0

Subtype of lumbosacral transitional vertebrae

The largest category found was the Type IIA LSTV at 40.7% (n=37/91) of the sample, which consisted of an articulation of the lumbar TVP with the ala of the sacrum. The second-largest category was the Type IIB LSTV, accounting for 25.3% (n=23/91) of the sample, which consisted of articulating of both lumbar TVP with the alae of the sacrum. The third most common category found was the Type IIIB LSTV, accounting for 14.3% (n=13/91) of the sample, which consisted of bilateral lumbar TVP fusion to the alae of the sacrum. The Type IV LSTV morphology was present in 13.2% (n=12/91) of the sample while the least common subtype of LSTV at 6.6 % (n=6/91) was Type IIIA, a fusion of a one lumbar TVP to the ala of the sacrum. Refer to Table 4.5 for a summary of the findings of subtypes of LSTV categorised within this cohort.

Table 4.5: Subtypes of lumbosacral transitional vertebrae in the osteological cohort.

Subtypes	Frequency	Percent	Cumulative Percent
Type IIA	36	39.6	40.7
Type IIB	23	25.3	65.9
Type IIIA	6	6.6	72.5
Type IIIB	14	15.4	86.8
Type IV	12	13.2	100.0
Total (N)	91	100.0	

Frequency of side of lumbosacral transitional vertebrae

The largest category for frequency of side was 'bilateral' which accounted for 40.7% (n=37/91) of the sample. The 'left' side followed this at 35.2% (n=32/91) of the sample while the 'right' side represented the least common frequency of side, accounting for 11.0% (n=10/91). Regarding 'other', which represented the Type IV LSTV, this type contributed to 13.2% (n=12/91) of the sample. Type IV cannot be sided. Refer to Table 4.6 to summarise the findings for the frequency of sides associated with LSTV within this cohort.

Table 4.6: Frequency of side of lumbosacral transitional vertebrae in the osteological cohort.

Side	Frequency	Percent	Cumulative Percent
Left	32	35.2	35.2
Right	10	11.0	46.2
Bilateral	37	40.7	86.8
Other	12	13.2	100.0
Total	91	100.0	

Subtype and frequency of side of lumbosacral transitional vertebrae

Lumbosacral transitional vertebrae subtypes and their frequency of side were found in the following proportions:

The largest category of LSTV subtype and their frequency of side was the 'Type IIA Left' at 31.9% (n=29) of the sample. The second-largest number was the 'Type IIB' at 25.3% (n=23/91) of the sample. Third by number was the 'Type IIIB' with 15.4% (n=14/91) followed by the 'Type IIA Right' which represented 7.7% (n=7) of the sample. The categories 'Type IIIA Left' (n=3/91) and 'Type IIIA right' (n=3) consisted of the same number and percentage at 3.3% of the sample. The Type IV LSTV accounted for 13.2% (12/91) of the total sample and it could not be sided. Refer to Table 4.7 to summarise the findings of LSTV Subtype and side preference categorised within this cohort.

Table 4.7: Subtype and frequency of side.

	SUBTYPE AND FREQUENCY OF SIDE							TOTAL
	TYPE IIA LEFT	TYPE IIA RIGHT	TYPE II Bilateral	TYPE IIIA LEFT	TYPE IIIA RIGHT	TYPE III Bilateral	TYPE IV	
COUNT	29	7	23	3	3	14	12	**91**
PERCENTAGE	31.9	7.7	25.3	3.3	3.3	15.4	13.2	**100.0**

Spinal enumeration

Lumbar spine enumeration was split into sacralisation and lumbarisation. The majority of spinal enumeration associated with LSTV was sacralisation representing 72.5% (n=66) while lumbarisation accounted for 27.5% (n=25) of the sample.

Osteometric Measurements

Twenty-three separate sets of measurements were labelled one to twenty-three for each of the dimensions (D). These were discussed individually to avoid confusion. Refer to Tables 4.8 and 4.9 for an overview of the LSTV and control cohort's measurements. Variability of number exists per dimension. Samples free of considerable damage or arthrosis were utilised in the data collection and analyses. Selected areas of damage and advanced arthrosis were found unilaterally or bilaterally, making measurement impossible for dimensions. This was attributed to the AD of the skeletal remains (aged spine) and wear of the skeletal remains from use and storage from previous research endeavours. Where possible, utilisation of the remainder of the viable intact skeletal remains was used to bolster the number of samples available for statistical analyses. Statistical comparison was performed for each measurement with four subcategories for each measurement (where possible).

The five main statistical comparisons were:

- LSTV cohort and the control cohort;
- Male and female LSTV cohorts;
- Male and female control cohorts;
- LSTV male cohort and male control cohort; and
- LSTV female cohort and female control cohort.

Additional analyses were performed on the Type II LSTV cohort comparing the facet joint angles (FA), sacral facet surface areas (FSA), sacral body surface areas (BSA) and accessory facet surface areas (AFSA) to one another. These additional analyses were discussed at the end of each of the Type II LSTV-containing osteometric dimensions. Refer to Table 4.10 for a summary of the statistically significant osteometric results.

The outliers were excluded from the statistical calculations when running the statistical analyses not to skew the results. Outliers are results or observations that differ greatly from the majority (Rousseeuw and Hubert, 2011). This may be as a result of human error, pathology or an aberrant individual. Outliers were demonstrated as numbered individual plot points on the boxplot graphs for visual representation without influencing the statistical results.

Tests for normality

Tests for normality were conducted on the four main statistical comparisons to assess the distribution of the samples. The Shapiro-Wilk test was used to test for normality for data that consisted of small sample size (<50) the Shapiro-Wilk test was used to test for normality. The p-value was set at $p \leq 0.05$ for all statistical tests.

Table 4.8: An overview of the measurements for the dimensions in the lumbosacral transitional vertebrae cohort.

DIMENSION	N *	MEAN (mm)	MEDIAN (mm)	STD. DEVIATION (±)	MINIMUM (mm)	MAXIMUM (mm)
D1. SH	83	102,11	100,76	16,68	69,13	153,01
D2. SBW	83	45,36	44,51	6,316	24,42	59,53
D3. SBL	76	30,35	29,91	3,73	24,53	54,53
D4. IAD	88	101,41	100,77	7,15	79,85	127,54
D5. IFD*lat*	85	48,130	48,48	5,28	38,52	62,23
D6. IFD*med*	86	25,52	25,75	4,62	2,93	38,23
D7. FD	81	15,08	14,28	4,46	4,26	36,16
D8. SFH (right)	77	15,38	15,36	2,72	8,77	24,48
D8. SFH (left)	79	14,99	14,83	2,75	7,54	21,42
D9. SFW (right)	79	13,95	13,98	2,85	8,11	20,80
D9. SFW (left)	80	13,63	13,40	2,59	6,14	19,54
D10. AL (right)	86	59,36	58,83	7,10	46,16	82,89
D10. AL (left)	88	59,84	60,60	9,02	6,65	79,17
D11. FA (right)	91	52,62°	52,61°	9,72°	30,81°	86,21°
D11. FA (left)	91	54,22°	53,90°	10,41°	37,57°	85,99°
D12. SHL	87	20,42	19,02	10,06	3,00	49,98

All measurements were measured in millimetres with the exception of:

Facet angle (FA) was measured in degrees (°)

Surface area measurements (ASA, TPC-ASA, FSA, BSA and AFSA) was measured in square millimetres (mm^2).

*** – Indicates the number of specimens that were utilised per dimension. Only samples free of damage or considerable arthrosis were utilised in the data collection and analyses.***

Table 4.8: (continued)

DIMENSION	N*	MEAN (mm)	MEDIAN (mm)	STD. DEVIATION (±)	MINIMUM (mm)	MAXIMUM (mm)
D13. TVPL (right)	56	19,32	19,04	4,03	7,76	27,63
D13. TVPL (left)	56	21,08	21,09	3,46	12,96	31,15
D14. TVPH (right)	60	20,34	20,42	5,47	8,33	33,01
D14. TVPH (left)	60	22,87	23,09	5,36	9,42	33,46
D15. ASA (right)	83	1177,86 mm^2	1162,31 mm^2	170,94 mm^2	823,38 mm^2	1705,39 mm^2
D15. ASA (left)	86	1185,61 mm^2	1174,73 mm^2	200,43 mm^2	774,84 mm^2	2028,00 mm^2
D16. TPC-ASA (right)	10	116,70 mm^2	88,10 mm^2	95,39 mm^2	15,47 mm^2	309,22 mm^2
D16. TPC-ASA (left)	14	154,23 mm^2	107,64 mm^2	112,39 mm^2	59,41 mm^2	405,02 mm^2
D17. FSA (right)	57	140,35 mm^2	144,02 mm^2	45,59 mm^2	47,71 mm^2	235,02 mm^2
D17. FSA (left)	58	136,63 mm^2	137,62 mm^2	39,74 mm^2	29,84 mm^2	233,84 mm^2
D18. BSA	57	1047,03 mm^2	1056,70 mm^2	172,18 mm^2	697,53 mm^2	1583,00 mm^2
D19. AFSA (right)	31	247,36 mm^2	231,46 mm^2	100,92 mm^2	119,54 mm^2	489,53 mm^2
D19. AFSA (left)	49	285,51 mm^2	282,24 mm^2	113,96 mm^2	101,58 mm^2	603,42 mm^2
D20. VBH1	89	26,55	26,37	1,80	22,53	32,05
D21. VBH2	90	25,71	25,63	1,90	22,10	32,45
D22. TLE	88	17,26	17,00	0,47	16	18

All measurements were measured in millimetres with the exception of:

Facet angle (FA) was measured in degrees (^{o})

Surface area measurements (ASA, TPC-ASA, FSA, BSA and AFSA) was measured in square millimetres (mm^2).

*** – Indicates the number of specimens that were utilised per dimension. Only samples free of damage or considerable arthrosis were utilised in the data collection and analyses.***

Table 4.9: An overview of the measurements for the dimensions in the control group cohort.

DIMENSION	N	MEAN (mm)	MEDIAN (mm)	STD. DEVIATION (±)	MINIMUM (mm)	MAXIMUM (mm)
D1. SH	60	97,81	97,61	8,63	76,22	113,05
D2. SBW	60	49,53	48,90	4,70	37,72	60,11
D3. SBL	60	30,05	30,33	2,69	25,59	37,91
D4. IAD	60	108,57	107,40	15,48	89,90	207,09
D5. IFD*lat*	60	50,72	50,15	4,93	39,52	61,03
D6. IFD*med*	60	26,94	27,03	4,57	18,32	47,82
D7. FD	60	17,70	17,69	2,30	13,46	22,65
D8. SFH (right)	60	16,17	16,08	1,62	12,19	20,06
D8. SFH (left)	60	16,27	16,27	1,65	12,59	21,72
D9. SFW (right)	60	15,69	15,31	1,99	11,76	20,92
D9. SFW (left)	60	15,70	15,70	1,67	11,86	19,40
D10. AL (right)	60	56,67	56,34	4,72	44,23	66,96
D10. AL (left)	60	56,95	56,73	5,22	45,33	70,93
D11. FA (right)	60	51,68^{o}	51,66^{o}	7,94^{o}	36,62^{o}	74,69^{o}
D11. FA (left)	60	50,80^{o}	51,54^{o}	8,46^{o}	27,35^{o}	80,36^{o}
D12. SHL	60	16,98	16,28	7,29	3,97	36,68
D13. TVPL (right)	60	17,39	17,09	3,29	9,33	24,34
D13. TVPL (left)	60	17,23	17,21	3,19	10,37	26,80

All measurements were measured and recorded in millimetres with the exception of:

Facet angle (FA) was measured and recorded in degrees (^{o})

Surface area measurements (ASA, FSA, BSA) was measured and recorded in square millimetres (mm^{2}).

Table 4.9: (Continued)

DIMENSION	N	MEAN (mm)	MEDIAN (mm)	STD. DEVIATION (±)	MINIMUM (mm)	MAXIMUM (mm)
D14. TVPH (right)	60	12,91	12,77	2,28	7,32	18,50
D14. TVPH (left)	60	12,72	12,38	2,045	8,39	18,78
D15. ASA (right)	60	1124,70mm^2	1112,50mm^2	162,81mm^2	780,53mm^2	1612,36mm^2
D15. ASA (left)	60	1131,11 mm^2	1121,33 mm^2	166,79 mm^2	825,36 mm^2	1515,05 mm^2
D17. FSA (right)	60	201,79 mm^2	202,70 mm^2	41,21 mm^2	130,30 mm^2	313,31 mm^2
D17. FSA (left)	60	204,22 mm^2	201,26 mm^2	39,48 mm^2	124,25 mm^2	315,87 mm^2
D18. BSA	60	1206,15 mm^2	1191,62 mm^2	215,54 mm^2	813,12 mm^2	1861,51 mm^2
D20. VBH1	60	25,96	25,89	1,92	20,12	30,00
D21. VBH2	60	25,78	25,90	1,83	19,73	29,27
D22. TLE	60	17,07	17,00	0,25	17	18

All measurements were measured and recorded in millimetres with the exception of:

Facet angle (FA) was measured and recorded in degrees (^{o})

Surface area measurements (ASA, FSA, BSA) was measured and recorded in square millimetres (mm^2).

Table 4.10: Summary of statistically significant osteometric results.

DIMENSION	Statistically significant	P-value	DIMENSION	Statistically significant	P- value
D1. SH	LSTV[+] vs control	*p*=0.047	**D8. SFH (right)**	LSTV male vs control male[+]	P=0.059
			D8. SFH (left)	LSTV vs control[+]	*p*=0.001
D2. SBW	LSTV vs control[+]	*p*<0.001		LSTV female vs control female[+]	*p*=0.002
	Control male[+] vs female	*p*=0.001		LSTV male vs control male[+]	*p*=0.037
	LSTV female vs control female[+]	*p*=0.002	**D9. SFW (right)**	LSTV vs control[+]	*p*<0.001
	LSTV male vs control male[+]	*p*<0.001		LSTV female vs control female[+]	*p*=0.012
D3. SBL	Control male[+] vs female	*p*=0.001		LSTV male vs control male[+]	*p*=0.003
D4. IAD	LSTV[+] and control	*p*=0.001	**D9. SFW (left)**	LSTV vs control[+]	*p*<0.001
	LSTV male vs control male[+]	*p*=0.003		LSTV female vs control female[+]	*p*<0.001
D5. IFD*lat*	LSTV vs control[+]	*p*=0.003		LSTV male vs control male[+]	*p*=0.001
	LSTV male vs control male[+]	*p*=0.010	**D10. AL (right)**	LSTV[+] vs control	*p*=0.007
D6. IFD*med*	Control male[+] vs female	*p*=0.019		LSTV male[+] vs female	*p*=0.039
	LSTV male vs control male[+]	*p*=0.031		Control male[+] vs female	*p*=0.007
D7. FD	LSTV vs control[+]	*p*<0.001	**D10. AL (left)**	LSTV[+] vs control	*p*=0.015
	LSTV female vs control female[+]	*p*=0.001		LSTV male[+] vs female	*p*=0.001
	LSTV male and control male[+]	*p*<0.001		Control male[+] vs female	*p*=0.045
D8. SFH (left)	LSTV vs control[+]	*p*=0.037		LSTV male[+] vs control male	*p*=0.011

+ – Indicates which cohort had the larger statistically significant mean measurement.

Table 4.10: Continued.

DIMENSION	Statistically significant	P-value	DIMENSION	Statistically significant	P-value
D11. FA (right)	Additional x 2	$p<0.001$	**D14. TVPH (right)**	LSTV$^+$ vs control	$p<0.001$
		$p=0.007$		LSTV female$^+$ vs control female	$p<0.001$
D11. FA (left)	LSTV vs control$^+$	$p=0.028$		LSTV male$^+$ vs control male	$p<0.001$
	LSTV male vs female$^+$	$p=0.023$	**D14. TVPH (left)**	LSTV$^+$ vs control	$p<0.001$
	LSTV female$^+$ vs control female	$p=0.003$		LSTV female$^+$ vs control female	$p<0.001$
	Additional x 1	$p<0.001$		LSTV male$^+$ vs control male	$p<0.001$
D12. SHL	LSTV$^+$ vs control	$p=0.025$	**D15. ASA (right)**	Control male$^+$ vs female	$p=0.010$
D13. TVPL (right)	LSTV$^+$ vs control	$p=0.005$		LSTV female$^+$ vs control female	$p=0.028$
	LSTV male$^+$ vs control male	$p=0.028$	**D15. ASA (left)**	LSTV male$^+$ vs female	$p=0.025$
D13. TVPL (left)	LSTV$^+$ vs control	$p<0.001$		Control male$^+$ vs female	$p=0.025$
	LSTV female$^+$ vs control female	$p<0.001$			
	LSTV male$^+$ vs control male	$p<0.001$			

+ – Indicates which cohort had the larger statistically significant mean measurement.

Table 4.10: Continued.

DIMENSION	Statistically significant	P-value	DIMENSION	Statistically significant	P-value
D17. FSA (right)	LSTV vs control[+]	$p<0.001$	**D18. BSA**	LSTV vs control[+]	$p<0.001$
	LSTV male vs female[+]	$p=0.029$		Control male[+] vs female	$p<0.001$
	LSTV female vs control female[+]	$p=0.012$		LSTV male vs male control[+]	$p<0.001$
	LSTV male vs control male[+]	$p<0.001$		Additional x 2	$p=0.005$
	Additional x 3	$p<0.001$			$p<0.001$
		$p=0.005$	**D19. AFSA (right)**	Additional x1	$p=0.045$
		$p=0.045$	**D22. TLE**	LSTV[+] vs control	$p=0.001$
D17. FSA (left)	LSTV vs control[+]	$p<0.001$		Control male[+] and female	$p=0.040$
	LSTV female vs control female[+]	$p<0.001$		LSTV female[+] vs control female	$p=0.008$
	LSTV male vs control male[+]	$p<0.001$	**D23L**	LSTV[+] vs control	$p<0.001$
	Additional x 2	$p<0.001$ $p<0.001$		Male cohort	$p<0.001$

+ – Indicates which cohort had the larger statistically significant mean measurement.

D1: Sacral height (SH)

The LSTV cohort (n=83) consisted of 63 males (n=63) and 20 females (n=20). The control cohort (n=60) consisted of 30 males (n=30) and 30 females (n=30).

Sacral height comparison of lumbosacral transitional vertebrae cohort and the control cohort

The mean SH in the LSTV cohort (102.11mm ± 16.68mm) was larger than the control cohort (97.81mm ±8.63mm). The SH of the LSTV cohort had a larger range in variation of length, between 69.13mm and 153.01mm, while the control cohort range was between 76.22mm and 113.05mm.

Sex comparison of lumbosacral transitional vertebrae and control cohorts

A sex comparison found that the mean SH of males in the LSTV cohort (103.34mm ± 20.90mm) was longer than that of the females within the same cohort (98.24mm ± 13.57mm). The SH measurements ranged in LSTV men from 69.13mm to 153.01mm, while LSTV females range was 76.91mm to 126.80mm in length.

Likewise, a sex comparison of the mean SH of men in the control cohort was longer (99.02mm ± 9.79mm) than the females (96.99mm ± 7.27mm) within the same cohort. The SH measurements ranged in the control cohort in males from 76.22mm to 113.05mm, while in the females, the measurement group ranged from 87.65mm to 112.34mm in length.

The mean SH of males in the LSTV cohort (103.34mm ± 20.90mm) was longer than the males in the control cohort (99.02mm ± 9.79mm). Similarly, the mean SH of females in the LSTV cohort was longer than the females in the control cohort. Refer to Tables 4.9 and 4.10 and Figures 4.4 and 4.5. Figure 4.6 demonstrates the SH variations associated with LSTV.

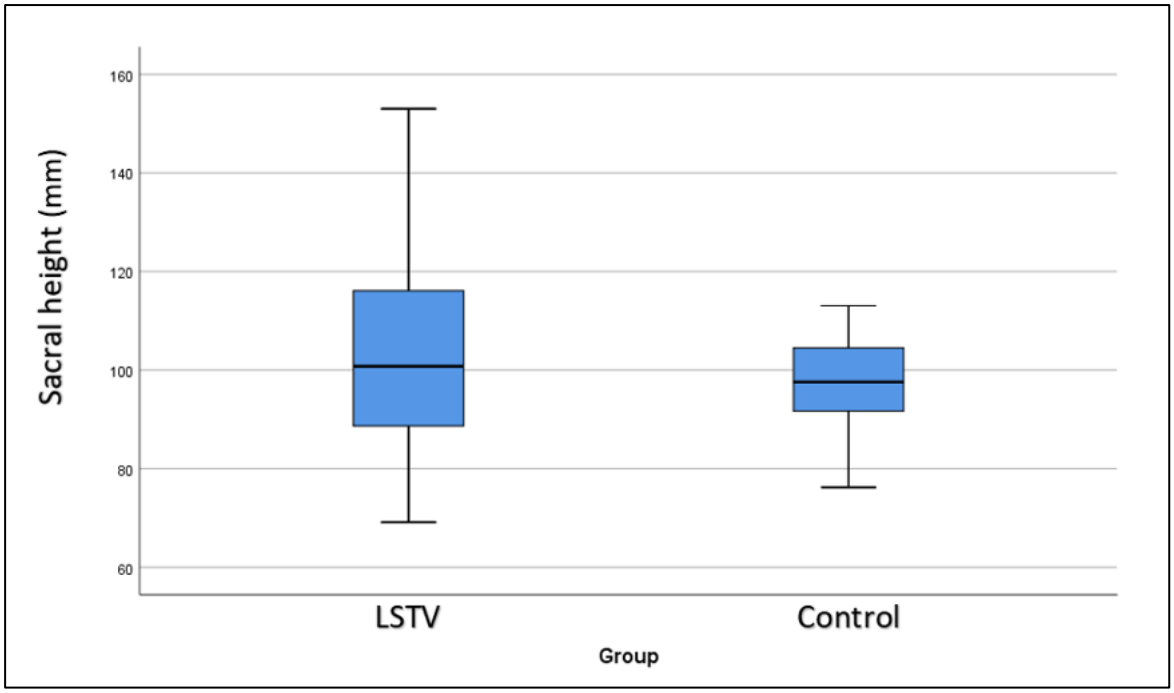

Figure 4.4: *A boxplot graph of the sacral height measurement for the LSTV and control cohorts.*

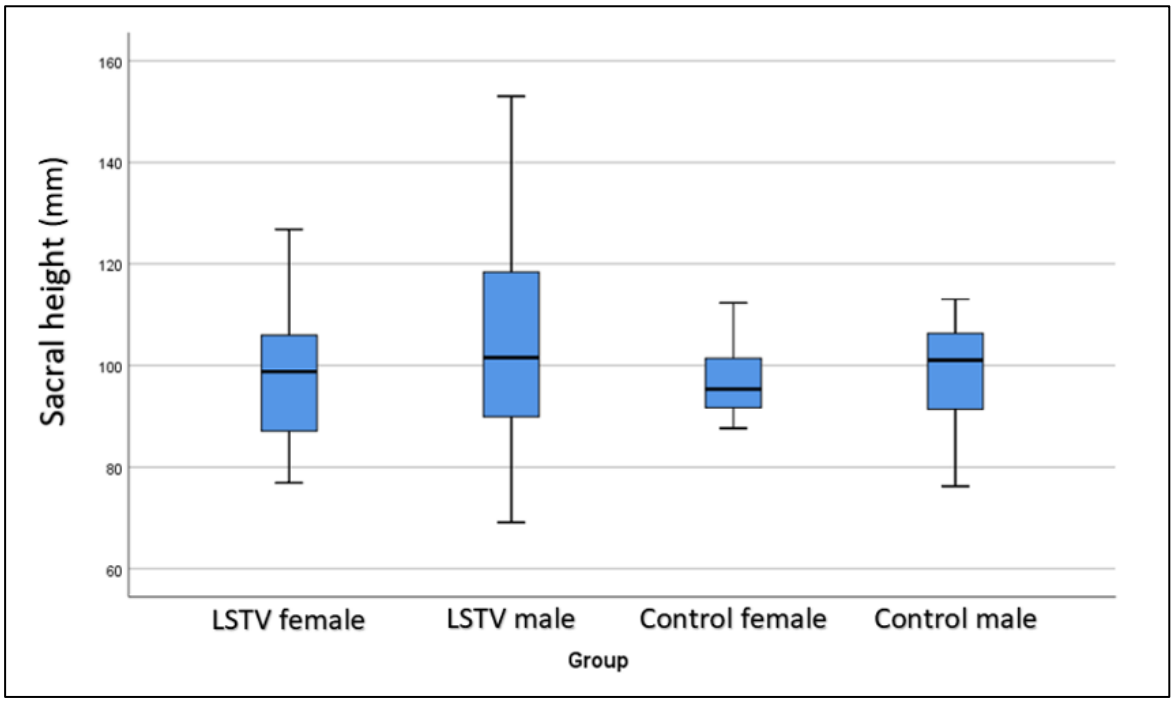

Figure 4.5: *A boxplot graph of the sacral height measurement for the LSTV and control cohorts comparing the sexes.*

Statistical analyses

Lumbosacral transitional vertebrae cohort and control cohort comparison

The T-test compared the mean rank values of SH in the LSTV (n=83) cohort and the control (n=60) cohort. Levene's test for variance was not equal. The unequal variance T-test (t=2.01, df=129.33, *p*=0.047) found a statistically significant difference in SH in the LSTV cohort (n=83) containing a longer sacrum compared to the control cohort (n=60).

Lumbosacral transitional vertebrae male and female cohort comparison

The Mann-Whitney U test compared the mean rank values of SH in the LSTV male cohort (n=63) and the LSTV female (n=20) cohort. There was no statistically significant difference (U=526.00, Z=-1.11, *p*=0.268) in SH between the LSTV male (mean rank 43.65) and female (mean rank 36.80) cohorts.

Control cohort male and female comparison

The Mann-Whitney U test compared the mean rank values of SH in the male (n=30) and the female (n=30) control cohorts. There was no statistically significant difference (U=377.00, Z=-1.08, *p*=0.280) in SH between the control male (mean rank 32.93) and female (mean rank 28.07) cohorts.

Female lumbosacral transitional vertebrae cohort and female control cohort comparison

The Mann-Whitney U test compared the mean rank values of the SH in the LSTV female (n=20) and the control female (n=30) cohorts. There was no statistically significant difference (U=285.00, Z=-0.30, *p*=0.766) in SH between the LSTV female (mean rank 26.25) and the control female (mean rank 25.00) cohorts.

Male lumbosacral transitional vertebrae cohort and male control cohort comparison

The Mann-Whitney U test compared the mean rank values of the SH in the LSTV male (n=63) and the control male (n=30) cohorts. There was no statistically significant difference (U=811.50, Z=-1.097, *p*=0.273) in SH between the LSTV female (mean rank 49.12) and the control female (mean rank 42.55) cohorts.

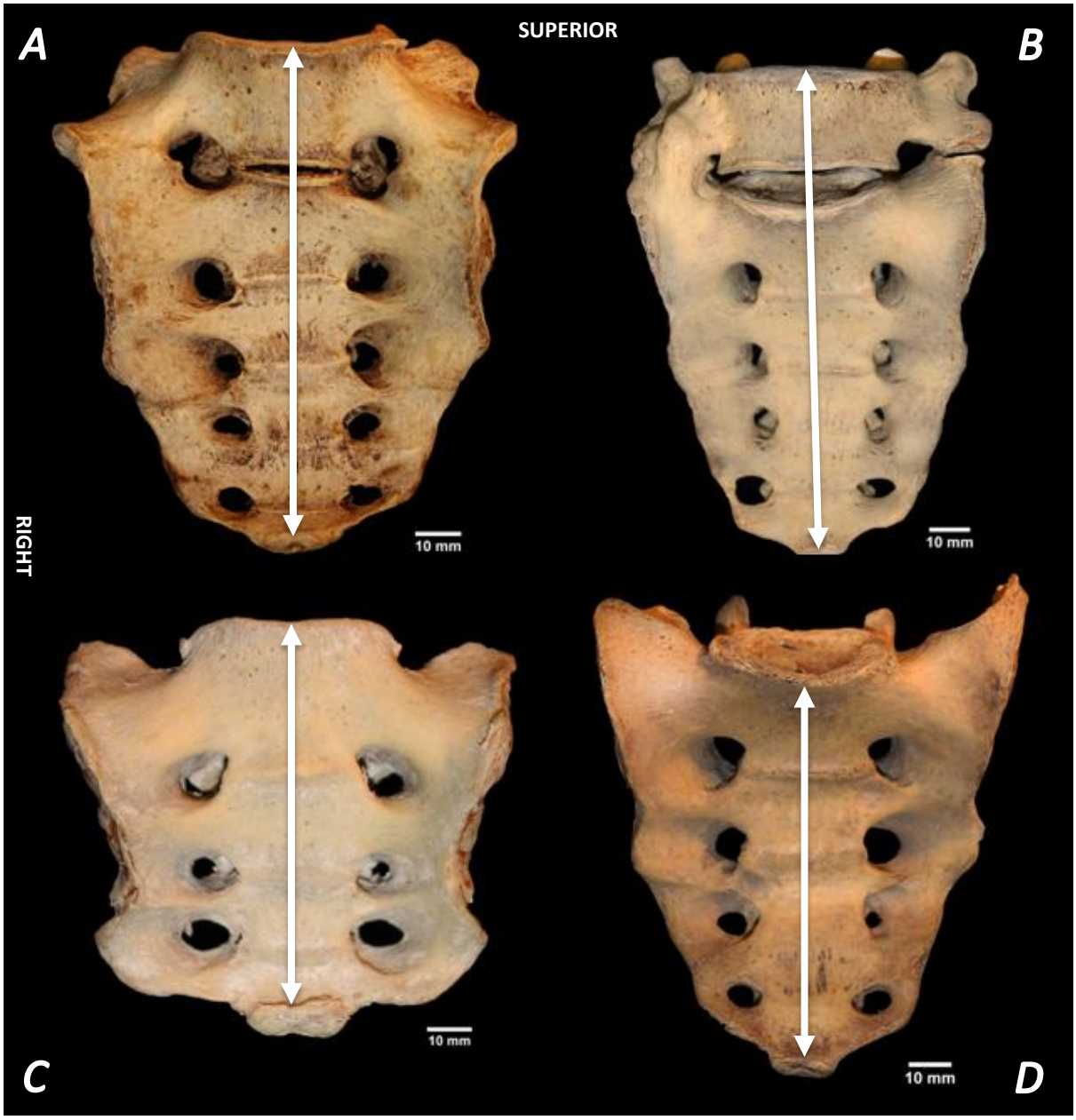

Figure 4.6: *Anterior view of sacra displaying the sacral length associated with lumbosacral transitional vertebrae.* ***A)*** *A Type IIIB lumbosacral transitional vertebra.* ***B)*** *A Type IV lumbosacral transitional vertebra.* ***C)*** *A Type IV lumbosacral transitional vertebra.* ***D)*** *A Type IIB lumbosacral transitional vertebra. The double arrows indicate the sacral height measurements.* ***Photography and editing:*** *GJ Paton.*

D2: Sacral Body Width (SBW)

The LSTV cohort (N=83) consisted of 59 males (n=59) and 24 females (n=24). The control cohort (N=60) consisted of 30 males (n=30) and 30 females (n=30).

Sacral body width comparison of lumbosacral transitional vertebrae and the control cohort

The mean SBW in the LSTV cohort (45.36mm ± 6.32mm) was longer than the control cohort (49.54mm ±4.70mm). The SBW of the LSTV cohort had a larger range in variation of width, between 40.42mm and 59.53mm, while the control cohort range was between 37.72mm and 60.11mm.

Sex comparison of lumbosacral transitional vertebrae and control cohorts

A sex comparison found that the mean SBW of males in the LSTV cohort (46.35mm ± 6.07mm) was longer than that of the LSTV female cohort (42.95mm ± 6.38). The SBW measurements ranged in LSTV males from 32.97mm to 59.53mm while LSTV female range was 24.42mm to 53.78mm in length.

Likewise, the sex comparison of the mean SBW in males in the control cohort (51, 57 ± 4, 68mm) was longer when compared to the female control cohort (47.51mm ± 3.80mm). The SBW measurements ranged in the control cohort in males from 76.22mm to 113.05mm while the female measurements ranged from 87.65mm to 112.34mm in length.

The mean SBW of males in the LSTV cohort (46.35mm ± 6.07mm) was shorter than the males in the control cohort (51.57 ± 4.68mm). Similarly, the mean SBW of females in the LSTV cohort was shorter than in the control cohort. Refer to Figures 4.7 and 4.8. Figure 4.9 demonstrates the SBW variations associated with LSTV.

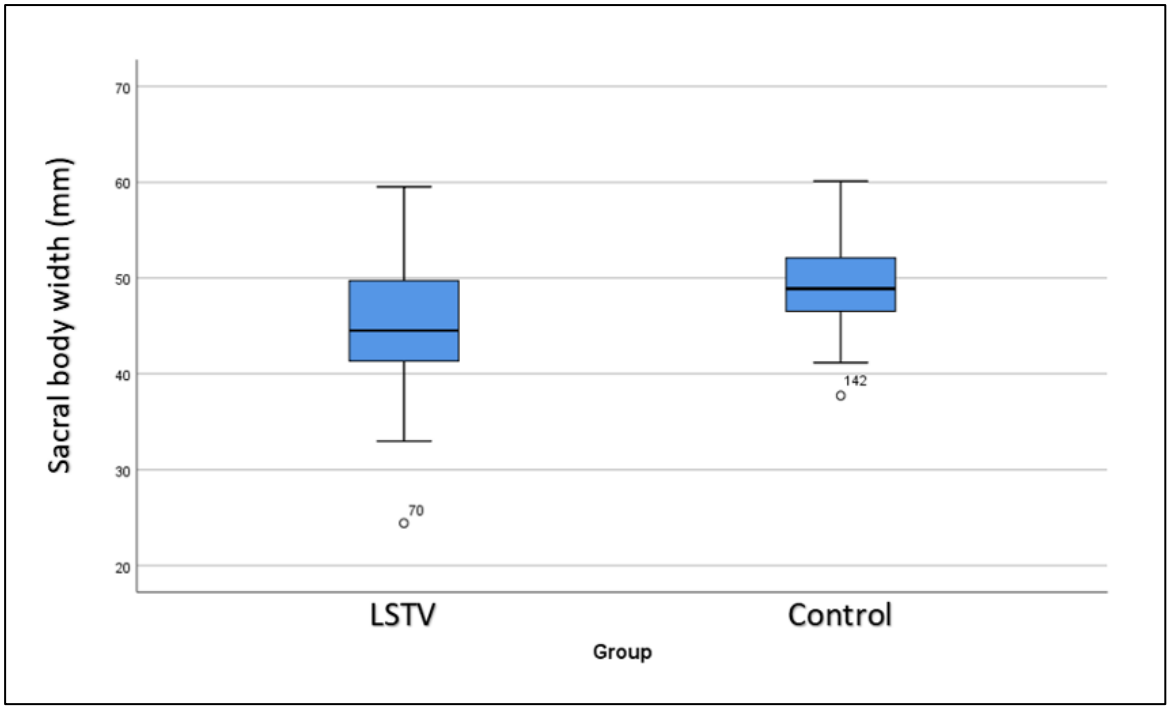

Figure 4.7: *A boxplot graph of the sacral body width measurement for the LSTV and control cohorts' measurements.*

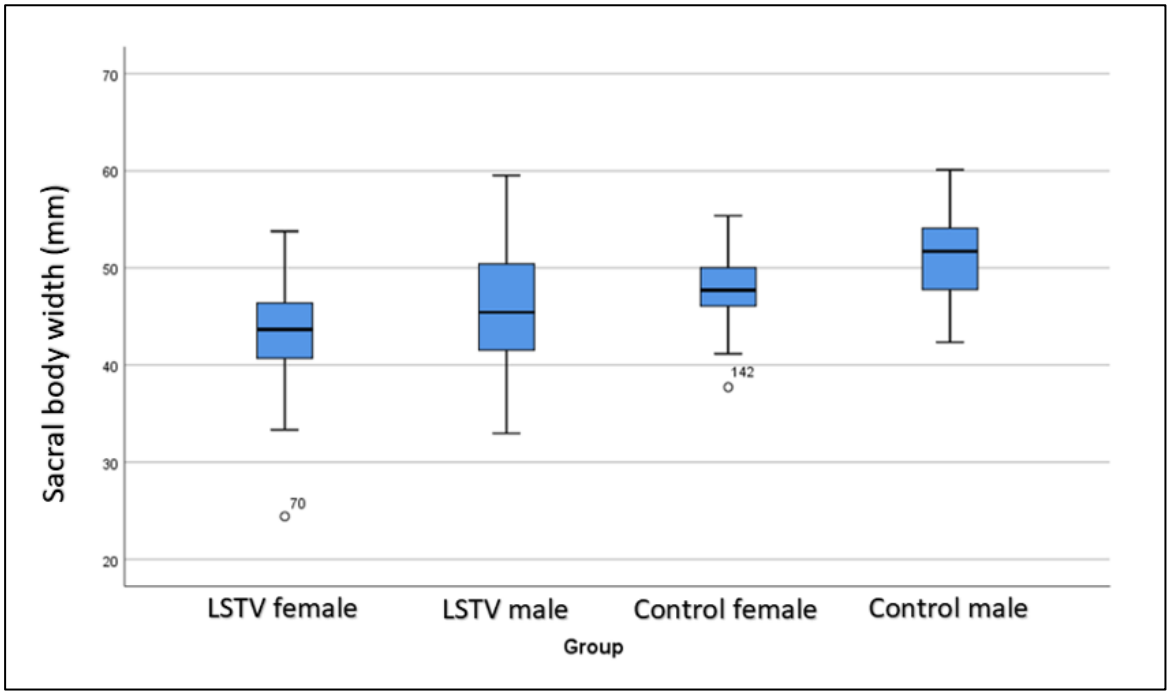

Figure 4.8: *A boxplot graph of the sacral body width measurement for the LSTV and control cohorts comparing the sexes.*

Statistical analyses

Lumbosacral transitional vertebrae and control cohort comparison

The T-test compared the mean rank values of SBW in the LSTV (n=83) cohort and the control (n=60) cohort. Levene's test for variance was not equal. The unequal variance T-test for equality of means (t=-4.53, df= 140.86, p<0.001) found a statistically significant difference in SBW with the LSTV cohort containing a smaller sacral body as measured in width compared to the control cohort.

Lumbosacral transitional vertebrae cohort male and female comparison

The Mann-Whitney U test compared the mean rank values of SBW in the LSTV male cohort (n=59) and the LSTV female (n=24) cohort. There was no statistically significant difference (U=518.00, Z=-1.91, p=0.056) in SBW between the LSTV male (mean rank 45.22) and female (mean rank 34.08) cohorts.

Control cohort male and female comparison

The Mann-Whitney U test compared the mean rank values of SBW in the male (n=30) and the female (n=30) control cohorts. There was a statistically significant difference (U=227.00, Z=-3.30, p=0.001) containing a larger sacral body width when comparing the control male (mean rank 37.93) and female (mean rank 23.07) cohorts.

Female lumbosacral transitional vertebrae cohort and female control cohort comparison

The Mann-Whitney U test compared the mean rank values of the SBW in the female LSTV (n=24) and the female control (n=30) cohorts. There was a statistically significant difference (U=179.00, Z=-3.15, p=0.002) in SBW between the LSTV female (mean rank 19.96) and the control female (mean rank 33.53) cohorts.

Male lumbosacral transitional vertebrae cohort and male control cohort comparison

The Mann-Whitney U test compared the mean rank values of the SBW in the male LSTV (n=59) and the male control (n=30) cohorts.

There was a statistically significant difference (U=442.50, Z=-3.481, p<0.001) in SBW between the LSTV male (mean rank 37.50) and the larger control male (mean rank 59.75) cohorts.

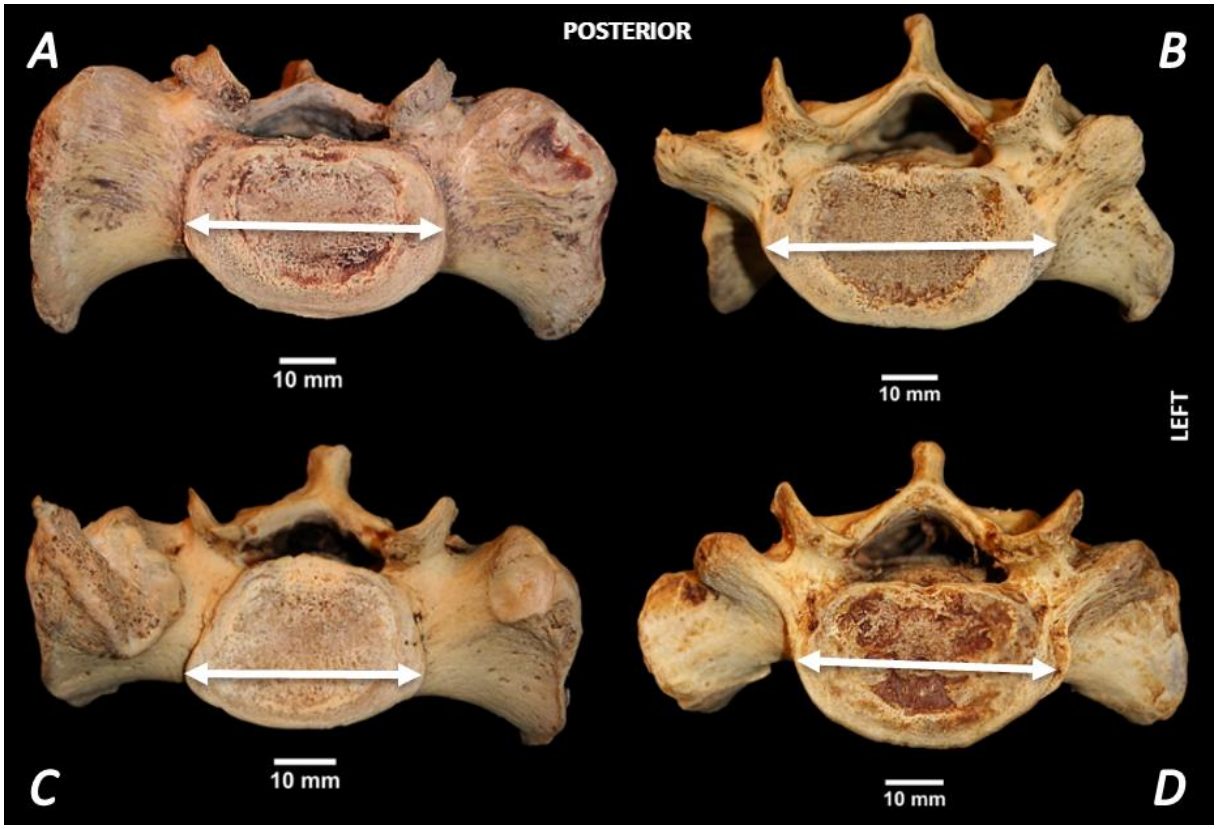

Figure 4.9: *Superior view of sacra displaying sacral body width associated with lumbosacral transitional vertebrae.* ***A)*** *Left sided Type IIA lumbosacral transitional vertebra.* ***B)*** *Left-sided Type IIIA lumbosacral transitional vertebra.* ***C)*** *Type IIB lumbosacral transitional vertebra.* ***D)*** *Type IIIB lumbosacral transitional vertebra. The double arrows indicate the sacral body width measurements.* ***Photography and editing:*** *GJ Paton.*

D3: Sacral body length (SBL)

The LSTV cohort (N=76) consisted of 53 males (n=53) and 23 females (n=23). The control cohort (N=60) consisted of 30 males (n=30) and 30 females (n=30).

Lumbosacral transitional vertebrae cohort compared to the control cohort

The mean SBL in the LSTV cohort (30.35mm ± 3.73mm) was marginally longer than the control cohort (30.05mm ±2.70mm). The SBL of the LSTV cohort had a larger range in variation of length, between 24.53mm and 54.53mm, while the control cohort range was between 25.59mm and 37.91mm in length.

Sex comparison of lumbosacral transitional vertebrae cohort and control cohorts

A sex comparison found that the mean SBL of males in the LSTV cohort (30.42mm ± 2.43mm) was marginally longer than that of the females within the same cohort (30.20mm ± 5.78mm). The SBL measurements ranged in LSTV males from 24.95mm to 36.33mm while LSTV female range was between 24.53mm and 54.53mm in length.

Likewise, sex comparison of the mean SBL in the control cohort was longer for males (31.38mm ± 2.45mm) when compared to the females (28.72mm ± 2.26mm). The SBL measurements ranged in the control cohort in males from 27.43mm to 37.91mm while the female measurements ranged from 25.59mm to 32.62mm in length.

The mean SBL of males in the LSTV cohort (30.42mm ± 2.43mm) was shorter than the males in the control cohort (31.38mm ± 2.45mm). The mean SBL of females in the LSTV cohort (30.20mm ± 5.78mm) was longer than the females in the control cohort (28.72mm ± 2.26mm). Refer to Figures 4.10 and 4.11. Figure 4.12 demonstrates the SBL variations associated with LSTV.

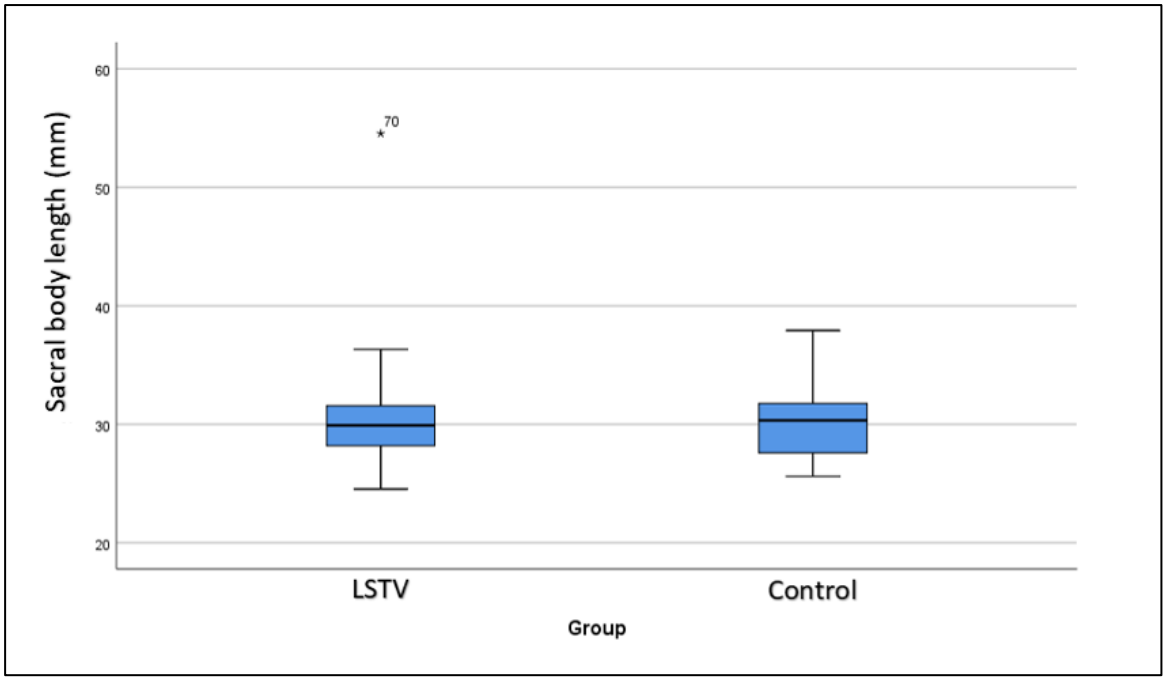

Figure 4.10: *A boxplot graph of the sacral body length measurement for the LSTV and control cohorts.*

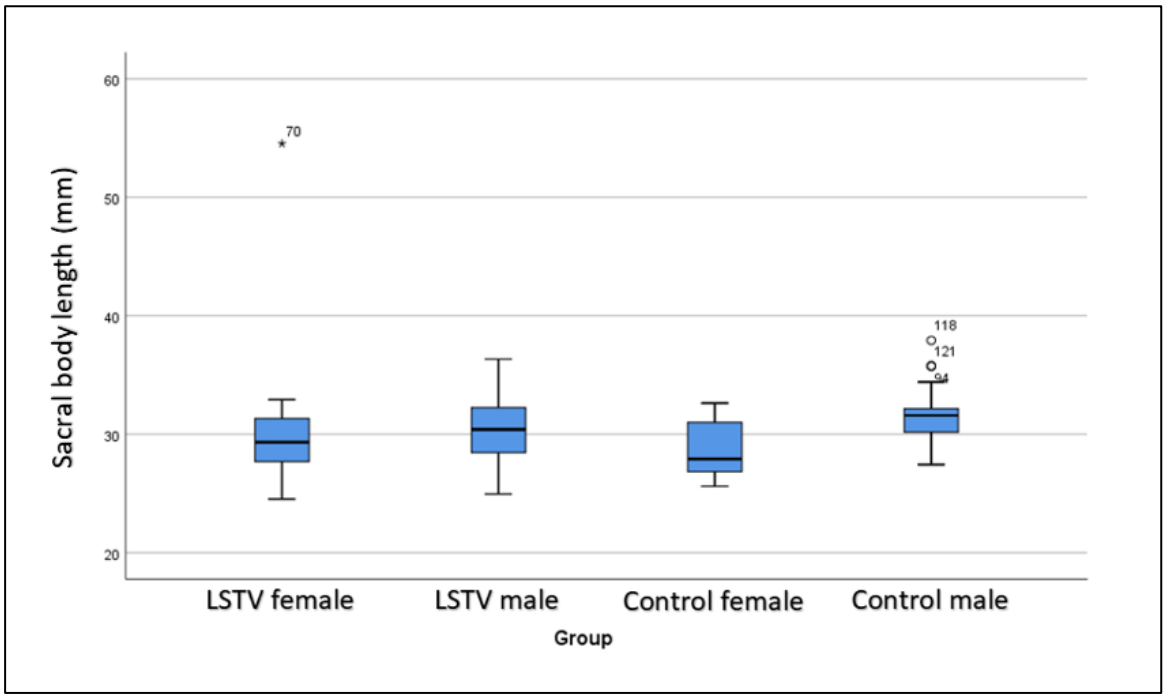

Figure 4.11: A boxplot graph of the sacral body length measurement for the LSTV and control cohorts comparing the sexes.

Statistical analyses

Lumbosacral transitional vertebrae and control cohort comparison

The T-test compared the mean rank values of SBL in the LSTV (n=76) cohort and the control (n=60) cohort. Levene's test for variance was equal. The T-test for equality of means (t=0.522, df= 134, *p*=0.603) found a non-statistically significant difference in SBL with the LSTV cohort containing a marginally longer sacrum compared to the control cohort.

Lumbosacral transitional vertebrae cohort male and female comparison

The Mann-Whitney U test compared the mean values of SBL in the LSTV male cohort (n=53) and the LSTV female (n=23) cohort. There was no statistically significant difference (U=478.00, Z=-1.48, *p*=0.139) in SBL between the LSTV male (mean rank 40.97) and female (mean rank 32.80) cohorts.

Control cohort male and female comparison

The Mann-Whitney U test compared the mean rank values of SBL in the male (n=30) and the female (n=30) control cohorts. There was no statistically significant difference (U=208.00, Z=-3.58, *p*=0.001) in SBL between the control male (mean rank 38.57) and female (mean rank 22.43) cohorts.

Female lumbosacral transitional vertebrae cohort and female control cohort comparison

The Mann-Whitney U test compared the mean rank values of the SBL in the female LSTV (n=23) and the female control (n=30) cohorts. There was no statistically significant difference (U=287.00, Z=-1.04, *p*=0.298) in SBL between the LSTV female (mean rank 29.52) and the control female (mean rank 25.07) cohorts.

Male lumbosacral transitional vertebrae cohort and male control cohort comparison

The Mann-Whitney U test compared the mean rank values of the SBL in the male LSTV (n=53) and the male control (n=30) cohorts. There was no statistically significant difference (U=609.50, Z=-1.758, *p*=0.079) in SBL between the LSTV male (mean rank 38.50) and the control male (mean rank 48.18) cohorts.

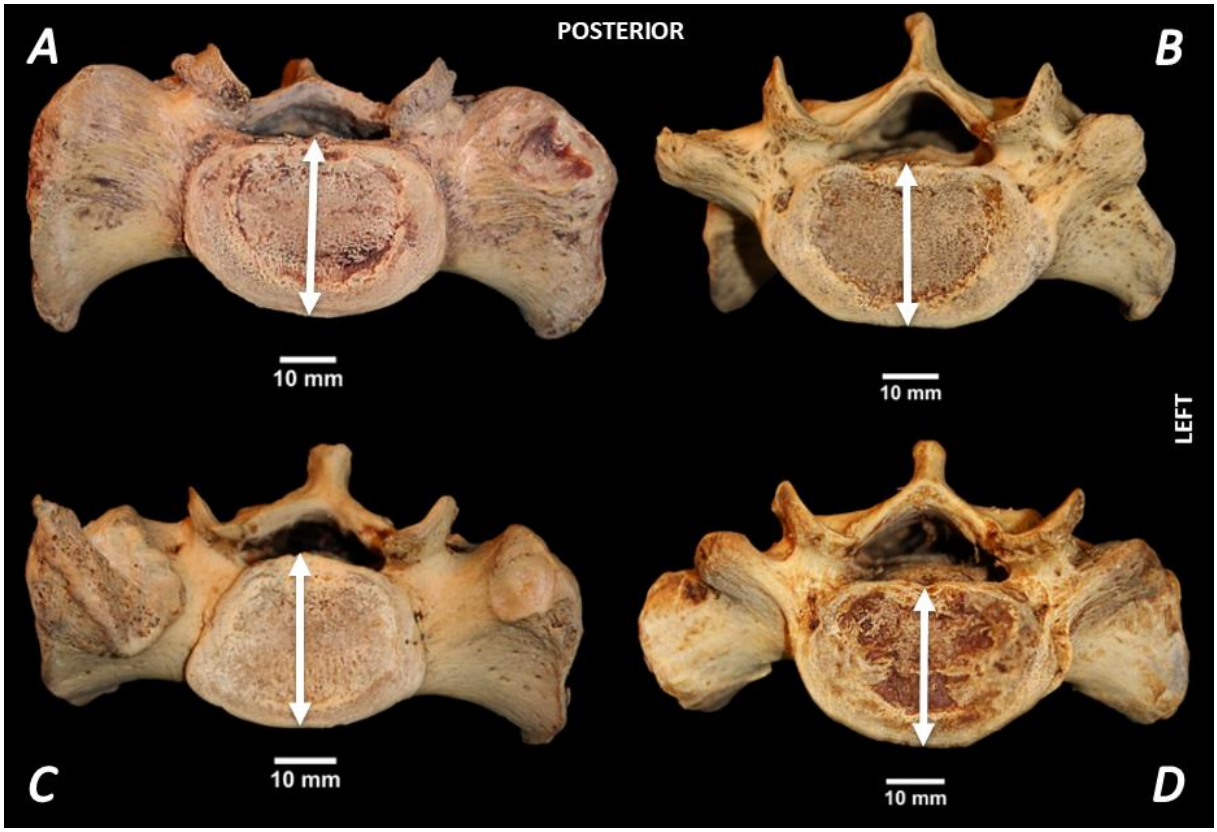

Figure 4.12: *Superior view of sacra displaying sacral body length associated with lumbosacral transitional vertebrae.* ***A)*** *Left-sided Type IIA lumbosacral transitional vertebra.* ***B)*** *Left-sided Type IIIA lumbosacral transitional vertebra.* ***C)*** *Type IIB lumbosacral transitional vertebra.* ***D)*** *Type IIIB lumbosacral transitional vertebra. The double arrows indicate the sacral body length measurements.* ***Photography and editing:*** *GJ Paton.*

D4: Inter-alae distance (IAD)

The LSTV cohort (N=88) consisted of 63 males (n=63) and 25 females (n=25). The control cohort (N=60) consisted of 30 males (n=30) and 30 females (n=30).

Lumbosacral transitional vertebrae cohort compared to the control cohort

The mean IAD in the LSTV cohort was smaller (101.41mm ± 7.15mm) than the control cohort (108.57mm ± 15.48mm). The IAD of the LSTV cohort had a larger range in variation of length, between 79.85mm and 127.54mm, while the control cohort range was 89.0mm and 207.09mm in length.

Sex comparison of lumbosacral transitional vertebrae and control cohorts

A sex comparison found that the mean IAD of males in the LSTV cohort (100.58mm ± 6.73mm) was shorter than that of the female within the same cohort (103.52mm ± 7.86mm). The IAD measurements ranged in LSTV males from 79.85mm to 115.96mm while LSTV female range was between 92.70mm and 127.54mm in length.

Likewise, sex comparison of the mean IAD in the control cohort was shorter for males (106.53mm ± 8.63mm) when compared to the females (110.61mm ± 20.11mm). The IAD measurements ranged in the control cohort in males from 89.90mm to 124.90mm while the female measurements ranged from 91.23mm to 207.09mm in length.

The mean IAD of males in the LSTV cohort (100.58mm ± 6.73mm) was shorter than the males in the control cohort (106.53mm ± 8.63mm). The mean IAD of females in the LSTV cohort (103.52mm ± 7.86mm) was shorter than the females in the control cohort (110.61mm ± 20.11mm). Refer to Figures 4.13 and 4.14. Figure 4.15 demonstrates the IAD variations associated with LSTV.

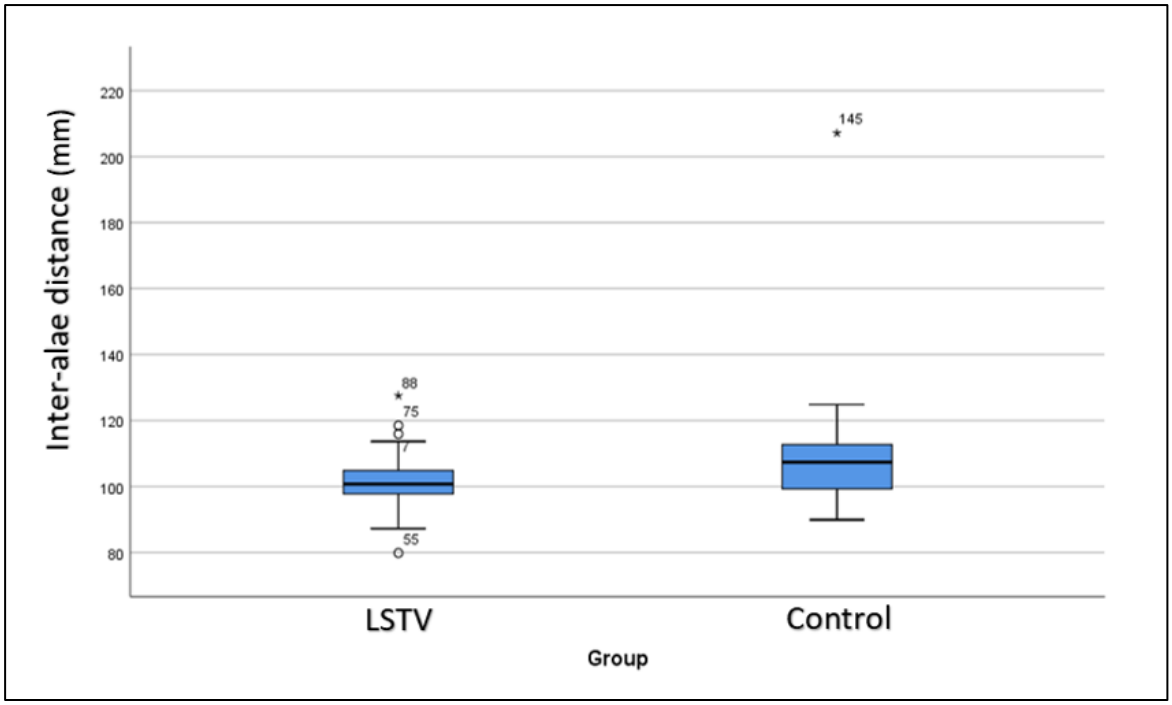

Figure 4.13: *A boxplot graph of the inter-alae distance measurement for the LSTV and control cohorts.*

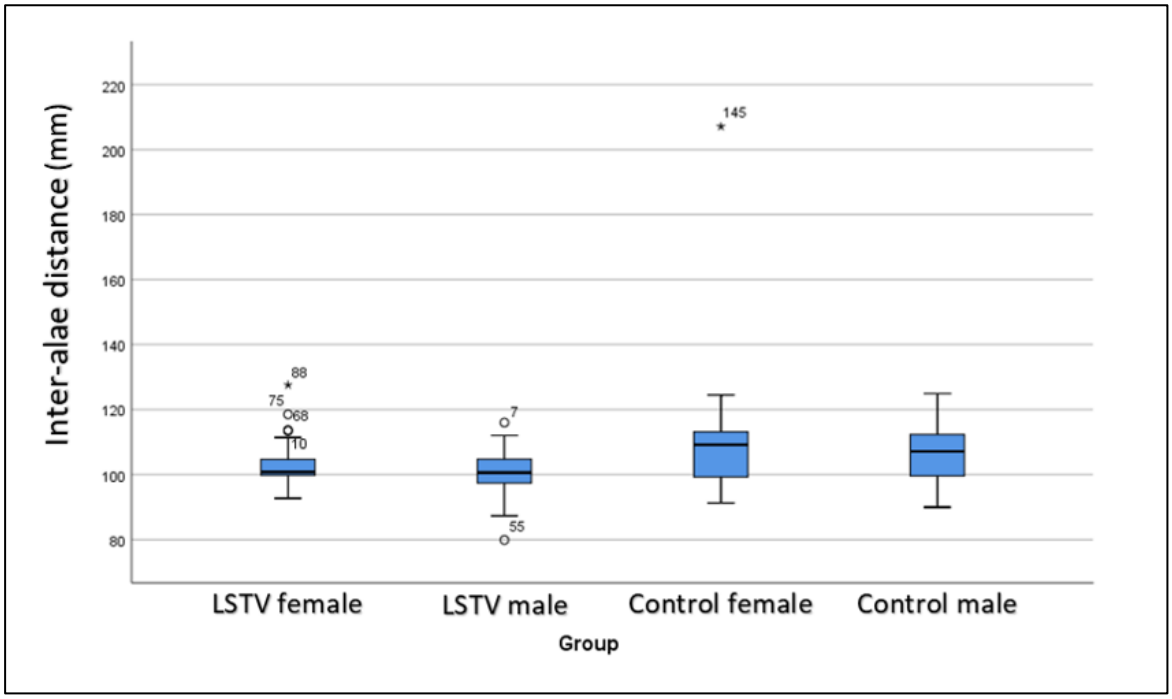

Figure 4.14: *A boxplot graph of the inter-alae distance measurement for the LSTV and control cohorts comparing the sexes.*

Statistical analyses

Lumbosacral transitional vertebrae and control cohort comparison

The T-test compared the mean rank values of IAD in the LSTV (n=88) cohort and the control (n=60) cohort. Levene's test for variance was not equal. The unequal variance T-test for equality of means (t=-3.35, df= 76.30, *p*=0.001) found a statistically significant difference in IAD with the LSTV cohort containing a narrower IAD as compared to the control cohort.

Lumbosacral transitional vertebrae cohort male and female comparison

The Mann-Whitney U test compared the mean rank values of IAD in the LSTV male cohort (n=63) and the LSTV female (n=25) cohort. There was no statistically significant difference (U=679.00, Z=-1.00, *p*=0.315) in IAD between the LSTV male (mean rank 42.78) and female (mean rank 48.84) cohorts.

Control cohort male and female comparison

The Mann-Whitney U test compared the mean rank values of IAD in the male (n=30) and the female (n=30) control cohorts. There was no statistically significant difference (U=425.00, Z=-0.37, *p*=0.712) in IAD between the control male (mean rank 34.23) and female (mean rank 31.33) cohorts.

Female lumbosacral transitional vertebrae cohort and female control cohort comparison

The Mann-Whitney U test compared the mean rank values of the IAD in the female LSTV (n=25) and the female control (n=30) cohorts. There was no statistically significant difference (U=275.00, Z=-1.69, *p*=0.091) in IAD between the LSTV female (mean rank 24.00) and the control female (mean rank 31.33) cohorts.

Male lumbosacral transitional vertebrae cohort and male control cohort comparison

The Mann-Whitney U test compared the mean rank values of the IAD in the male LSTV (n=63) and the male control (n=30) cohorts.

There was a statistically significant difference (U=584.00, Z= -2.967, *p*=0.003) in IAD between the LSTV male (mean rank 41.27) and the larger control male (mean rank 59.03) cohorts.

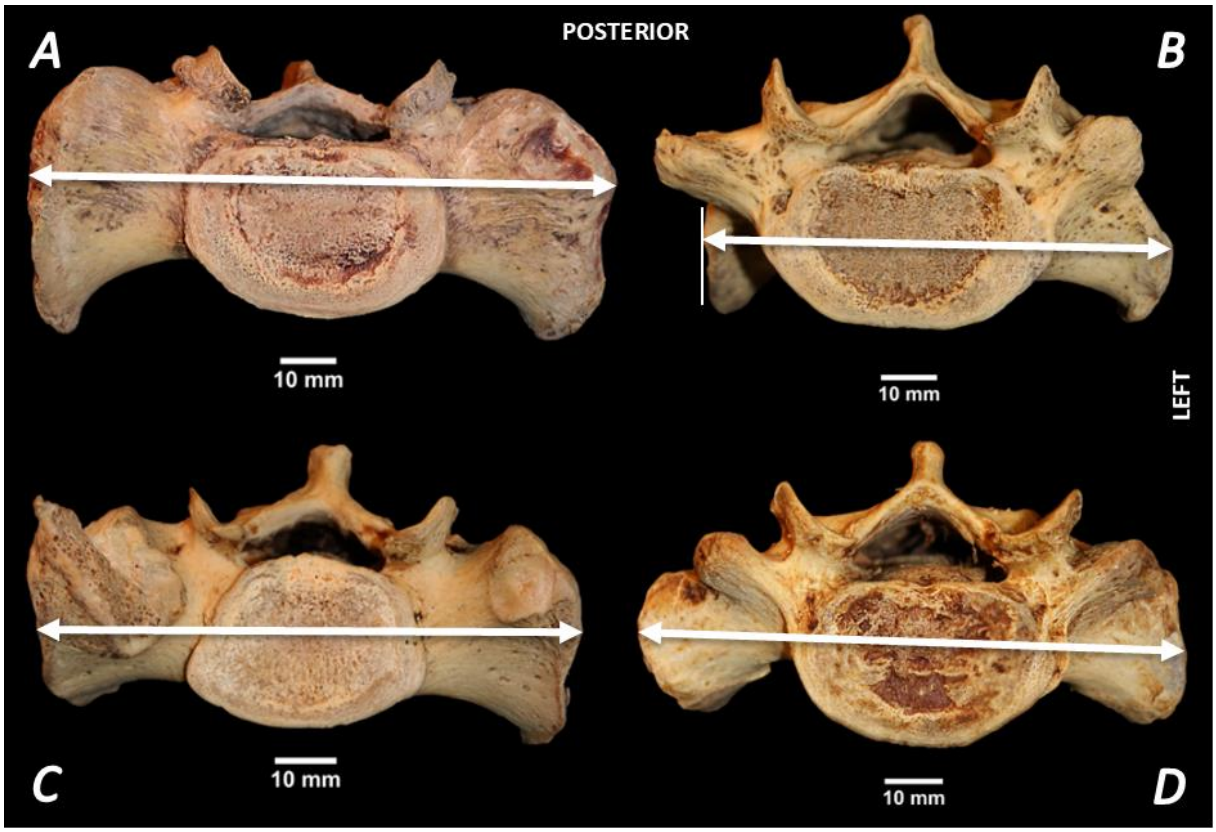

Figure 4.15: *Superior view of sacra displaying inter-alae distance associated with lumbosacral transitional vertebrae.* ***A)*** *Left-sided Type IIA lumbosacral transitional vertebra.* ***B)*** *Left-sided Type IIIA lumbosacral transitional vertebra.* ***C)*** *Type IIB lumbosacral transitional vertebra.* ***D)*** *Type IIIB lumbosacral transitional vertebra. The double arrows indicate the inter-alae measurements.* ***Photography and editing:*** *GJ Paton.*

D5: Inter-facet distance: lateral (IFD*lat*)

The LSTV cohort (N=85) consisted of 61 males (n=61) and 24 females (n=24). The control cohort (N=60) consisted of 30 males (n=30) and 30 females (n=30).

Lumbosacral transitional vertebrae cohort compared to the control cohort

The mean IFD*lat* in the LSTV cohort was larger (48.13mm ± 5.28mm) than the control cohort (50.72mm ± 4.93mm). The IFD*lat* of the LSTV cohort had a larger range in variation of length, between 38.52mm and 62.23mm, while the control cohort range was 39.52mm to 61.03mm in length.

Sex comparison of LSTV and control cohorts

A sex comparison found that the mean IFD*lat* of males in the LSTV cohort (48.49mm ± 5.43mm) was larger than that of the female within the same cohort (47.22mm ± 4.87mm). The IFD*lat* of the LSTV male cohort had a larger range in variation of length, between 38.52mm and 62.23mm, while the control female cohort range was 39.22mm to 55.36mm in length.

Likewise, sex comparison of the mean IFD*lat* in the control cohort was larger for males (51.77mm ± 5.41mm) when compared to the females (49.67mm ± 3.80mm). The IFD*lat* of the LSTV cohort had a larger range in variation of length, between 39.52mm and 61.03mm, while the female control cohort range was 42.38mm to 59.05mm in length.

The mean IFD*lat* of males in the LSTV cohort (48.49mm ± 5.43mm) was shorter than the males in the control cohort (51.77mm ± 5.41mm). The mean IFD*lat* of females in the LSTV cohort (47.22mm ± 4.87mm) was shorter than the females in the control cohort (49.67mm ± 3.80mm). Refer to Figures 4.16 and 4.17. Figure 4.18 demonstrates the IFD*lat* variations associated with LSTV.

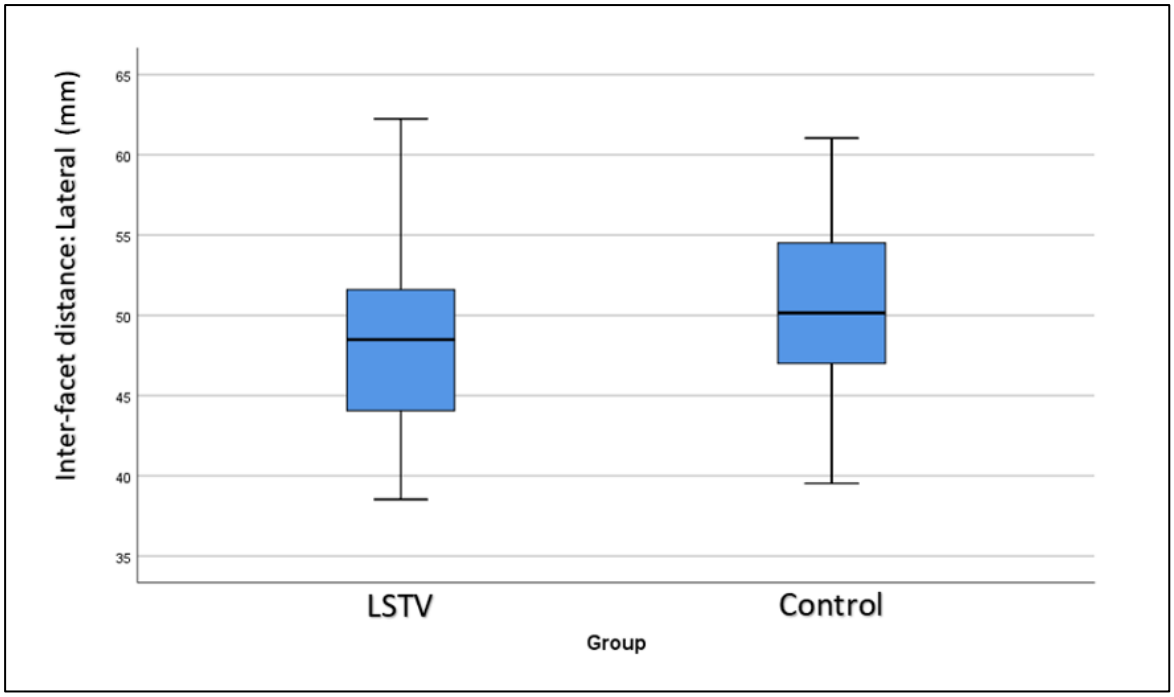

Figure 4.16: *A boxplot graph of the lateral inter-facet distance measurement for the LSTV and control cohorts.*

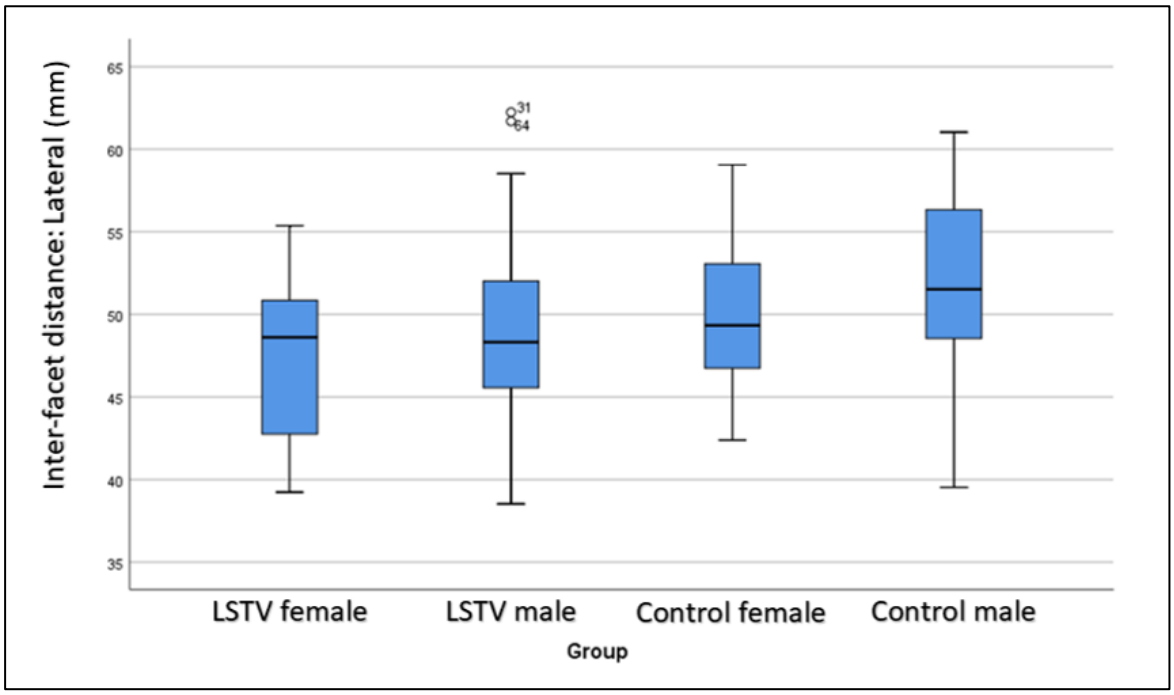

Figure 4.17: *A boxplot graph of the lateral inter-facet distance measurement for the LSTV and control cohorts comparing the sexes.*

Statistical analyses

Lumbosacral transitional vertebrae and control cohort comparison

The T-test compared the mean rank values of IFD*lat* in the LSTV (n=85) cohort and the control (n=60) cohort. Levene's test for variance was equal. The T-test for equality of means (t=-2.98, df= 143, *p*=0.003) found a statistically significant difference in IFD*lat* with the LSTV cohort containing a shorter IFD*lat* as compared to the control cohort.

Lumbosacral transitional vertebrae cohort male and female comparison

The Mann-Whitney U test compared the mean rank values of IFD*lat* in the LSTV male cohort (n=61) and the LSTV female (n=24) cohort. There was no statistically significant difference (U=650.00, Z=-0.80, *p*=0.423) in IFD*lat* between the LSTV male (mean rank 44.34) and female (mean rank 39.58) cohorts.

Control cohort male and female comparison

The Mann-Whitney U test compared the mean rank values of IFD*lat* in the male (n=30) and the female (n=30) control cohorts. There was no statistically significant difference (U=338.00, Z=-1.66, *p*=0.098) in IFD*lat* between the control male (mean rank 34.23) and female (mean rank 26.77) cohorts.

Female lumbosacral transitional vertebrae cohort and female control cohort comparison

The Mann-Whitney U test compared the mean rank values of the IFD*lat* in the female LSTV (n=24) and the female control (n=30) cohorts. There was no statistically significant difference (U=266.50, Z=-1.63, *p*=0.104) in IFD*lat* between the LSTV female (mean rank 23.60) and the control female (mean rank 230.62) cohorts.

Male lumbosacral transitional vertebrae cohort and male control cohort comparison

The Mann-Whitney U test compared the mean rank values of the IFD*lat* in the male LSTV (n=61) and the male control (n=30) cohorts. There was a statistically significant difference (U=608.50, Z=-2.153, *p*=0.010) in IFD*lat* between the LSTV male (mean rank 40.98) and the larger control male (mean rank 56.22) cohorts.

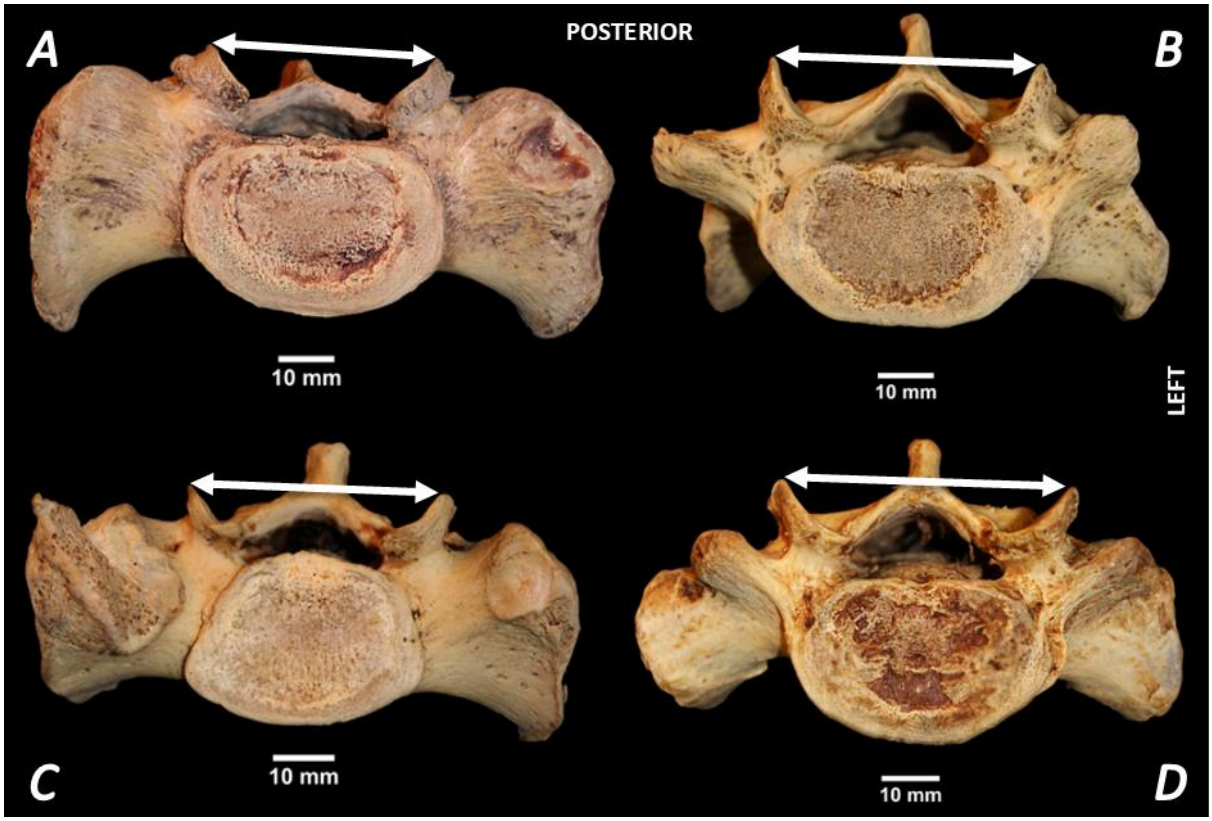

Figure 4.18: *Superior view of sacra displaying lateral inter-facet distance associated with lumbosacral transitional vertebrae.* ***A)*** *Left-sided Type IIA lumbosacral transitional vertebra.* ***B)*** *Left-sided Type IIIA lumbosacral transitional vertebra.* ***C)*** *Type IIB lumbosacral transitional vertebra.* ***D)*** *Type IIIB lumbosacral transitional vertebra. The double arrows indicate the lateral inter-facet distance measurements.* ***Photography and editing:*** *GJ Paton.*

D6: Inter-facet distance: medial (IFD*med)*

The LSTV cohort (N=86) consisted of 62 males (n=62) and 24 females (n=24). The control cohort (N=60) consisted of 30 males (n=30) and 30 females (n=30).

Lumbosacral transitional vertebrae cohort compared to the control cohort

The mean IFDm*ed* in the LSTV cohort was larger (25.52mm ± 4.62mm) than the control cohort (26.94mm ± 4.57mm). The IFDm*ed* of the LSTV cohort had a larger range in variation of length, between 2.93mm and 38.30mm, while the control cohort range was 18.32mm to 47.82mm in length.

Sex comparison of LSTV and control cohorts

A sex comparison found that the mean IFDm*ed* of males in the LSTV cohort (26.12mm ± 3.55mm) was larger than that of the female LSTV cohort (23.67mm ± 6.47mm). The IFDm*ed* of the LSTV male cohort had a smaller range in variation of length, between 17.27mm and 34.89mm, while the LSTV female cohort range was 2.93mm to 38.23mm in length.

Likewise, sex comparison of the mean IFDm*ed* in the control cohort was larger for males (27.77mm ± 3.75mm) when compared to the females (26.11mm ± 5.19mm). The IFDm*ed* of the LSTV cohort had a larger range in variation of length, between 19.44mm and 34.27mm, while the female control cohort range was 18.32mm to 47.82mm in length.

The mean IFDm*ed* of males in the LSTV cohort (26.12mm ± 3.55mm) was shorter than the males in the control cohort (27.77mm ± 3.75mm). The mean IFD*med* of females in the LSTV cohort (23.67mm ± 6.47mm) was shorter than the females in the control cohort (26.11mm ± 5.19mm). Refer to Figures 4.19 and 4.20. Figure 4.21 demonstrates the IFD*med* variations associated with LSTV.

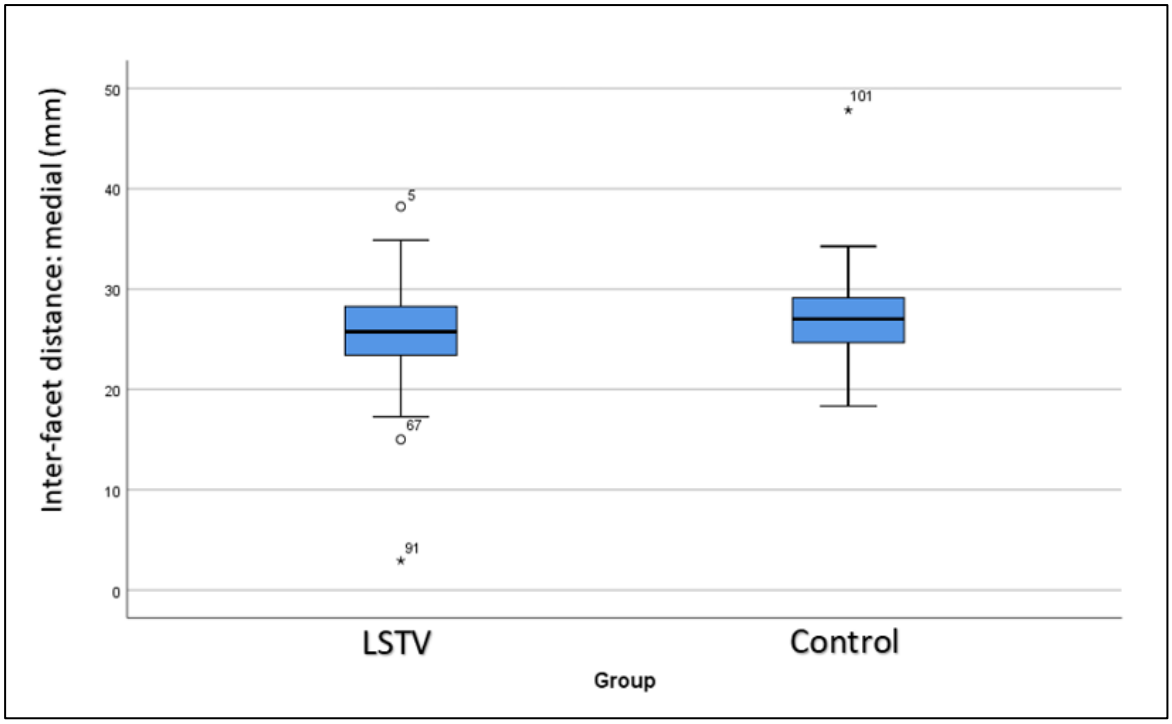

Figure 4.19: *A boxplot graph of the medial inter-facet distance measurement for the LSTV and control cohorts.*

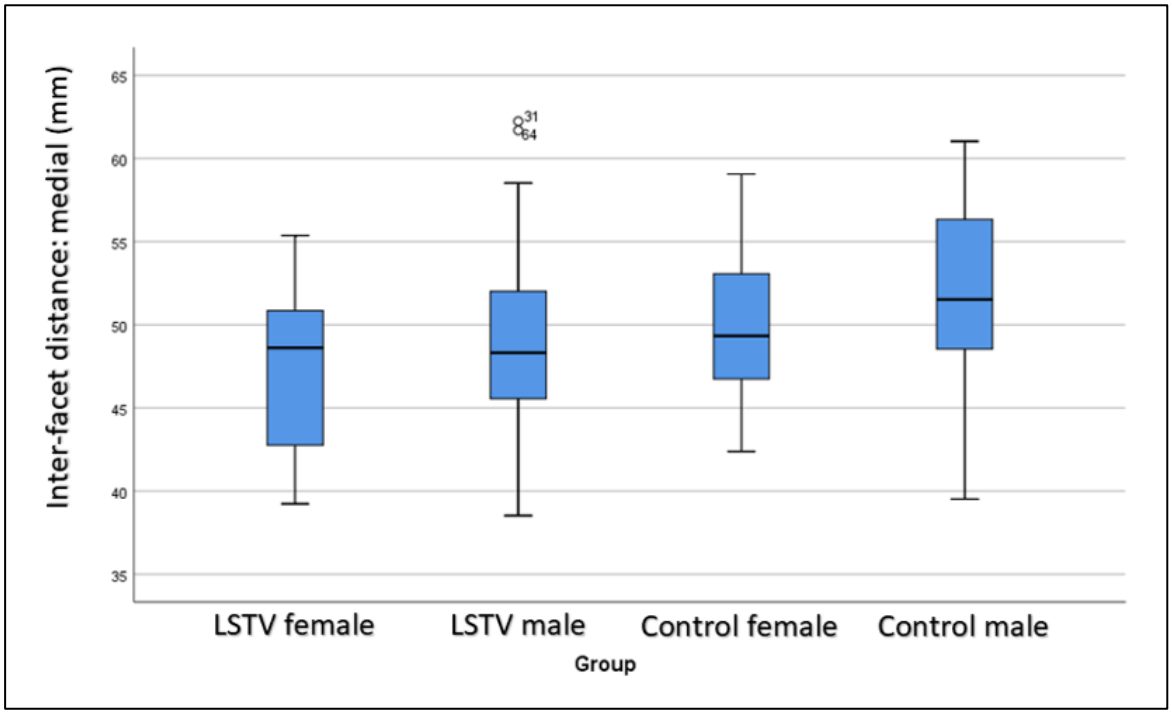

Figure 4.20: *A boxplot graph of the medial inter-facet measurement for the LSTV and control cohorts comparing the sexes.*

Statistical analyses

Lumbosacral transitional vertebrae and control cohort comparison

The T-test compared the mean rank values of IFD*med* in the LSTV (n=86) cohort and the control (n=60) cohort. Levene's test for variance was equal. The T-test for equality of means (t=-1.84, df= 144, *p*=0.069) found a statistically significant difference in IFD*med* with the LSTV cohort containing a shorter IFD*med* as compared to the control cohort.

Lumbosacral transitional vertebrae cohort male and female comparison

The Mann-Whitney U test compared the mean rank values of IFD*med* in the LSTV male cohort (n=62) and the LSTV female (n=24) cohort. There was no statistically significant difference (U=569.50, Z=-1.68, *p*=0.093) in IFD*med* between the LSTV male (mean rank 46.31) cohort and female (mean rank 36.23) cohorts.

Control cohort male and female comparison

The Mann-Whitney U test compared the mean rank values of IFD*med* in the male (n=30) and the female (n=30) control cohort. There was a statistically significant difference (U=292.00, Z=-2.34, *p*=0.019) in IFD*med* between the control male (mean rank 35.77) and female (mean rank 25.23) cohorts.

Female lumbosacral transitional vertebrae cohort and female control cohort comparison

The Mann-Whitney U test compared the mean rank values of the IFD*med* in the female LSTV (n=24) and the female control (n=30) cohorts. There was no statistically significant difference (U=301.00, Z=-1.03, *p*=0.304) in IFD*med* between the LSTV female (mean rank 25.04) and the control female (mean rank 29.47) cohorts.

Male lumbosacral transitional vertebrae cohort and male control cohort comparison

The Mann-Whitney U test compared the mean rank values of the IFD*med* in the male LSTV (n=63) and the male control (n=30) cohorts. There was a statistically significant difference (U=671.00, Z=-2.153, *p*=0.031) in IFD*med* between the LSTV male (mean rank 42.33) and the larger control male (mean rank 55.12) cohorts.

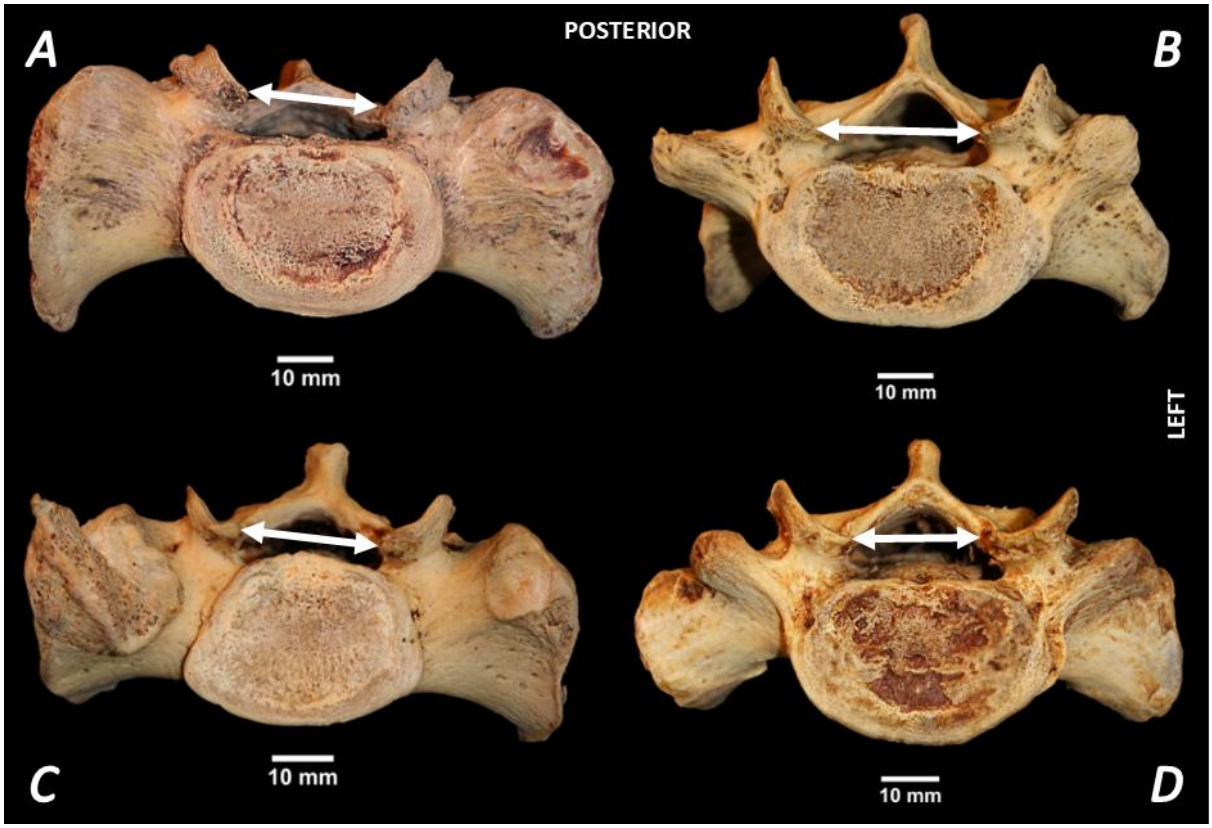

Figure 4.21: *Superior view of sacra displaying medial inter-facet distance associated with lumbosacral transitional vertebrae.* ***A)*** *Left-sided Type IIA lumbosacral transitional vertebra.* ***B)*** *Left-sided Type IIIA lumbosacral transitional vertebra.* ***C)*** *Type IIB lumbosacral transitional vertebra.* ***D)*** *Type IIIB lumbosacral transitional vertebra. The double arrows indicate the medial inter-facet distance measurements.* ***Photography and editing:*** *GJ Paton.*

D7: Facet distance (FD)

The LSTV cohort (N=81) consisted of 59 males (n=59) and 22 females (n=22). The control cohort (N=60) consisted of 30 males (n=30) and 30 females (n=30).

Lumbosacral transitional vertebrae cohort compared to the control cohort

The mean FD in the LSTV cohort was larger (15.08mm ± 4.46mm) than the control cohort (17.70mm ± 2.30mm). The FD of the LSTV cohort had a larger range in variation of length, between 4.26mm and 36.16mm, while the control cohort range was 13.46mm to 22.65mm in length.

Sex comparison of LSTV and control cohorts

A sex comparison found that the mean FD of males in the LSTV cohort (15.22mm ± 4.77mm) was larger than that of the females within the same cohort (14.71mm ± 3.57mm). The FD of the LSTV male cohort had a larger range in variation of length, between 4.26mm and 36.16mm, while the female cohort range was 10.48mm to 22.86mm in length.

Likewise, sex comparison of the mean FD in the control cohort was marginally longer for males (17.80mm ± 24.69mm) when compared to the females (17.59mm ± 1.87mm). The FD of the LSTV male cohort had a larger range in variation of length, between 13.46mm and 22.65mm, while the control female cohort range was 13.77mm to 21.99mm in length.

The mean FD of males in the LSTV cohort (15.22mm ± 4.77mm) was shorter than the males in the control cohort (17.80mm ± 24.69mm). The mean IFD*lat* of females in the LSTV cohort (14.71mm ± 3.57mm) was shorter than the females in the control cohort (17.59mm ± 1.87mm). Refer to Figures 4.22 and 4.23. Figure 4.24 demonstrates the FD variations associated with LSTV.

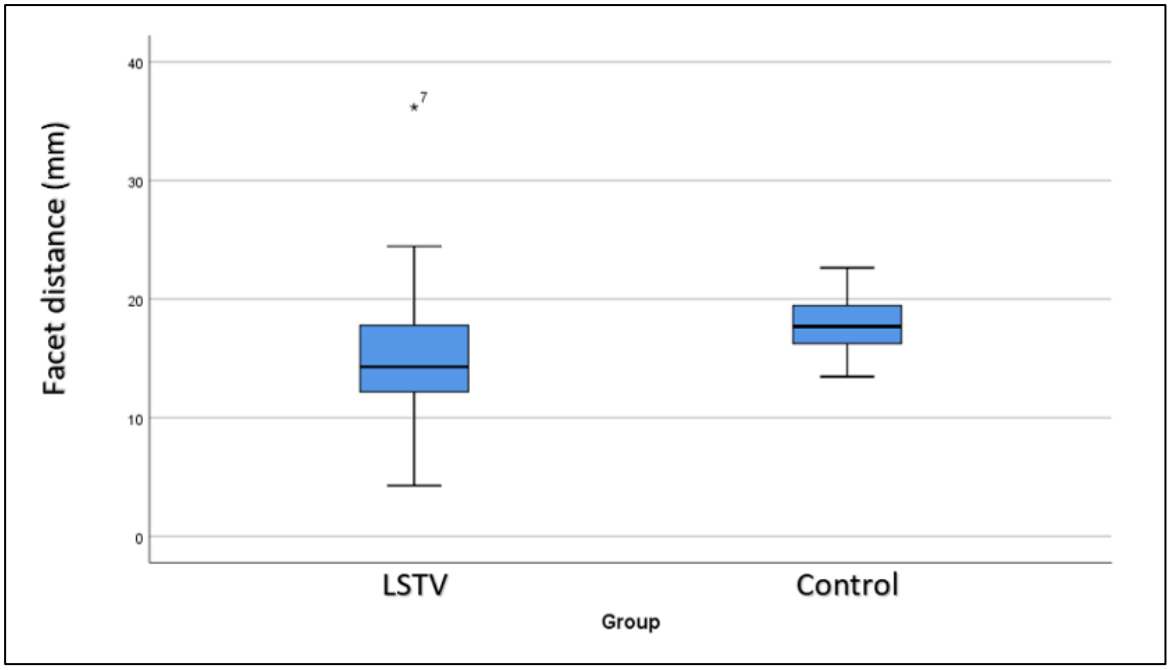

Figure 4.22: *A boxplot graph of the facet distance measurement for the LSTV and control cohorts.*

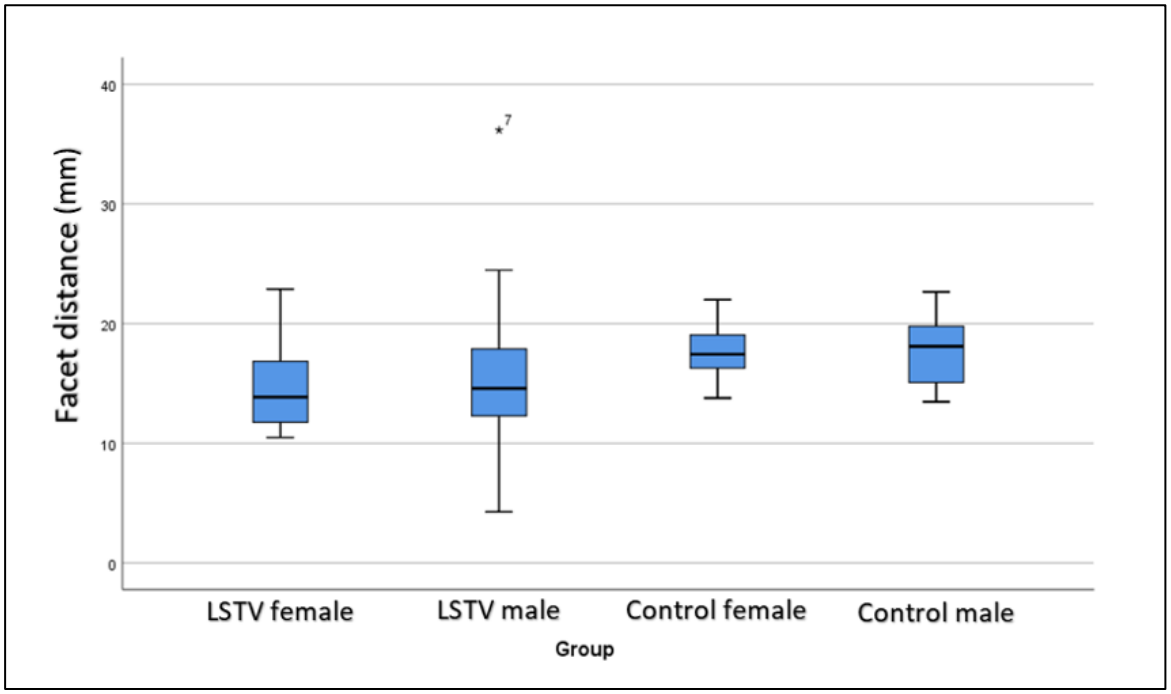

Figure 4.23: *A boxplot graph of the facet distance measurement for the LSTV and control cohorts comparing the sexes.*

Statistical analyses

Lumbosacral transitional vertebrae and control cohort comparison

The T-test compared the mean rank values of FD in the LSTV (n=81) cohort and the control (n=60) cohort. Levene's test for variance was not equal. The unequal variance T-test for equality of means (t=-4.53, df= 125.66, $p<0.001$) found a statistically significant difference in FD with the LSTV cohort containing a shorter FD as compared to the control cohort.

Lumbosacral transitional vertebrae cohort male and female comparison

The Mann-Whitney U test compared the mean rank values of FD in the LSTV male cohort (n=59) and the LSTV female (n=22) cohort. There was no statistically significant difference (U=596.00, Z=-0.56, $p=0.057$) in FD between the LSTV male (mean rank 41.90) and female (mean rank 38.59) cohorts.

Control cohort male and female comparison

The Mann-Whitney U test compared the mean rank values of FD in the male (n=30) and the female (n=30) control cohorts. There was no statistically significant difference (U=417.00, Z=-0.49, $p=0.626$) in FD between the control male (mean rank 31.60) and female (mean rank 29.40) cohorts.

Female lumbosacral transitional vertebrae cohort and female control cohort comparison

The Mann-Whitney U test compared the mean rank values of the FD in the female LSTV (n=24) and the female control (n=30) cohorts. There was a statistically significant difference (U=146.00, Z=-3.41, $p=0.001$) in FD between the LSTV female (mean rank 18.14) and the control female (mean rank 32.63) cohorts.

Male lumbosacral transitional vertebrae cohort and male control cohort comparison

The Mann-Whitney U test compared the mean rank values of the FD in the male LSTV (n=59) and the male control (n=30) cohorts.

There was no statistically significant difference (U=483.50, Z=-3.485, p<0.001) in FD between the LSTV male (mean rank 38.19) and the longer control male (mean rank 58.38) cohorts.

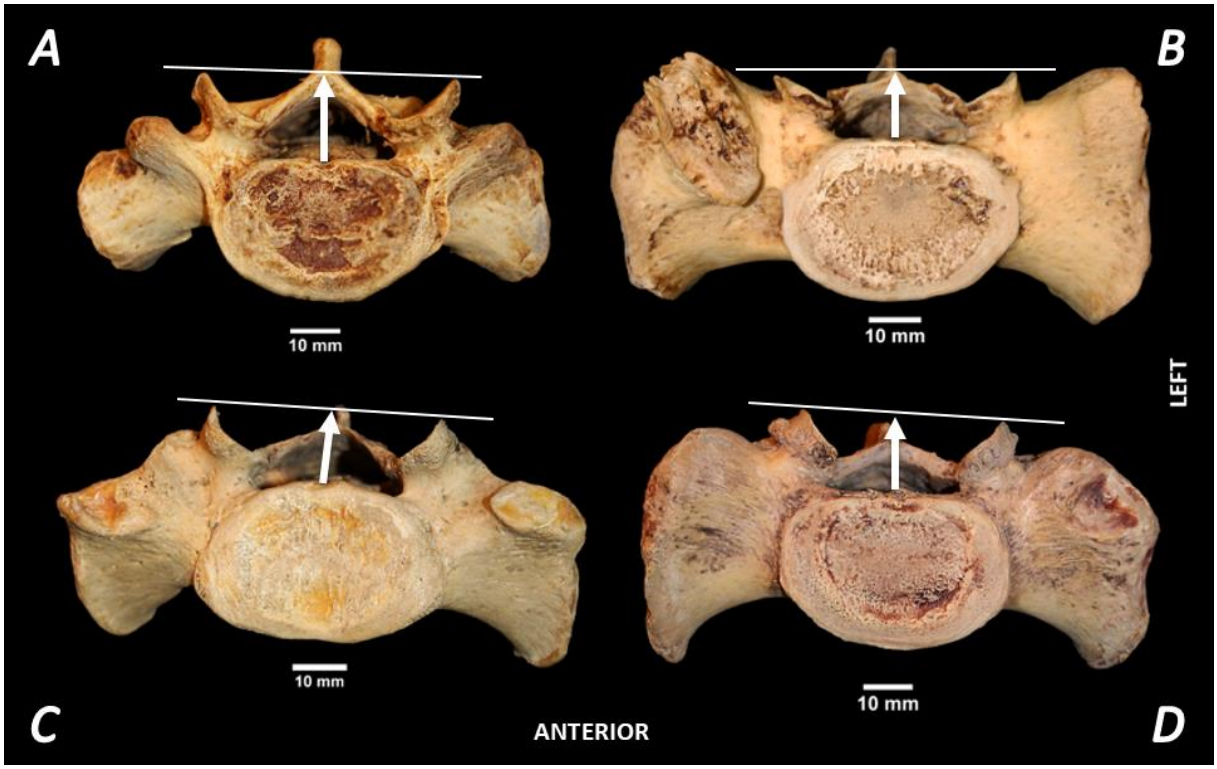

Figure 4.24: *Superior view of sacra displaying the sacral facet distance associated with lumbosacral transitional vertebrae.* ***A)*** *Left-sided Type IIA lumbosacral transitional vertebra.* ***B)*** *Left-sided Type IIIA lumbosacral transitional vertebra.* ***C)*** *Type IIB lumbosacral transitional vertebra.* ***D)*** *Type IIIB lumbosacral transitional vertebra. The arrows indicate the facet distance measurements.* ***Photography and editing:*** *GJ Paton.*

D8: Sacral Facet height (SFH), right and left

The right LSTV cohort (N=77) consisted of 57 males (n=57) and 20 females (n=20) and the left LSTV cohort (N=79) consisted of 58 males (n=58) and 21 females (n=21). The control cohort (N=60) consisted of 30 males (n=30) and 30 females (n=30).

Lumbosacral transitional vertebrae cohort compared to the control cohort

Right side

The mean SFH on the right side in the LSTV cohort was larger (15.38mm ± 2.72mm) than the control cohort (16.17mm ± 1.62mm). The SFH of the LSTV cohort had a larger range in variation of length, between 8.77mm and 24.48mm, while the control cohort range was 12.19mm to 20.06mm in length.

Left side

The mean SFH on the left side in the LSTV cohort was larger (14.99mm ± 2.76mm) than the control cohort (16.27mm ± 1.647mm). The SFH of the LSTV cohort had a larger range in variation of length, between 7.54mm and 21.42mm, while the control cohort range was 12.59mm to 21.72mm in length.

Sex comparison of lumbosacral transitional vertebrae and control cohorts

Right side

A sex comparison found that the mean SFH of males on the right side in the LSTV cohort (15.54mm ± 2.92mm) was larger than that of the females within the same cohort (14.93mm ± 2.08). The SFH of the LSTV male cohort had a larger range in variation of length, between 8.77mm and 24.48mm, while the female LSTV cohort range was 9.15mm to 18.99mm in length. Likewise, sex comparison of the mean SFH on the right side in the control cohort was larger for males (16.55 ± 1.88mm) when compared to the females (15.79mm ± 1. 23mm).

The SFH of the LSTV female cohort had a larger range in variation of length, between 12.19mm and 20.06mm, while the cohort range was 13.58mm to 18.27mm in length.

The mean SFH of males on the right side in the LSTV cohort (15.54mm ± 2.92mm) was shorter than the males in the control cohort (16.55 ± 1.88mm). The mean SFH of females in the LSTV cohort (14.93mm ± 2.08) was shorter than the females in the control cohort (15.79mm ± 1. 23mm). Refer to Figures 4.25 and 4.26.

Left side

Sex comparison of the mean SFH on the left side in the LSTV cohort was larger for males (15.28mm ± 2.90mm) when compared to the females (14.19mm ± 2.17mm). The SFH of the LSTV male cohort had a larger range in variation of length, between 7.54mm and 21.42mm, while the control female cohort range was 10.62mm to 18.05mm in length.

Likewise, sex comparison of the mean SFH on the left side in the male control cohort was larger for males (16.53mm ± 2.08mm) when compared to the females (16.00mm ± 1.04mm). The SFH of the LSTV male cohort had a larger range in variation of length, between 12.59mm and 21.72mm, while the control female cohort range was 14.23mm to 17.74mm in length.

The mean SFH of the male LSTV cohort on the left side (15.28mm ± 2.90mm) was shorter than the males in the control cohort (16.53mm ± 2.08mm). The mean IFD*lat* of females in the LSTV cohort (14.19mm ± 2.17mm) was shorter than the females in the control cohort (16.00mm ± 1.04mm). Refer to Figures 4.27 and 4.28. Figures 4.29 and 4.30 demonstrate the SFH variations associated with LSTV on the right and left sides.

Right side

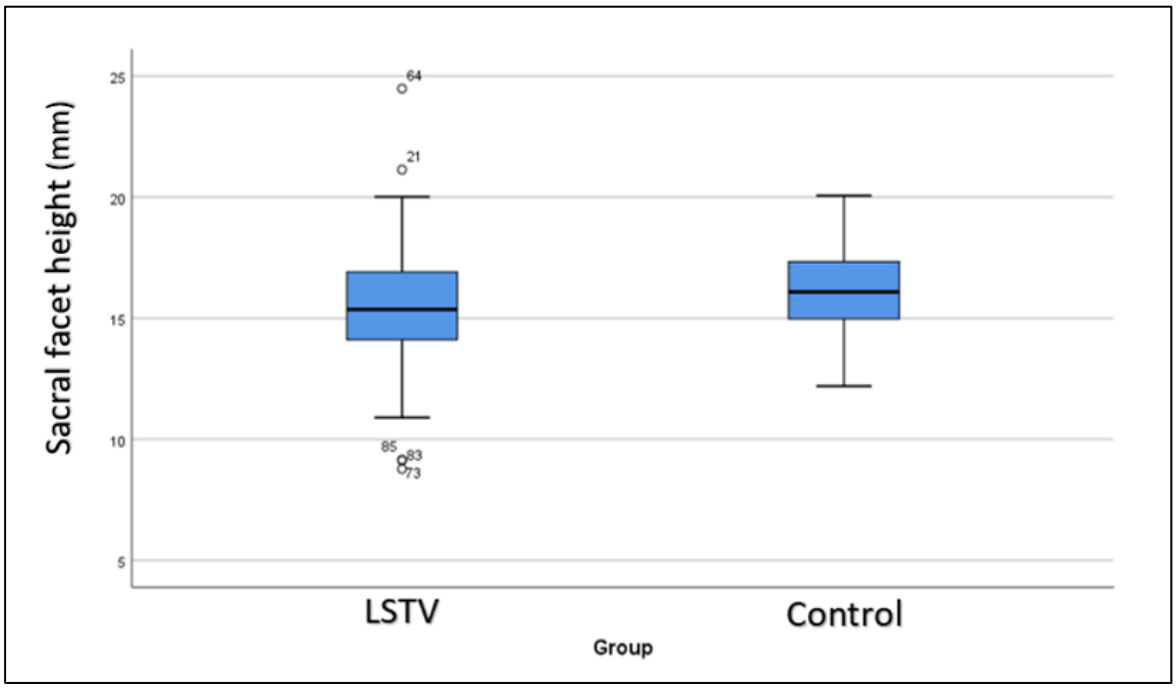

Figure 4.25: *A boxplot graph of the right sacral facet height measurement for the LSTV and control cohorts.*

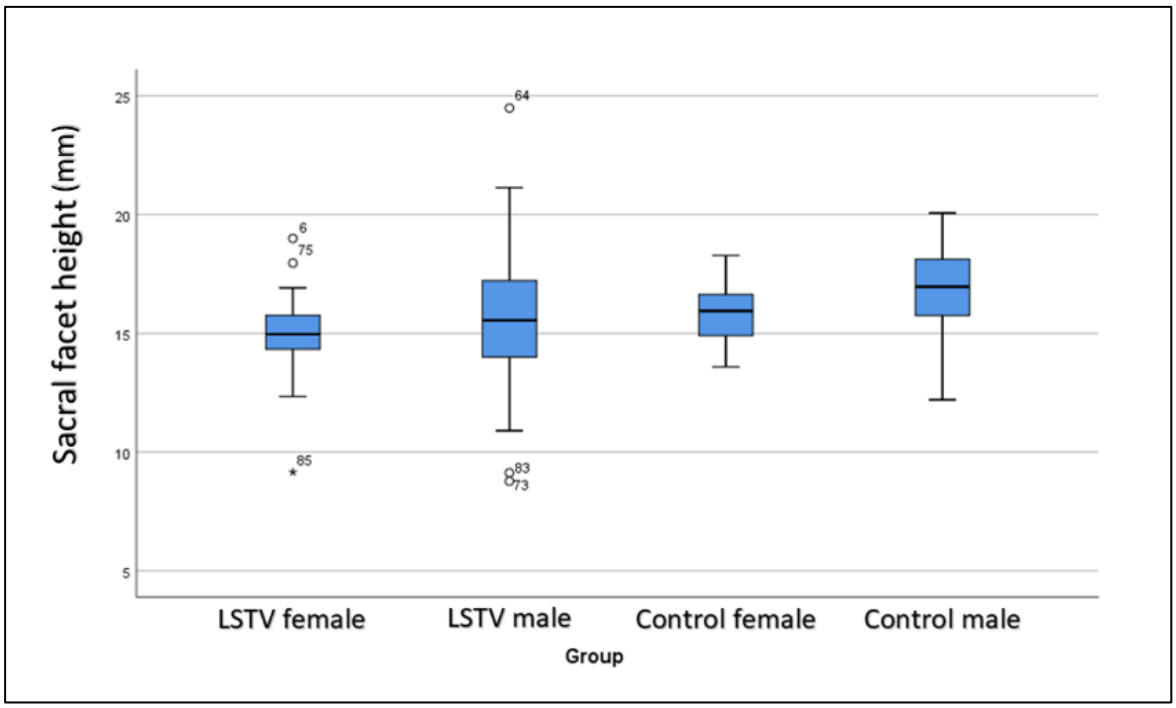

Figure 4.26: *A boxplot graph of the right sacral facet height measurement for the LSTV and control cohorts comparing the sexes.*

Left side

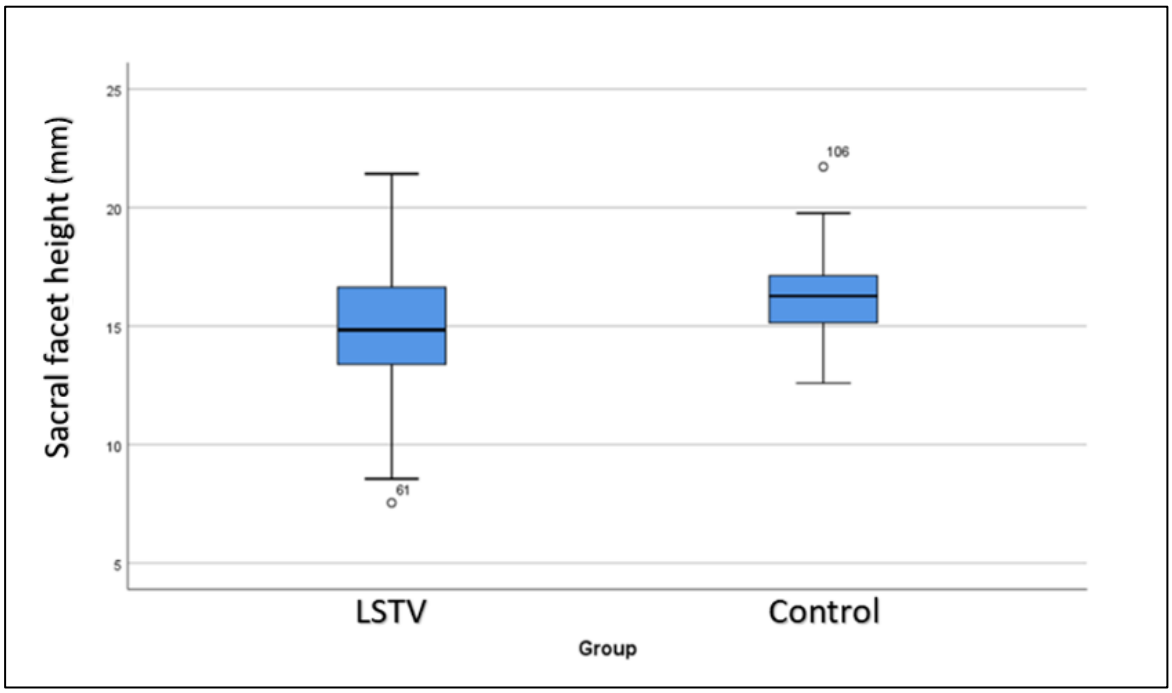

Figure 4.27: *A boxplot graph of the left sacral facet height measurement for the LSTV and control cohorts.*

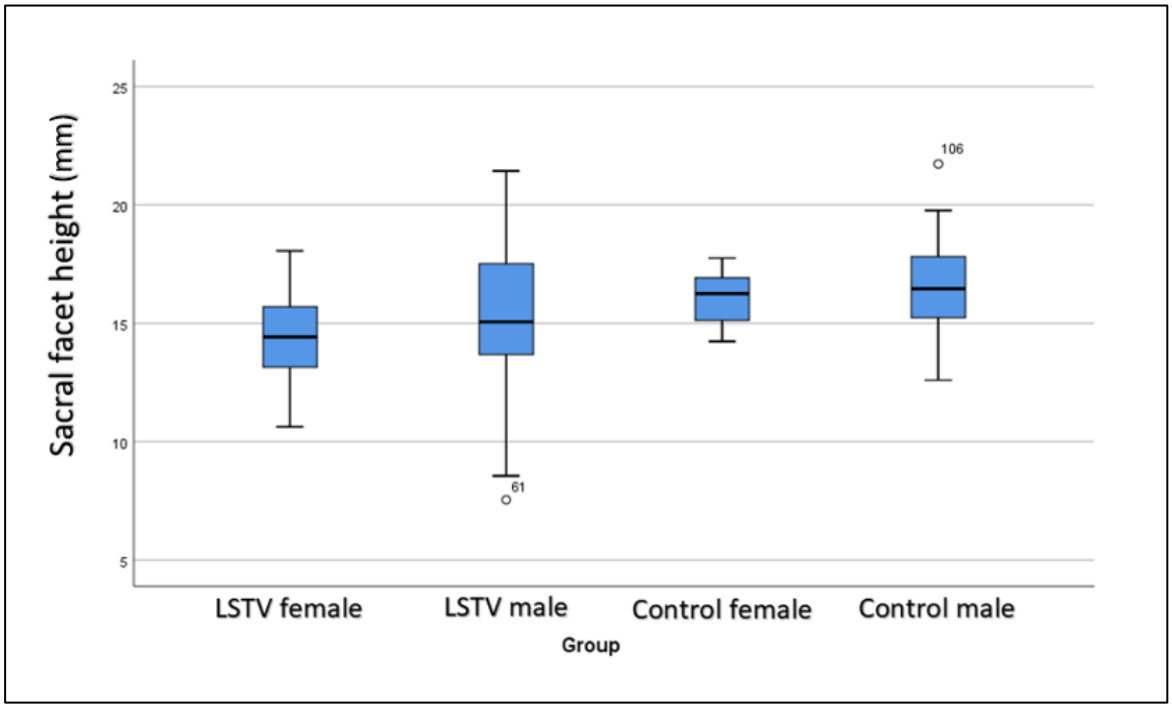

Figure 4.28: *A boxplot graph of the sacral facet height measurement for the LSTV and control cohorts comparing the sexes.*

Statistical analyses

Lumbosacral transitional vertebrae and control cohort comparison

Right side

The T-test compared the mean rank values of SFH in the LSTV (n=77) cohort and the control (n=60) cohort. Levene's test for variance was not equal. The unequal variance T-test for equality of means (t=-2.12, df= 127.00, *p*=0.036) found a statistically significant difference in right SFH with the LSTV cohort containing a shorter SFH as compared to the control cohort.

Left side

The T-test compared the mean rank values of SFH in the LSTV (n=79) cohort and the control (n=60) cohort. Levene's test for variance was not equal. The unequal variance T-test for equality of means (t=-3.39, df= 130.40, *p*=0.001) found a statistically significant difference in left SFH with the LSTV cohort containing a shorter SFH as compared to the control cohort.

Lumbosacral transitional vertebrae cohort male and female comparison

Right side

The Mann-Whitney U test compared the mean rank values of SFH in the LSTV male cohort (n=58) and the LSTV female (n=21) cohort. There was no statistically significant difference (U=495.00, Z=-0.87, *p*=0.384) in SFH between the LSTV male (mean rank 40.32) and female (mean rank 35.25) cohorts.

Left side

The Mann-Whitney U test compared the mean rank values of SFH in the LSTV male cohort (n=59) and the LSTV female (n=21) cohort. There was no statistically significant difference (U=454.50, Z=-1.72, *p*=0.086) in SFH between the LSTV male (mean rank 42.66) and female (mean rank 32.64) cohorts.

Control cohort male and female comparison

Right side

The Mann-Whitney U test compared the mean rank values of SFH in the male (n=30) and the female (n=30) control cohorts.

There was no statistically significant difference (U=319.50, Z=-1.93, *p*=0.054) in right SFH between the control male (mean rank 34.85) and female (mean rank 26.15) cohorts.

Left side

The Mann-Whitney U test compared the mean rank values of SFH in the male (n=30) and the female (n=30) control cohorts. There was no statistically significant difference (U=376.00, Z=-1.09, *p*=0.277) in left SFH between the control male (mean rank 32.95) and female (mean rank 28.05) cohorts.

Female lumbosacral transitional vertebrae cohort and female control cohort comparison

Right side

The Mann-Whitney U test compared the mean rank values of the SFH in the female LSTV (n=20) and the female control (n=30) cohorts. There was no statistically significant difference (U=211.50, Z=-1.75, *p*=0.080) in SFH between the LSTV female (mean rank 21.08) and the control female (mean rank 28.45) cohorts.

Left side

The Mann-Whitney U test compared the mean rank values of the SFH in the female LSTV (n=21) and the female control (n=30) cohorts. There was a statistically significant difference (U=151.50, Z=-3.13, *p*=0.002) in SFH between the LSTV male (mean rank 18.21) and the larger control male (mean rank 31.45) cohorts.

Male lumbosacral transitional vertebrae cohort and male control cohort comparison

Right side

The Mann-Whitney U test compared the mean rank values of the SFH in the male LSTV (n=57) and the male control (n=30) cohorts.

There was no statistically significant difference (U=643.50, Z=-1.889, *p*=0.059) in SFH between the LSTV male (mean rank 40.29) and the control male (mean rank 51.05) cohorts.

Left side

The Mann-Whitney U test compared the mean rank values of the SFH in the male LSTV (n=58) and the male control (n=30) cohorts.

There was a statistically significant difference (U=633.00, Z=-2.086, *p*=0.037) in SFH between the LSTV male (mean rank 40.41) and the control male (mean rank 51.40) cohorts.

Right side

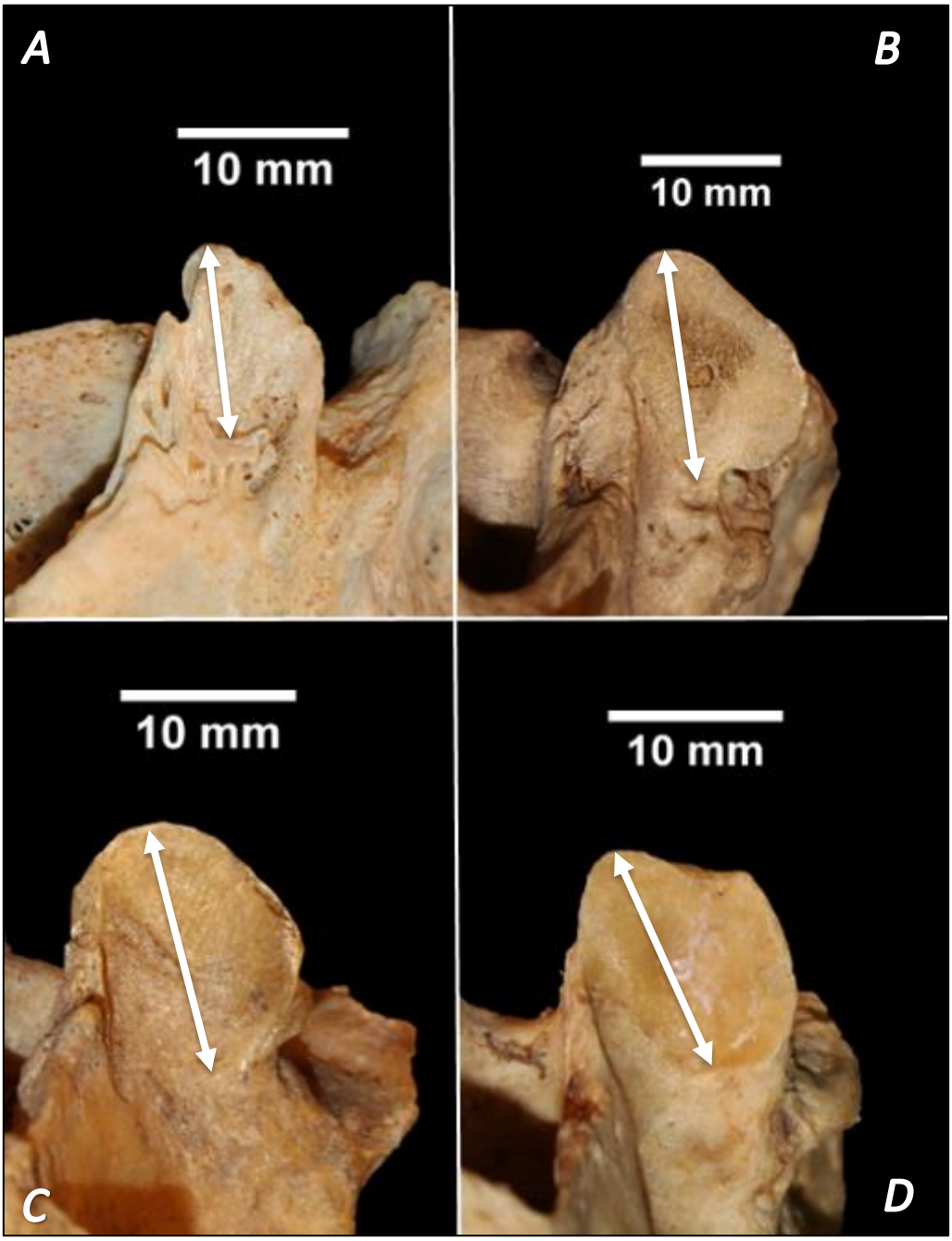

Figure 4.29: *Perpendicular view of the right-sided sacral facet heights associated with lumbosacral transitional vertebrae.* ***A)*** *A left sacral facet of a Type IIB lumbosacral transitional vertebra asymmetrical facet joint orientation.* ***B)*** *A left sacral facet of a left-sided Type IIIA lumbosacral transitional vertebra with roughly symmetrical facet joint orientation.* ***C)*** *A left sacral facet of a left-sided Type IIA lumbosacral transitional vertebra with slightly asymmetrical facet joint orientation.* ***D)*** *A left sacral facet of Type IIB lumbosacral transitional vertebra with roughly symmetrical facet joint orientation. The double arrows indicate the sacral facet height of the left sacral facet joints.* ***Photography and editing:*** *GJ Paton.*

Left side

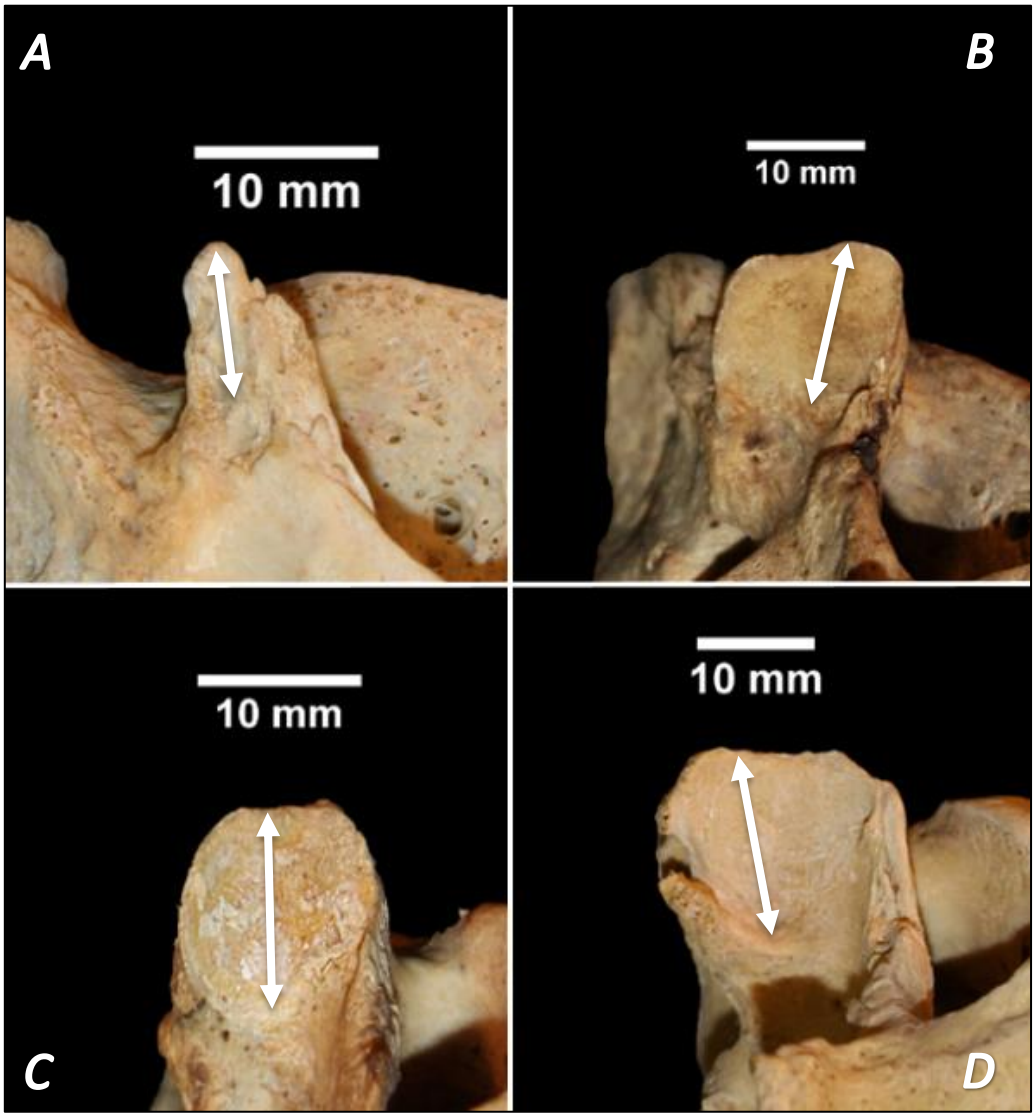

Figure 4.30: *Perpendicular view of the left-sided sacral facet heights associated with lumbosacral transitional vertebrae.* ***A)*** *A right sacral facet of a Type IIB lumbosacral transitional vertebra asymmetrical facet joint orientation.* ***B)*** *A right sacral facet of a left-sided Type IIIA lumbosacral transitional vertebra with roughly symmetrical facet joint orientation.* ***C)*** *A right sacral facet of a left-sided Type IIA lumbosacral transitional vertebra with slightly asymmetrical facet joint orientation.* ***D)*** *A right facet of a Type IIB lumbosacral transitional vertebra with roughly symmetrical facet joint orientation. The double arrows indicate the sacral facet height of the right facet joints.* ***Photography and editing:*** *GJ Paton.*

D9: Sacral Facet Width (SFW), right and left

The right LSTV cohort (N=79) consisted of 58 males (n=58) and 21 females (n=21) and the left LSTV cohort (N=80) consisted of 59 males (n=59) and 21 females (n=21). The control cohort (N=60) consisted of 30 males (n=30) and 30 females (n=30).

Lumbosacral transitional vertebrae cohort compared to the control cohort

Right side

The mean SFW on the right side in the LSTV cohort was shorter (13.95mm ± 2.85mm) than the control cohort (15.69mm ± 1.99mm). The SFW of the LSTV cohort had a smaller range in variation of length, between 8.11mm and 20.80mm, while the control cohort range was 11.70mm to 20.92mm in length.

Left side

The mean SFH on the left side in the LSTV cohort was shorter (13.63mm ± 2.59mm) than the control cohort (15.70mm ± 1.72mm). The SFW of the LSTV cohort had a larger range in variation of length, between 6.14mm and 19.54mm, while the control cohort range was 11.86mm to 19.40mm in length.

Sex comparison of lumbosacral transitional vertebrae and control cohorts

Right side

A sex comparison found that the mean SFW on the right of males in the LSTV cohort (13.97mm ± 3.08mm) was marginally larger than that of the female cohort (13.91mm ± 2.19mm). The SFW of the LSTV male cohort had a larger range in variation of length, between 8.11mm and 20.80mm, while the cohort range was 9.88mm to 17.68mm in length.

Likewise, sex comparison of the mean SFW on the right in the control cohort was larger for males (15.89mm ± 2.20mm) when compared to the females (15.50mm ± 1.77mm).

The SFW of the LSTV male cohort had a larger range in variation of length, between 12.56mm and 20.92mm, while the control cohort range was 11.76mm to 19.05 mm in length.

The mean SFW of the male LSTV cohort on the right side (13.97mm ± 3, 08mm) was shorter than the males in the control cohort (15.89mm ± 2.20mm). The mean SFW of females in the LSTV cohort (13.91mm ± 2.19mm) was shorter than the females in the control cohort (15.50mm ± 1.77mm). Refer to Figures 4.31 and 4.32.

Left side

A sex comparison found that the mean SFW on the left of males in the LSTV cohort (13.62mm ± 2.80mm) was larger than that of the female LSTV cohort (13.67mm ± 1.94mm). The SFW of the LSTV cohort had a larger range in variation of length, between 6.14mm and 19.54mm, while the female LSTV cohort range was 10.95mm to 18.74mm in length.

Likewise, sex comparison of the mean SFW on the left in the control cohort was larger for males (15.71mm ± 2.04mm) when compared to the females (15.69mm ± 1.24mm). The SFW of the LSTV cohort had a larger range in variation of length, between 11.86mm and 19.40mm, while the female control cohort range was 12.52mm to 17.77mm in length.

The mean SFW of the male LSTV cohort on the left side (13.62mm ± 2.80mm) was shorter than the males in the control cohort (13.67mm ± 1.94mm). The mean SFW of females in the LSTV cohort (14.19mm ± 2.17mm) was shorter than the females in the control cohort (15.69mm ± 1.24mm). Refer to Figures 4.33 and 4.34. Figures 4.35 and 4.36 demonstrate the SFW variations associated with LSTV on the right and left sides.

Right side

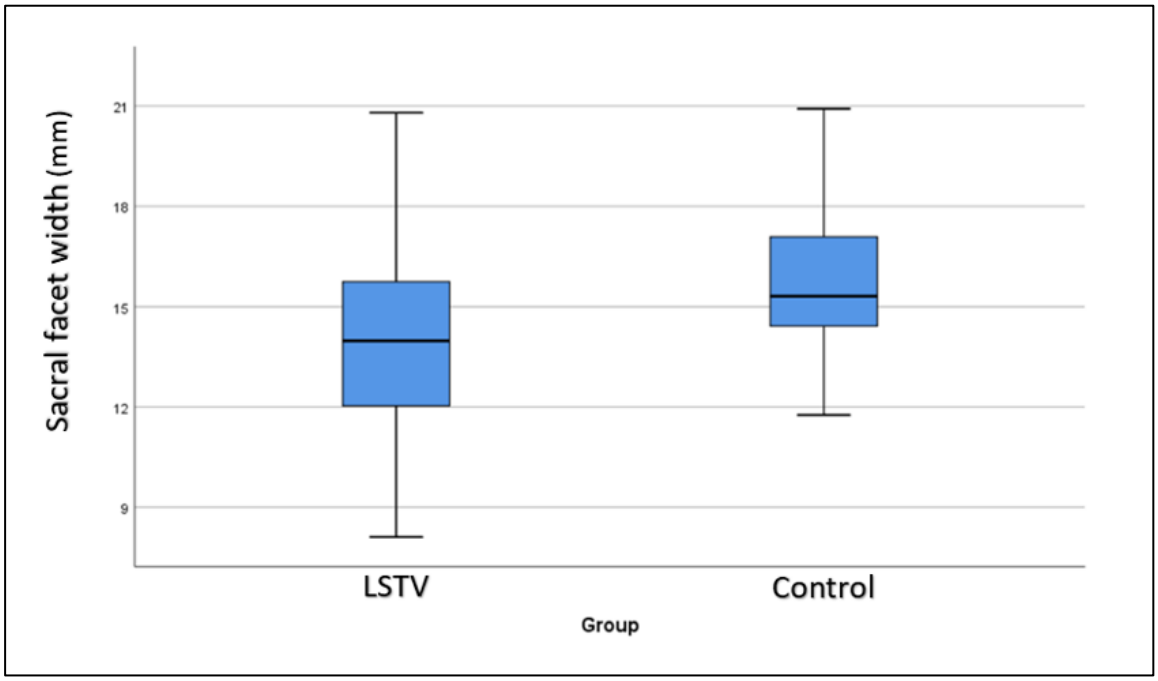

Figure 4.31: *A boxplot graph of the right sacral facet width measurement for the LSTV and control cohorts.*

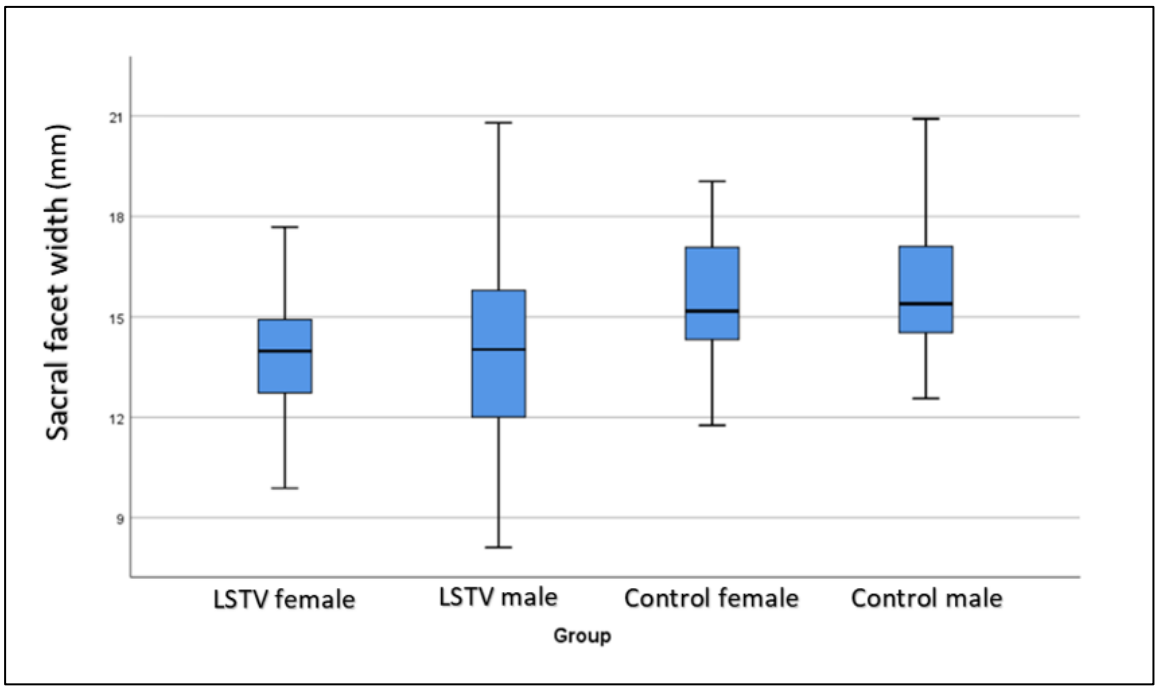

Figure 4.32: *A boxplot graph of the right sacral facet width measurement for the LSTV and control cohorts comparing the sexes.*

.**Left side**

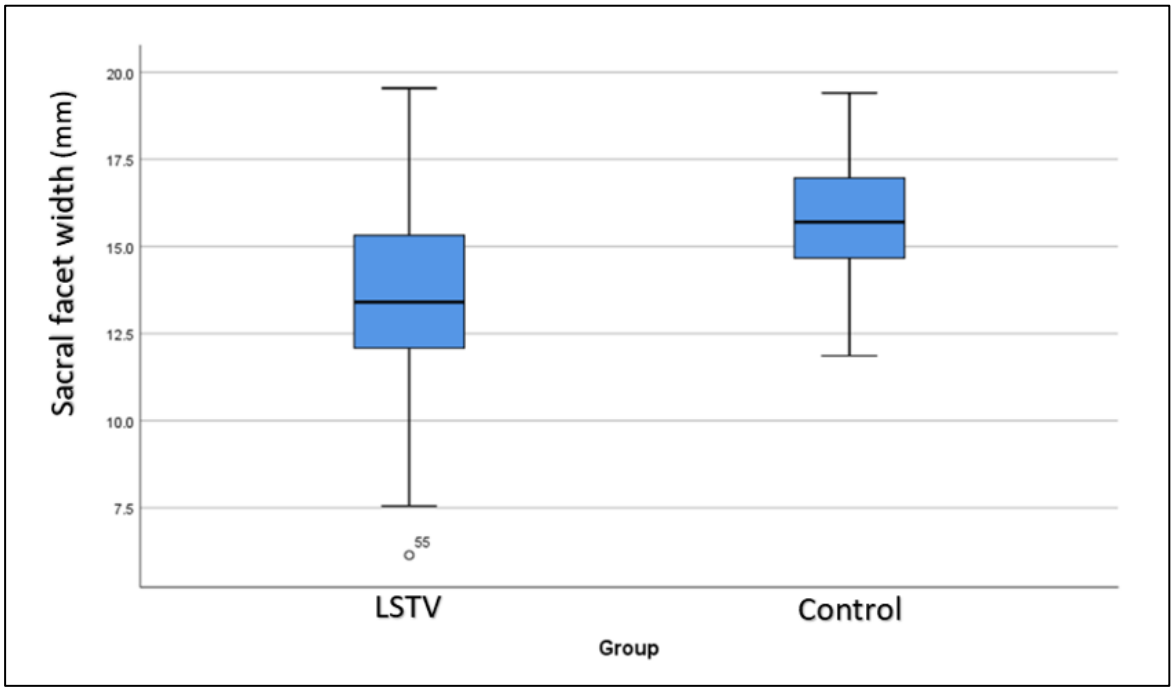

Figure 4.33: *A boxplot graph of the left sacral facet width measurement for the LSTV and control cohorts.*

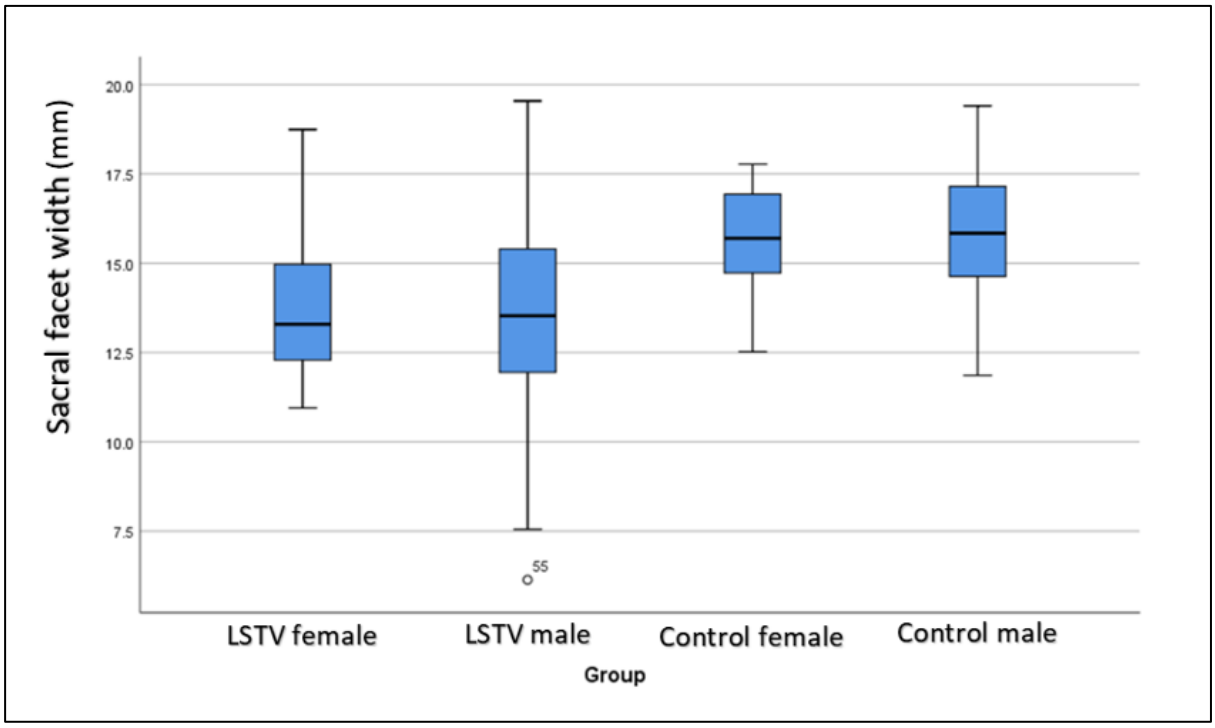

Figure 4.34: *A boxplot graph of the left sacral facet width measurement for the LSTV and control cohorts comparing the sexes.*

Statistical analyses

Lumbosacral transitional vertebrae and control cohort comparison

Right side

The T-test compared the mean rank values of SFW in the LSTV (n=79) cohort and the control (n=60) cohort. Levene's test for variance was not equal. The unequal variance T-test for equality of means (t=-4.23, df=136.01, p<0.001) found a statistically significant difference in right SFW with the LSTV cohort containing a shorter SFW compared to the control cohort.

Left side

The T-test compared the mean rank values of SFW in the LSTV (n=80) cohort and the control (n=60) cohort. Levene's test for variance was not equal. The unequal variance T-test for equality of means (t=-5.40, df=135.23, p<0.001) found a statistically significant difference in left SFW with the LSTV cohort containing a shorter SFW compared to the control cohort.

Lumbosacral transitional vertebrae cohort male and female comparison

Right side

The Mann-Whitney U test compared the mean rank values of SFW in the LSTV male cohort (n=58) and the LSTV female (n=21) cohort. There was no statistically significant difference (U=607.00, Z=-0.02, p=0.982) in SFW between the LSTV male (mean rank 40.03) and female (mean rank 39.90) cohorts.

Left side

The Mann-Whitney U test compared the mean rank values of SFW in the LSTV male cohort (n=59) and the LSTV female (n=21) cohort. There was no statistically significant difference (U=603.00, Z=-0.18, p=0.857) in SFW between LSTV male (mean rank 40.78) and female (mean rank 39.71) cohorts.

Control cohort male and female comparison

Right side

The Mann-Whitney U test compared the mean rank values of SFW in the male (n=30) and the female (n=30) control cohorts.

There was no statistically significant difference (U=415.00, Z=-0.52, *p*=0.605) in right SFW between the control male (mean rank 31.67) and female (mean rank 29.33) cohorts.

Left side

The Mann-Whitney U test compared the mean rank values of SFW in the male (n=30) and the female (n=30) control cohorts. There was no statistically significant difference (U=433.50, Z=-0.25; *p*=0.802) in left SFW between the control male (mean rank 31.07) and female (mean rank 29.93) cohorts.

Female lumbosacral transitional vertebrae cohort and female control cohort comparison

Right side

The Mann-Whitney U test compared the mean rank values of the SFW in the female LSTV (n=21) and the female control (n=30) cohorts.

There was a statistically significant difference (U=183.00, Z=-2.53, *p*=0.012) in SFW between the LSTV female (mean rank 19.71) and the control female (mean rank 30.40) cohorts.

Left side

The Mann-Whitney U test compared the mean rank values of the SFW in the female LSTV (n=21) and the female control (n=30) cohorts. There was a statistically significant difference (U=118.50, Z=-3.76, *p*<0.001 in SFW between the LSTV female (mean rank 16.54) and the control female (mean rank 32.55) cohorts.

Male lumbosacral transitional vertebrae cohort and male control cohort comparison

Right side

The Mann-Whitney U test compared the mean rank values of the SFW in the male LSTV (n=58) and the male control (n=30) cohorts. There was a statistically significant difference (U=527.00, Z=-3.019, *p*=0.003) in SFW between the LSTV male (mean rank 38.59) and the larger control male (mean rank 55.93) cohorts.

Left side

The Mann-Whitney U test compared the mean rank values of the SFW in the male LSTV (n=59) and the male control (n=30) cohorts.

There was a statistically significant difference (U=484.00, Z=-3.480, *p*=0.001) in SFW between the LSTV male (mean rank 38.20) and the larger control male (mean rank 58.37) cohorts.

Right side

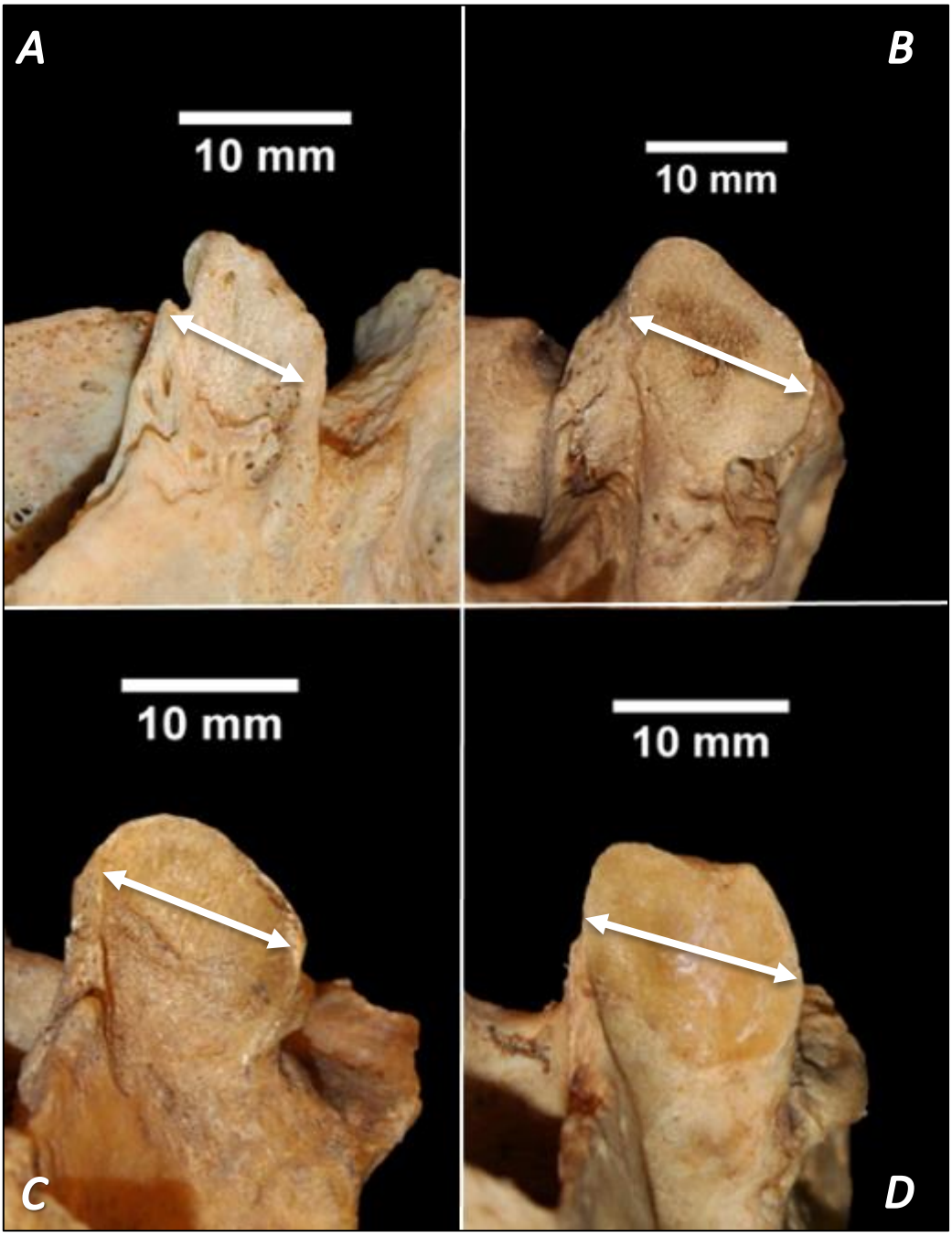

Figure 4.35: *Perpendicular view of the right-sided sacral facet widths associated with lumbosacral transitional vertebrae.* ***A)*** *A right-sided sacral facet of a Type IIB lumbosacral transitional vertebra asymmetrical facet joint orientation.* ***B)*** *A right-sided sacral facet of a left-sided Type IIIA lumbosacral transitional vertebra with roughly symmetrical facet joint orientation.* ***C)*** *A right-sided sacral facet of a right-sided Type IIA lumbosacral transitional vertebra with slightly asymmetrical facet joint orientation.* ***D)*** *A sacral facet of a Type IIB lumbosacral transitional vertebra with roughly symmetrical facet joint orientation. The double arrows indicate the sacral facet width of the right sacral facet joints.* ***Photography and editing:*** *GJ Paton.*

Left side

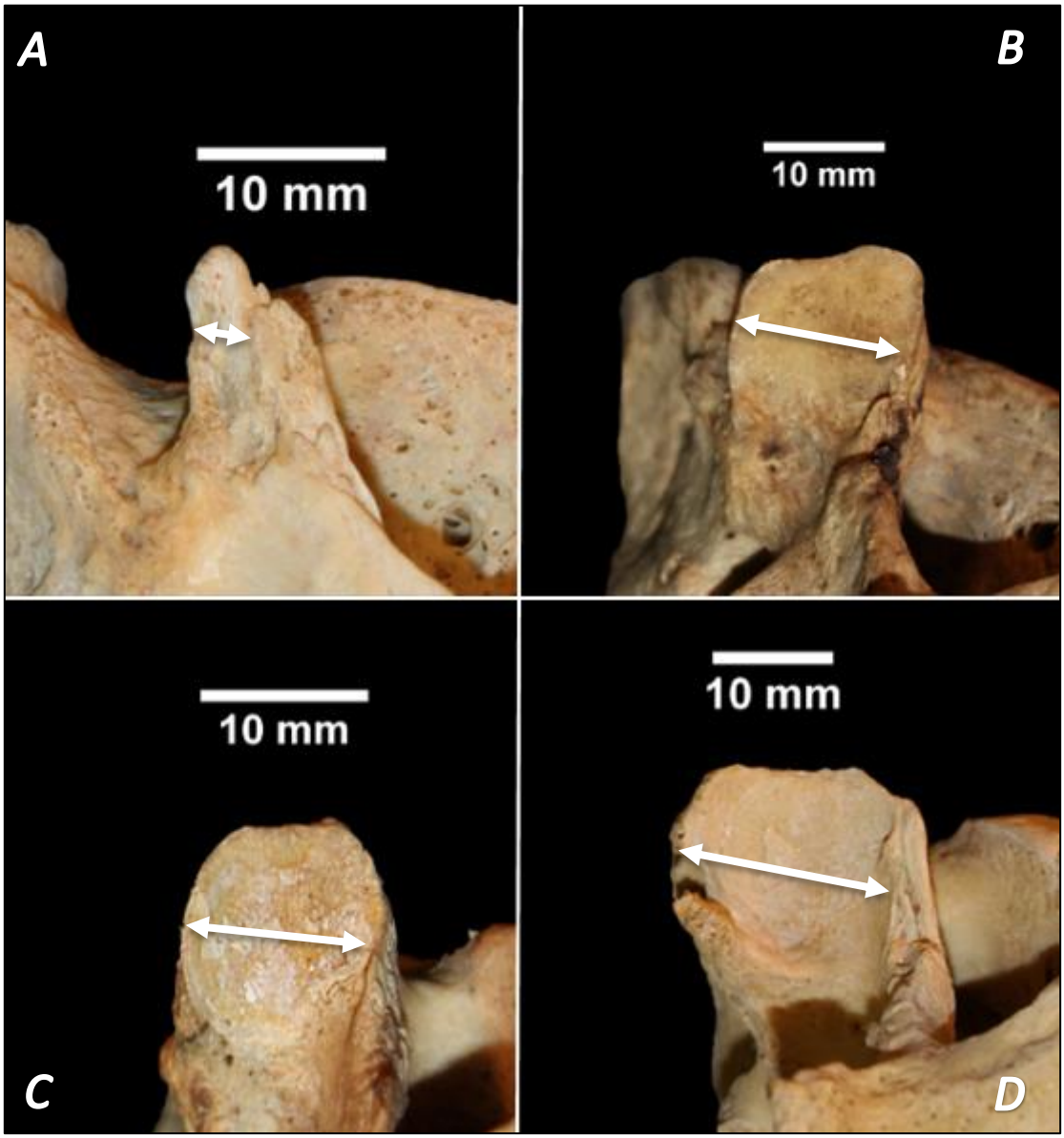

Figure 4.36: *Perpendicular view of the right-sided sacral facet widths associated with lumbosacral transitional vertebrae.* ***A)*** *A left-sided dysplastic sacral facet of a Type IIB lumbosacral transitional vertebra asymmetrical facet joint orientation.* ***B)*** *A left-sided sacral facet of a left-sided Type IIIA lumbosacral transitional vertebra with roughly symmetrical facet joint orientation.* ***C)*** *A left-sided sacral facet of a right-sided Type IIA lumbosacral transitional vertebra with slightly asymmetrical facet joint orientation.* ***D)*** *A left-sided sacral face of a Type IIB lumbosacral transitional vertebra with roughly symmetrical facet joint orientation. The double arrows indicate the sacral facet width of the left sacral facet joints.* ***Photography and editing:*** *GJ Paton.*

D10: Auricular length (AL); right and left

The right LSTV cohort (N=86) consisted of 62 males (n=62) and 24 females (n=24) and the left LSTV cohort (N=88) consisted of 64 males (n=64) and 24 females (n=24). The control cohort (N=60) consisted of 30 males (n=30) and 30 females (n=30).

Lumbosacral transitional vertebrae cohort compared to the control cohort

Right side

The mean AL on the right side in the LSTV cohort (59.36mm ± 7.10mm) was larger than the control cohort (56.67mm ± 4.72mm). The AL of the LSTV cohort had a larger range in variation of length, between 46.16mm and 82.89mm, while the control cohort range was 44.23mm and 66.96mm in length.

Left side

The mean AL on the left side in the LSTV cohort (59.84mm ± 9.02mm) was larger than the control cohort (56.95mm ± 5.22mm). The AL of the LSTV cohort had a smaller range in variation of length, between 69.65mm and 79.17mm, while the control cohort range was 45.33mm to 70.93mm in length.

Sex comparison of lumbosacral transitional vertebrae and control cohorts

Right side

A sex comparison found that the mean AL on the right side in the male LSTV cohort (60.37mm ± 7.06mm) was larger than that of the female cohort (56.76mm ± 6.64). The AL of the LSTV cohort had a larger range in variation of length, between 47.93mm and 82.89mm, while the female cohort range was 46.16mm to 71.52mm in length.

Likewise, sex comparison of the mean AL on the right side in the male control cohort was larger for males (58.036mm ± 5.14mm) when compared to the females (55.30mm ± 3.88mm).

The AL of the LSTV cohort had a smaller range in variation of length, between 44.23mm and 65.55mm, while the control cohort range was 49.10mm to 66.96mm in length.

The mean AL of the male LSTV cohort on the left side (60.37mm ± 7.06mm) was shorter than the males in the control cohort (58.036mm ± 5.14mm). The mean AL of females in the LSTV cohort (56.76mm ± 6.64mm) was shorter than the females in the control cohort (55.30mm ± 3.88mm). Refer to Figures 4.37 and 4.38.

Left side

A sex comparison found that the mean AL on the left side in the male LSTV cohort (61.65mm ± 7.04mm) was larger than that of the female cohort (55.00mm ± 11.76). The AL of the male LSTV cohort had a larger range in variation of length, between 46.96mm and 79.17mm, while the female LSTV cohort range was 69.65mm to 70.67mm in length.

Likewise, sex comparison of the mean AL on the left in the control cohort was larger for males (58.04 ± 5.85mm) when compared to the females (55.86mm ± 4.33mm). The AL of the male cohort had a larger range in variation of length, between 45.33mm and 70.93mm, while the female cohort range was 50.39mm to 65.99mm in length.

The mean AL of the male LSTV cohort on the left side (61.65mm ± 7.04mm) was longer than the males in the control cohort (55.00mm ± 11.76). The mean AL of females in the LSTV cohort (58.04 ± 5.85mm) was longer than the females in the control cohort (55.86mm ± 4.33mm). Refer to Figures 4.39 and 4.40. Figures 4.41 and 4.42 demonstrate the AL variations associated with LSTV on the right and left sides.

Right side

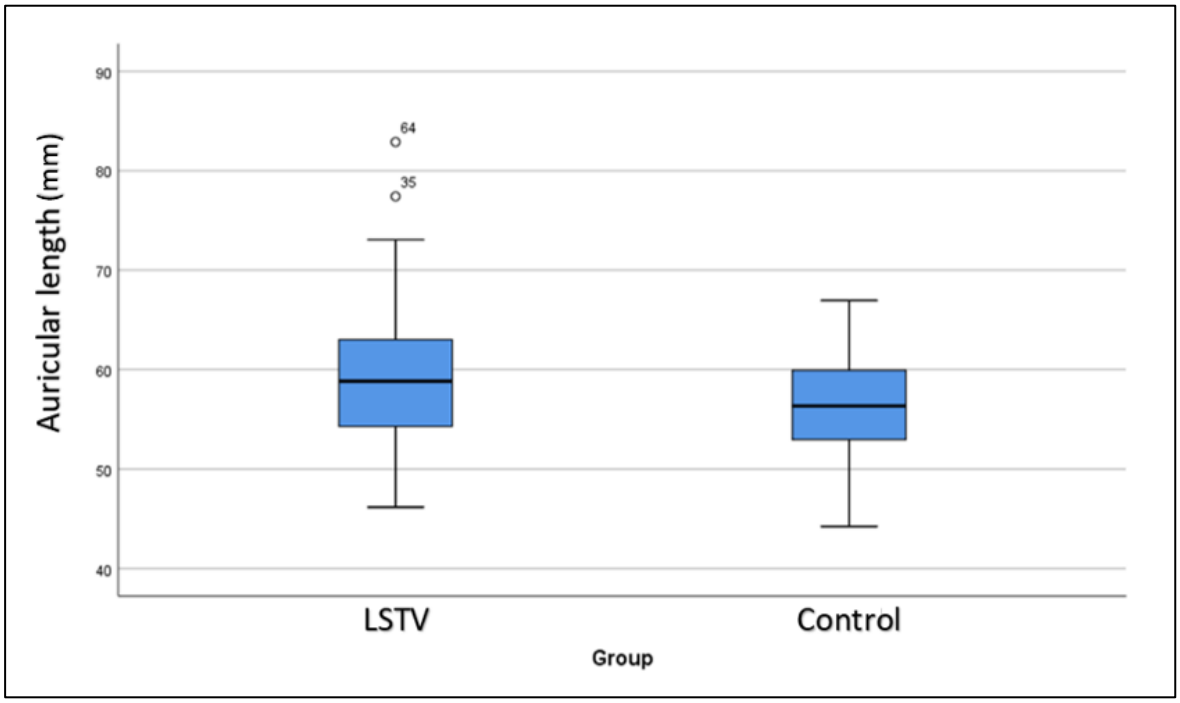

Figure 4.37: *A boxplot graph of the right auricular length measurement for the LSTV and control cohorts.*

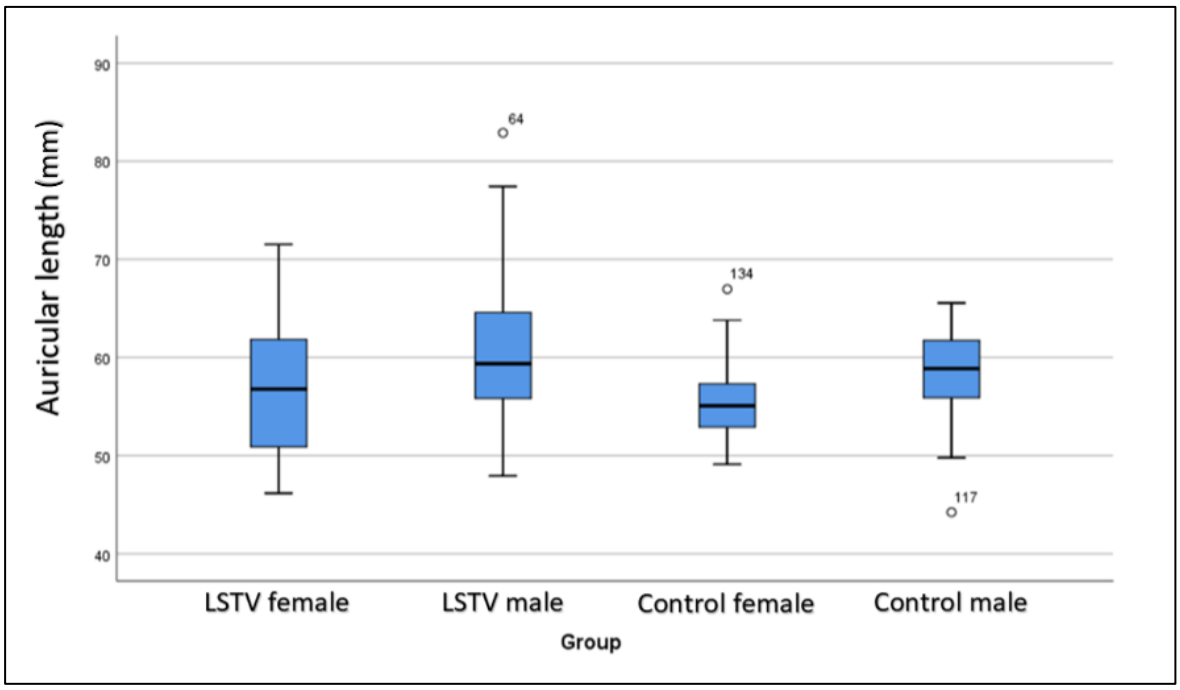

Figure 4.38: *A boxplot graph of the right auricular length measurement for the LSTV and control cohorts comparing the sexes.*

Left side

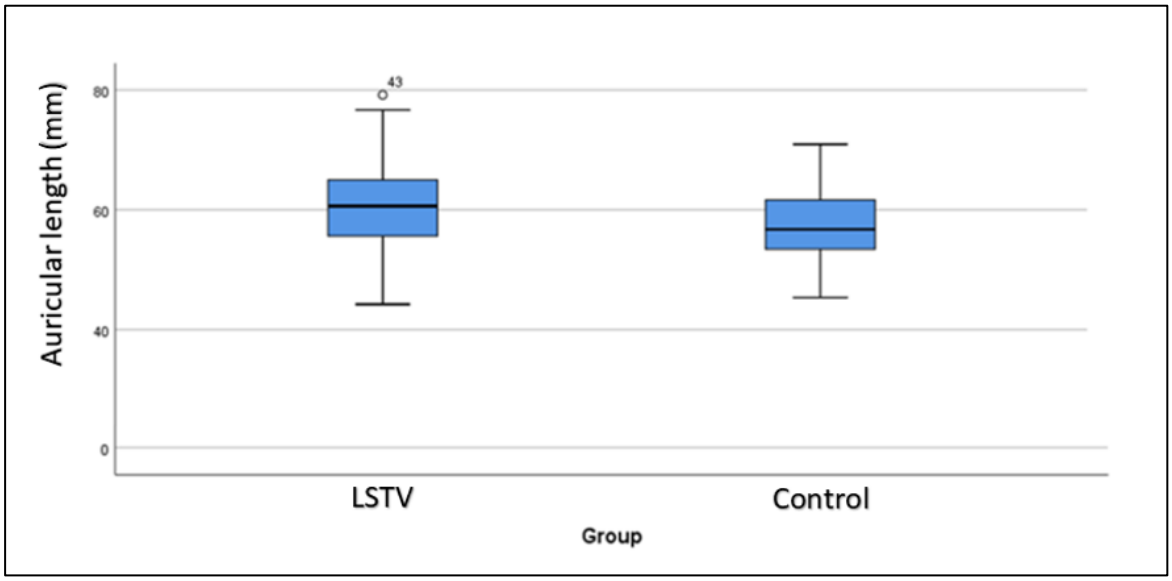

Figure 4.39: *A boxplot graph of the left auricular length measurement for the LSTV and control cohorts.*

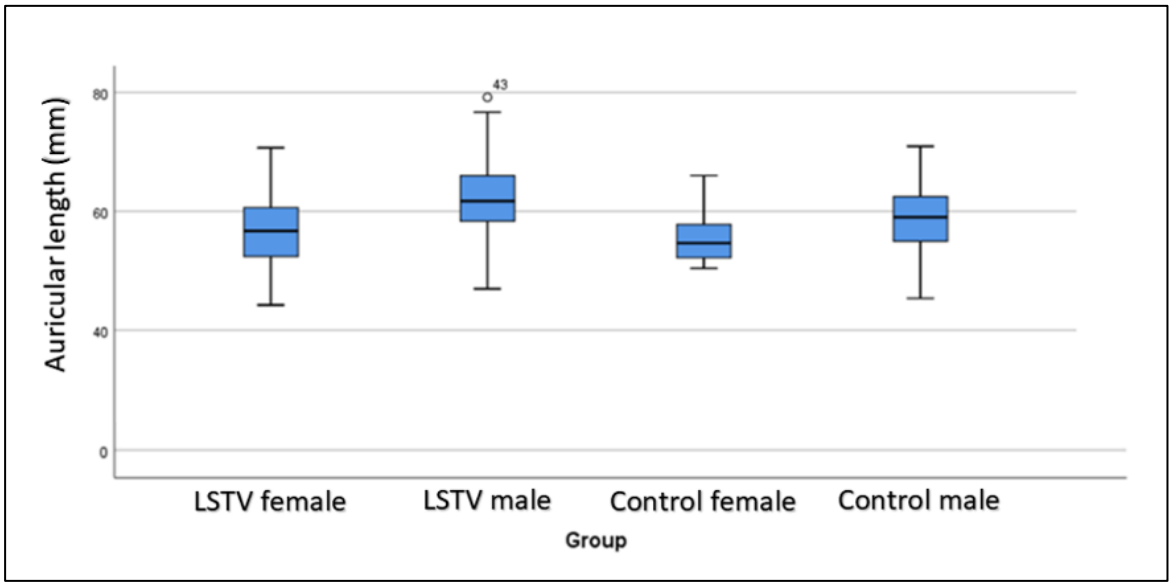

Figure 4.40: *A boxplot graph of the left auricular length measurement for the LSTV and control cohorts comparing the sexes.*

Statistical analyses

Lumbosacral transitional vertebrae and control cohort comparison

Right side

The T-test compared the mean rank values of AL in the LSTV (n=86) cohort and the control (n=60) cohort. Levene's test for variance was not equal. The unequal variance T-test for equality of means (t=2.57, df= 143.73, *p*=0.007) found a statistically significant difference in right AL with the LSTV cohort containing a longer AL compared to the control cohort.

Left side

The T-test compared the mean rank values of AL in the LSTV (n=88) cohort and the control (n=60) cohort. Levene's test for variance was not equal. The unequal variance T-test for equality of means (t=2.46, df= 142.70, *p*=0.015) found a statistically significant difference in left AL with the LSTV cohort containing a longer AL compared to the control cohort.

Lumbosacral transitional vertebrae cohort male and female comparison

Right side

The Mann-Whitney U test compared the mean rank values of AL in the LSTV male cohort (n=62) and the LSTV female (n=24) cohort. There was a statistically significant difference (U=530.00, Z=-2.06, *p*=0.039) in the right AL between the LSTV male (mean rank 46.95) and female (mean rank 34.58) cohorts.

Left side

The Mann-Whitney U test compared the mean rank values of AL in the LSTV male cohort (n=64) and the LSTV female (n=24) cohort. There was a statistically significant difference (U=429.00, Z=-3.18, *p*=0.001) in the left AL between the LSTV male (mean rank 49.80) and female (mean rank 30.38) cohorts.

Control cohort male and female comparison

Right side

The Mann-Whitney U test compared the mean rank values of AL in the male (n=30) and the female (n=30) control cohorts.

There was a statistically significant difference (U=267.00, Z=-2.71, *p*=0.007) in AL between the control male (mean rank 36.60) and female (mean rank 24.40) cohorts.

Left side

The Mann-Whitney U test compared the mean rank values of AL in the male (n=30) and the female (n=30) control cohorts. There was a statistically significant difference (U=314.50, Z=-2.00, *p*=0.045) in AL between the control male (mean rank 35.02) and female (mean rank 25.98) cohorts.

Female lumbosacral transitional vertebrae cohort and female control cohort comparison

Right side

The Mann-Whitney U test compared the mean rank values of the AL in the female LSTV (n=24) and the female control (n=30) cohorts. There was no statistically significant difference (U=318.00, Z=-0.73, *p*=0.465) in AL between the LSTV female (mean rank 29.25) and the control female (mean rank 26.10) cohorts.

Left side

The Mann-Whitney U test compared the mean rank values of the AL in the female LSTV (n=24) and the female control (n=30) cohorts. There was no statistically significant difference (U=323.00, Z=-0.64, *p*=0.520) in AL between the LSTV female (mean rank 29.04) and the control female (mean rank 26.27) cohorts.

Male lumbosacral transitional vertebrae cohort and male control cohort comparison

Right side

The Mann-Whitney U test compared the mean rank values of the AL in the male LSTV (n=62) and the male control (n=30) cohorts.

There was no statistically significant difference (U=797.00, Z=-1.108, *p*=0.268) in AL between the LSTV male (mean rank 48.65) and the control male (mean rank 42.07) cohorts.

Left side

The Mann-Whitney U test compared the mean rank values of the AL in the LSTV male (n=64) and the control male (n=30) cohorts.

There was a statistically significant difference (U=648.00, Z=-2.531, *p*=0.011) in AL between the LSTV male (mean rank 52.38) and the control male (mean rank 37.10) cohorts.

Right side

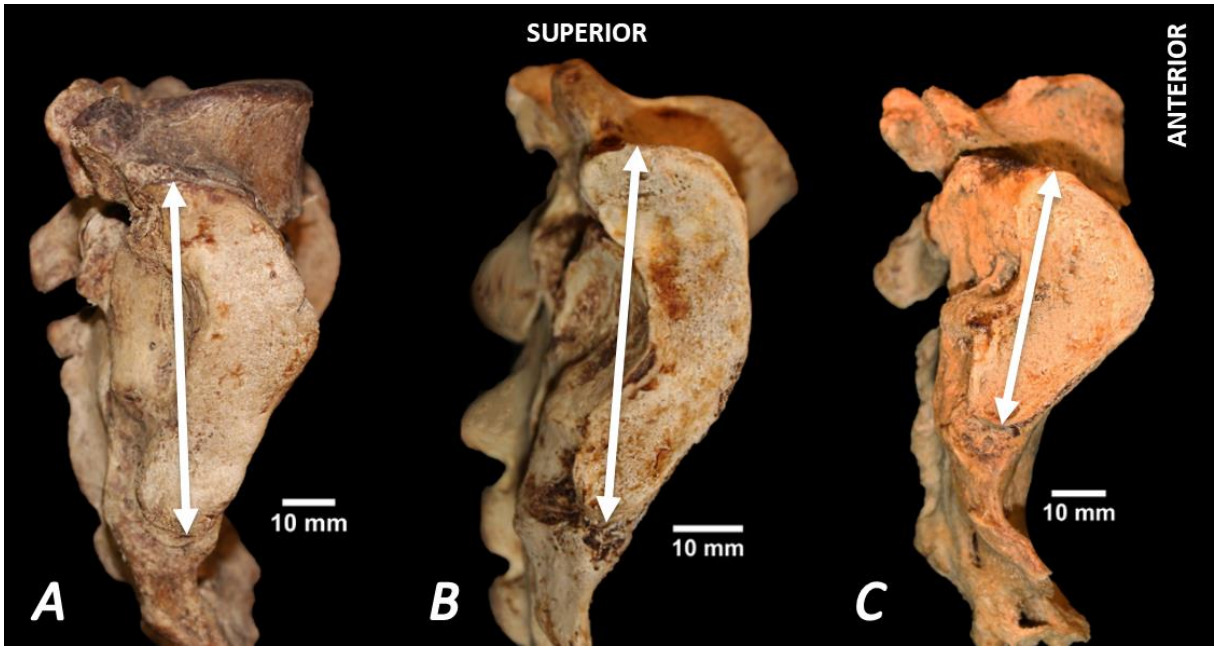

Figure 4.41: *Lateral view of sacra displaying the right-sided auricular lengths associated with lumbosacral transitional vertebrae.* ***A)*** *A Type IIIB lumbosacral transitional vertebra asymmetrical facet joint orientation.* ***B)*** *A Type IIIB lumbosacral transitional vertebra with roughly symmetrical facet joint orientation.* ***C)*** *A right-sided Type IIIA lumbosacral transitional vertebra with slightly asymmetrical facet joint orientation. The double arrows indicate the auricular length.* ***Photography and editing:*** *GJ Paton.*

Left side

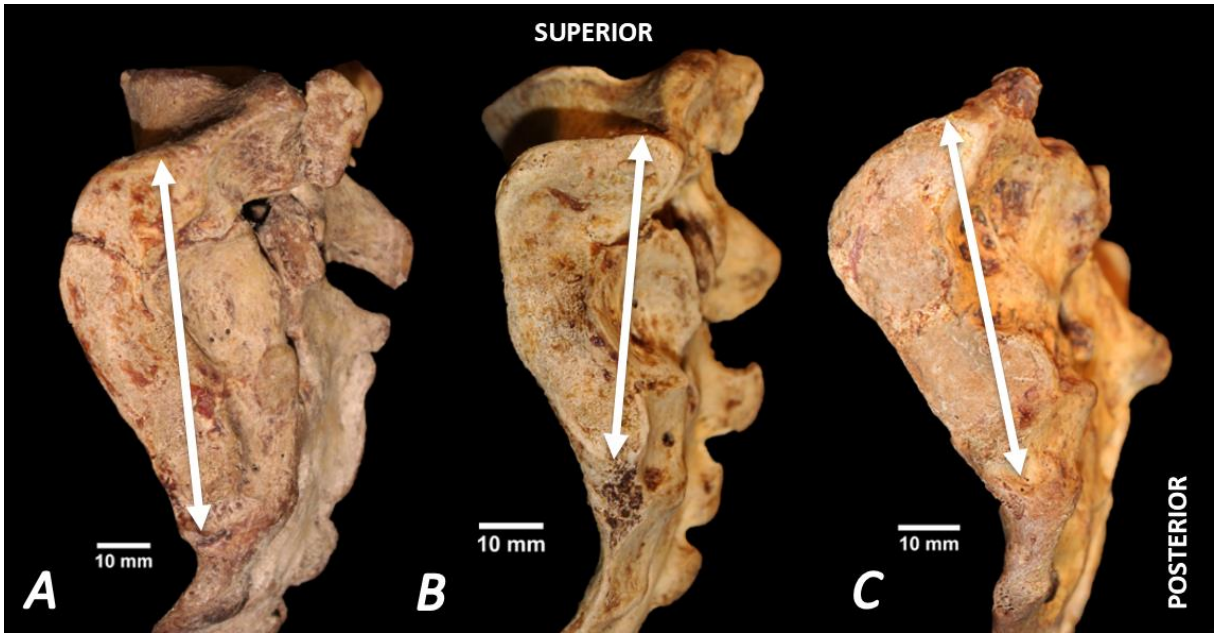

Figure 4.42: *Lateral view of sacra displaying the left-sided auricular lengths associated with lumbosacral transitional vertebrae.* ***A)*** *A Type IIIB lumbosacral transitional vertebra asymmetrical facet joint orientation.* ***B)*** *A Type IIIB lumbosacral transitional vertebra with roughly symmetrical facet joint orientation.* ***C)*** *A left-sided Type IIA lumbosacral transitional vertebra with slightly asymmetrical facet joint orientation. The double arrows indicate the auricular length.* ***Photography and editing:*** *GJ Paton.*

D11: Facet Joint Angle (FA), right and left

The right LSTV cohort (N=83) consisted of 66 males (n=66) and 25 females (n=25) and 17 females (n=17). The left LSTV cohort (N=83) consisted of 66 males (n=66) and 25 females (n=25). The control cohort (N=60) consisted of 30 males (n=30) and 30 females (n=30).

Lumbosacral transitional vertebrae cohort compared to the control cohort

Right side

The mean FA on the right side in the LSTV cohort was larger (52.62° ± 9.73°) than the control cohort (51.69° ± 7.94°). The right FA of the LSTV cohort had a larger range in variation of degrees of angulation, between 30.81° and 86.21°, while the control cohort range was 36.62° to 74.69° of angulation.

Left side

The mean FA on the left side in the LSTV cohort was larger (54.23° ± 10.41°) than the control cohort (50.81° ± 8.46°). The left FA of the LSTV cohort had a larger range in variation of degrees of angulation, between 37.57° and 85.99°, while the control cohort range was 27.35° to 80.36° of angulation.

Sex comparison of lumbosacral transitional vertebrae and control cohorts

Right side

A sex comparison found that the mean FA on the right side of males in the LSTV cohort (52.34° ± 9.34°) was larger than that of the female cohort (53.37° ± 10.86°). The right FA of the male LSTV cohort had a larger range in variation of degrees of angulation, between 30.81° and 86.21°, while the female LSTV cohort range was 34.95° to 76.22° of angulation.

Likewise, sex comparison of the mean FA on the right side in the control cohort was larger for males (50.29° ± 6.82°) when compared to the females (53.08° ± 8.81°).

The right FA of the male control cohort had a smaller range in variation of degrees of angulation, between 37.96° and 65.72°, while the female control cohort range was 36.62° to 74.69° of angulation.

The mean FA of the male LSTV cohort on the right side (52.34° ± 9.34°) was longer than the males in the control cohort (50.29° ± 6.82°). The mean FA of females in the LSTV cohort (53.37° ± 10.86°) was marginally longer than the females in the control cohort (53.08° ± 8.81°). Refer to Figures 4.43 and 4.44.

Left side

A sex comparison found that the mean FA on the left side of males in the LSTV cohort (52.87° ± 10.15°) was larger than that of the female cohort (57.81° ± 10.44°). The left FA of the male control cohort had a larger range in variation of degrees of angulation, between 37.70° and 85.99°, while the female control cohort range was 37.57° to 84.65° of angulation.

Likewise, sex comparison of the mean FA on the left side in the control cohort was larger for males (51.74° ± 8.42°) when compared to the females (49.86° ± 8.53°). The left FA of the male control cohort had a larger range in variation of degrees of angulation, between 34.46° and 80.36°, while the female control cohort range was 27.35° and 63.73° of angulation.

The mean FA of the male LSTV cohort on the right side (52.87° ± 10.15°) was larger than the males in the control cohort (51.74° ± 8.42°). The mean FA of females in the LSTV cohort (57.81° ± 10.44°) was larger than the females in the control cohort (49.86° ± 8.53°). Refer to Figures 4.45 and 4.46. Figure 4.49 demonstrate the FA variations associated with LSTV on the right and left sides.

Right side

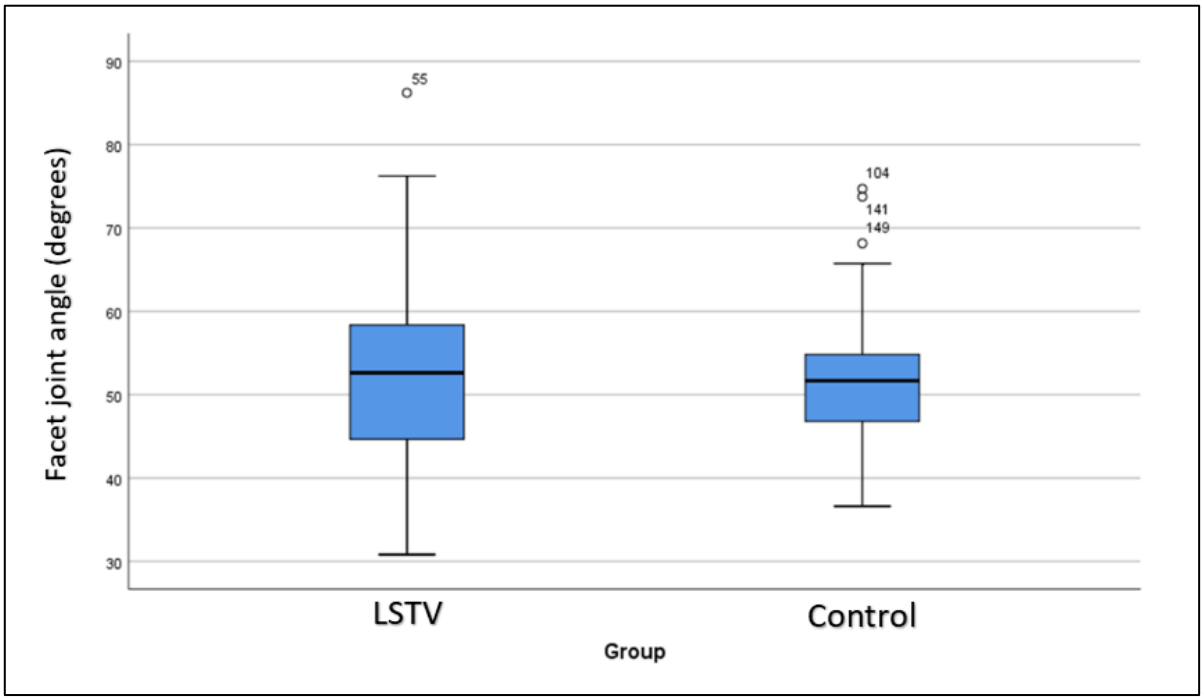

Figure 4.43: *A boxplot graph of the right sacral facet joint angle measurement for the LSTV and control cohorts.*

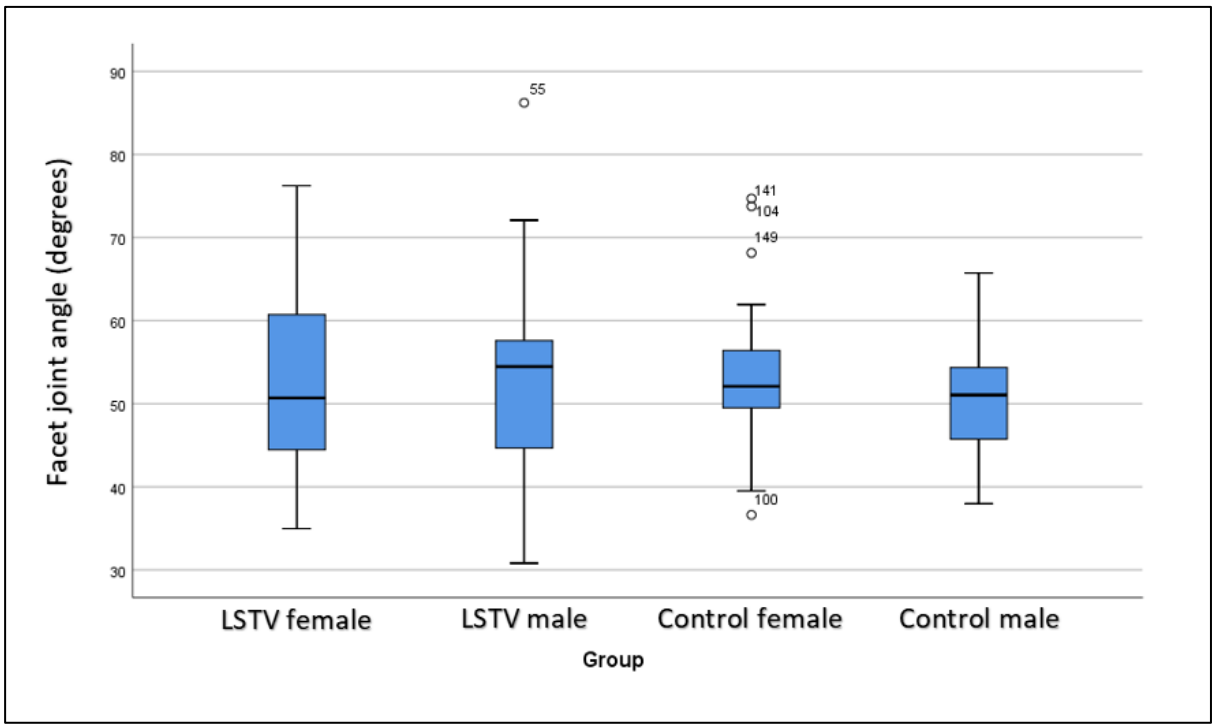

Figure 4.44: *A boxplot graph of the right sacral facet joint angle measurement for the LSTV and control cohorts compared to the sexes.*

Left side

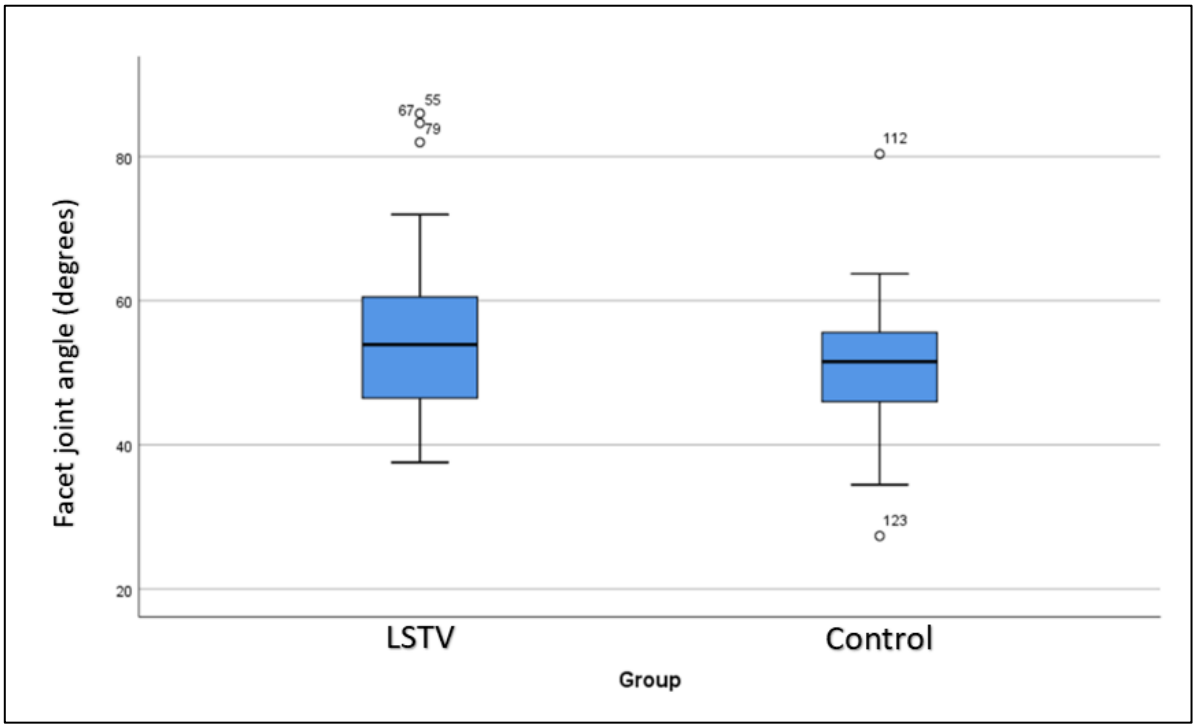

Figure 4.45: *A boxplot graph of the left sacral facet joint angle measurement for the LSTV and control cohorts.*

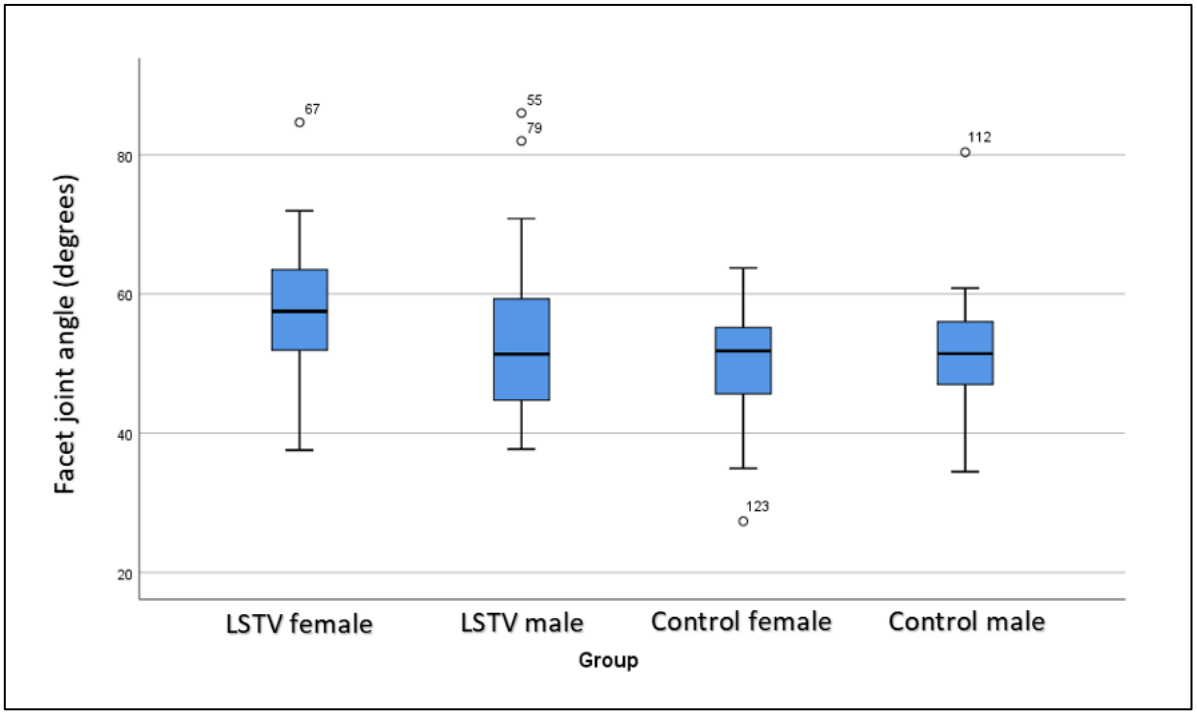

Figure 4.46: *A boxplot graph of the left sacral facet joint angle measurement for the LSTV and control cohorts compared to the sexes.*

Statistical analyses

Lumbosacral transitional vertebrae and control cohort comparison

Right side

The T-test compared the mean rank values of the right FA in the LSTV (n=91) cohort and the control (n=60) cohort. Levene's test for variance was not equal. The unequal variance T-test for equality of means (t=0.65, df=142.22, *p*=0.518) found no statistically significant difference in right FA with the LSTV cohort containing a greater angle as compared to the control cohort.

Left side

The T-test compared the mean rank values of the left FA in the LSTV (n=91) cohort and the control (n=60) cohort. Levene's test for variance was not equal. The unequal variance T-test for equality of means (t=2.22, df=142.52, *p*=0.028) found a statistically significant difference in left FA with the LSTV cohort containing a greater angle as compared to the control cohort.

Lumbosacral transitional vertebrae cohort male and female comparison

Right side

The Mann-Whitney U test compared the mean rank values of right FA in the LSTV male cohort (n=59) and the LSTV female (n=24) cohort. There was no statistically significant difference (U=787.00, Z=-0.34, *p*=0.735) in FA between the LSTV male (mean rank 45.42) and female (mean rank 47.52) cohorts.

Left side

The Mann-Whitney U test compared the mean rank values of left FA in the LSTV male cohort (n=59) and the LSTV female (n=24) cohort. There was a statistically significant difference (U=570.00, Z=-2.27, *p*=0.023) in FA angle on the left side between the LSTV male (mean rank 42.14) and female (mean rank 56.20) cohorts.

Control cohort male and female comparison

Right side

The Mann-Whitney U test compared the mean rank values of the right FA in the male (n=30) and the female (n=30) control cohorts. There was no statistically significant difference (U=370.00, Z=-1.18, *p*=0.237) in FA between the control male (mean rank 27.83) and female (mean rank 33.17) cohorts.

Left side

The Mann-Whitney U test compared the mean rank values of the left FA in the male (n=30) and the female (n=30) control cohorts. There was no statistically significant difference (U=420.00, Z=-0.44, *p*=0.657) in FA between the control male (mean rank 31.50) and female (mean rank 29.50) cohorts.

Female lumbosacral transitional vertebrae cohort and female control cohort comparison

Right side

The Mann-Whitney U test compared the mean rank values of the FA in the female LSTV (n=25) and the female control (n=30) cohorts. There was no statistically significant difference (U=365.00, Z=-0.17, *p*=0.866) in FA between the LSTV female (mean rank 27.26) and the control female (mean rank 28.33) cohorts.

Left side

The Mann-Whitney U test compared the mean rank values of the FA in the female LSTV (n=25) and the female control (n=30) cohorts. There was a statistically significant difference (U=201.00, Z=-2.94, *p*=0.003) in FA between the LSTV female (mean rank 34.96) and the control female (mean rank 22.20) cohorts.

Male lumbosacral transitional vertebrae cohort and male control cohort comparison

Right side

The Mann-Whitney U test compared the mean rank values of the FA in the male LSTV (n=66) and the male control (n=30) cohorts. There was no statistically significant difference (U=833.00, Z=-1.241, *p*=0.215) in right FA between the LSTV male (mean rank 50.88) and the control male (mean rank 43.27) cohorts.

Left side

The Mann-Whitney U test compared the mean rank values of the left FA in the LSTV male (n=66) and the control male (n=30) cohorts. There was no statistically significant difference (U=952, Z=-0.300, *p*=0.764) in FA between the LSTV male (mean rank 49.08) and the control male (mean rank 47.23) cohorts.

Additional analyses

Pearson's coefficient correlation was used to assess if a relationship exists between FA and the size of the FA, BSA and ASFA. Additionally correlation was assessed between FA left and right.

Right side

The FA on the right found no statistically significant relationship exists between the right FA (*p*= 0.110), left FA (*p*=0.094), BSA (*p*=0.057), right ASFA (*p*=0.077) and left ASFA (*p*=0.309). A statistically significant positive correlation was found between the right FA and the left FA (*p*<0.001), with a medium effect size (*r*=0.45). Refer to Figure 4.47.

Left side

The FA on the left found no statistically significant relationship exists between the right FA (*p*= 0.611), left SFA (*p*=0.222), right ASFA (*p*=0.970) and left ASFA (*p*=0.393). Refer to Figure 4.48.

Bilateral

A statistically significant negative correlation was found between the right FA and the BSA (p=0.007) with a medium effect size (r= -0.354).

Right side

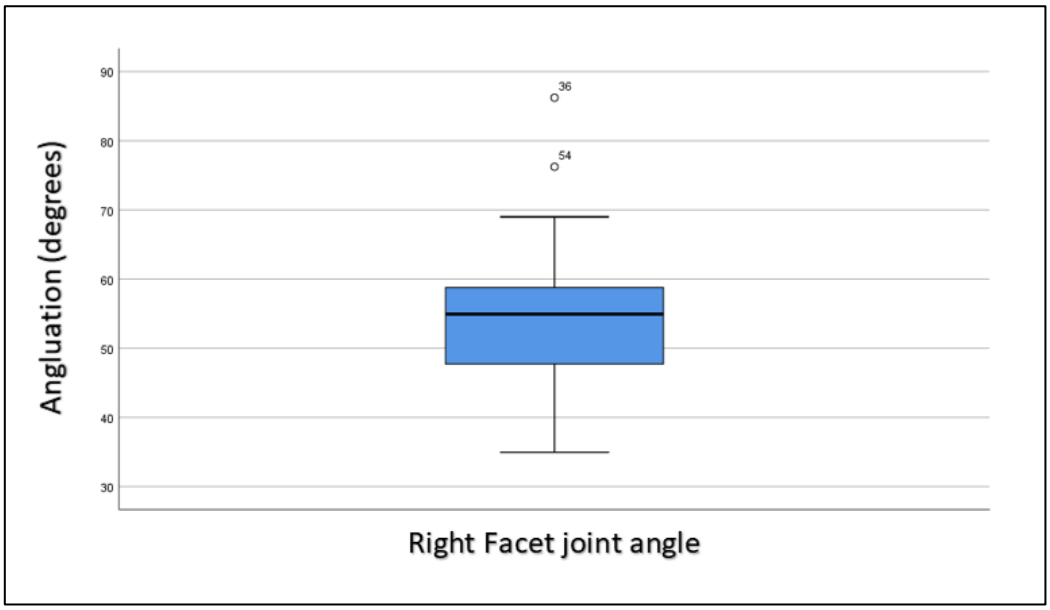

Figure 4.47: *A boxplot graph of the right sacral facet angle measurement associated with Type II lumbosacral transitional vertebrae.*

Left side

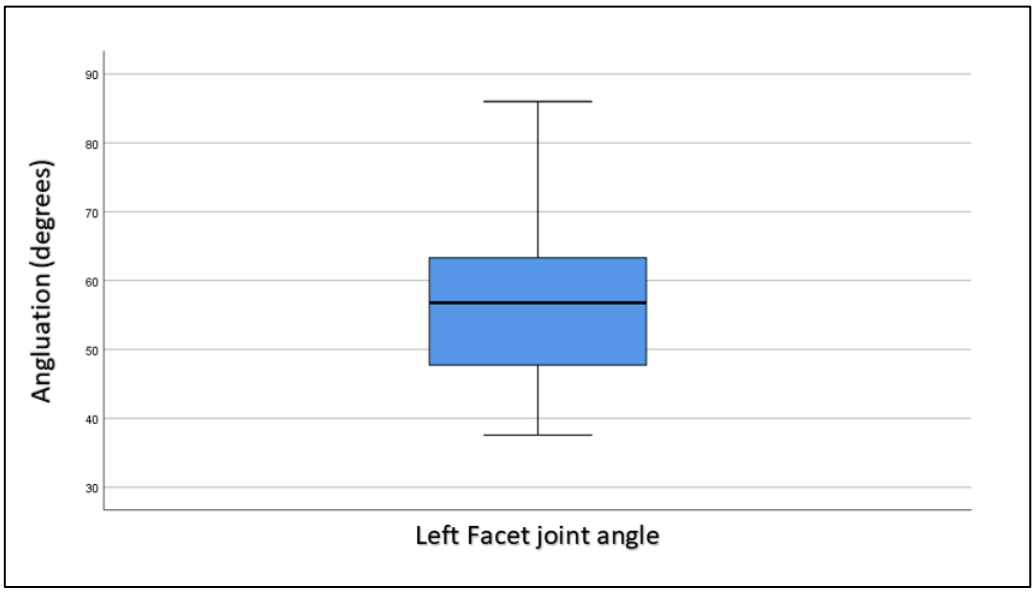

Figure 4.48*: A boxplot graph of the left sacral facet joint angle measurement associated with Type II lumbosacral transitional vertebrae.*

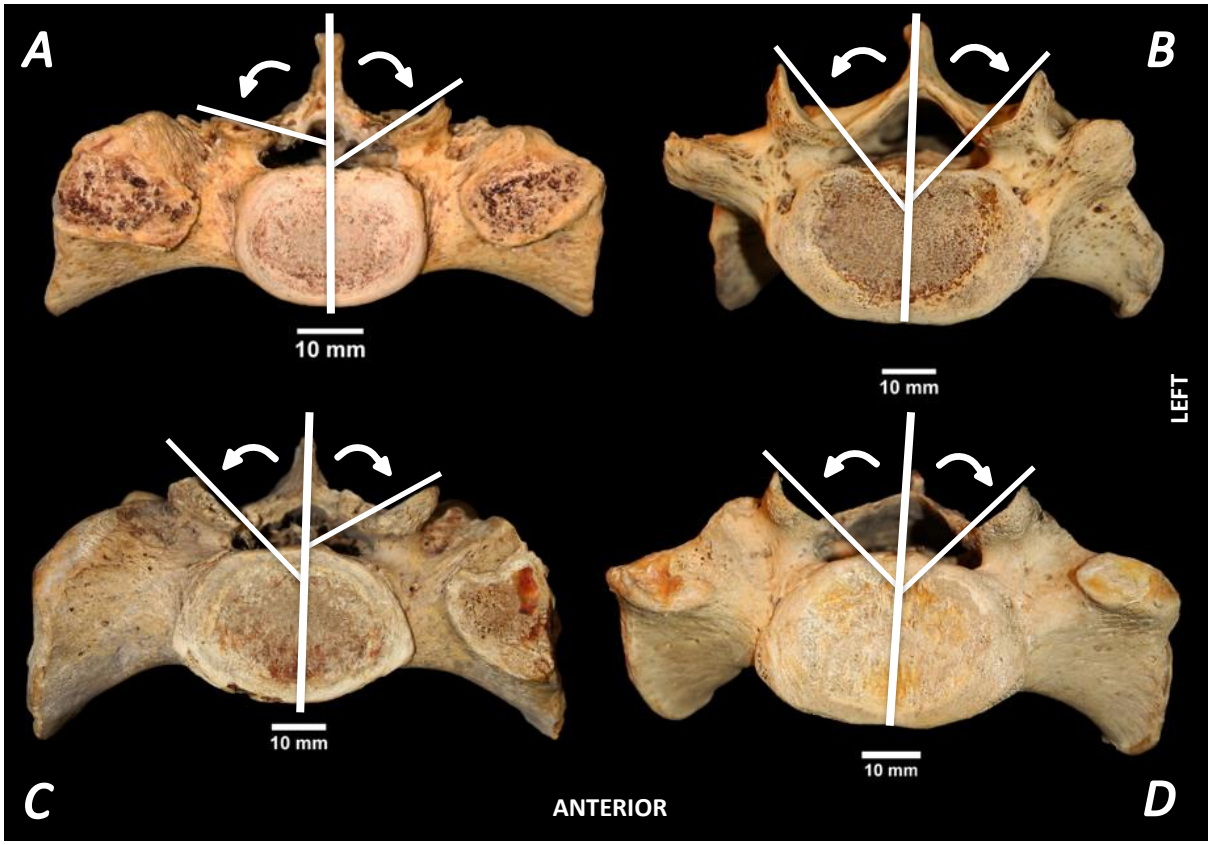

Figure 4.49: *Superior view of sacra displaying the facet joint angles associated with lumbosacral transitional vertebrae.* ***A)*** *A Type IIB lumbosacral transitional vertebra asymmetrical facet joint orientation.* ***B)*** *A left-sided Type IIIA lumbosacral transitional vertebra with roughly symmetrical facet joint orientation.* ***C)*** *A left-sided Type IIA lumbosacral transitional vertebra with slightly asymmetrical facet joint orientation.* ***D) A*** *Type IIB lumbosacral transitional vertebra with roughly symmetrical facet joint orientation. The arrows indicate the plane of the facet joints measured in degrees of angulation from the midline.* ***Photography and editing:*** *GJ Paton.*

D12: Sacral Hiatus Length (SHL)

The LSTV cohort (N=87) consisted of 63 males (n=63) and 24 females (n=24). The control cohort (N=60) consisted of 30 males (n=30) and 30 females (n=30).

Lumbosacral transitional vertebrae cohort compared to the control cohort

The mean SHL in the LSTV cohort was larger (20.42mm ± 10.06mm) than the control cohort (16.98mm ± 7.29mm). The SHL of the LSTV cohort had a larger range in variation of length, between 3.0mm and 49.98mm, while the control cohort range was between 3.97mm and 36.68mm in length.

Sex comparison of lumbosacral transitional vertebrae cohort compared to the control cohort

A sex comparison found that the mean SHL of males in the LSTV cohort (21.81mm ± 10.99mm) was larger than that of the female cohort (16.79mm ± 5.81mm). The SHL of the male LSTV cohort had a larger range in variation of length, between 3.0mm and 49.98mm, while the female LSTV cohort range was between 6.57mm and 26.50mm in length.

Likewise, sex comparison of the mean SHL in the control cohort was larger for males (17.52mm ± 7.23mm) when compared to the females (16.43mm ± 7.44mm). The SHL of the male control cohort had a larger range in variation of length, between 5.35mm and 36.68mm, while the female control cohort range was between 3.97mm and 29.21mm in length.

The mean SHL of the male LSTV cohort on the right side (21.81mm ± 10.99mm) was larger than the males in the control cohort (17.52mm ± 7.23mm). The mean SHL of females in the LSTV cohort (16.79mm ± 5.81mm) was larger than the females in the control cohort (16.43mm ± 7.44mm). Refer to Figures 4.50 and 4.51. Figure 4.52 demonstrates the SHL variations associated with LSTV.

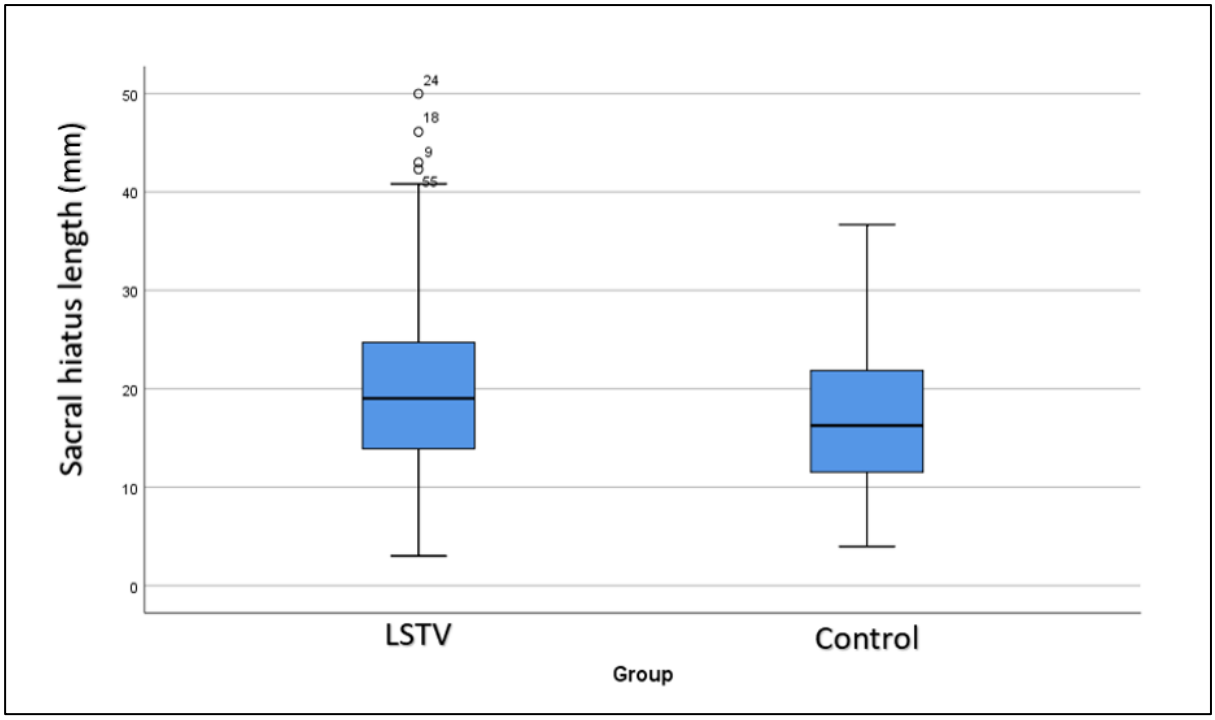

Figure 4.50: *A boxplot graph of the sacral hiatus length measurement for the LSTV and control cohorts.*

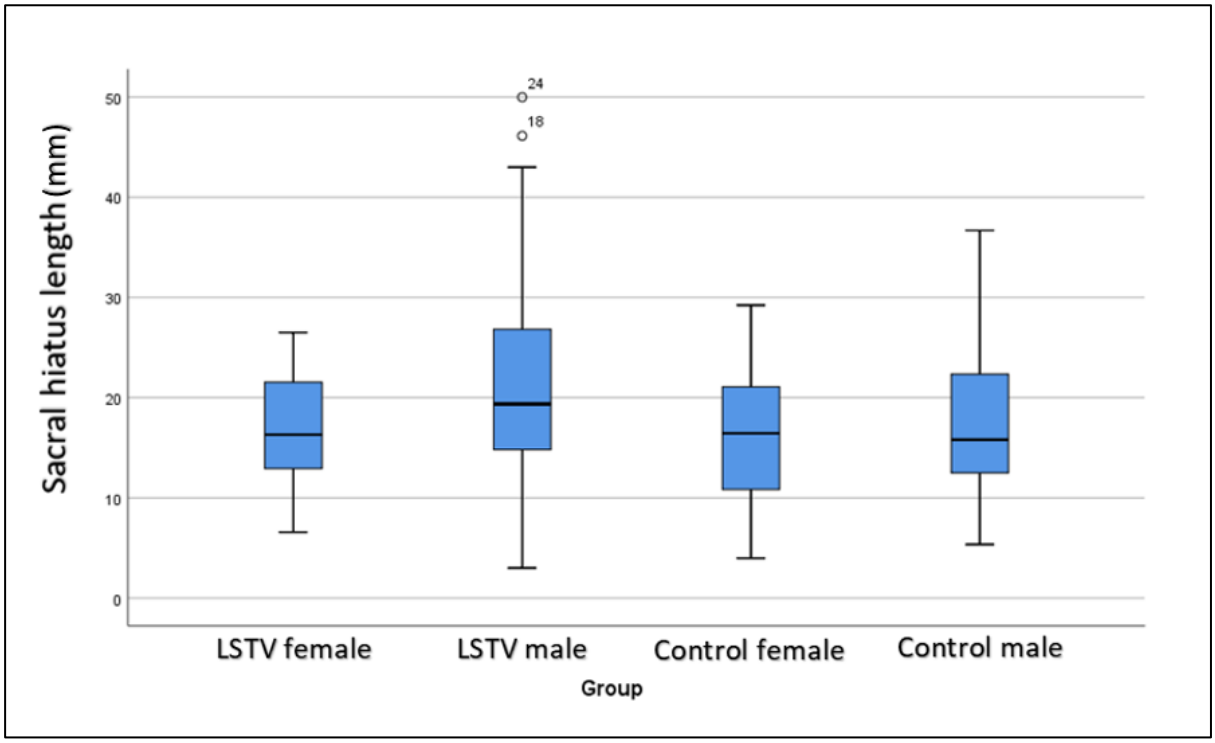

Figure 4.51: *A boxplot graph of the sacral hiatus length measurement for the LSTV and control cohorts comparing the sexes.*

Statistical analyses

Lumbosacral transitional vertebrae and control cohort comparison

The T-test compared the mean rank values of SHL in the LSTV (n=87) cohort and the control (n=60) cohort. Levene's test for variance was equal. The T-test for equality of means (t=2.27, df=145, *p*=0.025) found a statistically significant difference in SHL with the LSTV cohort containing a longer SHL compared to the control cohort.

Lumbosacral transitional vertebrae cohort male and female comparison

The Mann-Whitney U test compared the mean rank values of SHL in the LSTV male cohort (n=63) and the LSTV female (n=24) cohort. There was no statistically significant difference (U=586.00, Z=-1.61, *p*=0.106) in SBW between the LSTV male (mean rank 446.70) and female (mean rank 36.92) cohorts.

Control cohort male and female comparison

The Mann-Whitney U test compared the mean rank values of SHL in the male (n=30) and the female (n=30) control cohorts. There was no statistically significant difference (U=428.00, Z=-0.33, *p*=0.745) in SHL between the control male (mean rank 31.23) and female (mean rank 29.77) cohorts.

Female lumbosacral transitional vertebrae cohort and female control cohort comparison

The Mann-Whitney U test compared the mean rank values of the SHL in the female LSTV (n=24) and the female control (n=30) cohorts. There was no statistically significant difference (U=347.00, Z=-0.23, *p*=0.821) in SHL between the LSTV female (mean rank 28.04) and the control female (mean rank 27.07) cohorts.

Male lumbosacral transitional vertebrae cohort and male control cohort comparison

The Mann-Whitney U test compared the mean rank values of the SHL in the male LSTV (n=66) and the male control (n=30) cohorts. There was no statistically significant difference (U=744.00, Z=-1.65, *p*=0.099) in SHL between the LSTV male (mean rank 50.19) and the control male (mean rank 40.30) cohorts.

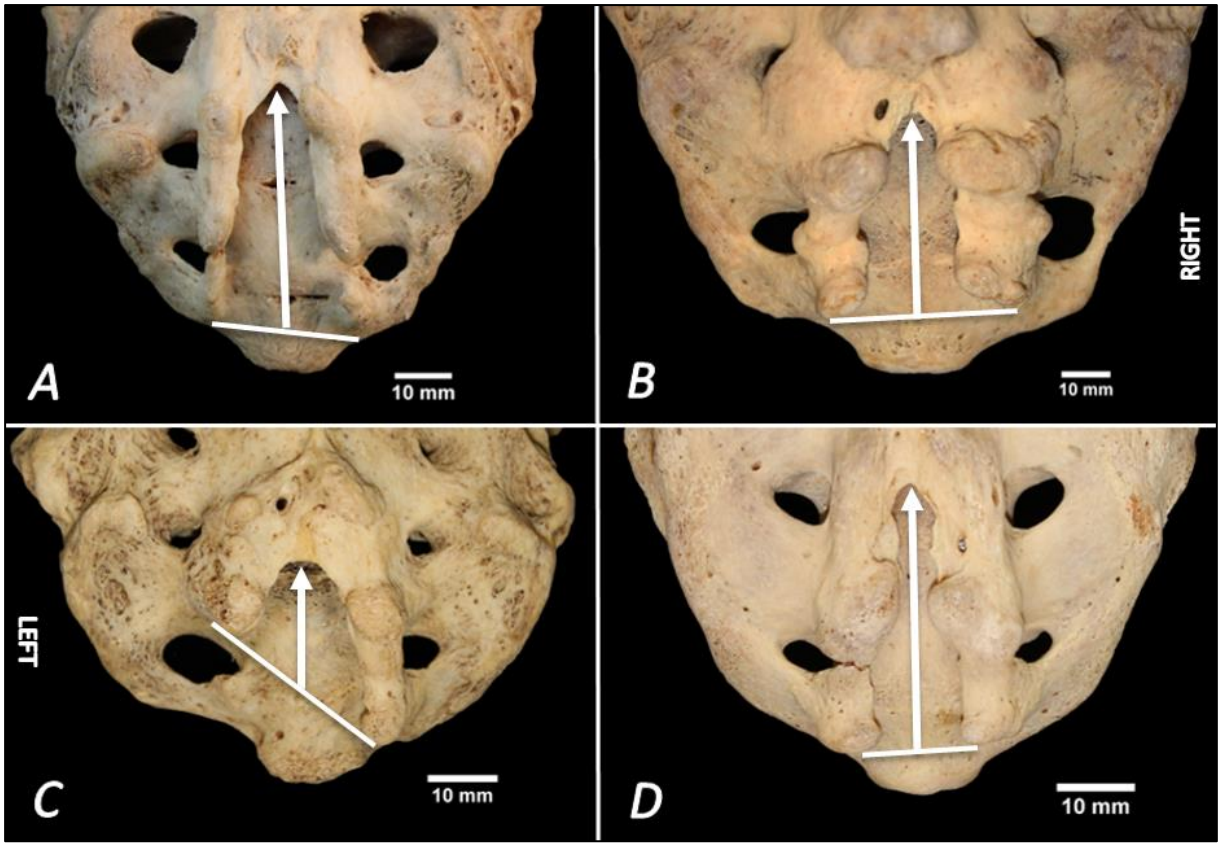

Figure 4.52: *Posterior view of inferior distal sacra displaying sacral hiatus length associated with lumbosacral transitional vertebrae.* ***A)*** *A Type IV lumbosacral transitional vertebra.* ***B)*** *A Type IV lumbosacral transitional vertebra.* ***C)*** *A left-sided Type IIIA lumbosacral transitional vertebra.* ***D)*** *A Type IIIB lumbosacral transitional vertebra. The arrows indicate the sacral hiatus length measurements.* ***Photography and editing:*** *GJ Paton.*

D13: Transverse Process Length (TVPL), right and left

The right LSTV cohort (N=56) consisted of 39 males (n=39) and 17 females (n=17) and the left LSTV cohort (N=56) consisted of 39 males (n=39) and 17 females (n=17). The control cohort (N=60) consisted of 30 males (n=30) and 30 females (n=30).

Lumbosacral transitional vertebrae cohort compared to the control cohort

Right side

The mean TVPL on the right side in the LSTV cohort was larger (19.32mm ± 4.03mm) than the control cohort (17.39mm ± 3.29mm). The TVPL of the LSTV cohort had a larger range in variation of length, between 7.76mm and 27.63mm, while the control cohort range was between 9.33mm and 24.34mm in length.

Left side

The mean TVPL on the left side in the LSTV cohort was larger (21.08mm ± 3.46mm) than the control cohort (17.23mm ± 3.19mm). The TVPL of the LSTV cohort had a larger range in variation of length, between 12.96mm and 31.15mm, while the control cohort range was between 10.37mm and 26.80mm in length.

Sex comparison of lumbosacral transitional vertebrae cohort compared to the control cohort

Right side

A sex comparison found that the mean TVPL on the right of males in the LSTV cohort (19.26mm ± 4.35mm) was marginally shorter than that of the female cohort (19.46mm ± 3.27mm). The TVPL of the male LSTV cohort had a larger range in variation of length, between 7.76mm and 27.63mm, while the female LSTV cohort range was between 13.79mm and 25.14mm in length.

Likewise, sex comparison of the mean TVPL on the right in the control cohort was larger for males (17.29mm ± 3.08mm) when compared to the females (17.49mm ± 3.54mm).

The TVPL of the control cohort had a smaller range in variation of length, between 11.67mm and 23.72mm, while the control cohort range was between 9.33mm and 24.34mm in length. The mean TVPL of the male LSTV cohort on the right side (19.26mm ± 4.35mm) was longer than the males in the control cohort (17.29mm ± 3.08mm). The mean TVPL of females in the LSTV cohort (19.46mm ± 3.27mm) was longer than the females in the control cohort (17.49mm ± 3.54mm). Refer to Figures 4.53 and 4.54.

Left side

Likewise, sex comparison of the mean TVPL on the left in the LSTV cohort was larger for males (21.13mm ± 3.73mm) when compared to the females (20.98mm ± 2.84mm). The TVPL of the LSTV cohort had a larger range in variation of length, between 12.96mm and 31.15mm, while the control cohort range was between 16.23mm and 27.17mm in length.

Likewise, sex comparison of the mean TVPL on the right in the control cohort was larger for males (17.52mm ± 3.54mm) when compared to the females (16.94mm ± 2.82mm). The TVPL of the male control cohort had a larger range in variation of length, between 10.37mm and 26.80mm, while the female cohort range was between 11.46mm and 22.91mm in length.

The mean TVPL of the male LSTV cohort on the left side (21.13mm ± 3.73mm) was longer than the males in the control cohort (17.52mm ± 3.54mm). The mean AL of females in the LSTV cohort (20.98mm ± 2.84mm) was longer than the females in the control cohort (16.94mm ± 2.82mm). Refer to Figures 4.55 and 4.56. Figure 4.57 demonstrate the TVPL variations associated with LSTV on the right and left sides.

Right side

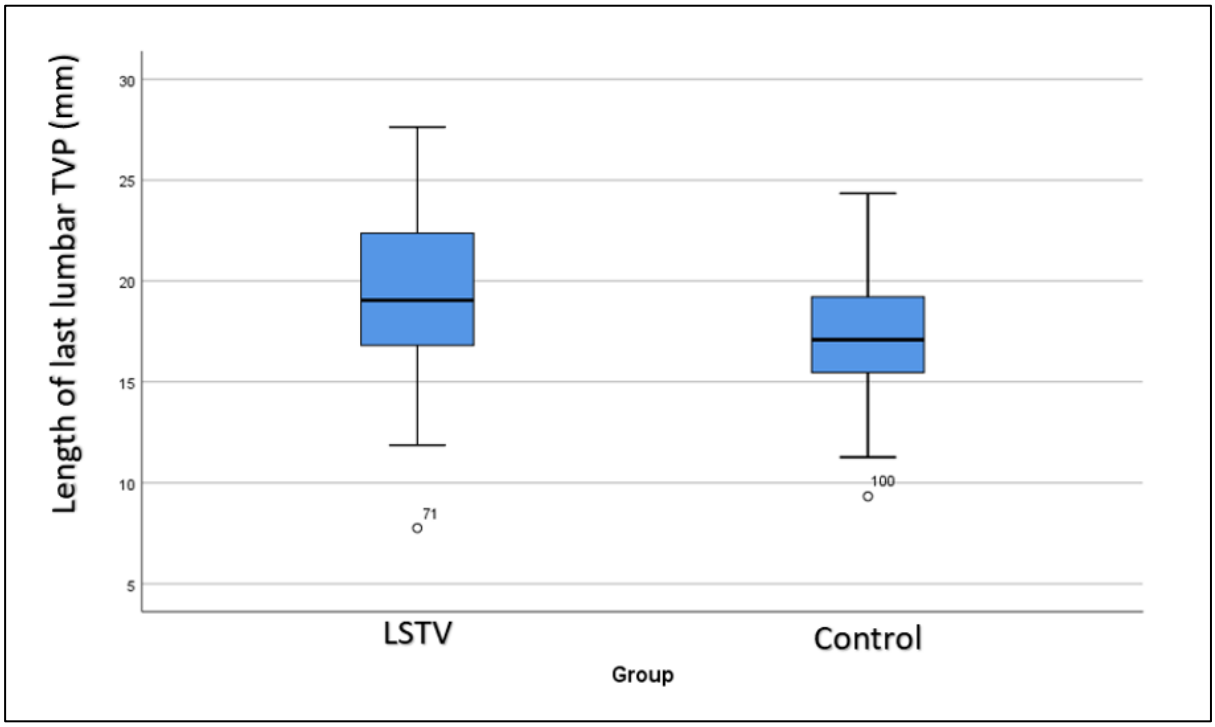

Figure 4.53: *A boxplot graph of the length of the right transverse process of the last lumbar vertebra measurement for the LSTV and control cohorts.*

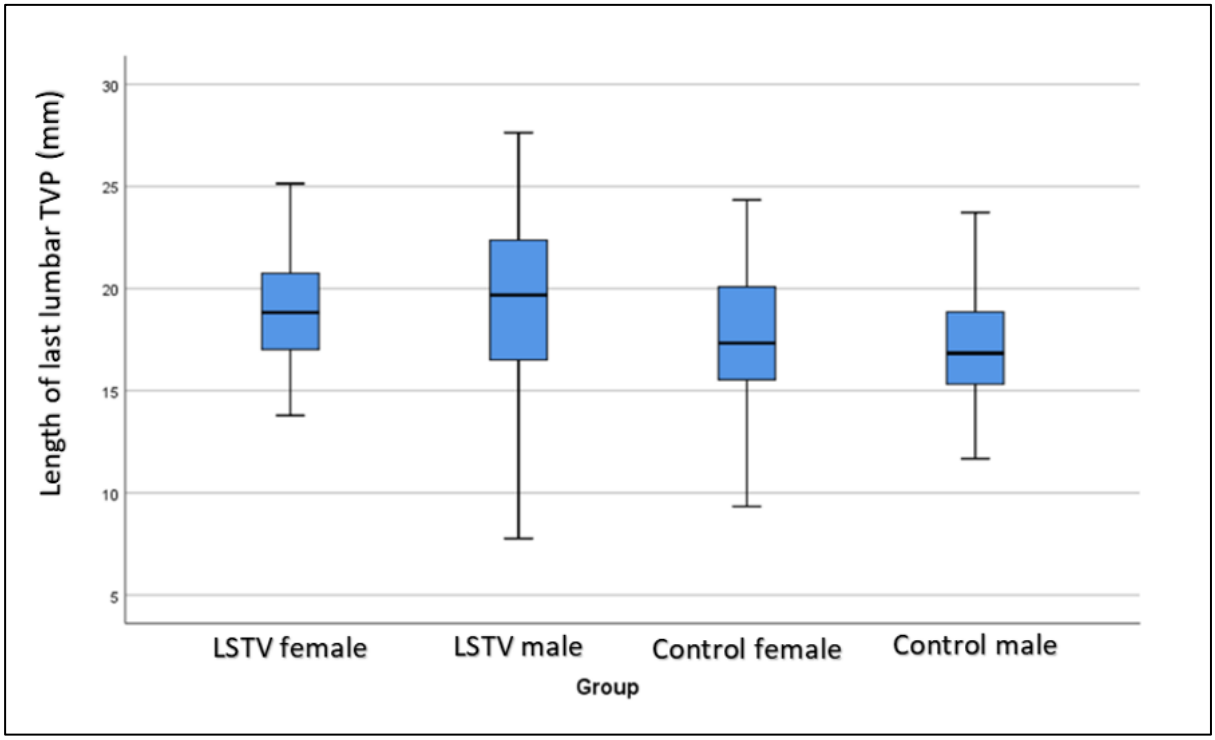

Figure 4.54: *A boxplot graph of the length of the left transverse process of the last lumbar vertebra for the LSTV and control cohorts compared to the sexes.*

Left side

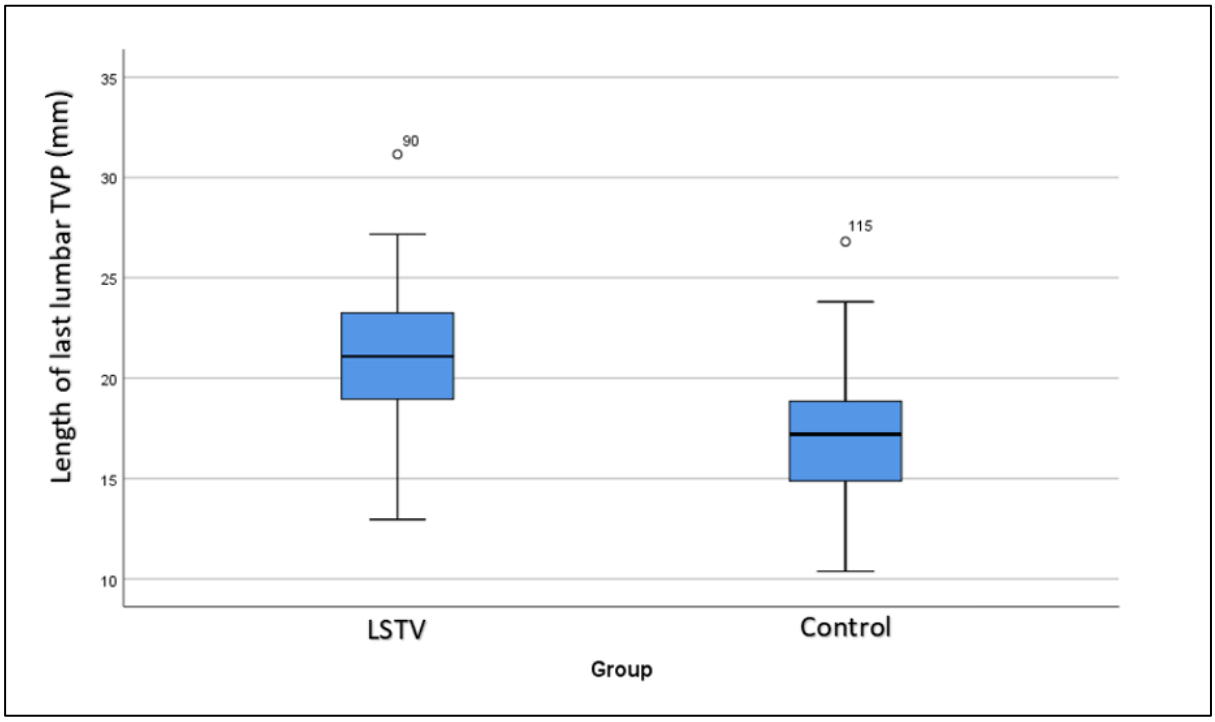

Figure 4.55: *A boxplot graph of the length of the transverse process of the last lumbar vertebra for the LSTV and control cohorts.*

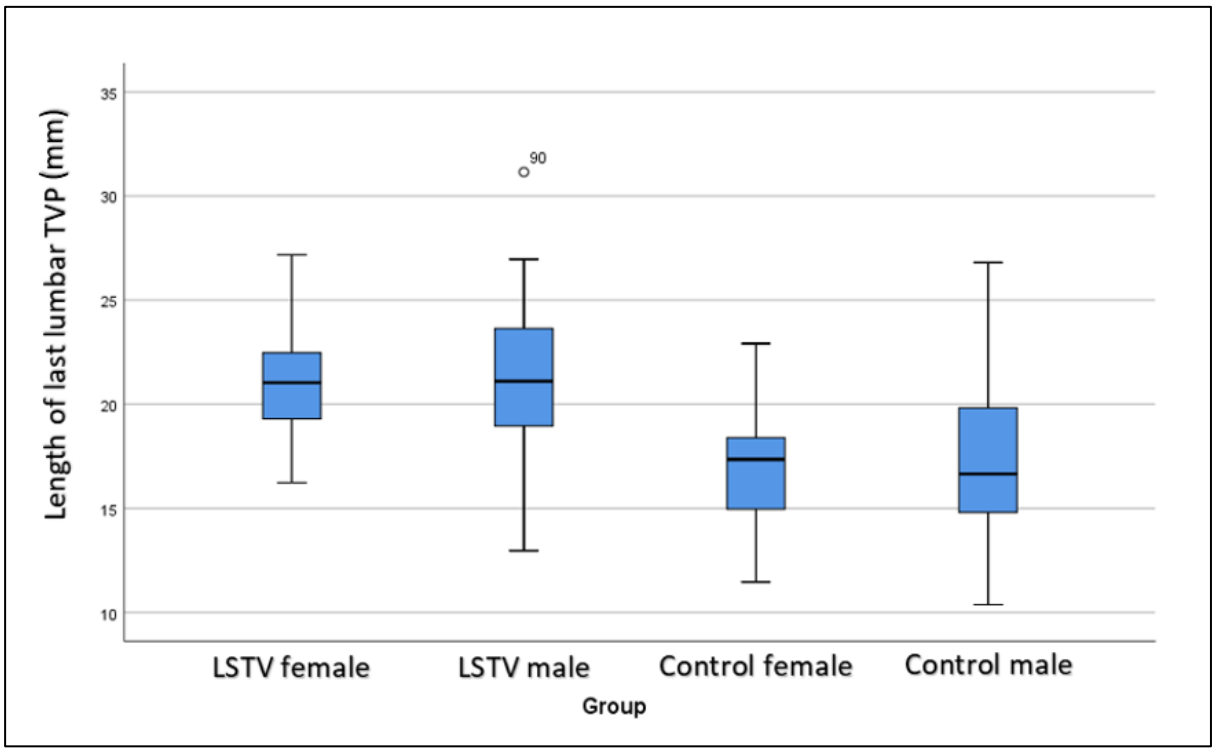

Figure 4.56: *A boxplot graph of the length of the transverse process of the last lumbar process for the LSTV and control cohorts compared to the sexes.*

Statistical analyses

Lumbosacral transitional vertebrae cohort and control cohort comparison

Right side

The T-test compared the mean rank values of TVPL in the LSTV (n=56) cohort and the control (n=60) cohort. Levene's test for variance was equal. The T-test for equality of means (t=2.84, df= 114, *p*=0.005) found a statistically significant difference in right TVPL with the LSTV cohort containing a longer right TVP as compared to the control cohort.

Left side

The T-test compared the mean rank values of TVPL in the LSTV (n=56) cohort and the control (n=60) cohort. Levene's test for variance was equal. The T-test for equality of means (t=6.24, df= 114, *p*<0.001) found a statistically significant difference in left TVPL with the LSTV cohort containing a longer left TVP as compared to the control cohort.

Lumbosacral transitional vertebrae cohort male and female comparison

Right side

The Mann-Whitney U test compared the mean rank values of TVPL in the LSTV male cohort (n=39) and the LSTV female (n=17) cohort. There was no statistically significant difference (U=329.50, Z=-0.04, *p*=0.972) in TVPL between the LSTV male (mean rank 28.55) and female (mean rank 28.38) cohorts.

Left side

The Mann-Whitney U test compared the mean rank values of TVPL in the LSTV male cohort (n=39) and the LSTV female (n=17) cohort. There was no statistically significant difference (U=322.00, Z=-0.17, *p*=0.866) in TPL between the LSTV male (mean rank 28.74) and female (mean rank 27.94) cohorts.

Control cohort male and female comparison

Right side

The Mann-Whitney U test compared the mean rank values of TVPL in the male (n=30) and the female (n=30) control cohorts. There was no statistically significant difference (U=418.00, Z=-0.47, *p*=0.636) in TVPL between the control male (mean rank 29.43) and female (mean rank 31.57) cohorts.

Left side

The Mann-Whitney U test compared the mean rank values of TVPL in the male (n=30) and the female (n=30) control cohorts. There was no statistically significant difference (U=430.00, Z=-0.30, *p*=0.767) in TVPL between the control male (mean rank 31.17) and female (mean rank 29.83) cohorts.

Female lumbosacral transitional vertebrae cohort and female control cohort comparison

Right side

The Mann-Whitney U test compared the mean rank values of the TVPL in the female LSTV (n=17) and the female control (n=30) cohorts. There was no statistically significant difference (U=181.00, Z=-1.64, *p*=0.101) in TVPL between the LSTV female (mean rank 28.35) and the control female (mean rank 21.35) cohorts.

Left side

The Mann-Whitney U test compared the mean rank values of the TVPL in the female LSTV (n=17) and the female control (n=30) cohorts. There was a statistically significant difference (U=77.00, Z=-3.94, *p*<0.001) in TVPL between the LSTV female (mean rank 34.47) and the control female (mean rank 18.07) cohorts.

Male lumbosacral transitional vertebrae cohort and male control cohort comparison

Right side

The Mann-Whitney U test compared the mean rank values of the TVPL in the male LSTV (n=39) and the male control (n=30) cohorts. There was a statistically significant difference (U=404.00, Z=-2.19, *p*=0.028) in TVPL between the LSTV male (mean rank 39.64) and the control male (mean rank 28.97) cohorts.

Left side

The Mann-Whitney U test compared the mean rank values of the TVPL in the male LSTV (n=39) and the male control (n=30) cohorts. There was a statistically significant difference (U=273.00, Z=-3.78, *p*<0.001) in TVPL between the LSTV male (mean rank 43.00) and the control male (mean rank 24.60) cohorts.

Figure 4.57: *Superior view of lumbosacral transitional vertebrae displaying the transverse process length associated with lumbosacral transitional vertebrae.* ***A)*** *A Type IIB lumbosacral transitional vertebra.* ***B)*** *A Type IIB lumbosacral transitional vertebra.* ***C)*** *A right-sided Type IIA lumbosacral transitional vertebra.* ***D)*** *A left-sided Type IIA lumbosacral transitional vertebra. The arrows indicate the transverse process measurements.* ***Photography and editing:*** *GJ Paton.*

D14: Transverse processes height (TVPH), right and left

The right LSTV cohort (N=60) consisted of 43 males (n=43) and 17 females (n=17) and the left LSTV cohort (N=60) consisted of 41 males (n=41) and 19 females (n=19). The control cohort (N=60) consisted of 30 males (n=30) and 30 females (n=30).

Lumbosacral transitional vertebrae cohort compared to the control cohort

Right side

The mean TVPH in the LSTV cohort was larger (20.34mm ± 5.47mm) than the control cohort (12.91mm ± 2.28mm). The TVPH of the LSTV cohort had a larger range in variation of length, between, 8.33mm and 33.01mm while the control cohort range was between 7.32mm and 18.50mm in length.

Left side

The mean TVPH in the LSTV cohort was larger (22.87mm ± 5.36mm) than the control cohort (12.72mm ± 2.05mm). The TVPH of the LSTV cohort had a larger range in variation of length, between 9.42mm and 33.46mm, while the control cohort range was between 8.39mm and 18.78mm in length.

Sex comparison of lumbosacral transitional vertebrae cohort compared to the control cohort

Right side

A sex comparison found that the mean TVPH on the right of males in the LSTV cohort (30.73mm ± 5.71mm) was marginally shorter than that of the female cohort (19.34mm ± 4.83mm). The TVPH of the male LSTV cohort had a larger range in variation of length, between 8.33mm and 33.01mm, while the female LSTV cohort range was between 12.58mm and 28.35mm in length.

Likewise, sex comparison of the mean TVPH on the right in the control cohort was larger for males (13.40mm ± 2.29mm) when compared to the females (12.42mm ± 2.19mm).

The TVPH of the male LSTV cohort had a larger range in variation of length, between 8.73mm and 18.50mm, while the female LSTV cohort range was between 7.32mm and 17.91mm in length. The mean TVPH of the male LSTV cohort on the right side (30.73mm ± 5.71mm) was larger than the males in the control cohort (13.40mm ± 2.29mm). The mean TVPL of females in the LSTV cohort (19.34mm ± 4.83mm) was larger than the females in the control cohort (12.42mm ± 2.19mm). Refer to Figures 4.58 and 4.59.

Left side

A sex comparison found that the mean TVPH on the left of males in the LSTV cohort (22.95mm ± 5.55mm) was marginally shorter than that of the female cohort (22.69mm ± 5.05mm). The TVPH of the male LSTV cohort had a larger range in variation of length, between 9.42mm and 33.46mm, while the female LSTV cohort range was between 14.87mm and 230.60mm in length.

Likewise, sex comparison of the mean TVPH on the left in the control cohort was larger for males (13.23mm ± 2.28mm) when compared to the females (12.22mm ± 1.67mm). The TVPH of the male LSTV cohort had a larger range in variation of length, between 8.39mm and 18.78mm, while the female LSTV cohort range was between 8.44mm and 15.77mm in length.

The mean TVPH of the male LSTV cohort on the right side (22.95mm ± 5.55mm) was larger than the males in the control cohort (13.23mm ± 2.28mm). The mean TVPL of females in the LSTV cohort (22.69mm ± 5.05mm) was larger than the females in the control cohort (12.22mm ± 1.67mm). Refer to Figures 4.60 and 4.62. Figure 4.63 demonstrate the TVPH variations associated with LSTV.

Right side

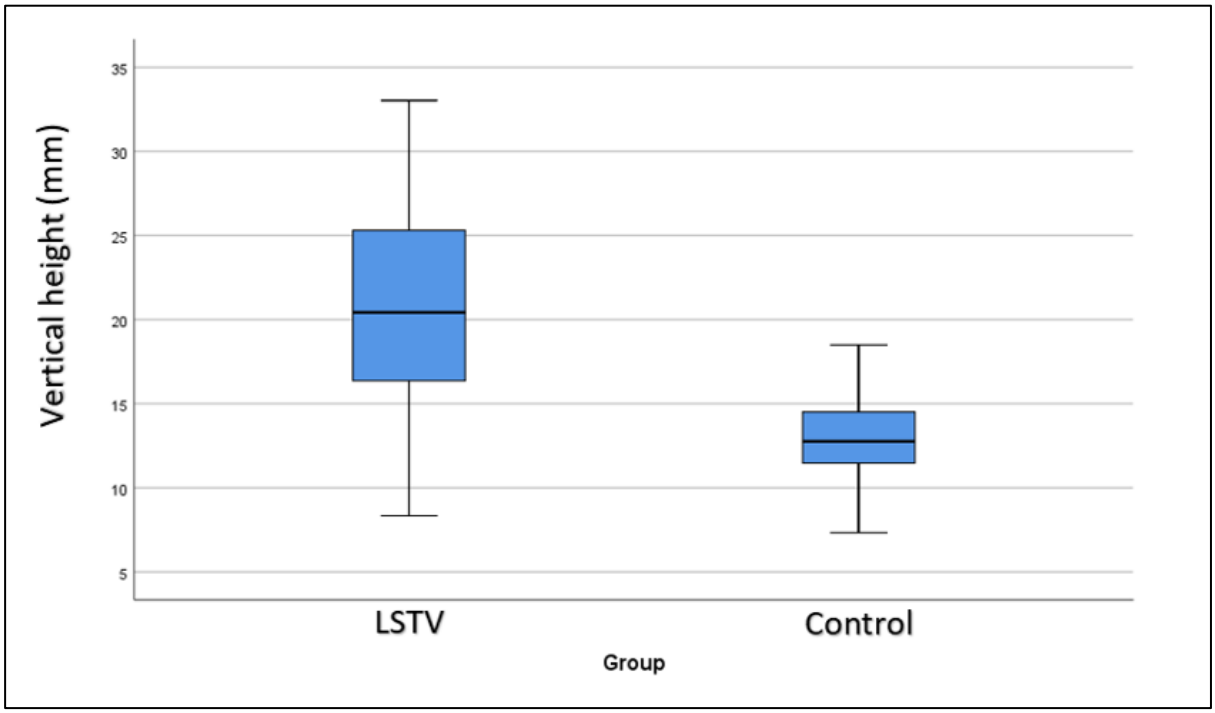

Figure 4.58: *A boxplot graph of the right transverse process height for the LSTV and control cohorts.*

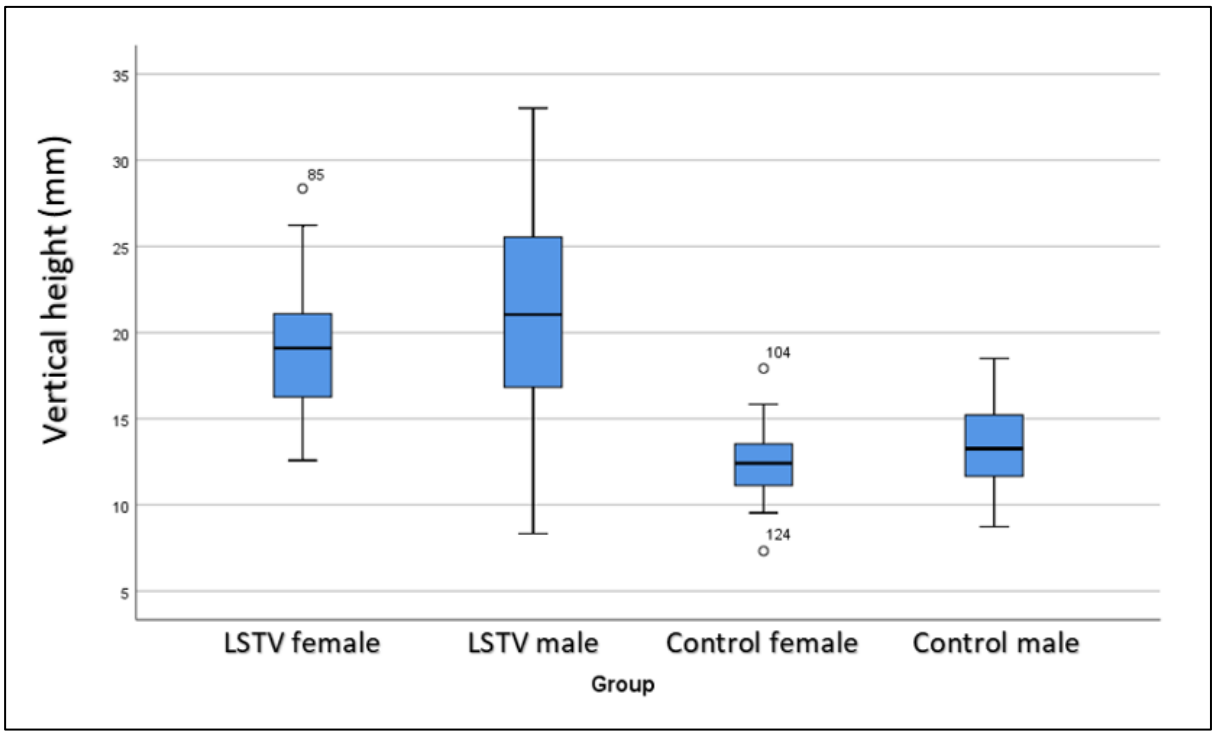

Figure 4.59: *A boxplot graph of the right transverse process height for the LSTV and control cohorts comparing the sexes.*

Left side

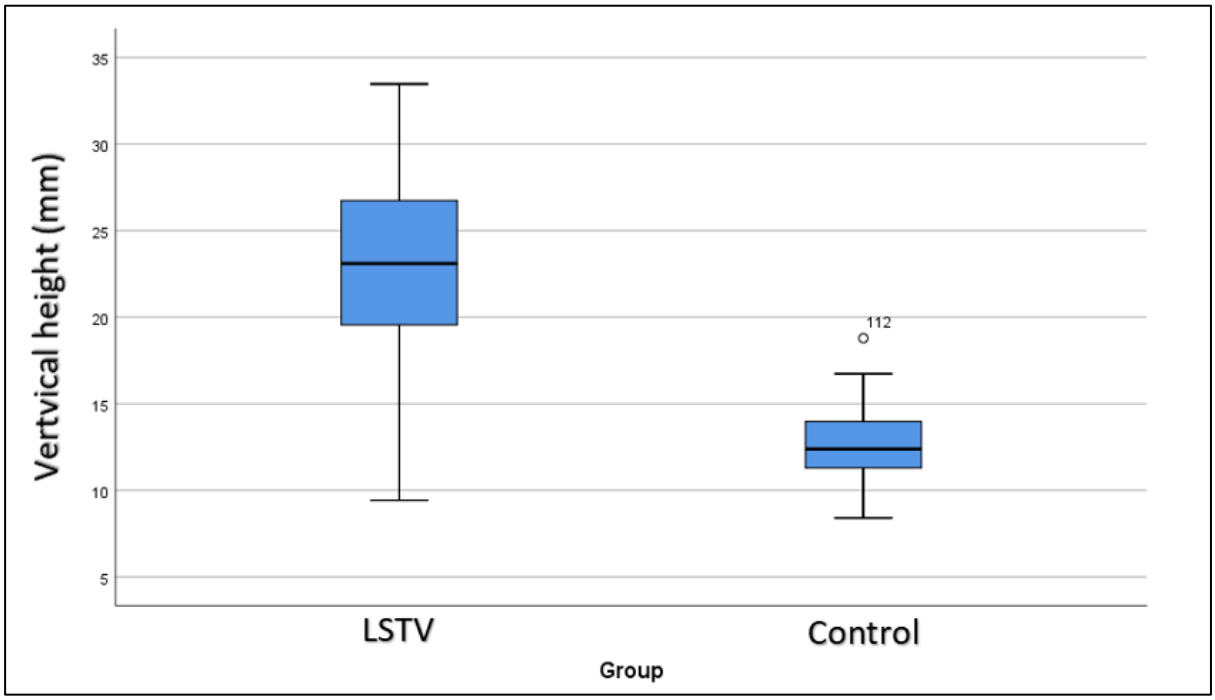

Figure 4.60: *A boxplot graph of the left transverse process height for the LSTV and control cohorts.*

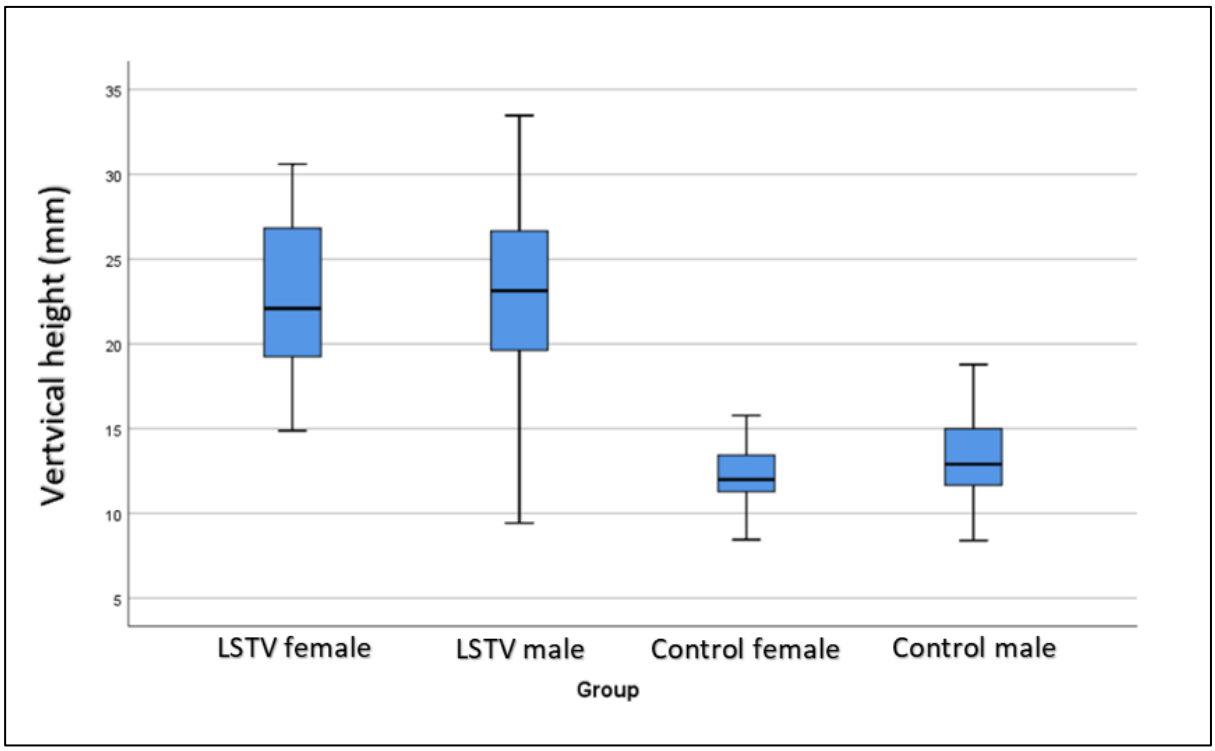

Figure 4.61: *A boxplot graph of the right transverse process height for the LSTV and control cohorts comparing the sexes.*

Statistical analyses

Lumbosacral transitional vertebrae and control cohort comparison

Right side

The T-test compared the mean rank values of TVPH in the LSTV (n=60) cohort and the control (n=60) cohort. Levene's test for variance was not equal. The unequal variance T-test for equality of means (t=9.71, df= 78.87, p<0.001) found a statistically significant difference in right TVPH with the LSTV cohort containing a TVP with greater height as compared to the control cohort.

Left side

The T-test compared the mean rank values of TVPH in the LSTV (n=60) cohort and the control (n=60) cohort. Levene's test for variance was not equal. The unequal variance T-test for equality of means (t=13.70, df= 75.84, p<0.001) found a statistically significant difference in left TVPH with the LSTV cohort containing a TVP with greater height compared to the control cohort.

Lumbosacral transitional vertebrae cohort male and female comparison

Right side

The Mann-Whitney U test compared the mean rank values of TVPH in the LSTV male cohort (n=43) and the LSTV female (n=17) cohort. There was no statistically significant difference (U=308.00, Z=-0.94, p=0.346) in TVPH between the LSTV male (mean rank 31.84) and female (mean rank 27.12) cohorts.

Left side

The Mann-Whitney U test compared the mean rank values of TVPH in the LSTV male cohort (n=41) and the LSTV female (n=19) cohort. There was no statistically significant difference (U=369.00, Z=-0.33, p=0.745) in TVPH between the LSTV male (mean rank 31.00) and female (mean rank 29.42) cohorts.

Control cohort male and female comparison

Right side

The Mann-Whitney U test compared the mean rank values of TVPH in the male (n=30) and the female (n=30) control cohorts. There was no statistically significant difference (U=344.00, Z=-1.57, *p*=0.117) in TVPH between the control male (mean rank 34.03) and female (mean rank 26.97) cohorts.

Left side

The Mann-Whitney U test compared the mean rank values of TVPH in the male (n=30) and the female (n=30) control cohorts. There was no statistically significant difference (U=340.00, Z=-1.63, *p*=0.104) in TVPH between the control male (mean rank 34.17) and female (mean rank 26.83) cohorts.

Female lumbosacral transitional vertebrae cohort and female control cohort comparison

Right side

The Mann-Whitney U test compared the mean rank values of the TVPH in the female LSTV (n=17) and the female control (n=30) cohorts. There was a statistically significant difference (U=44.00, Z=-4.67, *p*<0.001) in TVPH between the LSTV female (mean rank 36.41) and the control female (mean rank 19.67) cohorts.

Left side

The Mann-Whitney U test compared the mean rank values of the TVPH in the female LSTV (n=19) and the female control (n=30) cohorts. There was no statistically significant difference (U=3.00, Z=-5.79, *p*<0.001) in TVPH between the LSTV female (mean rank 39.84) and the control female (mean rank 15.60) cohorts.

Male lumbosacral transitional vertebrae cohort and male control cohort comparison

Right side

The Mann-Whitney U test compared the mean rank values of the TVPH in the male LSTV (n=43) and the male control (n=30) cohorts. There was a statistically significant difference (U=160.00, Z=-5.44, *p*<0.001) in TVPH between the LSTV male (mean rank 48.28) and the control male (mean rank 20.83) cohorts.

Left side

The Mann-Whitney U test compared the mean rank values of the TVPH in the male LSTV (n=41) and the male control (n=30) cohorts. There was a statistically significant difference (U=71.00, Z=-6.33, *p*<0.001) in TVPH between the LSTV male (mean rank 49.27) and the control male (mean rank 17.87) cohorts.

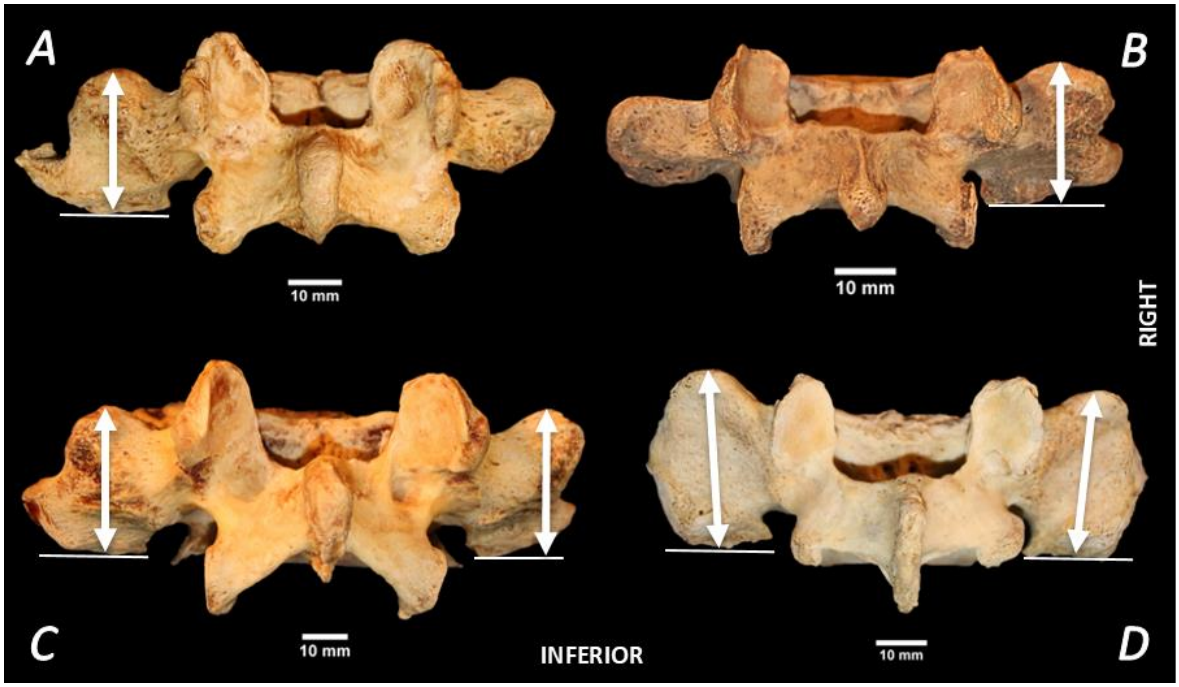

Figure 4.62: *Posterior view of lumbosacral transitional vertebrae displaying transverse process height/s.* ***A)*** *Left-sided Type IIA lumbosacral transitional vertebra.* ***B)*** *Right-sided Type IIIB lumbosacral transitional vertebra.* ***C)*** *Type IIB lumbosacral transitional vertebra.* ***D)*** *Type IIB lumbosacral transitional vertebra. The Arrows indicate the transverse process height measurements.* ***Photography and editing:*** *GJ Paton.*

D15: Auricular surface area (ASA), right and left

The right LSTV cohort (N=83) consisted of 59 males (n=59) and 24 females (n=24) and the left LSTV cohort (N=86) consisted of 62 males (n=62) and 24 females (n=24). The control cohort (N=60) consisted of 30 males (n=30) and 30 females (n=30).

Lumbosacral transitional vertebrae cohort compared to the control cohort

Right side

The mean ASA in the LSTV cohort was larger (1177.86mm^2 ± 170.94mm^2) than the control cohort (1124.70mm^2 ± 162.81mm^2). The ASA of the LSTV cohort had a larger range in variation of surface area, between, 823.38mm^2 and 1705.39mm^2 while the control cohort range was between 780.53mm^2 and 1612.36mm^2 in surface area.

Left side

The mean ASA in the LSTV cohort was larger (1185.61mm^2 ± 200.43mm^2) than the control cohort (1131.11mm^2 ± 116.79mm^2). The ASA of the LSTV cohort had a larger range in variation of surface area, between 774.84mm^2 and 2028.00mm^2, while the control cohort range was between 825.36mm^2 and 1515.05mm^2 in surface area.

Sex comparison of lumbosacral transitional vertebrae cohort compared to the control cohort

Right side

A sex comparison found that the mean ASA on the right of males in the LSTV cohort (1181.90mm^2 ± 173.91mm^2) was larger than that of the female cohort (1167.93mm^2 ± 116.62mm^2). The ASA of the male LSTV cohort had a larger range in variation of surface area, between 860.51mm^2 and 1705.39mm^2, while the female LSTV cohort range was between 823.38mm^2 and 1536.52mm^2 in surface area.

Likewise, sex comparison of the mean ASA on the right in the control cohort was larger for males (1181.76mm^2 ± 178.79mm^2) when compared to the females (1067.63mm^2 ± 123.40mm^2).

The ASA of the male LSTV cohort had a larger range in variation of surface area, between 826.08mm^2 and 1612.36mm^2, while the female LSTV cohort range was between 780.53mm^2 and 1321.42mm^2 in surface area.

The mean ASA of the male LSTV cohort on the right side (1181.90mm^2 ± 173.91mm^2) was marginally larger than the males in the control cohort (1181.76mm^2 ± 178.79mm^2). The mean ASA of females in the LSTV cohort (1167.93mm^2 ± 116.62mm^2) was larger than the females in the control cohort (1067.63mm^2 ± 123.40mm^2). Refer to Figures 4.63 and 4.64.

Left side

A sex comparison found that the mean ASA on the left of males in the LSTV cohort (1214.84mm^2 ± 209.58mm^2) was larger than that of the female cohort (1110mm^2 ± 153.96mm^2). The ASA of the male LSTV cohort had a larger range in variation of surface area, between 795.84mm^2 and 2028.00mm^2, while the female LSTV cohort range was between 774.84mm^2 and 1439.79mm^2 in surface area.

Likewise, sex comparison of the mean ASA on the right in the control cohort was larger for males (1179.72mm^2 ± 172.94mm^2) when compared to the females (1082.50mm^2 ± 147.66mm^2). The ASA of the male control cohort had a larger range in variation of surface area, between 863.12mm^2 and 1515.05mm^2, while the female control cohort range was between 825.36mm^2 and 1472.47mm^2 in surface area.

The mean ASA of the male LSTV cohort on the left side (1214.84mm^2 ± 209.58mm^2) was larger than the males in the control cohort (1179.72mm^2 ± 172.94mm^2). The mean ASA of females in the LSTV cohort (1110mm^2 ± 153.96mm^2) was larger than the females in the control cohort (1082.50mm^2 ± 147.66mm^2). Refer to Figures 4.65 and 4.66. Figures 4.67 and 4.68 demonstrate the FA variations associated with LSTV on the right and left sides.

Right side

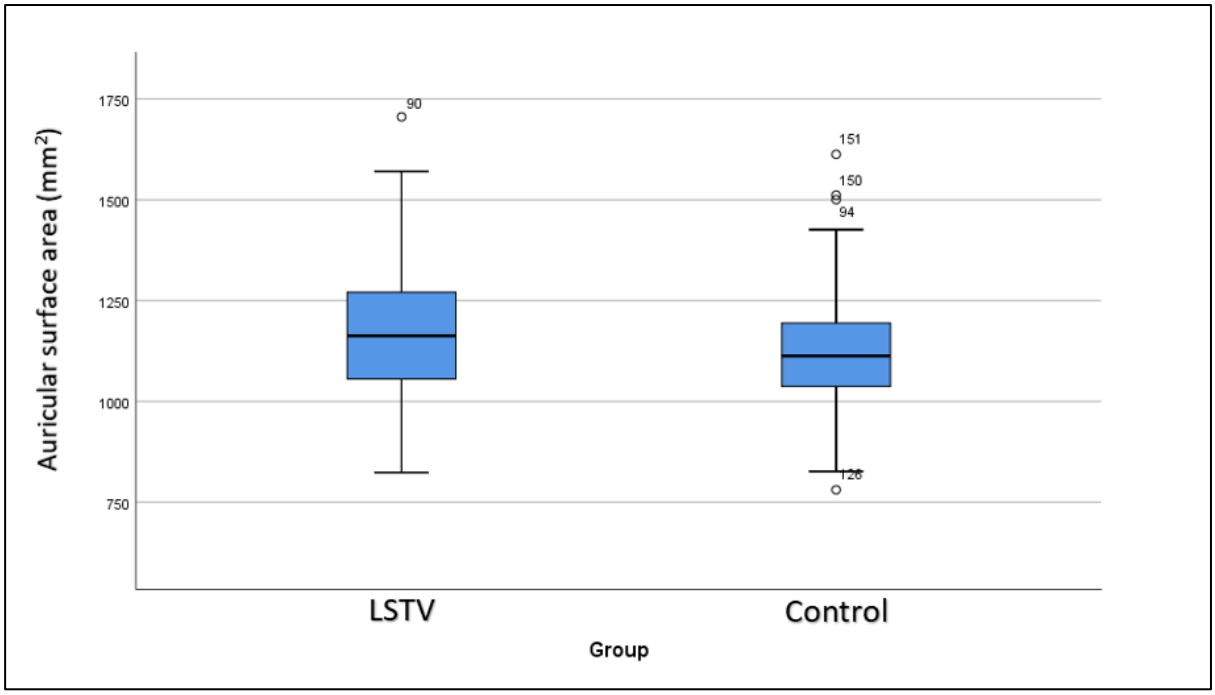

Figure 4.63: *A boxplot graph of the auricular surface area for the LSTV and control cohorts.*

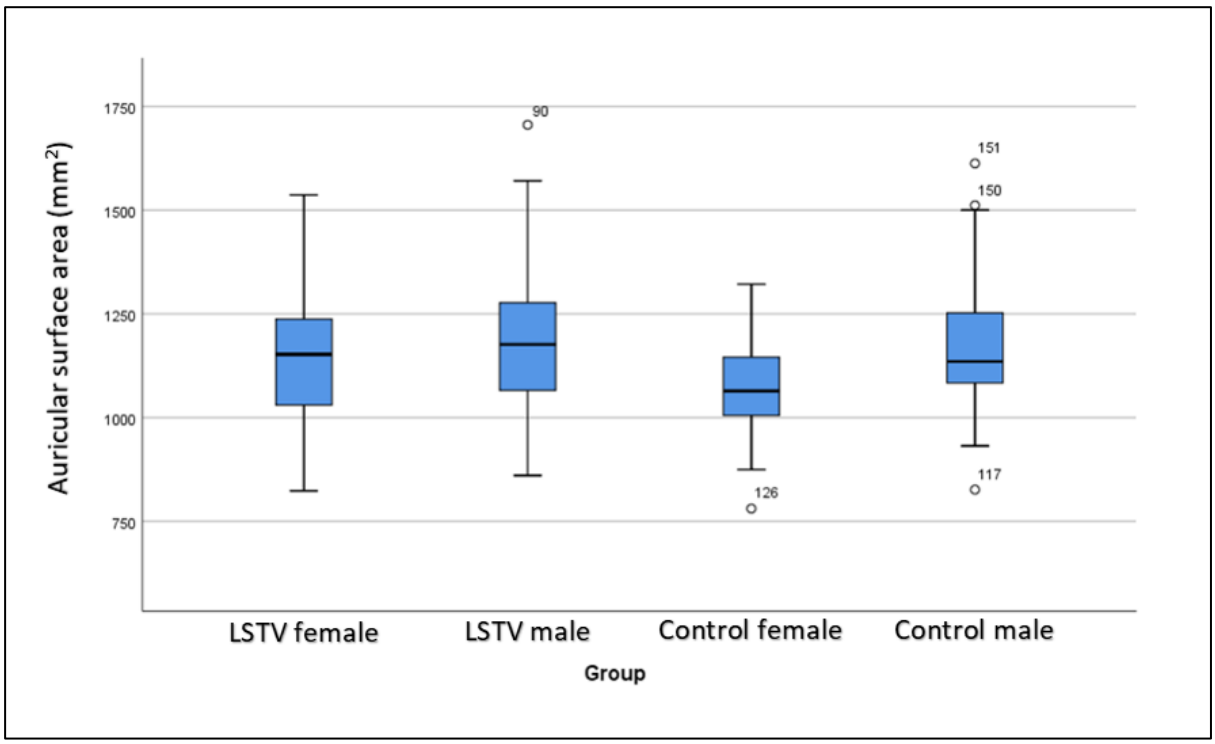

Figure 4.64: *A boxplot graph of the auricular surface areas for the LSTV and control cohorts comparing the sexes.*

Left side

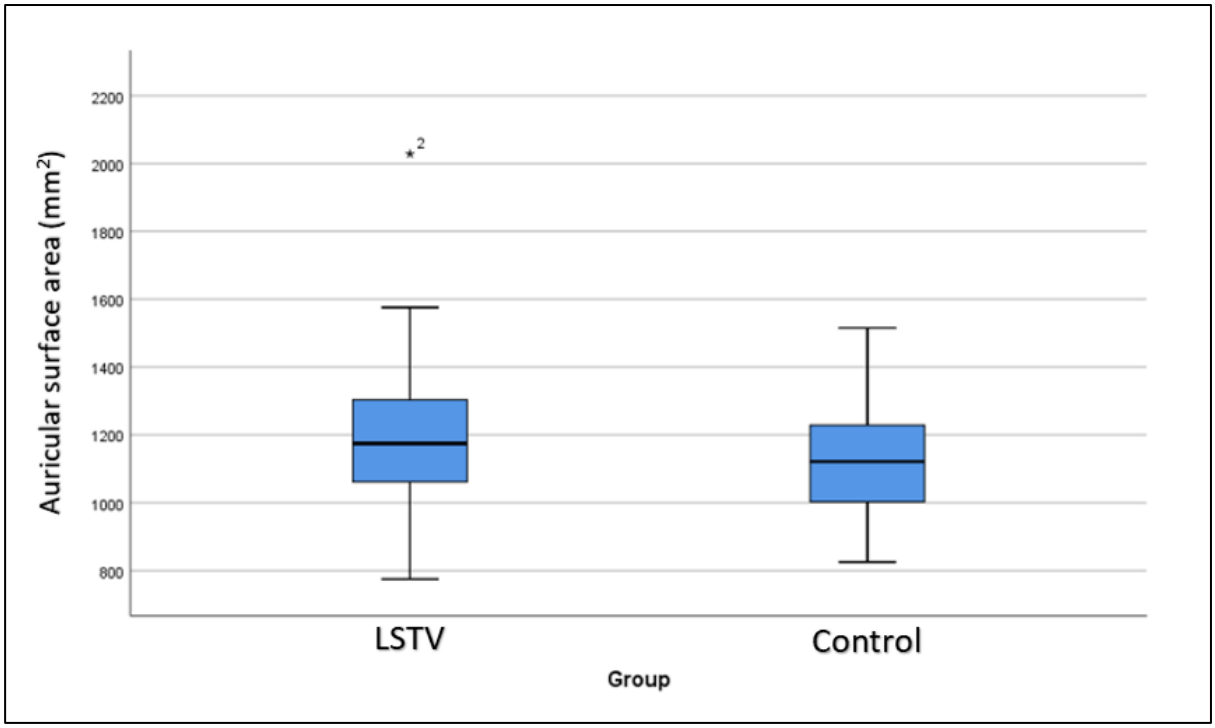

Figure 4.65: *A boxplot graph of the auricular surface area for the LSTV and control cohorts.*

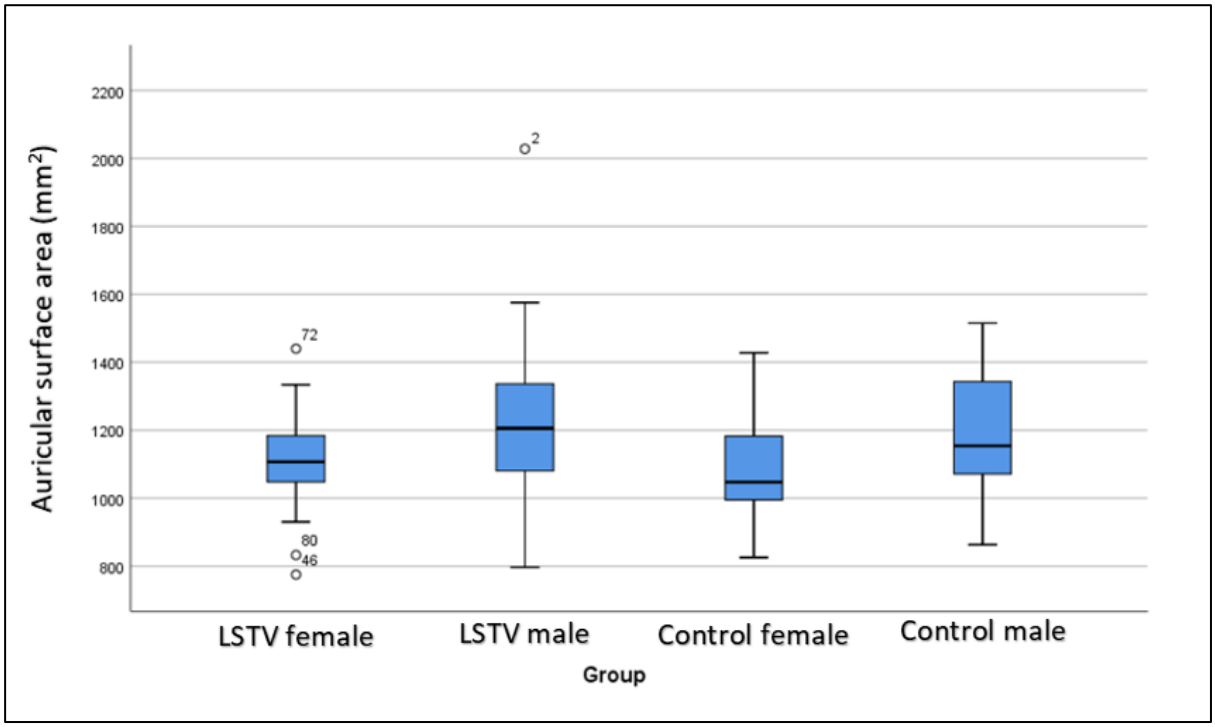

Figure 4.66: *A boxplot graph of the auricular surface area for the LSTV and control cohorts comparing the sexes.*

Statistical analyses

Lumbosacral transitional vertebrae and control cohort comparison

Right side

The T-test compared the mean rank values of ASA in the LSTV (n=83) cohort and the control (n=60) cohort. Levene's test for variance was equal. The T-test for equality of means (t=1.87, df= 141, *p*=0.061) found no statistically significant difference in right ASA with the LSTV cohort containing an ASA with greater surface area as compared to the control cohort.

Left side

The T-test compared the mean rank values of ASA in the LSTV (n=86) cohort and the control (n=60) cohort. Levene's test for variance was equal. The T-test for equality of means (t=1.73, df= 144, *p*=0.089) found no statistically significant difference in left ASA with the LSTV cohort containing a greater surface area as compared to the control cohort.

Lumbosacral transitional vertebrae cohort male and female comparison

Right side

The Mann-Whitney U test compared the mean rank values of ASA in the LSTV male cohort (n=59) and the LSTV female (n=24) cohort. There was no statistically significant difference (U=668.00, Z=0.40, *p*=0.069) in ASA between the LSTV male (mean rank 42.68) and female (mean rank 40.33) cohorts.

Left side

The Mann-Whitney U test compared the mean rank values of ASA in the LSTV male cohort (n=62) and the LSTV female (n=24) cohort. There was a statistically significant difference (U=511.00, Z=-2.24, *p*=0.025) in ASA, exhibiting a larger ASA between the LSTV male (mean rank 47.26) and female (mean rank 33.79) cohorts.

Control cohort male and female comparison

Right side

The Mann-Whitney U test compared the mean rank values of ASA in the male (n=30) and the female (n=30) control cohorts. There was a statistically significant difference (U=276.00, Z=-2.57, *p*=0.010) in ASA between the control male (mean rank 36.30) and female (mean rank 24.70) cohorts.

Left side

The Mann-Whitney U test compared the mean rank values of ASA in the male (n=30) and the female (n=30) control cohorts. There was a statistically significant difference (U=298.00, Z=-2.25, *p*=0.025) in ASA between the control male (mean rank 25.57) and female (mean rank 25.43) cohorts.

Female lumbosacral transitional vertebrae cohort and female control cohort comparison

Right side

The Mann-Whitney U test compared the mean rank values of the ASA in the female LSTV (n=24) and the female control (n=30) cohorts. There was a statistically significant difference (U=234.00, Z=-2.19 *p*=0.028) in ASA between the LSTV female (mean rank 32.75) and the control female (mean rank 23.30) cohorts.

Left side

The Mann-Whitney U test compared the mean rank values of the ASA in the female LSTV (n=24) and the female control (n=30) cohorts. There was no statistically significant difference (U=310.00, Z=-0.87, *p*=0.384) in ASA between the LSTV female (mean rank 29.58) and the control female (mean rank 25.83) cohorts.

Male lumbosacral transitional vertebrae cohort and male control cohort comparison

Right side

The Mann-Whitney U test compared the mean rank values of the ASA in the male LSTV (n=59) and the male control (n=30) cohorts. There was no statistically significant difference (U=871.00, Z=-0.12, *p*=0.903) in TVPL between the LSTV male (mean rank 45.24) and the control male (mean rank 44.53) cohorts.

Left side

The Mann-Whitney U test compared the mean rank values of the TVPL in the male LSTV (n=39) and the male control (n=30) cohorts. There was no statistically significant difference (U=839.00, Z=-0.76, *p*=0.448) in TVPL between the LSTV male (mean rank 47.97) and the control male (mean rank 43.47) cohorts.

Right side

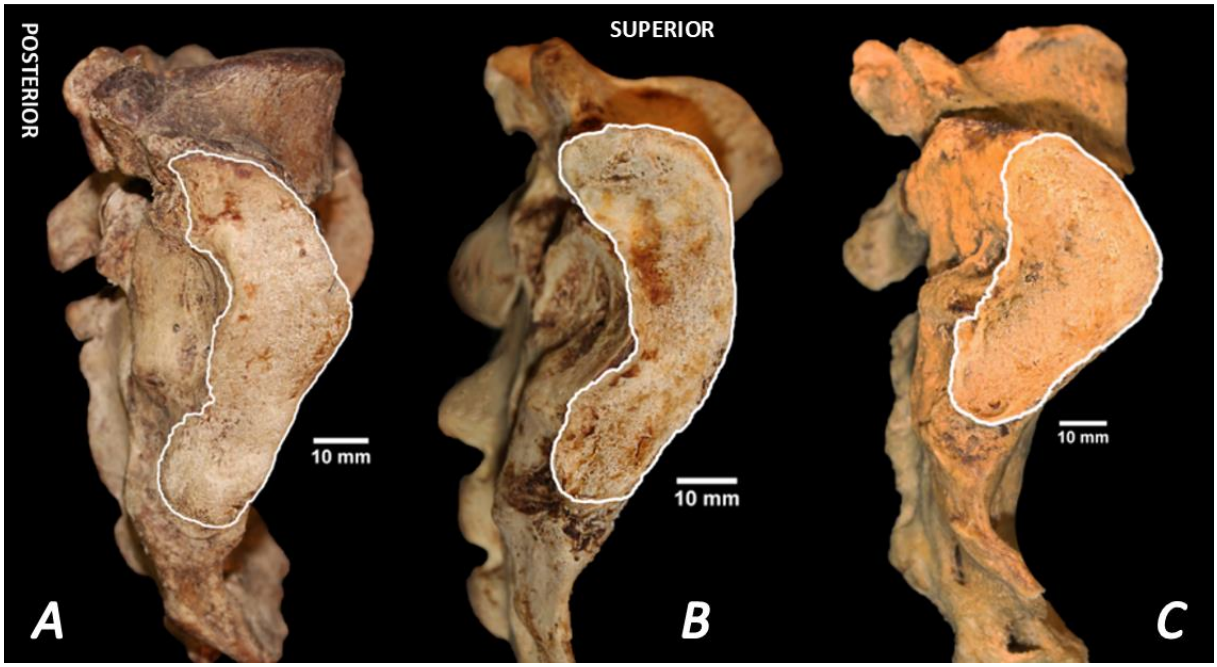

Figure 4.67: *Lateral view of sacra displaying the right-sided auricular surface area associated with lumbosacral transitional vertebrae.* ***A)*** *A Type IIIA lumbosacral transitional vertebra.* ***B)*** *A Type IIIB lumbosacral transitional vertebra.* ***C)*** *A left-sided Type IIIA lumbosacral transitional vertebra. The circumference of the auricular surface area is outlined in white.* ***Photography and editing:*** *GJ Paton.*

Left side

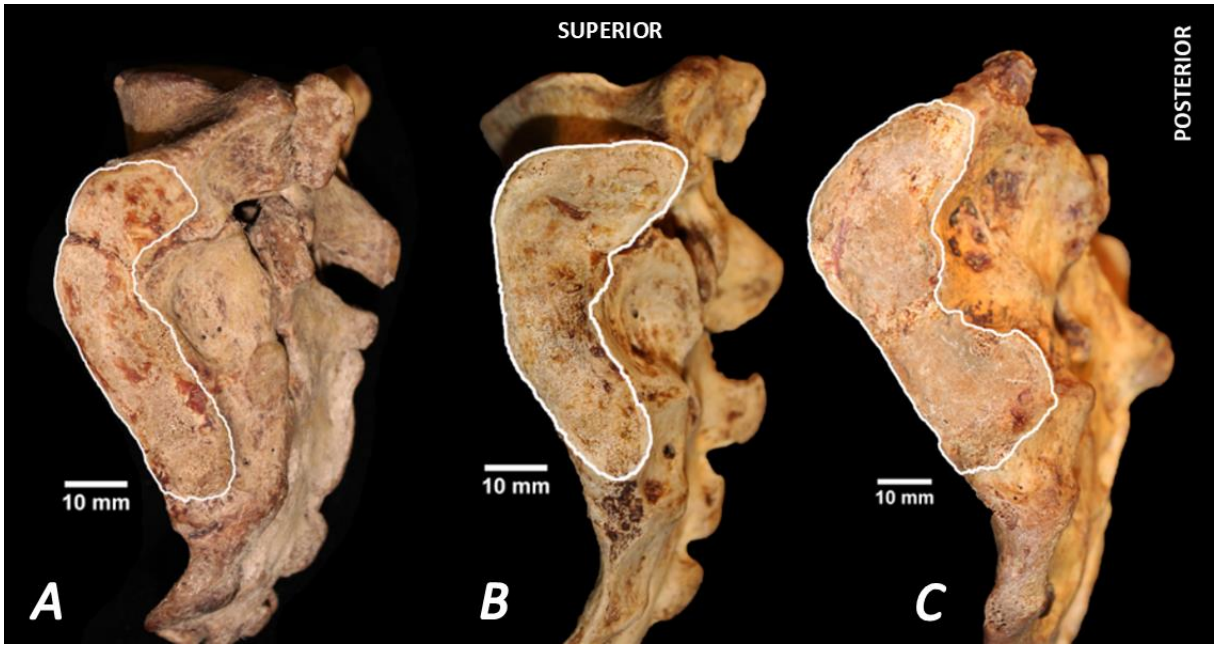

Figure 4.68: *Lateral view of sacra displaying the left-sided auricular surface area associated with lumbosacral transitional vertebrae.* ***A)*** *A Type IIIA lumbosacral transitional vertebra.* ***B)*** *A Type IIIB lumbosacral transitional vertebra.* ***C)*** *A left-sided Type IIA lumbosacral transitional vertebra. The circumference of the auricular surface is outlined in white.* ***Photography and editing:*** *GJ Paton.*

D16: Lumbar transverse process contribution to the ASA (TPC-ASA); right and left

The right LSTV cohort (N=10) consisted of seven males (n=7) and three females (n=3) and the left LSTV cohort (N=14) consisted of twelve males (n=12) and 2 females (n=2). There was no control cohort as this is a LTSV-related finding with no control possible for the variation.

Lumbosacral transitional vertebrae cohort

Right side

The mean TPC-ASA in the LSTV cohort was larger (116.70mm^2 ± 95.39mm^2) The TPC-ASA of the LSTV cohort had a range in variation of surface area, between 15.47mm^2 and 309.22mm^2.

Left side

The mean TPC-ASA in the LSTV cohort was larger (154.23mm^2 ± 112.39mm^2) The TPC-ASA of the LSTV cohort had a range in variation of surface area, between 59.41mm^2 and 405.02mm^2.

Sex comparison of lumbosacral transitional vertebrae cohort

Right side

A sex comparison found that the mean TPC-ASA on the right of males in the LSTV cohort (137.52mm^2 ± 108.28mm^2) was larger than that of the female cohort (68.11mm^2 ± 26.73mm^2). The ASA of the male LSTV cohort had a larger range in variation of surface area, between 15.47mm^2 and 309.22mm^2, while the female LSTV cohort range was 37.25mm^2 and 84.08mm^2 in length. Refer to Figures 4.69.

Left side

A sex comparison found that the mean TPC-ASA on the left of males in the LSTV cohort (156.88mm^2 ± 121.49mm^2) was larger than that of the female cohort (138.31mm^2 ± 35.53mm^2).

The ASA of the male LSTV cohort had a larger range in variation of surface area, between 59.41mm^2 and 405.02mm^2, while the female LSTV cohort range was between 113.19mm^2 and 163.43mm^2 in length. Refer to Figure 4.70. Figure 4.71 demonstrate the TPC-ASA variations associated with LSTV on the right and left sides.

Right side

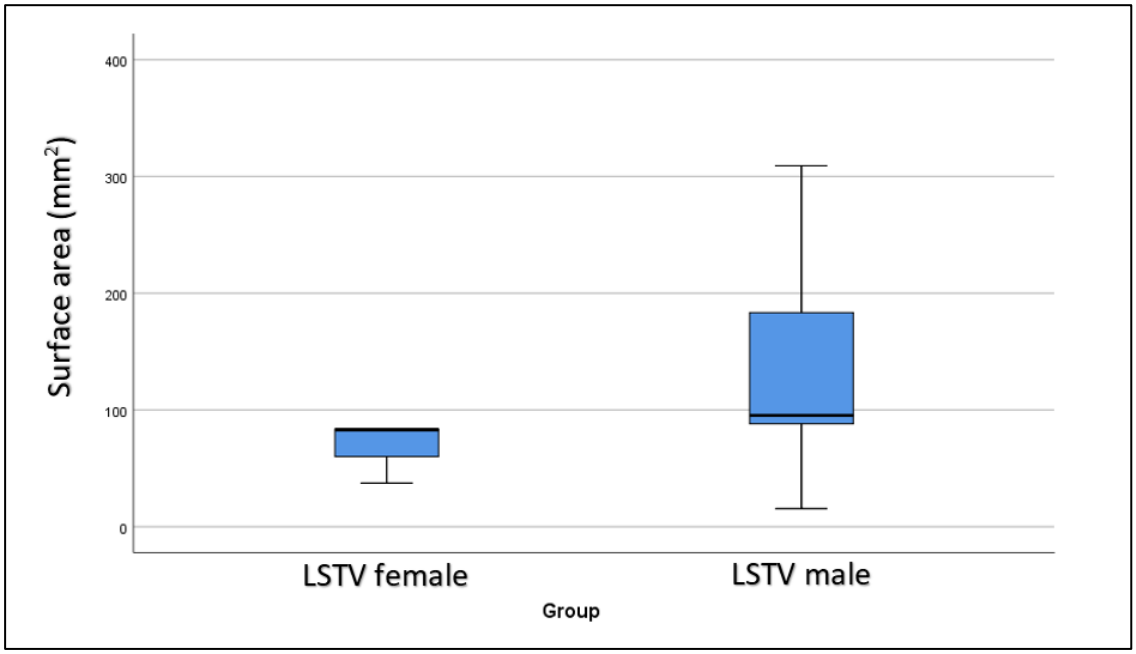

Figure 4.69: *A boxplot graph of the right lumbar contribution to the auricular surface area for the LSTV cohort comparing the sexes.*

Left side

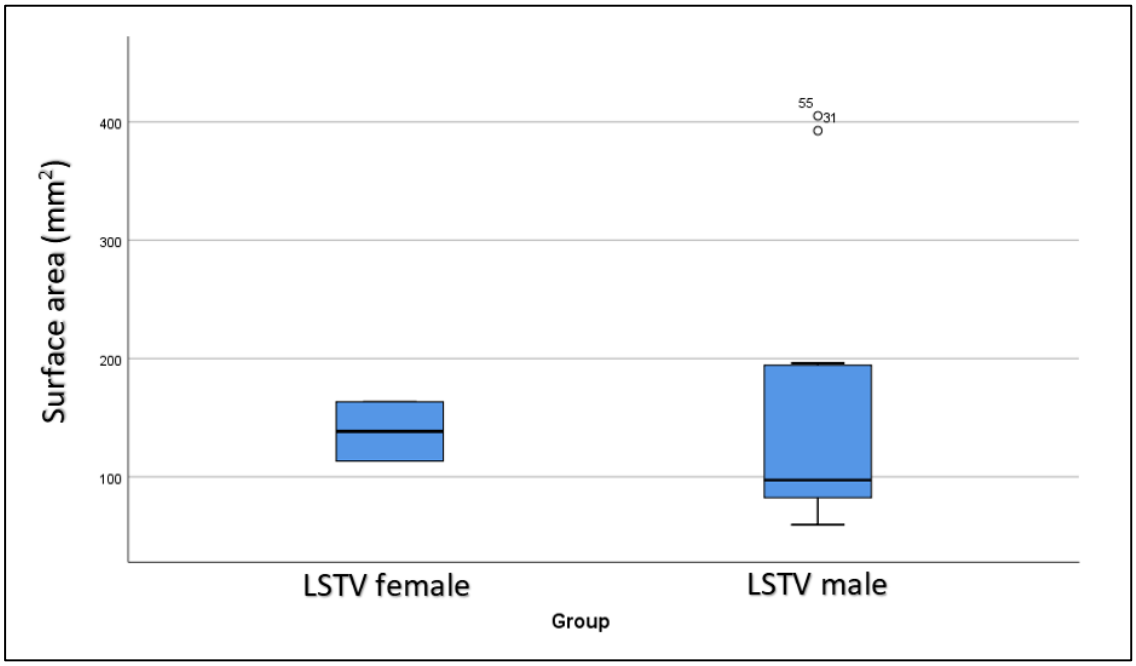

Figure 4.70: A boxplot graph of the left lumbar contribution to the auricular surface area for the LSTV cohort comparing the sexes.

Statistical analyses

No statistical analyses were performed for TPC-ASA as the control cohort did not contain a TPC-ASA. It is only found in LSTV-containing samples.

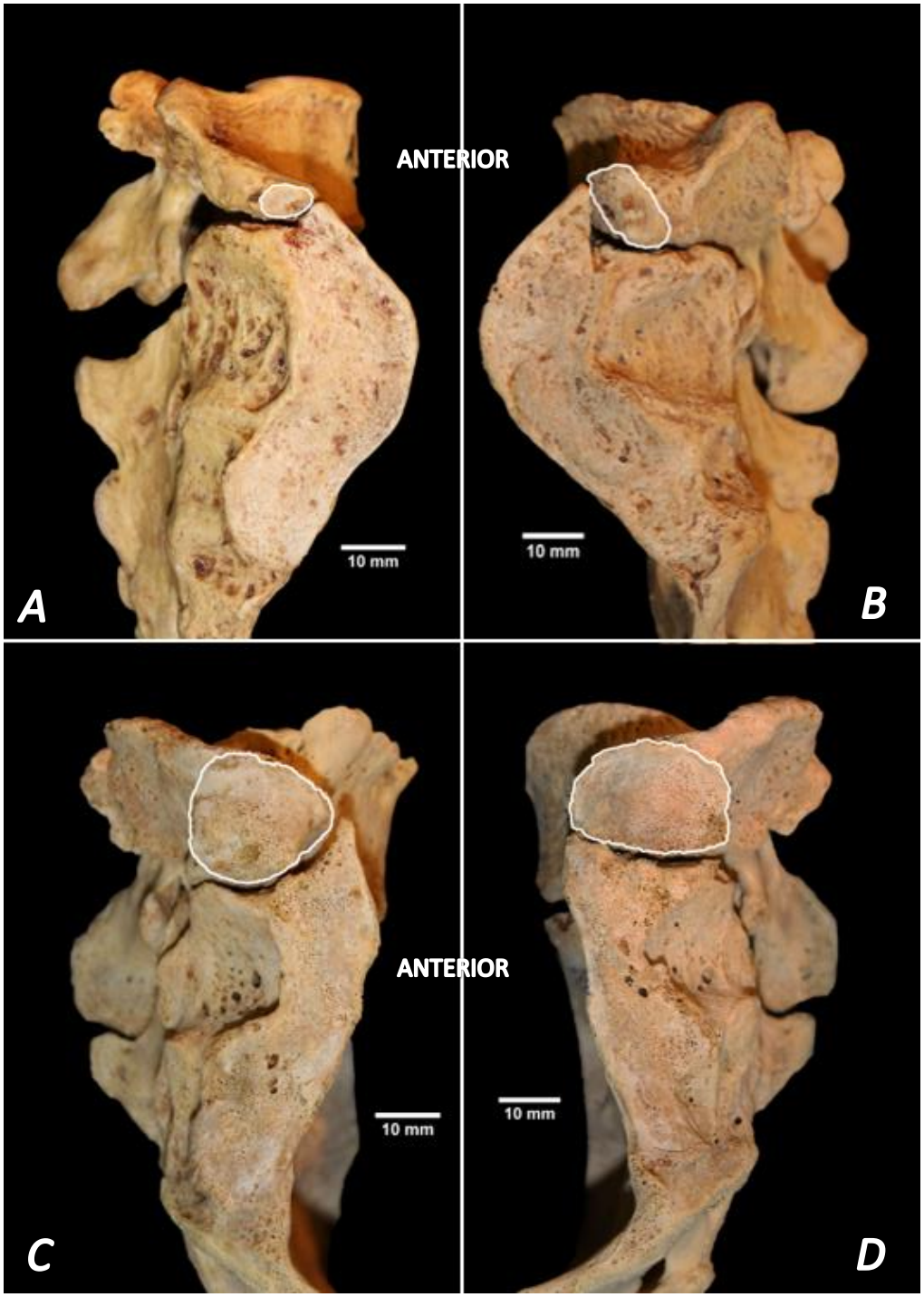

Figure 4.71: *Lateral view of sacra displaying the right and left lumbar transverse process contributions to the auricular surface area associated with lumbosacral transitional vertebrae.* ***A)*** *Right-sided auricular surface of a Type IIB lumbosacral transitional vertebra.* ***B)*** *Left-sided auricular surface a Type IIB lumbosacral transitional vertebra.* ***C)*** *Right sided auricular surface of a Type IIB lumbosacral transitional vertebra.* ***D)*** *Left-sided auricular surface of a Type IIB lumbosacral transitional vertebra. The arrows indicate the enlarged transverse processes that contributed to the auricular surface area.* ***Photography and editing:*** *GJ Paton.*

D17: Sacral facet surface area (FSA); right and left

Sacral facet surface area was measured in association with a Type II LSTV only. The right LSTV cohort (N=57) consisted of 39 males (n=39) and 18 females (n=18) and the left LSTV cohort (N=58) consisted of 40 males (n=40) and 18 females (n=18). The control cohort (N=60) consisted of 30 males (n=30) and 30 females (n=30).

Lumbosacral transitional vertebrae cohort compared to the control cohort

Right side

The mean FSA in the LSTV cohort (140.35mm^2 ± 45.59mm^2) was smaller than the control cohort (201.79mm^2 ± 41.21mm^2). The FSA of the LSTV cohort had a smaller range in variation of surface area, between, 47.71mm^2 and 235.02mm^2 while the control cohort range was between 130.30mm^2 and 313.31mm^2 in length.

Left side

The mean FSA in the LSTV cohort (136.63mm^2 ± 39.75mm^2) was smaller than the control cohort (204.22mm^2 ± 39.48mm^2). The FSA of the LSTV cohort had a smaller range in variation of surface area, between 29.84mm^2 and 233.84mm^2, while the control cohort range was between 124.25mm^2 and 315.87mm^2 in length.

Sex comparison of lumbosacral transitional vertebrae cohort compared to the control cohort

Right side

A sex comparison found that the mean FSA on the right of males in the LSTV cohort (131.14mm^2 ± 42.53mm^2) was smaller than that of the female cohort (160.30mm^2 ± 46.79mm^2). The FSA of the male LSTV cohort had a smaller range in variation of surface area, between 47.71mm^2 and 198.73mm^2, while the female LSTV cohort range was between 69.83mm^2 and 235.02mm^2 in surface area.

Conversely, a sex comparison of the mean FSA on the right in the control cohort was larger for males (208.60mm^2 ± 48.82mm^2) when compared to the females (194.97mm^2 ± 31.24mm^2).

The FSA of the male control cohort had a larger range in variation of surface area, between 130.30mm^2 and 313.31mm^2, while the female cohort range was between 143.32mm^2 and 272.13mm^2 in surface area.

The mean FSA of the male LSTV cohort on the right side (131.14mm^2 ± 42.53mm^2) was smaller than the males in the control cohort (208.60mm^2 ± 48.82mm^2). The mean FSA of females in the LSTV cohort (145.31mm^2 ± 35.50mm^2) was smaller than the females in the control cohort (160.30mm^2 ± 46.79mm^2). Refer to Figures 4.72 and 4.73.

Left side

A sex comparison found that the mean FSA on the left of males in the LSTV cohort (132.72mm^2 ± 41.34mm^2) was smaller than that of the female cohort (145.31mm^2 ± 35.50mm^2). The FSA of the male LSTV cohort had a larger range in variation of length, between 29.84mm^2 and 207.77mm^2, while the female LSTV cohort range was between 92.38mm^2 and 233.84mm^2 in length.

Conversely, a sex comparison of the mean FSA on the left in the control cohort was larger for males (207.58mm^2 ± 49.87mm^2) when compared to the females (200.86mm^2 ± 25.70mm^2). The FSA of the male control cohort had a larger range in variation of surface area, between 124.25mm^2 and 315.87mm^2, while the female LSTV cohort range was between 146.23mm^2 and 243.85mm^2 in surface area.

The mean FSA of the male LSTV cohort on the right side (132.72mm^2 ± 41.34mm^2) was smaller than the males in the control cohort (207.58mm^2 ± 49.87mm^2). The mean FSA of females in the LSTV cohort (145.31mm^2 ± 35.50mm^2) was smaller than the females in the control cohort (200.86mm^2 ± 25.70mm^2). Refer to Figures 4.74 and 4.75. Figures 4.76 and 4.77 demonstrate the FSA variations associated with LSTV on the right and left sides.

Right side

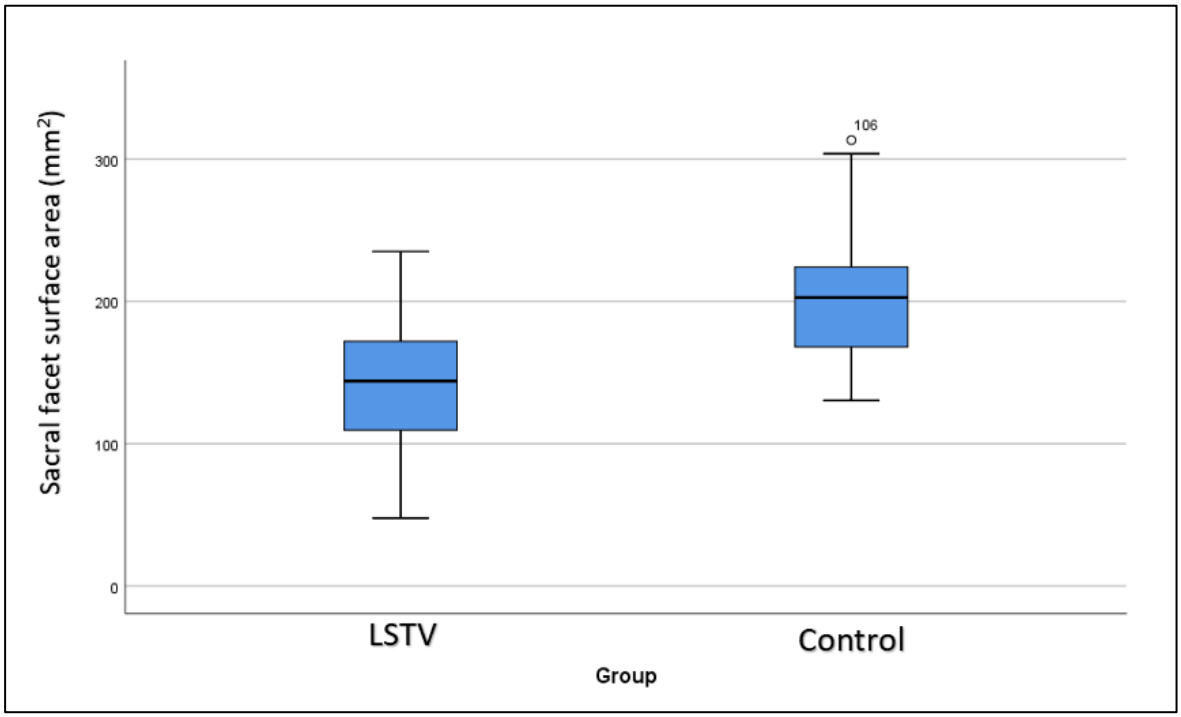

Figure 4.72: *A boxplot graph of the right sacral facet surface area for the LSTV and control cohorts.*

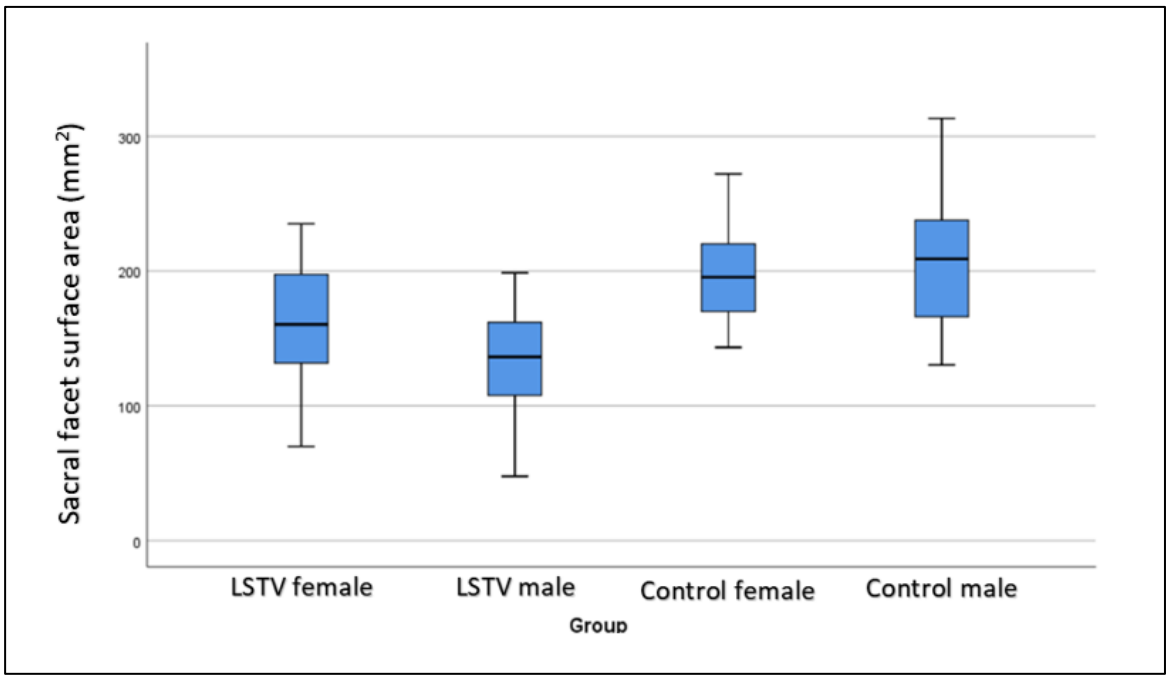

Figure 4.73: *A boxplot graph of the right sacral facet surface area for the LSTV and control cohort comparing the sexes.*

Left side

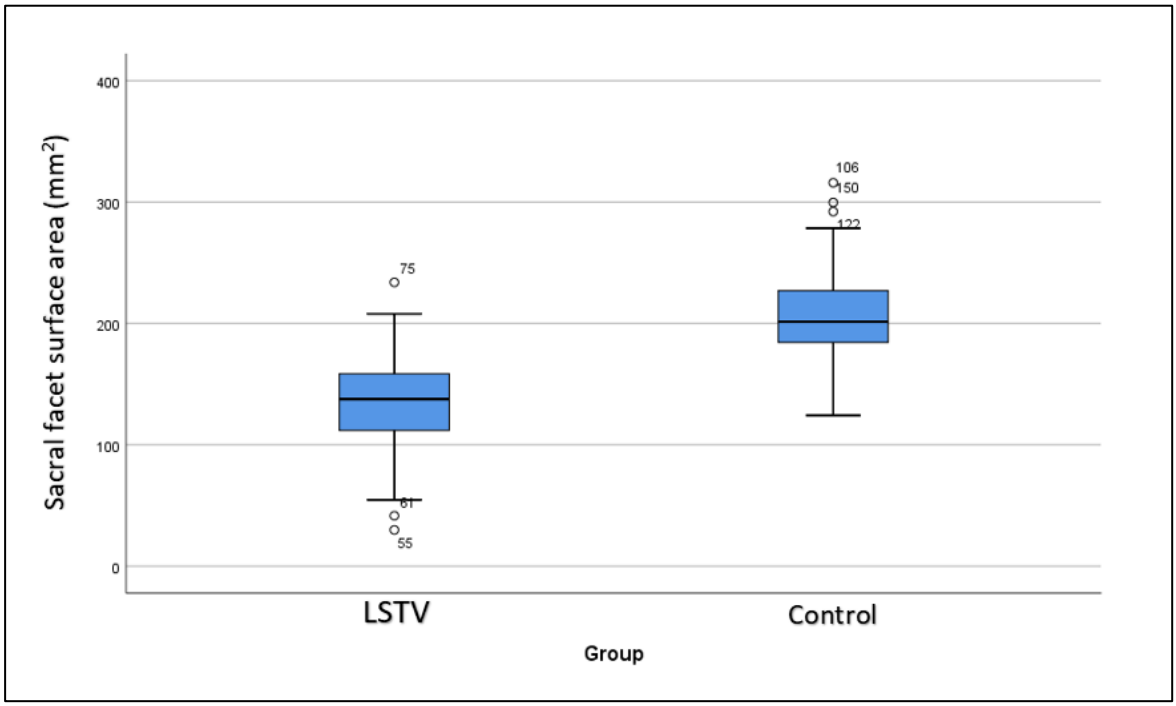

Figure 4.74: *A boxplot graph of the left sacral facet surface area for the LSTV and control cohorts.*

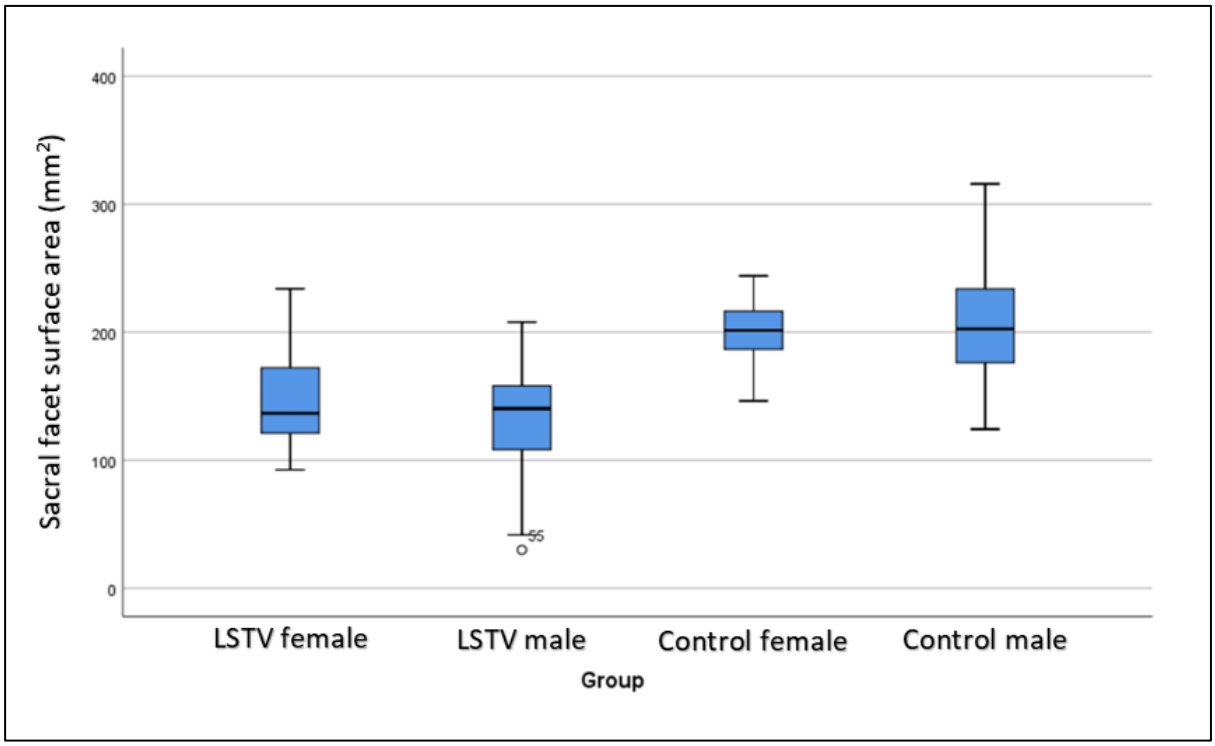

Figure 4.75: *A boxplot graph of the left sacral facet surface area for the LSTV and control cohorts comparing the sexes.*

Statistical analyses

Lumbosacral transitional vertebrae and control cohort comparison

Right side

The T-test compared the mean rank values of FSA in the LSTV (n=57) cohort and the control (n=60) cohort. Levene's test for variance was equal. The T-test for equality of means (t=-7.65, df= 115, p<0.001) found a statistically significant difference in right FSA with the LSTV cohort containing a smaller surface area as compared to the control cohort.

Left side

The T-test compared the mean rank values of FSA in the LSTV (n=58) cohort and the control (n=60) cohort. Levene's test for variance was equal. The T-test for equality of means (t=-9.27, df= 116, p<0.001) found a statistically significant difference in left FSA with the LSTV cohort containing a smaller surface area as compared to the control cohort.

Lumbosacral transitional vertebrae cohort male and female comparison

Right side

The Mann-Whitney U test compared the mean rank values of FSA in the LSTV male cohort (n=39) and the LSTV female (n=18) cohort. There was a statistically significant difference (U=223.50, Z=-2.19, p=0.029) in FSA between the LSTV male (mean rank 25.73) and LSTV female (mean rank 36.08) cohorts.

Left side

The Mann-Whitney U test compared the mean rank values of FSA in the LSTV male cohort (n=40) and the LSTV female (n=18) cohort. There was no statistically significant difference (U=311.00, Z=-0.82, p=0.410) in FSA between the LSTV male (mean rank 28.28) and LSTV female (mean rank 32.22) cohorts.

Control cohort male and female comparison

Right side

The Mann-Whitney U test compared the mean rank values of FSA in the male (n=30) and the female (n=30) control cohorts. There was no statistically significant difference (U=384.00, Z=-0.98, *p*=0.329) in FSA between the control male (mean rank 32.70) and the female (mean rank 28.30) cohorts.

Left side

The Mann-Whitney U test compared the mean rank values of FSA in the male (n=30) and the female (n=30) control cohorts. There was no statistically significant difference (U=423.00, Z=-0.40, *p*=0.690) in FSA between the control male (mean rank 31.40) and female (mean rank 29.60) cohorts.

Female lumbosacral transitional vertebrae cohort and female control cohort comparison

Right side

The Mann-Whitney U test compared the mean rank values of the FSA in the female LSTV (n=18) and the female control (n=30) cohorts. There was a statistically significant difference (U=152.00, Z=-2.51, *p*=0.012) in FSA between the smaller LSTV female (mean rank 17.94) and the larger control female (mean rank 28.43) cohorts.

Left side

The Mann-Whitney U test compared the mean rank values of the FSA in the female LSTV (n=18) and the female control (n=30) cohorts. There was a statistically significant difference (U=57.00, Z=-4.54, *p*<0.001) in FSA between the smaller LSTV female (mean rank 12.67) and the larger control female (mean rank 31.60) cohorts.

Male lumbosacral transitional vertebrae cohort and male control cohort comparison

Right side

The Mann-Whitney U test compared the mean rank values of the FSA in the male LSTV (n=39) and the male control (n=30) cohorts. There was a statistically significant difference (U=130.00, Z=-5.51, p<0.001) in FSA between the LSTV male (mean rank 23.33) and the larger control male (mean rank 50.17) cohorts.

Left side

The Mann-Whitney U test compared the mean rank values of the FSA in the male LSTV (n=40) and the male control (n=30) cohorts.

There was a statistically significant difference (U=158.00, Z=-5.25, p<0.001) in FSA between the LSTV male (mean rank 24.45) and the larger control male (mean rank 50.23) cohorts.

Additional analyses

Pearson's coefficient correlation was used to assess if a relationship exists between FSA and the size of the FA, BSA and ASFA. Additionally, the correlation was assessed between FSA left and right.

Right FSA

The FSA on the right found no statistically significant relationship exists between the right FA (p= 0.110), left FA (p=0.611) and left ASFA (p=0.200). A statistically significant positive relationship was found between the left FA and the left FSA (p<0.001), with a large effect size (r=0.656) and the right FSA and the BSA (p=0.005), with a medium effect size (r=0.374). A statistically significant negative relationship was found between the left FSA and the right ASFA (p=0.045), with a medium effect size (r= -0.374).

Left FSA

The FSA on the left found no statistically significant relationship exists between the right FA (p= 0.094), left FA (p=0.222), right ASFA (p=0.597) and left ASFA (p=0.807).

A statistically significant positive relationship was found between the left FSA and the right FSA (p<0.001) with a large effect size (r=0.656) and the right FSA and the BSA (p<0.001) with a medium effect size (r=0.462).

Right side

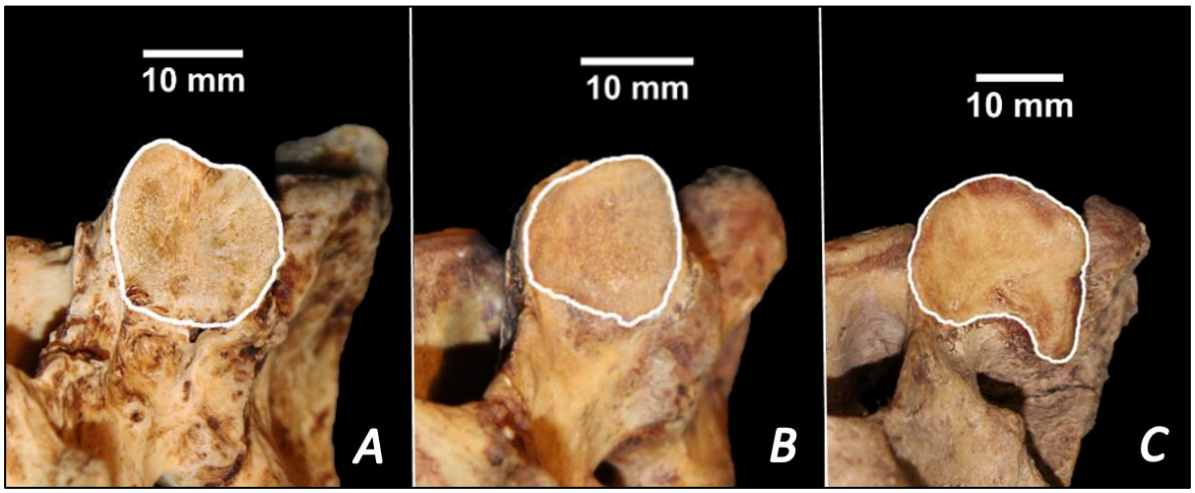

Figure 4.76: *Perpendicular view of the right-sided sacral facet surface area associated with lumbosacral transitional vertebrae.* ***A)*** *A right sacral facet of a Type IIB lumbosacral transitional vertebra.* ***B)*** *A right sacral facet surface area a Type IIB lumbosacral transitional vertebra.* ***C)*** *A right sacral facet surface area of a right-sided Type IIA lumbosacral transitional vertebra. The circumference of the sacral facet surface area is outlined in white.* ***Photography and editing:*** *GJ Paton.*

Left side

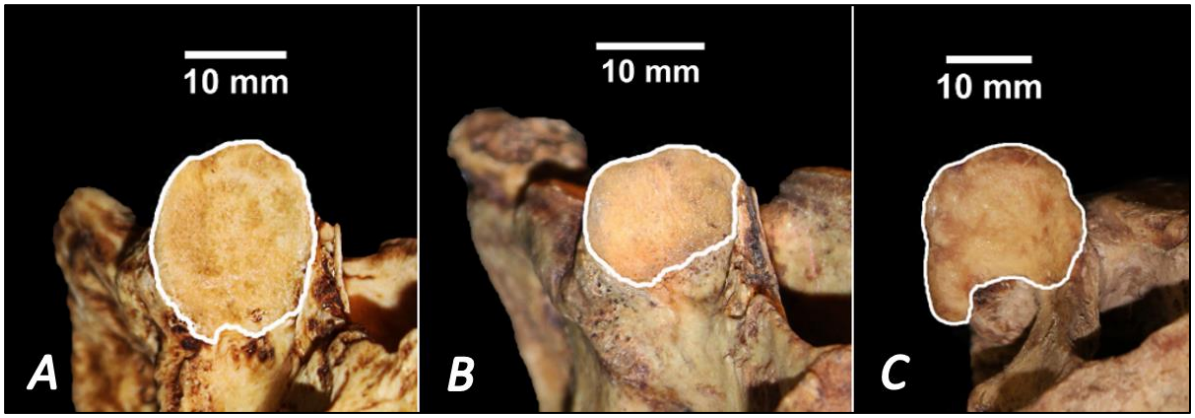

Figure 4.77: *Perpendicular view of the left-sided sacral facet surface area associated with lumbosacral transitional vertebrae.* ***A)*** *A left sacral facet surface area of a Type IIB lumbosacral transitional vertebra.* ***B)*** *A left sacral facet surface area of a Type IIB lumbosacral transitional vertebra.* ***C)*** *A left sacral facet surface area of a right-sided Type IIA lumbosacral transitional vertebra. The circumference of the sacral facet surface area is outlined in white****.*** ***Photography and editing:*** *GJ Paton.*

D18: Sacral body surface area (BSA)

The LSTV cohort (N=57) consisted of 39 males (n=39) and 18 females (n=18). The control cohort (N=60) consisted of 30 males (n=30) and 30 females (n=30).

Lumbosacral transitional vertebrae cohort compared to the control cohort

The mean BSA in the LSTV cohort (1047.03mm^2 ± 172.18mm^2) was smaller than the control cohort (1206.15mm^2 ± 215.54mm^2). The BSA of the LSTV cohort had a smaller range in variation of surface area, between 697.53mm^2 and 1583.00mm^2 while the control cohort range was between 813.12mm^2 and 1861.51mm^2 in surface area.

Sex comparison of lumbosacral transitional vertebrae cohort compared to the control cohort

A sex comparison found that the mean BSA of males in the LSTV cohort (1060.08mm^2 ± 170.05mm^2) was larger than that of the female cohort (1018.76mm^2 ± 178.29mm^2). The BSA of the male LSTV cohort had a larger range in variation of surface area, between 760.26mm^2 and 1583.00mm^2, while the female LSTV cohort range was between 697.53mm^2 and 1286.05mm^2 in surface area.

Likewise, sex comparison of the mean BSA in the control cohort was larger for males (1310.15mm ± 217.90mm) when compared to the females (1102.16mm ± 157.04mm^2). The BSA of the male control cohort had a larger range in variation of length, between 929.92mm^2 and 1861.51mm^2, while the female control cohort range was between 813.12mm2 and 1470.21mm^2 in length.

The mean BSA of the male LSTV cohort (1060.08mm^2 ± 170.05mm^2) was smaller than the males in the control cohort (1310.15mm ± 217.90mm^2). The mean BSA of females in the LSTV cohort (1018.76mm^2 ± 178.29mm^2) was smaller than the females in the control cohort (1102.16mm ± 157.04mm^2). Refer to Figures 4.78 and 4.79. Figure 4.80 demonstrate the BSA variations associated with LSTV.

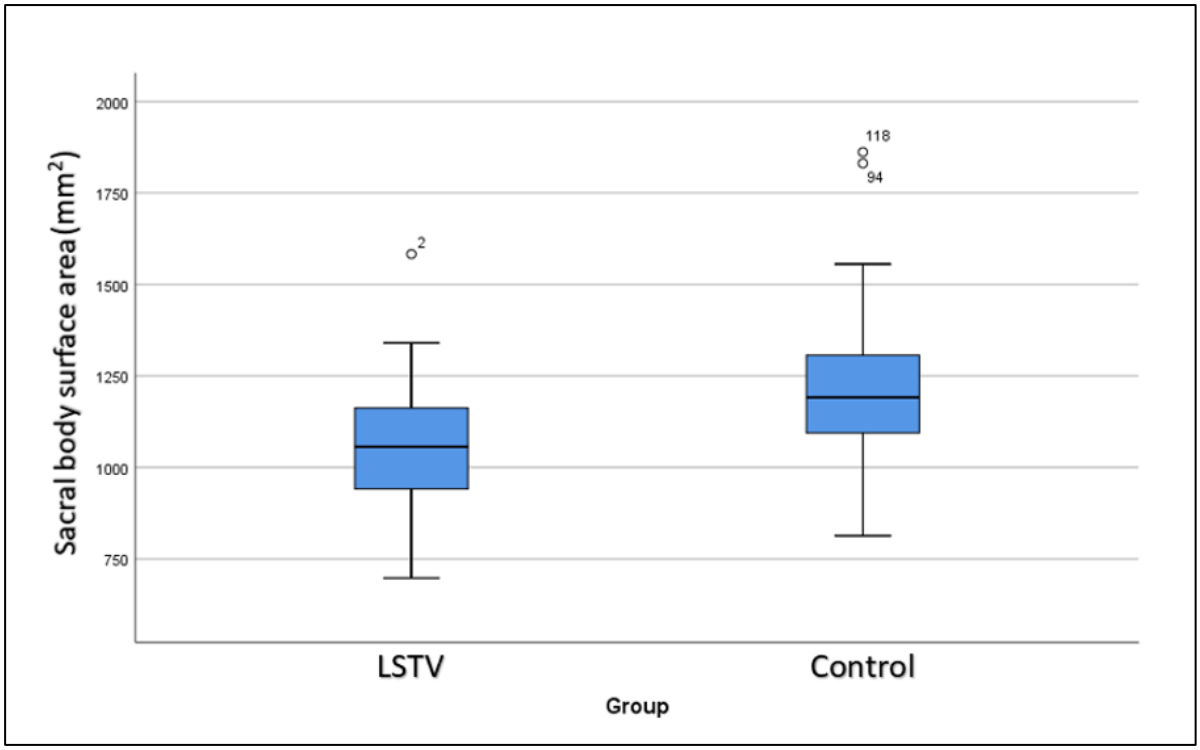

Figure 4.78: *A boxplot graph of the sacral body surface area for the LSTV and control cohorts.*

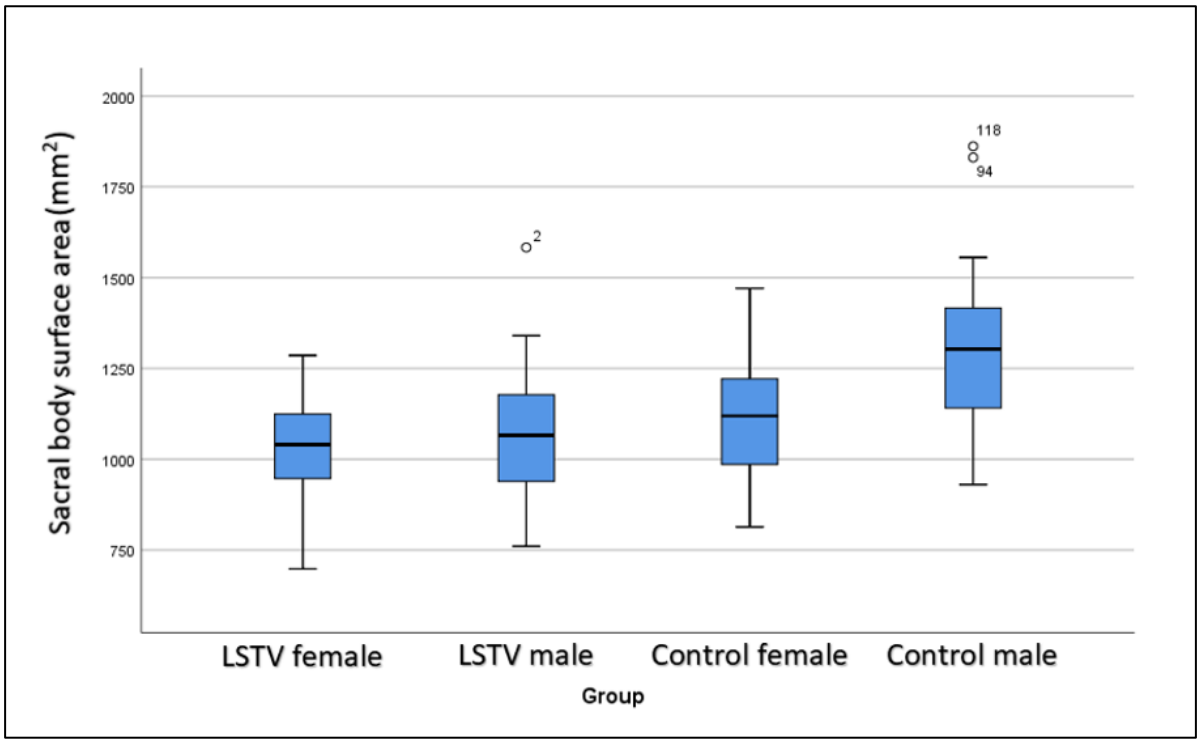

Figure 4.79: *A boxplot graph of the sacral body surface area for the LSTV and control cohorts comparing the sexes.*

Statistical analyses

LSTV and control cohort comparison

The T-test compared the mean rank values of BSA in the LSTV (n=57) cohort and the control (n=60) cohort. Levene's test for variance was equal. The T-test for equality of means (t=-4.40, df= 115, p<0.001) found a statistically significant difference in BSA with the LSTV cohort containing a smaller surface area as compared to the control cohort.

Lumbosacral transitional vertebrae cohort male and female comparison

The Mann-Whitney U test compared the mean rank values of BSA in the LSTV male cohort (n=39) and the LSTV female (n=18) cohort. There was no statistically significant difference (U=319.00, Z=-0.55, p=0.058) in BSA between the LSTV male (mean rank 29.82) and LSTV female (mean rank 27.22) cohorts.

Control cohort male and female comparison

The Mann-Whitney U test compared the mean rank values of BSA in the male (n=30) and the female (n=30) control cohorts. There was a statistically significant difference (U=191.00, Z=-3.83, p<0.001) in BSA between the control male (mean rank 39.13) and the female (mean rank 21.87) cohorts.

Female Lumbosacral transitional vertebrae cohort and female control cohort comparison

The Mann-Whitney U test compared the mean rank values of the BSA in the female LSTV (n=18) and the female control (n=30) cohorts. There was a statistically significant difference (U=198.00, Z=-1.53, p=0.125) in SH between the LSTV female (mean rank 20.50) and the control female (mean rank 26.90) cohorts.

Male Lumbosacral transitional vertebrae cohort and male control cohort comparison

The Mann-Whitney U test compared the mean rank values of the BSA in the male LSTV (n=39) and the male control (n=30) cohorts.

There was a statistically significant difference (U=195.00, Z=-4.72, p<0.001) in TVPL between the LSTV male BSA (mean rank 25.00) and the larger control male (mean rank 48.00) cohorts.

Additional analyses

Pearson's coefficient correlation was used to assess if a relationship exists between BSA and the size of the FA, FSA and ASFA. Additionally, the correlation was assessed between BSA left and right.

No statistically significant relationship exists between the right FA (p= 0.057), right ASFA (p=0.097) and left ASFA (p=0.436) with the BSA.

Statistically significant positive relationship was found between the BSA and the right FSA (p=0.005), with a medium effect size (r=0.374) and the BSA (p<0.001), with a medium effect size (r=0.462). Statistically significant negative relationship was found between the BSA and the left FA (r=0.007), with a medium effect size (r=-0.374).

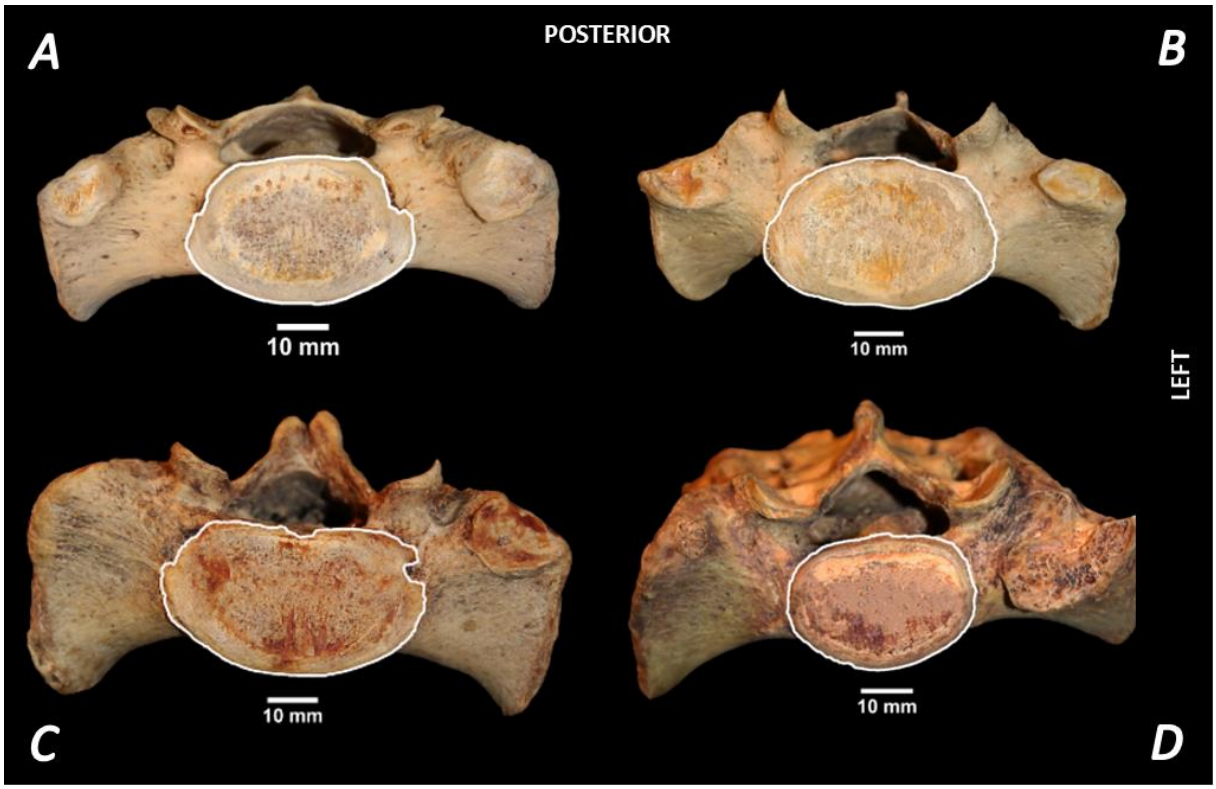

Figure 4.80: *Superior view of sacra displaying the sacral base surface area associated with lumbosacral transitional vertebrae.* ***A)*** *A Type IIB lumbosacral transitional vertebra.* ***B)*** *A Type IIB lumbosacral transitional vertebra.* ***C)*** *A left- sided auricular surface of a Type IIA lumbosacral transitional vertebra.* ***D)*** *A left-sided Type IIA lumbosacral transitional vertebra. The circumference of the sacral base surface area is outlined in white.* ***Photography and editing:*** *GJ Paton.*

D19: Accessory facet surface area (AFSA); right and left

Accessory facet surface area was measured in association with a Type II LSTV only. Bilateral accessory facets found on both the sacral alae were categorised into right and left groupings. The right LSTV cohort (N=31) consisted of 24 males (n=24) and 7 females (n=7) and the left LSTV cohort (N=49) consisted of 34 males (n=34) and 15 females (n=15). There was no control cohort as this is a LTSV-related finding.

Lumbosacral transitional vertebrae cohort

Right side

The mean AFSA in the LSTV cohort was (247.36mm^2 ± 100.92mm^2). The AFSA of the LSTV cohort had a range in variation of surface area, between 119.54mm^2 and 489.53mm^2.

Left side

The mean AFSA in the LSTV cohort was (285.51mm^2 ± 113.96mm^2). The AFSA of the LSTV cohort had a range in variation of surface area between 101.58mm^2 and 603.42mm^2.

Sex comparison of lumbosacral transitional vertebrae cohort

Right side

A sex comparison found that the mean AFSA on the right of males in the LSTV cohort (244.83mm^2 ± 99.85mm^2) was smaller than that of the female cohort (256.02mm^2 ± 112.20mm^2). The AFSA of the male LSTV cohort had a larger range in variation of surface area, between 119.54mm^2 and 489.53mm^2, while the female LSTV cohort range was between 121.54mm^2 and 423.47mm^2 in surface area. Refer to Figures 4.81 and 4.82.

Left side

A sex comparison found that the mean AFSA on the left of males in the LSTV cohort (284.56mm^2 ± 127.25mm^2) was smaller than that of the female cohort (287.65mm^2 ± 79.67mm^2).

The AFSA of the male LSTV cohort had a larger range in variation of surface area, between 101.58mm^2 and 603.422mm^2, while the female LSTV cohort range was between 128.82mm^2 and 481.41mm^2 in surface area. Refer to Figures 4.83 and 4.84. Figure 4.85 demonstrates the AFSA variations associated with LSTV on the right and left sides.

Right side

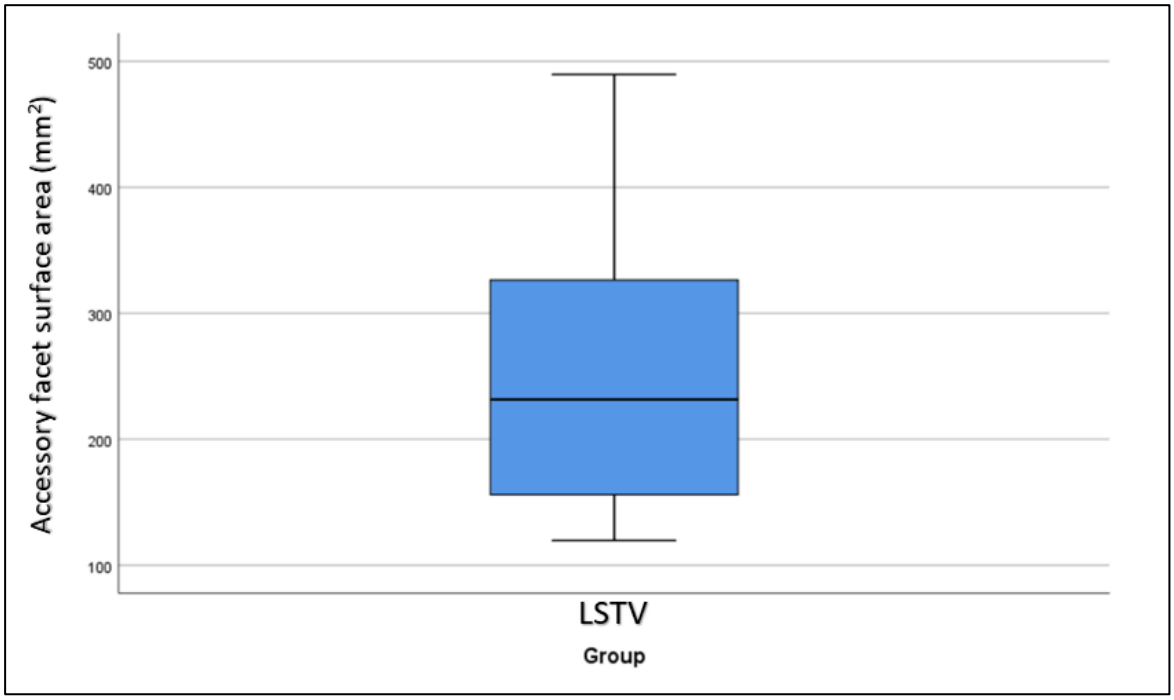

Figure 4.81: *A boxplot graph of the right accessory surface area for the LSTV cohort.*

Right side

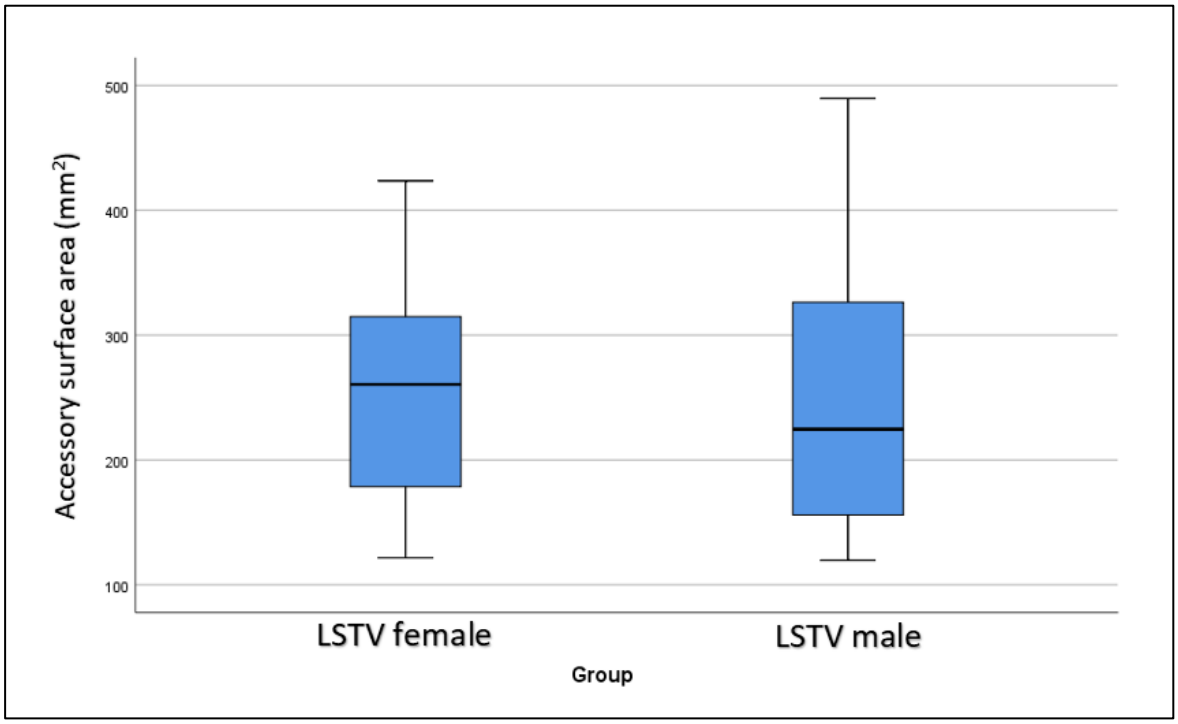

***Figure 4.82**: A boxplot graph of the right accessory surface area for the LSTV cohort comparing the sexes.*

Left side

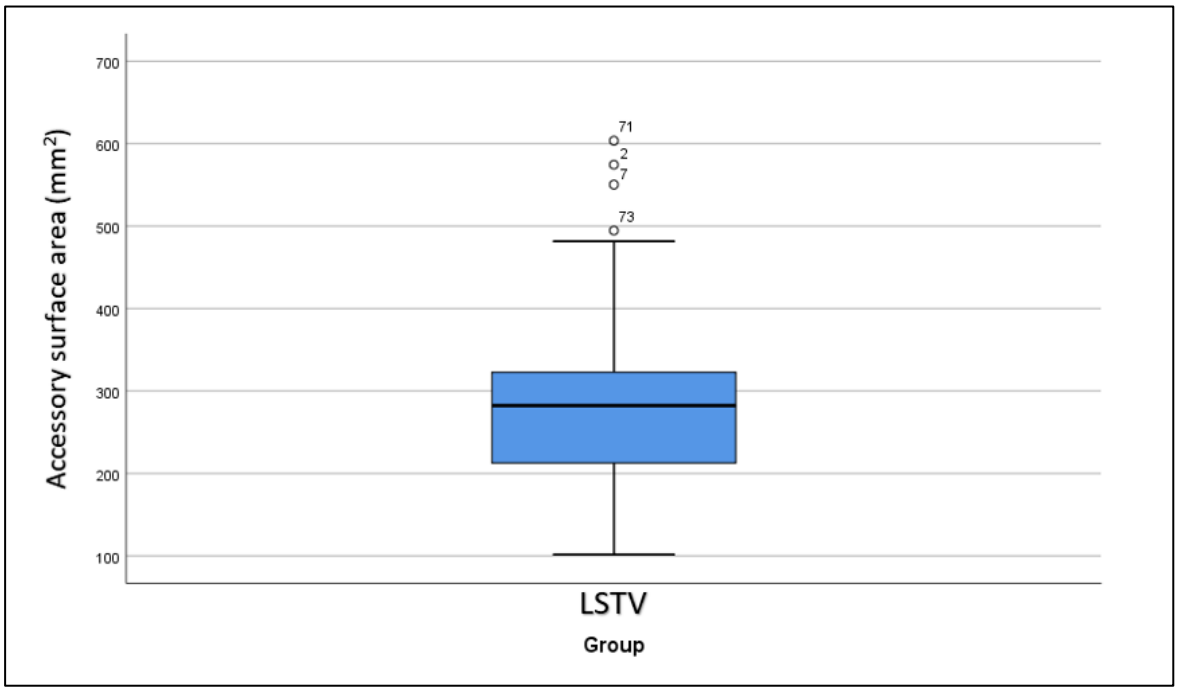

***Figure 4.83**: A boxplot graph of left accessory surface area for the LSTV cohort.*

Left side

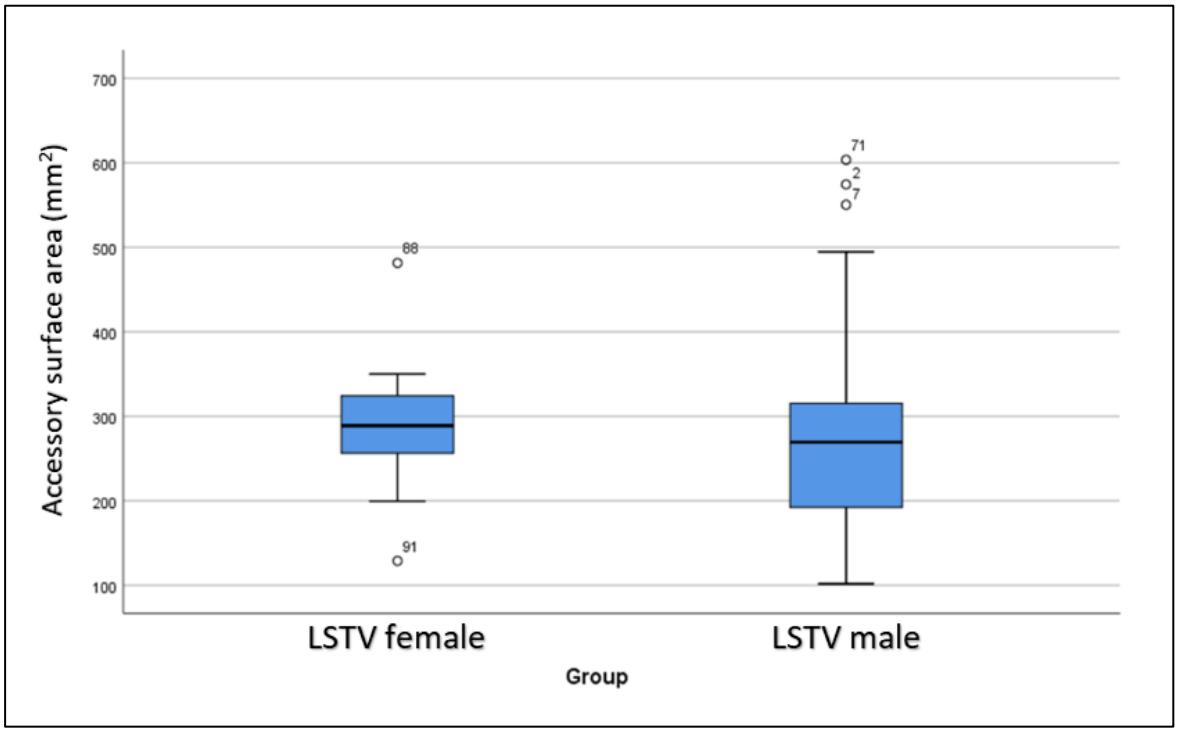

Figure 4.84: *A boxplot graph of the left accessory surface area for the LSTV cohort comparing the sexes.*

Statistical analyses

Lumbosacral transitional vertebrae and control cohort comparison

Comparison to control cohort could not be made as only LSTV contains an accessory facet joint needed for AFSA evaluation.

Lumbosacral transitional vertebrae cohort male and female comparison

Right side

The Mann-Whitney U test compared the mean rank values of AFSA in the LSTV male cohort (n=24) and the LSTV female (n=7) cohort. There was no statistically significant difference (U=80.00, Z=-0.19, *p*=0.850) in AFSA between the LSTV male (mean rank 15.83) and female (mean rank 16.57) cohorts.

Left side

The Mann-Whitney U test compared the mean rank values of AFSA in the LSTV male cohort (n=34) and the LSTV female (n=15) cohort.

There was no statistically significant difference (U=217.00, Z=-0.82 p=0.410) in AFSA between the LSTV male (mean rank 23.88) cohort and female (mean rank 27.53) cohorts.

Additional analyses

Pearson's coefficient correlation was used to assess if a relationship exists between AFSA and the size of the FA, FSA and BSA. Additionally correlation was assessed between AFSA left and right.

Right AFSA

The FSA on the right found no statistically significant relationship exists between the right FA (p= 0.077), left FA (p=0.970), left FSA (p=0.597), BSA (p=0.097) and left AFSA (p=0.859).

Statistically significant negative relationship was found between the right ASFA and the right FSA (p=0.045), with a medium effect size (r=0.656).

Left AFSA

The AFSA on the left found no statistically significant relationships when compared to the right FA (p= 0.077), left FA (p=0.393), right FSA (p=0.200), left FSA (p=0.807) and BSA (p=0.436) demonstrated insignificant p values.

Control cohort male and female comparison

Comparison of the control cohort could not be made as only LSTV contains an accessory facet joint needed for AFSA evaluation.

Female lumbosacral transitional vertebrae cohort and female control cohort comparison

Comparison of LSTV and the control cohort could not be made as only LSTV contains an accessory facet joint needed for AFSA evaluation.

Male lumbosacral transitional vertebrae cohort and male control cohort comparison

Comparison of LSTV and the control cohort could not be made as only LSTV contains an accessory facet joint needed for AFSA evaluation.

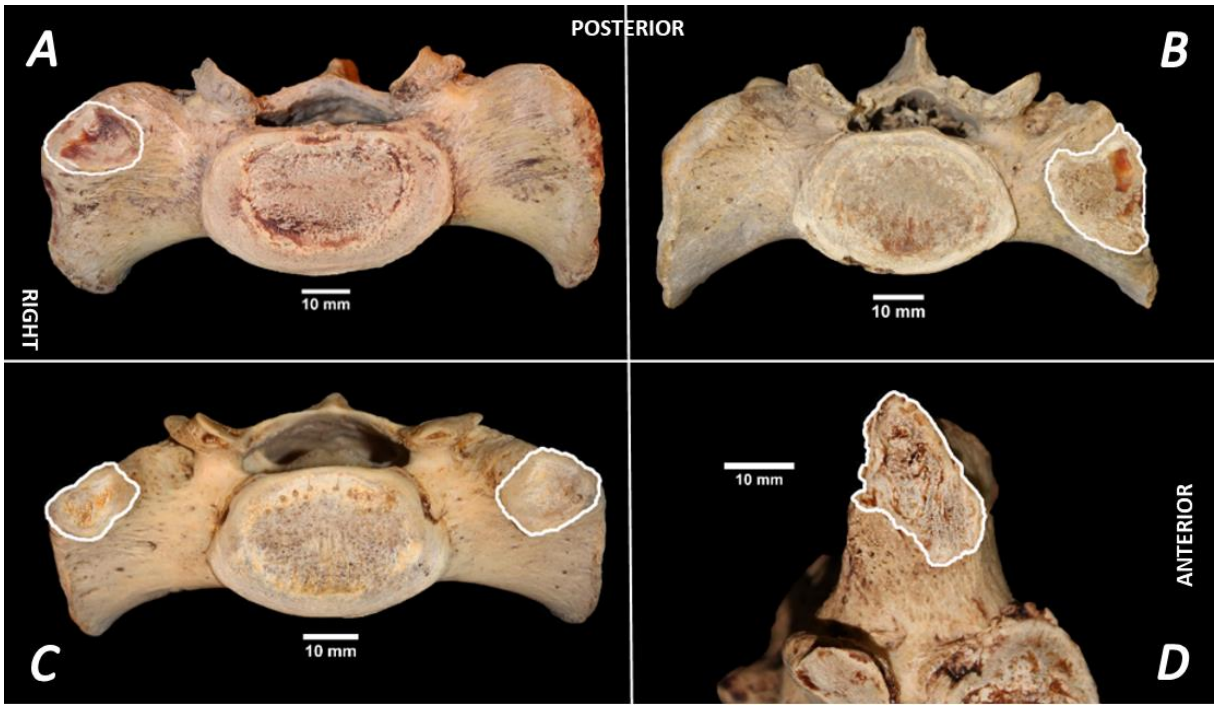

***Figure 4.85**: Superior view of sacra of lumbosacral transitional vertebrae displaying accessory facet articulations. **A)** Right-sided accessory facet articulation of a Type IIA lumbosacral transitional vertebra. **B)** Left-sided facet articulation of a Type IIA lumbosacral transitional vertebra. **C)** Right and left accessry facet articulations of a Type IIB lumbosacral transitional vertebra. **D)** Perpendicular view of an obliquely orientated accessory articulation of a left-sided Type IIA lumbosacral transtional vertebra. **Photography and editing:** GJ Paton.*

D20: Vertebral body height 1 (VBH1)

The LSTV cohort (N=89) consisted of 64 males (n=64) and 25 females (n=25). The control cohort (N=60) consisted of 30 males (n=30) and 30 females (n=30).

Lumbosacral transitional vertebrae cohort compared to the control cohort

The mean VBH1 in the LSTV cohort was larger (26.55mm ± 1.80mm) than the control cohort (25.96mm ± 1.92mm). The VBH1 of the LSTV cohort had a marginally smaller range in variation of height, between 22.53mm and 32.05mm, while the control cohort range was between 20.12mm and 30.00mm in height.

Sex comparison of lumbosacral transitional vertebrae cohort compared to the control cohort

A sex comparison found that the mean VBH1 of males in the LSTV cohort (26.50 ± 1.73mm) was smaller than that of the female cohort (26.66mm ± 2.00mm). The VBH1 of the male LSTV cohort had a smaller range in variation of height, between 22.53mm and 30.41mm, while the female LSTV cohort range was between 23.82mm and 32.05mm in height.

Conversely, a sex comparison of the mean VBH1 in the control cohort was larger for males (26.30mm ± 2.15mm) when compared to the females (25.62mm ± 7.44mm). The VBH1 of the male control cohort had a larger range in variation of height, between 20.12mm and 29.67mm, while the female control cohort range was between 22.16mm and 30.00mm in height.

The mean VBH1 of the male LSTV cohort on the right side (26.50 ± 1.73mm) was larger than the males in the control cohort (26.30mm ± 2.15mm). The mean VBH1 of females in the LSTV cohort (26.66mm ± 2.00mm) was larger than the females in the control cohort (25.62mm ± 7.44mm). Refer to Figures 4.86 and 4.87. Figure 4.88 demonstrate the VBH1 measurements associated with LSTV.

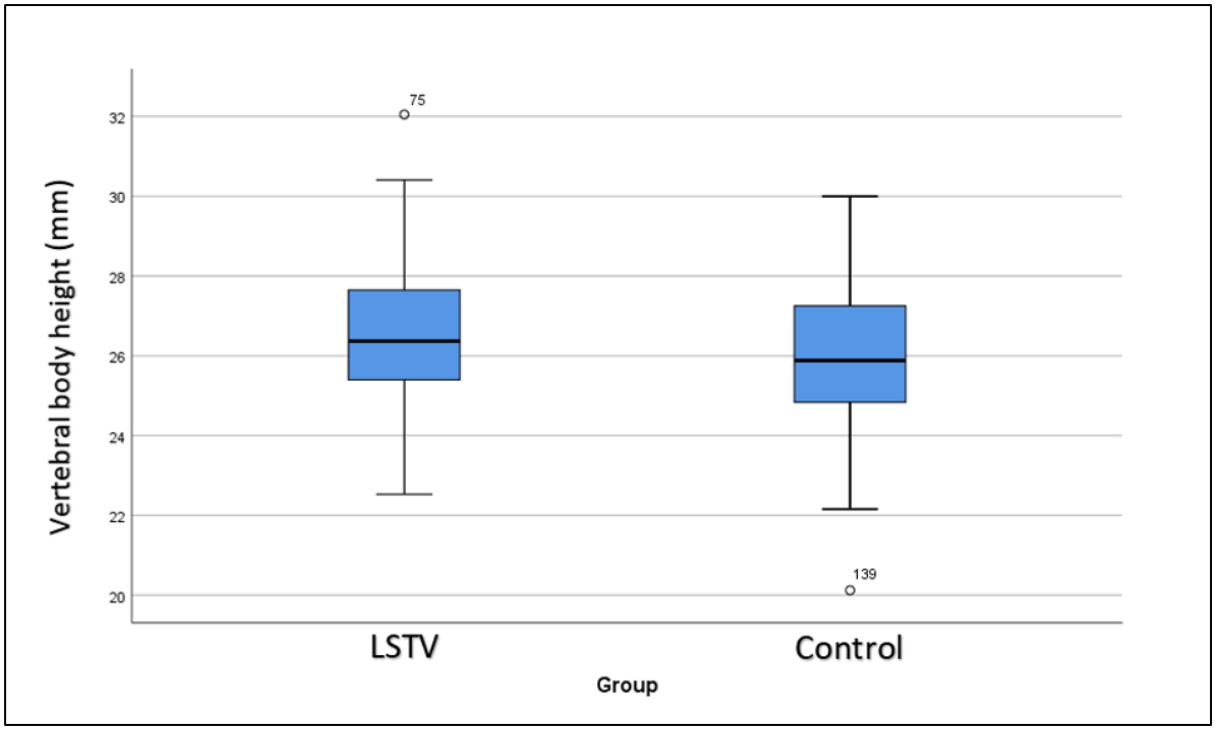

Figure 4.86: *A boxplot graph of the vertebral body height for the LSTV and control cohorts.*

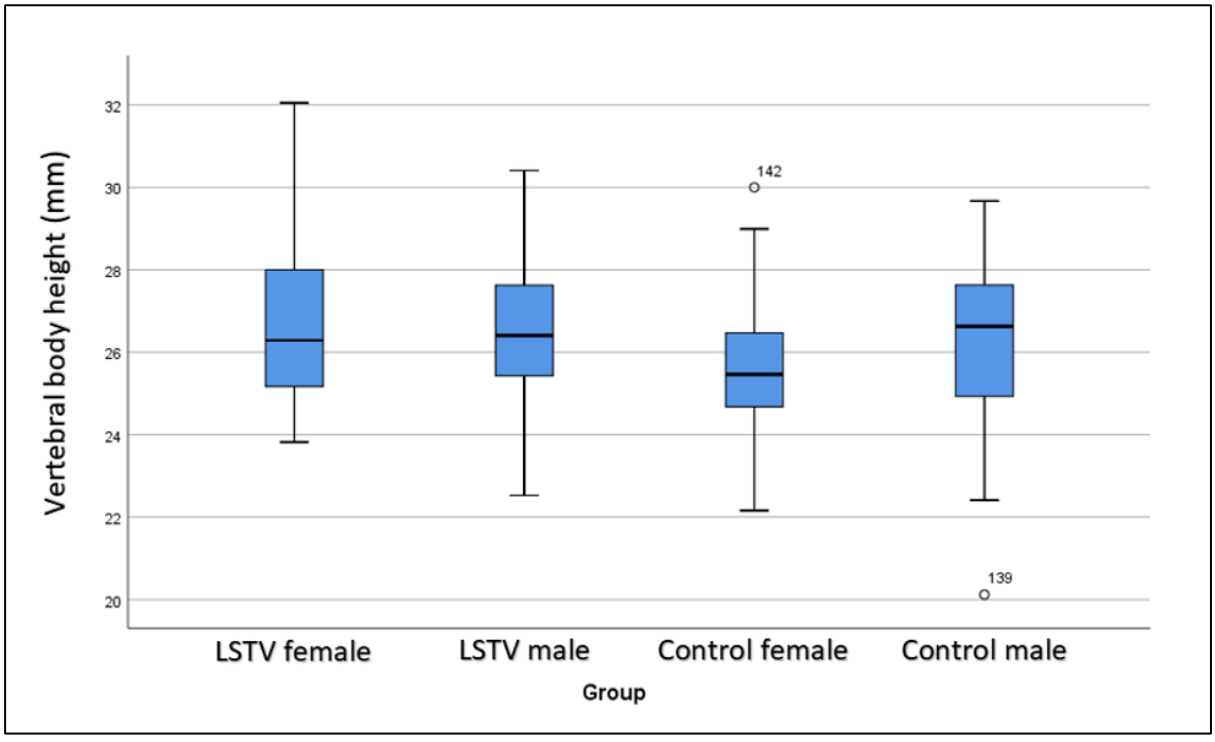

Figure 4.87: A boxplot graph of the vertebral body height for the LSTV and control cohorts comparing the sexes.

Statistical analyses

Lumbosacral transitional vertebrae and control cohort comparison

The T-test compared the mean rank values of VBH1 in the LSTV (n=89) cohort and the control (n=60) cohort. Levene's test for variance was equal. The T-test for equality of means (t=1.91, df= 147, *p*=0.058) found no statistically significant difference in VBH1 with the LSTV cohort containing a larger height as compared to the control cohort.

Lumbosacral transitional vertebrae cohort male and female comparison

The Mann-Whitney U test compared the mean rank values of VBH1 in the LSTV male cohort (n=64) and the LSTV female (n=25) cohort. There was no statistically significant difference (U=797.50, Z=-0.02, *p*=0.982) in VBH1 between the LSTV male (mean rank 45.04) and female (mean rank 44.90) cohorts.

Control cohort male and female comparison

The Mann-Whitney U test compared the mean rank values of VBH1 in the male (n=30) and the female (n=30) control cohorts. There was no statistically significant difference (U=324.50, Z=-1.86, *p*=0.064) in VBH1 between the control male (mean rank 34.68) and female (mean rank 26.32) cohorts.

Female lumbosacral transitional vertebrae cohort and female control cohort comparison

The Mann-Whitney U test compared the mean rank values of the VBH1 in the female LSTV (n=25) and the female control (n=30) cohorts. There was no statistically significant difference (U=261.50, Z=-1.92, *p*=0.055) in VBH1 between the LSTV female (mean rank 32.54) and the control female (mean rank 24.22) cohorts.

Male lumbosacral transitional vertebrae cohort and male control cohort comparison

The Mann-Whitney U test compared the mean rank values of the VBH1 in the male LSTV (n=64) and the male control (n=30) cohorts. There was no statistically significant difference (U=950.00, Z=-0.08, *p*=0.935) in VBH1 between the LSTV male (mean rank 47.66) and the control male (mean rank 47.17) cohorts.

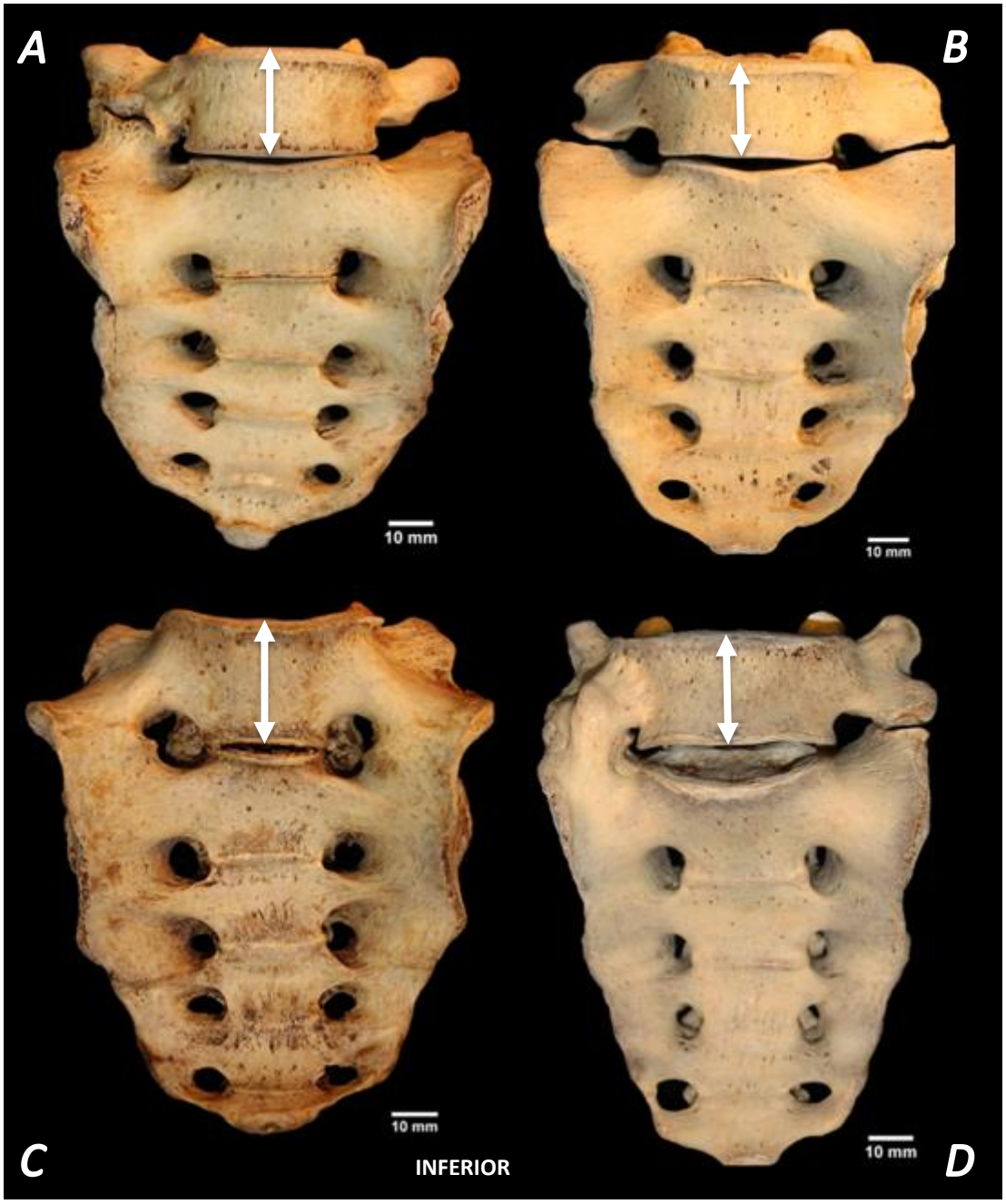

Figure 4.88: *Anterior view sacra displaying the vertebral body height of the lumbosacral transitional vertebrae.* ***A)*** *Right-sided Type IIA lumbosacral transitional vertebra.* ***B)*** *A Type IIB lumbosacral transitional vertebra.* ***C)*** *A Type IIIB lumbosacral transitional vertebra.* ***D)*** *A Type IV lumbosacral transitional vertebra. The double arrows indicate the vertebral body height measurements.* ***Photography and editing:*** *GJ Paton.*

D21: Vertebral body height 2 (VBH2)

The LSTV cohort (N=90) consisted of 65 males (n=65) and 25 females (n=25). The control cohort (N=60) consisted of 30 males (n=30) and 30 females (n=30).

Lumbosacral transitional vertebrae cohort compared to the control cohort

The mean VBH2 in the LSTV cohort was larger (25.71mm ± 1.90mm) than the control cohort (25.78mm ± 1.84mm). The VBH2 of the LSTV cohort had a larger range in variation of height, between 22.10mm and 32.45mm, while the control cohort range was between 19.73mm and 29.27mm in height.

Sex comparison of lumbosacral transitional vertebrae cohort compared to the control cohort

A sex comparison found that the mean VBH2 of males in the LSTV cohort (25.53mm ± 1.88mm) was smaller than that of the female cohort (26.17mm ± 1.91mm). The VBH2 of the male LSTV cohort had a smaller range in variation of height, between 22.10mm and 32.45mm, while the female LSTV cohort range was 22.89mm to 30.05mm in height.

Conversely, a sex comparison of the mean VBH1 in the control cohort was marginally larger for males (25.95mm ± 2.01mm) when compared to the females (25.60mm ± 7.44mm). The VBH2 of the male control cohort had a larger range in variation of height, between 19.73mm and 28.35mm, while the female control cohort range was 23.15mm to 29.27mm in height.

The mean VBH2 of the male LSTV cohort on the right side (25.53mm ± 1.88mm) was marginally smaller than the males in the control cohort (25.95mm ± 2.01mm). The mean VBH2 of females in the LSTV cohort (26.17mm ± 1.91mm) was larger than the females in the control cohort (25.60mm ± 7.44mm). Refer to Figures 4.89 and 4.90. Figure 4.91 demonstrates the VBH2 measurements associated with LSTV.

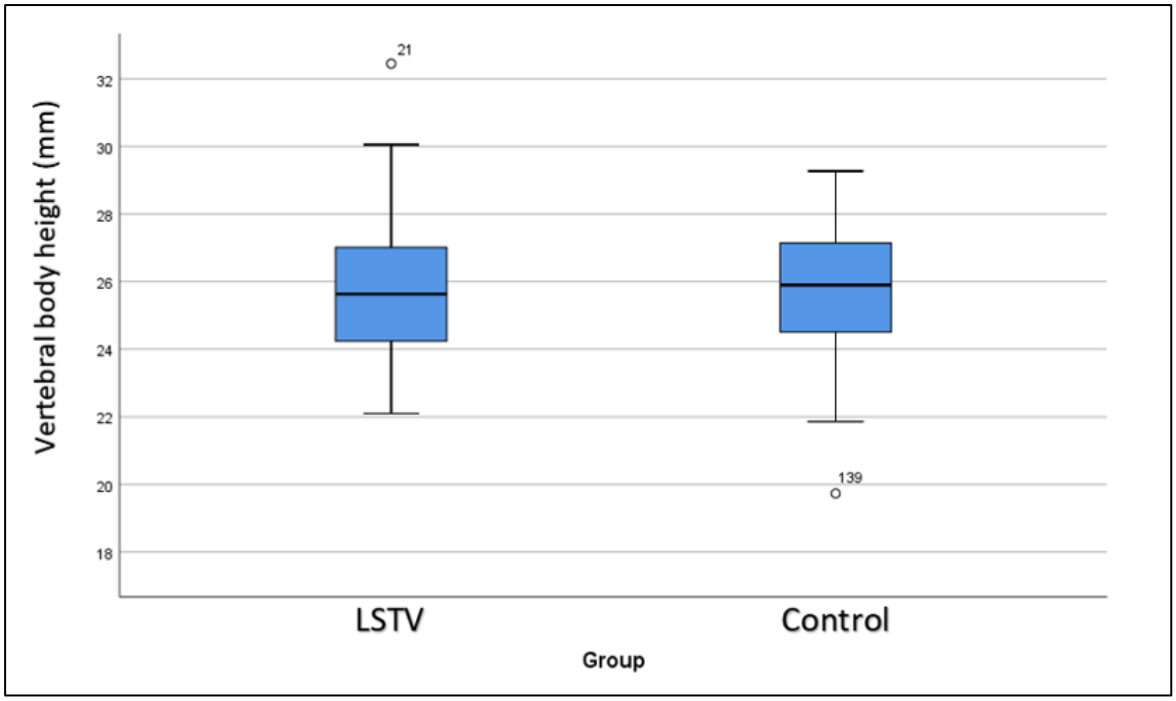

Figure 4.89: A boxplot graph of the vertebral body height for the LSTV and control cohorts.

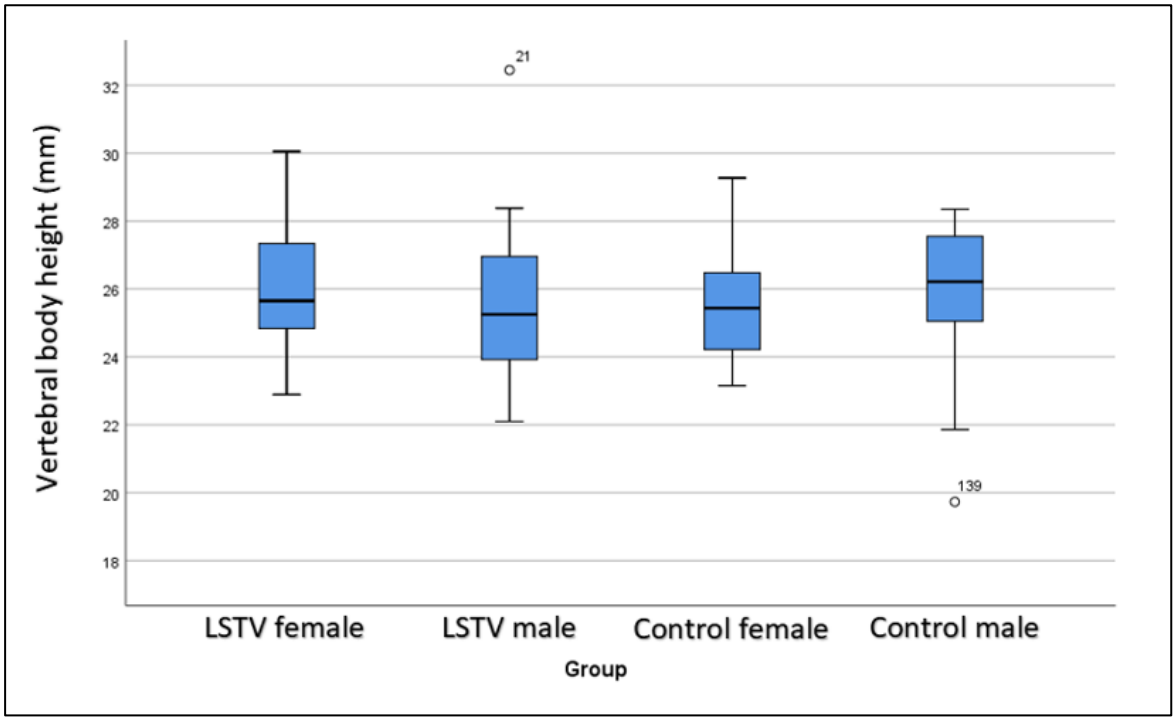

Figure 4.90: *A boxplot graph of the vertebral body height for the LSTV and control cohorts comparing the sexes.*

Statistical analyses

Lumbosacral transitional vertebrae and control cohort comparison

The T-test compared the mean rank values of VBH2 in the LSTV (n=90) cohort and the control (n=60) cohort. Levene's test for variance was equal. The T-test for equality of means (t=-0.21, df= 148*,* *p*=0.832) found no statistically significant difference in VBH2 with the LSTV cohort containing a marginally shorter height as compared to the control cohort.

Lumbosacral transitional vertebrae cohort male and female comparison

The Mann-Whitney U test compared the mean rank values of VBH2 in the LSTV male cohort (n=65) and the LSTV female (n=25) cohort. There was no statistically significant difference (U=677.00, Z=-1.22, *p*=0.022) in VBH2 between the LSTV male (mean rank 43.42) and female (mean rank 50.92) cohorts.

Control cohort male and female comparison

The Mann-Whitney U test compared the mean rank values of VBH2 in the male (n=30) and the female (n=30) control cohorts. There was no statistically significant difference (U=356.00, Z=-1.39, *p*=0.165) in VBH2 between the control male (mean rank 33.63) and female (mean rank 27.37) cohorts.

Female lumbosacral transitional vertebrae cohort and female control cohort comparison

The Mann-Whitney U test compared the mean rank values of the VBH2 in the female LSTV (n=25) and the female control (n=30) cohorts. There was no statistically significant difference (U=313.00, Z=-1.05, *p*=0.295) in VBH2 between the LSTV female (mean rank 30.48) and the control female (mean rank 25.93) cohorts.

Male lumbosacral transitional vertebrae cohort and male control cohort comparison

The Mann-Whitney U test compared the mean rank values of the TVPL in the male LSTV (n=65) and the male control (n=30) cohorts.

There was a statistically significant difference (U=770.00, Z=-1.64, *p*=0.102) in TVPL between the LSTV male (mean rank 44.85) and the control male (mean rank 54.82) cohorts.

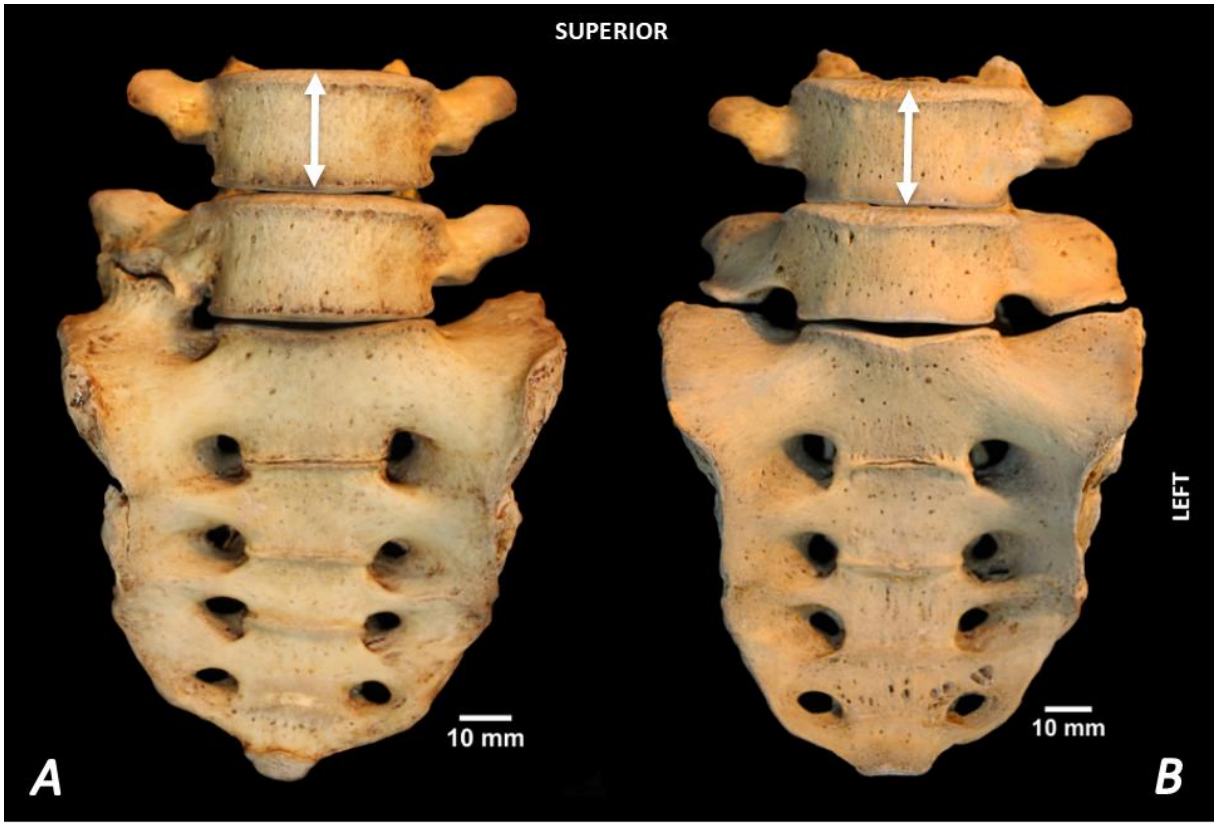

Figure 4.91: *Anterior view sacra displaying the vertebral body height of the lumbosacral transitional vertebrae.* ***A)*** *Right-sided Type IIA lumbosacral transitional vertebra.* ***B)*** *A Type IIB lumbosacral transitional vertebra. The double arrows indicate the vertebra body height above the lumbosacral transitional vertebrae.* ***Photography and editing:*** *GJ Paton.*

D22: Thoracolumbar enumeration (TLE)

The LSTV cohort (N=88) consisted of 65 males (n=65) and 23 females (n=23). The control cohort (N=60) consisted of 30 males (n=30) and 30 females (n=30).

Lumbosacral transitional vertebrae cohort compared to the control cohort

The mean TLE in the LSTV cohort was larger (17.26 ± 0.47) than the control cohort (17.07 ± 0.25). The TLE of the LSTV cohort had a larger range in variation of vertebrae number, between 16 and 18, while the control cohort range was 17 to 18 in vertebrae number.

Sex comparison of lumbosacral transitional vertebrae cohort compared to the control cohort

A sex comparison found that the mean TLE of males in the LSTV cohort (17.27 ± 0.48) was marginally larger than that of the female cohort (17.22 ± 0.42). The LTE of the male LSTV cohort had a larger range in variation of number, between 16 and 18, while the female LSTV cohort range was 17 to 18 in number.

Likewise, a sex comparison of the mean TLE in the control cohort was marginally larger for males (17.13 ± 0.35) when compared to the females (17.00 ± 0.00). The TLE of the male control cohort had a larger range in variation of number, between 17 and 18, while the female control cohort range was only 17 in number.

The mean TLE of the male LSTV cohort on the right side (17.27 ± 0.48) was marginally larger than the males in the control cohort (17.13 ± 0.35). The mean TLE of females in the LSTV cohort (17.22 ± 0.42) was larger than in the control cohort (17.00 ± 0.00). Refer to Figures 4.92 and 4.93.

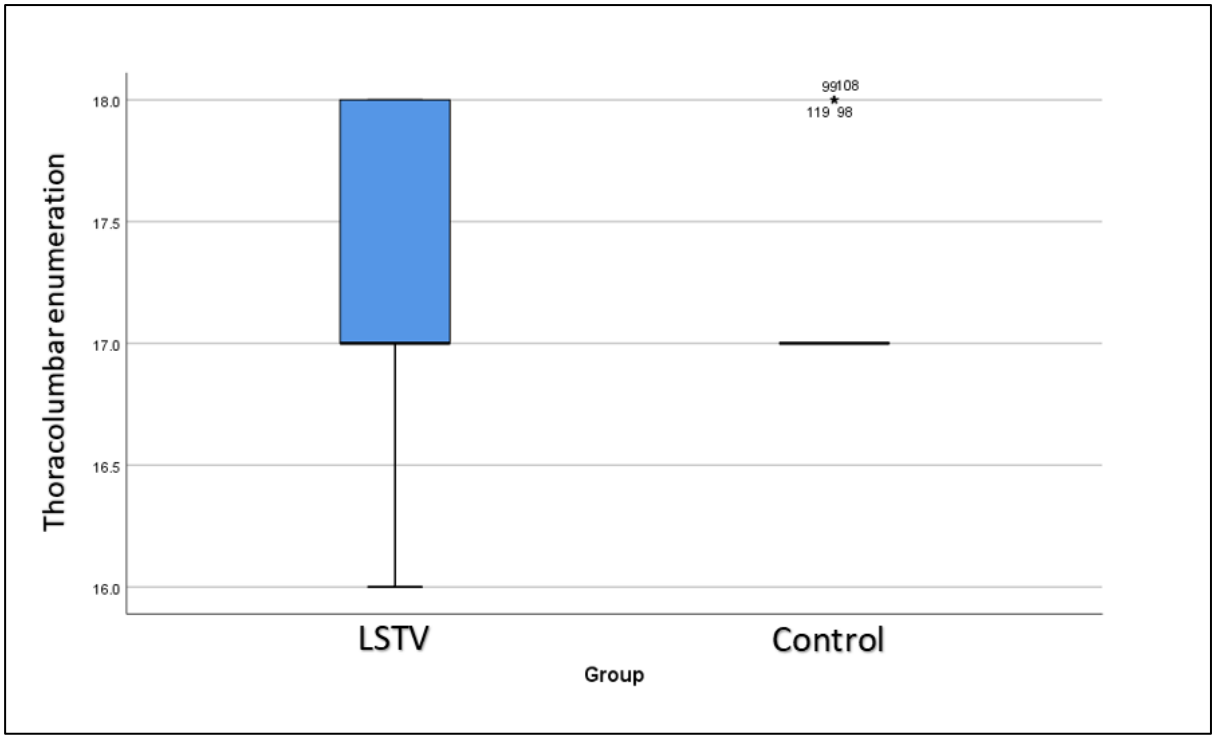

Figure 4.92: *A boxplot graph of the thoracolumbar enumeration for the LSTV and control cohorts.*

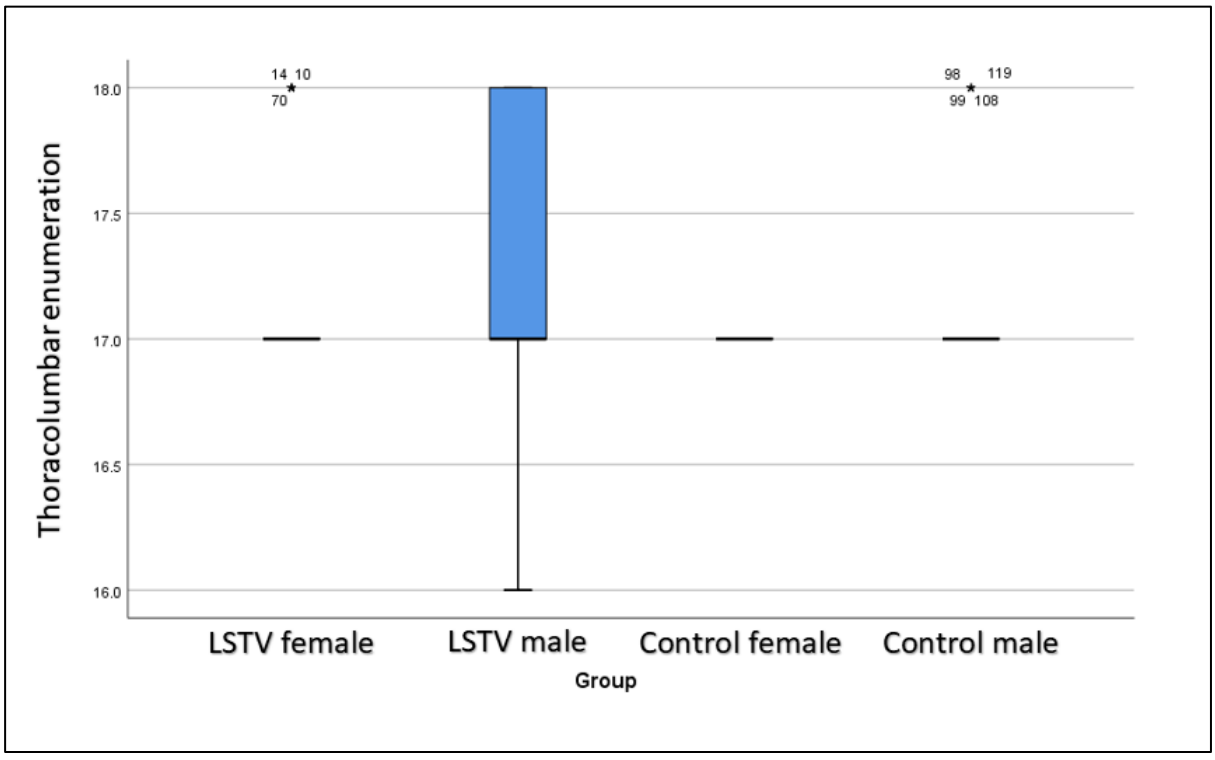

Figure 4.93*: A boxplot graph of the thoracolumbar enumeration for the LSTV and control cohorts comparing the sexes.*

Statistical analyses

Lumbosacral transitional vertebrae and control cohort comparison

The T-test compared the mean rank values of TLE in the LSTV (n=88) cohort and the control (n=60) cohort. Levene's test for variance was not equal. The unequal variance T-test for equality of means (t=3.28, df=139.52, *p*=0.001) found a statistically significant difference in TLE with the LSTV cohort containing a greater number of the thoracolumbar vertebra as compared to the control cohort.

Lumbosacral transitional vertebrae cohort male and female comparison

The Mann-Whitney U test compared the mean rank values of TLE in the LSTV male cohort (n=65) and the LSTV female (n=23) cohort. There was no statistically significant difference (U=700.50, Z=-0.57, *p*=0.569) in TLE between the LSTV male (mean rank 45.22) and female (mean rank 42.46) cohorts.

Control cohort male and female comparison

The Mann-Whitney U test compared the mean rank values of TLE in the control male cohort (n=30) and the control female (n=30) cohort. There was a statistically significant difference (U=390.00, Z=-2.05, *p*=0.040) in TLE between the control male (mean rank 32.50) and female (mean rank 28.50) cohorts.

Female lumbosacral transitional vertebrae cohort and female control cohort comparison

The Mann-Whitney U test compared the mean rank values of the TLE in the female LSTV (n=23) and the female control (n=30) cohorts. There was no statistically significant difference (U=270.00, Z=-2.66, *p*=0.008) in TLE between the LSTV female (mean rank 30.26) and the control female (mean rank 24.50) cohorts.

Male lumbosacral transitional vertebrae cohort and male control cohort comparison

The Mann-Whitney U test compared the mean rank values of the TLE in the male LSTV (n=65) and the male control (n=30) cohorts. There was no statistically significant difference (U=833.00, Z=-1.51, *p*=0.132) in TLE between the LSTV male (mean rank 50.18) and the control male (mean rank 43.27) cohorts.

D23: Thoracolumbar vertebral contribution to the TLE; comprising two components: **D23T** and **D23L**.

D23T: Thoracic vertebrae count

Spinal enumeration associated with lumbosacral transitional vertebrae and control cohorts

The X^2 test could not be used for statistical inference as it violated the second condition for its use; the expected per-cell count was lower than 4 for 66.7% of cells (X^2=2.546, df=2, *p*=0.280). The general trend demonstrated most individuals had twelve thoracic vertebrae greater variation in the LSTV group. There was not enough evidence to suggest an association between sex, subtype and side preference of LSTV. Refer to Figure 4.94.

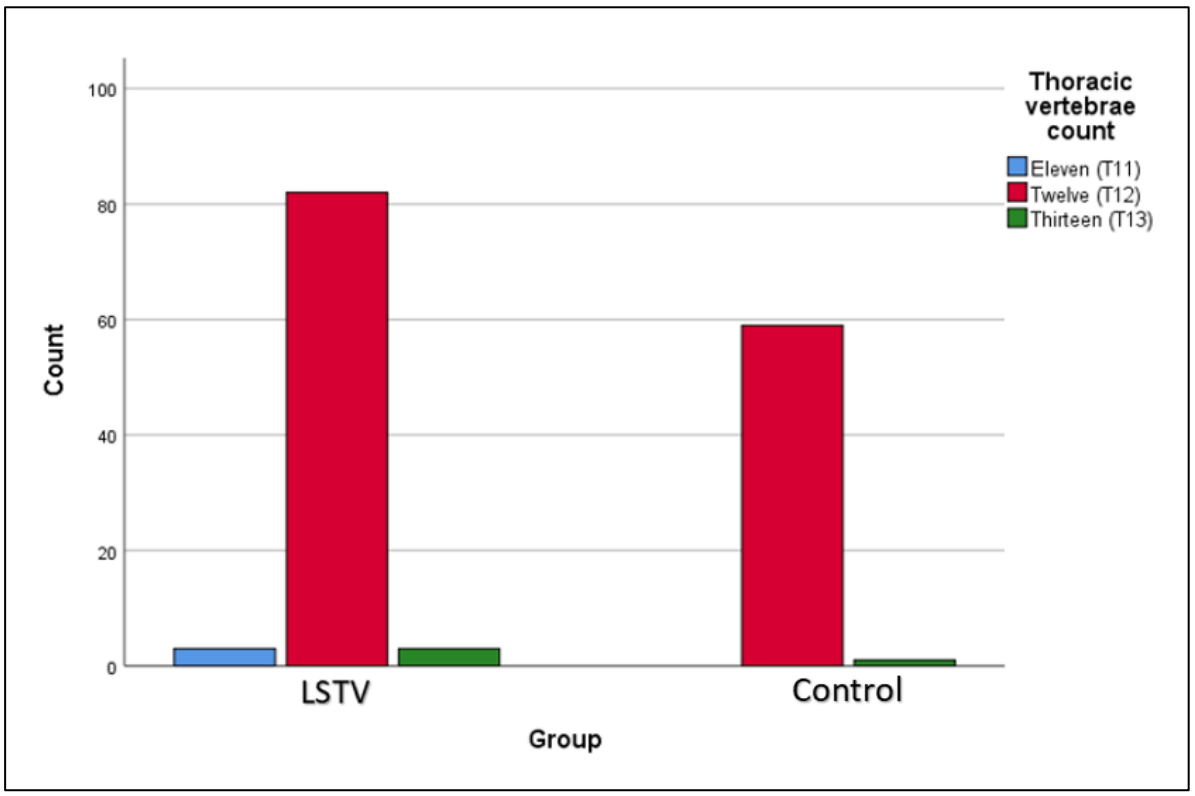

Figure 4.94: *A boxplot graph of the thoracic spinal enumeration for the LSTV and control cohorts.*

Sex and lumbosacral transitional vertebrae cohort

The X^2 test could not be used for statistical inference as it violated the second condition for its use; the expected per-cell count was lower than 4 for 66.7% of cells (X^2=1.6, df=2, *p*=0.559).

The general trend was that twelve thoracic vertebrae were the predominant finding with greater variability in the LSTV male cohort. There was not enough evidence to suggest an association between sex, subtype and side preference of LSTV. Refer to Figure 4.95.

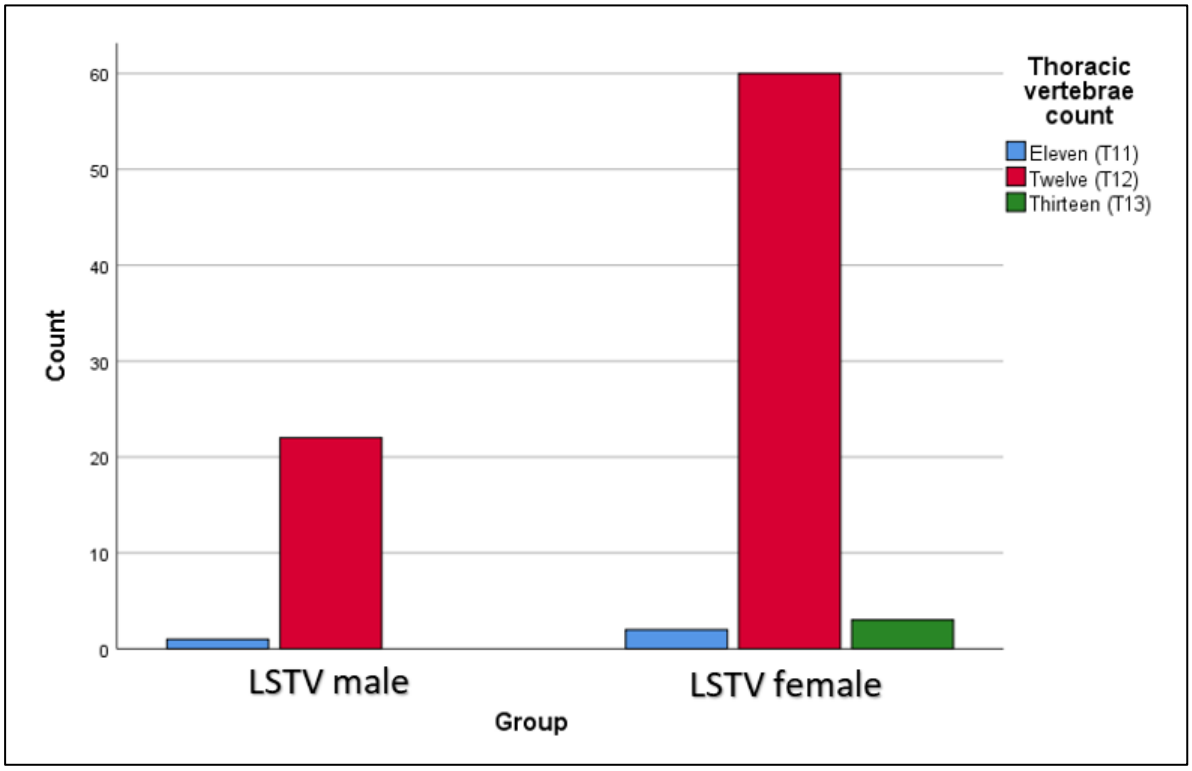

Figure 4.95: *A boxplot graph of the thoracic spinal enumeration for the LSTV cohort comparing the sexes.*

Sex and control cohort

The X^2 test could not be used for statistical inference as it violated the second condition for its use; the expected per-cell count was lower than 2 for 50.0% of cells (X^2=1.087, df=1, *p*=0.297). Fisher's exact test was used for the two-column and two-row (2x2) table (*p*=0.483). The general trend was that twelve thoracic vertebrae was the predominant thoracic count. There was not enough evidence to suggest an association between sexes, subtype and side preference of LSTV. Refer to Figure 6.96.

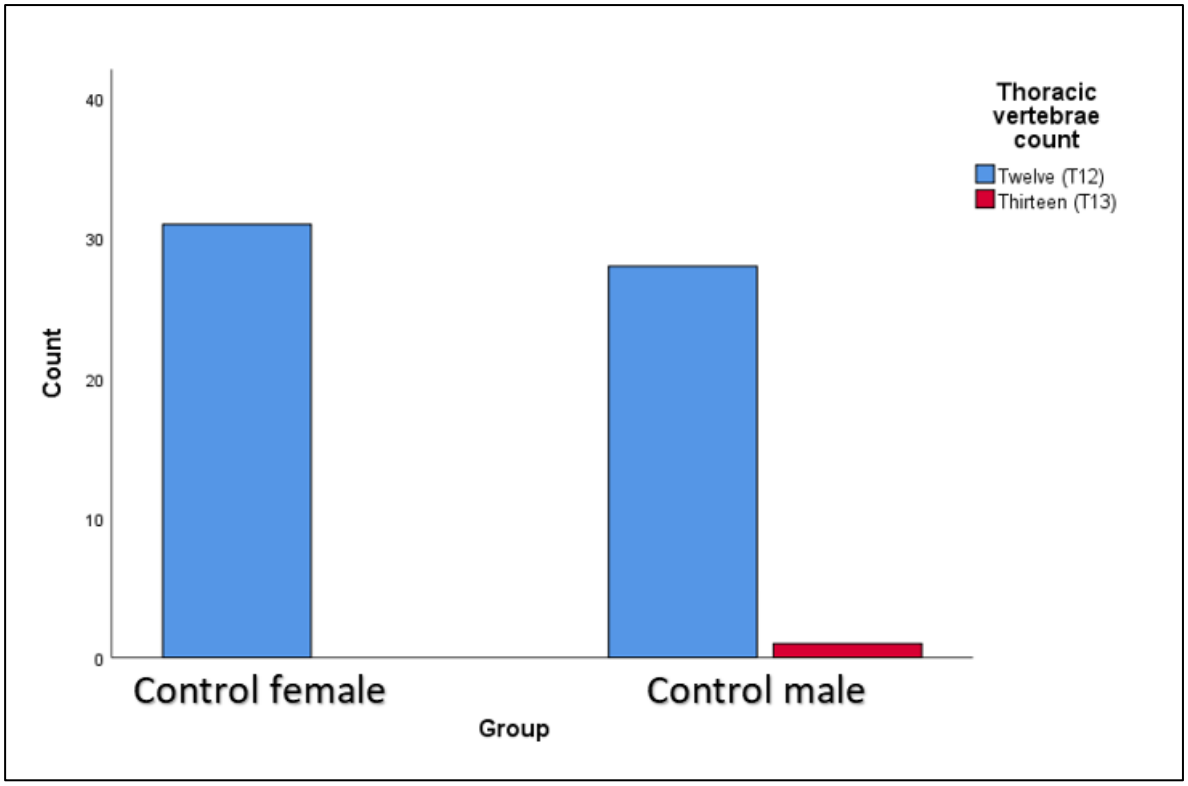

***Figure 4.96**: A boxplot graph of the thoracic spinal enumeration for the control cohort comparing the sexes.*

Sex and cohort comparison

Female

Comparison of the female sex was made between LSTV and control cohorts comparing thoracic spine enumeration. The X^2 test could not be used for statistical inference as it violated the second condition for its use; the expected per-cell count was lower than 4 for 66.7% of cells (X^2=1.373, df=1, *p*=0.241). Fisher's exact test was used to analyse of the two column and two-row (2x2) contingency table (*p*=0426). There was not enough evidence to suggest an association between the female sex, LSTV and control cohorts and spinal enumeration. Refer to Figure 4.97.

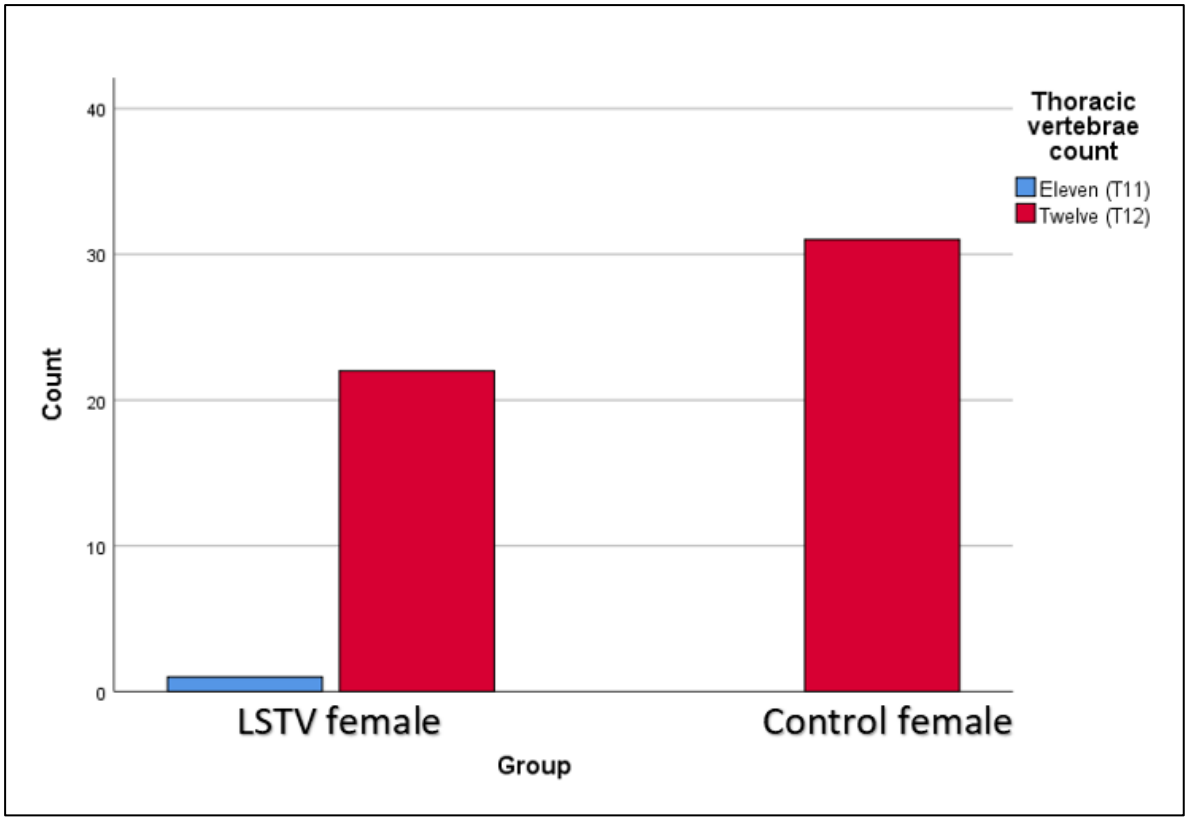

Figure 4.97: *A boxplot graph of the thoracic spinal enumeration comparing the females in the LSTV and control cohorts.*

Male

Comparison of the male sex was made between LSTV and control cohorts comparing thoracic spine enumeration. The X^2 test could not be used for statistical inference as it violated the second condition for its use; the expected per-cell count was lower than 4 for 66.7% of cells (X^2=0.995, df=2, *p*=0.601). The general trend was that twelve thoracic vertebrae were present in the thoracic spine with slight variability in the LSTV cohort. There was not enough evidence to suggest an association between the male sex, LSTV and control cohorts and spinal enumeration. Refer to Figure 4.98.

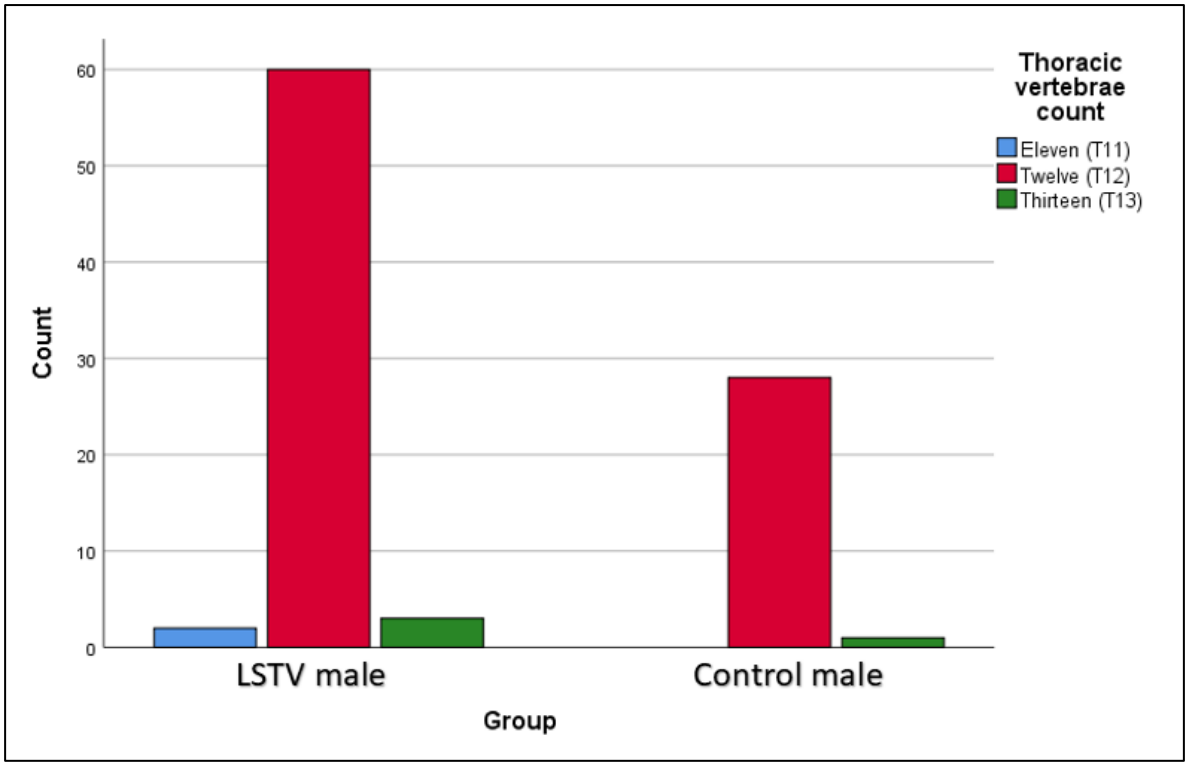

Figure 4.98: *A boxplot graph of the thoracic spinal enumeration comparing the males in the LSTV and control cohorts.*

D23L: Lumbar vertebrae count

Sacralisation was the most abundant finding in this study, meaning LSTV was present at the fifth vertebra in the lumbar spine. In order to analyse the findings of lumbar vertebral enumeration, the lumbar vertebrae were divided into mobile segments, four, five and six to avoid confusion with five mobile segments found in individuals free of LSTV. For example, an L5 LSTV would represent four mobile segments above the variation as the variation is seen to be an extension of the sacrum.

Spinal enumeration associated with lumbosacral transitional vertebrae and control cohorts

Spinal enumeration was compared in the LSTV and control cohorts assessing the number of mobile segments of the spine. The X^2 test could be conducted as it met the necessary parameters for statistical inference.

A statistical significance was found with greater variability in the lumbar spinal enumeration in the LSTV cohort (X^2=136.991, df=2, p<0.001), with a large effect size (V= 0.962) as indicated by the Cramer's V test. Refer to Figure 4.99.

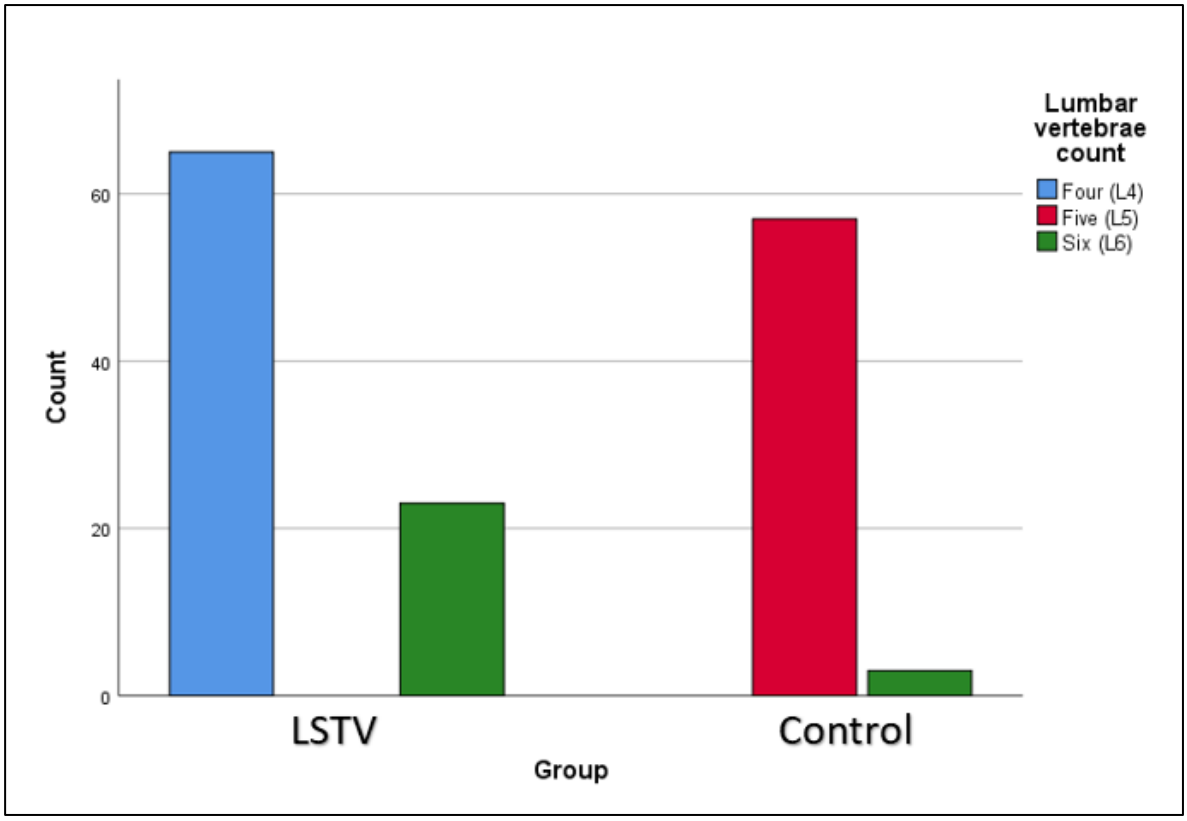

Figure 4.99*: A boxplot graph of the lumbar spinal enumeration for the LSTV and control cohorts.* **Note:** Six lumbar vertebrae in the control cohort does not represent LSTV. There was no dysplastic change of one or both of the transverse process height of the last lumbar vertebra. This is a known variation in lumbar enumeration.

Sex and lumbosacral transitional vertebrae cohort

The X^2 test could be conducted as it met the necessary parameters for statistical inference. Fisher's exact test was used for the analysis of the two column and two-row (2x2) contingency table. No statistical significance was found (X^2=0.00, df=1, *p*=0.995). Therefore, the null hypothesis stands, no relationship is demonstrated between the male sex and LSTV. Refer to 4.100.

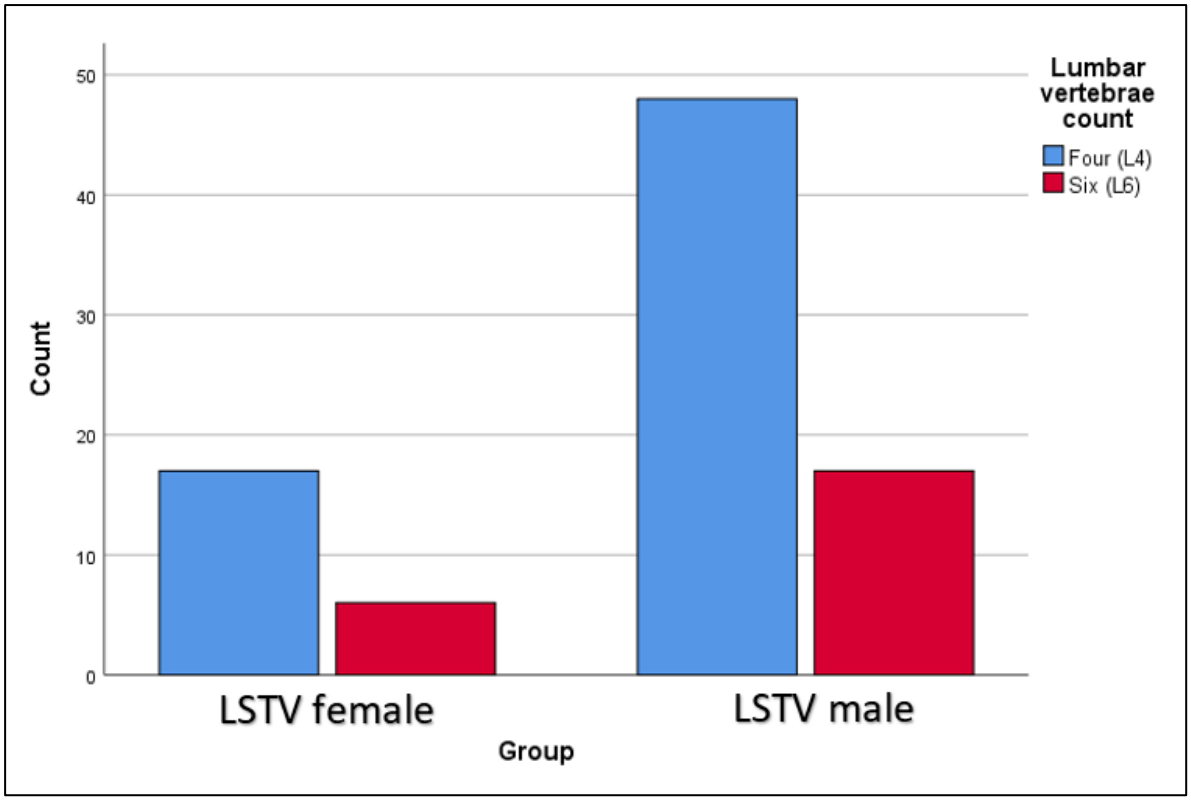

Figure 4.100: *A boxplot graph of the lumbar spinal enumeration for the LSTV cohort comparing the sexes.*

Sex and control cohort

The X^2 test could not be used for statistical inference as it violated the second condition for its use; the expected per-cell count was lower than 2 for 50.0% of cells (X^2=3.376, df=2, *p*=0.66). Fisher's exact test was used for the 2x2 contingency table (X^2=3.376, df=2, *p*=0.107). The general trend was five lumbar vertebrae was the predominant lumbar count. There was insufficient evidence to suggest an association between sex associated with the control cohort. Refer to Figure 4.101.

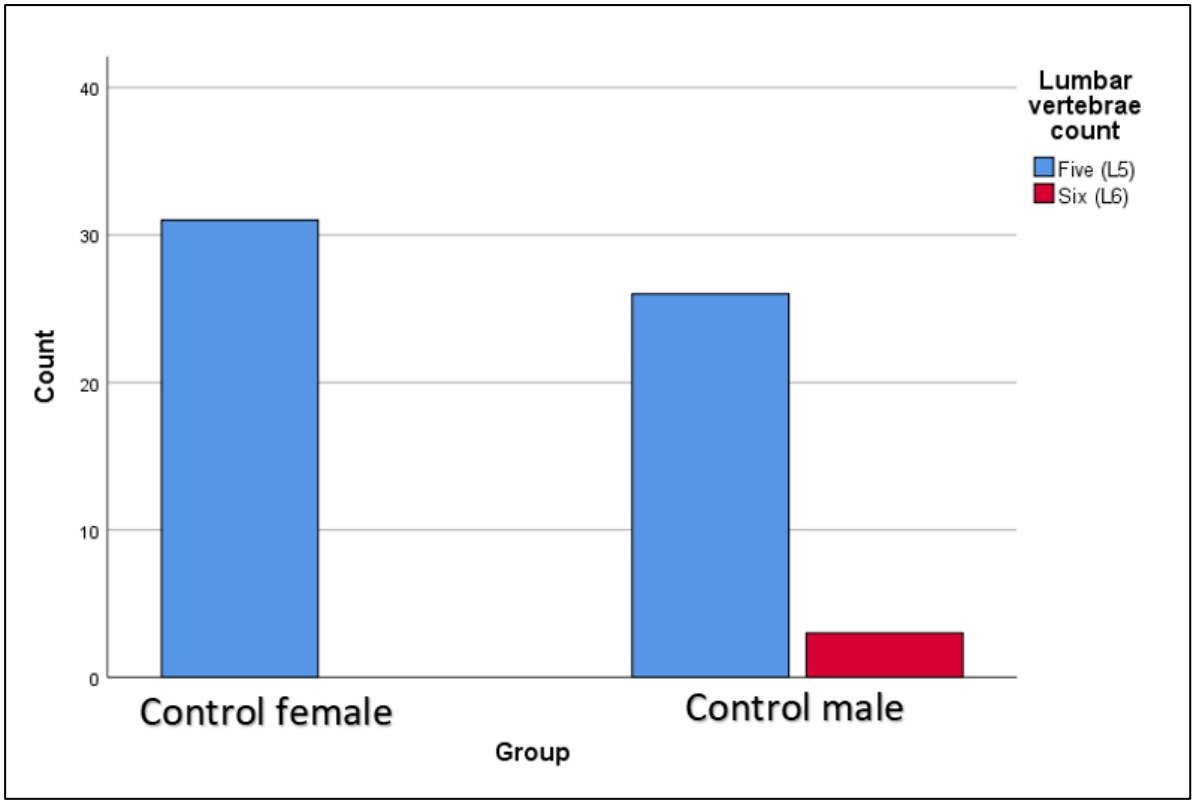

***Figure 4.101**: A boxplot graph of the lumbar spinal enumeration for the control cohort comparing the sexes.*

Sex and cohort comparison

Female

Comparison of the female sex was made between LSTV and control cohorts comparing thoracic spine enumeration. The X^2 test could not be used for statistical inference as it violated the second condition for its use; the expected per-cell count was lower than 2 for 33.3% of cells (X^2=54.00, df=2, p<0.001). There was not enough evidence to suggest an association between the female sex, LSTV and control cohorts and lumbar spinal enumeration changes. Refer to Figure 4.102.

Male

Comparison of the male sex was made between LSTV and control cohorts comparing thoracic spine enumeration. The X^2 test could be conducted as it met the necessary parameters for statistical inference. A statistical significance was found between LSTV and control cohorts of the male sex and lumbar spinal enumeration (X^2=82.047, df=2, p<0.001), with a large effect size as indicated by the Cramer's V test value.

Therefore, the null hypothesis is rejected, a relationship is demonstrated, with a large effect size between the LSTV and control cohorts of the male sex and lumbar spinal enumeration. Refer to Figure 4.103.

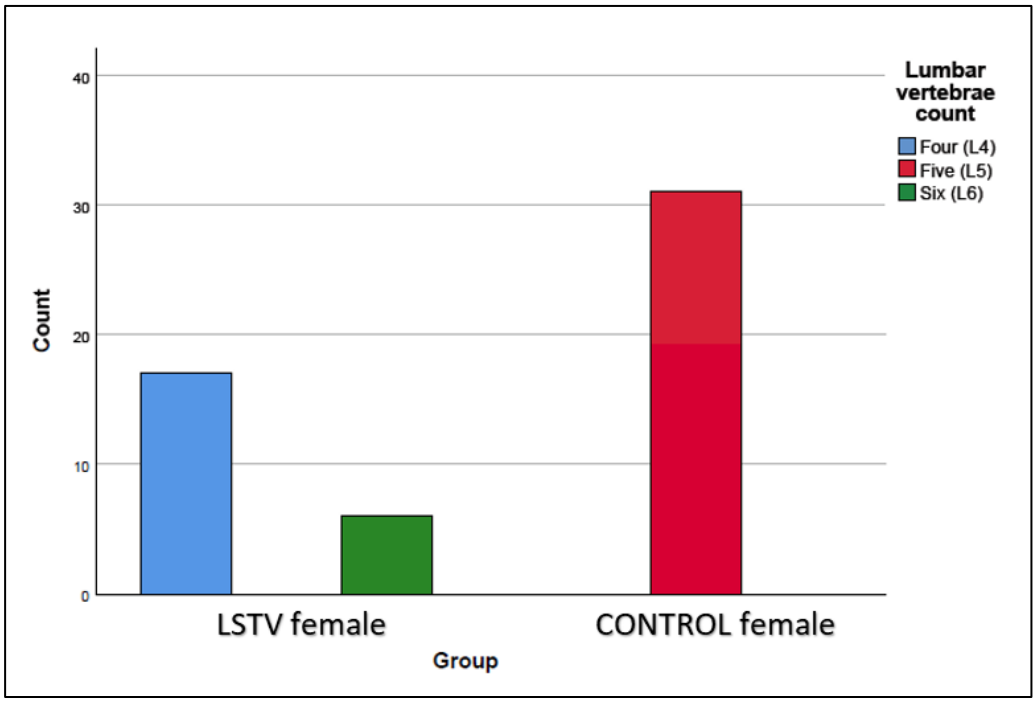

Figure 4.102: A boxplot graph of the lumbar spinal enumeration comparing the female cohorts.

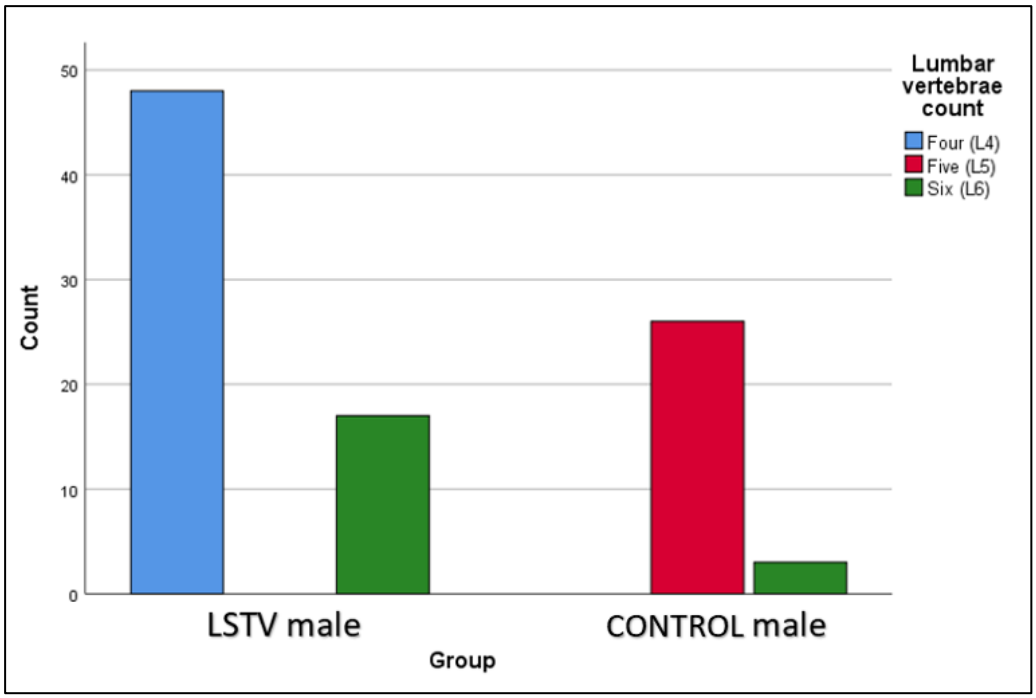

Figure 4.103: *A boxplot graph of the lumbar spinal enumeration comparing the males cohorts.*

Non-metric observations

Noteworthy non-metric observations are listed below and will be discussed in Chapter 5.

Iliolumbar articulation

An additional finding in the osteological cohort was an example of a right-sided Type IIA LSTV with a left-sided articulation between the L5 lumbar transverse process and the ilium. Refer to Figure 4.104.

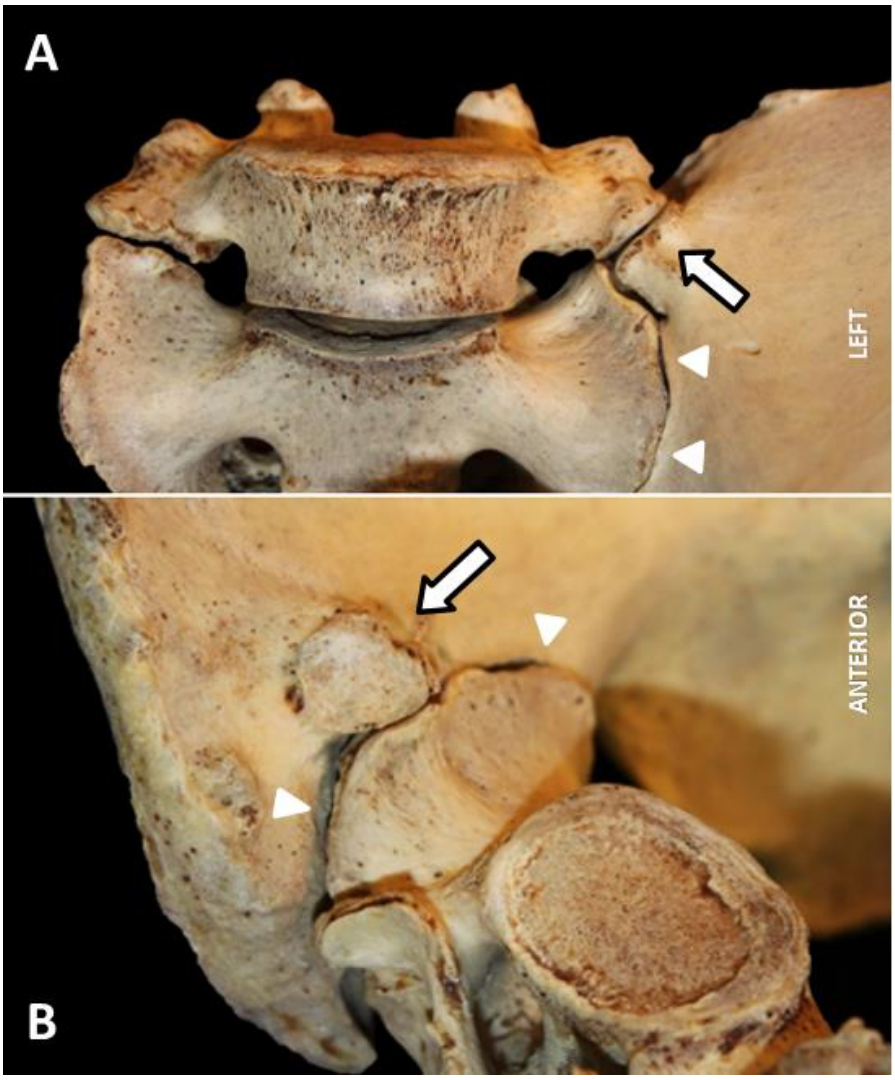

Figure 4.104: *An atypical right-sided Type IIA lumbosacral transitional vertebra.* ***A)*** *An anterior view of the approximate spatial relationship of the lumbosacral junction and sacroiliac articulation containing a right-sided Type IIA lumbosacral transitional vertebra.* ***B)*** *An oblique anterosuperior view of the approximate spatial relationship of the sacroiliac articulation. The arrows indicate iliac articulation for the left transverse processes of the L5 with the ilium. The arrowheads indicate the sacroiliac articulation. Both images are the skeletal remains of the same skeletal individual.* ***Photography and editing:*** *GJ Paton.*

Transverso-sacro-iliac articulation complex

An additional finding in the osteological cohort was examples of Type IIA LSTV of L5, which displayed three articulations. Firstly, the articulation of the auricular surface of the sacrum with the ilium of the pelvis forming the sacroiliac articulation is a normal spinopelvic joint found bilaterally. Furthermore, two additional accessory joints were identified, namely a unilateral or bilateral articulation between the L5 lumbar transverse process and the ala of the sacrum known as the lumbosacral articulation and an articulation of the lumbar transverse process with the ilium of the pelvis known as the iliolumbar articulation. These were found unilaterally (right and left) and bilaterally in the osteological cohort. The tripartite articulation formed a complex, which the author has named the transverso-sacro-iliac articulation complex. Refer to Figure 4.105.

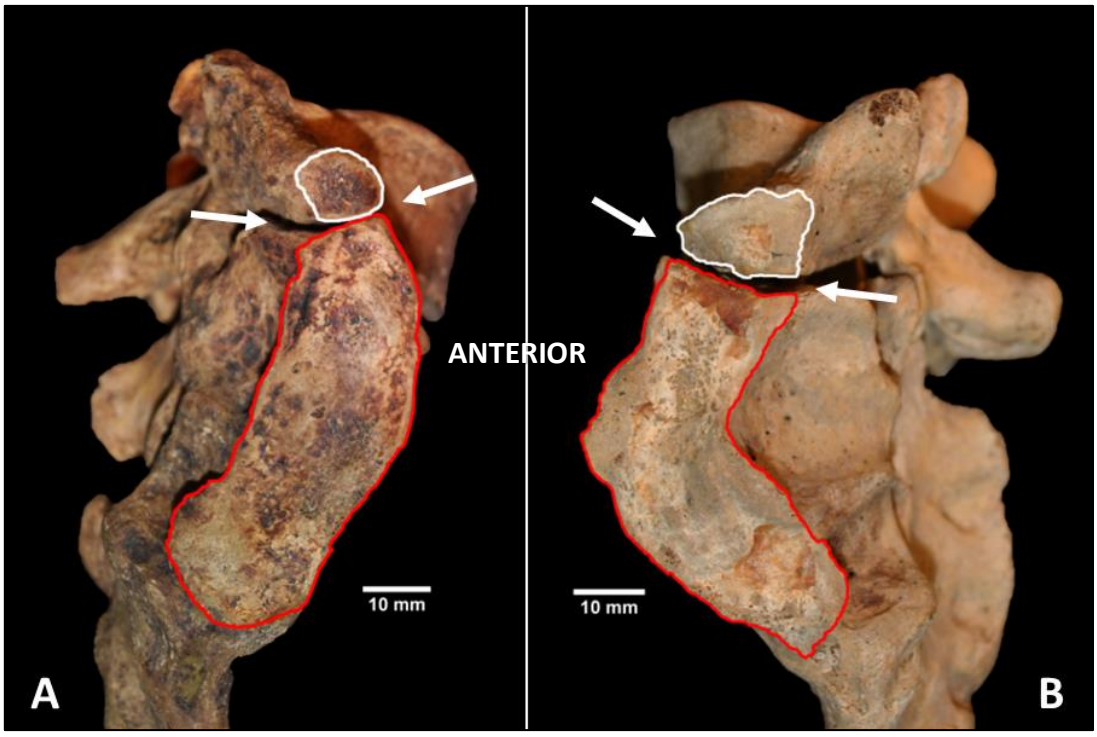

Figure 4.105: *Lumbosacral transitional vertebrae displaying three articulations that contribute to the sacroiliac joints of the pelvic girdle.* ***A)*** *A right lateral view (sacroiliac articulation perspective) of the approximate spatial relationship of the lumbosacral junction and containing a right-sided Type II lumbosacral transitional vertebra.* ***B)*** *A left lateral view (sacro-iliac articulation perspective) of the approximate spatial relationship of the lumbosacral junction and containing a left-sided Type II lumbosacral transitional vertebra. The red outline indicates the articulation of the sacra's auricular surfaces which forms part of the sacroiliac joint. The white outline indicates the articulation of the transverse processes of the lumbosacral transitional vertebrae, which forms part of the sacroiliac joint. The arrows indicate the lumbosacral articulation between the lumbosacral transitional vertebrae and the alae of the sacrum. These articulations together form the transverso-sacro-iliac joint complex.* ***Photography and editing:*** *GJ Paton.*

CHAPTER 5

DISCUSSION

This chapter sets out to discuss pertinent findings of this study. Part 1 relates to the imaging cohort, and Part 2 relates to the osteometric cohort of the study.

Epidemiological variables

Sex

Part 1:

In this study, there was a greater number of female individuals for both the total imaging cohort and the LSTV-containing cohort (n=1614, 52.1% and n=166, 53.9%) compared to male individuals for both cohorts (n=1482, 47.9% and n=142, 46.1%). Females account for 51.2% of the total population in South Africa (SAPSS, 2019). Moreover, females may seek medical services more frequently when compared to men, who tend to ignore symptoms, as has been observed (Hunt et al., 1999; Hunt et al., 2011).

The total sample cohort was marginally in favour of the female sex, which may have compounded a similar finding in the LSTV cohort within this study. A review of the literature suggested that the male sex has a higher rate of LSTV prevalence (Castellvi et al., 1984; O'Driscoll et al., 1996; Apazidis, 2011; Dharati et al., 2012; Nardo et al., 2012; Uçar 2013; Dzupa, 2014; Tang et al., 2014; Gopalan and Yerramshetty, 2018; Alblas, 2019; Park et al., 2019) with the exception of a few studies (Hasner et al., 1953; Radulovska-Chabukovska, 2014; Benlidayi, 2015; De Bruin, 2017; Table 5.1).

This study is in the minority of studies wherein the total imaging cohort, and the LSTV cohort contained a greater proportion of females. Likewise, Radulovska-Chabukovska et al. (2014), Benlidayi et al. (2015) and De Bruin et al. (2017) contained a greater proportion of females in their total cohort samples as well as the LSTV cohorts. Their average LSTV-containing female predominance was 57.3% (60%, 57.6% and 54.4%, respectively). Therefore, this study is similar to the three studies identified and is thought to be higher in LSTV favouring females due to the total cohort containing a greater ratio of female to male patients.

Part 2:

In this study, the osteological cohort demonstrated a male-biased sex distribution housed at WITS in the Dart Collection. Men were the predominant sex in the total osteological cohort as well as the LSTV-containing cohort (n=1307, 72.7% and n=66, 72.5%) when compared to the females for both cohorts (n=491, 27.3% and n=25, 27.5%). Similarly, Alblas (2019) found a male bias in the LSTV cohort (69.9%, n=58/83) from the South African population housed in the Kirsten Skeletal Collection in the Western Cape.

It has been reported that a male bias is common in many cadaveric skeletal collections both in South Africa and North America (Savage, 2005; Hunt & Albanese, 2005; L'Abbé et al., 2005; Komar & Grivas, 2008; Dayal et al., 2009; Alblas et al., 2018; Alblas, 2019). There is no single defined reason for the male sex bias seen in numerous skeletal collections. The author believes the predominance of males within the sample from the Dart Collection is due to unclaimed bodies being over-represented by males. Possible reasons for the male-biased sample may be explained by the migrant working practices in South Africa, where males, seen as the breadwinners, seek work in urban and peri-urban areas (Tal and Tau, 1983; Clark 2007). In the pre-mechanised world, free of large-scale automation, labour was needed. Men fulfilled the physical role needed for jobs such as mining. Job opportunities thus attracted men to the adjacent mines and industries in the vicinity of WITS. Upon their deaths, many of their bodies remained unclaimed which allowed the use of their bodies in medical training through cadaveric teaching. A bias towards unclaimed bodies from the early to late twentieth-century by WITS for medical training may have inadvertently led to more men than women in the cadaver medical programme. Due to the influx of men to Johannesburg and nearby surrounds, men would have been more prevalent as they sought job opportunities in the mining and industrial sectors (Lucas, 1985).

Conversely, Savage (2005) found that the LSTV-containing cohort contained a female bias of 8.2% while the male proportion was 6.7% of the total sample. This contrasts with the total sample cohort containing 83% (n=2340/2803) male skeletal remains.

Savage's (2005) study was the largest osteometric study containing LSTV (n=196/2803) in the literature. Although Savage's (2005) skeletal sample contained a greater male prevalence which is in line with the majority of skeletal collections (Hunt & Albanese, 2005, L'Abbé et al., 2005; Komar & Grivas, 2008; Dayal et al., 2009, Alblas et al., 2018; Alblas, 2019) the LSTV-containing cohort was female-biased. One possible explanation for the female-bias may be that the Hamann-Todd collection from which the skeletal remains were studied is located in Cleveland, Ohio, USA. Few skeletal remains were born in the area, thereby creating a heterogeneous mixture of populations in one skeletal collection. This mixture of population demographics may have allowed LSTV containing females to be included in the skeletal collection.

Age

Part 1

The average age for the entire imaging cohort group was 47.10 years (SD 15.26 years) (N=3096). The average age of males without LSTV was 47.31 years (n=1340) (SD 15.23 years) and the average age of females without LSTV was 47.13 years (n=1448) (SD 14.62 years). By contrast, the males within the LSTV cohort had an average age of 45.90 years (n=142) (SD 16.08 years) and the average age of females with the LSTV cohort was 47.40 years (n=166) (SD 13.03 years). The age range for both the males and females in the cohort without LSTV was between 16 and 88 years. Comparison to reviewed LSTV studies found that the age range was comparable. Tang et al. (2014) had an average age of 40.9 years, while Park et al. (2019) averaged 55.17 years. The average age ranges seen reflect criteria such as the subjects' geographical location, access to imaging, financial means, transport difficulties, and work commitments, to name a few.

Part 2

In the Dart Collection of skeletal samples, the average AD for the total sample group was 45.10 years (SD 12.23 years) (N=1797). The minimum AD was 21 years, and the maximum age was 65 years old for both male and female cohorts. The average AD for the male cohort was 45.63 years (standard deviation 11.81 years), and the female cohort was 43.62 years (SD 13.18 years).

By comparison the average AD for the LSTV skeletal cohort was 42.70 years (n=91) (SD 12.41 years). The minimum AD for the LSTV sample was 21 years while the maximum was 65 years old. The average AD for the male LSTV sample was 43.5 years (SD 11.76 years) and for the female LSTV sample was 40.67 years (SD 12.99 years). These ages reflect the skeletal samples housed in the Dart Collection and are influenced by their time of collection. The skeletal samples that had a younger AD may have been collected when life expectancy was lower as compared to now. The physically strenuous conditions may have contributed to earlier deaths, and social conditions resulted in more bodies being unclaimed. Other factors leading to early death may be styles of life from rural to urban and the change in diet that may be associated with geographical location. Kramer et al. (2019) reports that bequests/donations has become the main source of acquisitions to the Dart Collection in recent times. Thus the general age of cadavers at AD across ethnicities has steadily increased as bequests/donations are typically of the aged and life expectancies have increased (Kramer et al., 2019). The improved longevity of the population is likely due to improved medical technology, changes in lifestyle, and greater access to healthcare. This may lead to a bias for older-aged individuals over time due to bequests. Similarly, Alblas' (2019) osteological cohort contained an average age of 48.4 years.

Lumbosacral transitional vertebrae prevalence

The prevalence of LSTV in this study of the South African population was determined from radiographs (n=3096) and found to be 10.0% (Types II, III and IV). No statistically significant differences were found between the three ancestral groups for their prevalence of LSTV. A comparative literature search was conducted to compare the results of this study to comparable studies performed around the globe, since the introduction of the Castellvi et al. (1984) classification.

By contrast, the prevalence of LSTV in the literature is widely variable, 3.3% to 35.6% (Erken, 2002; Apazidis, 2011; Uçar et al., 2013) (see Table 1.10). The reasons for such greatly variable prevelance rates may be explained by cofounding variables within different populations, diagnostic criteria, imaging techniques, and natural variation in phenotypic expression (Mahato, 2011; Doo et al., 2020).

Sixty-six studies have been published globally between the years 1984 and 2021 that utilise the Castellvi et al. (1984) classification, which is the most widely used classification system of LSTV (Konin & Walz, 2010; Mahato, 2013; Jancuska et al., 2015; Matson et al., 2020) (see Table 1.10).

The average prevalence for LSTV, Types II, III and IV in Table 5.1 was 10.3% which is almost identical to prevalence rate found in this study at 10% of the South African population.

The similarity in prevalence of LSTV is likely due to the heterogeneous mixture of individuals within the South African population. Furthermore, it indicates that the South African population conforms to the average prevalence of LSTV and is not significantly affected by the lumbosacral spinal variation. Direct comparison is difficult as there is paucity in the literature for African-ancestry and Mixed-ancestry LSTV prevalence studies. Compounding the difficulty in comparison is the heterogeneous mixture of populations that has seen greater migration of formerly isolated ethnic and cultural groups.

The average prevalence of LSTV increases when Types I to IV is included and was 19.3%. The removal of Type I LSTV morphology decreases prevalence to 10.3% (Table 5.1). The sixty-six studies, including the infamous Castellvi et al. (1984) study, were appraised for their detail on LSTV classification. The appraisal of the literature found that 25 studies contained sufficient detail on LSTV classification. Within the 25 eligible studies, 16 studies contained the Type I LSTV morphological classification within their prevalence report of findings while nine studies contained Types II to IV LSTV morphological classification (see Table 5.1).

It is interesting to note, in the literature the prevalence of LSTV has been suggested to be higher in LBP studies compared to general population studies (Ileeze et al., 2018). However, when comparing studies that comprised LBP within their inclusion criteria (highlighted in red in Table 5.1), there appeared to be no substantial difference (Table 5.3) as suggested by Peterson et al. (2005) ; Seçer et al. (2009) and Nardo et at. (2012). Therefore, the literature does not seem to substantiate the assertion by many authors (Tini et al., 1977; Luoma et al., 2004; Apazidis et al., 2011) that LBP-focused sampling methods contain higher LSTV prevalence rates over general population sampling methods.

Non-specific LBP is complex in nature with a multifactorial aetiology (Mousavi et al., 2019) and this forms the basis for the limitation to these LBP studies. A causal link between LBP and increased prevalence of LSTV has not been established but the presence of LSTV may bias an individual to lumbosacral pain (Jönsson et al., 1989; Santavirta et al., 1993; Avimadje et al., 1999; Jancuska et al., 2015; Shinonara et al., 2021). Importantly, there are numerous cases of LBP in the literature which have been ascribed to the presence of LSTV (Jönsson et al., 1989; Santavirta et al., 1993; Avimadje et al., 1999; Brault et al., 2001; Connolly et al., 2003; Jancuska et al., 2015; Adams et al., 2018; Shinonara et al., 2021).

Savage (2005) found a greater prevalence of LSTV in the imaging cohort associated with LBP when compared to an osteological cohort. In the current study, the prevalence of LSTV in the imaging cohort (10.0%) was greater than that of the osteological cohort (6.3%). There may have been an unintentional selection bias in the imaging cohort for which LBP, in part, was at least one factor for medical consultation and imaging at hospitals selected for data collection.

From a West African perspective, Olofin et al. (1994); Oyinloye et al. (2009) and Njeze et al. (2018) studied African cohorts outside of South Africa, in Nigeria. Olofin and colleagues (1994) found a prevalence of 37% while Oyinloye et al. (2009) found 9.1% and Njeze et al. (2018) found 8.1% of the Nigerian population contained LSTV on radiographs. No details of the Types, subtypes, or frequency of side were contained within their studies. A possible reason for the great disparity in prevalence rate for Olofin et al. (1994) within the Nigerian population over the more recent Nigerian studies may be due the technological limitations of the time as radiographic technology 27 years ago did not produce images with the same clarity as today's equipment and computer software. Furthermore, Olofin et al. (1994) lacked images in their publication. The Castellvi et al. (1984) classification was known to Olofin et al. (1994) as they had cited the system of classification research in their publication. It remains an unknown why LSTV sub-classification was not detailed in their study of the prevalence of LSTV in a Nigerian population.

The prevalence of lumbosacral transitional vertebrae by Types

The prevalence of LSTV in imaging cohort by Type, namely Type II, III and IV in this study was 67.9% (n=209/308), 27.6% (n=85/308) and 4.5% (n=14/308) respectively (Table 3.5). When compared to 24 studies from around the world Type II, III and IV prevalence was 52.9%, 29.8% and 8.3% respectively (Table 5.1). The general global trend is in keeping with this study. The order from highest prevalence was Type II followed by Type III and lastly the least prevalent Type of LSTV is Type IV.

There is great variability in the prevalence rates of LSTV classified by Type (Table 5.1). Type II prevalence varied between 13.2% and 75.7%, Type III prevalence varied between 6.7% and 48%, and Type IV prevalence varied between 0% and 15.3% in the literature (Table 5.1).

The prevalence of lumbosacral transitional vertebrae by subtypes

The order of prevalence of LSTV classified by subtype found in this study was subtypes IIA, IIB and IIIA and IIIB in this study was 41.9% (n=129/308), 26.0% (n=80/308), 5.8% (n=18/308), 21.8% (n=67/308) respectively (Table 3.6). When the results of this current study are compared to the prevalence of LSTV by subtype in the literature it was found they had a similar pattern. Tables 5.1 and 5.2 found subtypes IIA, IIB, IIIA and IIIB prevalence was 25.2%, 18.2%, 5.6% and 17.9%. The general global trend was in keeping with this study albeit this study contained higher prevalence proportions for subtypes IIA and IIB. Interestingly, subtype IIIA had almost the same percentage corresponding to a Type IIIA in Table 5.2.

Type IIIA can be seen as a battle of two identities. One side represents fusion to the ala of the sacrum by the lumbar transverse process while the contralateral side is almost unmodified from the typical morphology of a lumbar vertebra. A possible explanation may be that this is a form of sagittal axial patterning where left and right sides developed independently rather than an axial patterning model. This would be controlled through HOX gene expression and may be a less common form of spinal development. As with axial patterning, partial failure of separation or fusion associated with segmentation and resegmentation processes of vertebrogenesis during embryonic development may be at fault. Barnes (2012) stated partial homeotic shifts exist in which incomplete or complete change in characteristics may be seen.

The prevalence of lumbosacral transitional vertebrae by frequency of side

The frequency of side namely left, right and bilateral in this study was 26.6% (n=82/308), 21.1% (n=65/308), 47.7% (n=147/308) respectively (Table 3.7). Unfortunately, when compared to Tables 5.2 encompassing 17 studies there was a failure to specify, in the literature, which side was affected or involved in unilateral LSTV morphology. Only two of the listed studies gave detail of the side associated with the subtypes of LSTV, namely Quinlan et al. (2006) and Hanhivaara et al. (2020).

No inference can be made on whether this study aligns with or differs from the trend in frequency of side globally due to lack of available information.

When compared to the three African studies, (Olofin et al., 1994; Oyinloye et al., 2009; Njeze et al., 2018), once again inadequate information prevents comparison as none of the three articles contained information on frequency of side.

The prevalence of lumbosacral transitional vertebrae by subtype and frequency of side

It was not possible to compare subtype and frequency of side due to a significant lack of information regarding frequency of side. This highlights the paucity of information regarding unilateral LSTV morphology and side of accessory articulation. The subtype and frequency of side in this study found Type IIA right 18.8% (n=58/308), Type IIA left 23.1% (n=71/308), Type IIB 26% (n=80/308), Type IIIA right and Type IIIA left contained 2.9% (n=9/308) of the sample for each and Type IIIB 21.8% (n=67/308) (Table 3.8).

Spinal enumeration associated with lumbosacral transitional vertebrae

In the current study, the lumbar vertebral column enumeration was subdivided into sacralisation and lumbarisation. The majority of spinal enumeration associated with LSTV was sacralisation which represented 64.0% (n=197/308) while lumbarisation accounted for 36.0% (n=111/308) of the sample. Sacralisation represented LSTV morphology at L5 while lumbarisation represented LSTV morphology present at L6.

Worldwide, sacralisation is the predominant spinal enumeration associated with LSTV (Table 1.10). From an African perspective, the Olofin et al. (1994) prevalence study recorded spinal enumeration in favour of sacralisation over lumbarisation (64%>36%). In similarity to Olofin and colleagues research, this study found in favour of a sacralisation over lumbarisation. The difference in spinal enumeration in percentage between this study and that of Olofin et al. (1994) may be due to increased X-ray quality for improved radiographic appraisal. All three of the ancestral groups featured in this study favoured sacralisation with the Mixed-ancestry containing the greatest percentage (72.9%, n=70/96) while the African-ancestry contained the greatest quantity (n=73/109, 67%). The European-ancestry cohort consisted of the least in both number and percentage (n=54/103, 52.4%) of the sample. Refer to Table 5.1.

Table 5.1: Lumbosacral transitional vertebrae prevalence comparison by Type and sex.

First Author	Year	Sample size	Transitional Vertebrae (I-IV)	Removal Type I Transitional Vertebrae (II-IV)	Type I	Type II	Type III	Type IV	Sex (LSTV)	
									Male	Female
Haffer	2021	819	**53** (6.5%)	**33** (4%)	**16** (30.2%)	**23** (43.4%)	**7** (13.2%)	**7** (13.2%)	**28** (52.8%)	**25** (47.2%)
Luo	2020	1180	**262** (13.9%)	**105** (5.6%)	**157** (59.9%)	**85** (32.4%)	**8** (3.1%)	**12** (0.64%)	*	*
Hanhivaara	2020	3855	**1101** (29%)	**347** (9.7%)	**754** (68.4%)	**171** (15.5%)	**143** (13.0%)	**33** (3.0%)	*	*
Tucker	2019	560	**71** (12.7%)	**24** (4.3%)	**46** (69.0%)	**15** (21.1%)	**7** (9.9%)	**3** (4.2%)	*	*
Ono	2018	347	*	**70** (20.17%)	N/A	**53** (75.7%)	**13** (18.6%)	**4** (5.7%)	*	*
Apaydin	2018	1875	**600** (32%)	**201** (10.7%)	**399** (66.5%)	**131** (21.8%)	**48** (8%)	**22** (3.6%)	*	*
Khan	2018	4939	**574** (11.6%)	**444** (9%)	**130** (22.6%)	**258** (44.9%)	**144** (25.1%)	**42** (7.3%)	**322** (56.1%)	**252** (43.9%)
Illeez	2018	500	**130** (26%)	**101** (20.2%)	**39** (30.0%)	**75** (57.7%)	**7** (5.4%)	**9** (6.9%)	*	*
Shaikh	2017	504	*	**75** (15%)	N/A	36 (48%)	**39** (52%)	0	*	*
De Bruin	2017	273	**68** (24.9%)	**33** (12.1%)	**35** (51.15%)	**11** (16.2%)	**17** (25.0%)	**5** (7.4%)	**31** (45.6%)	**37** (54.4%)
Sarawagi	2016	317	**81** (25.5%)	**69** (21.8%)	**12** (14.8%)	**36** (44.4%)	**31** (38.3%)	**2** (2.5%)	*	*
Benlidayi	2015	1588	*	96 (6.1%) (n=**85**[1])	N/A	**32** (37.6%)	**40** (47.1%)	**13** (15.3%)	**36** (42.4%)	**49** (57.6%)
French	2014	5429	*	**540** (9.9%)	N/A	**224** (41.5%)	**259** (48.0%)	**57** (10.6%)	*	*
Sekharappa	2014	3000	*	**390** (13%)	N/A	**177** (45.4%)	**173** (44.4%)	**28** (7.2%)	**240** (61.5%)	**150** (38.5%)
Tang	2014	5860	**928** (15.8%)	**512** (8.7%)	**416** (44.8%)	**400** (43.2%)	**67** (7.2%)	**45** (4.8%)	**567** (61.1%)	**361** (38.9%)
Radulovska-Chabukovska	2014	200	*	**64** (31.5%)	N/A	**24** (38.1%)	**22** (34.9%)	**4** (6.3)	**25** (40%)	**38** (60%)

Table 5.1: (Continued)

First Author	Year	Sample size	Transitional Vertebrae (I-IV)	Removal Type I Transitional Vertebrae (II-IV)	Type I	Type II	Type III	Type IV	Sex (LSTV)	
									Male	Female
Paik	2013	8280	*	**877** (10.6%)	N/A	**509** (58.0%)	**308** (35.1%)	**60** (6.8%)	*	*
Uçar	2013	3607	**683** (18.9%)	**483** (13.4%)	**335** (49.0%)	**125** (18.3%)	**119** (17.4%)	**41** (6.0%)	**369** (54%)	**314** (46%)
Bulut	2013	1000	**190** (19.0%)	**168** (16.8%)	*	*	*	*	**97** (51.1%)	**93** (49%)
Nardo	2012	4636	**841** (18.1%)	**492** (10.6)	**351** (41.72)%	**349** (41.4%)	**97** (11.5%)	**44** (5.2%)	**539** (64.1%)	**302** (35.9%)
Sharma	2011	206	**38** (18.6%)	**24** (11.7%)	**14** (36.8%)	**5** (13.2%)	**17** (44.7%)	**2** (5.3%)	**26** (68.4%)	**12** (31.6%)
Apazidis	2011	211	**75** (35.6%)	**49** (23.2%)	**49** (65.3%)	**17** (22.7)%	**7** (9.3%)	**2** (0.9%)	**40** (53%)	**35** (46.7%)
Quinlan	2006	769	*	**35** (4.6%)	N/A	**35** (100%)	**0**	**0**	**22** (63%)	**13** (37%)
Hsieh	2000	1668	*	**67** (4%)	N/A	**21** (45%)	**18** (39%)	**6** (13%)	**35** (52.2%)	**32** (47.8%)
Castellvi	1984	200	**60 ^** (30%)	**35** (17.5%)	**25** (41.7%)	**23** (38.3%)	**5** (6.7%)	**3** (5%)	**43** (71.7%)	**17** (28.5%)
TOTAL		**50623**	**5625/29109** [a] **(19.3%)**	**5363/51823** [b] **(10.3%)**	**2778/5625** [c] **(49.4%)**	**2835/5363** [d] **(52.9%)**	**1596/5363** [e] **(29.8%)**	**444/5363** [f] **(8.3%)**	**2420/4287** [g] **(56.4%)**	**1730/4287** [h] **(40.4%)**

***** – Lack of detailed information regarding LSTV Type I classification counts.***

***a** – Indicates the total sample size that contains information on LSTV Types I to IV numbers (n=29109).*

***b** – Indicates the total sample size that contains information on LSTV Types II to IV numbers (n=50623).*

***c** – Indicates the total sample size of lumbosacral transitional vertebrae Types I to IV.*

***d, e, f** – Indicates a total sample size of lumbosacral transitional vertebrae Types II to IV.*

***g, h** – Indicates studies that contained sex count including Type I lumbosacral transitional vertebrae as only 5 studies contained sex counts which excluded Type I lumbosacral transitional vertebrae.*

***^** – 4 patients presented with full lumbarisation of the first sacral vertebra (six lumbar vertebrae without any change of the lumbar transverse processes).*

***1** – 11 patients were excluded from frequency count and analyses. Percentages reflect n=85 for the LSTV cohort.*

Sex percentages were calculated on the number of individuals in the LSTV cohort and not the total sample cohort.

Authors in red text represent studies that included low back pain or studied Bertolotti's syndrome.

Table 5.2: Lumbosacral transitional vertebrae categorised by subtype and frequency of side from the literature.

FIRST AUTHOR	YEAR	SUBTYPE and FREQUENCY OF SIDE					
		TYPE IIA		TYPE IIB	TYPE IIIA		TYPE IIIB
		TYPE IIA LEFT	TYPE IIA RIGHT		TYPE IIIA LEFT	TYPE IIIA RIGHT	
Haffer	2021	**14** (26.4%)		**9** (17%)	**5** (9.4%)		**2** (3.8%)
Luo	2020	**60** (3.2%) #		**25** (1.3%)	**8** (0.4%) #		**0**
Hanhivaara	2020	* (Left>Right)+		*	* (Left >Right) +		*
Tucker	2019	**27** (28.0%)		**19** (26.8%)	**2** (0.4%)		**5** (7.0%)
Ono	2018	**29** (41.4%)		**24** (34.3%)	**8** (11.4%)		**5** (7.1%)
Apaydin	2018	**43** (7.2%)		**88** (14.7%)	**22** (3.7%)		**26** (4.3%)
Illeez	2018	**134** (26.9%)		**154** (30.8%)	**4** (0.8%)		**24** (4.6%)
Khan	2018	*	*	*	*	*	*
Shaikh	2017	*	*	*	*	*	*
De Bruin	2017	**4** (5.9%)		**7** (10.3%)	**1** (1.5%)		**16** (23.5%)
Sarawagi	2016	**11** (13.6%)		**25** (30.9%)	**4** (4.9%)		**27** (33.3)
Benlidayi	2015	**20** (23.5%)		**12** (14.1%)	**9** (10.6%)		**31** (36.5%)
French	2014	*	*	*	*	*	*
Sekharappa	2014	**157** (40.3%)		**20** (5.1%)	**22** (5.6%)		**151** (38.7%)
Tang	2014	*	*	*	*	*	*
Radulovska-Chabukovska	2014	**24** (38.1%)		**22** (34.9%)	**4** (6.3%)		**4** (6.3%)
Paik	2013	**349** (39.8%)		**160** (18.2%)	**46** (5.2%)		**262** (29.9%)
Uçar	2013	**75** (11.0%)		**50** (7.3%)	**36** (5.3%)		**83** (12.2%)
Bulut	2013	**75** (39.5%)		**50** (26.3%)	**36** (18.9%)		**41** (21.6%)
Nardo	2012	*	*	*	*	*	*
Sharma	2011	**4** (10.5%)		**1** (2.6%)	**6** (15.8%)		**11** (28.9%)
Apazidis	2011	4.3%		3.8%	1.9%		1.4%
Quinlan	2006	**5** (14.3%)	**3** (8.6%)	**27** (77.1%)	**0**	**0**	**0**
Hsieh	2000	**14** (30%) *		**7** (15%)	**4** (9%) *		**8** (17%)
Olofin	1994	*		*	*		*
Castellvi	1984	**12** (20%)		**11** (18.6%)	**1** (1.6%)		**4** (6.7%)
TOTAL		**985/3905** [a] **(25.2%)**		**711/3905** [a] **(18.2%)**	**218/3905** [a] **(5.6%)**		**700/3905** [a] **(17.9%)**

***** – *Indicates no data on frequency of side was available in the literature.*

+ – *Study indicated unilateral LSTV was more common on left side than the right.*

– *Left-sided LSTV was found in 52% (n=89) and right-sided LSTV was found in 49% (n=43) of 172 unilateral LSTV cases. No breakdown for frequency of side for each Type of LSTV was provided.*

a – *Indicates the total sample size that contains information on subtype and or frequency of side numbers (n=3905).*

Authors in blue font were excluded because of lack of detail or participant numbers.

Table 5.3: Literary comparison of lumbosacral transitional vertebrae prevalence rates associated with and without low back pain.

Lumbosacral transitional vertebrae studies	Total LSTV number Types I-IV	Total LSTV number Types II-IV	Total number of participants
LSTV studies including LBP	**4349** (15.1%)	**3074** (10.7%)	28832
LSTV studies excluding LBP	**3545** (15.6%)	**2185** (9.6%)	22791

Ancestry in the literature

In the current study no statistically significant differences were found between the three ancestries and LSTV prevalence. This finding is supported by earlier work performed by Nardo et al. (2012) who found no statistically significant difference in the rate of LSTV prevalence amongst various ancestral groups. No link has been identified to favour one ancestry over another. Reports of prevalence of LSTV, even among the same population groups, have a high range of variability (Table 1.10).

The report of findings of ancestry in the literature is lacking. Many studies considered population homogenisation (e.g. Australian or Asian population) when reporting their findings and did not include a breakdown of ancestry, ethnic groupings or racial background (Castellvi et al., 1984; Vergauwen et al., 1997; Nardo et al., 2012; French et al., 2014; Park et al., 2019; Hanhivaara et al., 2020; Luo et al., 2021). This can be seen in the majority of LSTV studies, especially those with large sample sizes (Paik et al., 2013; Uçar et al., 2013; French et al., 2014; Sekharappa et al., 2014; Tang et al., 2014; Hanhivaara et al., 2020). Three African-based studies were identified in literature, all from Nigeria, namely Olofin et al. (1994); Oyinloye et al. (2009) and Njeze et al. (2018). Their prevalence of LSTV findings were 37%, 9.1% and 8.1%, respectively.

Savage (2005) osteological study found African-American (African-ancestry) cohort had 7.5% prevalence of LSTV (females > males) while the European-ancestry cohort had 6.7% prevalence of LSTV (females > males). Minor variances were noted but no statistically significant differences were found between ancestries and sexes.

Imaging cohort statistical findings

Two significant results were found in the imaging cohort when comparing lumbarisation and sacralisation.

Firstly, a statistical significance with small effect size (V=0.178) was identified between ancestry and spinal enumeration (p=0.008). The African-ancestry (67.0%) and Mixed-ancestry (72.9%) demonstrated a greater affinity for sacralisation over the European-ancestry which demonstrated only marginally in favour of sacralisation (52.4%) preference.

In the literature, sacralisation ranged from 14.1% to 100% of the LSTV cohorts and lumbarisation ranged from 1.7% to 100% (Table 1.10). The average for sacralisation from Table 1.10 was 52.7% and lumbarisation was lower at 47.3%.

In the literature, Hald et al. (1995) found sacralisation to be higher than lumbarisation, at 7.8% versus 5.9%, respectively, in a German population sample. By contrast, French et al. (2014) found in their Australian population that the prevalence of lumbarisation was 58.3% while sacralisation accounted for 41.7% of the sample. In this study the European-ancestry cohort was found to contain 47.6% lumbarisation. It appears there is variability in the presentation of sacralisation and lumbarisation in European-ancestry populations. Migration is likely the main contributor to the genetic variability. Migration across Europe over many centuries has been led by urbanisation with greater work prospects in cities. Other reasons include conflict and spread of religious beliefs (Tilly, 1976).

In a West African specific study, Olofin et al. (1994) found lumbarisation accounted for 34% while the predominant finding was sacralisation (64%). The African-ancestry cohort in this current study contained the greatest frequency of sacralisation which was similar to Olofin et al. (1994). (n=73/109, 67%).

Alblas (2019) studied the largest cohort of Mixed-ancestry skeletal remains containing LSTV in South Africa but did not report on spinal enumeration. No comparison could be made for the Mixed-ancestry cohort in this current study. The Mixed-ancestry cohort contained the greatest percentage of sacralisation (72.9%, n=70/96) of all three ancestries in this current study.

Secondly, a statistical significance with a medium effect size (*V*=0.256) was found in males (*p*=0.010) when comparing ancestry and spinal enumeration. This was interpreted as there being a difference in spinal enumeration between the three ancestral cohorts in the male sex cohort. The African-ancestry (n=34/48) and Mixed-ancestry (n=33/42) contained 71% and 79% sacralisation while the European-ancestry accounted for only 50% sacralisation (n=26/52). In the literature, sacralisation has a higher frequency in men (Erken et al., 2002; Mahato, 2010; Mahato, 2011). The reason believed to influence sacralisation in males is that males generally contain more overall body mass, which may lead to higher stress loads on the lumbosacral junction and thus may contribute to the ultimate form of the LSTV (Mahato, 2011).

The finding in the European-ancestry represents a deviation from the male-dominant pattern of sacralisation reported to date as well as for the African-ancestry and Mixed-ancestry groups in this study. A possible reason for this may lie in the homeotic shifting of the transitional areas of the spine. Homeotic shifts may occur at both the lumbosacral border and the thoracolumbar junction leading to concomitant LSTV and thoracolumbar transitional vertebrae (TLTV) (Hughes and Saifuddin, 2004; Park et al., 2016). It has been reported that abnormal rib counts may occur in association with LSTV as high as 12.6% (Nakajima et al., 2014; Park et al., 2016; Doo et al., 2020). The European-ancestry cohort may have experienced a higher prevalence in TLTV leading to greater lumbarisation due to the method of enumeration relying on thoracic rib count.

Osteometric findings

There were multiple statistically significant findings for the osteometric analyses of LSTV. These were clustered and discussed in five designated groupings used for the statistical analyses to reduce the complexity of the discussion. Refer to Table 4.10 for a summary of the significant results.

Lumbosacral transitional vertebrae prelude

The lumbar vertebral column, free of pathologies, is composed of three joint joints per vertebral level. These include a central articulation of the IVD with adjacent superior and inferior vertebral bodies and two zygapophyseal joints. The addition of Type II LSTV morphology would add one or two extra articulations at the lumbosacral level.

In effect, the base-of-support at the Type II LSTV will be expanded and may contain up to five areas of load transmission, thereby creating a stabilising effect at the lumbosacral junction. It is unequivocal that there is increased stability between LSTV and the sacrum as long as there is contact between the lumbar TVP and ala of the sacrum. This stabilising effect is irrespective of morphological Type (II-IV) (Wigh and Anthony, 1981; Catsellvi et al., 1984; Luoma et al., 2004; Aihara et al., 2005; Konin and Walz, 2010; Mahato, 2013b; Zhang et al., 2017; Hanhivaara et al., 2020). The osteometric finding of a statistically significant increase in TVPH associated with the LSTV cohort for both sexes is a characteristic feature for LSTV morphology.

Interestingly, accompanying the change in TVPH was a statistically significant increase in TVPL for all the LSTV cohorts, male and female. This is thought to be due to the size of the accessory articulation requiring greater length to accommodate the accessory facet.

Control male and female cohort comparison

The following osteometric dimensions demonstrated statistically significant differences between the control sex cohorts for males and females. All findings were in favour of the larger male osteometric dimensions. These were D2 (SBW), D3 (SBL), D6 (IFD*med*), D10 (AL) right and left, D15 (ASA) right and left, D18 (BSA) and D22 (TLE). Refer to Table 4.10 for a summary of the statistically significant osteometric results.

Males generally contain a larger overall body mass, which necessitates greater stability and support from the vertebral column to perform daily tasks. Taylor and Twomey (1984) reported that males presented with a smaller vertebral body height/ transverse diameter index.

Similarly, Zlolniski et al. (2019) found female vertebrae to have a greater vertebral body height whereas male vertebrae showed larger transverse and anteroposterior lengths relative the vertebral body height. These findings are in similarity to the findings in this study.

The SBW, SBL, IFD*med*, bilateral AL and bilateral ASA increase the base-of-support necessary for weight bearing and stabilise the forces of the increased mass carried by males. The bilaterally elongated AL as well as the enlarged ASA, which forms part of the sacroiliac joints, enables greater spinopelvic stability by increasing both form and force closure mechanisms of stability during bipedal ambulation.

Lumbosacral transitional vertebrae cohort and control cohort comparison

The following osteometric dimensions demonstrated statistically significant differences between the LSTV and control cohorts. The control cohort demonstrated larger values for D2 (SBW), D5 (IFD*lat*), D7 (FD), bilateral D8 (SFH), bilateral D9 (SFW), D11 (FA) left side, D12 (SHL), bilateral D17 (FSA) and D18 (BSA).

The LSTV cohort demonstrated larger values for D1 (SH), D4 (IAD), bilateral D10 (AL), bilateral D13 (TVPL) and D14 (TVPH), D22 (TLE) and D23L. Refer to Table 4.10 for a summary of the statistically significant osteometric results.

Sacralisation associated with LSTV Types III and IV increased the mass of the sacrum through assimilation of the LSTV to the sacrum, thereby increasing the overall length of the sacrum. Consequently, the SH demonstrated a statistically significant increase in length for the LSTV cohort when compared to the control cohort. It has been demonstrated by Mahato (2013b), Golubovsky et al. (2019) and Mahato et al. (2019) that the load transmission of the upper body through the LSTV is borne through the accessory articulation/s associated with Type IIA and B morphology. It is hypothesized in the current study that LSTV enables enlarged distribution of load transmission borne through multiple surfaces at the lumbosacral junction, not least the accessory articulation/s.

The accessory articulation/s would result in diminishment of the size of the typical weight bearing surfaces at the lumbosacral junction, namely the sacral body dimensions and the zygapophyseal joint dimensions.

Reduction of sacral zygapophyseal joint size would reduce sacral facet surface area size. This was demonstrated in the current study by a statistically significant reduction in size of the SBW, bilateral SFH, bilateral SFW and surfaces area reduction of the both the sacral facet joints (FSA) as well as the superior surface of the sacral vertebral body (BSA).

Sequelae of the inherent increased stability associated with LSTV, reduction of the IFD*lat* and FD were found as a result of the smaller sacral facet joints and decreased demand for robust posterior element passive restraint mechanisms of the sacrum. The increased IAD can be explained as a result of the statistically increased length of the TVPs of the LSTV (TVPL), thereby extending the divergent proximal side of the sacrum which widened the IAD. This once again increases the base-of-support at the lumbosacral junction in conjunction with LSTV. All combined, the features of LSTV advocate for form over function. There is a sacrifice of mobility for greater stability. This imposes less demand for passive restraint mechanisms and increases the weight-bearing base-of-support for effective transfer of load transmission along the kinematic chain.

Lumbosacral transitional vertebrae are associated with variability in thoracolumbar enumeration. Regional homeotic shifting may take place at both the lumbosacral and thoracolumbar borders concomitantly (Nakajima et al., 2014; Doo et al., 2020). Therefore, the TLE was found to have greater variation in number for the LSTV cohort over the control cohort.

Furthermore, lumbar vertebral enumeration shows greater variability with LSTV, namely sacralisation and lumbarisation, of the last lumbar vertebra. A statistically significant change over the control cohort was seen. This is an expected result as LTSV is characterised by change in number of mobile segments of the lumbar vertebral column.

Lumbosacral transitional vertebrae male and female cohort comparison

The following osteometric dimensions demonstrated statistically significant differences between males and females in the LSTV cohort. The male LSTV cohort demonstrated larger values for bilateral D10 (AL) and D15 (ASA) left side.

The female LSTV cohort demonstrated larger values for D11 (FA) left side and D17 (FSA) right side. Refer to Table 4.10 for a summary of the statistically significant osteometric results.

The LSTV male cohort exhibited longer bilateral AL and larger ASA on the left. It is hypothesized that due to males exhibiting larger mass, elongated bilateral AL and enlarged left ASA enables greater spinopelvic stability by increasing both form and force closure mechanisms during bipedal ambulation. Additionally, Virgile and Bishop (2021) found that leg dominance is highly dependent on the task being performed.

They found 90% of people exhibit right-hand preference with 90% of their cohort preferred the right limb to kick a soccer ball. This may explain why the ASA was statistically larger on the left as it would be used as a pivot and increased size may increase spinopelvic stability associated with right-side lower limb dominance in performing tasks. Moreover, the left sided FA demonstrated less angulation on males than females and this is thought to be related to the need to have greater movement over a more common left-sided pivotal stance leg (non-dominant leg) (Virgile and Bishop, 2021).

The right FSA for LSTV males was smaller. In this study, the most common frequency of side was a bilateral presentation of LSTV (40.7%), after which left was the next most common (35.2%). The Type IIA morphology was the most frequent morphological Type of LSTV (39.6%). The finding of the right FSA demonstrating smaller surface area may be seen as the body's attempt to allow for more motion at the lumbosacral junction towards the right side. The right side was the least common frequency of side (11.0%) and therefore had less impedance for limited motion created by the LSTV.

Female lumbosacral transitional vertebrae cohort and female control cohort comparison

The following osteometric dimensions demonstrated statistically significant differences between the female LSTV cohort and female control cohort.

The female LSTV cohort demonstrated statistically larger values for (D11) FA left side, left D13 (TVPL) left side, D14 (TVPH) right side, (D15) ASA right and (D22) TLE.

The female control cohort demonstrated larger values for D2 (SBW), (D7) FD, (D8) SFH left side, bilateral (D9) SFW and bilateral (D17) FSA.

As with the male LSTV cohort, LSTV has a stabilising effect of the lumbosacral junction. As a result, the female control cohort demonstrated larger values for SBW, FD, SFH left side, bilateral SFW and bilateral FSA as a non-variant lumbosacral junction requires greater support and stabilisation from the anatomical structures of the sacral vertebral body, sacral zygapophysial joint size and orientation (greater coronal orientation) as well as surface area. In the LSTV cohort, the second most common frequency of side found in the current study after bilateral was left. The most common subtype and frequency of side was Type IIA left side at 31.9% (Table 4.7).

This may explain why only the mean average of the left TVPL was statistically larger in female LSTV cohort. Note, the mean average of the right TVPL was larger in the LSTV cohort than the female control cohort but was not statistically significant. Assimilation of the LTSV would increase the ASA and the right side was enlarged. As discussed earlier, LSTV is associated with variability in thoracolumbar enumeration (Nakajima et al., 2014; Doo et al., 2020).

Male lumbosacral transitional vertebrae cohort and male control cohort comparison

The following osteometric dimensions demonstrated statistically significant differences between the male LSTV cohort and male control cohort. The male control cohort demonstrated larger measurements for D2 (SBW), D4 (IAD), D5 (IFD*lat*), D6 (IFD*med*), D7 (FD), bilateral D8 (SFH), bilateral D9 (SFW), bilateral D17 (FSA) and D18 (BSA).

The male LSTV cohort demonstrated larger measurements for D10 (AL) left side, bilateral D13 (TVPL) and D14 (TVPH).

As previously discussed, LSTV inherently affords greater stability at the lumbosacral junction. As such, the male control cohort demonstrates larger SBW, IFD*lat*, IFD*med*, FD values that reflect a need for more stability.

The bilateral sacral zygapophyseal joints were on average larger in height (SFH), width (SFW) and surface area (FSA) in the male control cohort when compared to the male LSTV cohort. It is thought that the larger sacral zygapophyseal joints produced a larger IFD*lat* and FD. Combined with the larger BSA, these features aid in lumbosacral stability.

The increased span of the left AL for the male LSTV cohort is believed to allow for more stable pivoting on the left leg. The right leg is more commonly the dominant leg and therefore tasks that involve a right-sided dominant leg would require weight transfer of the upper body to the left hip joint which would act as a pivot and thus involve the left sacroiliac joint as the connection from the spine to the lower limb. A larger AL would create greater resistance to sheering and increase the force closure aspect of the sacroiliac joint (Virgile and Bishop, 2021).

Additional findings of lumbosacral transitional vertebrae

Comparison of D11, D17 and D18 and D19: FA, FSA, BSA and AFSA

Pearson's coefficient correlation was used to assess if a relationship exists between the sizes of FA, FSA, BSA and ASFA. Additionally, an investigation of the FSA was conducted to assess if correlation existed between the sizes of right and left FSA.

Right and left facet angle side and sacral base surface area comparison

The comparison revealed a statistically significant positive correlation between the right and left FA (p<0.001) with a medium effect size (r=0.45) for the LSTV cohort. This finding suggests that a change in angulation of one the sacral zygapophyseal joints may influence the angulation of the other. This is likely due to result in the dissipation of load and stress force distribution so as not to unevenly increase stress reaction forces onto a single side.

Furthermore, a statistically significant negative correlation was found between the bilateral FA and the BSA (p=0.007) with a medium effect size (r=-0.354).

These findings suggest that an increase in the BSA would lead to a decrease in the size of the FA of both right and left facet joints. This is likely due to the weight bearing and stabilising effect of the BSA in relation to its size.

The larger a base of support, the more stable an object would be and there is therefore less need for mechanical restraint from the sacral zygapophyseal joints.

Right and left sacral facet areas

A statistically significant positive relationship was found between the left FSA and the right FSA (p<0.001), with a large effect size (r=0.656), and the right FSA and the BSA (p=0.005), with a medium effect size (r=0.374).

The greater the angle of the FA the more gliding force will be restrained by the sacral zygapophyseal joints (Kapandji, 2008) leading to larger surface area of the sacral zygapophysial joints. This may be explained by proposing that the body seeks to distribute stress and load forces of the vertebral column evenly. This aids locomotion and mechanical efficiency in movement.

Bilateral sacral zygapophyseal joint surface area relative symmetry enables distribution of gliding stress forces as a form of restraint mechanism at the lumbosacral junction (Kapandji, 2008).

The left and right FSA were positively correlated. This is likely due to right side dominance being more common and therefore the left articular column will be responsible for more pivoting as it will be the stance side (Virgile and Bishop, 2021).

Right accessory facet surface area

A statistically significant negative relationship was found between the right ASFA and the right FSA (p=0.045), with a medium effect size (r=0.656).

Left accessory facet surface area

A statistically significant negative relationship was found between the left FSA and the right ASFA (p=0.045), with a medium effect size (r=-0.374). The findings for the negative relationship between the right and left AFSA compared with their homolateral FSA can be explained biomechanically. Load transmission of the upper body is borne through the accessory facet joints of the LSTV which reduces the stress forces on the homolateral sacral zygapophyseal joint facet joint.

The larger the surface area of the facet accessory articulation the smaller the surface area of the homolateral sacral zygapophyseal joint facet joint is in response and vice versa. The stabilising effect of the Type II LSTV negates the need for larger sacral zygapophyseal joints as a restraining mechanism at the lumbosacral junction. This finding strengthens the concept of the inherent quality that LSTV stabilises the lumbosacral junction as long as there is contact of the TVP with the ala of the sacrum, either unilaterally or bilaterally.

Novel findings of this research

South African specific population study of lumbosacral transitional vertebrae

This study found that the prevalence of LSTV in the South African population was 10%.

Many South African researchers have made variable contributions towards the finding of LSTV (Wells, 1963; De Beer Kaufman, 1974; Einstein, 1978; Morris, 1984; Du Plessis, 2017; Alblas, 2019). This is the only dedicated study of LSTV prevalence in South Africa and was the largest on the African continent.

Ancestry and lumbosacral transitional vertebrae

No statistically significant results were found when comparing LSTV and ancestry. This in itself is a significant finding and may suggest that ancestry plays little to no role in LSTV phenotypic expression. However, there is a lack of ethnic information in the literature. Many authors use homogenised sample populations, e.g., an American population. Further studies are needed to determine the prevalence in different ancestral groups in order to confirm or oppose the findings in the current study. Based on the lack of information regarding prevalence of LSTV in a Mixed-ancestry cohort, this current study fills the gap in knowledge and allows for future comparison for Mixed-ancestry specific comparative cohort analyses to be conducted.

Morphology of lumbosacral transitional vertebrae

Based on the lack of information regarding subtype and frequency of side, this study fills the gap in knowledge and allows for future comparison for African-specific and Mixed-ancestral comparative cohort analyses.

Iliolumbar articulation

The iliolumbar articulation is also known as lumbo-iliac or transverse-iliac articulation which has been sparsely reported in the literature (White and Klauber, 1976; Avimadje et al. 1999; Magee, 2008; Mitra and Carlisle, 2008). It can be defined as an accessory articulation formed by contact of the transverse process of the last vertebra with the ilium on the same side. Three examples were found in this current study (Figures 3.44, 3.45 and 4.104) which demonstrated a unilateral iliolumbar articulation between the last lumbar TVP and the ilium of the pelvis, right-sided and left-sided examples were recorded. The iliolumbar articulations found in this study were associated with Type IIA LSTV morphology on the contralateral side. Interestingly, both male and female LSTV cohorts demonstrated a statistically significant change in TVP length on the side/s of the dysplastic TVP. It has been proposed that the presence of an iliolumbar articulation may contribute partially or wholly to the generation of back pain associated with Bertolotti syndrome (Avimadje et al. 1999; Mitra and Carlisle, 2008).

Iliolumbar articulation remains a clinically significant entity and should be recognised alongside LSTV morphology in diagnostic imaging. It is hypothesized by the author that an increase in TVP length may be a previously unrecognised morphological trait associated with LSTV.

Two features which ascribe to change in length were statistically significantly increased in the current study in the LSTV cohort, namely IAD and TVPL. It is possible that the developing vertebral column underwent a form of sagittal axial patterning whereby the left and right sides developed independently, but instead of a single characteristic change in morphology such as TVPH there was an additional change with opposing side for TVPL. Such a change may represent a homolateral change in TVPH and a contralateral change in TVPL. This would be controlled through HOX gene expression and is a rare sub-variant of LSTV morphology. The presence of an LSTV with concomitant iliolumbar articulation is novel, and at present is not described as part of the Castellvi et al. (1984) classification for LSTV morphology. Consequently, it is the author's recommendation for its inclusion into a modified Castellvi et al. (1984) classification of LSTV within the Type II subtype class of morphological variation (see Figure 5.1).

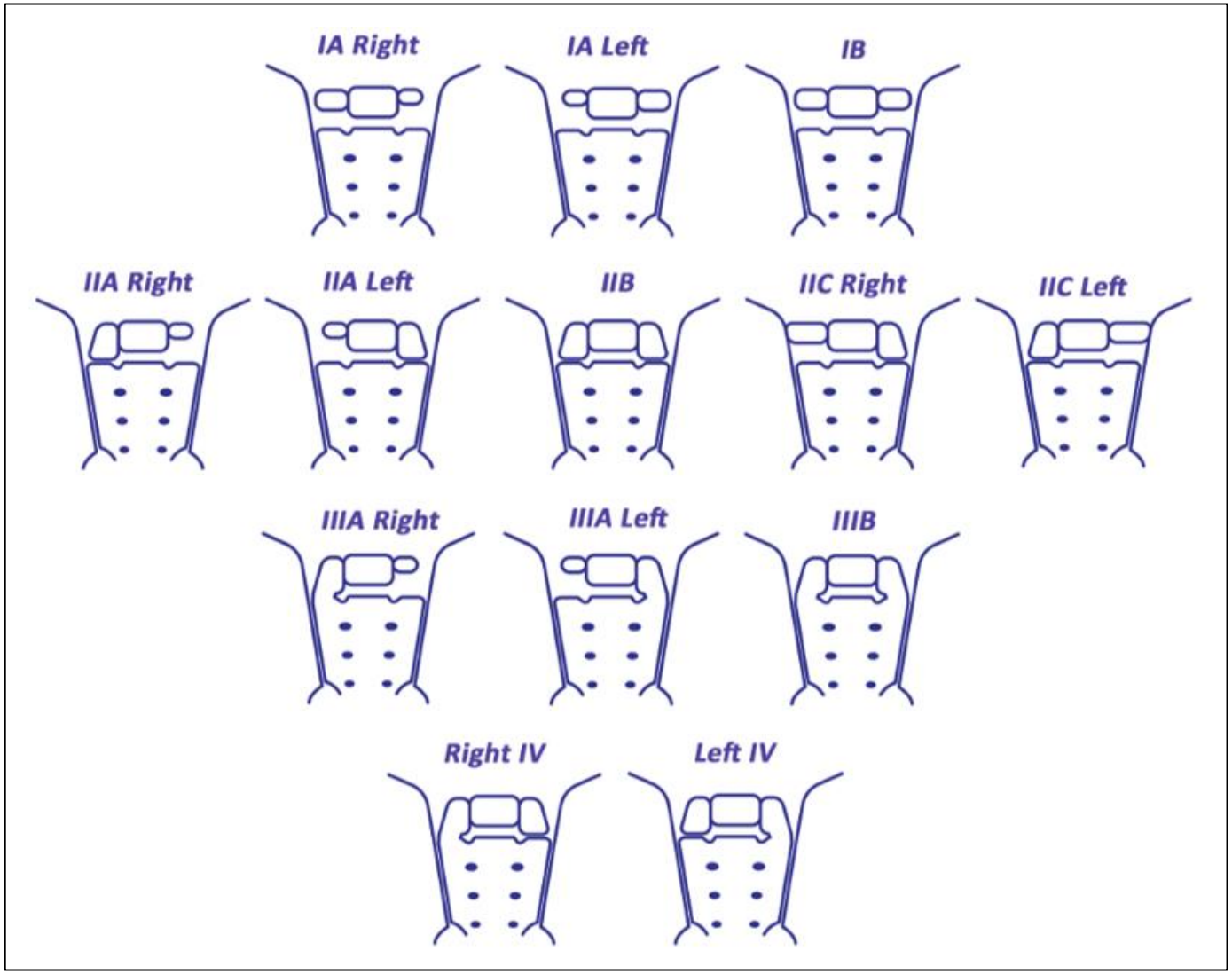

Figure 5.1: *A proposed new classification for lumbosacral transitional vertebrae. Displayed is the modified Castellvi et al., (1984) classification representing the four main Types (I-IV) with their new subtypes.* ***Type I****: top row.* ***Type II****: second row from the top.* ***Type III****: third row from the top.* ***Type IV****: bottom row. There is inclusion of the iliolumbar articulation as a sub-classification to the Type II lumbosacral transitional vertebrae category (IIC right and left). Additionally, there is modification of the Type IV lumbosacral transitional vertebrae category which demonstrates the inclusion of a side preference (right and left).*

Type IV Lumbosacral transitional vertebrae

The Castellvi et al. (1984) classification system fails to subdivide the Type IV LSTV by side. It was found in the current study that there are two distinct morphological forms that represent mirror images of each other (see Figure 5.2). As yet, no proposed sub-classification by frequency of side of the Type IV LSTV has been recommended. This is problematic as the literature is ambiguous with respect to which morphological representations were found as well as if any clinically significant symptoms may be attributed to one morphology over the other. Table 5.1 displays proportions of LSTV found in the literature including the unspecified Type IV morphology. The unilateral fusion and formation of the bony bridge-like structure formed by the fusion of the TVP to the ala of the sacrum is deemed to be the unchanging and unequivocal feature of the Type IV LSTV morphology. The contralateral side to the fusion is deemed to be analogous to the category of a Type IIA LSTV which may be difficult to interpret on radiographs due to a number of reasons. Obscurity of the joint space due to obliquity in patient position may to lead superimposition of structures which would impede visualisation of the unfused side on a radiograph. Similarly, hypertrophy and undulation of the joint may affect recognition. As a result of ageing, the Type IIA component of the Type IV morphology may be subject to degradation. This may change the appearance on imaging and make interpretation more difficult. The side of fusion cannot change in its morphological representation over time and it is therefore proposed by the author to be the side by which the Type IV LSTV should be named.

In a clinical setting it would be important to side a Type IV LSTV. It has been confirmed that a Type III LSTV has been associated with pain generation (Adams et al., 2018), likely as a result of micro-movement and axial loading of the unilateral fused bony bridge leading to a stress fracture. A Type IV LSTV could be viewed as having similar loading properties and biomechanical traits as Type IIIA LSTV as the side contralateral to the fused segment may not participate as significantly in weight bearing and distribution of load transmission forces. Therefore, knowledge of which morphological Type IV LSTV is present may be useful when considering pain generation aetiology and appropriate treatment planning for individuals associated with possible Bertolotti syndrome.

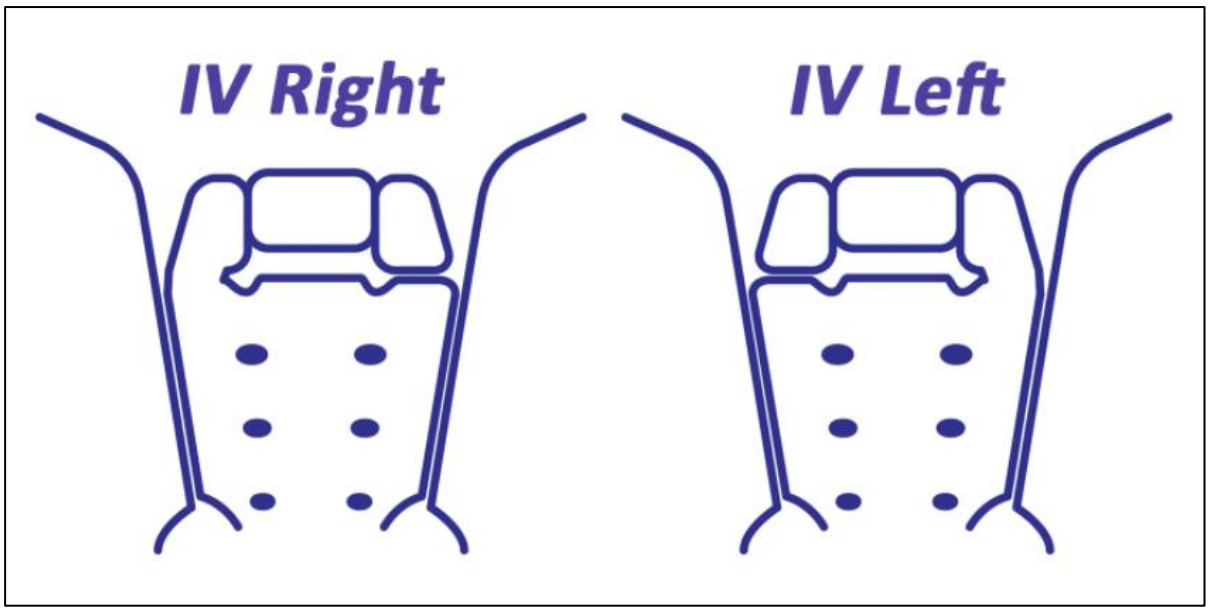

Figure 5.2: *Proposed classification subdivision for the Type IV lumbosacral transitional vertebra morphology. Siding of Type IV morphology relies on the side of fusion of the lumbar transverse process to the sacral ala.* ***Left)*** *A Type IV lumbosacral transitional vertebra demonstrating a right fusion of the right lumbar transverse process to the ala of the sacrum.* ***Right)*** *A Type IV lumbosacral transitional vertebra demonstrating a left fusion of the left lumbar transverse process to the ala of the sacrum.*

Bipartition of the sacral foramen

On review of spinal images in this study, a bipartite foramen was found of the left first anterior sacral foramen (Figure 3.46). In a literature search for bipartition of a sacral foramen no description or comparative case study could be found. It is hypothesised that the appearance seen in Figure 3.46 may be due to ligament ossification creating an osseous division of the left first anterior sacral foramen leading to the radiographic appearance of a bipartite foramen. It has been found that the outer fibres of the annulus fibrosus may ossify in association with LSTV (Savage, 2005 and Figure 4.2A and B) which may support the idea that adjacent ligaments may ossify in association with LSTV. Speculation in symptomology of this bipartite foramen is ongoing and it is unfortunate that no further information could be acquired on this unique case. Possible sequela may include irritation of the left S1 nerve.

Intra-articular vacuum phenomenon

On review of spinal images in this study, intra-articular vacuum phenomenon (VP) was seen at the accessory joints of Type IIA and IIB LSTV as well as iliotransverse joints in a 55-year old female, 52-year old male and a 41-year old female, Figure 3.47.

These examples were too few to ascribe the female sex as significant proponent for VP as described by Faflia et al. (1998), Lo et al., (2011), Gohil et al. (2014) and Takata et al. (2016). The vacuum phenomena seen in Figures 3.47A, B and C, were incidental and were not an objective for this current study. For that reason, the complete complement of medical images was not scrutinised or recorded for the purpose of visualisation of VP during the data collection phase of the current study associated with LSTV morphology.

Since VP is associated with a stress response over time leading to degeneration, Mahato et al. (2019) and Golubovsky et al. (2019) found that loads that increased the stress patterns at the accessory articulation of LSTV were found in all three planes of movement, namely extension, lateral flexion (towards the accessory articulation) and axial rotation (away from the articulation). Mahato et al. (2019) provides a theoretical basis for the explanation that mechanical changes may occur with the presence of LSTV through stress loading pattern changes as well as models that map the ROM associated with a left-sided LSTV. Mahato et al. (2019) and Golubovsky et al. (2019) further demonstrated by use of cadaveric and computational modelling that there is increased stress associated with LSTV at both the vertebral endplates as well as at the accessory articulations during motion of the vertebral column. It is therefore possible that increased stress loads at the accessory articulations of LSTV may lead to arthrosis of the accessory articulation over time. Moreover, Mahato (2011, 2012, 2013a) found that a transitional vertebra may exhibit change in morphology due to an acquired functional response to load transmission and stress. This change may contribute to accessory articulation arthrosis. Asymmetrical mechanical loading may accompany LSTV accessory joint/s and may lead to arthrosis whereby vacuum phenomenon may be visualised on imaging of the lumbar vertebral column.

Vacuum phenomenon of the iliotransverse joints was explained by Illeez et al. (2018), who found a statistically significant association between sacroiliac joint dysfunction and LSTV. Illeez et al. (2018) commented that sacroiliac joint dysfunction causes pain and should be considered when evaluating LBP aetiology. Additionally, Mahato et al. (2019) found loss of mobility at the lumbosacral junction in relation to a unilateral Type II LSTV. With this in mind, Savage (2005) and Tague (2009) found that fusion may occur at any three possible sites at the lumbosacral junction in association with LSTV. These sites were the facet joints, transverse processes where they make contact with the alae of the sacrum and finally around the IVD.

Farshad-Amacker et al. (2015) found that LSTV stabilised the lumbosacral segment leading to protection of the lumbosacral IVD but increased the degeneration at adjacent spinal segments, especially the cephalad segment. The effect of LSTV Types II may be seen as stabilising and in Types III and IV similar to a surgical arthrodesis of the lumbosacral segment. Many authors have found that lumbosacral arthrosis leads to SIJ degeneration and pain (Elster 1989; Ha et al., 2008; Unoki et al., 2016; Baria et al., 2020). It is therefore believed that intra-articular VP in the sacroiliac joint/s in the presence of LSTV, especially if sacralisation (loss of mobile segments of the lumbar vertebral column) is present, could be due in part to degeneration of the sacroiliac joint from the stabilising effect of the LSTV over time. Two of the three examples were over the age of 50 years and the VP may be related to arthrosis due to ageing as an additional factor. Further research in this area is recommended.

Enlargement of the lumbar transverse process without articulation

The measurement of the lumbar TVP exhibiting change in vertical height greater than 19mm associated with LSTV was proposed by Southworth and Bersack in 1950. Since Southworth and Bersack (1950) description of the most rudimentary form of LSTV, a Type I morphology, subsequent authors (Tini et al., 1977; McCulloch and Waddell, 1980 and Castellvi et al., 1984) did not define enlargement of the lumbar TVP without contact or fusion to the sacral alae as representing a sub-classification when associated with a unilateral Type II or III morphology. Hanhivaara et al. (2020) described enlargement of the last lumbar TVP in association with unilateral Types II and III LSTV as a potential sub-type classification when considering the complete complement of the Castellvi et al. (1984) classification.

Although this study excluded Type I LSTV morphology, the author observed examples of the enlargement of the lumbar TVP in agreement with Hanhivaara et al. (2020) prior to reading their paper (Figure 4.48). This reinforces that Hanhivaara et al.'s (2020) findings are not isolated and in the author's opinion would be welcomed as an adjunct to a sub-classification to the Castellvi et al. (1984) classification.

The clinical significance of a unilaterally enlarged TVP coinciding with a Type IIA or Type IIIA LSTV remains unknown and future research should be undertaken in this area.

Lumbar ossified bridging syndrome

In this study, while reviewing spinal images, LOBS was identified in a 53-year old female with the concomitant presence of LSTV. For reasons that are unknown to the author, she sought spinal imaging (Figure 3.49). The concurrent finding of LOBS and LSTV may indicate that this example may be as a result of unilateral sagittal plane patterning where the left side developed independently from the right side, instead of symmetrical patterning changes, allowing for unilateral multilevel changes in morphology. Trauma could be a possible reason for the LOBS appearance whereby the individual had a pre-existing LSTV.

Transverso-sacro-iliac articulation complex

A novel finding associated with LSTV, the transverso-sacro-iliac articulation complex, represents a tripartite articulation when present unilaterally. The first articulation is of the auricular surface of the sacrum with the ilium of the pelvis forming the sacroiliac articulation which is a normal spinopelvic joint found bilaterally. Furthermore, two additional accessory joints were identified, namely an articulation between the L5 lumbar transverse process and the ala of the sacrum known as the lumbosacral articulation and an articulation of the lumbar transverse process with the ilium of the pelvis known as the iliolumbar articulation, refer to Figure 3.50 and Figure 4.105. Lumbosacral transitional vertebrae, however, pose a unique biomechanical effect on spinal and lumbopelvic motion as the biomechanical model proposed by Mahato et al., (2019) has demonstrated. However, after a thorough review of the literature (Table 1.10), none of the other studies considered the effect of LSTV on SIJ motion. There is paucity in the literature on whether the SIJs are vulnerable to adjacent segment disease as a result of the presence of LSTV. It is unknown if the transverso-sacro-iliac articulation complex alters biomechanical behaviour of load transmission during static posture and motion during locomotion. The clinical implications of the transverso-sacro-iliac articulation complex may have multiple consequences.

One, it may create an additional diagnostic challenge in cases of LBP due to the presence of three articulations on one side which may be involved in pain generation. De Bruin et al. (2017) validated the concept that two sites of pain can arise in the presence of LSTV.

De Bruin et al. (2017) described LBP arising from the sacroiliac joint below the LSTV, visualised as bone marrow oedema on MRI, while concomitantly demonstrating bone marrow oedema at the accessory articulation of the unilateral LSTV. Clinicians would need to be aware of their existence when considering pain generation and therapeutic interventions thereof. A method sensitive to detecting stress-induced changes in bone is skeletal scintigraphy (Connolly et al., 2003). A method to confirm site of pain generation would include the use of analgesic intra-articular steroid injections which would decrease pain if placed at the correct site.

Two, the presence of the transverso-sacro-iliac articulation complex may contribute to alteration of sacroiliac joint anatomy with a predisposition to tongue-in-groove morphology. This would be of particular interest for therapeutic interventions such as spinopelvic manipulation performed by chiropractors, osteopaths and physiotherapists. Figures 3.50A (left side) and 3.50B (bilateral) demonstrate a tongue-in-groove appearance to the sacroiliac articulation which appears to be accentuated by the iliolumbar component of the transverso-sacro-iliac articulation complex. A tongue-in-groove appearance has been attributed to sacral dysmorphism (Kaiser et al., 2014; Weigelt et al., 2019). Sacral dysmorphism has no rigid anatomical definition (Kaiser et al., 2014; Weigelt et al., 2019) but may be described as interdigitation of the sacroiliac joint that creates convolution to the articular surfaces thereby creating a ridge-like appearance that deepens the sacroiliac joint (Miller and Routt, 2012; Vleeming et al., 2012). Biomechanically, the sacroiliac joint experiences two types of anatomically-mediated stability mechanisms, namely form closure and force closure (Vleeming et al., 2012; Zlomislic and Garfin, 2019). Form closure may be described as closely fitting surfaces of a joint that confer stability (Zlomislic and Garfin, 2019). Force closure can be seen as joint compression in which friction and dynamic lateral forces are utilised to withstand vertical load forces and transfer of forces (Zlomislic and Garfin, 2019).

Three, tongue-in-groove sacroiliac joint morphology would represent increased joint congruity between the sacrum and the ilium and may inhibit the sacroiliac joint's mobility in sacrifice for stability. It is therefore theoretically possible that the transverso-sacro-iliac articulation complex may have an influence on sacroiliac joint mobility due to the ridge-like structure known as a tongue-in-groove sacroiliac dysmorphism. Further research is needed in this area.

Alternate classification for the lumbosacral transitional vertebrae

In light of the LSTV morphological appearances of Figures 3.47C, 3.48A, B, C and D, and the transverso-sacro-iliac articulation (Figure 3.50) as well as the morphology displayed in Figure 4.2A, B and C, and Figure 4.3A and B, an alternate classification is proposed here. The proposed alternate classification differs in morphology from the classification seen in Figure 5.1 by demonstrating an additional attribute. The attribute is an iliolumbar articulation of the dysplastic side of the LSTV which may be present unilaterally or bilaterally. This attribute when present on a fused LSTV (Types III and unilateral side of IV) would change the sacroiliac joint length and when present on an unfused LTSV (Types II and unilateral side of IV) is associated with the transverso-sacro-iliac articulation complex. The alternate classification seen in Figure 5.3 builds on the newly proposed classification seen in Figure 5.1 by highlighting the supplementary morphological variation within LSTV whereby the TVP of the LTSV articulates with the ilium. The superscript representation of a star symbol (*) is proposed to be used to denote that the Type or subtype of LSTV is articulating with the ilium. For example, a unilateral Type IIA articulating with the ilium will be represented as 'IIA*'. Since the introduction of the Castellvi et al. (1984) classification, a number of authors have displayed the LSTV morphological classification in varying stylistic versions with no alterations to the original (Konin & Walz 2010; Nakajimaet al., 2014; Kapetanakis et al., 2017; Jeon et al., 2018). Although LSTV is aptly named for its lumbosacral morphology, many authors have failed to recognise the iliotransverse articulation component that may accompany the LSTV. Without the presence of the pelvis flanking the sacrum in their morphological depictions of LSTV as reference source, these iliotransverse articulations may remain unrecognised when viewed by healthcare professions unfamiliar with the intricacies of LSTV. Bertolotti syndrome has been discussed multiple times in this current study. While under dispute globally, LSTV has been demonstrated to be pain-generating in multiple cases. One possible site of pain generation is the iliolumbar articulation or the sacroiliac joint adjacent to the LSTV.

The Type IIC classification seen in Figure 5.1 remains an unmodified feature in Figure 5.3 as it has not been found to a have an iliolumbar articulation on the dysplastic TVP side.

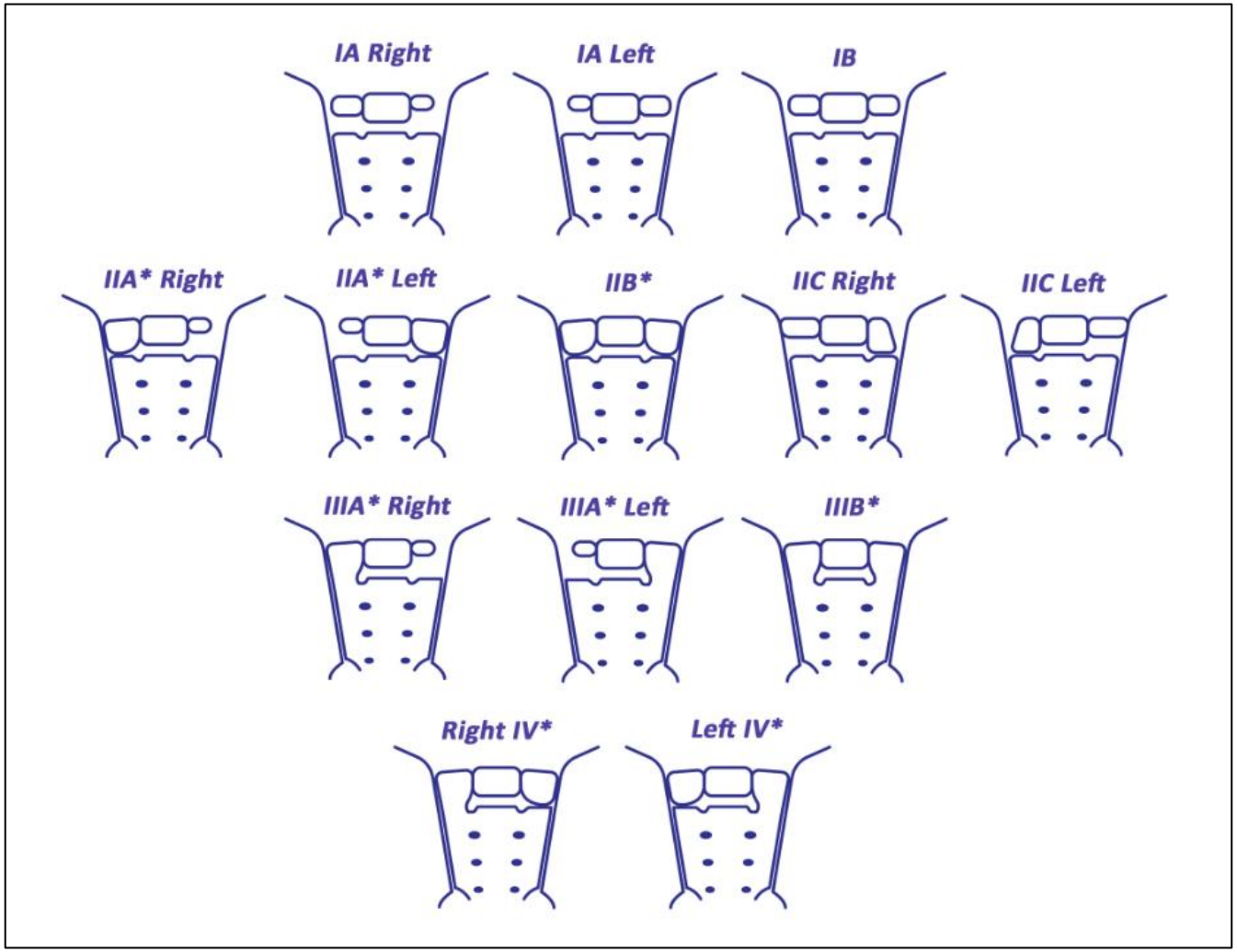

Figure 5.3: *A proposed alternate classification for lumbosacral transitional vertebrae. Displayed is an alternate Castellvi et al., (1984) classification representing the four main Types (I-IV) with the new subtypes (IIC).* ***Type I****: top row.* ***Type II****: second row from the top. Articulation of the lumbosacral and iliolumbar articulations is represented. The triad is known as the transverso-sacro-iliac articulation.* ***Type III****: third row from the top. Demonstrates the elongation of the sacroiliac joint on the side of the fused lumbosacral transitional vertebra.* ***Type IV****: bottom row. Elongation of the sacroiliac joint on the side of the fused lumbosacral transitional vertebra. Articulation of the unfused side of demonstrates articulation with the ilium. Additionally, there is modification of the Type IV lumbosacral transitional vertebrae category which demonstrates the inclusion of a side preference (right and left).* ***** *represents articulation of the lumbosacral transitional vertebrae with the ilium.*

Future research

Although this study did not attempt to link LSTV with LBP, it may be of value to research the prevalence of LBP associated with LSTV in the South African population. It is recommended by the author that prevalence studies of LSTV containing LBP should seek to select for the area of LBP, focussing on lumbosacral pain and gluteal pain, to better assess whether LSTV may predispose individuals to LBP. This would help inform spinal conservative care professionals as well as interventional clinicians in recognition of LBP and identification of LSTV.

Further research should be conducted on symptoms related to the two distinct morphological sub-types, right and left, Type IV LSTV.

Vacuum phenomenon was seen associated with accessory articulation of LSTV in this study. Future research should undertake to explore the prevalence of VP associated with accessory articulation in LSTV. It is unknown whether VP may be an incidental finding or have clinical implications.

The clinical relevance of a unilaterally enlarged TVP (increased TVPH) coinciding with a Type IIA or Type IIIA LSTV is unknown. Further research can be targeted to researching any possible clinical significance which may be ascribed to this morphological variant.

Future research should be conducted to determine if an increase in TVP length may be a previously unrecognised morphological trait associated with LSTV. If so, investigation into the implications for a biomechanical model of the lumbosacral junction could be pursued.

Tongue-in-groove sacroiliac morphology associated with the transverso-sacro-iliac articulation complex should be explored further. Computer-aided biomechanical models would prove very useful in assessment of sacroiliac mobility.

Future investigations should be sought to increase the knowledge on African-ancestry divided by regions within Africa and Mixed-ancestral cohorts. These are either sparsely reported or have no reported observations in association with LSTV.

Reflections

The idea to combine medical images with osteometric morphological appraisal of skeletal remains for LSTV was ambitious. It made for a very time-consuming and labour-intensive process. However, the combined information from both parts of the study proved invaluable.

Strengths of the study

This study is the first to indicate the prevalence of LSTV in the South African population (10%) as well as the three largest sub-groups. The prevalence in the African-ancestry was 10.6%, Mixed-ancestry was 9.3% and European-ancestry contained 10.0% LSTV respectively.

This study evaluated a sizeable quantity of individuals, both alive and deceased. A total sample size for the medical imaging cohort and osteological cohort of LSTV amounting to 4893 individuals were screened. Four hundred and twenty-two LSTV were found with an overall prevalence rate of LSTV in a sample of the South African population of 8.6% when combined.

Two recommendations were made to modify the Castellvi et al. (1984) morphological classification of LSTV. The practical extrapolations of this study may help inform medical doctors, radiologists, anaesthetists, chiropractors, osteopaths, physiotherapists and rehabilitation practitioners to better identify LSTV and how to record the findings of medical imaging. Additionally, this current study may help inform clinicians by adapting current treatment protocols for patients with the anatomical variation of LSTV.

Low back pain is multifactorial and the presence of LSTV does not exclusively designate origin of LBP but it may help inform clinicians of possible sites of pain generation. Moreover, exercise and rehabilitation may need to be tailored due to the anatomical variation at the lumbosacral junction.

Limitations of the research

A limitation of the study was that it was conducted in only two medical facilities however the facilities are found in the two largest populated metropoles in South Africa (Arndt et al., 2019).

As the sample was derived from medical facilities this may have produced a selection bias in the sample.

It is unknown what pathology each person may have had but spinal pain may have been one of the reasons to image the vertebra column which may be associated with LSTV (Castellvi et al., 1984; Jönsson et al., 1989; Avimadje et al., 1999; Nardo et al., 2012; Jancuska et al., 2015). It is reiterated that LSTV has been found to cause LBP but not all persons with LSTV will have LBP.

This study did not consider the Type I LSTV due to its lack of clinical significance (Castellvi et al., 1984; Konin & Walz, 2010; Paik et al., 2013; Hanhivaara et al., 2020; Hou et al., 2020). Inclusion of the Type I LSTV would likely have increased the overall prevalence rate of LSTV, albeit for academic purposes only.

Although this study represents the 11th largest study conducted globally (refer to Table 1.10), limitations existed when conducting the statistical analyses. These limitations were as a result of the number of subtypes of LSTV in the imaging cohort being too low for statistical inferences. Further research could aim to increase the quantity of LSTV samples to support statistical comparisons.

In LSTV appraisal, classification of the morphology is the primary goal with the enumeration serving as secondary modifier. Lumbar vertebral column enumeration is of great importance for the purposes of therapeutic interventions such as intra- or peri-facet infiltrations of zygapophyseal joints and surgical procedures. The literature reports incorrect vertebral level surgery and errors in intra-articular infiltrations have occurred from misidentification of lumbar vertebral level (Malanga and Cooke, 2004; Konin and Walz, 2010; Apazidiset al., 2011; Sharma et al., 2011; Nakagawa et al., 2017). Complete vertebral counts were not possible in this study as most patients only had images taken of one spinal region.

The only method to correctly count the lumbar vertebrae with complete confidence is entire vertebral column imaging, which therefore, is the gold standard method (Hahn, Strobel and Hahn, 1992; Farshad-Amacker et al., 2015; Sarawagi et al., 2016; Tins and Balain, 2016; Lian et al., 2018; Doo et al., 2020).

An alternative technique to entire vertebral column imaging would be to image the vertebral column from the level of T1 and count inferiorly to the lumbosacral junction (Doo et al., 2020). This can be done with serial X-rays or a scouting MRI scan (Doo et al., 2020).

Finally, in this study the lumbar vertebral column enumeration relied on the presence of thoracic ribs for determining the terminal thoracic vertebra, T12. This may be problematic as there is an anatomical variation that occurs at the thoracolumbar junction known as thoracolumbar transitional vertebrae (TLTV). There is no universally accepted classification for TLTV (Park et al., 2016; Doo et al., 2020). Thus, Park et al. (2016) proposed a classification system for TLTV that takes out the ambiguity from previous authors' versions, see Figure 5.4. Thoracolumbar transitional vertebrae have been associated with variable rib counts or LSTV (Nakajima et al., 2014; Doo et al., 2020). The presence of TLTV and LSTV on spinal imaging necessitates further examination for better understanding of lumbar vertebral enumeration, especially if invasive methods of pain management are deemed necessary, such as spinal surgery (Doo et al., 2020).

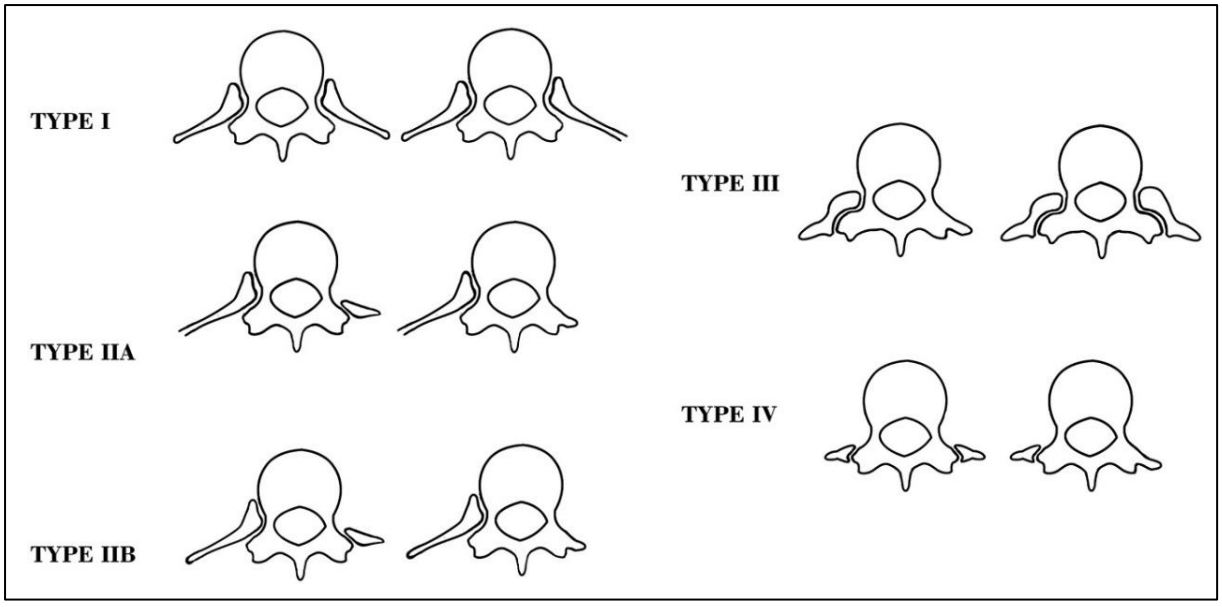

Figure 5.4: *Park et al., (2016) proposed classification of the thoracolumbar transitional vertebra. Four Types of thoracolumbar transitional vertebrae morphology has been suggested. Images obtained from the British Journal of Radiology, an open access publication, creative commons licence.*

CHAPTER 6

CONCLUSIONS

There is currently no dedicated study on lumbosacral transitional vertebrae prevalence (LSTV) and morphology in the South African population. This study aimed to establish baseline data on the prevalence rates of LSTV and describe the morphological characteristics of LSTV in a South African population.

Therefore, this study is the first to describe the prevalence of LSTV in the South African population. Moreover, this is the first study to document the sex and number of individuals from the three largest ancestral groupings in such a population. Of importance is LSTV associated with Mixed-ancestry as there is no other comparative investigation anywhere else in the world. This study creates a baseline description for the Mixed-ancestry cohort. Finally, this is the first study to incorporate an *in situ* and an *ex situ* study of the same population examining spinal morphology of LSTV obtained from medical images and cadaveric skeletal remains for descriptive analyses.

This study was subdivided into two main sections, namely Part 1 and Part 2.

Significant findings in Part 1

The study purpose was to determine the prevalence rates in the South African population. It assessed stored medical images, namely radiographs, MRI and CT scan images obtained from Groote Schuur Hospital and Charlotte Maxeke Johannesburg Academic Hospital. Randomised consecutive cohort sampling was used to assess the radiographs of 3096 (N_t=3096) individuals' radiographs. The total cohort was subdivided into three groups/ subgroups based on the most prevalent ancestral groups in South Africa, namely African-ancestry (n=1032), Mixed-ancestry (n=1032) and European-ancestry (n=1032). The Castellvi et al. (1984) classification, the most widely used in the world, was used to categorise LSTV. Frequency of side as well as spinal enumeration were also reported.

The study found the overall prevalence of LSTV in the South Africa population to be 10% (n=308/3096). The prevalences of LSTV in the three ancestral groups were 10.5% (n=109/1032), 9.3% (n=96/1032) and 9.9% (n=103/1032) for the African, Mixed and European-ancestries respectively.

Sex distribution of LSTV was found in favour of females over males (52.1%>47.9%). Sacralisation (64%, n=197/308) was the predominant finding over lumbarisation (36.0%, n= 111/308).

The morphological assessment found the prevalence of LSTV by Type was Type II (67.9%) followed by Types III (27.6%) and IV (4.5%). The most frequent subtype by prevalence was Type IIA (41.9%) followed by Type IIB (26%), Type IIIB (21.8%), and Type IV (5.8%). Moreover, the frequency of side was bilateral (47.7%), left (26.6%), right (21.1%), and other (4.5%).

Statistically significant results for Part 1

Ancestry and spinal enumeration analyses found that individuals of African-ancestry (67.0%) and Mixed-ancestry (72.9%) demonstrated a greater affinity of prevalence for sacralisation over the European-ancestry subgroup, which demonstrated marginal prevalence of sacralisation (52.4%). This was statistically significant (p=0.008) with a small effect size (V=0.178).

A statistical significance with a medium effect size (V=0.256) was found in males (p=0.010) when comparing ancestry and spinal enumeration. This was interpreted as there is a difference in the spinal enumeration in the male sex cohort between the three ancestral cohorts. The males of African-ancestry (n=34/48) and Mixed-ancestry (n=33/42) contained significantly higher proportions of sacralisation, 71% and 79% respectively, while the males of European-ancestry accounted for only 50% sacralisation (n=26/52).

Significant findings in Part 2

The study assessed 1797 (N_t=1797) cadaveric skeletal remains of known sex and ancestry between 21 and 65 years of age at death (AD). These skeletal remains were studied in the Dart Collection at WITS for metric and non-metric observations.

One hundred and fourteen individuals were identified as containing LSTV with a skeletal sample prevalence rate of 6.3%. Due to extensive damage or loss of vertebrae, 23 samples were excluded from the study. Therefore, 91 LSTV samples (n=91) met the inclusion criteria to be studied.

The total number of males identified was 1308 (72.8%) compared to 489 (27.2%) females. A sex balanced control group cohort (N=60) of 30 males (n=30) and 30 females (n=30), was selected at random from the Dart Collection.

The morphological assessment found the most common Type of LSTV was Type II at 64.8%, the second largest category was the Type III LSTV, accounting for 22.0% and the Type IV LSTV was the smallest category, accounting for only 13.2% of the sample.

The morphological assessment identified the most common subtype of LSTV by prevalence as Type IIA (40.7%) followed by Type IIB (5.3%), Type IIIB (14.3%), and Type IV (13.2%). Moreover, the most common frequency of side was bilateral (40.7%), left (35.2%), other (4.5%) and right (11.0%).

The majority of spinal enumeration associated with LSTV was sacralisation, representing 72.5% (n=66/91) while lumbarisation accounted for 27.5% (n=25/91) of the sample.

Statistically significant results for Part 2

Numerous osteometric comparisons were statistically significant, as set out in Table 4.10. The foundation of the Castellvi et al. (1984) classification relies on a change in transverse process height (TVPH) for which LSTV morphology is known. This study found that the TVPH of the last lumbar vertebra in the Type II LTSV morphology to be statistically significant in height over the control cohort. Furthermore, an additional finding pertinent to the TVP of the last lumbar vertebra was a statistically significant elongation of the transverse process length (TVPL) associated with the LSTV cohort.

Likewise, it was evident that there were morphometric changes associated with LSTV when compared to control cohorts with a general trend of the diminished size of the articulations at the lumbosacral junction, namely the sacral zygapophyseal joints [sacral facet width (SFW), sacral facet height (SFH), and sacral facet surface area (FSA)]. Similarly, the sacral base demonstrated diminished size of the articulations at the lumbosacral junction in multiple directions [sacral body width (SBW), sacral body length (SBL), and sacral body surface area (BSA)]. These changes in articulation dimensions are thought to be as a result, by the author, of a stabilising effect that LSTV affords the lumbosacral junction.

The size of the weight-bearing articulations was generally smaller in the LSTV cohort irrespective of the sex comparison to the control cohort. Bilateral observations of the AL were also longer in LSTV. Moreover, there was a direct positive correlation between the accessory sacral facet surface area (AFSA) and articulations of the lumbosacral junction. The larger the ASFA, the more diminutive the size of the BSA and sacral zygapophyseal size and surface areas. The load transmission was partially borne at the accessory articulation/s thereby negating larger articulations for stabilisation.

Novel findings

This study is the first to indicate the prevalence of LSTV in the South African population (10%) and, its three largest sub-groups. The prevalence in the African-ancestry subgroup was 10.6%, Mixed-ancestry was 9.3% and European-ancestry contained 10.0% LSTV, respectively.

Further novel findings associated with LSTV include the discovery of iliolumbar articulation, bipartition of the sacral foramen, intra-articular vacuum phenomenon of accessory articulations of LSTV, enlargement of the contralateral TVP associated with Types III and IV LSTV (confirming the finding of Hanhivaara et al., 2020), LOBS and a novel complex named the transverso-sacro-iliac articulation.

This study suggested three modifications to the Castellvi et al. (1984) classification:

1) There should be a sub-classification of the Type IV LSTV into right and left nomenclature;

2) The inclusion of a new subtype of Type II LSTV morphology, a unilateral right or left iliolumbar articulation associated with contralateral Type IIA morphology.

3) A modified morphological classification of LSTV based on the presence of an extended sacroiliac articulation either directly or via the transverso-sacro-iliac articulation. This finding effectively increases the size of the sacroiliac joint and is thought to increase the spinopelvic stability. The transverso-sacro-iliac articulation was demonstrated for all clinically significant LSTV Types (II-IV), both unilateral (right or left) and bilateral.

Overall impression of Lumbosacral transitional vertebrae

Considerable variability seems to exist in the prevalence and sub classification of LSTV from study to study (Table 5.1). This is thought to be due to regional population differences, methodological differences of the studies, imaging technique utilised and selection bias.

It appears that LSTV is highly variable in its phenotypic expression and that the genotypic traits are likely to be random in their expression. No clear link has been defined for ancestry as a significant contributor to LSTV prevalence. This is likely, in part, due to increased travel between regions and countries where previously cross border travel would be difficult or limited. There is greater population diversity and mixing of gene pools over time which may influence the phenotypic expression of LSTV.

Future opportunities for research related to LSTV that arose from this study include:

- The clinical significance (effect on biomechanics, possible links to pain generation or altered soft tissue anatomy) of enlarged TVPs without contact to the sacrum.
- The cut-off criteria for the classification of LSTV of 19mm of TVPH should be re-evaluated. It seems there is no substantiation or corroboration to this seemly arbitrary number proposed by Southworth and Bersack (1950).
- *Pain* is a contentious issue associated with LSTV. Narrowing the scope for inclusion criteria for imaging studies of LSTV prevalence that contain patient information regarding LBP should be limited to lumbosacral or gluteal pain (Nardo et al., 2012). This will better evaluate the role of LSTV in pain generation.

- There is a paucity of published studies on LSTV prevalence on the African continent, outside of Nigeria. Future research should seek to sample more African populations and compare African regions to one another.
- Besides the current study, LSTV associated with Mixed-ancestry has not been actively studied in the South African population or abroad.
- The sub-classification of Type IV LSTV by frequency of side should be considered for description in future studies.
- The frequency of side preference associated with LSTV is almost non-existent in the literature. Reporting of frequency of side as well as morphological classification is of great importance, especially if symptomatology is present.
- The lumbosacral transitional vertebrae effect on sacroiliac morphology should be evaluated *in situ* utilising medical imaging.
- Future studies should be targeted to assess if the newly described classifications of LSTV, namely the new subtype (Type IIc) and the alternate LSTV classification may be pain-generating. The gold standard for evaluating pain generation remains infiltration of local anaesthetic into the site of articulation.

REFERENCES

Abbas, J., Peled, N., Hershkovitz, I. and Hamoud, K., (2019). Is Lumbosacral Transitional Vertebra Associated with Degenerative Lumbar Spinal Stenosis? *BioMedical Research International*, 2019. pp. 1-7.

Adams, R., Herrera-Nicol, S. and Jenkins III, A.L., (2018). Surgical Treatment of a Rare Presentation of Bertolotti's Syndrome from Castellvi Type IV Lumbosacral Transitional Vertebra: Case Report and Review of the Literature. *Journal of neurological surgery reports*, 79(03), pp.e70-e74.

Aihara, T., Takahashi, K., Ogasawara, A., Itadera, E., Ono, Y. and Moriya, H., (2005). Intervertebral disc degeneration associated with lumbosacral transitional vertebrae: a clinical and anatomical study. *The Journal of bone and joint surgery*. British volume, 87(5), pp.687-691.

Akoglu, H., (2018). User's guide to correlation coefficients. *Turkish journal of emergency medicine*, 18(3), pp.91-93.

Alblas, A., Greyling, L.M. and Geldenhuys, E.M., (2018). Composition of the Kirsten skeletal collection at Stellenbosch University. *South African Journal of Science*, 114(1-2), pp.1-6.

Alblas, A., (2019). Assessment of health status in a 20th century skeletal collection from the Western Cape. Doctoral Thesis. Stellenbosch University. Stellenbosch, South Africa. pp.117-185.

Alderink, G.J., (1991). The sacroiliac joint: review of anatomy, mechanics, and function. *Journal of Orthopaedic & Sports Physical Therapy*, 13(2), pp.71-84.

Almeida, D.B.D., Mattei, T.A., Sória, M.G., Prandini, M.N., Leal, A.G., Milano, J.B. and Ramina, R., (2009). Transitional lumbosacral vertebrae and low back pain: diagnostic pitfalls and management of Bertolotti's syndrome. *Arquivos de neuro-psiquiatria*, 67(2A), pp.268-272.

Al Riyami, K.S., Alahmed, S.M., Saad, Z.Z. and Bomanji, J., (2017). Evaluation and identification of lumbosacral transitional vertebra causing intractable low back pain utilizing bone single-photon emission tomography with computed tomography. *World journal of nuclear medicine*, 16(4), pp.328, 329.

Apazidis, A., Ricart, P.A., Diefenbach, C.M. and Spivak, J.M., (2011). The prevalence of transitional vertebrae in the lumbar spine. *The Spine Journal*, 11(9), pp.858-862.

Apaydin, M., Uluc, M.E. and Sezgin, G., (2019). Lumbosacral transitional vertebra in the young men population with low back pain: anatomical considerations and degenerations (transitional vertebra types in the young men population with low back pain). *La radiologia medica*, 124(5), pp.375-381.

Arndt, C., Davies, R. and Thurlow, J., (2019). Urbanization, structural transformation, and rural-urban linkages in South Africa. Southern Africa, Towards Inclusive Economic Development, *SA-TIED Working Paper*, (41), pp.1-35.

Avimadje, M., Goupille, P., Jeannou, J., Gouthiere, C. and Valat, J.P., (1999). Can an anomalous lumbo-sacral or lumbo-iliac articulation cause low back pain? A retrospective study of 12 cases. *Revue du rhumatisme* (English ed.), 66(1), pp.35-39.

Avimadje, M., Zomalhèto, Z., Adjadohoun, S. and Gounongbé, M., (2015). Clinical characteristics and outcome of young West African patients with Bertolotti's syndrome. *The Egyptian Rheumatologist*, 37(2), pp.93-96.

Baria, D., Lindsey, R.W., Milne, E.L., Kaimrajh, D.N. and Latta, L.L., (2020). Effects of lumbosacral arthrodesis on the biomechanics of the sacroiliac joint. *JBJS Open Access*, *5*(1), pp.1-6.

Barnes, E., (2012). Atlas of developmental field anomalies of the human skeleton: a paleopathology perspective. John Wiley & Sons. pp.68-69.

Barzo, P., Vörös, E. and Bodosi, M., (1993). Clinical significance of lumbosacral transitional vertebrae (Bertolotti syndrome). *Orvosi hetilap*, 134(46), pp.2537-2540.

Basadonna, P.T., Gasparini, D. and Rucco, V., (1996). Iliolumbar ligament insertions: in vivo anatomic study. *Spine*, 21(20), pp.2313-2316.

Benlidayi, I.C., Coskun, N.C. and Basaran, S., (2015). Does lumbosacral transitional vertebra have any influence on sacral tilt? *Spine*, 40(22), pp.E1176-E1179.

Benoist, M., (2005). Natural history of the aging spine. In The aging spine. Springer, Berlin, Heidelberg. pp.4-7.

Bertolotti. M. (1917). Contributo alla conoscenza dei vizi di differenzazione regionale del rachide con speciale riguardo all' assimilazione sacrale della V lombare. *Radiol Med*, 4(1), pp.113–144.

Billet, F.P., Schmitt, W.G. and Böhmer, E., (1991). Bony bridges of the lumbar transverse processes. *RoFo: Fortschritte auf dem Gebiete der Rontgenstrahlen und der Nuklearmedizin*, 155(2), pp.171-178.

Blumensaat, C. and Clasing, C., (1932). Anatomie und Klinik der lumbosacralen Übergangswirbel (Sakralisation und Lumbalisation). In Ergebnisse der Chirurgie und Orthopädie. Springer, Berlin, Heidelberg. pp.1-59.

Bogduk, N., (2005). Clinical anatomy of the lumbar spine and sacrum. Elsevier Health Sciences. pp.1-173

Bogduk, N., (2012). Clinical and Radiological Anatomy of the Lumbar Spine E-Book. Elsevier Health Sciences. pp.63-75.

Brault, J.S., Smith, J. and Currier, B.L., (2001). Partial lumbosacral transitional vertebra resection for contralateral facetogenic pain. *Spine*, 26(2), pp.226-229.

Brent, A.E., Schweitzer, R. and Tabin, C.J., (2003). A somitic compartment of tendon progenitors. *Cell*, 113(2), pp.235-248.

Brezina, V., (2018). Statistics in corpus linguistics: A practical guide. Cambridge University Press. pp. 102-138.

Brinjikji, W., Luetmer, P.H., Comstock, B., Bresnahan, B.W., Chen, L.E., Deyo, R.A., Halabi, S., Turner, J.A., Avins, A.L., James, K. and Wald, J.T., (2015). Systematic literature review of imaging features of spinal degeneration in asymptomatic populations. *American Journal of Neuroradiology*, 36(4), pp.811-816.

Bron, J.L., van Royen, B.J. and Wuisman, P.I.J.M., (2007). The clinical significance of lumbosacral transitional anomalies. *Acta Orthopaedica Belgica*, 73(6), pp.687-693.

Bulut, M., Uçar, B.Y., Uçar, D., Azboy, İ., Demirtaş, A., Alemdar, C., Gem, M. and Özkul, E., (2013). Is Sacralization Really a Cause of Low Back Pain?. *International Scholarly Research Notices*,pp.1-3.

Burke, A.C., Nelson, C.E., Morgan, B.A. and Tabin, C., (1995). Hox genes and the evolution of vertebrate axial morphology. *Development*, 121(2), pp.333-346.

Burke, A.C. and Nowicki, J.L., (2001). Hox genes and axial specification in vertebrates. *American Zoologist*, 41(3), pp.687-697.

Cadeddu, J.A., Benson, J.E., Silver, R.I., Lakshmanan, Y., Jeffs, R.D. and Gearhart, J.P., (1997). Spinal abnormalities in classic bladder exstrophy. *British journal of urology*, 79(6), pp.975-978.

Carapuço, M., Nóvoa, A., Bobola, N. and Mallo, M., (2005). Hox genes specify vertebral types in the presomitic mesoderm. *Genes & Development*, 19(18), pp.2116-2121.

Cardoso, H.F. and Rios, L., (2011). Age estimation from stages of epiphyseal union in the presacral vertebrae. *American Journal of Physical Anthropology*, 144(2), pp.238-247.

Cardoso, H.F., Pereira, V. and Rios, L., (2014). Chronology of fusion of the primary and secondary ossification centers in the human sacrum and age estimation in child and adolescent skeletons. *American Journal of Physical Anthropology*, 153(2), pp.214-225.

Carrino, J.A., Campbell Jr, P.D., Lin, D.C., Morrison, W.B., Schweitzer, M.E., Flanders, A.E., Eng, J. and Vaccaro, A.R., (2011). Effect of spinal segment variants on numbering vertebral levels at lumbar MR imaging. *Radiology*, 259(1), pp.196-202.

Castellvi, A.E., Goldstein, L.A. and Chan, D.P., (1984). Lumbosacral transitional vertebrae and their relationship with lumbar extradural defects. *Spine*, 9(5), pp.493-495.

Caverly, R.H., (2015). MRI fundamentals: RF aspects of magnetic resonance imaging (MRI). *IEEE Microwave Magazine*, 16(6), pp.20-33.

Chakraverty, R., Pynsent, P. and Isaacs, K., (2007). Which spinal levels are identified by palpation of the iliac crests and the posterior superior iliac spines? *Journal of Anatomy*, 210(2), pp.232-236.

Chal, J. and Pourquié, O., (2009). 3 Patterning and Differentiation of the Vertebrate Spine. *Cold Spring Harbor Monograph Archive*, 53, pp.41-116.

Chalian, M., Soldatos, T., Carrino, J.A., Belzberg, A.J., Khanna, J. and Chhabra, A., (2012). Prediction of transitional lumbosacral anatomy on magnetic resonance imaging of the lumbar spine. *World journal of radiology*, 4(3), pp.97-101.

Chang, H.S. and Nakagawa, H., (2004). Altered function of lumbar nerve roots in patients with transitional lumbosacral vertebrae. *Spine*, 29(15), pp.1632-1635.

Chithriki, M., Jaibaji, M. and Steele, R., (2002). The anatomical relationship of the aortic bifurcation to the lumbar vertebrae: a MRI study. *Surgical and Radiologic Anatomy*, 24(5), pp.308-312.

Chowdhury, A. and Sharma, H., (2018). A review of 571 radiographs on Tuffier's inter-cristal line and its' application in lumbar spinal surgery. *Journal of Spine Surgery*, 4(2), pp.383-386.

Christ, B., Huang, R. and Wilting, J., (2000). The development of the avian vertebral column. *Anatomy and embryology*, 202(3), pp.179-194.

Christ, B., Huang, R. and Scaal, M., (2007). Amniote somite derivatives. *Developmental dynamics*, 236(9), pp.2382-2396.

Clark, S.J., Collinson, M.A., Kahn, K., Drullinger, K. and Tollman, S.M., (2007). Returning home to die: circular labour migration and mortality in South Africa 1. *Scandinavian Journal of Public Health*, 35(69), pp.35-44.

Cochard, L.R., (2012). Netter's Atlas of Human Embryology E-Book: Updated Edition. Elsevier Health Sciences. pp.1-344.

Corallo, D., Trapani, V. and Bonaldo, P., (2015). The notochord: structure and functions. *Cellular and molecular life sciences*, 72(16), pp.2989-3008.

Connolly, L.P., d'Hemecourt, P.A., Connolly, S.A., Drubach, L.A., Micheli, L.J. and Treves, S.T., (2003). Skeletal scintigraphy of young patients with low-back pain and a lumbosacral transitional vertebra. *Journal of Nuclear Medicine*, 44(6), pp.909-914.

Cox, J.M., (2012). Low back pain: mechanism, diagnosis and treatment. Lippincott Williams & Wilkins. pp.1-215.

Dai, L., (1999). Lumbosacral transitional vertebrae and low back pain. *Bulletin (Hospital for Joint Diseases (New York, NY)*), 58(4), pp.191-193.

Dayal, M.R., Kegley, A.D., Štrkalj, G., Bidmos, M.A. and Kuykendall, K.L., (2009). The history and composition of the Raymond A. Dart Collection of human skeletons at the University of the Witwatersrand, Johannesburg, South Africa. *American Journal of Physical Anthropology*, 140(2), pp.324-335.

De Beer Kaufman, P. (1974). Variation in the number of presacral vertebrae in Bantu-speaking South African Negroes. *American Journal of Physical Anthropology*, 40(3), pp.369-374.

Decoding your South African ID number. 2019. Western Cape Government (producer), (2019). Cape Town. https://www.westerncape.gov.za/general-publication/decoding-your-south-african-id-number-0

Delport, E.G., Cucuzzella, T.R., Kim, N., Marley, J., Pruitt, C. and Delport, A.G., (2006). Lumbosacral transitional vertebrae: incidence in a consecutive patient series. *Pain physician*, 9(1), pp.53-56.

de Bruin, F., Ter Horst, S., Bloem, J.L., van den Berg, R., de Hooge, M., van Gaalen, F., Dagfinrud, H., van Oosterhout, M., Landewé, R., van der Heijde, D. and Reijnierse, M., (2017). Prevalence and clinical significance of lumbosacral transitional vertebra (LSTV) in a young back pain population with suspected axial spondyloarthritis: results of the Spondyloarthritis caught early (SPACE) cohort. *Skeletal radiology*, 46(5), pp.633-639.

Deora, H., Srinivas, D., Shukla, D., Devi, B.I., Mishra, A., Beniwal, M., Kannepalli, N.R. and Somanna, S., (2019). Multiple-site neural tube defects: embryogenesis with complete review of existing literature. *Neurosurgical Focus*, 47(4), pp.1-9.

DeWitte, S.N. and Stojanowski, C.M., (2015). The osteological paradox 20 years later: past perspectives, future directions. *Journal of Archaeological Research*, 23(4), pp.397-450.

Dharati, K., Nagar, S.K., Ojaswini, M., Dipali, T., Paras, S. and Sucheta, P., (2012). A study of sacralisation of fifth lumber vertebra in Gujarat. *National Journal of Medical research*, 2(2), pp.211-213.

Dias, M.S., (2007). Normal and abnormal development of the spine. *Neurosurgery Clinics of North America*, 18(3), pp.415-429.

Doo, A.R., Lee, J., Yeo, G.E., Lee, K.H., Kim, Y.S., Mun, J.H., Han, Y.J. and Son, J.S., (2020). The prevalence and clinical significance of transitional vertebrae: a radiologic investigation using whole spine spiral three-dimensional computed tomographic images. *Anesthesia & Pain Medicine*, 15(1), pp.103-110.

Dubrulle, J. and Pourquie, O., (2003). Welcome to syndetome: a new somitic compartment. *Developmental cell*, 4(5), pp.611-612.

Dulhunty, J., (2015). The measurement and correction of sacral obliquity PH.D Thesis. Macquarie University. Sydney, Australia. pp.1-315.

Dunsworth, H.M., (2020). Expanding the evolutionary explanations for sex differences in the human skeleton. *Evolutionary Anthropology*, 29(3), pp.1-116.

Du Plessis, A.M., (2017). Congenital anomalies in the vertebral column associated with thoracolumbar transitional vertebrae. Masters Thesis. Stellenbosch University. Stellenbosch, South Africa. pp.1-52.

Durrheim, K. and Tredoux, C., (2014). Numbers, hypotheses & conclusions: A course in statistics for the social sciences. Second Edition. Juta and Company Ltd. pp. 1-394.

Dzupa, V., Slepanek, M., Striz, M., Krbec, M., Chmelova, J., Kachlik, D. and Baca, V., (2014). Developmental malformations in the area of the lumbosacral transitional vertebrae and sacrum: differences in gender and left/right distribution. *Surgical and Radiologic Anatomy*, 36(7), pp.689-693.

Eisenstein, S.M. (1978). Spondylolysis: A skeletal investigation of two population groups. *Journal of Bone and Joint Surgery*. 60(4), pp.488-494.

Elster, A.D., (1989). Bertolotti's Syndrome Revisited: Transitional Vertebrae of the Lumbar Spine. *Spine*, 14(12), pp.1373-1377.

Erken, E., Ozer, H.T., Gulek, B. and Durgun, B., (2002). The association between cervical rib and sacralization. *Spine*, 27(15), pp.1659-1664.

Eubanks, J.D., Lee, M.J., Cassinelli, E. and Ahn, N.U., (2007). Prevalence of lumbar facet arthrosis and its relationship to age, sex, and race: an anatomic study of cadaveric specimens. *Spine*, 32(19), pp.2058-2062.

Faflia, C.P., Prassopoulos, P.K., Daskalogiannaki, M.E. and Gourtsoyiannis, N.C., (1998). Variation in the appearance of the normal sacroiliac joint on pelvic CT. *Clinical radiology*, 53(10), pp.742-746.

Farshad, M., Aichmair, A., Hughes, A.P., Herzog, R.J. and Farshad-Amacker, N.A., (2013). A reliable measurement for identifying a lumbosacral transitional vertebra with a solid bony bridge on a single-slice midsagittal MRI or plain lateral radiograph. *The Bone & Joint Journal*, 95(11), pp.1533-1537.

Farshad-Amacker, N.A., Lurie, B., Herzog, R.J. and Farshad, M., (2014a). Is the iliolumbar ligament a reliable identifier of the L5 vertebra in lumbosacral transitional anomalies? *European radiology*, 24(10), pp.2623-2630.

Farshad-Amacker, N.A., Lurie, B., Herzog, R.J. and Farshad, M., (2014b). Interreader and intermodality reliability of standard anteroposterior radiograph and magnetic resonance imaging in detection and classification of lumbosacral transitional vertebra. *The Spine Journal*, 14(8), pp.1470-1475.

Farshad-Amacker, N.A., Aichmair, A., Herzog, R.J. and Farshad, M., (2015). Merits of different anatomical landmarks for correct numbering of the lumbar vertebrae in lumbosacral transitional anomalies. *European Spine Journal*, 24(3), pp.600-608.

Farshad-Amacker, N.A., Herzog, R.J., Hughes, A.P., Aichmair, A. and Farshad, M., (2015). Associations between lumbosacral transitional anatomy types and degeneration at the transitional and adjacent segments. *The Spine Journal*, 15(6), pp.1210-1216.

Fleming, A., Keynes, R.J. and Tannahill, D., (2001). The role of the notochord in vertebral column formation. *The Journal of Anatomy*, 199(1-2), pp.177-180.

Forlani, S., Lawson, K.A. and Deschamps, J., (2003). Acquisition of Hox codes during gastrulation and axial elongation in the mouse embryo. *Development*, 130(16), pp.3807-3819.

Fromental-Ramain, C., Warot, X., Lakkaraju, S., Favier, B., Haack, H., Birling, C., Dierich, A. and Chambon, P., (1996). Specific and redundant functions of the paralogous Hoxa-9 and Hoxd-9 genes in forelimb and axial skeleton patterning. *Development*, 122(2), pp.461-472.

French, H.D., Somasundaram, A.J., Schaefer, N.R. and Laherty, R.W., (2014). Lumbosacral transitional vertebrae and its prevalence in the Australian population. *Global Spine Journal*, 4(04), pp.229-232.

Frymoyer, J.W., Newberg, A., Pope, M.H., Wilder, D.G., Clements, J. and MacPherson, B., (1984). Spine radiographs in patients with low-back pain. An epidemiological study in men. *The Journal of Bone and Joint Surgery*. American volume, 66(7), pp.1048-1055.

Fujiwara, A., Tamai, K., Yoshida, H., Kurihashi, A., Saotome, K., A, H.S. and Lim, T.H., (2000). Anatomy of the iliolumbar ligament. *Clinical Orthopaedics and Related Research*, 380, pp.167-172.

Giles, R.G., (1931). Vertebral anomalies. *Radiology*, 17(6), pp.1262-1266.

Gohil, I., Vilensky, J.A. and Weber, E.C., (2014). Vacuum phenomenon: clinical relevance. *Clinical Anatomy*, 27(3), pp.455-462.

Golubovsky, J.L., Colbrunn, R.W., Klatte, R.S., Nagle, T.F., Briskin, I.N., Chakravarthy, V.B., Gillespie, C.M., Reith, J.D., Jasty, N., Benzel, E.C. and Steinmetz, M.P., (2020). Development of a novel in vitro cadaveric model for analysis of biomechanics and surgical treatment of Bertolotti syndrome. *The Spine Journal*, 20(4), pp.638-656.

Gopalan, B. and Yerramshetty, J.S., (2018). Lumbosacral transitional vertebra-related low back pain: resolving the controversy. *Asian Spine Journal*, 12(3), pp.407-415.

Guan, W., Yu, W., Lin, Q., Zhang, Z., Du, G., Tian, J., Xu, Y. and Hsieh, E., (2018). Lumbar Vertebrae Morphological Analysis and an Additional Approach for Vertebrae Identification in Lumbar Spine DXA Images. *Journal of Clinical Densitometry*. 23(3), pp.395-402.

Gündüz, N., Günaydin, G.D., Eser, M.B., Aslan, A. and Kabaalioğlu, A., (2019). Role of iliac crest tangent in correct numbering of lumbosacral transitional vertebrae. *Turkish Journal of Medical Sciences*, 49(1), pp.184-189.

Ha, K.Y., Lee, J.S. and Kim, K.W., (2008). Degeneration of sacroiliac joint after instrumented lumbar or lumbosacral fusion: a prospective cohort study over five-year follow-up. *Spine*, 33(11), pp.1192-1198.

Haeusler, M., Martelli, S.A. and Boeni, T., (2002). Vertebrae numbers of the early hominid lumbar spine. *Journal of Human Evolution*, 43(5), pp.621-643.

Hahn, P.Y., Strobel, J.J. and Hahn, F.J., (1992). Verification of lumbosacral segments on MR images: identification of transitional vertebrae. *Radiology*, 182(2), pp.580-581.

Hald, H.J., Danz, B., Schwab, R., Burmeister, K. and Bähren, W., (1995). Radiographically demonstrable spinal changes in asymptomatic young men. *RoFo: Fortschritte auf dem Gebiete der Rontgenstrahlen und der Nuklearmedizin*, 163(1), pp.4-8.

Haffer, H., Becker, L., Putzier, M., Wiethölter, M., Ziegeler, K., Diekhoff, T., Pumberger, M. and Hardt, S., (2021). Changes of Fixed Anatomical Spinopelvic Parameter in Patients with Lumbosacral Transitional Vertebrae: A Matched Pair Analysis. *Diagnostics*, 11(1), pp.1-12.

Hammer, N., Steinke, H., Böhme, J., Stadler, J., Josten, C. and Spanel-Borowski, K., (2010). Description of the iliolumbar ligament for computer-assisted reconstruction. *Annals of Anatomy-Anatomischer Anzeige*r, 192(3), pp.162-167.

Hanhivaara, J., Määttä, J.H., Niinimäki, J. and Nevalainen, M.T., (2020). Lumbosacral transitional vertebrae are associated with lumbar degeneration: retrospective evaluation of 3855 consecutive abdominal CT scans. *European Radiology*, pp.1-8.

Hasner, E., Jacobsen, H.H., Schalimtzek, M. and Snorrason, E., (1953). Lumbosacral transitional vertebrae: a clinical and roentgenologic study of 400 cases of low back pain. *Acta radiologica*, (3), pp.225-230.

Hermanek, P., Rathore, J.S., Aloisi, V. and Carmignato, S., (2018). Principles of X-ray computed tomography. In Industrial X-Ray Computed Tomography. Springer, Cham. pp.25-67

Hinkle, D.E. and Wiersma, W., (2009). Applied Statistics for Behavioral Sciences, International 5th Edition, Cengage Learning. Inc., Boston. pp.95-115

Hou, L., Bai, X., Li, H., Gao, T., Li, W., Wen, T., He, Q., Ruan, D., Shi, L. and Bing, W., (2020). Lumbar plain radiograph is not reliable to identify lumbosacral transitional vertebra types according to Castellvi classification principle. *BMC Musculoskeletal Disorders*, 21, pp.1-8.

Hsieh, C.Y.J., Vanderford, J.D., Moreau, S.R. and Prong, T., (2000). Lumbosacral transitional segments: classification, prevalence, and effect on disk height. *Journal of Manipulative and Physiological Therapeutics*, 23(7), pp.483-489.

Huang, R., Zhi, Q., Brand-Saberi, B. and Christ, B., (2000). New experimental evidence for somite resegmentation. *Anatomy and Embryology*, 202(3), pp.195-200.

Hughes, R.J. and Saifuddin, A., (2004). Imaging of lumbosacral transitional vertebrae. *Clinical Radiology*, 59(11), pp.984-991.

Hughes, R.J. and Saifuddin, A., (2006). Numbering of lumbosacral transitional vertebrae on MRI: role of the iliolumbar ligaments. *American Journal of Roentgenology*, 187(1), pp.W59-W65.

Hunt, K., Ford, G., Harkins, L. and Wyke, S., (1999). Are women more ready to consult than men? Gender differences in family practitioner consultation for common chronic conditions. *Journal of Health Services Research & Policy*, 4(2), pp.96-100.

Hunt, D.R. and Albanese, J., (2005). History and demographic composition of the Robert J. Terry anatomical collection. *American Journal of Physical Anthropology*, 127(4), pp.406-417.

Hunt, K., Adamson, J., Hewitt, C. and Nazareth, I., (2011). Do women consult more than men? A review of gender and consultation for back pain and headache. *Journal of Health Services Research & Policy*, 16(2), pp.108-117.

IBM Corporation. (2017). IBM SPSS Statistics for Windows, version 25.0. Armonk, New York: IBM Corp. United States of America.

il Ju, C., Kim, S.W., Kim, J.G., Lee, S.M., Shin, H. and Lee, H.Y., (2017). Decompressive L5 transverse processectomy for Bertolotti's syndrome: A preliminary study. *Pain Physician*, 20, pp.E923-E932.

Illeez, O.G., Atıcı, A., Ulger, E.B., Kulcu, D.G., Ozkan, F.U. and Aktas, I., (2018). The transitional vertebra and sacroiliac joint dysfunction association. *European Spine Journal*, 27(1), pp.187-193.

Jancuska, J.M., Spivak, J.M. and Bendo, J.A., (2015). A Review of Symptomatic Lumbosacral Transitional Vertebrae: Bertolotti's Syndrome. *International Journal of Spine Surgery*, 9(1), pp.1-18.

Jacoby, G.W., (1895). Lumbar puncture of the subarachnoid space. *New York Medical Journal*, 62, pp.813-818.

Jeon, J.Y., Jeong, Y.M., Lee, S.W., Kim, J.H., Choi, H.Y. and Ahn, Y., (2018). The termination level of the dural sac relevant to caudal epidural block in lumbosacral transitional vertebrae: a comparison between sacralization and lumbarization groups. *Pain Physician*, 21(1), pp.73-82.

Jönsson, B., Strömqvist, B. and Egund, N., (1989). Anomalous lumbosacral articulations and low-back pain. Evaluation and treatment. *Spine*, 14(8), pp.831-834.

Josiah, D.T., Boo, S., Tarabishy, A. and Bhatia, S., (2017). Anatomical differences in patients with lumbosacral transitional vertebrae and implications for minimally invasive spine surgery. *Journal of Neurosurgery*: *Spine*, 26(2), pp.137-143.

Kaiser, S.P., Gardner, M.J., Liu, J., Routt Jr, M.C. and Morshed, S., (2014). Anatomic determinants of sacral dysmorphism and implications for safe iliosacral screw placement. *Journal of Bone and Joint Surgery*, 96(14), pp.1-8.

Kalcheim, C., (2015). Epithelial–mesenchymal transitions during neural crest and somite development. *Journal of Clinical Medicine*, 5(1), pp.1-15.

Kalender, W.A., (2006). X-ray computed tomography. *Physics in Medicine & Biology*, 51(13), pp.R29-43.

Kanematsu, R., Hanakita, J., Takahashi, T., Minami, M., Tomita, Y. and Honda, F., (2020). Extraforaminal entrapment of the fifth lumbar spinal nerve by nearthrosis in patients with lumbosacral transitional vertebrae. *European Spine Journal*, pp.1-7.

Kapandji, A.I., (2008). The physiology of the joints, Volume3: The spinal column, pelvic girdle and head. Edinburgh: Churchill Livingstone. Copyright Éditions Maloine, pp.89-141.

Kapetanakis, S., Chaniotakis, C., Paraskevopoulos, C. and Pavlidis, P., (2017). An unusual case report of Bertolotti's syndrome: extraforaminal stenosis and L5 unilateral root compression (Castellvi Type III an LSTV). *Journal of Orthopaedic Case Reports*, 7(3), pp.1-9.

Kaplan, K.M., Spivak, J.M. and Bendo, J.A., (2005). Embryology of the spine and associated congenital abnormalities. *The Spine Journal*, 5(5), pp.564-576.

Kassir, M.A., Al-Faham, Z., Abel, N. and Balon, H.R., (2015). Lumbosacral Transitional Vertebra Diagnosed on 99mTc-Methylene Diphosphonate SPECT/CT. *Journal of Nuclear Medicine Technology*, 43(2), pp.137-138.

Keith, A., (1902). The extent to which the posterior segments of the body have been transmuted and suppressed in the evolution of man and allied primates. *Journal of Anatomy And Physiology*, 37(Pt 1), pp.1-18.

Keller, R., (2005). Cell migration during gastrulation. *Current Opinion in Cell Biology*, 17(5), pp.533-541.

Kellgren, J.H. and Lawrence, J.S., (1956). Rheumatoid arthritis in a population sample. *Annals of The Rheumatic Diseases*, 15(1), pp.1-11.

Keynes, R., (2018). Patterning spinal nerves and vertebral bones. *Journal of Anatomy*, 232(4), pp.534-539.

Khan, M.B., Khan, M.Z., Waqar, M., Satar, A., Saeed, M. and Arif, M., (2018). Prevalence of Lumbosacral Transitional Vertebrae Among Patients Presented to Hayatabad Medical Complex, Peshawar. *Journal of Pakistan Orthopaedic Association*, 30(01), pp.9-12.

Khanna, A.J., (2014). MRI essentials for the spine specialist. New York: *Thieme*. pp.3-18.

Kim, N.H. and Suk, K.S., (1995). The Role of Transitional Vertebra in Spondylolysis and Spondyloytic Spondylolisthesis. *Journal of the Korean Orthopaedic Association*, 30(2), pp.286-290.

Kim, J.T., Jung, C.W., Lee, J.R., Min, S.W. and Bahk, J.H., (2003). Influence of lumbar flexion on the position of the intercrestal line. *Regional Anesthesia & Pain Medicine,*, 28(6), pp.509-511.

Kim, J.H., Kim, S.W. and Kim, H.S., (2012). Congenital osseous bridging of lumbar transverse processes. *Journal of Korean Neurosurgical Society*, 52(2), pp.159-160.

Kim, H.Y., (2017). Statistical notes for clinical researchers: Chi-squared test and Fisher's exact test. *Restorative Dentistry & Endodontics*, 42(2), pp.152-155.

Komar, D.A. and Grivas, C., (2008). Manufactured populations: what do contemporary reference skeletal collections represent? A comparative study using the Maxwell Museum documented collection. *American Journal of Physical Anthropology*, 137(2), pp.224-233.

Konin, G.P. and Walz, D.M., (2010). Lumbosacral transitional vertebrae: classification, imaging findings, and clinical relevance. *American Journal of Neuroradiology*, 31(10), pp.1778-1786.

Kotrlik, J.W., Williams, H.A. and Jabor, M.K., (2011). Reporting and Interpreting Effect Size in Quantitative Agricultural Education Research. *Journal of Agricultural Education*, 52(1), pp.132-142.

Kramer, B., Hutchinson, E.F., Brits, D.M. and Billings, B.K., (2019). Making the ethical transition in South Africa: Acquiring human bodies for training in anatomy. *Anatomical Sciences Education*, 12(3), pp.264-271.

Kubota, Y., Toyoda, Y. and Kubota, H., (1992). Jacoby's line rather than Tuffier's line as a guide to lumbar puncture. *Anesthesia & Analgesia*, 74(6), pp.939.

L'Abbé, E.N., Loots, M. and Meiring, J.H., (2005). The Pretoria bone collection: a modern South African skeletal sample. *Homo*, 56(2), pp.197-205.

Laloo, F., Herregods, N., Varkas, G., Jaremko, J.L., Baraliakos, X., Elewaut, D., Van den Bosch, F., Verstraete, K. and Jans, L., (2017). MR signal in the sacroiliac joint space in spondyloarthritis: a new sign. *European Radiology*, 27(5), pp.2024-2030.

Latimer, B. and Ward, C.V., (1993). The thoracic and lumbar vertebrae. The Nariokotome Homo erectus skeleton. Cambridge, MA: Harvard University Press. pp.266-293.

Lawrence, J.S., Bremner, J.M., Ball, J. and Burch, T.A., (1966). Rheumatoid arthritis in a subtropical population. *Annals of The Rheumatic Diseases*, 25(1), pp.59-66.

Leboeuf, C., Kimber, D. and White, K., (1989). Prevalence of spondylolisthesis, transitional anomalies and low intercrestal line in a chiropractic patient population. *Journal of Manipulative and Physiological Therapeutics*, 12(3), pp.200-204.

Lee, C.H., Seo, B.K., Choi, Y.C., Shin, H.J., Park, J.H., Jeon, H.J., Kim, K.A., Park, C.M. and Kim, B.H., (2004). Using MRI to evaluate anatomic significance of aortic bifurcation, right renal artery, and conus medullaris when locating lumbar vertebral segments. *American Journal of Roentgenology*, 182(5), pp.1295-1300.

Lee, C.H., Park, C.M., Kim, K.A., Hong, S.J., Seol, H.Y., Kim, B.H. and Kim, J.H., (2007). Identification and prediction of transitional vertebrae on imaging studies: anatomical significance of paraspinal structures. *Clinical Anatomy*, 20(8), pp.905-914.

Li, Y., Lubelski, D., Abdullah, K.G., Mroz, T.E. and Steinmetz, M.P., (2014). Minimally invasive tubular resection of the anomalous transverse process in patients with Bertolotti's syndrome: presented at the 2013 Joint Spine Section Meeting. *Journal of Neurosurgery: Spine*, 20(3), pp.283-290.

Lian, J., Levine, N. and Cho, W., (2018). A review of lumbosacral transitional vertebrae and associated vertebral numeration. *European Spine Journal*, 27(5), pp.995-1004.

Lo, S.S., Atceken, Z., Carone, M. and Yousem, D.M., (2011). Sacroiliac joint vacuum phenomenon—underreported finding. *Clinical Imaging*, 35(6), pp.465-469.

Lovejoy, C.O., Suwa, G., Simpson, S.W., Matternes, J.H. and White, T.D., (2009). The great divides: Ardipithecus ramidus reveals the postcrania of our last common ancestors with African apes. *Science*, 326(5949), pp.73-106.

Lovejoy, C.O. and McCollum, M.A., (2010). Spinopelvic pathways to bipedality: why no hominids ever relied on a bent-hip–bent-knee gait. Philosophical Transactions of the Royal Society B: *Biological Sciences*, 365(1556), pp.3289-3299.

Lovejoy. C.O., Latimer, B.M., Spurlock, L. and Haile-Selassie, Y., (2016). 'Chapter 8: The Pelvic Girdle and Limb Bones of KSD-VP-1/1', in Haile-Selassie, Y. and Su, D.F. (eds.), The Postcranial Anatomy of Australopithecus Afarensis: New Insights from KSD-VP-1/1. Springer, pp.167-169.

Lucas, R.E., (1985). Mines and migrants in South Africa. *The American Economic Review*, pp.1094-1108.

Luk, K.D., Ho, H.C. and Leong, J.C., (1986). The iliolumbar ligament. A study of its anatomy, development and clinical significance. *The Journal of Bone and Joint Surgery*. British volume, 68(2), pp.197-200.

Luo, R., Barsoum, D., Ashraf, H., Cheng, J., Hurwitz, N.R., Goldsmith, C.Y. and Moley, P.J., (2021). Prevalence of lumbosacral transitional vertebrae in patients with symptomatic femoroacetabular impingement requiring hip arthroscopy. Arthroscopy: *The Journal of Arthroscopic & Related Surgery*. 37(1), pp.149-155.

Luoma, K., Vehmas, T., Raininko, R., Luukkonen, R. and Riihimäki, H., (2004). Lumbosacral transitional vertebra: relation to disc degeneration and low back pain. *Spine*, 29(2), pp.200-205.

McIntyre, D.C., Rakshit, S., Yallowitz, A.R., Loken, L., Jeannotte, L., Capecchi, M.R. and Wellik, D.M., (2007). Hox patterning of the vertebrate rib cage. *Development*, 134(16), pp.2981-2989.

Magee, D.J. (2008). Orthopedic Physical Assessment. 5th Edition. St. Louis, Mo, Saunders Elsevier. pp.590.

Mahato, N.K., (2010). Morphometric analysis and identification of characteristic features in sacra bearing accessory articulations with L5 vertebrae. *The Spine Journal*, 10(7), pp.616-621.

Mahato, N.K., (2011a). Facet dimensions, orientation, and symmetry at L5–S1 junction in lumbosacral transitional States. *Spine*, 36(9), pp.E569-E573.

Mahato, N.K., (2011b). Disc spaces, vertebral dimensions, and angle values at the lumbar region: a radioanatomical perspective in spines with L5–S1 transitions. *Journal of Neurosurgery: Spine*, 15(4), pp.371-379.

Mahato, N.K., (2013a). Redefining lumbosacral transitional vertebrae (LSTV) classification: integrating the full spectrum of morphological alterations in a biomechanical continuum. *Medical Hypotheses*, 81(1), pp.76-81.

Mahato, N.K., (2013b). Complexity of neutral zones, lumbar stability and subsystem adaptations: probable alterations in lumbosacral transitional vertebrae (LSTV) subtypes. *Medical Hypotheses*, 80(1), pp.61-64.

Mahato, N.K., (2016). Implications of structural variations in the human sacrum: why is an anatomical classification crucial? *Surgical and Radiologic Anatomy*, 38(8), pp.947-954.

Mahato, N.K., Dhason, R. and Ram, D.R., (2019). Quantifying range of motion and stress patterns at the transitional lumbosacral junction: Pilot study using a computational model for load-bearing at accessory L5-S1 articulation. *International Journal of Spine Surgery*, 13(1), pp.17-23.

Malanga, G.A. and Cooke, P.M., (2004). Segmental anomaly leading to wrong level disc surgery in cauda equina syndrome. *Pain Physician*, 7(1), pp.107-110.

Mamo, G., Batra, R. and Steinig, J., (2021). A Case of Diastematomyelia Presenting With Minimal Neurologic Deficits in a Middle-Aged Patient. *Cureus*, 13(1), pp.1-5.

Manmohan, S., Dzulkarnain, A., Azlin, Z.N. and Fazir, M., (2015). Bertolotti's syndrome: A commonly missed cause of back pain in young patients. *Malaysian Family Physician*, 10(2), pp.55-57.

Marić, D.L., Krstonošić, B., Erić, M., Marić, D.M., Stanković, M. and Milošević, N.T., (2015). An anatomical study of the lumbar external foraminal ligaments: appearance at MR imaging. *Surgical and Radiologic Anatomy*, 37(1), pp.87-91.

Masud, R., Rehman, K., Sadiq, A. and Ahmed, S., (2016). Lumbosacral transitional vertebrae: incidence in patients with low back pain. *Pakistan Journal of Radiology*, 21(4), pp.159-162.

Matson, D.M., MacCormick, L.M., Sembrano, J.N. and Polly, D.W., (2020). Sacral Dysmorphism and Lumbosacral Transitional Vertebrae (LSTV) Review. *International Journal of Spine Surgery*, 14(s1), pp.S14-S19.

Matveeva, N., Papazova, M., Zhivadinovik, J., Zafirova, B., Dodevski, A. and Poposka, V., (2015). Morphologic characteristics of sacra associated with assimilation of the last lumbar vertebra. *Folia Morphologica*, pp.196-203.

McBride, G.B., (2005). A proposal for strength-of-agreement criteria for Lin's concordance correlation coefficient. NIWA client report: HAM2005-062, pp.62-65.

McCollum, M.A., Rosenman, B.A., Suwa, G., Meindl, R.S. and Lovejoy, C.O., (2010). The vertebral formula of the last common ancestor of African apes and humans. *Journal of Experimental Zoology Part B: Molecular and Developmental Evolution*, 314(2), pp.123-134.

McCulloch, J.A. and Waddell, G, (1980). Variation of the lumbosacral myotomes with bony segmental anomalies. *The Journal of Bone and Joint Surgery*. British volume, 62(4), pp.475-480.

McHugh, M.L., (2013). The chi-square test of independence. *Biochemia medica*, 23(2), pp.143-149.

Miller, A.N. and Routt Jr, M.L.C., (2012). Variations in sacral morphology and implications for iliosacral screw fixation. *Journal of the American Academy of Orthopaedic Surgeons*, 20(1), pp.8-16.

Mirjalili, S.A., McFadden, S.L., Buckenham, T., Wilson, B. and Stringer, M.D., (2012). Anatomical planes: are we teaching accurate surface anatomy?. *Clinical Anatomy*, 25(7), pp.819-826.

Mitra, R. and Carlisle, M., (2008). Bertolotti's syndrome: a case report. *Pain Practice*, 9(2), pp.152-154.

Mohamed Abith Ali, I., (2011). A study of Lumbosacral Transitional Vertebra and its significance in Lumbar Disc Surgery. Masters Dissertation, Stanley Medical College, Chennai. pp.38-50.

Moore, B.H., (1925). Sacralization of the fifth lumbar vertebra. *Journal of Bone and Joint Surgery*, 7(2), pp.271-278.

Moore, K.L., Dalley, A.F., and Agur, A.M.R. (2014). Clinically Orientated Anatomy. Seventh Edition. Lippincott William and Wilkins. Philadelphia. pp.440-450

Moore, K.L., Persaud, T.V.N. and Torchia, M.G., (2018). The Developing Human-E-Book: Clinically Oriented Embryology. Elsevier Health Sciences. pp.337-353.

Morimoto, T., Sonohata, M., Kitajima, M., Konishi, H., Otani, K., Kikuchi, S.I. and Mawatari, M., (2013). The termination level of the conus medullaris and lumbosacral transitional vertebrae. *Journal of Orthopaedic Science*, 18(6), pp.878-884.

Morris, A.G. (1984). An Osteological Analysis of the Protohistoric Populations of the Northern Cape and Western Orange Free state, South Africa. PhD Thesis. University of Witwatersrand, Johannesburg. pp.269-270.

Mould, R.F., (1995). The early history of X-ray diagnosis with emphasis on the contributions of physics 1895-1915. *Physics in Medicine & Biology*, 40(11), pp.1741-1785.

Mousavi, S.J., van Dieën, J.H. and Anderson, D.E., (2019). Low back pain: Moving toward mechanism-based management. *Clinical Biomechanics*, 61, pp.190-191.

Nachemson, A.L.F., (1975). Towards a better understanding of low-back pain: a review of the mechanics of the lumbar disc. *Rheumatology*, 14(3), pp.129-143.

Naciye, K.I.Ş. and Düzkalir, H.G., (2017). Analysis of Iliolumbar Ligament on Lumbosacral Transitional Anomalies. *The Journal of Turkish Spinal Surgery*, 28(3), pp.155-157.

Nakagawa, T., Hashimoto, K., Tsubakino, T., Hoshikawa, T., Inawashiro, T. and Tanaka, Y., (2017). Lumbosacral Transitional Vertebrae Cause Spinal Level Misconception in Surgeries for Degenerative Lumbar Spine Disorders. *The Tohoku Journal of Experimental Medicine*, 242(3), pp.223-228.

Nakajima, A., Usui, A., Hosokai, Y., Kawasumi, Y., Abiko, K., Funayama, M. and Saito, H., (2014). The prevalence of morphological changes in the thoracolumbar spine on whole-spine computed tomographic images. *Insights into Imaging*, 5(1), pp.77-83.

Nardo, L., Alizai, H., Virayavanich, W., Liu, F., Hernandez, A., Lynch, J.A., Nevitt, M.C., McCulloch, C.E., Lane, N.E. and Link, T.M., (2012). Lumbosacral transitional vertebrae: association with low back pain. *Radiology*, 265(2), pp.497-503.

Nevalainen, M.T., McCarthy, E., Morrison, W.B., Zoga, A.C. and Roedl, J.B., (2018). Lumbosacral transitional vertebrae: significance of local bone marrow edema at the transverse processes. *Skeletal Radiology*, 47(8), pp.1145-1149.

Nicholson, A.A., Roberts, G.M. and Williams, L.A., (1988). The measured height of the lumbosacral disc in patients with and without transitional vertebrae. *The British Journal of Radiology*, 61(726), pp.454-455.

Nieves, J.W., (2017). Sex-differences in skeletal growth and aging. *Current Osteoporosis Reports*, 15(2), pp.70-75.

Nikitovic, D., (2018). Sexual dimorphism (humans). *The International Encyclopedia of Biological Anthropology*, pp.1-4.

Njeze, N.R., Ezeofor, S.N. and Agwu-Umahi, O.R., (2018). Plain radiograghs of lumbar spine in patients with low back pain. *Archives of Osteoporosis*, 13(1), pp.1-6.

Oatis, C.A., (2017). Kinesiology: The Mechanics and Pathomechanics of Human Movement. Third Edition. Lippincott Williams & Wilkins. Philadelphia. pp.600-680.

O'Driscoll, C.M., Irwin, A. and Saifuddin, A., (1996). Variations in morphology of the lumbosacral junction on sagittal MRI: correlation with plain radiography. *Skeletal Radiology*, 25(3), pp.225-230.

Olofin, M.U., Noronha, C. and Okanlawon, A., (2001). Incidence of lumbosacral transitional vertebrae in low back pain patients. *West African Journal of Radiology*, 8, pp.1-6.

Ono, T., Tarukado, K., Tono, O., Harimaya, K., Morishita, Y., Nakashima, Y. and Doi, T., (2018). The morphological relationship between lumbosacral transitional vertebrae and lumbosacral pedicle asymmetry. *Spine Surgery and Related Research*, 2(1), pp.77-81.

Otani, K., Konno, S. and Kikuchi, S., (2001). Lumbosacral transitional vertebrae and nerve-root symptoms. *The Journal of Bone and Joint Surgery*. British volume, 83(8), pp.1137-1140.

O'Rahilly, R., Müller, F. and Meyer, D.B., (1990). The human vertebral column at the end of the embryonic period proper. 4. The sacrococcygeal region. *Journal of Anatomy*, 168, pp.95-110.

O'Rahilly, R. and Müller, F., (2003). Somites, spinal ganglia, and centra. *Cells Tissues Organs*, 173(2), pp.75-92.

Oyinloye, O.I., Abdulkadir, A.Y. and Babalola, M., (2009). Incidence and patterns of lumbosacral transitional vertebrae, in patients with low backpain in a Nigerian hospital. *Nigerian Quarterly Journal of Hospital Medicine*, 19(2), pp.96-99.

Paik, N.C., Lim, C.S. and Jang, H.S., (2013). Numeric and morphological verification of lumbosacral segments in 8280 consecutive patients. *Spine*, 38(10), pp.E573-E578.

Pallant, J., (2013). Statistical techniques to compare groups: A step by step guide to data analysis using SPSS. SPSS survival Manual, 5, pp.201-238.

Pang, D., Zovickian, J. and Moes, G.S., (2011). Retained medullary cord in humans: late arrest of secondary neurulation. *Neurosurgery*, 68(6), pp.1500-1519.

Papadakis, M., Sapkas, G., Papadopoulos, E.C. and Katonis, P., (2011). Pathophysiology and biomechanics of the aging spine. *The Open Orthopaedics Journal*, 5, pp.335-343.

Park, S.K., Park, J.G., Kim, B.S., Huh, J.D. and Kang, H., (2016). Thoracolumbar junction: morphologic characteristics, various variants and significance. *The British Journal of Radiology*, 89(1064), pp.1-8.

Park, T.S., Lim, Y.S., Baek, S.Y. and Yoon, S., (2019). Incidence Rate of Lumbosacral Transitional Vertebrae and Measurement of their Cross-sectional Areas of Vertebral Canal and Dural Sac Using Magnetic Resonance Imaging. *Anatomy & Biological Anthropology*, 32(1), pp.31-42.

Peterson, C.K., Bolton, J., Hsu, W. and Wood, A., (2005). A cross-sectional study comparing pain and disability levels in patients with low back pain with and without transitional lumbosacral vertebrae. *Journal of Manipulative and Physiological Therapeutics*, 28(8), pp.570-574.

Peh, W.C., Siu, T.H. and Chan, J.H., (1999). Determining the lumbar vertebral segments on magnetic resonance imaging. *Spine*, 24(17), pp.1852.

Pilbeam, D., (2004). The anthropoid postcranial axial skeleton: comments on development, variation, and evolution. *Journal of Experimental Zoology Part B: Molecular and Developmental Evolution*, 302(3), pp.241-267.

Pool-Goudzwaard, A., van Dijke, G.H., Mulder, P., Spoor, C., Snijders, C. and Stoeckart, R., (2003). The iliolumbar ligament: its influence on stability of the sacroiliac joint. *Clinical Biomechanics*, 18(2), pp.99-105.

Porter, N.A., Lalam, R.K., Tins, B.J., Tyrrell, P.N., Singh, J. and Cassar-Pullicino, V.N., (2014). Prevalence of extraforaminal nerve root compression below lumbosacral transitional vertebrae. *Skeletal Radiology*, 43(1), pp.55-60.

Quinlan, J.F., Duke, D. and Eustace, S., (2006). Bertolotti's syndrome: a cause of back pain in young people. *The Journal of Bone and Joint Surgery*. British volume, 88(9), pp.1183-1186.

Radulovska-Chabukovska, J., Matveeva, N. and Poposka, A., (2014). Lumbosacral transitional anatomy types and disc degenerative changes. *Sanamed*, 9(2), pp.131-136.

Rafieyan, V., (2016). Relationship between acculturation attitude and translation of culture-bound texts. *Journal of Studies in Education*, 6(2), pp.144-156.

Ramesh, T., Nagula, S.V., Tardieu, G.G., Saker, E., Shoja, M., Loukas, M., Oskouian, R.J. and Tubbs, R.S., (2017). Update on the notochord including its embryology, molecular development, and pathology: a primer for the clinician. *Cureus*, 9(4). pp.1-11.

Remak, R., (1855). Untersuchungen über die Entwickelung der Wirbelthiere (Vol. 1). G. Reimer. pp.1-189.

Rilliet B. (2008). Diastematomyelia. In: The Spina Bifida. Springer, Milano. pp.487-489.

Ríos, L., Weisensee, K. and Rissech, C., (2008). Sacral fusion as an aid in age estimation. *Forensic Science International*, 180(2), pp.111-13.

Ríos, L., Munoz, A., Cardoso, H. and Pastor, F., (2014). Traits unique to genus Homo within primates at the cervical spine (C2–C7). *Annals of Anatomy-Anatomischer Anzeiger*, 196(2-3), pp.167-173.

Robinson, J. (1972). Early Hominid Posture and Locomotion. The University of Chicago Press. Chicago. pp.365.

Rousseeuw, P.J. and Hubert, M., (2011). Robust statistics for outlier detection. *Wiley Interdisciplinary Reviews: Data Mining and Knowledge Discovery*, 1(1), pp.73-79.

Rowton, M., (2013). The Role of PARAXIS as a Mediator of Epithelial-mesenchymal Transitions During the Development of the Vertebrate Musculoskeletal System. Doctoral dissertation. Arizona State University. United States of America. pp.1-50.

Rucco, V., Basadonna, P.T. and Gasparini, D., (1996). ANATOMY OF THE ILIOLUMBAR LIGAMENT: A Review of its Anatomy and a Magnetic Resonance Study1. *American Journal of Physical Medicine & Rehabilitation*, 75(6), pp.451-455.

Sahin, O., Gurel, K., Gurel, S. and Gulekon, N., (2007). Osseous bridging of lumbar transverse processes causing low back pain: a case report and review of the literature. *Journal of Back and Musculoskeletal Rehabilitation*, 20(2-3), pp.127-130.

Sakamoto, F.A., Winalski, C.S., Schils, J.P., Parker, R.D. and Polster, J.M., (2011). Vacuum phenomenon: prevalence and appearance in the knee with 3 T magnetic resonance imaging. *Skeletal Radiology*, 40(10), pp.1275-1285.

Sanchis-Gimeno, J.A., Llido, S. and Nalla, S., (2018). Double Retrotransverse Foramen of Atlas (C1). *World neurosurgery*, 114, pp.e869-e872.

Sangari, S.K., Dossous, P.M., Heineman, T. and Mtui, E.P., (2015). Dimensions and anatomical variants of the foramen transversarium of typical cervical vertebrae. *Anatomy Research International*, 2015. pp.1-4.

Santavirta, S., Tallroth, K., Ylinen, P. and Suoranta, H., (1993). Surgical treatment of Bertolotti's syndrome. *Archives of Orthopaedic and Trauma Surgery*, 112(2), pp.82-87.

Santiago, F., Milena, G., Herrera, R., Romero, P. and Plazas, P., (2001). Morphometry of the lower lumbar vertebrae in patients with and without low back pain. *European Spine Journal*, 10(3), pp.228-233.

Sarawagi, R., Kankanala, S. and Gupta, S.K., (2016). Detection of numeric and morphological variation at lumbosacral junction: Role of whole spine magnetic resonance imaging. *West African Journal of Radiology*, 23(2), pp.95-100.

Savage, C. (2005). Lumbosacral Transitional Vertebrae: Classification of Variation and Associated with Low Back Pain. M.A. Thesis. University of Missouri-Columbia. Columbia, United States of America. pp.1-41.

Scaal, M., (2016). Early development of the vertebral column. *Seminars in Cell & Developmental Biology*. Academic Press. Vol. 49, pp.83-91.

Schneider, C.A., Rasband, W.S. and Eliceiri, K.W., (2012). NIH Image to ImageJ: 25 years of image analysis. *Nature Methods*, 9(7), pp.671-675.

Schmorl, G., (1971). The human spine in health and disease. *In The human spine in health and disease*. pp.1-504.

Schoenwolf, G.C., Bleyl, S.B., Brauer, P.R. and Francis-West, P.H., (2009). Development of the musculoskeletal system. Larsen's human embryology. 5th ed. Philadelphia, PA: Churchill Livingstone, pp.172-96.

Schultz, A.H., (1930). The skeleton of the trunk and limbs of higher primates. *Human Biology*, 2(3), pp.303-438.

Schultz, A.H., (1960). Vertebral column and thorax (Vol. 4). Karg*er Medical and Scientific Publishers*. pp.1–66.

Seçer, M., Muradov, J. M., Dalgiç, A., (2009). Evaluation of congenital lumbosacral malformations and neurological findings in patients with low back pain. *Turkish Neurosurgery*, 19(2), pp.145-148.

Sekharappa, V., Amritanand, R., Krishnan, V. and David, K.S., (2014). Lumbosacral transition vertebra: prevalence and its significance. *Asian Spine Journal*, 8(1), pp.51-58.

Shaikh, A., Khan, S.A., Hussain, M., Soomro, S., Adel, H., Adil, S.O., Huda, F. and Khanzada, U., (2017). Prevalence of lumbosacral transitional vertebra in individuals with low back pain: evaluation using plain radiography and magnetic resonance imaging. *Asian Spine Journal*, 11(6), pp.892-397.

Shapiro, S.S. and Wilk, M.B., (1965). An analysis of variance test for normality (complete samples). *Biometrika*, 52(3/4), pp.591-611.

Sharma, V.A., Sharma, D.K. and Shukla, C.K., (2011). Oesteogenic study of lumbosacral transitional vertebra in central India region. *Journal of Anatomical Society of India*, 60(2), pp.212-217.

Shellshear, J.L., (1949). The transverse process of the fifth lumbar vertebra. *Surveys of Anatomical Fields*. Sydney: Grahame. Ch3. pp.21-32.

Shinonara, K., Kaneko, M., Ugawa, R., Arataki, S. and Takeuchi, K., (2021). The effectiveness of preoperative assessment using a patient-specific three-dimensional pseudoarticulation model for minimally invasive posterior resection in a patient with Bertolotti's syndrome: a case report. *Journal of Medical Case Reports*, 15(1), pp.1-6.

Sims, J.A. and Moorman, S.J., (1996). The role of the iliolumbar ligament in low back pain. *Medical Hypotheses*, 46(6), pp.511-515.

Skórzewska, A., Grzymisławska, M., Bruska, M., Łupicka, J. and Woźniak, W., (2013). Ossification of the vertebral column in human foetuses: histological and computed tomography studies. *Folia Morphologica*, 72(3), pp.230-238.

Smith, L.J., Nerurkar, N.L., Choi, K.S., Harfe, B.D. and Elliott, D.M., (2011). Degeneration and regeneration of the intervertebral disc: lessons from development. *Disease Models & Mechanisms*, 4(1), pp.31-41.

Snider, K.T., Kribs, J.W., Snider, E.J., Degenhardt, B.F., Bukowski, A. and Johnson, J.C., (2008). Reliability of Tuffier's line as an anatomic landmark. *Spine*, 33(6), pp.E161-E165.

Southworth, J.D. and Bersack, S.R., (1950). Anomalies of the lumbosacral vertebrae in 550 individuals without symptoms referable to the low back. *The American Journal of Roentgenology and Radium Therapy*, 64(4), pp.624-634.

Statistics South Africa. Mid-Year Population Estimates 2019 (dataset). Statistical Release version P0302. Pretoria. Statistics South Africa (producer), (2019). South Africa. http://www.statssa.gov.za/publications/P0302/P03022019.pdf

Steinberg, E.L., Luger, E., Arbel, R., Menachem, A. and Dekel, S., (2003). A comparative roentgenographic analysis of the lumbar spine in male army recruits with and without lower back pain. *Clinical Radiology*, 58(12), pp.985-989.

Stemple, D.L., (2005). Structure and function of the notochord: an essential organ for chordate development. *Development*, 132(11), pp.2503-2512.

Stinchfield, F.E. and Sinton, W.A., (1955). Clinical significance of the transitional lumbosacral vertebra: relationship to back pain, disk disease, and sciatica. *Journal of the American Medical Association*, 157(13), pp.1107-1109.

Susai Manickam, P. and Dhason, R., (2006). A Biomechanical Study of Lumbosacral Transitional Vertebrae (L4/S1) Using Finite Element Method. *Journal of Engineering and Applied Sciences*, 11(12), pp.7898-7901.

Tague, R.G., (2009). High assimilation of the sacrum in a sample of American skeletons: prevalence, pelvic size, and obstetrical and evolutionary implications. *American Journal of Physical Anthropology*, 138(4), pp.429-438.

Tague, R.G., (2011). Fusion of coccyx to sacrum in humans: prevalence, correlates, and effect on pelvic size, with obstetrical and evolutionary implications. *American Journal of Physical Anthropology*, 145(3), pp.426-437.

Takata, Y., Higashino, K., Morimoto, M., Sakai, T., Yamashita, K., Abe, M., Nagamachi, A. and Sairyo, K., (2016). Vacuum phenomenon of the sacroiliac joint: Correlation with sacropelvic morphology. *Asian Spine Journal*, 10(4), pp.762-766.

Tang, M., Yang, X.F., Yang, S.W., Han, P., Ma, Y.M., Yu, H. and Zhu, B., (2014). Lumbosacral transitional vertebra in a population-based study of 5860 individuals: Prevalence and relationship to low back pain. *European Journal of Radiology*, 83(9), pp.1679-1682.

Taskaynatan, M.A., Izci, Y., Ozgul, A., Hazneci, B., Dursun, H. and Kalyon, T.A., (2005). Clinical significance of congenital lumbosacral malformations in young male population with prolonged low back pain. *Spine*, 30(8), pp.E210-E213.

Taylor, J.R. and Twomey, L.T., (1984). Sexual dimorphism in human vertebral body shape. *Journal of anatomy*, 138(Pt 2), pp.281-286.

Thawait, G.K., Chhabra, A. and Carrino, J.A., (2012). Spine Enumeration Segmentation and Normal and Variants. Spine Imaging, *An Issue of Radiologic Clinics of North America-E-Book*, 50(4), pp.587-598.

Tilly, C., (1976). Migration in modern European history. University of Michigan, USA. pp 1-46.

Tini, P.G., Wieser, C. and Zinn, W.M., (1977). The transitional vertebra of the lumbosacral spine: its radiological classification, incidence, prevalence, and clinical significance. *Rheumatology*, 16(3), pp.180-185.

Tins, B.J. and Balain, B., (2016). Incidence of numerical variants and transitional lumbosacral vertebrae on whole-spine MRI. *Insights into Imaging*, 7(2), pp.199-203.

Tom, W.R., Pham, T.M. and Shirvalkar, P., (2021). A Tale of Two Cords: Diastematomyelia. *Pain Medicine*, 22(4), pp.1000-1001.

Toyohara, R., Kurosawa, D., Hammer, N., Werner, M., Honda, K., Sekiguchi, Y., Izumi, S.I., Murakami, E., Ozawa, H. and Ohashi, T., (2020). Finite element analysis of load transition on sacroiliac joint during bipedal walking. *Scientific Reports*, 10(1), pp.1-10.

Tucker, B.J., Weinberg, D.S. and Liu, R.W., (2019). Lumbosacral Transitional Vertebrae. *Clinical Spine Surgery*, 32(7), pp.E330-E334.

Tuffier, T., (1900). Anesthesie medullaire chirurgicale par injection sous-arachnoidienne lombaire de cocaine; technique et resultats. *Sem Med*, 20, pp.167-9.

Tureli, D., Ekinci, G. and Baltacioglu, F., (2014). Is any landmark reliable in vertebral enumeration? A study of 3.0-Tesla lumbar MRI comparing skeletal, neural, and vascular markers. *Clinical Imaging*, 38(6), pp.792-796.

Ubelaker, D.H. and DeGaglia, C.M., (2017). Population variation in skeletal sexual dimorphism. *Forensic Science International*, 278, pp.407-409.

Uçar, D., Uçar, B.Y., Coşar, Y., Emrem, K., Gümüşsuyu, G., Mutlu, S., Mutlu, B., Çaçan, M.A., Mertsoy, Y. and Gümüş, H., (2013). Retrospective cohort study of the prevalence of lumbosacral transitional vertebra in a wide and well-represented population. *Arthritis*. pp.1-5.

Uhthoff, H.K., (1993). Prenatal development of the iliolumbar ligament. *The Journal of Bone and Joint Surgery*. British volume, 75(1), pp.93-95.

Umeh, R., Fisahn, C., Burgess, B., Iwanaga, J., Moisi, M., Oskouian, R.J. and Tubbs, R.S., (2016). Transforaminal ligaments of the lumbar spine: A comprehensive review. *Cureus*, 8(10), pp.2-5.

Unoki, E., Abe, E., Murai, H., Kobayashi, T. and Abe, T., (2016). Fusion of multiple segments can increase the incidence of sacroiliac joint pain after lumbar or lumbosacral fusion. *Spine*, 41(12), pp.999-1005.

Vergauwen, S., Parizel, P.M., Van Breusegem, L., Van Goethem, J.W., Nackaerts, Y., Van den Hauwe, L. and De Schepper, A.M., (1997). Distribution and incidence of degenerative spine changes in patients with a lumbo-sacral transitional vertebra. *European Spine Journal*, 6(3), pp.168-172.

Verma, J.P. and Abdel-Salam, A.S.G., (2019). Testing statistical assumptions in research. John Wiley & Sons. Hoboken, New Jersey. USA. pp.141-147.

Vieira, S.M., Kaymak, U. and Sousa, J.M., (2010). Cohen's kappa coefficient as a performance measure for feature selection. In International Conference on Fuzzy Systems. *IEEE*. pp.1-8.

Virgile, A. and Bishop, C., (2021). A narrative review of limb dominance: Task specificity and the importance of fitness testing. *The Journal of Strength & Conditioning Research*, 35(3), pp.846-858.

Vleeming, A., Schuenke, M.D., Masi, A.T., Carreiro, J.E., Danneels, L. and Willard, F.H., (2012). The sacroiliac joint: an overview of its anatomy, function and potential clinical implications. *Journal of Anatomy*, 221(6), pp.537-567.

Wahba, G.M., Hostikka, S.L. and Carpenter, E.M., (2001). The paralogous Hox genes Hoxa10 and Hoxd10 interact to pattern the mouse hindlimb peripheral nervous system and skeleton. *Developmental Biology*, 231(1), pp.87-102.

Wang, J.M., Kirkpatrick, C. and Loukas, M., (2018). The Iliolumbar Ligament Does Not Have a Direct Nerve Supply. *The Spine Scholar*, pp.1-5.

Ward, C.V. and Latimer, B., (2005). Human evolution and the development of spondylolysis. *Spine*, 30(16), pp.1808-1814.

Wayne, C.R., 2016. Metric Variation in the Human Sacrum: Costal Process Length among Black and White South Africans. M.A. Thesis. University of Central Florida. Florida, United States of America. pp.1-34.

Weigelt, L., Laux, C.J., Slankamenac, K., Ngyuen, T.D., Osterhoff, G. and Werner, C.M., (2019). Sacral dysmorphism and its implication on the size of the sacroiliac joint surface. *Clinical Spine Surgery*, 32(3), pp.E140-E144.

Wells, L.H. (1963). Variation in the human vertebral column, with particular reference to the lumbo-sacral junction. *South Africa Medical Journal*. 37, pp.60-64.

Wellik, D.M. and Capecchi, M.R., (2003). Hox10 and Hox11 genes are required to globally pattern the mammalian skeleton. *Science*, 301(5631), pp.363-367.

Wellik, D.M., (2007). Hox patterning of the vertebrate axial skeleton. *Developmental Dynamics*, 236(9), pp.2454-2463.

Wellik, D.M., (2009). Hox genes and vertebrate axial pattern. *Current Topics in Developmental Biology*, 88, pp.257-278.

Wenzel. C. (1824). Über die Krankheiten am Rückgrathe [Diseases of the spine]. Wilhelm Ludwig Wesché, Bamberg, Plate 7, Figure 1. pp.458.

Whitcome, K.K., (2012). Functional implications of variation in lumbar vertebral count among hominins. *Journal of Human Evolution*, 62(4), pp.486-497.

White, R.I. and Klauber, G.T., (1976). Sacral agenesis: Analysis of 22 cases. *Urology*, 8(6), pp.521-525.

White, T.D., Black, M.T. and Folkens, P.A., (2012). Human osteology. Academic press. pp.143-147, 219-225.

Wigh, R.E. and Anthony JR, H.F., (1981). Transitional Lumbosacral Discs: Probability of Herniation. *Spine*, 6(2), pp.168-171.

Williams, S.A., (2011). Evolution of the hominoid vertebral column. Doctoral dissertation, University of Illinois at Urbana-Champaign. pp. 1-170.

Williams, S.A., (2012). Variation in anthropoid vertebral formulae: implications for homology and homoplasy in hominoid evolution. *Journal of Experimental Zoology Part B: Molecular and Developmental Evolution*, 318(2), pp.134-147.

Williams, S.A. and Russo, G.A., (2015). Evolution of the hominoid vertebral column: the long and the short of it. *Evolutionary Anthropology,* 24(1), pp.15-32.

Williams, S.A., Middleton, E.R., Villamil, C.I. and Shattuck, M.R., (2016). Vertebral numbers and human evolution. *American Journal of Physical Anthropology*, 159(S61), pp.S19-S36.

Williams, S.A., Spear, J.K., Petrullo, L., Goldstein, D.M., Lee, A.B., Peterson, A.L., Miano, D.A., Kaczmarek, E.B. and Shattuck, M.R., (2019). Increased variation in numbers of presacral vertebrae in suspensory mammals. *Nature Ecology & Evolution*, 3(6), pp.949-956.

Wolpert, L., (1969). Positional information and the spatial pattern of cellular differentiation. *Journal of Theoretical Biology*, 25(1), pp.1-47.

Wood, J.W., Milner, G.R., Harpending, H.C., Weiss, K.M., Cohen, M.N., Eisenberg, L.E., Hutchinson, D.L., Jankauskas, R., Cesnys, G., Katzenberg, M.A. and Lukacs, J.R., (1992). The osteological paradox: problems of inferring prehistoric health from skeletal samples. *Current Anthropology*, 33(4), pp.343-370.

Wu, L.P., Li, Y.K., Li, Y.M., Zhang, Y.Q. and Zhong, S.Z., (2009). Variable morphology of the sacrum in a Chinese population. *Clinical Anatomy*, 22(5), pp.619-626.

Yanagawa, Y., Ohsaka, H., Jitsuiki, K., Yoshizawa, T., Takeuchi, I., Omori, K., Oode, Y. and Ishikawa, K., (2016). Vacuum phenomenon. *Emergency Radiology*, 23(4), pp.377-382.

Yoshida, H., Shinomiya, K., Nakai, O., Kurosa, Y. and Yamaura, I., (1997). Lumbar nerve root compression caused by lumbar intraspinal gas: report of three cases. *Spine*, 22(3), pp.348-351.

Yoslow, W. and Becker, M.H., (1968). Osseous Bridges between the Transverse Processes of the Lumbar Spine: Report of Three Cases and Review of the Literature. *Journal of Bone and Joint Surgery*, 50(3), pp.513-520.

Zhang, B., Wang, L., Wang, H., Guo, Q., Lu, X. and Chen, D., (2017). Lumbosacral Transitional Vertebra: Possible Role in the Pathogenesis of Adolescent Lumbar Disc Herniation. *World Neurosurgery*. 107, pp.983-989.

Zinn, W.M. (1972). Die konservative Behandlung des Kreuzschmerzes. *Orthopade*. 1, pp.177-84.

Zlolniski, S., Torres-Tamayo, N., García-Martínez, D., Blanco-Pérez, E., Mata-Escolano, F., Barash, A., Nalla, S., Martelli, S., Sanchis-Gimeno, J.A. and Bastir, M., (2019). 3D geometric morphometric analysis of variation in the human lumbar spine. *American Journal of Physical Anthropology*, 170(3), pp.361-372.

Zlomislic, V. and Garfin, S.R., (2019). Anatomy and Biomechanics of the Sacroiliac Joint. *Techniques in Orthopaedics*, 34(2), pp.70-75.

APPENDICES

Appendix 1: University of Cape Town Ethics Approval

UNIVERSITY OF CAPE TOWN
Faculty of Health Sciences
Human Research Ethics Committee

Room E53-46 Old Main Building
Groote Schuur Hospital
Observatory 7925
Telephone [021] 406 6626
Email: shureta.thomas@uct.ac.za
Website: www.health.uct.ac.za/fhs/research/humanethics/forms

22 June 2017

HREC REF: 195/2017

Prof G Louw
Clinical Anatomy and Biological Anthropology
Human Biology
Anatomy Building

Dear Prof G Louw

PROJECT TITLE: LUMBOSACRAL TRANSITIONAL VERTEBRA MORPHOLOGY; A SOUTH AFRICAN POPULATION (PhD-candidate-Dr G Paton)

Thank you for submitting your response to the Faculty of Health Sciences Human Research Ethics Committee dated 6 June 2017.

It is a pleasure to inform you that the HREC has **formally approved** the above-mentioned study.

Approval is granted for one year until the 30 June 2018.

Please submit a progress form, using the standardised Annual Report Form if the study continues beyond the approval period. Please submit a Standard Closure form if the study is completed within the approval period.
(Forms can be found on our website: www.health.uct.ac.za/fhs/research/humanethics/forms)

Please quote the HREC REF in all your correspondence.

Please note that the ongoing ethical conduct of the study remains the responsibility of the principal investigator.

Please note that for all studies approved by the HREC, the principal investigator **must** obtain appropriate institutional approval before the research may occur.

The HREC acknowledge that the student, Dr Glen James Paton will also be involved in this study.

Yours sincerely

Signature Removed

PROFESSOR M BLOCKMAN
CHAIRPERSON, FHS HUMAN RESEARCH ETHICS COMMITTEE
Federal Wide Assurance Number: FWA00001637.
Institutional Review Board (IRB) number: IRB00001938

HREC 195/2017

Appendix 1B: University of Cape Town Extension of Ethics Approval

HUMAN RESEARCH ETHICS COMMITTEE
20 JUL 2018
HEALTH SCIENCES FACULTY UNIVERSITY OF CAPE TOWN

UNIVERSITY OF CAPE TOWN
FACULTY OF HEALTH SCIENCES
Human Research Ethics Committee

FHS016: Annual Progress Report / Renewal

HREC office use only (FWA00001637; IRB00001938) This serves as notification of annual approval, including any documentation described below.			
☑ Approved	Annual progress report	Approved until/next renewal date	30/07/2019
☐ Not approved	See attached comments		
Signature Chairperson of the HREC		Date Signed	23/7/2018

Comments to PI from the HREC

Principal Investigator to complete the following:

1. Protocol information

Date (when submitting this form)	19/7/2018		
HREC REF Number	195/2017	Current Ethics Approval was granted until	30 June 2018
Protocol title	LUMBOSACRAL TRANSITIONAL VERTEBRA MORPHOLOGY: A SOUTH AFRICAN POPULATION		
Protocol number (if applicable)			
Are there any sub-studies linked to this study?	☐ Yes ✓ No		
If yes, could you please provide the HREC Ref's for all sub-studies? Note: A separate FHS016 must be submitted for each sub-study			
Principal Investigator	Prof Graham Louw, student: Dr Glen James Paton		
Department / Office Internal Mail Address	Graham.louw@uct.ac.za		
1.1 Does this protocol receive US Federal funding?		☐ Yes	✓ No

(Note: Please complete the Closure form (FHS010) if the study is completed within the approval period)

Signature Removed

Appendix 2: University of Witwatersrand Ethics Approval

School of Anatomical Sciences
University of the Witwatersrand, Johannesburg
7 York Rd, Parktown 2193, South Africa • Tel: +27 11 717 2713 • Fax: +27 11 717 2422 • www.wits.ac.za

SCHOOL OF ANATOMICAL SCIENCES COLLECTIONS COMMITTEE

APPROVAL TO CONDUCT RESEARCH IN COLLECTION

NAME: Glen Paton
(Principal investigator)

AFILIATION/S: Anatomy Department, University of Cape Town

REFERENCE NUMBER:

PROJECT TITLE: Lumbosacral transitional vertebra: A South African population

COLLABORATORS:

N/A

COLLECTION TO BE ACCESSED:

Raymond A. Dart Collection of Human Skeletons

DECISION: Approved

CONDITIONS:

The validity of this approval extends up to **2 years** from the date on this approval document.

APPROVED BY: Signature Removed

Mr Brendon Billings, Chair of Collections Committee

DATE OF APPROVAL: 14/02/2018

Anatomical Sciences

Appendix 3: Ethics Approval for Charlotte Maxeke Johannesburg Academic Hospital

GAUTENG PROVINCE
HEALTH
REPUBLIC OF SOUTH AFRICA

CHARLOTTE MAXEKE JOHANNESBURG ACADEMIC HOSPITAL

Enquiries:
Ms. N. Mzila
Office of the Clinical Director
Tell: (011): 488-4812
Email: Nolwazi.Mzila@gautemg.gov.za
20 August 2018

GP_201807_050

Dear Dr. Glen James Paton

STUDY TITLE: Lumbosacral Transitional Vertebra Morphology: A South African Population

Permission is granted for you to conduct the above recruitment activities as described in your request provided:

1. Charlotte Maxeke Johannesburg Academic Hospital will not anyway incur or inherit costs as result of the said study.
2. Your study shall not disrupt services at the study sites.
3. Strict confidentiality shall be observed at all times.
4. Informed consent shall be solicited from patients participating in your study.

Please liaise with the HOD and Unit Manager or sister in charge to agree on the dates and time that would suit all parties.

Kindly forward this office with the results of your study on completion of the research.

Supported / ~~not supported~~

Dr. M.I. Mofokeng
Clinical Director
DATE: 22/8/2018

Approved/~~not approved~~

Ms. G. Ngogoshi
Chief Executive Officer
Date: 23/8/2018

Signatures Removed

Appendix 4: Ethics Approval for Groote Schuur Hospital

Western Cape Government
Health

GROOTE SCHUUR HOSPITAL
Enquiries: Dr Bernadette Eick
E-mail : Bernadette.Eick@westerncape.gov.za

Professor Graham Louw
Clinical Anatomy & Biological Anthropology

E-mail: Graham.Louw@uct.ac.za / gipchiro@gmail.com

Dear Dr Louw,

RESEARCH PROJECT EXTENSION: Lumbosacral Transitional Vertebra Morphology: A South African Population

Your recent communication to the hospital refers.

The extension of your research is approved in accordance with UCT Ethics clearance, until **30 July 2019, subject to the approval of Professor Steve Beningfield.**

As previously mentioned:

a) Your research may not interfere with normal patient care.
b) Hospital staff may not be asked to assist with the research.
c) No hospital consumables and stationary may be used.
d) **No patient folders may be removed from the premises or be inaccessible.**
e) Please provide the research assistant/field worker with a copy of this letter as verification of approval.
f) Confidentiality must be maintained at all times.
g) Once the research is complete, please submit a copy of the publication or report.

I would like to wish you every success with the project.

Yours sincerely

Signature Removed

DR BERNADETTE EICK
CHIEF OPERATIONAL OFFICER
Date: 3 October 2018

C.C. Mr L. NaidooT
Dr H. Aziz
Professor S. Beningfield

G46 Management Suite, Old Main Building,
Observatory 7925

Tel: +27 21 404 6288 fax: +27 21 404 6125

Private Bag X,
Observatory, 7935

www.capegateway.go.v.za